Development and application of consistent path size route choice models

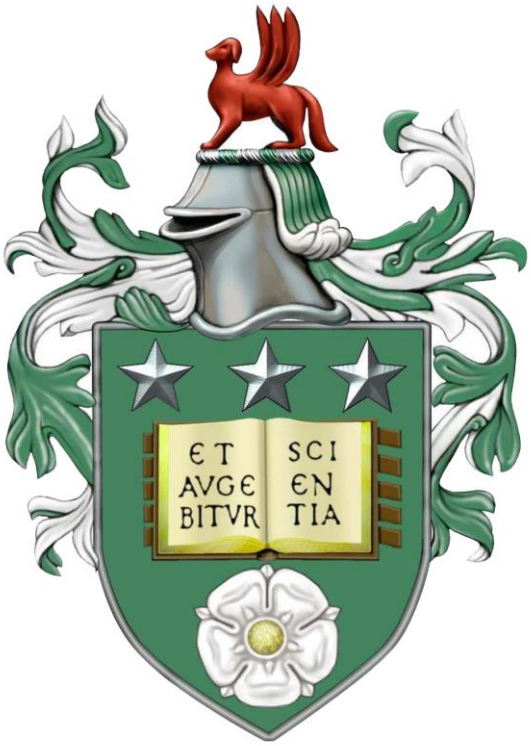

Submitted in accordance with the requirements
for the degree of Doctor of Philosophy
by

Lawrence Christopher Duncan

University of Leeds
February 2021

Intellectual Property and Publications

The candidate confirms that the work submitted is his own, except where work which has formed part of jointly authored publications has been included. The contribution of the candidate and the other authors to this work has been explicitly indicated below. The candidate confirms that appropriate credit has been given within the thesis where reference has been made to the work of others.

The work in Chapter 2 of this thesis has appeared in publication as follows:

Duncan L, Watling D, Connors R, Rasmussen T, & Nielsen O, (2020). *Path Size Logit route choice models: Issues with current models, a new internally consistent approach, and parameter estimation on a large-scale network with GPS data*. Transportation Research Part B, 135, p.1-40.

I developed the main idea for the work together with all co-authors. I performed the theoretical analysis, wrote the computer code to implement the models, conducted the numerical experiments, and was lead author on the written manuscript. All co-authors provided recommendations on the modelling and comments on the results. The manuscript was improved by comments from all the co-authors.

The work in Chapter 3 of this thesis is a manuscript under review:

Duncan L, Watling D, Connors R, Rasmussen T, & Nielsen O, (under review). *Formulation and solution of Adaptive Path Size Logit Stochastic User Equilibrium – addressing choice set robustness and internal consistency*.

I developed the main idea for the work together with all co-authors. I performed the theoretical analysis, wrote the computer code to implement the models, conducted the numerical experiments, and was lead author on the written manuscript. All co-authors provided recommendations on the modelling and comments on the results. The manuscript was improved by comments from all the co-authors.

The work in Chapter 4 of this thesis has appeared in publication as follows:

Duncan L, Watling D, Connors R, Rasmussen T, & Nielsen O, (2021). *A bounded path size route choice model excluding unrealistic routes: Formulation and estimation from a large-scale GPS study. Transportmetrica A: Transport Science.*

I developed the main idea for the work together with all co-authors. I performed the theoretical analysis, wrote the computer code to implement the models, conducted the numerical experiments, and was lead author on the written manuscript. All co-authors provided recommendations on the modelling and comments on the results. The manuscript was improved by comments from all the co-authors.

The work in Chapter 5 of this thesis is a manuscript in preparation:

Duncan L, Watling D, Connors R, Rasmussen T, & Nielsen O, (in preparation). *Formulation and solution of bounded path size stochastic user equilibrium models – consistently addressing route overlap and unrealistic routes*.

I developed the main idea for the work together with all co-authors. I performed the theoretical analysis, wrote the computer code to implement the models, conducted the numerical experiments, and was lead author on the written manuscript. All co-authors provided recommendations on the modelling and comments on the results. The manuscript was improved by comments from all the co-authors.

Acknowledgements

First and foremost, I would like to express my sincere gratitude for all the guidance that my supervisors David Watling and Richard Connors have given me. They have both been incredibly supportive and inspirational throughout my time in Leeds. Their passion for the field and expertise in it were apparent from the outset and I have very quickly grown to share their enthusiasm. Under their exemplary supervision I have learnt valuable skills in how to be an independent academic researcher, and I owe a lot of my achievements to them. I would specifically like to thank David for encouraging me to pursue a PhD, helping me to obtain funding, and believing in my ability to complete it.

I would also like to say a big thank you to my co-authors Thomas Kjær Rasmussen and Otto Anker Nielsen. I have benefitted immeasurably from the collaboration of research my supervisors and I have had with colleagues at the Technical University of Denmark (DTU). Thomas and Otto have both shown great enthusiasm to assist me in my research. Our meetings have been highly constructive, and their comments have greatly improved the quality of the papers. I extend my thanks to DTU for allowing me to use their data, and for also giving me access to their supercomputers, which I could not have conducted my experiments without. I thank Thomas, Otto, and DTU for their kind hospitality when I have visited.

Additionally, I would like to thank Dave Milne for giving me the opportunity to be module assistant, which I enjoyed immensely and gained invaluable experience in teaching. And, I thank the Spatial Modelling and Dynamics group for giving me feedback on my presentations. I also acknowledge the financial support provided by the University of Leeds for awarding me a Doctoral Scholarship.

Abstract

The congestion of road traffic has a negative effect on the environment, the economy, and the well-being of people. It has therefore long been the aim of transport agencies to reduce congestion levels by improving transport infrastructure. It is essential that decision processes related to improving transport infrastructure, are supported by a well-functioning transport model which gives a realistic representation of the route choices of travellers. The ability to predict driver route choice means that route flows can be calculated and areas of potentially high levels of congestion can be identified, in turn allowing us to investigate many eventualities, and assess any possible remedial measures. This thesis develops new route choice models, specifically: path size route choice models, and investigates their applicability for use in real-life, e.g. parameter estimation and solution within network equilibrium.

Path Size Logit route choice models attempt to capture the correlation between overlapping routes by including correction terms within the route utility functions. This provides a convenient closed-form solution for implementation in traffic network models. The path size terms measure distinctiveness of routes; a route is penalised based on the number of other routes sharing its links, and the costs of those shared links. Typically, real road networks have many very long routes that should be considered unrealistic and excluded from route choice. Such unrealistic routes are problematic for the Path Size Logit (PSL) model because they negatively impact the choice probabilities of realistic routes when links are shared. The Generalised Path Size Logit (GPSL) model attempts to address this problem by weighting the contributions of routes to path size terms according to the ratio of route travel costs. However, the GPSL model is not internally consistent in how it defines routes as being unrealistic: the path size terms consider only travel cost, whereas the route choice probability relation considers disutility including the correction term.

To solve these challenges, this thesis formulates a new internally consistent Adaptive Path Size Logit (APSL) model wherein routes contribute to path size terms according to the ratio of route choice probabilities, ensuring that routes defined as unrealistic by the path size terms, are exactly those with very low choice probabilities.

While the GPSL and APSL models improve upon PSL in reducing the negative effects of unrealistic routes, the issue is not solved entirely; this thesis also investigates how one might eliminate unrealistic route contributions entirely, as well as remove all the negative effects of unrealistic routes by also assigning them zero choice probabilities. In order to do so, the integration of PSL concepts with the recently developed Bounded Choice Model (BCM) (Watling et al, 2018) is explored. A mathematically well-defined Bounded Path Size (BPS) route choice model is then derived that utilises a consistent criterion for assigning zero choice probabilities to unrealistic routes while eliminating their path size contributions.

Parameter estimation for the APSL and BPS models is explored in simulation studies and on a real-life large-scale network using GPS data, where computational feasibility is demonstrated. And, their application to Stochastic User Equilibrium is investigated, where it is proven that solutions are guaranteed to exist, and solution uniqueness is explored numerically.

Contents

List of Tables

List of Figures

List of Abbreviations

AON	All-Or-Nothing
APSL	Adaptive Path Size Logit
BAPS	Bounded Adaptive Path Size
BBPS	Bounded Bounded Path Size
BCM	Bounded Choice Model
BPS	Bounded Path Size
BRUE	Bounded Rational User Equilibrium
BSUE	Bounded Stochastic User Equilibrium
CCL	Congestion-based C-Logit
CL	C-Logit
CMM	Cross-Moment Model
CNL	Cross-Nested Logit
DP	Desired Property
DUE	Deterministic User Equilibrium
FAA	Flow-Averaging Algorithm
FPIM	Fixed-Point Iteration Method
GEV	Generalised Extreme Value
GNL	Generalised Nested Logit
GPS	Global Positioning System
GPSL	Generalised Path Size Logit
IID	Independently and Identically Distributed
LCL	Length-based C-Logit
LL	Log-Likelihood
MDM	Marginal Distribution Model
MFD	Macroscopic Fundamental Diagram
MLE	Maximum Likelihood Estimation
MNG	Multinomial Gammit
MNL	Multinomial Logit
MNP	Multinomial Probit
MNW	Multinomial Weibit
MP	Mathematical Programming
MSA	Method of Successive Averages
MSE	Mean Squared Error
MSWA	Method of Successive Weighted Averages
OD	Origin-Destination
PCL	Paired Combinatorial Logit
PSCL	Path Size Correction Logit
PSH	Path Size Hybrid
PSL	Path Size Logit
PSW	Path Size Weibit
RMSE	Route Mean Squared Error
RP	Required Properties
RRM	Random Regret Minimization
RSUE	Restricted Stochastic User Equilibrium
RSUET	Restricted Stochastic User Equilibrium with a Threshold
RUM	Random Utility Model
RUT	Random Utility Theory
SUE	Stochastic User Equilibrium

Chapter 1. Introduction

1. Background & Motivation

Road users worldwide waste many hours in congestion every day, which constitutes a large annual societal loss (see INRIX (2020) for figures in different countries). Moreover, a significant share of air pollution emissions is generated by road transport (e.g. over a quarter in Denmark (Klimarådet, 2020)), and it is well-documented that these transport related emissions have numerous negative effects on e.g. the climate and public health (Krzyzanowski et al, 2005; Ortiz, 2019; Stanley et al, 2011). Lower traffic volumes – such as those experienced during the Covid-19 pandemic – also reduces the frequency of on-road vehicle collisions (INRIX, 2020), which also have a significant economic impact (Blincoe et al, 2002). On-the-other-hand, due to increased vehicle speeds experienced with lower traffic volumes, fatality rates of the vehicle collisions actually increased during the pandemic (INRIX, 2020). All of this evidence points to the need to understand the interplay between traffic congestion and economic, environmental, and safety issues.

There is a consensus among researchers that neither the congestion challenge nor vehicle emission reduction goals (e.g. Klimarådet, 2020) can be fulfilled solely and cost-effectively through technological advancements (such as with biofuels or a transition to electric vehicles). A behavioural change of road users is therefore considered essential, and it is an aim of transport agencies to develop and introduce transport policies and interventions which instigate behavioural changes that reduce or beneficially displace congestion. For example, tolling schemes have proven successful in changing behaviour in cities such as Singapore, Stockholm, and London (Chin, 1996; Johansson, 2009; Tonne, 2008), and promise has been shown for region perimeter control schemes (e.g. in Nanjing (Du et al, 2015)).

In order to evaluate the impacts of different potential policy schemes and interventions, and provide evidence to either support or oppose different strategies, it is essential that policy makers have a well-functioning transport model, which gives a realistic representation of travel behaviour for travel adjustment predictions. Numerous models and computational methods have been constructed to capture the behaviour of drivers on road networks. These behavioural models classically involve predicting traffic flows on each road of the physical network with route choice traffic assignment models. Recent years have seen the emergence of more computationally attractive but less detailed approaches, however, that model traffic at an aggregated level exchanging between regions, for example using Macroscopic Fundamental Diagrams (e.g. Yildirimoglu & Geroliminis (2014), Batista & Leclercq (2019), Mariotte et al (2020)). This thesis, however, focuses on developing the traditional route choice traffic assignment model. There are two types of such model: Dynamic Traffic Assignment (DTA) and Static Traffic Assignment (DTA).

DTA models how the traffic on the network evolves over time, such as how vehicle flow propagates through the network interacting with each other and road conditions such as traffic lights. Several traffic simulation software packages such as VISSIM (Fellendorf & Vortisch, 2010), METROPILIS (Marchal, 2001), AIMSUN (Casas et al, 2010; Barcelo & Casas, 2005), and DynusT (Chiu & Bustillos, 2009; Chiu et al, 2010; Chiu et al, 2011; Nava & Chiu, 2012) have been developed based on DTA, as tools for policy makers to simulate travel behaviour. DTA and associated software packages have been used to investigate policy interventions in real-life case studies, such as road pricing schemes in Maryland (Chen et al, 2015; Chen et al, 2016), Tehran (Hosseinlou et al, 2016), and Athens (Gkotsis, 2006).

STA on-the-other-hand provides an aggregate representation of the traffic flow on the network links for a given period of time, supposing the vehicle flow is omnipresent across the route links. Generally, STA models are unable to properly account for the effects of congestion, such as how bottlenecks lead to flow-metering and spillbacks (Brederode et al, 2019), though ‘quasi-dynamic’ approaches have been developed to extend STA models to approximate such phenomena (e.g. Bleimer et al, 2014; Brederode et al, 2019). Three quasi-dynamic traffic assignment models in use in strategic transport model systems that, to some extent, capture flow metering and spillback effects are: QBLOK (Bakker et al, 1994) used solely in the Dutch national models system, SATURN (Van Vliet et al, 1980) used in e.g. London Highway Assignment Models, and the blocking back assignment in PTV VISUM (Bundschuh et al, 2006) used in e.g. the UK west midlands PRISM model and Flemish strategic traffic models (Brederode et al, 2019).

Although DTA models are able to produce the most realistic traffic flows and travel times, they have a much higher computational complexity, require more sophisticated calibration techniques, have poor convergence/mathematical properties, and are less scalable (Bleimer, 2014). Furthermore, despite having the

potential to provide more accuracy than traditional STA models, quasi-dynamic approaches tend not to have a solid theoretical basis, presented merely as algorithms with no underlying mathematical problem formulation and without specified assumptions. This leads to poor accountability and makes calibration cumbersome and model-specific (Brederode et al, 2019). Standard STA models on-the-other-hand are attractive due to their ease of use, comprehensibility, computational convenience, well-behaved convergence properties, and mathematical rigour (Bleimer, 2014). This thesis therefore focuses on advancing STA models, though the concepts developed are relevant and applicable also for DTA and quasi-dynamic models.

To set the background, the following details generic network modelling concepts. A typical road network has many spatially aggregated origins and destinations for trips, where a single Origin and Destination trip is known as an OD movement. Furthermore, each OD movement has a travel demand representing the number of drivers who make this trip in a given period of time (most commonly an hour). For each OD movement, there is a universal choice set of routes that a driver can take from the origin node to the destination node. A common assumption is that this set includes all 'simple' routes, i.e. where there are no cycles and no link is traversed more than once; this is to adhere to what one might consider as being sensible driving behaviours, though this assumption is not always upheld (Akamatsu, 1996).

In order to model the route choice behaviour of drivers, it has been proposed that each link in a network has a generalised travel cost that relates to some observable attributes of that link. The most basic travel cost is link/road length, though travel time is the most commonly used. Other attributes, for example any existing toll along the road, can also be incorporated into the generalised travel cost, usually by quantifying that cost in terms of time. This means that all drivers in the network have a perception of the travel cost (time penalty) associated with traversing along each link. Furthermore, it is assumed that the generalised travel cost for each route in the network can be calculated by summing up the generalised travel costs of the links that make up that route, hence, for each OD movement, the drivers have a perception of the generalised travel time cost for each available route.

As noted by e.g. Papola et al (2018), there are several distinct and unique aspects about route choice modelling that makes it a more challenging task than modelling other types of transport choices. The literature highlights four key aspects in particular.

The first aspect, as discussed by e.g. Damberg et al (1996), is that the exact characteristics of each available route are not necessarily known to the driver, for example the exact lengths of each route, nor are the route characteristics necessarily perceived uniformly among the drivers, for example different drivers may perceive a toll charge differently. Furthermore, as noted by Watling et al (2015), there is likely to be uncertainty from the modeller in terms of quantifying the attractiveness of each route, for example unobserved attributes. Consider the example network in Fig. 1.1. The travel costs as stipulated on the links result in Route 2 being the cheapest alternative. However, supposing there is some imprecision in measuring the travel costs, and that the 0.3 costing link in Route 3 was actually less, Route 3 could well be the best alternative.

The second aspect, as Papola et al (2018) describes, is that the choice that drivers have of choosing between routes is often correlated due to the topological overlapping of routes on a road network. Correlation between alternatives is common in choice modelling, but the particular difficulty for route choice is that the correlation structure of overlapping routes on the physical network is highly complex, which causes computational problems. It is widely acknowledged, however, that not accounting for the correlations between routes leads to unrealistic route flow predictions (e.g. Hoogendoorn-Lanser et al, 2005; Chen et al, 2012). Considering again Fig. 1.1, Routes 2&3 both share the 0.8 costing link and a significant proportion of their journeys. Clearly, the decision to take Route 2 is closely aligned with the decision to take Route 3 and the two routes should not be considered independently. It is worth noting also that *firstly*, it has been questioned whether travellers are fully aware of the topological overlapping of routes (e.g. Hoogendoorn-Lanser et al, 2005). Although two given routes may physically overlap and thus in theory drivers should perceive the two trips as being correlated, if the driver does not have a very good knowledge of the physical network structure (but does have an idea of the attractiveness of the two routes), then the fact that that the routes overlap is irrelevant. *Secondly*, regardless of the knowledge of the physical network structure, the correlation network structure that driver's actual consider may be different to the physical one (Frejinger & Bierlaire, 2007; Frejinger et al, 2009). It is questioned whether it is behaviourally realistic for drivers to have full knowledge of the physical network and/or that they take into account correlation between all parts that overlap. Frejinger & Bierlaire (2007) suppose for example that drivers only consider correlation between subnetworks consisting of the key most prevalent parts, such as motorways. Also, in the DTA framework there can be correlation

between leaving at different times (Bhat, 1998), e.g. the decision to set-off at 8:00am is likely to be correlated with the decision to set-off at 8:05am as there may be similar travel experiences, however setting off at perhaps 10:00am the congestion state will be different entirely.

The third aspect is that typical road networks have many possibilities for routes that should be considered unrealistic and excluded from route choice (Watling et al, 2015; Watling et al, 2018). It is important to point out here the distinction between an 'unrealistic route' and 'low probability route'. *Unrealistic routes* are routes that exist as possible options from the network, but drivers would not realistically consider taking them, i.e. they are not in the choice set for drivers and have zero probability of being chosen. *Low probability routes*, however, are routes that are within the choice set for drivers but have a very low likelihood of being chosen. On real-life networks, enumerating and performing route choice with the universal set of routes is behaviourally unrealistic and computationally infeasible, as the set contains millions of routes even in medium-sized networks, the majority of which are not routes that drivers would realistically consider taking. However, there is nothing physical that can be measured to determine with certainty whether a route is realistic or unrealistic, it can be a matter of opinion. A useful modelling concept is that there are cut-offs in travel costs that can define realistic and unrealistic routes, for example a cut-off in terms of the length of a route (e.g. Watling et al, 2015; Rasmussen et al, 2015; Watling et al, 2018). But, there is no exact science to determining exactly where the cut-offs are, and these may not be uniform across all drivers. Nonetheless, there is often a large number of routes that would clearly not be considered in the mental map that travellers build in their mind when making their route choice decisions, e.g. very long routes. Considering Fig. 1.1, it is clear that Route 1 is so costly that no driver would realistically consider taking it. It is less clear, however, whether the travel cost of Route 4 should mean it is considered unrealistic. It is worth noting route 'outliers' are common in tracked route data (e.g. GPS data), where the route an individual has taken between the origin and destination appears to be unrealistic/illogical. However, this is often because either: a) there is a model mis-specification error in that there are attributes of the route not captured by the modeller that the driver considered (for example the route passing by nicer scenery), and/or, b) there is a data error in that the data did not capture the true origins and true destinations of trips where a single route observation may actually contain multiple different trips (for example a driver may travel to drop a kid off at school and then to work, captured as one trip, but it is actually two). Thus, when the term 'realistic' is used for a route it means realistic as defined by the model and the utility attributes assumed.

The fourth aspect is that trips are affected by congestion; as Patriksson (2015) describes, as the number of drivers travelling on a road increases, the limited capacity of the road results in increased congestion, and hence increases in travel time. Congestion is known to highly influence travel behaviour and the distribution of traffic. It is thus crucial that the effects of congestion are incorporated into modelling route choice, and this is done through traffic assignment. Considering Fig. 1.1, supposing that the travel demand is $d = 100$, and the capacity of each link is 80 before a jamming scenario occurs, one might expect the drivers to distribute themselves in such a way to avoid the jamming situation, for example by 70 using the cheaper Routes 2&3 and 30 using Route 4.

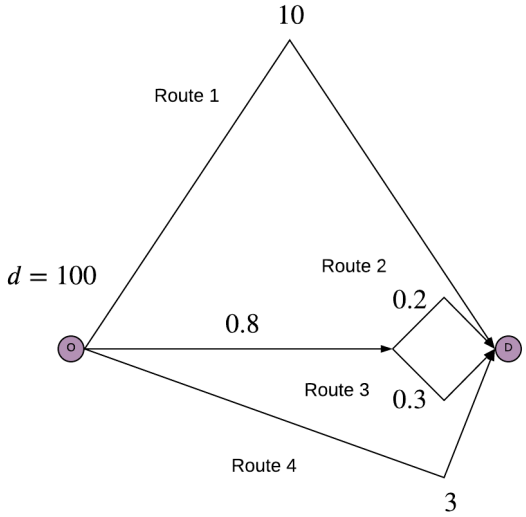

Fig. 1.1. Example network.

For behaviourally realistic traffic flow predictions, one must address these four key challenging aspects of route choice modelling. Numerous modelling approaches have been developed to address these challenges; however, as will be discussed in the subsequent sections and explored in more detail in the thesis, some of the models/approaches have issues with theoretical consistency, robustness, and/or being mathematically well-defined. The motivation for the research in this thesis was therefore to solve this by developing a new route choice modelling framework.

Before deciding on the approach to pursue, there were some requirements. The aim was to develop a model that would be suitable for traffic flow predictions on real-life networks, which are typically large-scale in size and present a greater computational challenge due to the greater number of links, nodes, routes, and OD movements. It was therefore considered crucial that the developed model could be solved in feasible computation times on large-scale networks, which would hence allow for rigorous analyses of policy schemes, rather than potentially only being able to test a handful of scenarios for a scheme in a feasible amount of time. Furthermore, the ability to successfully estimate the parameters of a model is crucial in order to be able to apply the model for e.g. policy testing, and hence the other requirement was that the proposed model could be successfully estimated. In order to set the background for the research in this thesis, and to set out the motivation for the research directions pursued, *the following four subsections* below discuss existing modelling approaches for the four key challenging aspects of route choice modelling, and review their potential suitability for the requirements set out above.

1.1 Aspect 1: Allowing for Driver/Modelling Uncertainties

In choice theory, the utility of a product or service is a scalar measure of its attractiveness; hence, the utility of a route relates to its travel cost. The Utility Maximisation concept states that when a driver is choosing between routes they will attempt to choose the route that maximises their utility, i.e. that will minimise their travel time cost. The all-or-nothing (AON) model could be considered as the most primitive route choice model, which proposes that all drivers will opt to travel upon the lowest costing route(s) in each OD choice set: maximising total utility. The AON model has however been widely discredited for being unrealistic. One of the reasons for this is that the model assumes all drivers have a uniform perception of the cost of each route, and that there is no uncertainty from the modeller in terms of any unobserved attributes or any unobserved heterogeneity in the utilities.

The well-known Random Utility Theory acknowledges the difficulties in analysing route choice behaviour and supposes that the utilities are not known with any certainty. To compensate for this, the utilities are treated as random variables, and thus include random error terms. The probability that the utility of a route is perceived to be greater than another depends upon the distribution of the error terms. Thus, assuming drivers (travellers) wish to maximise their utility (i.e. wish to choose the lowest costing route (path)), Watling et al (2015) state Stochastic User Conditions:

> *"For any OD movement, the proportion of travellers on a path is equal to the probability that the path has a perceived utility greater than [or equal to] the perceived utility of all alternative paths."*

Random Utility Models (RUMs) propose different distributions for the random error terms. For example, Multinomial Logit (MNL) (Dial, 1971), Multinomial Probit (MNP) (Daganzo & Sheffi, 1977), Multinomial Gammit (MNG) (Cantarella & Binetti, 2002), and Multinomial Weibit (MNW) (Castillo et al, 2008), propose that the error terms assume Gumbel, Normal, Gamma, and Weibit distributions, respectively.

1.2 Aspect 2: Capturing Route Correlations

The deficiency of the MNL model in its inability to capture correlations between overlapping routes is well-known. This issue stems from the underlying assumption made by the MNL model that the random error terms are Independently and Identically Distributed (IID) with the same, fixed variances (Sheffi, 1985). Numerous adaptations of the MNL model have been proposed in the literature which relax the IID assumption – specifically the independently distributed assumption – to attempt to capture the correlation between routes. These extended Logit models can be classified into three groups according to the model structures as suggested by Prashker & Bekhor (2004): GEV structures, Mixed Logit models, and MNL-modification models. Alternative RUMs to MNL either capture route correlations implicitly or utilise concepts from

extended Logit models to similarly adapt the model. Collating extended Logit models and alternative RUMs, there are three general types of correlation-based route choice models: GEV structure models, simulation models, and correction term models. Each of these categories is reviewed in turn below.

1.2.1 GEV Structure Models

GEV structure models are those that are based on the Generalized Extreme Value (GEV) theory (McFadden, 1978), which use a multi-level tree structure to capture the similarity among routes through the random error component of the utility function. These models include: Cross-Nested Logit (CNL) (Vovsha, 1997; Bekhor & Prashker, 1999), Paired Combinatorial Logit (PCL) (Chu, 1989; Bekhor & Prashker, 1999; Gliebe et al, 1999; Pravinvongvuth & Chen, 2005), Generalized Nested Logit (GNL) (Bekhor & Prashker, 2001; Wen & Koppelman, 2001), and the Network GEV model (Bierlaire, 2002; Daly & Bierlaire, 2006). For PCL, the logic is that each pair of routes in a choice set form a nest and routes are chosen from each nest. For CNL/GNL, each link in the network corresponds to a nest and routes using each link are chosen from that nest. The Network GEV model uses a fairly general class of networks to generalise the use of trees to represent nested logit models to a network representation.

Computational features: Although GEV structure models have closed-form probability expressions, due to their multi-level tree structure the choice probabilities are complex to compute, where the computational burden escalates significantly as the scale of network / choice set sizes increase. This is because the number of nests increases exponentially as the number of links/routes increases. This raises concerns over the applicability of GEV structure models to real-life large-scale networks, where there are potentially thousands of links and routes.

Estimation features: There are numerous different issues involved in estimating the numerous different specifications of the CNL model for route choice, and several studies have discussed issues in detail, for example see Bierlaire (2006), Abbe et al (2007), Marzano & Papola (2008). To summarise a few of the issues documented: a) there may be infinite specifications with different choice probabilities that lead to the same covariance figures (Marzano & Papola, 2008); b) the number of unknown parameters to be estimated increases as the number of routes increases (Marzano & Papola, 2008); c) several studies have found that when estimating the nesting coefficients the model tends to collapse to MNL (Ramming, 2002; Prato, 2005; Prato & Bekhor, 2006); d) the maximum likelihood estimation functions are not concave which significantly complicates the identification of a global maximum (Bierlaire, 2006); and, e) because of d), nonlinear programming methods tend to converge towards local maxima of the log-likelihood function, and in practice, one observes a significant influence of the initial values provided to the algorithm on the estimated parameters (Abbe et al, 2007). GNL requires the estimation of an additional parameter over CNL which makes parameter estimation more difficult.

1.2.2 Simulation Models

Simulation models include Mixed Logit models (Ben-Akiva & Bolduc, 1996; McFadden & Train, 2000) such as the Factor Analytic Logit Kernel model (Bekhor et al, 2002), as well as alternative RUMs to MNL such as MNP and MNG. Mixed Logit models divide the error terms into two Gumbel and Gaussian distributed variable components which ensures the Logit structure is kept while allowing for capturing interdependencies between routes. MNP and MNG etc. do not suffer from the same issue as MNL, as the similarity between each pair of routes is accounted for by allowing for covariance between the error terms, and route correlations are thus captured implicitly.

Computational features: The main problem for simulation models is that they do not have closed-form expressions and solving the choice probabilities requires either Monte Carlo simulation or alternative methods, all of which are computationally burdensome. Many analytical approximation methods have been proposed to solve the MNP model, all aiming to provide the best compromise between speed and accuracy (reviews can be seen in e.g. Rosa (2003), Connors et al (2014)); however, performance of these approaches are assessed with a very limited number of routes, typically up to just 25 alternatives. It is generally considered infeasible to accurately compute MNP, MNG etc. probabilities on large-scale networks with thousands of routes.

Estimation features: Studies have discussed/found difficulties in estimating the parameters of the Factor Analytic Logit Kernel model: Ramming (2002) finds instable estimates of the covariance parameters, despite the very large number of random draws, while Prato (2005) discusses the difficulty in obtaining significant

estimates. And, there are also issues involved in estimating the MNP model, including: identification issues arising from the number of parameters that may need to be estimated (Dansie, 1985; Bunch, 1991; Keane, 1992); and, difficulties in accurately computing small choice probabilities (Connors et al, 2014).

1.2.3 Correction Terms Models

Correction term models modify the deterministic utilities / probability relations by including correction terms that adjust the choice probabilities in order to approximate the correlation between routes. These models include: C-Logit (CL) (Cascetta et al, 1996), Path Size Correction Logit (PSCL) (Bovy et al, 2008), Path Size Logit (PSL) (Ben-Akiva & Ramming, 1998), Path Size Hybrid (PSH) (Xu et al, 2015), and Path Size Weibit (PSW) (Kitthamkesorn & Chen, 2013). CL proposes that the correction terms are based upon commonality factors that measure the similarity of routes, and penalises the utilities accordingly. In contrast, path size models propose that the correction terms are based upon path size terms that measure route distinctiveness: a route is penalised based on the number of other routes sharing its links, and the lengths/costs of those shared links.

Computational features: The main attraction of correction term models is that they all retain the single-level tree structure as MNL and have simple closed-form expressions. This means that the route choice probabilities are generally easy and quick to compute, though as the size of network increases, so does the computational effort required to enumerate the overlap between all routes in a choice set. They are a useful and practical approach to approximating the correlation, however more complex models can capture route correlations more accurately.

Estimation features: Correction term models are frequently estimated on real-life large-scale networks. Their simplicity means that reasonable estimates for parameters can be obtained with relative ease. Examples of estimation studies for correction term models are: Ramming (2002), Bovy et al (2008), Hoogendoorn-Lanser et al (2005), Frejinger & Bierlaire (2007), and Prato (2013).

1.3 Aspect 3: Dealing with Unrealistic Routes

The typical route choice modelling approach for dealing with unrealistic routes, is to employ some kind of heuristic method that attempts to explicitly pre-generate a route choice set containing just the routes considered realistic. Numerous choice set generation schemes have been proposed, such as: distance-bounded enumeration (Leurent, 1997), constrained enumeration (Friedrich et al, 2001; Prato & Bekhor, 2006), probabilistic generation techniques (Cascetta & Papola, 2001; Frejinger et al, 2009), and various deterministic or stochastic shortest path algorithms (e.g. Dijkstra, 1959; Sheffi & Powell, 1982; Ben-Akiva et al, 1984).

The choice set generation approach is problematic, however. *Firstly*, it leads to theoretical inconsistencies, since the route generation criteria is not consistent with the calculation of the choice probabilities among generated routes. Consequently, a route found by the generation criteria may be considered unrealistic by the choice probability criteria, and vice versa, thus leading to inaccurate results. *Secondly*, generating the exact choice sets of realistic routes is very difficult to do, especially on large-scale networks, where there are a greater number of possible routes to generate spanning over a greater distance, and hence there is a greater amount uncertainty on where the cut-off is between realistic and unrealistic. In large-scale case studies, choice sets are typically generated to be large enough so that one can be fairly certain the realistic alternatives are present, regardless of how many unrealistic routes are generated. This is particularly problematic for many correlation-based models since many are not choice set robust, and results are thus negatively influenced by the presence of the unrealistic routes as well as highly sensitive to the choice set generation method adopted (Bovy et al, 2008; Bliemer & Bovy, 2008; Ramming, 2002; Ben-Akiva & Bierlaire, 1999; Bekhor et al, 2008). *Thirdly*, several of the methods are based on Monte Carlo simulation, which introduces a lack of repeatability of results due to this additional source of randomness.

Since it is difficult to obtain choice sets of realistic routes with absolute certainty for the PSL model to be suitable, a pragmatic approach that has been proposed is to utilise a weighted path size contribution technique along with choice set generation to attempt to reduce the impact any present unrealistic routes may have on the choice probabilities of realistic routes. Weighted path size contribution techniques weight the contribution of routes to path size terms with a path size contribution factor. Ben-Akiva & Bierlaire (1999) initially proposed that the contribution factor should be the ratio of the length/cost of each route compared to the shortest/cheapest alternative in the choice set. Hence, contributions of high costing routes compared to the

cheapest alternative are reduced. This was criticised by Ramming (2002) however, since a route that is completely distinct may have a non-zero path size correction term, thus resulting in an undesired penalisation upon the utility of that route.

To combat this, Ramming (2002) proposes the Generalised Path Size Logit (GPSL) model. The GPSL model proposes that the contribution factor is based upon ratios of either length or travel cost between routes, and hence routes with excessively long lengths / large travel costs have a diminished impact upon the correction terms of routes with short lengths / small travel costs, and consequently the choice probabilities of those routes. GPSL requires the estimation of an additional parameter over the PSL model which makes parameter estimation more difficult. Estimates for the parameter can be justified by assessing the goodness-of-fit, though the best estimates in case studies tend to be very large values meaning that it is difficult to provide a behavioural interpretation for the parameter.

An approach that has recently been proposed for consistently dealing with unrealistic routes is the Bounded Choice Model (BCM) (Watling et al, 2018). The BCM has a consistent criterion for determining restricted choice sets of realistic routes, and route choice probability: a bound is applied to the difference in random utility between each given route and an imaginary reference route alternative, so that routes only receive a non-zero choice probability if the difference between its random utility and the random utility of the reference alternative is within the bound. Furthermore, the probability by which each route is chosen relates to the odds associated with choosing each alternative versus the reference alternative. A special case of the BCM is where the reference alternative is that with the maximum deterministic utility i.e. the route with the cheapest generalised travel cost, so that a route only receives a non-zero probability if its cost is within some bound of the cheapest route. The BCM has a simple closed-form probability relation that is similar to MNL and the model is thus suited for large-scale network applications, though estimation of the model has not yet been explored. The key behavioural issue for the BCM however is that it does not account for route correlations.

1.4 Aspect 4: Incorporating the Effects of Congestion

As Patriksson (2015) describes, the travel speed on a link tends to decrease as the volume of traffic on that link increases, slowly at first, but as the effects of congestion become more significant, average speed decreases more rapidly, until the congestion level has developed into a jamming situation, where very little flow can be observed. Each link in a network thus has a link cost function that relates travel time for the link with vehicle flow upon it, where travel time increases with flow. There is thus a feedback effect in that drivers make decisions on which routes to take according to the travel times they perceive for the routes, which in turn depend upon the route choice decisions and the consequent route and link flows.

To model this feedback effect, the concept of road network user equilibrium was introduced. In urban areas such as cities, the travel demand is so large that high levels of congestion are often experienced, particularly during peak hour times. Time wasted in congestion has a big influence on how travellers organize their lives and decide between available routes. Moreover, it is well-known that travel behaviours tend to be habitual. Wardrop (1952) thus proposed the Deterministic User Equilibrium (DUE) model, based upon Wardrop's first principle of equilibrium:

"The journey times on all the routes actually used are equal, and less than those which would be experienced by a single vehicle on any unused route."

This principle makes some important assumptions about driver behaviour. As Damberg et al (1996) and Patriksson (2015) describe, the principle assumes that all drivers have complete and accurate information about all available routes, including the travel cost (time) for each route, where every driver has the exact same perception of travel cost. Furthermore, it is assumed that the routes chosen by drivers are those which are individually perceived as having the lowest cost, i.e. all drivers look to minimise their travel cost. The result from such conditions is a distribution of route flows such that no driver can improve upon their travel cost by unilaterally changing routes, hence resulting in a user equilibrium. For low travel demand, the DUE model is equivalent to the AON model where all drivers opt to take the single minimum costing route (providing there are no ties). As the travel demand increases, the lower costing routes increase in travel time (due to greater flows along them) and thus routes previously unused become more attractive and the flows are distributed across more minimum costing routes.

The DUE model makes some behaviourally questionable assumptions about driver behaviour, however. Similar to AON, the model assumes that all drivers have complete and accurate information about all

available routes, including the travel costs for each of the routes (which are flow-dependent), where every driver has the exact same perception of travel cost. Moreover, it assumes that there is no uncertainty from the modeller in terms of any unobserved attributes or any unobserved heterogeneity in the utilities. The DUE model is heavily dependent upon these behavioural assumptions, and it would be natural to assume that traffic flows do not satisfy the user equilibrium conditions when these assumptions are not true, for example if drivers do not all have perfect information about the cost of each route, or perceive travel costs differently (Damberg et al, 1996). The DUE model does, however, implicitly capture route correlations, and deals with unrealistic routes, since zero flows are given to routes that are not minimum costing.

Since it is behaviourally questionable (due to e.g. driver/modelling uncertainty) that a route with a cost only slightly higher than the minimum costing routes goes unused (i.e. as in DUE), one approach that has been proposed for addressing this is the Boundedly Rational User Equilibrium (BRUE) model (Mahmassani & Chang, 1987; Guo & Liu, 2011; Lou et al, 2010; Di et al, 2013; Di & Liu, 2016). In the context of route choice, the theory of bounded rationality has been interpreted as establishing the existence of 'indifference bands' on the excess cost of a route relative to the minimum costing route (Mahmassani & Chang, 1987; Hu & Mahmassani, 1997; Jayakrishnan et al, 1994; Mahmassani & Liu, 1999; Srinivasan & Mahmassani, 1999). BRUE proposes that drivers are indifferent to route cost differences within their indifference bands, and thus a space of route flow equilibrium solutions exists that represents drivers' inertia to route-switching. This extends the used route selection of DUE to include some sub-optimal routes while still excluding those that are unrealistic. A big issue however is that the deliberate non-uniqueness of solutions makes the approach unsuitable for real-life applications (such as policy testing).

To compensate for driver/modelling uncertainty of the route travel costs, Daganzo & Sheffi (1977) extend the DUE model to include a random component in the travel cost function, thus forming the Stochastic User Equilibrium (SUE) model. The probability that a specific route is chosen, given the actual cost of the route, is then dependent upon the probability distribution of the random component, i.e. dependent upon the underlying RUM. Solutions to the SUE model are such that the route flows result in travel costs (and thus route utilities) that satisfy the Stochastic User Conditions as described above, where the proportion of the travel demand flow on each route is equal to the probability that that route has the perceived highest utility.

SUE is expressed as a fixed-point problem and computing the SUE route flows thus requires a solution algorithm. These algorithms involve weighting the route flows between iterations with step-sizes, to eventually converge towards a solution. There are three main types of step-size scheme, as suggested by Chen et al (2014). Some SUE models can be expressed as equivalent Mathematical Programming (MP) formulations, and thus SUE for these models can be obtained through solving some convex optimisation problem where the step-sizes are *exact*. For SUE models that are not expressed as MP formulations, step-sizes are either *pre-determined* e.g. the method of successive averages and its variants such as the method of successive weighted averages (Liu et al, 2009) or the self-regulated averaging method (e.g. Yang et al, 2013; Xu & Chen, 2013; Kitthamkesorn & Chen 2013, 2014; Chen et al, 2014; Yao et al, 2014), or *inexact* such as Armijo's step-size strategy (Armijo, 1966; Bertsekas, 1976) or self-adaptive schemes such as those described by Chen et al (2012, 2013), Xu et al (2012), and Zhou et al (2012).

Like there are different computational challenges for solving the route choice probabilities for the different correlation-based route choice models, there are also different computational challenges involved in their application to SUE. The SUE application of each correlation-based route choice model category is reviewed in turn below.

GEV structure models. Equivalent MP formulations for CNL, GNL, and PCL are given by Bekhor & Prashker (1999, 2001). Bekhor & Prashker (2001), Chen et al (2003) and Bekhor et al (2008) provide path-based partial linearization algorithms for solving GNL SUE, PCL SUE, and CNL SUE, respectively. Due to their multi-level tree structure, the choice probabilities and in particular MP formulations are complex to compute, where the computational burden escalates significantly as the scale of network / choice set sizes increase. This raises concerns over their applicability to SUE on large-scale networks. Pre-determined, exact, and inexact step-size schemes have been investigated to assess computational trade-off, i.e. where the computation time required to perform each iteration is compared with the number of iterations required for convergence (Bekhor & Prashker, 2001; Bekhor et al, 2008; Chen et al, 2014).

Simulation models. Sheffi (1985) formulates MNP SUE as a mathematical programme and presents a flow-averaging solution algorithm. Cantarella & Binetti (2002) give flow-averaging and cost-averaging algorithms for solving MNG SUE. These models are attractive behaviourally due to their ability to accurately

capture route correlations, however there are computational issues for SUE. As discussed previously, computing the choice probabilities comes with a high computational cost, and increasing the accuracy of choice probability computation substantially adds to the computational burden. However, as Sheffi (1985) explores, in SUE application, one can trade-off the accuracy of the probabilities (and thus computation times of each iteration) with rate of SUE convergence. Nonetheless, due to the random nature in which the search direction is obtained in typical simulation-based algorithms, there are difficulties in suitably measuring flow convergence (Sheffi, 1985). Moreover, numerous studies have found convergence very slow on large-scale networks (Rich et al, 2015; Manzo et al, 2015; Rasmussen et al, 2017; Connors et al, 2014).

Correction term models. Zhou et al (2012) give equivalent MP formulations for Length-based CL SUE (LCL SUE) and Congestion-based CL SUE (CCL SUE), where length and congestion based refers to whether the correction term is computed using length or congestion-dependent travel cost. Chen et al (2012), Kitthamkesorn & Chen (2013), and Xu et al (2015) give equivalent MP formulations for PSL SUE, PSW SUE, and PSH SUE, respectively. Chen et al (2012) present a path-based partial linearization algorithm for solving LCL SUE and PSL SUE. Zhou et al (2012) present a path-based Gradient Projection algorithm for solving LCL SUE and CCL SUE, and Xu et al (2012) and Chen et al (2013) assess the computational trade-off for different step-size strategies. Kitthamkesorn & Chen (2013) develop a path-based partial linearization algorithm for solving PSW SUE, and Kitthamkesorn & Chen (2014) propose a link-based algorithm. These models have probability relations and MP formulations that are relatively easy and quick to compute, which makes them more suitable for SUE applications on large-scale networks. However, they are a heuristic approach to capturing route correlations, and as discussed in more detail below, theoretical consistency is often overlooked in the SUE formulations so that solution methods are simpler/quicker to implement.

GEV structure and correction term models do not require random simulation to compute choice probabilities, and search directions can be computed exactly. This means that convergence can be suitably measured, and more optimal step-size schemes / algorithms can be developed for better convergence. However, internal consistency is often overlooked in the SUE formulations for these models so that solution methods are simpler/quicker to implement. An SUE model is internally consistent if the same definition of generalised cost is used in all components of the specification. In SUE application where the travel costs within the deterministic utilities are flow-dependent (congested), the route similarity features (PCL, CL) or link-route prominence features (CNL, GNL, PSL, PSW, PSH) in the correlation components should also be based upon the congested cost. Most studies use topological length or uncongested cost (free-flow travel time) for these features, however this may be inaccurate behaviourally since a short route can have a large congested travel cost, and vice versa. Studies that have been implemented with flow-dependent correction terms include CCL SUE by Zhou et al (2012), Xu et al (2012), and Chen et al (2013), and PSL Restricted SUE (discussed below) by Rasmussen et al (2015).

Just as for route choice probability computations, the typical approach for dealing with unrealistic routes for SUE modelling is to attempt to exactly generate the realistic routes using some kind of heuristic method. There are however two ways in which route generation is typically done for SUE. The first way is also through choice set pre-generation which leads to the same issues as discussed above. The second way is to employ a column generation approach within implementation of the SUE algorithm, thereby generating routes as the algorithm progresses until the convergence criteria are met. The column generation approach is likely to have improved theoretical consistency over the choice set pre-generation approach, since routes are typically generated given the current link costs at the algorithm iterations, however the route generation and route flow distribution criteria are not guaranteed to be consistent. Furthermore, solutions emitted by the column generation algorithms have the potential to differ dramatically depending on the initial conditions set, especially for many correlation-based SUE models that are not choice set robust. For simulation SUE models, typical solution methods do not require explicit route generation and thus the accuracy of results is not dependent upon the choice sets generated, although the routes generated may vary from different algorithm runs.

Recent years have seen the emergence of some promising SUE approaches for dealing with unrealistic routes in a consistent way. Watling et al (2015) and Rasmussen et al (2015) develop a Restricted Stochastic User Equilibrium (RSUE) approach whereby the choice set of used routes is determined by some explicit constraint that is dependent on the equilibrium solution. Rasmussen et al (2015) then formulate the RSUE with a Threshold (RSUET) model which further extends the approach to include a second restriction, determined partly by an exogenously defined cost threshold. PSL correction terms are added to both of these

approaches to also deal with the route overlap problem. The disadvantage with these approaches, however, is that equilibrium solutions are not guaranteed to exist, and even in cases where solutions do exist, there is no guarantee of the uniqueness of the solution. This lack of theoretical guarantee of existence and uniqueness is a major price to pay when one considers the typical use of such models in policy testing, meaning that one cannot guarantee to attribute a unique forecasted benefit to any tested measure. Furthermore, the lack of a mathematically well-defined underlying route choice model with a continuous choice probability function means that the approach is not robust (i.e. potentially sensitive to small changes to network/model specifications).

Motivated by the desire to develop an SUE model that consistently addresses unrealistic routes but has guaranteed existence and uniqueness of solutions, as well as a mathematically well-defined underlying route choice model, Watling et al (2018) formulated the BCM (as described above) and applied it to SUE, thus formulating Bounded SUE (BSUE). BSUE applies a bound upon congested cost so that the choice sets of realistic routes are equilibrated along with the route flows. The issue for the BCM (and thus BSUE), however, as previously mentioned, is its inability to capture route correlations.

Table 1.1 summarises the features of the network equilibrium models mentioned above. A model which does not have an implicit mechanism for dealing with unrealistic routes, does it explicitly through e.g. choice set pre-generation.

Network Equilibrium Model	Well-defined underlying route choice model	Allows for driver/modelling uncertainty	Mechanism for capturing route correlations	Implicit mechanism for dealing with unrealistic routes
DUE	No	No	-	Yes
BRUE	No	No	-	Yes
MNL SUE	Yes	Yes	None	No
CNL SUE	Yes	Yes	Explicit	No
GNL SUE	Yes	Yes	Explicit	No
PCL SUE	Yes	Yes	Explicit	No
MNP SUE	Yes	Yes	Implicit	No
MNG SUE	Yes	Yes	Implicit	No
MNW SUE	Yes	Yes	None	No
(L/C)CL SUE	Yes	Yes	Explicit	No
PSL SUE	Yes	Yes	Explicit	No
PSW SUE	Yes	Yes	Explicit	No
PSH SUE	Yes	Yes	Explicit	No
MNL RSUE	No	Yes	None	Yes
PSL RSUE	No	Yes	Explicit	Yes
PSL RSUET	No	Yes	Explicit	Yes
BSUE	Yes	Yes	None	Yes

Table 1.1. Features of different network equilibrium models.

2. Research Directions & Thesis Outline

The previous section discussed modelling approaches for addressing four key challenging aspects of route choice modelling highlighted in the literature: allowing for driver/modelling uncertainty, capturing correlations between overlapping routes, dealing with unrealistic routes, and incorporating the effects of congestion. While many promising approaches have been developed, no approach has been developed thus far that addresses all four of these challenges in a theoretically consistent, robust, and mathematically well-defined way, and moreover, has been shown to be both computationally feasible and estimatable on real-life large-scale networks. Below, existing approaches are reviewed in summary, followed by a discussion on how the directions to pursue were decided upon.

Summary review of existing route choice modelling approaches

Simulation models are the most behaviourally attractive approach for addressing the route overlap problem, since route correlations are captured implicitly and consequently accurately. Furthermore, solution methods for computing choice probabilities and solving SUE do not necessarily require explicit route generation, and thus the accuracy of results is not necessarily dependent upon the choice sets generated nor highly influenced by unrealistic routes. However, there are major concerns over their suitability for real-life large-scale network applications. Accurately computing route choice probabilities on large-scale networks where there are potentially thousands of links/routes requires an extremely high computational cost, while there are also uncertainties involved in successfully estimating model parameters. Moreover, there are also issues in their SUE application, for example difficulties measuring convergence and slow convergence on large-scale networks.

GEV structure models can in theory capture route correlations accurately. However, due to the immense number of routes and the complexity in which they overlap on large-scale networks, estimating each individual e.g. similarity/nesting/inclusion parameter is infeasible, and instead, heuristic functional relationships have been proposed – using knowledge of network topology – in order to represent these parameters and simplify estimation. With this, it is uncertain exactly how accurately route correlations are captured, and there is some uncertainty in which functional relationships are best to adopt. Moreover, there are questions whether the functional relationships adopted thus far in SUE formulations are suitable given the lack

of consistency between the costs used in different components. Numerous difficulties have been documented in estimating GEV structure models, including in some studies results implying a collapse to MNL, while the complexity of the probability relations / MP formulations raise concerns over computational feasibility on large-scale networks. Furthermore, results can be sensitive to the adopted choice sets, but generating exact choice sets of realistic route alternatives is very difficult to do on large-scale networks.

Correction term models take a heuristic approach to capturing route correlations, and as such, are typically less accurate than the other approaches, but are very attractive for real-life large-scale applications. They have choice probabilities and MP formulations that are relatively easy and quick to compute, meaning SUE can be solved in feasible computation times on large-scale networks, and have also been shown to be estimatable in large-scale applications. A key issue, however, is that results also can be sensitive to the adopted choice sets and negatively influenced by the presence of unrealistic routes in the choice sets. This highlights the importance of obtaining exact choice sets of realistic routes to perform route choice / SUE with, which is very difficult to do on large-scale networks, while it also leads to theoretical inconsistencies.

Due to the attractiveness of correction term models for real-life large-scale network applications, and inspired by some promising approaches that have been proposed for addressing issues with unrealistic routes for these models, the following two research directions were chosen to pursue. Below, these research directions are detailed, and the contents of the thesis is outlined.

2.1 Research Direction 1 – A New Internally Consistent Weighted Path Size Contribution Technique

The PSL model attempts to capture correlations between routes by including correction terms within the route utility functions. These correction terms depend upon path size terms which measure the distinctiveness of routes: a route is penalised based on the number of other routes sharing its links, and the costs of those shared links. The key issue for PSL, however, is that the choice probabilities are extremely sensitive to the choice sets adopted since all routes contribute equally to path size terms, and as such, results are extremely sensitive to the choice set generation method adopted. Moreover, it is crucial for PSL that the choice sets contain realistic alternatives only, as the inclusion of a single unrealistic alternative can have a considerable and negative effect on the choice probabilities of the realistic routes.

Acknowledging the difficulties in obtaining exact choice sets of realistic routes for PSL to be suitable, a pragmatic approach that has been proposed is to utilise a weighted path size contribution technique along with choice set generation, to attempt to reduce the impact any present unrealistic routes may have on the choice probabilities of realistic routes. The idea is that instead of all routes having equal path size contributions to the path size terms of other routes (i.e. PSL) – and therefore the utilities and consequently the choice probabilities of realistic routes are undesirably adjusted to capture correlations between routes not even considered by drivers – the contributions are weighted so that the probabilities of realistic routes are only minorly adjusted from link sharing with generated unrealistic routes. This is a promising approach as it relaxes the importance of generating exact choice sets of realistic routes; however, the path size contribution factors proposed thus far have deficiencies, and the first research direction was to address this by developing a new contribution factor.

As discussed previously, the initial contribution factor proposed – where routes are weighted according to their length/cost compared to the shortest/cheapest route – is problematic, since a route that is completely distinct may have a non-zero path size correction term, thus resulting in an undesired penalisation upon the utility of that route.

The GSPL model attempts to address this by proposing each route contributes to the path size term of another according the ratio of length/cost between the routes. An issue that has not yet been brought to attention, however, nor addressed, is internal consistency. There may be many ways in which a model can be internally (in)consistent, however internal consistency is used in this thesis to describe two specific features of path size logit route choice models.

The *first feature* is how the path size model components define travel cost. Typically, path size logit models use length or free-flow travel time costs within the path size terms to measure link-route prominence. However, this is potentially inconsistent as generalised travel cost is used to measure the attractiveness of routes within the utility component. For example, a short route may have a large generalised travel cost, and vice versa.

The *second feature* is how the path size model components define routes as unrealistic. The GPSL path size correction terms define a route as unrealistic if it has a large length / travel cost, however the route choice probability relation considers disutility including the correction term. There are hence potentially inconsistent definitions for unrealistic routes within the model, which may lead to inaccurate results. Moreover, due to these internal inconsistency issues, an additional scaling parameter is required to scale the path size contributions which makes parameter estimation more difficult.

In **Chapter 2** of this thesis, the first journal manuscript, these internal inconsistency issues for GPSL are discussed and demonstrated on small example networks. Addressing these issues, **Chapter 2** then formulates the Adaptive Path Size Logit (APSL) model where a new path size contribution factor is proposed. The APSL model proposes that the contribution factors are based upon ratios of choice probability between routes, thus ensuring that routes defined as unrealistic by the path size terms, are exactly those with very low choice probabilities. APSL is hence internally consistent in how routes are defined as (un)realistic. Also, by defining the path size contribution factor as the ratio of choice probabilities, the scaling of the path size contributions is controlled implicitly through the scaling of the route choice probabilities (i.e. with the Logit parameter and path size parameter), and hence there is no additional path size contribution parameter for estimation. The APSL route choice probability relation is an implicit function involving the choice probabilities, and solutions to the model are solutions to the fixed-point problem. A solution algorithm is provided for computing the APSL choice probabilities, APSL solutions are proven to exist, and conditions for unique APSL solutions are given.

Given that the requirements set out for a developed model were that one should be able to solve it in computationally feasible times on large-scale networks, as well as successfully estimate the parameters of the model, in the second part of **Chapter 2** these properties are investigated for APSL. To show that the parameters of the APSL model can be estimated a Maximum Likelihood Estimation procedure is first proposed for estimating APSL with tracked route observation data, then this procedure is investigated in a simulation study on the Sioux Falls network, where it is shown it is generally possible to reproduce assumed true parameters. Then, in a real-life case study, the APSL model is estimated using real tracked route GPS data on a large-scale network. Computational feasibility is then assessed for solving and estimating APSL on the Sioux Falls and real-life large-scale network.

Chapter 3 of this thesis, the second journal manuscript, explores the integration of APSL within a SUE model, thereby developing a modelling approach that addresses all four of the key challenging aspects of route choice modelling. SUE conditions are established for the APSL model, where – for full internal consistency – flow-dependent, generalised costs are used in all components: route costs as well as path size correction terms. APSL SUE solutions are proven to exist.

APSL comes at a price of needing to solve a fixed-point problem even to compute route choice probabilities at given travel cost/utility levels. Thus, before the research was conducted, there was a question of whether it would be computationally feasible to implement such a method within an SUE framework, since it apparently needs to embed a fixed-point problem (for calculating choice probabilities) within another fixed-point problem (for equilibrating flows). However, as the paper shows, the potentially onerous requirement of solving fixed-point problems to compute APSL choice probabilities can be circumvented, since at SUE the route flow proportions and choice probabilities equate. The useful relationship between choice probabilities and route flow proportions in SUE context allows for a considerable flexibility in solving APSL SUE, as is explored, where one can trade-off the accuracy of APSL probabilities (and thus computation times of each iteration) with rate of SUE convergence.

Using a flow-averaging algorithm to solve the SUE models, the advantages of APSL SUE are demonstrated in numerical experiments on the Sioux Falls and Winnipeg networks, where computational performance, choice set robustness, and flow results are compared with the internally consistent SUE formulations of GEV structure and correction term correlation-based route choice models. APSL SUE solution uniqueness is explored numerically where results suggest that uniqueness conditions exist.

It is worth noting that, so far, standard PSL is the most common path size approach adopted in practice. It is hoped

2.2 Research Direction 2 – A Bounded Path Size Route Choice Model

Although the weighted path contribution technique is a promising approach for addressing the deficiency of the PSL model, in its sensitivity to unrealistic routes in the adopted choice sets, it does not solve the issue

entirely, since the path size contributions of routes defined as unrealistic are only reduced instead of eliminated. Moreover, as well as non-zero path size contributions, unrealistic routes also receive non-zero choice probabilities. Thus, while under the GPSL and APSL models each unrealistic route may only have a small path size contribution / choice probability, the total sum of these unrealistic route contributions / probabilities may be significant, consequently impacting the accuracy of results. This problem becomes greater as the scale of network increases and a greater amount of uncertainty comes with choice set generation, where, typically, choice sets are generated as large as the computational resources are deemed to allow, in order to minimise the possibility of excluding what would later turn out to be a plausible route.

In contrast to these issues with PSL models, the BCM has a consistent criterion for determining restricted choice sets of realistic routes and route choice probability, but does not account for route correlations. An approach that was therefore deemed promising was to explore the integration of PSL model concepts with the BCM, thereby harnessing the contrasting strengths of the two approaches. **Chapter 4** of this thesis, the third journal manuscript, explores formulating a Bounded Path Size (BPS) route choice model, where route correlations and unrealistic routes are fully dealt with in a consistent, robust, and mathematically-well defined way. The aim is to develop a model that eliminates unrealistic route path size contributions entirely, as well as removes all the negative effects of unrealistic routes by also assigning them zero choice probabilities.

A natural form for a BPS model can be derived by inserting path size choice model utilities into the standard BCM formula. However, as shown, this natural form for a BPS model is deeply problematic and there are no behaviourally and practically desirable formulations. This is because appropriately defining the path size contribution factors within the path size terms is challenging, and from demonstrating with different options, desired properties are established for a mathematically well-defined BPS choice model that utilises a consistent criterion for assigning zero choice probabilities to unrealistic routes while eliminating their path size contributions.

To develop a BPS model that satisfies these properties, an alternative BPS model form is the derived and two BPS models are consequently proposed: one that is closed-form (the Bounded Bounded Path Size (BBPS) model) and another expressed as a fixed-point problem (the Bounded Adaptive Path Size (BAPS) model). The BBPS model path size contribution factors consider ratios of the odds that routes are within the bound, and its limit model – where the bound is large enough so that all routes have non-zero choice probabilities – is a GPSL variant. The BAPS model utilises probability ratio contribution factors and its limit model is APSL. The BAPS model has a greater appeal behaviourally since it is fully internally consistent, while the BBPS model offers a more computationally practical alternative.

Again, given that the requirements set out for a developed model were that one should be able to solve it in computationally feasible times on large-scale networks, as well as successfully estimate the parameters of the model, the second part of **Chapter 4** investigates these properties for the BBPS & BAPS models. Similar to that for APSL, a Maximum Likelihood Estimation procedure is proposed for estimating the BBPS & BAPS models with tracked route observation data, then this procedure is investigated in a simulation study on the Sioux Falls network, where it is shown that it is generally possible to reproduce assumed true parameters. Then, in a real-life case study, the BBPS & BAPS models are estimated using real tracked route GPS data on a large-scale network. Computational feasibility is assessed for solving and estimating the BAPS model (since it is not closed-form) on the Sioux Falls and real-life large-scale network.

Chapter 5 of this thesis, the fourth manuscript, explores the integration of BPS models within a SUE model, thereby developing a second modelling approach that addresses all four of the key challenging aspects of route choice modelling. SUE conditions are established for the BPS models, where the restricted choice sets of realistic routes are equilibrated. BBPS SUE solutions are proven to exist.

A generic algorithm is proposed for solving BPS SUE models. The algorithm is an adaptation of the generic algorithm proposed by Watling et al (2018) for the BSUE model. To equilibrate the choice sets of realistic routes, the BSUE algorithm generates realistic routes from the network as the algorithm progresses. With the current techniques available for generating these routes, there are questions over the suitability of the approach for large-scale networks. A more heuristic approach is thus taken for the proposed BPS SUE algorithm, by pre-generating approximated universal choice sets.

For BAPS SUE, just like for APSL SUE, the potentially onerous requirement of solving fixed-point problems to compute BAPS model probabilities can be circumvented, since at SUE the route flow proportions and choice probabilities equate. The trade-off between the accuracy of BAPS model probabilities (and thus computation times of each iteration) with rate of SUE convergence is explored. Numerical experiments are

conducted on the Sioux Falls and Winnipeg networks, assessing computational performance for solving the BPS SUE models, comparing flow results between the models, and exploring numerically the uniqueness of BAPS SUE solutions. Computational performance, choice set robustness, and flow results are also compared related non-bounded SUE models, i.e. BSUE, PSL SUE models.

Chapter 6 concludes the thesis and discusses scope for further research.

Fig. 1.2 below summarises the structure and content of the thesis.

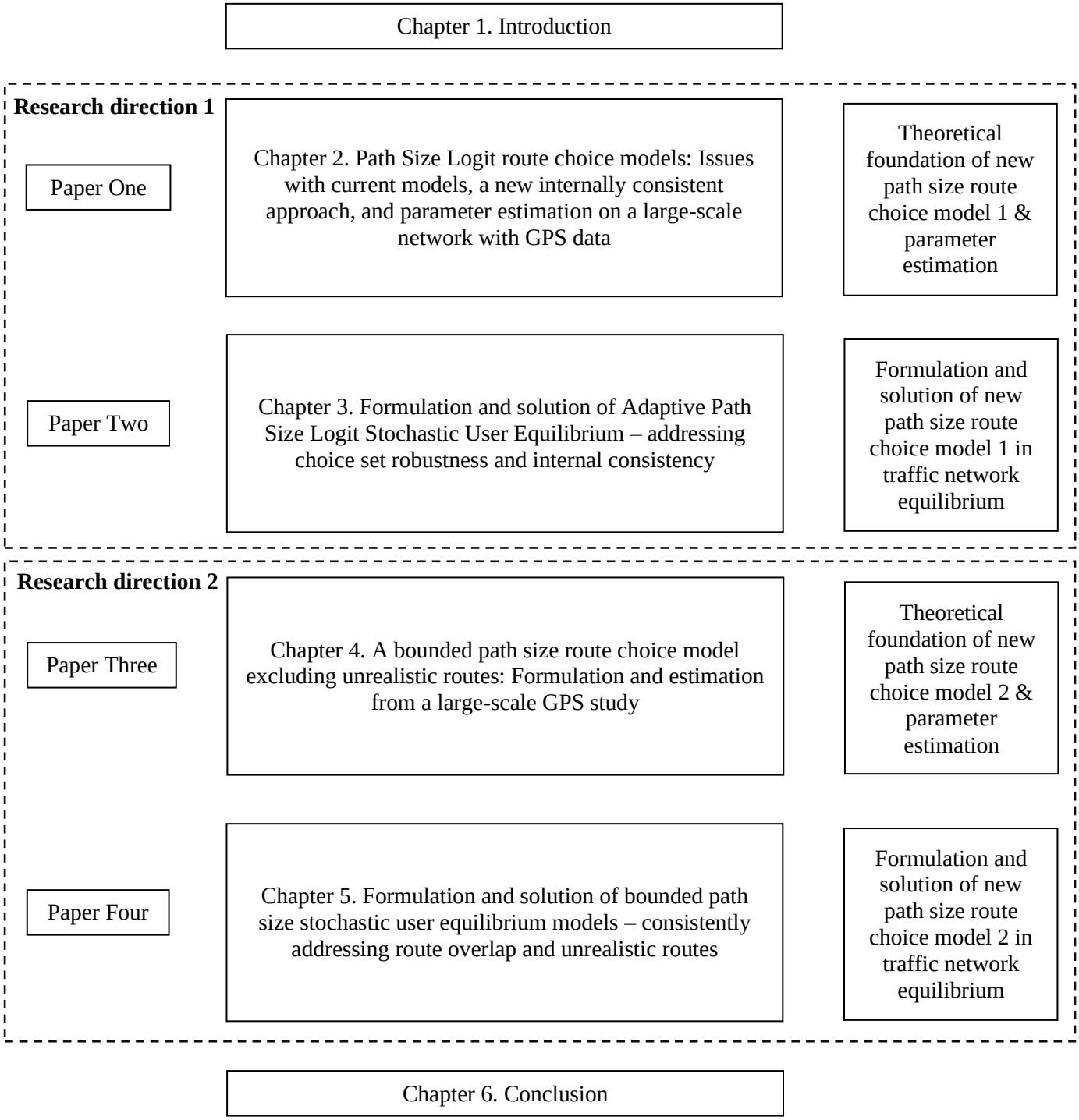

Fig. 1.2. Thesis structure.

3. References

Abbe E, Bierlaire M, & Toledo T, (2007). Normalization and correlation of cross-nested logit models. Transportation Research Part B, 41(7), p.795-808.

Akamatsu T, (1996). Cyclic Flows, Markov Process and Traffic Assignment. Transportation Research B, 30(5), p.369-386.

Armijo L, (1966). Minimization of functions having continuous partial derivatives. Pacific Journal of Mathematics, 16(1), p.1–3.

Bakker D, Mijjer P, & Hofman F, (1994). QBLOK: An Assignment Technique for Modelling the Dependency Between Bottlenecks and the Prediction of Grid Lock. In Proceedings of Colloquium Vervoersplanologisch Speurwerk, Delft, p.313–332.

Barceló J & Casas J, (2005). Dynamic Network Simulation with AIMSUN. In: Kitamura R., Kuwahara M. (eds) Simulation Approaches in Transportation Analysis. Operations Research/Computer Science Interfaces Series, vol 31. Springer, Boston, MA.

Batista S & Leclercq L, (2019). Regional Dynamic Traffic Assignment Framework for Macroscopic Fundamental Diagram Multi-regions Models. Transportation Science, 53(6), p.1563-1590.

Bekhor S & Prashker J, (1999). Formulations of extended logit stochastic user equilibrium assignments. In: Proceedings of the 14th International Symposium on Transportation and Traffic Theory, Jerusalem, Israel, p.351–372.

Bekhor S, & Prashker J, (2001) Stochastic user equilibrium formulation for the generalized nested logit model. Transportation Research Record, 1752, p.84–90.

Bekhor S, Ben-Akiva M, & Ramming M, (2002). Adaptation of logit kernel to route choice situation. Transportation Research Record, 1805, p.78–85.

Bekhor S, Toledo T, & Prashker J, (2008). Effects of choice set size and route choice models on path-based traffic assignment. Transportmetrica, 4(2), p.117-133.

Ben-Akiva M, Bergman M, Daly A, & Ramaswamy R, (1984). Modeling inter-urban route choice behaviour. In: Volmuller, J., Hamerslag, R. (Eds.), Proceedings of the 9th International Symposium on Transportation and Traffic Theory. VNU Science Press, Utrecht, The Netherlands, p.299–330.

Ben-Akiva M, & Bolduc D, (1996). Multinomial probit with a logit kernel and a general parametric specification of the covariance structure. Working Paper.

Ben-Akiva M, & Ramming S, (1998). Lecture notes: discrete choice models of traveler behavior in networks. Prepared for Advanced Methods for Planning and Management of Transportation Networks. Capri, Italy.

Ben-Akiva M, & Bierlaire M, (1999). Discrete choice methods and their applications to short term travel decisions. In: Halled, R.W. (Ed.), Handbook of Transportation Science. Kluwer Publishers.

Bertsekas D, (1976). On the Goldstein–Levitin–Polyak gradient projection method. IEEE Transactions on automatic control, 21(2), p.174–184.

Bhat C, (1998). Analysis of travel mode and departure time choice for urban shopping trips. Transportation Research B, 32, p.361-371.

Bierlaire M, (2002). The Network GEV Model. Conference paper STRC 2002.

Bierlaire M, (2006). A theoretical analysis of the cross-nested logit model. Annals of operations research, 144, p.287-300.

Bliemer M & Bovy P, (2008). Impact of Route Choice Set on Route Choice Probabilities. Transportation Research Record: Journal of the Transportation Research Board, 2076, p.10–19.

Bliemer M, Raadsen M, Smits E, Zhou B, & Bell M, (2014). Quasi-dynamic traffic assignment with residual point queues incorporating a first order node model. Transportation Research Part B: Methodological, 68, p.363-384.

Blincoe L, Seay A, Zaloshnja E, Miller T, Romano E, Luchter S, & Spicer R, (2002). The Economic Impact of Motor Vehicle Crashes. US Department of Transportation and the National Highway Traffic Safety Administration, Washington, DC.

Bovy P, Bekhor S, & Prato C, (2008). The Factor of Revisited Path Size: Alternative Derivation. Transportation Research Record: Journal of the Transportation Research Board, 2076, Transportation Research Board of the National Academies, Washington, D.C., p.132–140.

Brederode L, Pel A, Wismans L, de Romph E, & Hoogendoorn S, (2019). Static Traffic Assignment with Queuing: model properties and applications. Transportmetrica A: Transport Science, 15(2), p.179-214.

Bunch, D, (1991). Estimability in the multinomial probit model. Transportation Research Part B: Methodological, 25, p.1–12.

Bundschuh M, Vortisch P, & Van Vuuren T, (2006). Modelling Queues in Static Traffic Assignment. Proceedings of the European Transport Conference.

Cantarella G & Binetti M, (2002). Stochastic assignment with gammit path choice models. Patriksson, M., Labbé's, M. (Eds.), Transportation Planning: State of the Art, p.53–68.

Casas J, Ferrer J, Garcia D, Perarnau J, & Torday A, (2010). Traffic Simulation with Aimsun. In: Barceló J. (eds) Fundamentals of Traffic Simulation. International Series in Operations Research & Management Science, vol 145. Springer, New York.

Cascetta E, Nuzzolo A, Russo F, & Vitetta A, (1996). A modified logit route choice model overcoming path overlapping problems: specification and some calibration results for interurban networks. In: Proceedings of the 13th International Symposium on Transportation and Traffic Theory, Leon, France, p.697–711.

Cascetta E & Papola A, (2001). Random utility models with implicit availability perception of choice travel for the simulation of travel demand. Transport. Res. Part C: Emer. Technol., 9(4), p.249–263.

Castillo E, Menéndez J, Jiménez P, & Rivas A, (2008). Closed form expression for choice probabilities in the Weibull case. Transportation Research Part B, 42(4), p.373–380.

Chen A, Kasikitwiwat P, & Ji Z, (2003). Solving the overlapping problem in route choice with paired combinatorial logit model. Transportation Research Record 1857, p.65–73.

Chen A, Pravinvongvuth S, Xu X, Ryu S, & Chootinan P, (2012). Examining the scaling effect and overlapping problem in logit-based stochastic user equilibrium models. Transportation Research Part A, 46, p.1343-1358.

Chen A, Xu X, Ryu S, & Zhou Z, (2013). A self-adaptive Armijo stepsize strategy with application to traffic assignment models and algorithms. Transportmetrica A: Transport Science, 9(8), p.695–712.

Chen A, S Ryu, Xu X, & Choi K, (2014). Computation and Application of the Paired Combinatorial Logit Stochastic User Equilibrium Problem. Computers and Operations Research, 43, p.68–77.

Chen M, Zhub Z, & Zhang L, (2015). Simulation-based optimization of mixed road pricing policies in a large real-world network. Transportation Research Procedia, 8, p.215 – 226.

Chin A, (1996). Containing air pollution and traffic congestion: Transport policy and the environment in Singapore. Atmospheric Environment, 30, p.787-801.

Chiu Y, Bottom J, Mahut M, Paz A, Balakrishna R, Waller T, & Hicks J, (2011). Dynamic traffic assignment: A primer. Transp. Res. E-Circ. (E-C153).

Chiu Y & Bustillos B, (2009). A gap function vehicle-based solution procedure for consistent and robust simulation-based dynamic traffic assignment. In: Transportation Research Board 88th Annual Meeting, Washington, DC, USA. No. 09-3721.

Chiu Y, Zhou L, & Song H, (2010). Development and calibration of the anisotropic mesoscopic simulation model for uninterrupted flow facilities. Transp. Res. Part B, 44(1), p.152–174.

Chu C, (1989). A paired combinatorial logit model for travel demand analysis. In: Proc. Fifth World Conference on Transportation Research, Ventura, Calif. 4, p.295–309.

Connors R, Hess S, & Daly A, (2014). Analytic approximations for computing probit choice probabilities, Transportmetrica A: Transport Science, 10(2), p.119-139.

Daganzo C, & Sheffi Y, (1977). On stochastic models of traffic assignment. Transportation Science, 11, p.253–274.

Daly A, & Bierlaire M, (2006). A general and operational representation of Generalised Extreme Value models. Transportation Research Part B, 40, p.285–305.

Damberg O, Lundgren J & Patriksson M, (1996). An algorithm for the stochastic user equilibrium problem. Transport. Res. Part B: Methodol. 30(2), p.115-131.

Dansie, B, (1985). Parameter estimability in the multinomial probit model. Transportation Research Part B: Methodological, 19, p526–528.

Dial R, (1971). A Probabilistic Multipath Traffic Assignment Model Which Obviates Path Enumeration. Transportation Research, 5, p.83-111.

Dijkstra E, (1959). A note on two problems in connection with graphs. Numer. Math., 1, p.269–271.

Di X & Liu H, (2016). Boundedly rational route choice behavior: a review of models and methodologies. Transp. Res. Part B: Methodol., 85, p.142–179.

Di X, Liu H, & Pang J, & Ban X, (2013). Boundedly rational user equilibria (BRUE): mathematical formulation and solution sets. Transp. Res. Part B: Methodol., 57, p.300–313.

Du Y, Jia Y, Wu J, Xu M, & Yang S, (2015). Traffic Environmental Capacity and MFD Based Traffic Emission Dynamic Control Model. Journal of Residuals Science & Technology, 12(4), p.221-229.

Fellendorf M & Vortisch P, (2010). Microscopic Traffic Flow Simulator VISSIM. In: Barceló J. (eds) Fundamentals of Traffic Simulation. International Series in Operations Research & Management Science, vol 145. Springer, New York, NY.

Frejinger E, & Bierlaire M, (2007). Capturing correlation with subnetworks in route choice models. Transportation Research Part B, 41(3), p.363-378.

Frejinger E, Bierlaire M, & Ben-Akiva M, (2009). Sampling of alternatives for route choice modeling. Transport. Res. Part B: Methodol. 43(10), p.984–994.

Friedrich M, Hofsass I, & Wekeck S, (2001). Timetable-based transit assignment using branch and bound. Transport. Res. Rec. 1752, p.100–107.

Gkotsis I, Milioti C, Triantafyllos D, Vlahogianni E, Kepaptsoglou K, & Golias I, (2016). An ex-ante evaluation framework of dynamic congestion pricing: application to Athens, Greece. Advances in Transportation Studies, 40, p87-100.

Gliebe J, Koppleman F, & Ziliaskopoulos A, (1999). Route choice using a paired combinatorial logit model. Presented at the 78th Annual Meeting of the Transportation Research Board, Washington, DC.

Guo X & Liu H, (2011). Bounded rationality and irreversible network change. Transp. Res. Part B: Methodol., 45(10), p.1606–1618.

Hoogendoorn-Lanser S, van Nes R, & Bovy P, (2005). Path Size Modeling in Multimodal Route Choice Analysis. Transportation Research Record: Journal of the Transportation Research Board, 1921, p.27–34.

Hosseinlou M, Zolfaghari A, & Yazdanpanah M, (2016). Road Pricing Effect on the Emission of Traffic Pollutants, a Case Study in Tehran. Civil Engineering Journal, 2(7), p.306-315.

Hu T & Mahmassani H, (1997). Day-to-day evolution of network flows under real-time information and reactive signal control. Transp. Res. Part C: Emerg. Technol., 5(1), p.51–69.

INRIX, (2020). INRIX Global Traffic Scorecard. Available online: http://inrix.com/scorecard/. Accessed 15/6-2021.

Jayakrishnan R, Mahmassani H, & Hu T, (1994). An evaluation tool for advanced traffic information and management systems in urban networks. Transp. Res. Part C: Emerg. Technol., 2(3), p.129–147 .

Johansson C, Burman L, & Forsberg B, (2009). The effects of congestions tax on air quality and health. Atmospheric Environment, 43, p.4843- 4854.

Keane M, (1992). A note on identification in the multinomial probit model. Journal of Business & Economic Statistics, 10, p.193–200.

Kitthamkesorn S, & Chen A, (2013). Path-size weibit stochastic user equilibrium model. Transportation Research Part B, 57, p.378-397.

Kitthamkesorn S & Chen A, (2014). Unconstrained weibit stochastic user equilibrium model with extensions. Transportation Research Part B, 59, p.1–21.

Klimarådet, (2020). Kendte veje og nye spor til 70 procents reduktion - Retning og tiltag for de næste ti års klimaindsats i Danmark. Technical Report.

Krzyzanowski M, Kuna-Dibbert B, & Schneider J, (2005). Health effects of transport-related air pollution. Technical Report. WHO Regional Office for Europe.

Leurent F, (1997). Curbing the computational difficulty of the logit equilibrium assignment model. Transportation Research Part B, 31(4), p.315–326.

Liu H, He X, & He B, (2009). Method of successive weighted averages (MSWA) and self regulated averaging schemes for solving stochastic user equilibrium problem. Networks and Spatial Economics, 9(4), p.485–503.

Lou Y, Yin Y, & Lawphongpanich S, (2010). Robust congestion pricing under boundedly rational user equilibrium. Transp. Res. Part B: Methodol., 44(1), p.15–28 .

Mahmassani H & Chang G, (1987). On boundedly rational user equilibrium in transportation systems. Transp. Sci., 21(2), p.89–99.

Mahmassani H & Liu Y, (1999). Dynamics of commuting decision behaviour under advanced traveller information systems. Transp. Res. Part C: Emerg. Technol., 7(2-3), p.91–107.

Manzo S, Prato C & Nielsen O, (2015). How uncertainty in input and parameters influences transport model outputs: a four-stage model case-study. Elsevier, Transport Policy, 38, p.64-72.

Marchal F, (2001). Contribution to dynamic transportation models. Ph.D. dissertation.

Mariotte G, Leclercq L, Batista F, Krug J, & Paipuri M, (2020). Calibration and validation of multi-reservoir MFD models: A case study in Lyon. Transportation Research Part B, 136, p.62-86.

Marzano V & Papola A, (2008). On the covariance structure of the cross-nested logit model. Transportation Research Part B, 42(2), p.83–98.

McFadden D, (1978). Modeling the choice of residential location. In: Anders, Karlqvist., Lars, Lundqvist., Folke, Snickars., Jorgen, Weibull. (Eds.), Special interaction theory and planning models. North-Holland, Amsterdam, p.75–96.

McFadden D, & Train K, (2000). Mixed MNL models for discrete response. Journal of Applied Econometrics, 15 (5), p.447–470.

Nava E & Chiu Y, (2012). A temporal domain decomposition algorithmic scheme for large-scale dynamic traffic assignment. Int. J. Transp. Sci. Technol. 1(1), p.1–24.

Ortiz A, (2019). Air quality in Europe – 2019 report. Technical Report. European Environment Agency report 10/2019.

Papola A, Tinessa F, & Marzano V, (2018). Application of the Combination of Random Utility Models (CoRUM) to route choice. Transportation Research Part B, 111, p.304-326.

Patriksson M, (2015). The traffic assignment problem: models and methods. Courier Dover Publications.

Prashker J, & Bekhor S, (2004). Route choice models used in the stochastic user equilibrium problem: a review. Transport Reviews, 24 (4), p.437–463.

Prato C, (2005). Latent factors and route choice behaviour. Ph.D. Thesis, Turin, Polytechnic, Italy.

Prato C & Bekhor S, (2006). Applying branch & bound technique to route choice set generation. Transportation Research Record, 1985, p.19-28.

Pravinvongvuth S, & Chen A, (2005). Adaptation of the paired combinatorial logit model to the route choice problem. Transportmetrica, 1 (3), p.223–240.

Ramming S, (2002). Network knowledge and route choice. Ph.D. Thesis, Massachusetts Institute of Technology, Cambridge, USA.

Rasmussen T, Nielsen O, Watling D, & Prato C, (2015). Stochastic user equilibrium with equilibrated choice sets: Part II – Solving the restricted SUE for the logit family. Transportation Research Part B, 77, p.146–165.

Rasmussen T, Nielsen O, Watling D, & Prato C, (2017). The Restricted Stochastic User Equilibrium with Threshold model: Large-scale application and parameter testing. European Journal of Transport and Infrastructure Research, 15 (1), p.1-24.

Rich J & Nielsen, O (2015). System convergence in transport models: algorithms efficiency and output uncertainty. European Journal of Transport Infrastructure Research (EJTIR), 15 (3), p.38-62.

Rosa, A (2003). Probit based methods in traffic assignment and discrete choice modelling, (unpublished PhD Thesis), Napier University.

Sheffi Y, (1985). Urban Transportation Networks: Equilibrium Analysis with Mathematical Programming Methods. Prentice-Hall.

Sheffi Y & Powell W, (1982). An algorithm for the equilibrium assignment problem with random link times. Networks, 12(2), p.191–207.

Srinivasan K & Mahmassani H, (1999). Role of congestion and information in trip-makers' dynamic decision processes: experimental investigation. Transp. Res. Rec., 1676, p.44–52.

Stanley J, Hensher D, & Loader C, (2011). Road transport and climate change: Stepping off the greenhouse gas. Transportation Research Part A: Policy and Practice, 45(10), p.1020-1030.

Tonne C, Beevers S, Armstrong B, Kelly F, & Wilkinson P, (2008). Air pollution and mortality benefits of the London Congestion Charge: Spatial and socioeconomic inequalities. Occupational and Environmental Medicine, 65, p.620-627.

Van Vliet D, Hall M, & Willumsen L, (1980). A Simulation Assignment Model for the Evaluation of Traffic Management Schemes. Traffic Engineering & Control, 21, p.168–176.

Vovsha P, (1997). Application of cross-nested logit model to mode choice in Tel Aviv, Israel, Metropolitan Area. Transportation Research Record 1607, p.6–15.

Wardrop J, (1952). Some theoretical aspects of road traffic research. Proc. Institute of Civil Engineers, Part II, 1, p.325-378.

Watling D, Rasmussen T, Prato C, & Nielsen O, (2015). Stochastic user equilibrium with equilibrated choice sets: Part I – Model formulations under alternative distributions and restrictions. Transportation Research Part B (77), p.166-181.

Watling D, Rasmussen T, Prato C, & Nielsen O, (2018). Stochastic user equilibrium with a bounded choice model. Transportation Research Part B, 114, p.254-280.

Wen C, & Koppelman F, (2001). The generalized nested logit model. Transportation Research Part B, 35(7), p.627–641.

Xu X, Chen A, Zhou Z, & Behkor S, (2012). Path-based algorithms for solving C-logit stochastic user equilibrium assignment problem. Transportation Research Record, 2279, p.21–30.

Xu X, & Chen A, (2013). C-logit stochastic user equilibrium model with elastic demand. Transportation Planning and Technology, 36(5), p.463–478.

Xu X, Chen A, Kitthamkesorn S, Yang H, & Lo H.K, (2015). Modeling absolute and relative cost differences in stochastic user equilibrium problem. Transportation Research Part B, 81, p.686-703.

Yang C, Chen A, & Xu X, (2013). Improved partial linearization algorithm for solving the combined travel-destination-mode-route choice problem. Journal of Urban Planning and Development, 139(1), p.22–32.

Yao J, Chen A, Ryu S, & Shi F, (2014). A general unconstrained optimization formulation for the combined distribution and assignment problem. Transportation Research Part B, 59, p.137–160.

Yildirimoglu M & Geroliminis N, (2014). Approximating dynamic equilibrium conditions with macroscopic fundamental diagrams. Transportation Research Part B: Methodological, 70, p.186–200.

Zhou Z, Chen A, & Bekhor S, (2012). C-logit stochastic user equilibrium model: formulations and solution algorithm. Transportmetrica, 8(1), p.17–41.

Chapter 2. Path Size Logit route choice models: Issues with current models, a new internally consistent approach, and parameter estimation on a large-scale network with GPS data

Lawrence Christopher DUNCAN [a], David Paul WATLING [a], Richard Dominic CONNORS [a,b], Thomas Kjær RASMUSSEN [c], Otto Anker NIELSEN [c]

[a] Institute for Transport Studies, University of Leeds
36-40 University Road, Leeds, LS2 9JT, United Kingdom.

[b] University of Luxembourg, Faculté des Sciences, des Technologies et de Médecine,
Maison du Nombre, 6 Avenue de la Fonte, L-4364, Esch-sur-Alzette, Luxembourg.

[c] Department of Technology, Management and Economics, Technical University of Denmark
Bygningstorvet 116B, 2800 Kgs. Lyngby, Denmark.

Highlights

- Demonstrate issues with existing Path Size Logit (PSL) models
- Propose a new internally consistent Adaptive PSL that addresses these issues
- Proof of existence and uniqueness conditions for Adaptive PSL solutions
- Adaptive PSL Likelihood formulation and tracked route data MLE procedure
- Estimation of PSL models on a large-scale network using real GPS data

Abstract

Path Size Logit route choice models attempt to capture the correlation between routes by including correction terms within the route utility functions. This provides a convenient closed-form solution for implementation in traffic network models. The path size terms measure distinctiveness of routes; a route is penalised based on the number of other routes sharing its links, and the costs of those shared links. Typically, real road networks have many very long routes that should be considered unrealistic. Such unrealistic routes are problematic for the Path Size Logit (PSL) model because they negatively impact the choice probabilities of realistic routes when links are shared. The Generalised Path Size Logit (GPSL) model attempts to address this problem by weighting the contributions of routes to path size terms according to the ratio of route travel costs. However, the GPSL model is not internally consistent in how it defines routes as being unrealistic: the path size terms consider only travel cost, whereas the route choice probability relation considers disutility *including* the correction term.

To solve these challenges, this paper formulates a new internally consistent Adaptive Path Size Logit (APSL) model wherein routes contribute to path size terms according to the ratio of route choice probabilities, ensuring that routes defined as unrealistic by the path size terms, are exactly those with very low choice probabilities. The APSL route choice probability relation is an implicit function, naturally expressed as a fixed-point problem. A proof is provided for the guaranteed existence of solutions, as well as conditions for the uniqueness of solutions. A Maximum Likelihood Estimation procedure is given for estimating the APSL model with tracked route observation data, and this procedure is investigated in a simulation study where it is shown it is generally possible to reproduce assumed true parameters. APSL is then estimated using real tracked route GPS data on a large-scale network, and results are compared with other PSL models.

Key Words: path size logit, route choice, random utility, fixed-point problem, overlapping routes, parameter estimation

1. Introduction

It is well known that the Multinomial Logit (MNL) Random Utility Model (RUM) often provides unrealistic choice probabilities when applied to real road network route choice. One of the main reasons for this is that the MNL model does not capture the correlation between routes. This issue stems from the underlying assumption made by the MNL model that the random error terms are independently and identically distributed (IID) with the same, fixed variances (Sheffi, 1985). Numerous adaptations of the MNL model have been proposed in the literature which relax the IID assumption – specifically the independently distributed assumption – and attempt to capture the correlation between the routes. These extended Logit models can be classified into three groups according to the model structures as suggested by Prashker & Bekhor (2004): GEV structures, Mixed Logit models, and MNL-modification models. The fourth group of route choice models that provide an option for overcoming the weakness of MNL are those which propose an alternative probability distribution for the random error terms, i.e. alternative RUMs, that capture the correlation implicitly. To set the background for the research in the present paper, we consider each of these categories in turn below:

GEV structures: The first group of extended Logit models are those which are based on the Generalized Extreme Value (GEV) theory (McFadden, 1978), which use a two-level tree structure to capture the similarity among routes through the random error component of the utility function. These models include the Cross-Nested Logit (CNL) model (Vovsha, 1997; Bekhor & Prashker, 1999; Marzano & Papola, 2008), the Paired Combinatorial Logit (PCL) model (Chu, 1989; Bekhor & Prashker, 1999; Gliebe et al, 1999; Pravinvongvuth & Chen, 2005), the Generalized Nested Logit (GNL) model (Bekhor & Prashker, 2001; Wen & Koppelman, 2001), and the Network GEV model (Bierlaire, 2002; Daly & Bierlaire, 2006) which uses a fairly general class of networks to generalise the use of trees to represent nested logit models to a network representation. The PCL, CNL, and GNL models all have closed-form probability expressions, though due to their two-level tree structure the route choice probabilities are complex to compute for large-scale network applications. Furthermore, several studies have found that when estimating the nesting coefficients for the CNL model, the model tends to collapse to MNL (Ramming, 2002; Prato, 2005; Prato & Bekhor, 2006), and the GNL model requires the estimation of an additional parameter over the CNL model which makes parameter estimation more difficult.

Mixed Logit models: The second group of extended Logit models are Mixed Logit models (Ben-Akiva & Bolduc, 1996; McFadden & Train, 2000), also known as Logit Kernel, Random Parameter Logit, Error Component Logit, and Hybrid Logit. Mixed Logit models attempt to capture the correlation between routes by dividing the random error terms into two components; the first component is a set of IID Gumbel variables ensuring that the Logit structure is kept, and the second component is a set of Gaussian distributed variable terms that attempt to capture the interdependencies among the routes. Bekhor et al (2002) propose a Factor Analytic Logit Kernel model that attempts to capture the similarities among routes by assuming the covariance between utilities relates to overlap lengths. The main drawback of Mixed Logit models however, is that they do not possess closed-form expressions and therefore solving the route choice probabilities requires either Monte Carlo simulation or similar methods, which are computationally burdensome. There are also difficulties in estimating the parameters of the Factor Analytic Logit Kernel model: Ramming (2002) finds instable estimates of the covariance parameters, while Prato (2005) discusses the difficulty in obtaining significant estimates.

MNL-modification models: The third group of extended Logit models are the MNL-modification models which modify the deterministic part of the route utilities by including a correction term that adjusts the route choice probabilities to approximate the correlation between the routes. These models include C-Logit (CL) (Cascetta et al, 1996), Path Size Logit (PSL) (Ben-Akiva & Ramming, 1998), and Path Size Correction Logit (PSCL) (Bovy et al, 2008). Ramming (2002) proposes a Generalised Path Size Logit (GPSL) model which includes a component that attempts to reduce the impact that infeasibly long routes have on the correction terms (and thus choice probabilities) of feasible routes. The main attraction of MNL-modification models is that they all retain the single-level tree structure as MNL and have simple closed-form expressions, meaning the route choice probabilities are generally easy and quick to compute, and estimating the parameters of the CL, PSL, and PSCL models is a comparatively simple task, though as the size of network increases, so does

the computational effort required to enumerate the overlap between all routes in a choice set. The GPSL model requires the estimation of an additional parameter over the PSL model which makes parameter estimation more difficult; estimates for the parameter can be justified by assessing the goodness-of-fit, though the best estimates in case studies tend to be very large values meaning that it is difficult to provide a behavioural interpretation for the parameter.

Alternative RUMs: Another option is to utilise an alternative RUM. There are many RUMs that do not suffer from the same issue as MNL as the similarity between each pair of routes is accounted for by allowing for covariance between the error terms. The MNL RUM proposes that the random error terms assume a Gumbel distribution (Dial, 1971), while the Multinomial Probit (MNP) model (Daganzo & Sheffi, 1977) and the Multinomial Gammit (MNG) model (Cantarella & Binetti, 2002), propose that the error terms assume a Normal distribution and Gamma distribution, respectively. Other distributions include Log-Normal and Uniform, while Nielsen (2000) argues that Gamma distributed error terms is preferred since the error term is positive and link-additive (Nielsen & Frederiksen, 2006). These models however, do not have closed-form probability expressions and hence solving the route choice probabilities also requires either Monte Carlo simulation or similar methods which are computationally burdensome and converge very slowly on large scale networks (Rich et al, 2015; Manzo et al, 2015; Rasmussen et al, 2016; Connors et al, 2014). Mishra et al (2012), Ahipasaoglu et al (2013), and Ahipasaoglu et al (2015) explore a Cross Moment (CMM) choice model where the exact distribution of the random error terms is unknown and instead belongs to a set, where the distribution employed is that which maximises the expected utility given known mean and covariance information of the utilities. Efficient convex optimisation techniques are developed to solve the CMM, though computation times increase dramatically as the number of routes increases.

There are numerous examples of alternative RUMs where the correlation between routes is not explicitly captured (like MNL) and have been adapted accordingly utilising concepts from extended Logit models. These models thus share the same associated strengths/weaknesses of the approaches. Castillo et al (2008) proposed a Multinomial Weibit (MNW) model – where the random error terms assume a Weibull distribution – to address the other underlying assumption made by the MNL model that the error terms are identically distributed. Kitthamkesorn & Chen (2013) then integrated the ideas of the MNW and PSL models to formulate a Path Size Weibit (PSW) model that simultaneously addresses both the independently distributed and identically distributed assumptions made of the MNL error terms. Xu et al (2015) formulate a Hybrid closed-form route choice model to alleviate the contrasting scaling issues of MNL and MNW by simultaneously considering absolute cost difference and relative cost difference, and is extended to include a path size correction factor to capture the correlation between routes. Chikaraishi & Nakayama (2016) extend concepts from the q-Generalised Logit model (Nakayama & Chikaraishi, 2015) to introduce a q-Product Logit model in which the relationship between the deterministic and random components of utilities can be either additive, multiplicative, or in-between, depending on the value of the parameter q, where MNL and MNW are special cases of the model. A q-Product Nested Logit model is presented to capture correlation, where the CNL model is a special case, as well as a nested equivalent of the Weibit model. Li (2011) proposes a Semi-Parametric choice model that relaxes the assumption of underlying distributions from either Gumbel or Weibull to a wider distribution class where the underlying choice model is unknown, and integrates Mixed Logit concepts to postulate a Mixed Semi-Parametric choice model. Ahipasaoglu et al (2016) consider the application of the Marginal Distribution Model (MDM) (Natarajan et al, 2009) to route choice, where the marginal distributions of the route utilities are specified but the joint distributions are not, and the focus is on the particular joint distribution that maximizes expected utility. Incorporating information on the marginal distributions makes the MDM model flexible and MNL, CL, PSL, MNW, and PSW are all special cases. Numerous variants of the MDM are explored and PSL and CL concepts are integrated to form new MDMs. Chorus (2010) and Bekhor et al (2012) introduce a Random Regret Minimization (RRM) model which assumes that individuals minimise anticipated regret, rather than maximize expected utility, when choosing routes, and Prato (2014) develops a Path Size RRM model and a Path Size Correction RRM model.

To summarise, the greatest hindrance for the GEV structures, Mixed Logit models, and alternative RUMs is the considerable computational cost required to solve the route choice probabilities for large-scale networks, while another issue that has been noted for some of the GEV structures and Mixed Logit models is the difficulty in obtaining reasonable estimates for parameters. MNL-modification models are a useful and

practical approach to approximating the correlation; more complex models can capture the correlation more accurately, but due to the comparatively low computational cost and the relative ease in obtaining reasonable estimates for parameters, they are the most commonly used models in practice, and are the focus of this paper, in particular: Path Size Logit models.

One of the main issues for most MNL-modification models is that results are highly sensitive to the inclusion and exclusion of routes from the choice set. The CL model proposes that the correction terms are based upon commonality factors that measure the similarity of routes, and penalises the utilities accordingly. In contrast, the PSL and PSCL models propose that the correction terms are based upon path size terms that measure route distinctiveness: a route is penalised based on the number of other routes sharing its links, and the costs of those shared links. The inclusion of a route to a choice set can thus have a substantial effect upon the choice probability of any route that shares its links, as the correction terms adjust the route utilities attempting to capture the correlation.

In real-life applications where the size of the network is often large, route choice is rarely performed upon the full choice sets of routes, and choice sets are either pre-generated or a column generation approach is employed with implementation. This is often because it is computationally infeasible to both/either enumerate the full choice sets of routes and/or perform route choice upon the full choice sets of routes. Furthermore, typical road networks contain many very long routes that should be considered unrealistic and excluded from route choice. The key issue for the PSL model is that the choice probabilities are extremely sensitive to the utilised choice sets since all routes contribute equally to path size terms, and as such, results are extremely sensitive to the choice set generation / column generation method adopted. Moreover, it is crucial for the PSL model that the choice sets contain realistic alternatives only, as the inclusion of a single unrealistic alternative can have a considerable and negative effect on the choice probabilities of the realistic routes.

Thus, since it is difficult to obtain choice sets of realistic routes with absolute certainty for PSL to be suitable, a pragmatic approach is to utilise a weighted path size contribution technique along with choice set generation to attempt to reduce the impact any present unrealistic routes may have on the choice probabilities of realistic routes. Weighted path size contribution techniques weight the contribution of routes to path size terms with a path size contribution factor, i.e. so that the contribution of route k to the path size term of route i is reduced for unrealistic routes.

The GPSL model proposes that the path size contribution factor is based upon ratios of travel cost between routes, and hence routes with excessively large travel costs have a diminished impact upon the correction terms of routes with small travel costs, and consequently the choice probabilities of those routes. How the GPSL path size contribution factor is formulated, however, means that: a) the model is not always internally consistent with how it assesses routes to be (un)realistic, and b) an additional scaling parameter is required to scale the path size contributions which makes parameter estimation more difficult. The main contribution of the present paper is thus the formulation of an Adaptive Path Size Logit (APSL) model where a new path size contribution factor is proposed so that the model is always internally consistent with how it assesses routes to be unrealistic, and so that no additional parameters are required for estimation.

For Path Size Logit models, the probability that a route is chosen (i.e. how feasible of an alternative the route is perceived to be) is a trade-off between its relative attractiveness due to travel cost and its relative attractiveness due to distinctiveness, and two independent scaling parameters (Logit parameter and path size parameter) affect the relativeness of how attractive each component is. The GPSL path size contribution factors however, are inconsistent with this in two ways: a) they assess the feasibility of a route according to its relative attractiveness due to travel cost only; and, b) they scale the relativeness of how attractive routes are due to travel cost with an additional independent path size contribution parameter, which is not necessarily proportional to the Logit parameter that scales travel cost within the probability relation.

The APSL model proposes that the path size contribution factors are based upon ratios of choice probability between routes, thus ensuring that routes defined as unrealistic by the path size terms, are exactly those with very low choice probabilities. The APSL route choice probability relation is an implicit function involving the choice probabilities, and solutions to the model are solutions to the fixed-point problem. Also, by defining the path size contribution factor as the ratio of choice probabilities, the scaling of the path size contributions is controlled implicitly through the scaling of the route choice probabilities (i.e. with the Logit parameter and path size parameter), and hence there is no additional path size contribution parameter for estimation.

Fig. 2.1 displays a network with a single OD movement and three routes. As x varies, the travel cost of each route stays constant (though different from one another), meaning that the GPSL path size terms always assess the feasibility of each route as being the same. However, as x is varied between 0 and 1, the correlation between Route 1 and Route 2 varies, thus altering the choice probabilities and how feasible of an alternative each route is perceived to be. A key point is that the behaviour of the choice probabilities as x is varied is highly dependent upon the values of the scaling parameters; different ranges for the Logit / path size parameters imply different theoretical route choice behaviours consequently altering how feasible each route is deemed to be. This makes it difficult to state what behaviours we should expect to happen as x is varied, without knowing the parameter values we wish to set, to model specific behaviours. Due to its internal consistency, the APSL model is adaptable to whichever values are set for the scaling parameters, and the path size contribution factors will assess the feasibility of routes by how relatively attractive they are due to travel cost and distinctiveness as the scaling parameters dictate.

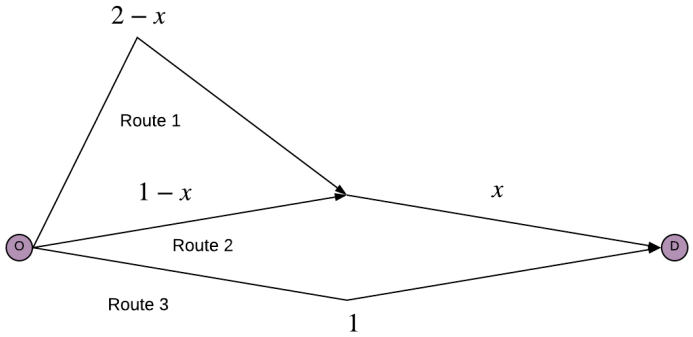

Fig. 2.1. Example network to demonstrate the inconsistency of the GPSL model.

The structure of the paper is as follows. In Section 2 we introduce some basic network notation as well as the definitions of the MNL, PSL, and GPSL models, and several numerical experiments on small-scale networks to demonstrate some of the key issues with PSL and GPSL, and the potential negative implications of an internally inconsistent PSL model. In Section 3 we detail the new APSL model, give results from several numerical experiments that demonstrate the key properties of the APSL model, and detail a solution method. Section 4 addresses existence and uniqueness of APSL solutions. In Section 5 we investigate estimating the APSL model. To show that the parameters of the APSL model can be estimated we first propose a Maximum Likelihood Estimation procedure for estimating APSL with tracked route observation data, then investigate this procedure in a simulation study on the Sioux Falls network where we show that it is generally possible to reproduce assumed true parameters. Then, in a real-life case study, we estimate the APSL model using real tracked route GPS data on a large-scale network. Section 6 concludes the paper.

2. Notation, Definitions, and Demonstrations of Key Issues with Existing Path Size Logit Models

2.1 Basic Network Notation

The model developed in this paper is applicable to general networks with multiple OD movements and flow-dependent link costs. However, without compromising the model derivation, we simplify notation by considering a single OD movement with fixed link costs. The network consists of link set A. For the OD movement, R is the choice set of all simple routes (without cycles), having size $N = |R|$. $A_i \subseteq A$ is the set of links belonging to route $i \in R$, and $\delta_{a,i} = \begin{cases} 1 & if\ a \in A_i \\ 0 & otherwise \end{cases}$. Each link $a \in A$ has a fixed generalised travel cost t_a, and supposing that the travel cost for a route can be attained through summing up the total cost of its links, then the generalised travel cost for route $i \in R$, c_i, can be computed as follows: $c_i = \sum_{a \in A_i} t_a$.

The route choice probability for route $i \in R$ is P_i, where $\boldsymbol{P} = (P_1, P_2, \dots, P_N)$ is the vector of route choice probabilities, and D is the set of all possible route choice probability vectors:

$$D = \left\{ \boldsymbol{P} \in \mathbb{R}^N_{\geq 0} : 0 \leq P_i \leq 1, \forall i \in R, \sum_{j=1}^{N} P_j = 1 \right\}.$$

And, $D^{>0} \subset D$ is the subset of all possible route choice probability vectors where no route has zero choice probability:

$$D^{>0} = \left\{ \boldsymbol{P} \in \mathbb{R}^N_{>0} : 0 < P_i < 1, \forall i \in R, \sum_{j=1}^{N} P_j = 1 \right\}.$$

2.2 Multinomial Logit

The Multinomial Logit (MNL) choice model is formulated as follows. The deterministic utility of alternative $i \in R$ is V_i, and the random utility of alternative $i \in R$ is U_i such that $U_i = V_i + \varepsilon_i$, where the ε_i terms are the individually and identically distributed random variable error terms. Assuming individuals seek the alternative with highest utility, the probability that an individual selects alternative $i \in R$ is:

$$P_i = \Pr\left(U_i \geq U_j, \forall j \in R, j \neq i\right) = \Pr\left(V_i + \varepsilon_i \geq V_j + \varepsilon_j, \forall j \in R, j \neq i\right).$$

The defining characteristic of Logit models is that the random variable error terms assume a Gumbel distribution. Consequently:

$$P_i(\boldsymbol{V}) = \frac{e^{V_i}}{\sum_{j \in R} e^{V_j}}$$

where $\boldsymbol{V}$ is the vector of deterministic utilities.

The MNL model in the context of route choice states that the deterministic utility of route $i \in R$ is given by $V_i = -\theta c_i$, where $\theta > 0$ is the Logit scaling parameter, and thus:

$$P_i = \frac{e^{-\theta c_i}}{\sum_{j \in R} e^{-\theta c_j}} = \frac{1}{\sum_{j \in R} e^{-\theta (c_j - c_i)}}. \tag{2.1}$$

The MNL model assumes the route utilities are independent from one another, however routes with overlapping links share unobserved attributes, and the assumption that the random error terms are all independently and identically distributed is no longer valid. The famous example for this is the 'loop hole' network (also known as the red-bus/blue-bus network) presented in Cascetta et al (1996).

2.3 Path Size Logit Models

Path Size Logit models include correction terms to penalise routes that share links with other routes, so that the deterministic utility of route $i \in R$ is $V_i = -\theta c_i + \kappa_i$, where $\kappa_i \leq 0$ is the correction term for route $i \in R$. The probability that a driver chooses route $i \in R$ is therefore:

$$P_i = \frac{e^{-\theta c_i + \kappa_i}}{\sum_{j \in R} e^{-\theta c_j + \kappa_j}}.$$

Path Size Logit models adopt the form $\kappa_i = \beta \ln(\gamma_i)$, where $\beta \geq 0$ is the path size scaling parameter, and $\gamma_i \in (0,1]$ is the path size term for route $i \in R$. A distinct route with no shared links has path size term equal to 1, resulting in no penalisation. Less distinct routes have smaller path size terms and incur greater penalisation. The probability that a driver chooses route $i \in R$ is:

$$P_i = \frac{e^{-\theta c_i + \beta \ln(\gamma_i)}}{\sum_{j \in R} e^{-\theta c_j + \beta \ln(\gamma_j)}} = \frac{(\gamma_i)^\beta e^{-\theta c_i}}{\sum_{j \in R} (\gamma_j)^\beta e^{-\theta c_j}} = \frac{1}{\sum_{j \in R} \left(\frac{\gamma_j}{\gamma_i}\right)^\beta e^{-\theta (c_j - c_i)}}. \tag{2.2}$$

2.3.1 Path Size Logit

The Path Size Logit (PSL) model was first proposed by Ben-Akiva & Ramming (1998), and states that the PSL path size term for route $i \in R$, γ_i^{PS}, is defined as follows:

$$\gamma_i^{PS} = \sum_{a \in A_i} \frac{t_a}{c_i} \frac{1}{\sum_{k \in R} \delta_{a,k}}. \tag{2.3}$$

To dissect the PSL path size term for route $i \in R$ defined in (2.3): each link a in route i is penalised (in terms of decreasing the path size term and hence the utility of the route) according to the number of routes in the choice set that also use that link $\left(\sum_{k \in R} \delta_{a,k}\right)$, and the significance of the penalisation is weighted according to how prominent link a is in route i, i.e. the cost of route a in relation to the total cost of route i $\left(\frac{t_a}{c_i}\right)$.

PSL Key Issue: *Unrealistic routes negatively impact the choice probabilities of realistic routes when links are shared.*

The key issue with the PSL model is that all routes contribute equally to path size terms (i.e. the path size contribution factors are simply all 1), and hence the choice probabilities of realistic routes are affected by link sharing with unrealistic routes. To demonstrate this, consider example network 1 in Fig. 2.2A where there are 3 routes: Routes 2 & 3 have travel cost 1 and Route 1 has travel cost $1 + \upsilon$, Routes 1 & 2 are correlated while Route 3 is distinct. Fig. 2.2B displays the example network 1 PSL choice probabilities as υ is increased from 0.5 to 3, $\theta = \beta = 1$. For $\upsilon = 0.5$, Routes 1 & 2 have the same unshared travel cost and are thus considered equally attractive. As υ is increased, Route 1 increases in travel cost and decreases in choice probability. As Route 1 becomes an unrealistic alternative, the choice probability of Route 2 should not be penalised for overlapping with Route 1. The PSL path size terms dictate though that Route 1 contributes equally to the path size term of Route 2 for all υ, and hence the choice probability of Route 2 is always significantly penalised. As υ is increased and the choice probability of Route 1 approaches zero, the contribution of Route 1 to the path size term of Route 2 should decrease, and the choice probability of Route 2 should converge to the choice probability of Route 3.

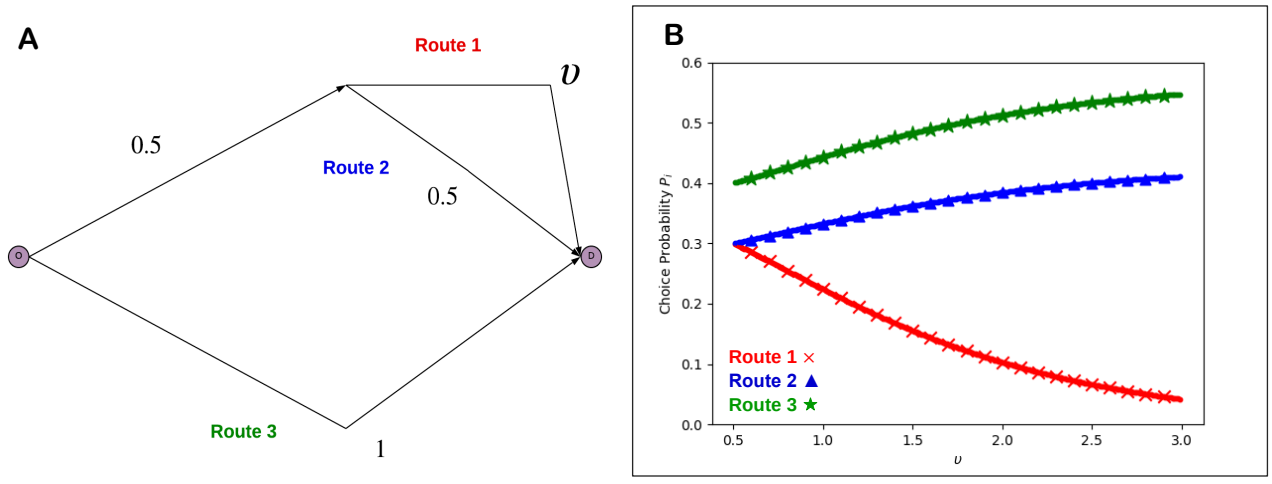

Fig. 2.2. A: Example network 1. **B:** Example network 1: PSL route choice probabilities for increasing υ ($\theta = \beta = 1$).

2.3.2 Generalised Path Size Logit

Ben-Akiva & Bierlaire (1999) formulate an alternative PSL model (PSL′) that attempts to reduce the contributions of excessively expensive routes to the path size terms of more realistic routes in the choice set. The PSL′ model states that the PSL′ path size term for route $i \in R$, $\gamma_i^{PS'}$, is defined as follows:

$$\gamma_i^{PS'} = \sum_{a \in A_i} \frac{t_a}{c_i} \frac{1}{\sum_{k \in R} \left(\frac{\min(c_l : l \in R)}{c_k}\right) \delta_{a,k}}, \tag{2.4}$$

As (2.4) shows, the contribution of route k to path size terms is weighted according to the ratio of route k and the cheapest route in the choice set $\left(\frac{\min(c_l : l \in R)}{c_k}\right)$, and hence contributions of high costing routes compared to the cheapest alternative are reduced.

As Ramming (2002) describes, however, when a route is completely distinct its path size term is not always equal to 1 which results in an undesired penalisation upon the utility of that route. To combat this, Ramming (2002) proposes the Generalised Path Size Logit (GPSL) model. The GPSL model states that the GPSL path size term for route $i \in R$, γ_i^{GPS}, is defined as follows:

$$\gamma_i^{GPS} = \sum_{a \in A_i} \frac{t_a}{c_i} \frac{1}{\sum_{k \in R} \left(\frac{c_i}{c_k}\right)^{\lambda} \delta_{a,k}}, \tag{2.5}$$

where $\lambda \geq 0$, noting that the GPSL model is equivalent to the PSL model when $\lambda = 0$. In (2.5), the contribution of route k to the path size term of route i (the path size contribution factor) is weighted according to the cost ratio between the routes, $\left(\left(\frac{c_i}{c_k}\right)^{\lambda}\right)$, and hence the contributions of high costing routes to the path size terms of low costing routes is reduced. $\lambda \geq 0$ is the path size contribution scaling parameter to be estimated.

Fig. 2.3 displays the example network 1 GPSL choice probabilities as υ is increased from 0.5 to 3, $\theta = \beta = 1$, $\lambda = 3$. As Fig. 2.3 shows, as υ is increased and the travel cost of Route 1 increases, the contribution of Route 1 to the path size term of Route 2 decreases, and consequently the choice probability of Route 2 converges to the choice probability of Route 3.

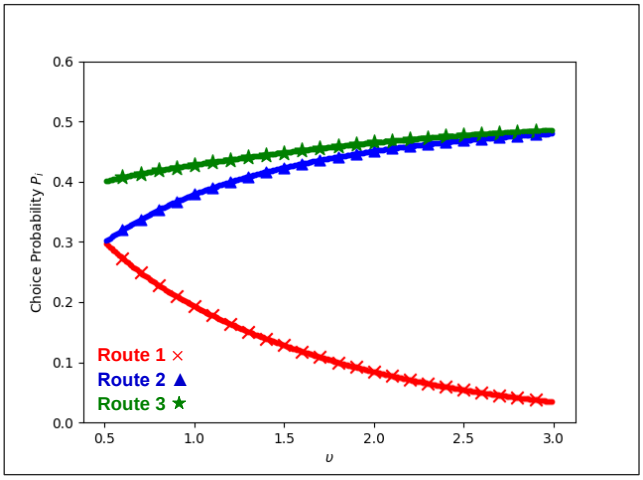

Fig. 2.3. Example network 1: GPSL route choice probabilities for increasing υ ($\theta = \beta = 1$, $\lambda = 3$).

GPSL Key Issue 1: *For large λ, GPSL path size terms are highly sensitive to small differences in route travel cost.*

It is mentioned numerous times in the literature that the GPSL model can be problematic for large λ values, especially when overlapping routes only have marginally different travel costs (Ramming, 2002; Frejinger & Bierlaire, 2007; Hoogendoorn-Lanser, 2005). Hoogendoorn-Lanser et al (2005) describe how λ should be set to 0 when overlapping routes have more-or-less equal travel costs, as the overlap between those alternatives should not affect their choice probabilities differently. However, when overlapping routes have very different travel costs λ should not be set to 0, as the effects that routes with high travel costs have on the path size terms of routes with low travel costs should be dampened. Example network 2 in Fig. 2.4A shows a network where both cases exist: Routes 1 & 2 are overlapping routes with more-or-less equal travel costs ($c_1 = 2.01$, $c_2 = 2$), and Routes 3 & 4 are overlapping routes with very different travel costs ($c_3 = 2$, $c_4 = 6$). Fig. 2.4B shows the example network 2 GPSL choice probabilities as λ is increased from 0 to 400, $\theta = \beta = 1$. When $\lambda = 0$ (i.e. GSPL is equivalent to PSL), Routes 1, 2 & 3 have approximately equal choice probabilities as they all have similar travel costs and all share approximately half of their journey with one other route. Route 4 induces a penalty on Route 3, but this should be less than the path size penalties Routes 1 & 2 impose on each other, and thus P_3 should be greater than P_1 and P_2, which should be approximately equal, for these values of θ and β. Although this is the case when $\lambda \cong 10$, increasing λ amplifies the difference in costs between Routes 1 & 2 so that P_1 and P_2 diverge, which is not desired.

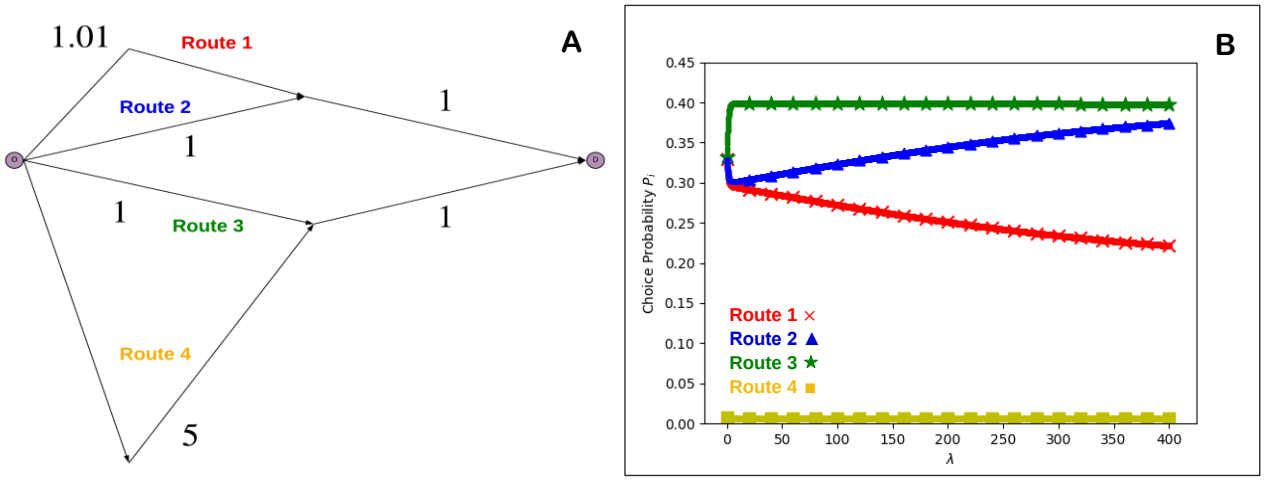

Fig. 2.4. A: Example network 2. **B:** Example network 2: GPSL route choice probabilities for increasing λ ($\theta = \beta = 1$).

As (2.2) shows, how feasible route i is perceived to be by drivers (i.e. its choice probability) is a trade-off between its relative attractiveness due to travel cost $e^{-\theta(c_j - c_i)}$ and its relative attractiveness due to distinctiveness $\left(\frac{\gamma_j}{\gamma_i}\right)^{\beta}$, where the θ parameter scales relative attractiveness due to travel cost and β scales relative attractiveness due to distinctiveness. The GPSL path size contribution factors in (2.5), however, assess the feasibility of route i according to its relative attractiveness due to travel cost only $\left(\frac{c_i}{c_k}\right)^{\lambda}$, where an additional parameter λ scales relative attractiveness due to travel cost. The internal inconsistency issues of the GPSL model between the probability relation and path size terms are thus twofold: a) there is an inconsistent assessment of the feasibility of routes; and, b) there are inconsistent parameters that scale relative attractiveness due to travel cost. We demonstrate both issues below.

GPSL Key Issue 2: *Internally inconsistent assessment of the feasibility of routes.*

Fig. 2.5A shows a network with 6 routes: Routes 1-5 are highly correlated with each other with fixed travel cost 1.2, and Route 6 has a fixed cost of 2 and is either a distinct route when $\eta = 1$ or correlated with Routes 1-5 when $\eta < 1$. As η is decreased, the correlation between Route 6 and Routes 1-5 increases, but the travel costs don't change. Supposing that $\theta = \beta = 1$, then one might expect Route 6 to have a choice probability greater than each of Routes 1-5 when $\eta = 1$ due to being distinct, and a choice probability smaller than each of Routes 1-5 when $\eta = 0$ due to having the larger detour. There should thus be a point $\eta_{eq} \in (0,1)$ where all routes have equal choice probability. At this point, each route is considered equally attractive and all routes should contribute equally to path size terms. By the definition of the PSL model all routes always contribute equally to path size terms; Fig. 2.5B shows the example network 3 PSL choice probabilities for increasing η, $\theta = \beta = 1$, and $\eta_{eq} = 0.27$ is the point where all routes have equal choice probabilities. For $\eta \neq \eta_{eq}$ however, it is not necessarily required for routes to contribute equally to path size terms, for example when $\eta = 0$ the contribution of Route 6 to Routes 1-5 may wish to be reduced, and the PSL model is incapable of this. Fig. 2.5C & Fig. 2.5D show the example network 3 GPSL choice probabilities for increasing η, $\theta = \beta = 1$, for $\lambda = 1$ and $\lambda = 10$, respectively. The GPSL model proposes that the contribution of Route 6 to the path size terms of Routes 1-5 is a constant $\left(\frac{1.2}{2}\right)^{\lambda}$ for all η, and thus the points where all routes have equal choice probabilities are $\eta_{eq} = 0.37$ and $\eta_{eq} = 0.48$ for $\lambda = 1$ and $\lambda = 10$, respectively, which are greater than 0.27, and larger values for λ moves η_{eq} further away from 0.27.

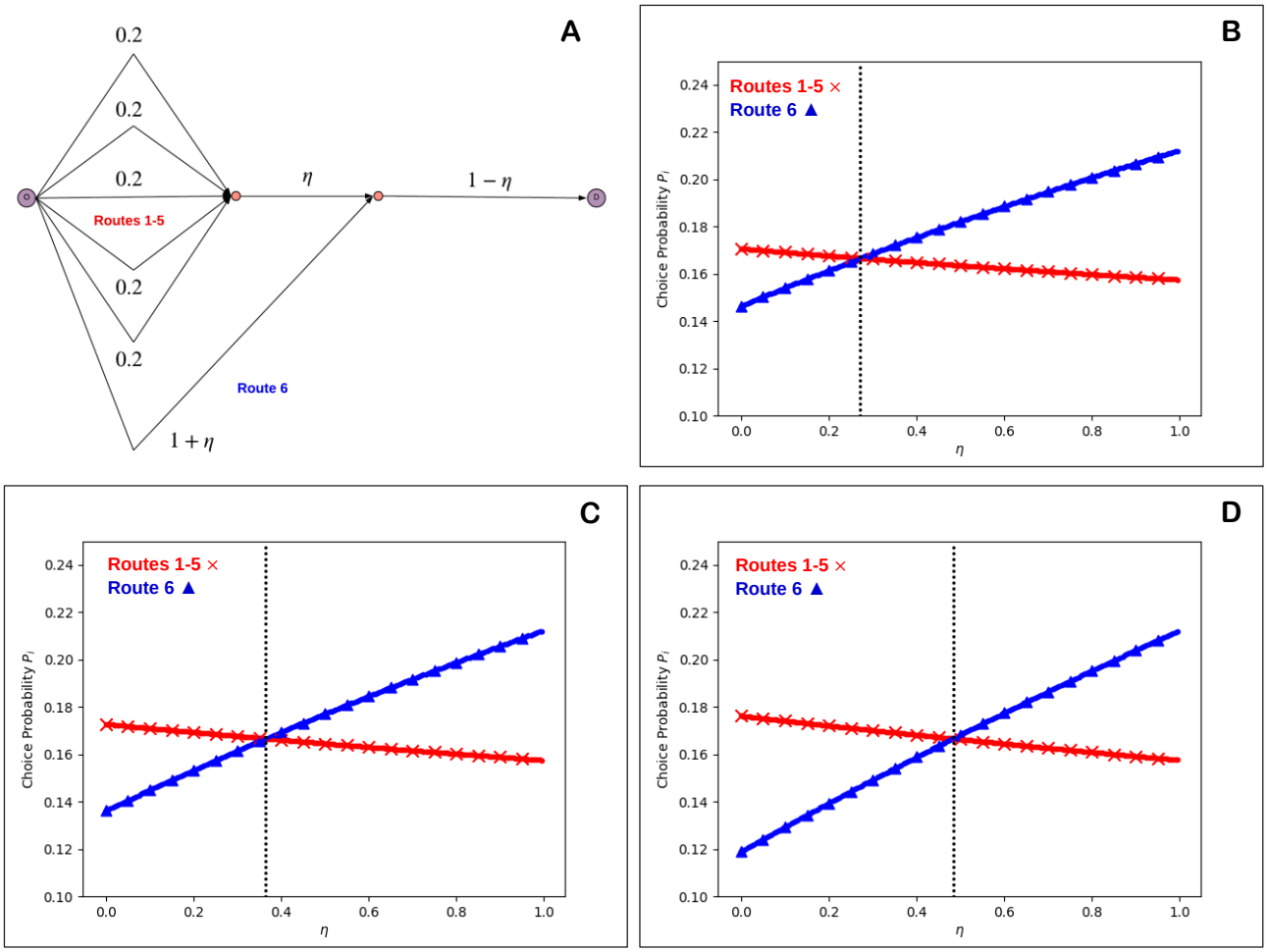

Fig. 2.5. A: Example network 3. Example network 3: Route choice probabilities for increasing η ($\theta = \beta = 1$). **B:** PSL, $(\eta_{eq} = 0.27)$. **C:** GPSL ($\lambda = 1$), $(\eta_{eq} = 0.37)$. **D:** GPSL ($\lambda = 10$), $(\eta_{eq} = 0.48)$.

GPSL Key Issue 3: *Internally inconsistent scaling parameters.*

Fig. 2.6A displays a network with 4 routes: Routes 1 & 4 have travel cost 3 and Routes 2 & 3 have travel cost 1, Routes 1 & 2 are distinct and Routes 3 & 4 are correlated, with Route 4 being more distinct than Route 3. Different ranges for the θ and β parameters have different implications for how relatively attractive the routes are due to travel cost and distinctiveness. Fig. 2.6B shows the example network 4 GPSL choice probabilities for increasing θ, $\beta = 1$, $\lambda = 4$. The GPSL model diminishes Route 4's contribution to the path size term of Route 3 to $\left(\frac{1}{3}\right)^4$, and thus Routes 2 & 3 have near identical choice probabilities for all θ. For low θ however, the sensitivity to the differences in travel cost is dampened within the probability relation, yet Route 4's path size term contribution to Route 3 accentuates the difference in cost, and the GPSL model is thus inconsistent.

To try and overcome this inconsistency issue, one must attempt to represent λ proportional to θ. Because θ scales travel cost difference, and λ scales travel cost ratios, it is difficult to know how λ should relate to θ, e.g. $\lambda = \theta^5$? A potential solution could be to adjust the GPSL path size contribution factor to resemble the relative attractiveness due to travel cost component within the Path Size Logit probability relation in (2.2) (and the MNL probability relation in (2.1)), thus formulating an alternative Generalised Path Size Logit (GPSL′) model, where the GPSL′ path size term for route $i \in R$, $\gamma_i^{GPS'}$, is defined as follows:

$$\gamma_i^{GPS'} = \sum_{a \in A_i} \frac{t_a}{c_i} \frac{1}{\sum_{k \in R} e^{-\lambda(c_k - c_i)} \delta_{a,k}}. \tag{2.6}$$

By setting $\lambda = \theta$, the relative attractiveness due to travel cost components within the GPSL′ model match exactly. Fig. 2.6C shows the example network 4 GPSL′$_{(\lambda=\theta)}$ choice probabilities for increasing θ, $\beta = 1$. For

low θ, the sensitivity to the difference in cost between Routes 3 & 4 is dampened within the probability relation *and* within the path size contribution factor, and Route 3 has the lowest choice probability due to being the least distinct. As θ is increased, the sensitivity to the difference in cost between Routes 3 & 4 is accentuated within the path size contribution factor and Route 4's contribution to Route 3 decreases, and the choice probability of Route 3 converges to the choice probability of Route 2.

The GPSL$'_{(\lambda=\theta)}$ model only partially improves the internal consistency of the GPSL model though. Fig. 2.6D shows the example network 4 GPSL$'_{(\lambda=\theta)}$choice probabilities for increasing θ, $\beta = 2$. An increase in β increases the sensitivity to distinctiveness within the probability relation; attractiveness due to distinctiveness is not considered within the GPSL & GPSL$'$ path size contribution factors however, and hence as Route 3 becomes unattractive for low θ due to being the least distinct, its path size contribution to Route 4 is not reduced, though approaching being considered unrealistic as the parameters dictate.

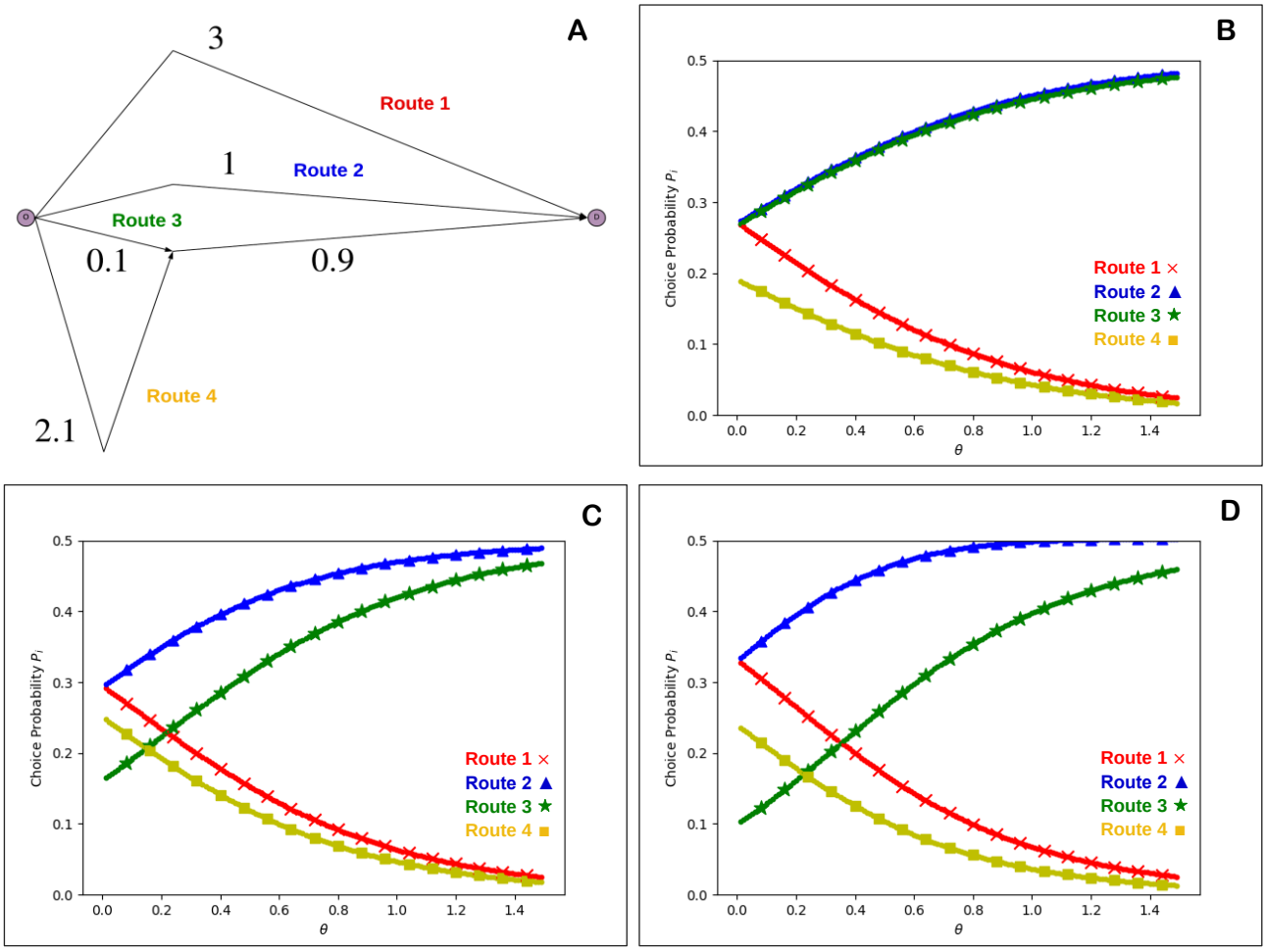

Fig. 2.6. A: Example network 4. Example network 4: Route choice probabilities for increasing θ: **B:** GPSL ($\beta = 1, \lambda = 4$). **C:** GPSL$'$ ($\lambda = \theta, \beta = 1$). **D:** GPSL$'$ ($\lambda = \theta, \beta = 2$).

3. The Adaptive Path Size Logit Model

In the PSL model, all routes contribute equally to path size terms so that unrealistic routes negatively impact the choice probabilities of realistic routes when links are shared. The GPSL model attempts to overcome this issue by including a path size contribution factor based upon travel cost ratios, but has issues with internal inconsistency. The alternative GPSL (GPSL$'_{(\lambda=\theta)}$) model partially addresses this inconsistency but does not take into account the relative attractiveness of routes due to distinctiveness. We thus propose in this section a fully internally consistent PSL model where all components assess the feasibility of routes according to its relative attractiveness due to travel cost and distinctiveness. Formulation of the APSL model was complicated by the desire to establish existence and uniqueness of solutions. First, we provide a simpler formulation of the

APSL model, then we detail the final more complicated definition, which has been constructed solely so that solutions exist and can be unique (proven in Section 4).

3.1 Preliminary Definition of APSL

Definition

The preliminary definition of APSL ($APSL_0$) is defined as follows. The $APSL_0$ choice probabilities, $\boldsymbol{P}^*$, are a solution to the fixed-point problem $\boldsymbol{P} = \boldsymbol{g}\left(\boldsymbol{\gamma}^{APS}(\boldsymbol{P})\right)$, where g_i for route $i \in R$ is:

$$g_i\left(\boldsymbol{\gamma}^{APS}(\boldsymbol{P})\right) = \frac{e^{-\theta c_i + \beta \ln\left(\gamma_i^{APS}(\boldsymbol{P})\right)}}{\sum_{j\in R} e^{-\theta c_j + \beta \ln\left(\gamma_j^{APS}(\boldsymbol{P})\right)}} = \frac{\left(\gamma_i^{APS}(\boldsymbol{P})\right)^{\beta} e^{-\theta c_i}}{\sum_{j\in R}\left(\gamma_j^{APS}(\boldsymbol{P})\right)^{\beta} e^{-\theta c_j}} = \frac{1}{\sum_{j\in R}\left(\frac{\gamma_j^{APS}(\boldsymbol{P})}{\gamma_i^{APS}(\boldsymbol{P})}\right)^{\beta} e^{-\theta(c_j - c_i)}}, \tag{2.7}$$

and γ_i^{APS} for route $i \in R$ is:

$$\gamma_i^{APS}(\boldsymbol{P}) = \sum_{a\in A_i} \frac{t_a}{c_i} \frac{P_i}{\sum_{k\in R} P_k \delta_{a,k}} = \sum_{a\in A_i} \frac{t_a}{c_i} \frac{1}{\sum_{k\in R}\left(\frac{P_k}{P_i}\right)\delta_{a,k}}, \qquad \forall \boldsymbol{P} \in D^{>0}. \tag{2.8}$$

The model parameters are $\theta > 0$ and $\beta \geq 0$. $\gamma_i^{APS}(\boldsymbol{P})$ in (2.8) is the APSL path size term function for route $i \in R$ that is a function involving the route choice probabilities. $g_i\left(\boldsymbol{\gamma}^{APS}(\boldsymbol{P})\right)$ in (2.7) is the APSL route choice probability function for route $i \in R$ which is a function involving the path size term functions and hence also the choice probabilities of routes. The choice probability relation for route $i \in R$ is given by $P_i = g_i\left(\boldsymbol{\gamma}^{APS}(\boldsymbol{P})\right)$, which is an implicit equation involving choice probabilities, and hence the $APSL_0$ route choice probabilities, $\boldsymbol{P}^*$, are a solution such that $P_i^* = g_i\left(\boldsymbol{\gamma}^{APS}(\boldsymbol{P}^*)\right), \forall i \in R$.

Property 1: For an $APSL_0$ route choice probability solution vector $\boldsymbol{P}^*$, $\gamma_i^{APS}(\boldsymbol{P}^*)$ is the APSL path size term for route $i \in R$, $\kappa_i = \beta \ln\left(\gamma_i^{APS}(\boldsymbol{P}^*)\right)$ is the correction term, and the deterministic utility is given by:

$$V_i = -\theta c_i + \beta \ln\left(\gamma_i^{APS}(\boldsymbol{P}^*)\right). \tag{2.9}$$

If the random utility for route $i \in R$ is $U_i = -\theta c_i + \beta \ln\left(\gamma_i^{APS}(\boldsymbol{P}^*)\right) + \varepsilon_i$, and if the random variable error terms, ε_i, are i.i.d Gumbel, then the probability relation in (2.7) is obtained.

As (2.8) shows, for a choice probability solution $\boldsymbol{P}^*$, the contribution of route k to the APSL path size term of route i is weighted according to the ratio of choice probabilities between the routes $\left(\frac{P_k^*}{P_i^*}\right)$, and hence unrealistic route alternatives with very low choice probabilities have a diminished contribution to the path size terms of realistic routes with relatively large choice probabilities. The choice probability ratio path size contribution factor can also be formulated as follows:

$$\frac{P_k^*}{P_i^*} = \frac{g_k\left(\boldsymbol{\gamma}^{APS}(\boldsymbol{P}^*)\right)}{g_i\left(\boldsymbol{\gamma}^{APS}(\boldsymbol{P}^*)\right)} = \left(\frac{\gamma_k^{APS}(\boldsymbol{P}^*)}{\gamma_i^{APS}(\boldsymbol{P}^*)}\right)^{\beta} e^{-\theta(c_k - c_i)}. \tag{2.10}$$

So, it is clear to see that the path size contribution factor in (2.10) matches the probability relation in (2.7), where both consider how attractive a route is by measuring its relative attractiveness due to travel cost and distinctiveness, and hence there is some clear consistency within the model's framework. Furthermore, not only do the path size contribution factors become more consistent with the eventual route choice probabilities (i.e. they both define a route as being unrealistic if it has a relatively unattractive combination of travel cost and distinctiveness) the model does not require the estimation of any additional parameters. Whereas the scaling of the path size contributions in the GPSL model depends upon an independent parameter λ, the scaling of the path size contributions in the $APSL_0$ model depends implicitly on the scaling of the choice probability relation with the θ and β parameters, and one cannot independently adjust the scaling within the path size contribution factors without scaling the choice probability relation as well.

In Random Utility Theory (RUT), RUMs are derived based on the deterministic utility function and random error term. As (2.9) shows, however, the deterministic utility function for the $APSL_0$ model is not in fact deterministic since it is dependent upon the route choice probabilities. $APSL_0$ is thus not a member of the RUM family, though it is derived using RUT. This is analogous to the way that Stochastic User Equilibrium (SUE) is a consistency condition derived using RUT but an SUE model is not a member of the RUM family. The key difference can be understood in considering a policy test: having solved the $APSL_0$ fixed-point problem for the 'before' case, the path size terms are not fixed. The 'after' case would require $APSL_0$ to be re-solved and the path size terms would be updated. If instead one fixed the APSL path size terms from the 'before' case, then the 'after' case would be a regular Path Size Logit model and hence a RUM. Making this explicit, imagine examining the impact on route choice of a new road added to the network. For pre-existing routes not overlapping with the new routes generated, the path size terms of the regular Path Size Logit models would remain the same, and hence so does the attractiveness of those routes. For the $APSL_0$ model, however, the fixed-point probability system must be re-solved, and the path size terms for *all* pre-existing routes may be adjusted to account for the updated attractiveness of the routes, and thus to alter the path size contributions.

The Issue

Standard proofs for existence and uniqueness of fixed-point solutions require the domain of the fixed-point function (in this case $\boldsymbol{g}$) to be a compact convex set. The issue with the $APSL_0$ model as defined in (2.7) and (2.8) is that the domain of the fixed-point function $\boldsymbol{g}$, $D^{>0}$, is open and bounded (not compact) as the function is not always defined for zero choice probabilities where $\frac{0}{0}$ can occur in the path size terms. Altering the definition of the path size terms so that the domain of the fixed-point function $\boldsymbol{g}$ is the closed and bounded set D, where routes can have zero choice probabilities, is however problematic as issues arise with ensuring that $\boldsymbol{\gamma}^{APS}(\boldsymbol{P})$ remains a continuous function (see Appendix A for a demonstration).

3.2 Proposed APSL Definition

While the preliminary definition of the APSL model defined in the previous subsection is the model we originally aimed to propose, as discussed, we could not prove that solutions were guaranteed to exist nor be unique according to standard proofs, and hence we provide here an altered model for use where solutions are guaranteed to exist and where conditions for uniqueness can be defined.

Definition

The APSL choice probabilities, $\boldsymbol{P}^*$, (for a choice set of size N) are a solution to the fixed-point problem $\boldsymbol{P} = \boldsymbol{G}\left(\boldsymbol{g}\left(\boldsymbol{\gamma}^{APS}(\boldsymbol{P})\right)\right)$, where G_i for route $i \in R$ is:

$$G_i\left(g_i\left(\boldsymbol{\gamma}^{APS}(\boldsymbol{P})\right)\right) = \tau + (1 - N\tau) \cdot g_i\left(\boldsymbol{\gamma}^{APS}(\boldsymbol{P})\right), \tag{2.11}$$

g_i for route $i \in R$ is:

$$g_i\left(\boldsymbol{\gamma}^{APS}(\boldsymbol{P})\right) = \frac{e^{-\theta c_i + \beta \ln\left(\gamma_i^{APS}(\boldsymbol{P})\right)}}{\sum_{j \in R} e^{-\theta c_j + \beta \ln\left(\gamma_j^{APS}(\boldsymbol{P})\right)}} = \frac{\left(\gamma_i^{APS}(\boldsymbol{P})\right)^{\beta} e^{-\theta c_i}}{\sum_{j \in R}\left(\gamma_j^{APS}(\boldsymbol{P})\right)^{\beta} e^{-\theta c_j}}, \tag{2.12}$$

and γ_i^{APS} for route $i \in R$ is:

$$\gamma_i^{APS}(\boldsymbol{P}) = \sum_{a \in A_i} \frac{t_a}{c_i} \frac{P_i}{\sum_{k \in R} P_k \delta_{a,k}} = \sum_{a \in A_i} \frac{t_a}{c_i} \frac{1}{\sum_{k \in R}\left(\frac{P_k}{P_i}\right) \delta_{a,k}}, \qquad \forall \boldsymbol{P} \in D^{(\tau)}, \tag{2.13}$$

$$D^{(\tau)} = \left\{ \boldsymbol{P} \in \mathbb{R}^N_{>0} : \tau \le P_i \le (1 - (N-1)\tau), \forall i \in R, \sum_{j=1}^{N} P_j = 1 \right\}.$$

The model parameters are $\theta > 0,\ \beta \ge 0,\ 0 < \tau \le \frac{1}{N}$. (2.12) and (2.13) are equivalent to (2.7) and (2.8) for the preliminary definition: $\gamma_i^{APS}(\boldsymbol{P})$ in (2.13) is the APSL path size term function for route $i \in R$ that is a

function involving the route choice probabilities, and $g_i\left(\boldsymbol{\gamma}^{APS}(\boldsymbol{P})\right)$ in (2.12) is the unadjusted choice probability function for route $i \in R$ which is a function involving the path size term functions and hence also the choice probabilities of routes. The choice probability relation for route $i \in R$ is given by $P_i = G_i\left(g_i\left(\boldsymbol{\gamma}^{APS}(\boldsymbol{P})\right)\right)$, which is an implicit equation involving choice probabilities, and hence the APSL route choice probabilities, $\boldsymbol{P}^*$, are a solution such that $P_i^* = G_i\left(g_i\left(\boldsymbol{\gamma}^{APS}(\boldsymbol{P}^*)\right)\right), \forall i \in R$. The key difference between this final model here and the preliminary definition is the adjustment function G_i. $G_i\left(g_i\left(\boldsymbol{\gamma}^{APS}(\boldsymbol{P})\right)\right)$ in (2.11) is the APSL choice probability adjustment function for route $i \in R$ which adjusts the choice probability function g_i for reasons given below.

Motivation

G_i is a fixed-point function, and its construction was motivated by some desired behaviours, as well as some required properties for proving existence and uniqueness:

1. G_i must map into itself.
2. G_i must be continuous for all $\boldsymbol{P}$.
3. G_i must be continuously differentiable with respect to $\boldsymbol{P}$ for all $\boldsymbol{P}$.
4. The domain of G_i must be closed and bounded.
5. The domain of G_i must not allow for zero choice probabilities.
6. G_i should be able to approximate g_i.
7. The domain of G_i should allow for choice probabilities to be approximately close to zero.

Desired Properties (DP) 1-4 are required for existence and uniqueness proofs. DP 5 is required since the path size term function $\gamma_i^{APS}(\boldsymbol{P})$ in (2.13) and thus $G_i\left(g_i\left(\boldsymbol{\gamma}^{APS}(\boldsymbol{P})\right)\right)$ in (2.11) can be undefined for zero choice probabilities where $\frac{0}{0}$ can occur. DP 6 is desired as it is not our intention for the choice probabilities acquired from this final APSL model to be different to the choice probabilities from the preliminary definition (where one would exist), and we wish them to be as close as possible. DP 7 is desired as we wish to be able to obtain choice probability solutions where there are unrealistic routes with extremely small choice probabilities.

So, the formulation of G_i in (2.11) and its domain $D^{(\tau)}$ have been constructed to satisfy DP 1-7. In Section 4 we prove that DP 1-3 are satisfied. The parameter τ is introduced, and the domain $D^{(\tau)}$ is such that $P_i \geq \tau, \forall i \in R$, and since the choice probabilities for all routes sum up to 1: $P_i \leq (1 - (N-1)\tau), \forall i \in R$. DP 4 is thus satisfied as $D^{(\tau)}$ is closed and bounded. Moreover, τ is restricted to the range $0 < \tau \leq \frac{1}{N}$ and thus DP 5 is satisfied as zero choice probabilities are not in the domain. As $\tau \to 0$, $G_i \to g_i$ satisfying DP 6 and the lower bound for P_i in $D^{(\tau)}$ tends towards zero satisfying DP 7.

It is important to note that **the τ parameter is not a model parameter that requires estimating**, it is simply a mathematical construct that ensures DP 1-7 are satisfied. While the proposed APSL model provides the capability, it is not our intention for this final APSL model to purposefully compute different choice probabilities to those obtained from the preliminary definition for any given theoretical reason. In fact, we desire the choice probabilities to be as close as possible, and hence we advise that only small values of τ are used. For the rest of the paper, i.e. for the demonstrations and estimation work, we set $\tau = 10^{-16}$, unless stated otherwise. In Section 5.3.2.2 we briefly investigate the impact of the τ parameter upon parameter estimation.

3.3 Demonstrations of Key Properties

APSL Key Property 1: *Unrealistic routes have a diminished impact upon the choice probabilities of realistic routes when links are shared.*

Referring to the PSL Key Issue in Section 2.3.1, Fig. 2.7 displays the example network 1 APSL choice probabilities as υ is increased from 0.5 to 3, $\theta = \beta = 1$. As Fig. 2.7 shows, as the travel cost of Route 1 increases, so does the relative unattractiveness of Route 1, thus decreasing the choice probability for that route and its influence upon the correction term of Route 2. The choice probability of Route 2 thus converges to match the choice probability of Route 3 as υ is increased.

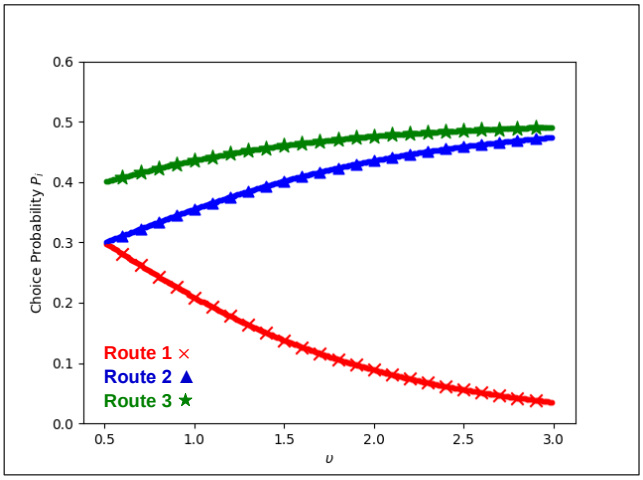

Fig. 2.7. Example network 1: APSL route choice probabilities for increasing υ ($\theta = \beta = 1$).

APSL Key Property 2: *APSL path size terms aren't highly sensitive to small differences in route travel cost.*

Referring to GPSL Key Issue 1 in Section 2.3.2, it was demonstrated how GPSL path size terms can be highly sensitive to small differences in route travel cost when λ values are large. It was also demonstrated how setting $\lambda = 0$ (i.e. equivalating GPSL and PSL) can also have adverse effects, as the routes with large travel costs negatively impact the choice probabilities of routes with low travel costs when links are shared. For example network 2 in Fig. 2.4A, a good compromise was found by setting $\lambda = 10$. APSL path size terms do not suffer from the same issues GPSL path size terms have when $\lambda = 0$ and when λ is large. Table 2.1 displays the example network 2 GPSL choice probabilities when $\lambda = 0$, $\lambda = 10$, and $\lambda = 400$, as well as the APSL choice probabilities, $\theta = \beta = 1$. As Table 2.1 shows, the APSL choice probabilities resemble the 'optimised' GPSL choice probabilities for $\lambda = 10$.

	PSL (= GPSL $\lambda = 0$)	GPSL ($\lambda = 10$)	GPSL ($\lambda = 400$)	APSL
P_1	0.329	0.294	0.222	0.297
P_2	0.332	0.301	0.374	0.301
P_3	0.332	0.399	0.398	0.397
P_4	0.007	0.006	0.006	0.006

Table 2.1. Example network 2: choice probabilities for different PSL models; $\theta = \beta = 1$.

APSL Key Property 3: *Internally consistent assessment of the feasibility of routes.*

Referring to GPSL Key Issue 2 in Section 2.3.2 where it was demonstrated how the GPSL model is not internally consistent with the assessment of the feasibility of routes, Fig. 2.8 shows the example network 3 APSL choice probabilities for increasing η, $\theta = \beta = 1$. At the point $\eta = \eta_{eq} = 0.27$, all routes have equal choice probabilities; the APSL model proposes that routes contribute to path size terms according to choice probability ratios and thus the path size contributions all cancel out at that point resulting in the PSL model, as desired.

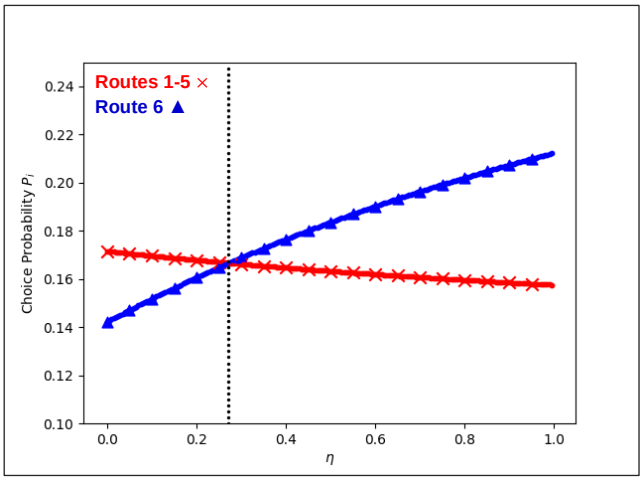

Fig. 2.8. Example network 3: APSL route choice probabilities for increasing η ($\theta = \beta = 1$).

APSL Key Property 4: *Internally consistent scaling parameters.*

Referring to GPSL Key Issue 3 in Section 2.3.2, it was demonstrated how the GPSL model has internally inconsistent scaling parameters, and how the GPSL$'_{(\lambda=\theta)}$ model partially improves the internal consistency of the GPSL model. Fig. 2.9A shows the example network 4 APSL choice probabilities for increasing θ, $\beta = 1$. As shown in (2.7) and (2.10), the APSL model, like the GPSL$'_{(\lambda=\theta)}$ model, uses the θ parameter to scale differences in travel cost within both the probability relation and the path size contribution factor, and thus for low θ Route 3 has the lowest choice probability due to being the least distinct, and for larger θ Route 3's choice probability converges to Route 2 as Route 4's path size contribution diminishes. Fig. 2.9B shows the example network 4 APSL choice probabilities for increasing θ, $\beta = 1.4$. An increase in β further decreases Route 3's choice probability for low θ, and as a consequence Route 3's path size contribution to Route 4 diminishes and Route 4 converges to the choice probability of Route 1.

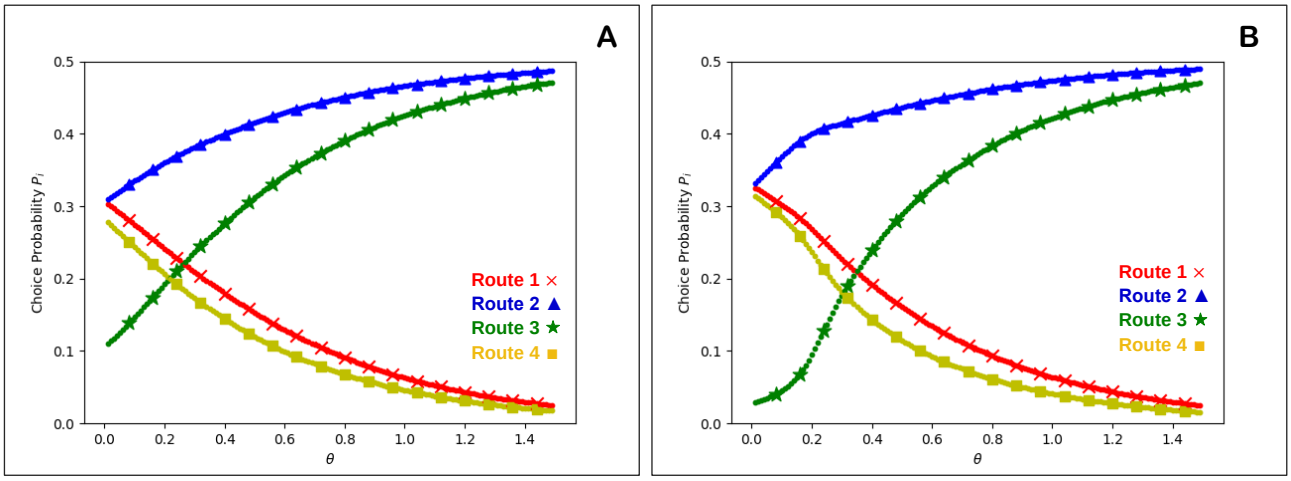

Fig. 2.9. Example network 4: APSL route choice probabilities for increasing θ. **A:** $\beta = 1$. **B:** $\beta = 1.4$.

3.4 Solution Method

There are many fixed-point algorithms available for solving the APSL fixed-point system $\boldsymbol{P} = \boldsymbol{G}\left(\boldsymbol{g}\left(\boldsymbol{\gamma}^{APS}(\boldsymbol{P})\right)\right)$. In the studies in this paper we utilise the simplest fixed-point algorithm available: the Fixed-Point Iteration Method (FPIM) (Isaacson & Keller, 1966). The FPIM is the most basic fixed-point algorithm, and other algorithms aim to accelerate the convergence of the FPIM, though require more complicated computations at each iteration. The FPIM for solving the APSL fixed-point system $\boldsymbol{P} = \boldsymbol{G}\left(\boldsymbol{g}\left(\boldsymbol{\gamma}^{APS}(\boldsymbol{P})\right)\right)$ is formulated as follows:

$$P_i^{(s+1)} = G_i\left(g_i\left(\boldsymbol{\gamma}^{APS}\left(\boldsymbol{P}^{(s)}\right)\right)\right), \qquad s = 0,1,2,\dots$$

such that

$$\lim_{s\to\infty} P_i^{(s+1)} = \lim_{k\to\infty} G_i\left(g_i\left(\boldsymbol{\gamma}^{APS}\left(\boldsymbol{P}^{(s)}\right)\right)\right) = P_i^*, \qquad \boldsymbol{P}^{(0)} \in D^{(\tau)}, \qquad \forall i \in R.$$

A standard convergence statistic we chose to observe in this study is $\ln\left(\sum_{i\in R}\left|P_i^{(s+1)} - P_i^{(s)}\right|\right)$, and the FPIM is said to have converged sufficiently to an APSL choice probability solution if:

$$\ln\left(\sum_{i\in R}\left|P_i^{(s+1)} - P_i^{(s)}\right|\right) < \ln\left(10^{-\xi}\right),$$

where $\xi > 0$ is a predetermined convergence parameter. In Sections 5.3.2.2 & 5.4.1.2 we assess the computational performance of the APSL model in calculating choice probabilities and parameter estimation.

4. Existence and Uniqueness of APSL Solutions

In this section we establish a series of theoretical results concerning the APSL model as defined in (2.11), (2.12), and (2.13), where the guaranteed existence of solutions is proven, and sufficient conditions for the uniqueness of solutions are detailed.

4.1 Properties

First, we note the relationship between the $APSL_0$ and APSL models.

Property 2. *A solution to the APSL model as defined in* (2.11), (2.12), *and* (2.13) *approaches the $APSL_0$ model as defined in* (2.7) *and* (2.8) *in the limit as* $\tau \to 0$.

Proof. This follows by inspection from the definition of G_i in (2.11) noting that $G_i \to g_i$, as $\tau \to 0$. ■

From Property 2, the APSL model will thus satisfy Property 1 in the limit as $\tau \to 0$.

We next provide two important properties of the fixed-point function $\boldsymbol{G}$. In Lemma 1 we establish the continuity property of $\boldsymbol{G}$.

Lemma 1. $G_i\left(g_i\left(\boldsymbol{\gamma}^{APS}(\boldsymbol{P})\right)\right)$ *is a continuous function for* $\boldsymbol{P} \in D^{(\tau)}, \forall i \in R$.

Proof. From the definition (2.13) above it follows that $\boldsymbol{\gamma}^{APS}$ is continuous in $\boldsymbol{P}$ for all $\boldsymbol{P} \in D^{(\tau)}$:

$$\lim_{\boldsymbol{P}\to\boldsymbol{q}} \boldsymbol{\gamma}^{APS}(\boldsymbol{P}) = \boldsymbol{\gamma}^{APS}(\boldsymbol{q}), \qquad \forall \boldsymbol{q} \in D^{(\tau)}. \tag{2.14}$$

If we let Γ be the set of possible path size terms:

$$\Gamma = \left\{\boldsymbol{\gamma}^{APS} \in \mathbb{R}^N_{>0} : 0 < \gamma_i^{APS} \leq 1, \forall i \in R\right\},$$

then from definition (2.12) above it follows that g_i is continuous in $\boldsymbol{\gamma}^{APS}$ for all $\boldsymbol{\gamma}^{APS} \in \Gamma$:

$$\lim_{\boldsymbol{\gamma}^{APS}\to\boldsymbol{\gamma}_0} g_i(\boldsymbol{\gamma}^{APS}) = g_i(\boldsymbol{\gamma}_0), \qquad \forall \boldsymbol{\gamma}_0 \in \Gamma, \qquad \forall i \in R. \tag{2.15}$$

And, from definition (2.11) above it follows that G_i is continuous in x for all $x \in (0,1)$:

$$\lim_{x\to x_0} G_i(x) = G_i(x_0), \qquad \forall x_0 \in (0,1). \tag{2.16}$$

It then follows from (2.14), (2.15), and (2.16) that $G_i\left(g_i\left(\boldsymbol{\gamma}^{APS}(\boldsymbol{P})\right)\right)$, as a composition of continuous functions, is itself continuous in $\boldsymbol{P}$ for all $\boldsymbol{P} \in D^{(\tau)}$:

$$\lim_{\boldsymbol{P}\to\boldsymbol{q}} G_i\left(g_i\left(\boldsymbol{\gamma}^{APS}(\boldsymbol{P})\right)\right) = G_i\left(g_i\left(\boldsymbol{\gamma}^{APS}(\boldsymbol{q})\right)\right), \qquad \forall \boldsymbol{q} \in D^{(\tau)}, \qquad \forall i \in R.$$

■

We now in Lemma 2 show that the domain of $\boldsymbol{G}$ maps to itself.

Lemma 2. $\boldsymbol{G}\left(\boldsymbol{g}\left(\boldsymbol{\gamma}^{APS}(\boldsymbol{P})\right)\right)$ *maps* $D^{(\tau)}$ *into* $D^{(\tau)}$.

Proof. From definition (2.13) above it follows that the function $\boldsymbol{\gamma}^{APS}$ maps $D^{(\tau)} \rightarrow \Gamma$, from definition (2.12) it follows that the function $\boldsymbol{g}$ maps $\Gamma \rightarrow D^{>0}$, and, from definition (2.11) it follows that the function $\boldsymbol{G}$ maps $D^{>0} \rightarrow D^{(\tau)}$. It thus follows that the composition of the functions $\boldsymbol{\gamma}^{APS}$, $\boldsymbol{g}$, and $\boldsymbol{G}$, $\boldsymbol{G}\left(\boldsymbol{g}\left(\boldsymbol{\gamma}^{APS}(\boldsymbol{P})\right)\right)$, maps $D^{(\tau)} \rightarrow D^{(\tau)}$.

■

4.2 Existence of Solutions

Having established some properties regarding the APSL fixed-point function $\boldsymbol{G}$, we consider the existence of APSL solutions.

Proposition 1. *At least one APSL fixed-point solution,* $\boldsymbol{P}^*$*, to the system* $\boldsymbol{P} = \boldsymbol{G}\left(\boldsymbol{g}\left(\boldsymbol{\gamma}^{APS}(\boldsymbol{P})\right)\right)$ *is guaranteed to exist in* $D^{(\tau)}$.

Proof. $\boldsymbol{G}\left(\boldsymbol{g}\left(\boldsymbol{\gamma}^{APS}(\boldsymbol{P})\right)\right)$ is a continuous function by Lemma 1, which maps $D^{(\tau)}$ into $D^{(\tau)}$ by Lemma 2, and thus since $D^{(\tau)}$ is a compact convex set, and by Brouwer's Fixed-Point Theorem at least one fixed-point solution, $\boldsymbol{P}^*$, is guaranteed to exist for the system $\boldsymbol{P} = \boldsymbol{G}\left(\boldsymbol{g}\left(\boldsymbol{\gamma}^{APS}(\boldsymbol{P})\right)\right)$ in $D^{(\tau)}$.

■

4.3 Uniqueness of Solutions

Having proven that APSL solutions are guaranteed to exist, the next question is whether sufficient conditions exist which ensure APSL solutions are unique. In order to do this, we must first establish two key properties of $J_{\boldsymbol{G}}(\boldsymbol{P};\beta)$ which is the Jacobian matrix of first partial derivatives of $\boldsymbol{G}$ evaluated at $\boldsymbol{P}$ and β.

Lemma 3. *The maximum Jacobian matrix norm of* $\boldsymbol{G}\left(\boldsymbol{g}\left(\boldsymbol{\gamma}^{APS}(\boldsymbol{P});\beta\right)\right)$ *for all* $\boldsymbol{P} \in D^{(\tau)}$ *at* $\beta = 0$ *is equal to zero:* $\max\left(\|J_{\boldsymbol{G}}(\boldsymbol{P};0)\| : \forall \boldsymbol{P} \in D^{(\tau)}\right) = 0$.

Proof. From definitions (2.11) and (2.12) above it follows that:

$$G_i\left(g_i\left(\boldsymbol{\gamma}^{APS}(\boldsymbol{P});0\right)\right) = \tau + (1 - N\tau) \cdot \left(\frac{e^{-\theta c_i}}{\sum_{j \in R} e^{-\theta c_j}}\right), \qquad \forall i \in R. \tag{2.17}$$

It then follows from (2.17) that:

$$\frac{\partial G_i\left(g_i\left(\boldsymbol{\gamma}^{APS}(\boldsymbol{P});0\right)\right)}{\partial P_l} = 0, \qquad \forall \boldsymbol{P} \in D^{(\tau)}, \qquad \forall i,l \in R. \tag{2.18}$$

It thus follows from (2.18) that $\|J_{\boldsymbol{G}}(\boldsymbol{P};0)\| = 0, \forall \boldsymbol{P} \in D^{(\tau)}$, and hence $\max\left(\|J_{\boldsymbol{G}}(\boldsymbol{P};0)\| : \forall \boldsymbol{P} \in D^{(\tau)}\right) = 0$.

■

Lemma 4. *The maximum Jacobian matrix norm of* $\boldsymbol{G}\left(\boldsymbol{g}\left(\boldsymbol{\gamma}^{APS}(\boldsymbol{P});\beta\right)\right)$, $\max\left(\|J_{\boldsymbol{G}}(\boldsymbol{P};\beta)\| : \forall \boldsymbol{P} \in D^{(\tau)}\right)$, is a continuous function for $\beta \in [0,\infty)$.

Proof. It follows from the definitions (2.11), (2.12), and (2.13) above that:

$$\frac{\partial G_i\left(g_i\left(\boldsymbol{\gamma}^{APS}(\boldsymbol{P})\right)\right)}{\partial P_l}$$

$$= (1 - N\tau) \cdot \left(\frac{\left(\gamma_i^{APS}(\boldsymbol{P})\right)^{\beta} e^{-\theta c_i}}{\sum_{j \in R}\left(\gamma_j^{APS}(\boldsymbol{P})\right)^{\beta} e^{-\theta c_j}}\right) \cdot \left(\frac{\beta \frac{\partial \gamma_i^{APS}(\boldsymbol{P})}{\partial P_l}}{\left(\gamma_i^{APS}(\boldsymbol{P})\right)} - \frac{\left(\sum_{j \in R} \beta \frac{\partial \gamma_j^{APS}(\boldsymbol{P})}{\partial P_l}\left(\gamma_j^{APS}(\boldsymbol{P})\right)^{\beta-1} e^{-\theta c_j}\right)}{\left(\sum_{j \in R}\left(\gamma_j^{APS}(\boldsymbol{P})\right)^{\beta} e^{-\theta c_j}\right)}\right), \tag{2.19}$$

$$\forall i,l \in R,$$

$$\frac{\partial \gamma_i^{APS}(\boldsymbol{P})}{\partial P_i} = \sum\nolimits_{a\in A_i} \frac{t_a}{c_i}\left(\frac{\sum_{k\in R;k\neq i} P_k\delta_{a,k}}{\left(\sum_{k\in R} P_k\delta_{a,k}\right)^2}\right), \qquad \forall i \in R, \tag{2.20}$$

and,

$$\frac{\partial \gamma_i^{APS}(\boldsymbol{P})}{\partial P_l} = -\sum\nolimits_{a\in A_i} \frac{t_a}{c_i}\frac{P_i\delta_{a,l}}{\left(\sum_{k\in R} P_k\delta_{a,k}\right)^2}, \qquad \forall i,l \in R, l \neq i. \tag{2.21}$$

From the definitions (2.20) and (2.21) above it follows that $\frac{\partial \boldsymbol{\gamma}^{APS}(\boldsymbol{P})}{\partial \boldsymbol{P}}$ is continuous in $\boldsymbol{P}$ for all $\boldsymbol{P} \in D^{(\tau)}$:

$$\lim_{\boldsymbol{P}\to\boldsymbol{q}} \frac{\partial \boldsymbol{\gamma}^{APS}(\boldsymbol{P})}{\partial \boldsymbol{P}} = \frac{\partial \boldsymbol{\gamma}^{APS}(\boldsymbol{q})}{\partial \boldsymbol{P}}, \qquad \forall \boldsymbol{q} \in D^{(\tau)}. \tag{2.22}$$

It then follows from (2.14) and (2.22) that $\frac{\partial G_i\left(g_i\left(\boldsymbol{\gamma}^{APS}(\boldsymbol{P})\right)\right)}{\partial P_l}$ as defined in (2.19), being a composition of continuous functions, is itself continuous in $\boldsymbol{P}$ for all $\boldsymbol{P} \in D^{(\tau)}$:

$$\lim_{\boldsymbol{P}\to\boldsymbol{q}} \frac{\partial G_i\left(g_i\left(\boldsymbol{\gamma}^{APS}(\boldsymbol{P})\right)\right)}{\partial P_l} = \frac{\partial G_i\left(g_i\left(\boldsymbol{\gamma}^{APS}(\boldsymbol{q})\right)\right)}{\partial P_l}, \qquad \forall \boldsymbol{q} \in D^{(\tau)}, \qquad \forall i,l \in R.$$

Since $\frac{\partial G_i\left(g_i\left(\boldsymbol{\gamma}^{APS}(\boldsymbol{P})\right)\right)}{\partial P_l}$ is a continuous function for $\boldsymbol{P} \in D^{(\tau)}$, $\forall i,l \in R$, $\frac{\partial G_i\left(g_i\left(\boldsymbol{\gamma}^{APS}(\boldsymbol{P});\beta\right)\right)}{\partial P_l}$ is also a continuous function for $\beta \in [0,\infty)$, $\forall i,l \in R$:

$$\lim_{\beta\to\beta_0}\left(\frac{\partial G_i\left(g_i(\boldsymbol{\gamma}^{APS}(\boldsymbol{P});\beta)\right)}{\partial P_l}\right) = \frac{\partial G_i\left(g_i(\boldsymbol{\gamma}^{APS}(\boldsymbol{P});\beta_0)\right)}{\partial P_l}, \qquad \forall \beta_0 \in [0,\infty), \qquad \forall i,l \in R.$$

Hence, since $\max\left(\|J_{\boldsymbol{G}}(\boldsymbol{P};\beta)\|: \forall \boldsymbol{P} \in D^{(\tau)}\right)$ is a composition of continuous functions then it itself is a continuous function for $\beta \in [0,\infty)$:

$$\lim_{\beta\to\beta_0}\left(\max\left(\|J_{\boldsymbol{G}}(\boldsymbol{P};\beta)\|: \forall \boldsymbol{P} \in D^{(\tau)}\right)\right) = \max\left(\|J_{\boldsymbol{G}}(\boldsymbol{P};\beta_0)\|: \forall \boldsymbol{P} \in D^{(\tau)}\right), \qquad \forall \beta_0 \in [0,\infty).$$

■

These two key properties of $J_{\boldsymbol{G}}(\boldsymbol{P};\beta)$ allow us to establish conditions for the uniqueness of solutions.

Proposition 2. *There always exist values of $b > 0$ such that when the β parameter is within the range $0 \leq \beta \leq b$, there are unique APSL fixed-point solutions, $\boldsymbol{P}^*$, to the system $\boldsymbol{P} = \boldsymbol{G}\left(\boldsymbol{g}(\boldsymbol{\gamma}^{APS}(\boldsymbol{P});\beta)\right)$ in $D^{(\tau)}$.*

Proof. $\boldsymbol{G}$ is a *contraction mapping* on the domain $D^{(\tau)}$ if:

a) $\boldsymbol{G}$ maps $D^{(\tau)}$ into itself, so $\boldsymbol{G}\left(\boldsymbol{g}(\boldsymbol{\gamma}^{APS}(\boldsymbol{q});\beta)\right) \in D^{(\tau)}, \forall \boldsymbol{q} \in D^{(\tau)}$, and

b) There exists a constant $0 \leq \sigma < 1$ such that:

$$\|J_{\boldsymbol{G}}(\boldsymbol{P};\beta)\| \leq \sigma, \qquad \forall \boldsymbol{P} \in D^{(\tau)},$$

where $J_{\boldsymbol{G}}(\boldsymbol{P};\beta)$ is the Jacobian matrix of first partial derivatives of $\boldsymbol{G}$ evaluated at $\boldsymbol{P}$.

If the link cost vector $\boldsymbol{t}$ is fixed (and thus the route cost vector $\boldsymbol{c}$ is fixed), and θ is fixed, then for any given β, if $\boldsymbol{G}$ is a contraction mapping, then since $D^{(\tau)}$ is a compact convex set, and by Lemma 1, Lemma 2, and the Contraction Mapping Theorem, $\boldsymbol{G}$ emits a unique fixed-point solution $\boldsymbol{P}^* \in D^{(\tau)}$.

It remains to establish the conditions under which $\boldsymbol{G}$ is a contraction mapping. Since by Lemma 3 the maximum Jacobian matrix norm of $\boldsymbol{G}$ for all $\boldsymbol{P} \in D^{(\tau)}$ at $\beta = 0$ is equal to zero $\left(\max\left(\|J_{\boldsymbol{G}}(\boldsymbol{P};0)\|: \forall \boldsymbol{P} \in D^{(\tau)}\right) = 0\right)$, and by Lemma 4 $\max\left(\|J_{\boldsymbol{G}}(\boldsymbol{P};\beta)\|: \forall \boldsymbol{P} \in D^{(\tau)}\right)$ is a continuous function for $\beta \in [0,\infty)$, then there must always exist values $b > 0$ such that when β is within the range $0 \leq \beta \leq b$ $\boldsymbol{G}$ is a contraction mapping and the sufficient conditions for unique APSL solutions are always met.

■

There are cases where the APSL model has unique solutions for all $\beta > 0$ (i.e. for all values of b), for example where all routes are non-overlapping and the path size terms are consequently all 1 so that G_i

collapses to (2.17), and hence in these cases a maximum value for b does not exist. However, in most cases APSL solutions are not unique for all values of β and in these cases a maximum value for b exists (denoted b_{max}) such that Proposition 2 holds. However, Proposition 2 is only a sufficient condition for unique APSL solutions and solutions are not necessarily non-unique for $\beta > b_{max}$. In Section 4.4 below we explore how $0 \leq \beta \leq b_{max}$ relates to the true maximum range $0 \leq \beta \leq \beta_{max}$ in which APSL solutions are unique.

4.4 Investigating the Conditions for Uniqueness

b_{max} is the maximum value such that the sufficient conditions for unique APSL solutions in Proposition 2 are satisfied for all β in the range $0 \leq \beta \leq b_{max}$. β_{max} is the true maximum value such that APSL solutions are unique for all β in the range $0 \leq \beta \leq \beta_{max}$, where $\beta_{max} \geq b_{max}$. The purpose of this section is to explore how close b_{max} is to β_{max}, and demonstrate that multiple solutions can exist when β is greater than β_{max}. We specify and demonstrate how to calculate b_{max}, and suggest and demonstrate a method for estimating β_{max}.

Calculating b_{max} can be formulated as either of the following optimisation problems:

b_{max} Optimisation Problem 1

$$b_{max} = \max\{\beta\}$$

subject to

$$\|J_{\boldsymbol{G}}(\boldsymbol{P};\beta)\| < 1, \qquad \forall \boldsymbol{P} \in D^{(\tau)}.$$

b_{max} Optimisation Problem 2

$$b_{max} = \max\{\beta\}$$

subject to

$$\|J_{\boldsymbol{G}}(\overline{\boldsymbol{P}};\beta)\| < 1$$

where

$$\overline{\boldsymbol{P}} = \arg\max_{\boldsymbol{P}}\{\|J_{\boldsymbol{G}}(\boldsymbol{P};\beta)\| : \forall \boldsymbol{P} \in D^{(\tau)}\}.$$

Example

Consider example network 5 in Fig. 2.10 where there are 2 routes: Route 1 has travel cost $u + w$ and Route 2 has travel cost $v + w$. Fig. 2.11A-D display the maximum Jacobian matrix norm of $\boldsymbol{G}$ for increasing β for four different network parameter settings.

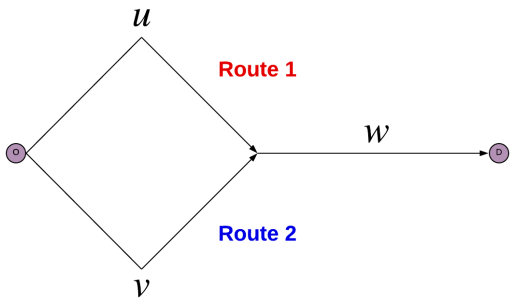

Fig. 2.10. Example network 5.

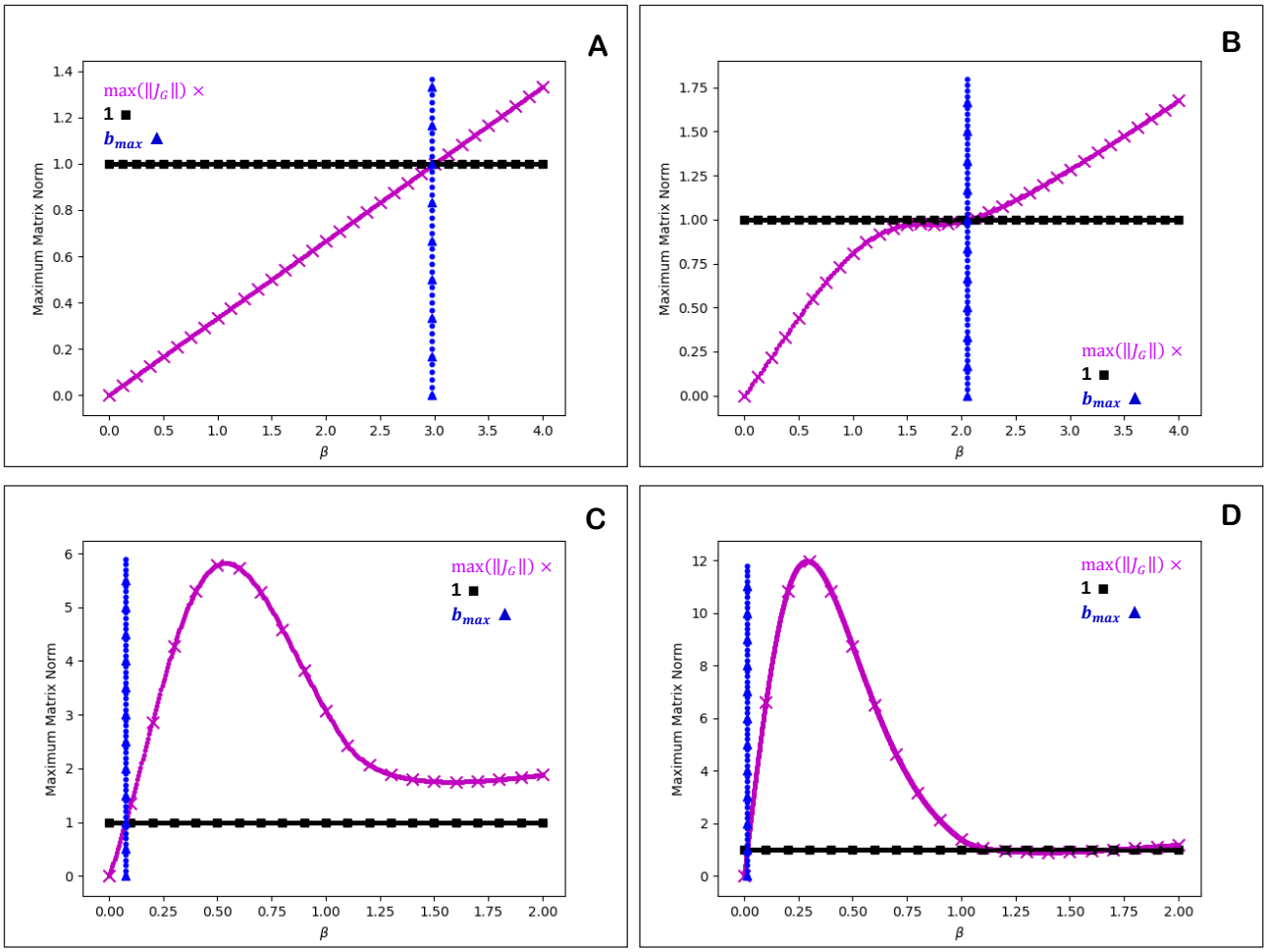

Fig. 2.11. Example network 5: Maximum Jacobian matrix norm of APSL fixed-point function $\boldsymbol{G}$ for increasing β.
A: $u = v = w = \theta = 1$, ($b_{max} \cong 2.95$). **B:** $u = 0.5$, $v = w = \theta = 1$, ($b_{max} \cong 2.05$).
C: $u = 0.1$, $v = 1$, $w = 4$, $\theta = 1$, ($b_{max} \cong 0.075$). **D:** $u = 0.1$, $v = w = 20$, $\theta = 10^{-5}$, ($b_{max} \cong 0.0125$).

β_{max} can be estimated by plotting trajectories of APSL solutions for varying β, and identifying where a unique trajectory of solutions ends and multiple trajectories begin. We briefly detail here a simple method for obtaining trajectories of APSL solutions:

Step 1. Identify a suitably large value for β.

Step 2. Solve the APSL fixed-point system for this large β with a randomly generated initial condition (see Section 3.4).

Step 3. Decrement β and obtain the next APSL solution with initial condition set as the APSL solution for the previous β.

Step 4. Continue until $\beta = 0$ or $\beta = b_{max}$ if known.

By plotting the choice probabilities at each decremented β, and repeating this method several times, one can determine where non-unique solution trajectories end and hence estimate β_{max}. If after several repetitions (with different randomly generated initial conditions) only a single trajectory of solutions is shown, then the initial large β value is increased. We illustrate the approach graphically, but there is no need to draw graphs for general networks. One can instead observe the choice probability values, where a finer grained decrement of β will provide a more accurate estimation of β_{max}.

To demonstrate, consider again example network 5 in Fig. 2.10; Fig. 2.12A-D display trajectories of APSL solutions as the β parameter is varied for the same network parameter settings as Fig. 2.11A-D, respectively. β was decremented by 0.01, and the initial large β value was $\beta = 10$, (though trajectories are only plotted for part of this range for illustrative purposes). The solution trajectory plotting was repeated until multiple clear trajectories were shown. As each of Fig. 2.12A-D show, there is a unique trajectory of choice

probability solutions up until $\beta = \beta_{max}$ where there then becomes multiple trajectories. As Fig. 2.12A shows, the estimated β_{max} value in this case is equal to b_{max} in Fig. 2.11A, however in the cases of Fig. 2.12B-D, the estimated β_{max} values are all greater than the b_{max} values in Fig. 2.11B-D.

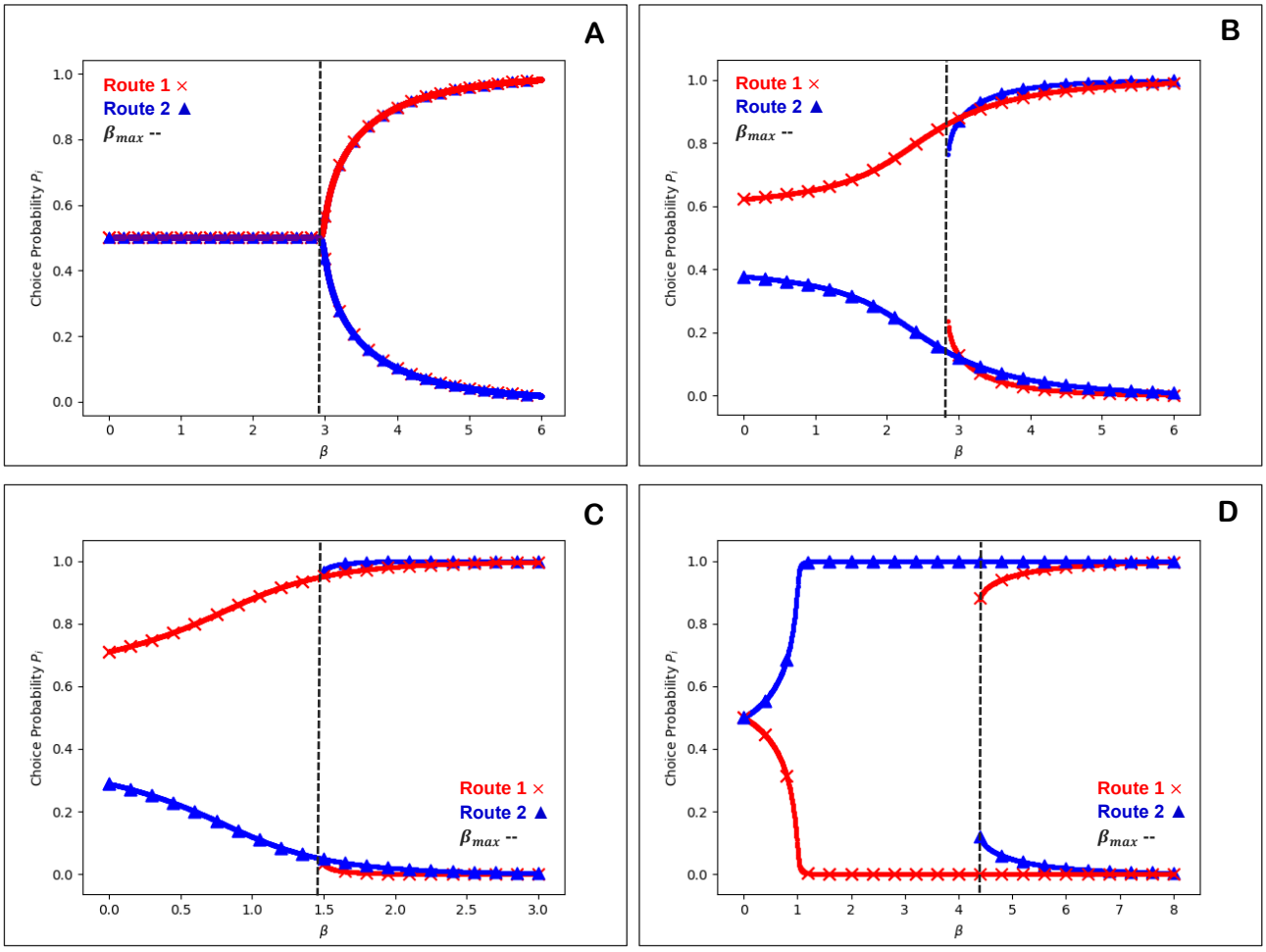

Fig. 2.12. Example network 5: Trajectories of APSL choice probability solutions as β is varied.
A: $u = v = w = \theta = 1$, ($\beta_{max} \cong 2.95$). **B:** $u = 0.5$, $v = w = \theta = 1$, ($\beta_{max} \cong 2.8$).
C: $u = 0.1$, $v = 1$, $w = 4$, $\theta = 1$, ($\beta_{max} \cong 1.5$). **D:** $u = 0.1$, $v = w = 20$, $\theta = 10^{-5}$, ($\beta_{max} \cong 4.3$).

As we have shown, b_{max} can be a conservative estimate of β_{max}. On the other hand, we have shown that for large enough values of β multiple solutions can exist, and therefore is an issue that should be considered in practice in real-life applications. The experiments above provide a computationally feasible method for revealing multiple solutions, and thus β_{max}, that can be applied in realistic sized networks (see Sections 5.3.2.3 / 5.4.1.3).

5. Estimating the APSL Model

In this section, we provide a Maximum Likelihood Estimation (MLE) procedure for estimating the APSL model with tracked route observations. This procedure for estimating the APSL model is then investigated in a simulation study, and the possibility of retrieving APSL parameter estimates is assessed. The APSL model is then estimated on a large-scale network using real route choice observation data tracked with GPS units, and results are compared with other Path Size Logit models.

5.1 Notation and Definitions for Estimation with Multiple OD Movements

5.1.1 Notation

To consider the estimation of the APSL model and other Path Size Logit models, we extend definitions here for estimation on a network with multiple OD movements, but where the travel costs remain fixed. The road

network consists of link set A and $m = 1, \dots, M$ OD movements. R_m is the choice set of all simple routes (no cycles) for OD movement m of size $N_m = |R_m|$, and $A_{m,i} \subseteq A$ is the set of links belonging to route $i \in R_m$, and $\delta_{a,m,i} = \begin{cases} 1 & if\ a \in A_{m,i} \\ 0 & otherwise \end{cases}$. Suppose that the generalised travel cost t_a of each link $a \in A$ is a weighted sum (by parameter vector $\boldsymbol{\alpha}$) of variables $\boldsymbol{w}_a$, i.e. $t_a(\boldsymbol{w}_a; \boldsymbol{\alpha})$, and that the generalised travel cost for route $i \in R_m$, $c_{m,i}$, can be attained through summing up the total cost of its links so that $c_{m,i}\big(\boldsymbol{t}(\boldsymbol{w}; \boldsymbol{\alpha})\big) = \sum_{a \in A_{m,i}} t_a(\boldsymbol{w}_a; \boldsymbol{\alpha})$, where $\boldsymbol{t}$ is the vector of all link travel costs and $\boldsymbol{w}$ is the vector of all link variables. Let the route choice probability for route $i \in R_m$ be $P_{m,i}$, where $\boldsymbol{P}_m = \big(P_{m,1}, P_{m,2}, \dots, P_{m,N_m}\big)$ is the vector of route choice probabilities for OD movement m, and D_m is the domain of possible route choice probability vectors for OD movement m, $m = 1, \dots, M$.

5.1.2 Model Definitions

5.1.2.1 Multinomial Logit

MNL choice probability relation for route $i \in R_m$:

$$P_{m,i}(\boldsymbol{t}) = \frac{1}{\sum_{j \in R_m} e^{-\theta\left(c_{m,j}(\boldsymbol{t}) - c_{m,i}(\boldsymbol{t})\right)}}. \tag{2.23}$$

5.1.2.2 Regular Path Size Logit Models

Regular Path Size Logit model choice probability relation for route $i \in R_m$:

$$P_{m,i}(\boldsymbol{t}) = \frac{1}{\sum_{j \in R_m} \left(\frac{\gamma_{m,j}(\boldsymbol{t})}{\gamma_{m,i}(\boldsymbol{t})}\right)^{\beta} e^{-\theta\left(c_{m,j}(\boldsymbol{t}) - c_{m,i}(\boldsymbol{t})\right)}}. \tag{2.24}$$

PSL path size term for route $i \in R_m$:

$$\gamma_{m,i}^{PS}(\boldsymbol{t}) = \sum_{a \in A_{m,i}} \frac{t_a}{c_{m,i}(\boldsymbol{t})} \frac{1}{\sum_{k \in R_m} \delta_{a,m,k}}. \tag{2.25}$$

GPSL path size term for route $i \in R_m$:

$$\gamma_{m,i}^{GPS}(\boldsymbol{t}) = \sum_{a \in A_{m,i}} \frac{t_a}{c_{m,i}(\boldsymbol{t})} \frac{1}{\sum_{k \in R_m} \left(\frac{c_{m,i}(\boldsymbol{t})}{c_{m,k}(\boldsymbol{t})}\right)^{\lambda} \delta_{a,m,k}}. \tag{2.26}$$

GPSL$'_{(\lambda=\theta)}$ path size term for route $i \in R_m$:

$$\gamma_{m,i}^{GPS'}(\boldsymbol{t}) = \sum_{a \in A_{m,i}} \frac{t_a}{c_{m,i}(\boldsymbol{t})} \frac{1}{\sum_{k \in R_m} e^{-\theta\left(c_{m,k}(\boldsymbol{t}) - c_{m,i}(\boldsymbol{t})\right)} \delta_{a,m,k}}. \tag{2.27}$$

5.1.2.3 Adaptive Path Size Logit

The APSL choice probabilities for OD movement m, $\boldsymbol{P}_m^*$, are a solution to the fixed-point problem $\boldsymbol{P}_m = \boldsymbol{G}_m\left(\boldsymbol{g}_m\big(\boldsymbol{c}_m(\boldsymbol{t}), \boldsymbol{\gamma}_m^{APS}(\boldsymbol{t}, \boldsymbol{P}_m)\big)\right)$, where $G_{m,i}$ for route $i \in R_m$ is:

$$G_{m,i}\left(g_{m,i}\big(\boldsymbol{c}_m(\boldsymbol{t}), \boldsymbol{\gamma}_m^{APS}(\boldsymbol{t}, \boldsymbol{P}_m)\big)\right) = \tau_m + (1 - N_m\tau_m) \cdot g_{m,i}\big(\boldsymbol{c}_m(\boldsymbol{t}), \boldsymbol{\gamma}_m^{APS}(\boldsymbol{t}, \boldsymbol{P}_m)\big), \tag{2.28}$$

$g_{m,i}$ for route $i \in R_m$ is:

$$g_{m,i}\big(\boldsymbol{c}_m(\boldsymbol{t}), \boldsymbol{\gamma}_m^{APS}(\boldsymbol{t}, \boldsymbol{P}_m)\big) = \frac{\left(\gamma_{m,i}^{APS}(\boldsymbol{t}, \boldsymbol{P}_m)\right)^{\beta} e^{-\theta c_{m,i}(\boldsymbol{t})}}{\sum_{j \in R_m} \left(\gamma_{m,j}^{APS}(\boldsymbol{t}, \boldsymbol{P}_m)\right)^{\beta} e^{-\theta c_{m,j}(\boldsymbol{t})}}, \tag{2.29}$$

and $\gamma_{m,i}^{APS}$ for route $i \in R_m$ is:

$$\gamma_{m,i}^{APS}(\boldsymbol{t}, \boldsymbol{P}_m) = \sum_{a \in A_{m,i}} \frac{t_a}{c_{m,i}(\boldsymbol{t})} \frac{P_{m,i}}{\sum_{k \in R_m} P_{m,k} \delta_{a,m,k}}, \qquad \boldsymbol{P}_m \in D_m^{(\tau_m)}, \tag{2.30}$$

$$D_m^{(\tau_m)} = \left\{ \boldsymbol{P}_m \in \mathbb{R}_{>0}^{N_m} : \tau_m \leq P_{m,i} \leq (1 - (N_m - 1)\tau_m), \forall i \in R_m, \sum_{j=1}^{N_m} P_{m,j} = 1 \right\},$$

The model parameters are $\theta > 0$, $\beta \geq 0$, and $0 < \tau_m \leq \frac{1}{N_m}$, $m = 1, \dots, M$. Each OD movement has its own range restrictions for τ_m based on the number of routes in the choice set, but the τ_m parameters are not model parameters that require estimating, they are simply a mathematical construct that ensure solutions to the APSL model exist and can be unique. As discussed in Section 3.2, only small values of τ_m should be used, and we set $\tau_m = 10^{-16}$, $m = 1, \dots, M$. APSL choice probability solutions are computed using the FPIM with initial conditions set as the MNL route choice probabilities, and convergence statistic set at $\xi = 10$ (see Section 3.4), unless specified otherwise.

5.2 Adaptive Path Size Logit Likelihood Formulation & Estimation Procedure

5.2.1 Likelihood Formulation

Suppose that we have available a set of Z observed routes, e.g. collected through GPS units or smart phones, and consider a situation where it is not needed to distinguish individuals in their preferences (the approach is, of course, readily generalised to permit multiple user classes differing in their parameters). Let m_z denote the OD movement of route observation z, and for each trip observation $z = 1,2, \dots, Z$, let R_{m_z} be the choice set of all simple routes between the origin and destination of the trip. Suppose that the observation data is contained in a vector $\boldsymbol{x}$ of size Z where:

$$x_z = i \quad \text{if alternative } i \in R_{m_z} \text{ is chosen,} \qquad z = 1, \dots, Z.$$

The Likelihood for a sample of size Z, can be formulated as:

$$L(\boldsymbol{\alpha}, \theta, \beta | \boldsymbol{x}) = \prod_{z=1}^{Z} P_{m_z, x_z}^{*}(\boldsymbol{t}(\boldsymbol{w}; \boldsymbol{\alpha}), \theta, \beta), \tag{2.31}$$

where $P_{m_z,x_z}^{*}(\boldsymbol{t}(\boldsymbol{w}; \boldsymbol{\alpha}), \theta, \beta)$ is the APSL choice probability solution for route $x_z \in R_{m_z}$ to the fixed-point problem $\boldsymbol{P}_{m_z} = \boldsymbol{G}_{m_z}\left(\boldsymbol{g}_{m_z}\left(\boldsymbol{c}_{m_z}(\boldsymbol{t}), \boldsymbol{\gamma}_{m_z}^{APS}(\boldsymbol{t}, \boldsymbol{P}_{m_z})\right)\right)$ for OD movement m_z, where $G_{m,i}$ and $g_{m,i}$ are as in (2.28) and (2.29) for route $i \in R_m$, respectively. The Log-Likelihood function is thus:

$$LL(\boldsymbol{\alpha}, \theta, \beta | \boldsymbol{x}) = \ln\left(\prod_{z=1}^{Z} P_{m_z,x_z}^{*}(\boldsymbol{t}(\boldsymbol{w}; \boldsymbol{\alpha}), \theta, \beta)\right) = \sum_{z=1}^{Z} \ln\left(P_{m_z,x_z}^{*}(\boldsymbol{t}(\boldsymbol{w}; \boldsymbol{\alpha}), \theta, \beta)\right). \tag{2.32}$$

5.2.2 Estimation Procedure

Standard MLE procedures can be used to estimate the parameters of the APSL model for a given network. Using a standard iterative estimation procedure, APSL model parameters can be found that maximise the Log-Likelihood function as formulated in (2.32) above for a given set of data. Algorithm 2.1 outlines pseudo-code for the estimation procedure.

Step 1: Initialisation. For each route observation $z = 1, \dots, Z$, generate the corresponding universal choice set and store the link attributes and link-route information. Define an initial set of parameter values $\left(\tilde{\boldsymbol{\alpha}}^{(1)}, \tilde{\theta}^{(1)}, \tilde{\beta}^{(1)}\right)$ for MLE, and set $n = 1$.

Step 2: Recalculate choice probabilities and LL. Given the set of parameter values $\left(\tilde{\boldsymbol{\alpha}}^{(n)}, \tilde{\theta}^{(n)}, \tilde{\beta}^{(n)}\right)$ for iteration n, calculate the link costs $\boldsymbol{t}\left(\boldsymbol{w}; \tilde{\boldsymbol{\alpha}}^{(n)}\right)$ and solve each of the fixed-point problems

$$\boldsymbol{P}_{m_z} = \boldsymbol{G}_{m_z}\left(\boldsymbol{g}_{m_z}\left(\boldsymbol{c}_{m_z}\left(\boldsymbol{t}\left(\boldsymbol{w};\tilde{\boldsymbol{\alpha}}^{(n)}\right)\right),\boldsymbol{\gamma}_{m_z}^{APS}\left(\boldsymbol{t}\left(\boldsymbol{w};\tilde{\boldsymbol{\alpha}}^{(n)}\right),\boldsymbol{P}_{m_z}\right);\tilde{\theta}^{(n)},\tilde{\beta}^{(n)}\right)\right)$$

for $z = 1, \dots, Z$. Given the fixed-point choice probability solutions $P^*_{m_z,x_z}$ for each of the route observations $z = 1, \dots, Z$, calculate the Log-Likelihood $LL^{(n)}\left(\tilde{\boldsymbol{\alpha}}^{(n)}, \tilde{\theta}^{(n)}, \tilde{\beta}^{(n)} \middle| \boldsymbol{x}\right)$ for iteration n.

Step 3: Compute new set of parameters. Based on $LL^{(s)}$ and the associated parameters $\left(\tilde{\boldsymbol{\alpha}}^{(s)}, \tilde{\theta}^{(s)}, \tilde{\beta}^{(s)}\right)$ for all $s \leq n$, compute a new set of parameters $\left(\tilde{\boldsymbol{\alpha}}^{(n+1)}, \tilde{\theta}^{(n+1)}, \tilde{\beta}^{(n+1)}\right)$ to test in the following iteration.

Step 4: Stopping criteria. If $\left|LL^{(n)} - LL^{(n-1)}\right| < \zeta$, stop. Otherwise, set $n = n + 1$ and return to Step 2.

Algorithm 2.1: Pseudo-code for estimating the APSL model.

In general, Step 3 could apply procedures from standard numerical optimisation methods to identify the parameters to evaluate in the next iteration. Utilising gradient approaches such as Newton-Raphson or BHHH, however, is complicated by the difficulties in differentiating the APSL Log-Likelihood function, which involves differentiating the fixed-point choice probabilities with respect to the parameters, which is not straightforward. Other optimisation algorithms such as BFGS and alternative quasi-Newton algorithms use methods to approximate the differentials, and while are more computationally burdensome and typically less accurate, are readily useable. For the experiments in this paper, we utilise the L-BFGS-B bound-constraint, quasi-Newton minimisation algorithm (Byrd et al, 1995) for Steps 2-4 of Algorithm 2.1 (where we minimise $-LL$). The parameter bounds and initial conditions are given in each study.

Note that Algorithm 2.1 computes one set of parameter estimates, estimated from one set of observations. It is possible to calculate standard errors for the estimated APSL parameters analytically, but this is again complicated by the requirement to differentiate the APSL Log-Likelihood function with respect to the parameters. Instead, the robustness of the parameters estimated (variation of the estimates) can be investigated numerically by applying Algorithm 2.1 multiple times through resampling-approaches such as Bootstrap or Jackknife.

5.3 Simulation Study

In this section we investigate the formulated likelihood function for the APSL route choice model in a simulation study, evaluating the likelihood-surface and assessing the possibility of estimating reasonable parameters that reproduces observed behaviour.

5.3.1 Experiment Setup

In general, the approach is to sample observations according to an assumed 'true' model, and then use these in combination with the log-likelihood function to evaluate the ability to reproduce the assumed 'true' parameters. The simulation study consists of three steps:

(i) Postulate a true APSL choice model including specification and parameter values.

(ii) Sample a set of observed route choices according to the true model using the specified link travel costs.

(iii) Apply MLE approach to obtain parameter estimates based on the observed route choices.

The estimation procedure in Algorithm 2.1 is altered for simulation studies, by modifying **Step 1: Initialisation** as outlined below to reflect (i) and (ii) in the above:

Step 1: Initialisation.

1.1 For OD movements $m = 1, \dots, M$, generate the choice sets and store the link attributes and link-route information.

1.2. Postulate a true set of parameters $(\boldsymbol{\alpha}^{true}, \theta_{true}, \beta_{true})$ for the APSL model, and given these parameters and

the generated choice sets, solve each of the fixed-point problems

$$\boldsymbol{P}_m = \boldsymbol{G}_m\left(\boldsymbol{g}_m\left(\boldsymbol{c}_m\left(\boldsymbol{t}(\boldsymbol{w};\boldsymbol{\alpha}^{true})\right),\boldsymbol{\gamma}_m^{APS}(\boldsymbol{t}(\boldsymbol{w};\boldsymbol{\alpha}^{true}),\boldsymbol{P}_m);\theta_{true},\beta_{true}\right)\right)$$

for $m = 1, \dots, M$.

1.3. Based on the fixed-point choice probability solutions $\boldsymbol{P}_m^*$ for $m = 1, \dots, M$ (obtained in 1.2), sample Z observed routes.

1.4. Define an initial set of parameter values $\left(\tilde{\boldsymbol{\alpha}}^{(1)}, \tilde{\theta}^{(1)}, \tilde{\beta}^{(1)}\right)$ for MLE, and set $n = 1$.

Algorithm 2.1 (Step 1): Pseudo-code, initialisation of simulation experiments.

The number of observed routes to sample, Z, is exogenously defined. The robustness of the estimated parameters estimated can be investigated numerically by applying Algorithm 2.1 multiple times and then analysing the variation of the estimated parameters.

5.3.2 Sioux Falls Application

The Sioux Falls network in Fig. 2.13 consists of 76 links, 528 OD movements with non-zero travel demands, and 1,632,820 total routes. The travel cost of link a is specified as the free-flow travel time $w_{a,1}$ only, such that:

$$t_a(\boldsymbol{w}_a;\boldsymbol{\alpha}) = w_{a,1} \cdot \alpha_1,$$

where $\alpha_1 > 0$ is the free-flow travel time parameter, and thus the travel cost for route $i \in R_m$ is:

$$c_{m,i}\left(\boldsymbol{t}(\boldsymbol{w};\boldsymbol{\alpha})\right) = \sum_{a \in A_{m,i}} t_a(\boldsymbol{w}_a;\boldsymbol{\alpha}) = \alpha_1 \sum_{a \in A_{m,i}} w_{a,1}.$$

The model requires the specification of three parameters: α_1, θ, and β, but to ensure identification θ is fixed at $\theta = 1$ throughout.

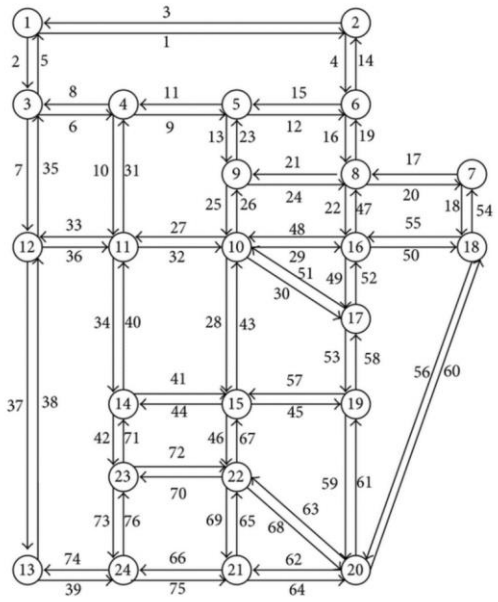

Fig. 2.13. Sioux Falls network.

Since the travel costs of the links (and thus routes) correspond to a single variable, to generate the utilised choice sets we employ k-shortest path to generate 150 of the lowest costing routes for each choice set. We also remove the short trip OD movements where the cheapest route has a free-flow travel time cost less than 10. The result is that there are 316 remaining OD movements, and a total of 47,400 routes.

5.3.3 Experiment Results

We begin the simulation study by investigating the Log-Likelihood surface. By evaluating the Log-Likelihood function in (2.32) for various configurations of α_1 and β the Log-Likelihood surface can be visualised for a sample of observed routes. Fig. 2.14 displays the log-likelihood surface for a single estimation experiment, with $\alpha_1^{true} = 0.3$, $\beta_{true} = 0.6$, and $Z = 2000$. As Fig. 2.14 shows, the Log-Likelihood surface is smooth and approximately maximal around the true parameters, where the estimated parameters are $\hat{\alpha}_1 = 0.294 \pm 0.002$ and $\hat{\beta} = 0.57 \pm 0.01$.

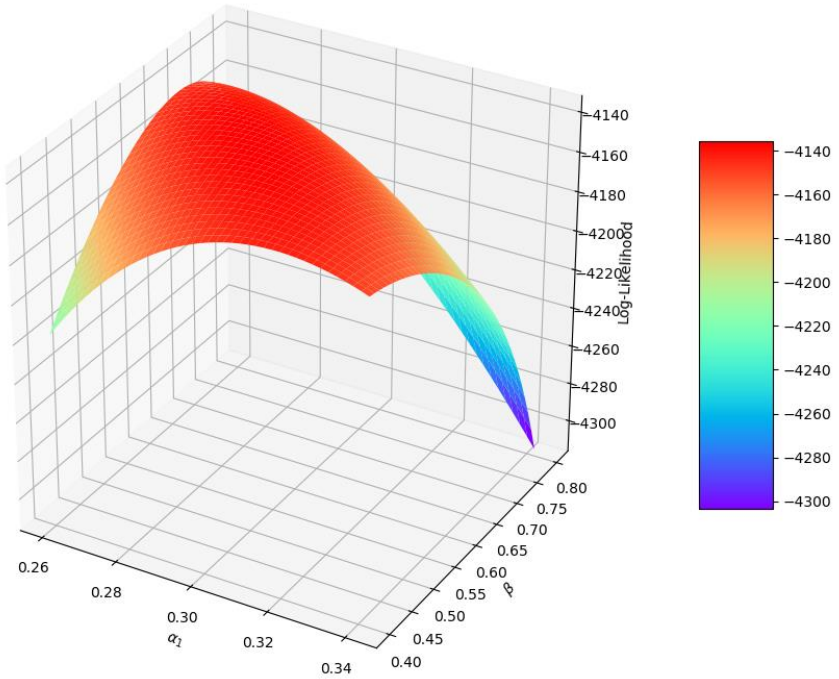

Fig. 2.14. Sioux Falls simulation study: Log-Likelihood surface ($\theta_{true} = 0.3$, $\beta_{true} = 0.6$, $Z = 2000$).

Next, we investigate the stability of the estimated parameters over multiple experiment replications. Each experiment utilises a Log-Likelihood maximisation algorithm (see Section 5.2.2) to obtain the parameter estimates with initial conditions $\left(\tilde{\alpha}_1^{(0)}, \tilde{\beta}^{(0)}\right) = (0.15,0)$, and bounds $\tilde{\alpha}_1, \tilde{\beta} \in [0,1]$.

Fig. 2.15A-D display for different settings of α_1^{true} and β_{true}, the distribution of the estimated parameters after $q = 100$ experiment replications of $Z = 1000$ simulated observations.

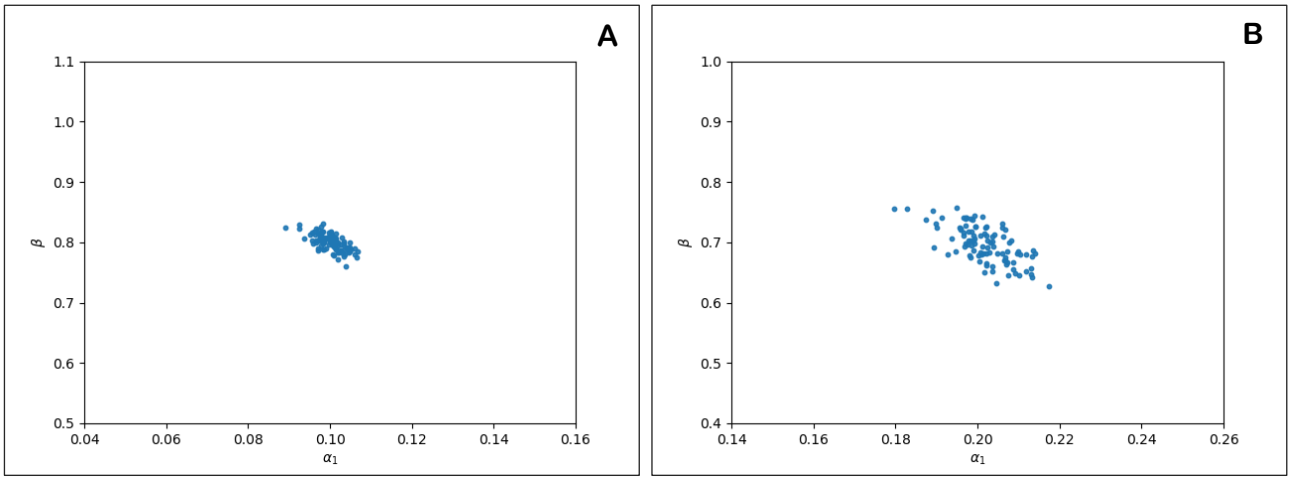

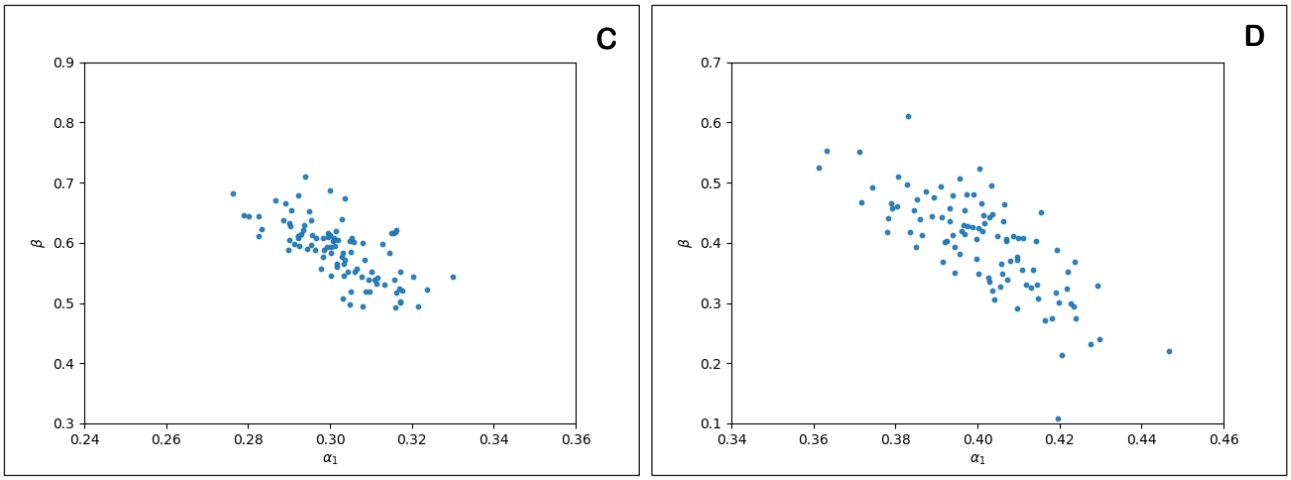

Fig. 2.15. Sioux Falls simulation study: Distribution of estimated parameters after multiple experiment replications ($Z = 1000$, $q = 100$). **A:** $\alpha_1^{true} = 0.1$ $\beta_{true} = 0.8$. **B:** $\alpha_1^{true} = 0.2$ $\beta_{true} = 0.7$. **C:** $\alpha_1^{true} = 0.3$ $\beta_{true} = 0.6$. **D:** $\alpha_1^{true} = 0.4$ $\beta_{true} = 0.4$.

Table 2.2 reports, for various settings of the true parameters (same as Fig. 2.15A-D), the mean value (μ), standard deviation (σ), and Mean Squared Error (MSE) of the estimates across $q = 100$ experiment replications with $Z = 1000$ simulated observations. Table 2.2 also displays the estimated covariance between the α_1 and β parameters. As shown, the mean estimates of α_1 and β are close to the true values for all settings tested (i.e. there is no evidence of bias in the parameter estimates). However, as measured by the MSE, the precision of estimating α_1 decreases as α_1^{true} increases, and the precision of estimating β decreases as β_{true} decreases. This seems reasonable as increasing α_1 in this case corresponds to lower perception error of travel cost and decreasing β corresponds to lower perception of distinctiveness.

Table 2.2 and Fig. 17A-D both indicate that, with this network and the generated choice sets, there appears to be some negative correlation between the $\hat{\alpha}_1$ and $\hat{\beta}$ estimates. This is likely due to the large number of unrealistic routes present within the choice sets and the consequent small path size contribution factors for these routes from the true parameters; these factors can be reduced by increasing α_1 or β and hence negative correlation appears from balancing the parameters to obtain small contributions.

α_1^{true}	β_{true}	$\hat{\alpha}_1$			$\hat{\beta}$			$cov(\hat{\boldsymbol{\alpha}}_1, \hat{\boldsymbol{\beta}})$
		μ	σ	MSE	μ	σ	MSE	
0.1	0.8	0.1000	0.0032	0.0000	0.8003	0.0136	0.0002	-0.00003
0.2	0.7	0.2016	0.0068	0.0001	0.6972	0.0305	0.0009	-0.00014
0.3	0.6	0.3021	0.0105	0.0001	0.5876	0.0485	0.0025	-0.00034
0.4	0.4	0.4012	0.0153	0.0002	0.3984	0.0817	0.0067	-0.00096

Table 2.2. Sioux Falls simulation study: Stability of estimated parameters across multiple experiment replications ($Z = 1000$, $q = 100$).

5.3.3.1 Computation Analysis

In this subsection we analyse the computational performance of the APSL model in the Sioux Falls MLE application. The computer used has a 2.10GHz Intel Xeon CPU, 512GB RAM, and 64 Logical Processors (of which 50 were utilised). The code was implemented in Python. Results are reported throughout this section for a single simulation experiment where $Z = 1000$ route choice observations were simulated from the true model $\alpha_1^{true} = 0.3$, $\beta_{true} = 0.6$. $\hat{\alpha}_1 = 0.295$ and $\hat{\beta} = 0.611$ are the consequent maximum likelihood estimates.

Fig. 2.16A shows for different values of the APSL choice probability convergence parameter ξ (and thus convergence statistic, See Section 3.4), the average number of fixed-point iterations per OD movement and computation time required to solve all of the 316 APSL fixed-point problems $\boldsymbol{P}_m = \boldsymbol{G}_m\left(\boldsymbol{g}_m\left(\boldsymbol{c}_m(\boldsymbol{t}), \boldsymbol{\gamma}_m^{APS}(\boldsymbol{t}, \boldsymbol{P}_m)\right)\right)$, and consequently compute the Log-Likelihood value of the maximum likelihood estimates. As shown, computation time and average number of fixed-point iterations per OD

increase roughly linearly as the convergence parameter is increased. As expected, computation times relate to the number of iterations required for convergence. Fig. 2.16B shows the value of the Log-Likelihood obtained as ξ is increased. As shown, the Log-Likelihood increases in value and accuracy as the APSL choice probabilities become more accurate.

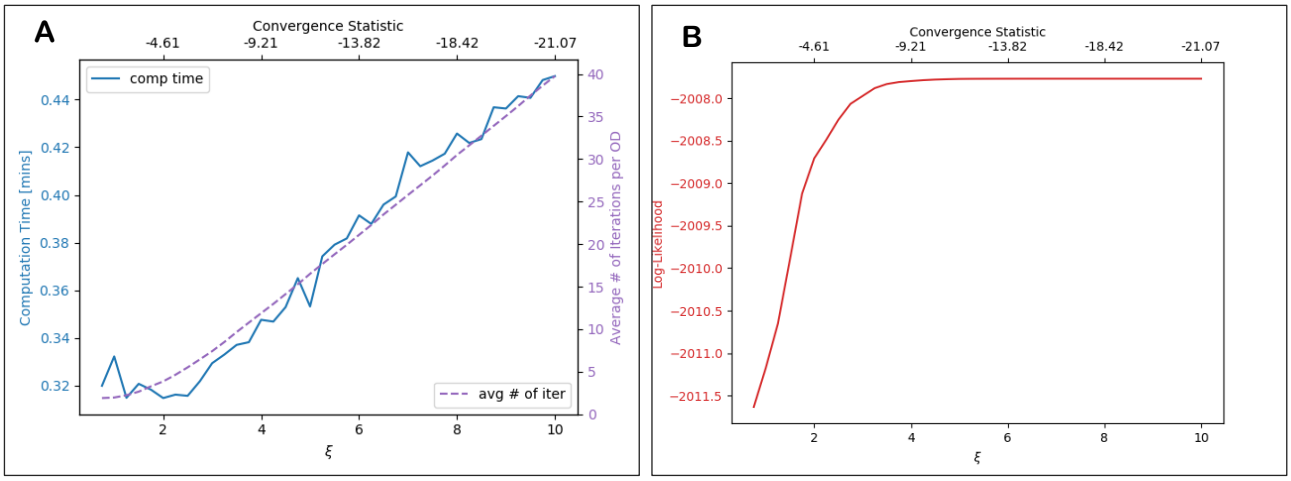

Fig. 2.16. Sioux Falls simulation study: Computational statistics for calculating APSL Log-Likelihoods as the APSL choice probability convergence parameter ξ is increased.
A: Average number of fixed-point iterations per OD / computation time [mins]. **B:** Log-Likelihood value.

Fig. 2.17 shows for different values of $\tilde{\beta}$ the average number of fixed-point iterations per OD movement and computation time required to calculate the Log-Likelihood, with $\xi = 7$ and $\tilde{\alpha}_1$ set as the maximum likelihood estimate $\hat{\alpha}_1 = 0.295$. As shown, the average number of iterations per OD required for convergence increases as $\tilde{\beta}$ increases, and thus so do the required computation times.

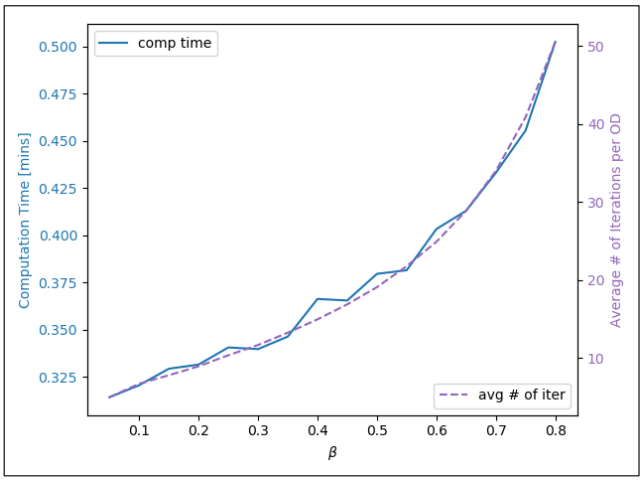

Fig. 2.17. Sioux Falls simulation study: Average number of fixed-point iterations per OD movement and computation time required to calculate the Log-Likelihood for different $\tilde{\beta}$ values ($\tilde{\alpha}_1 = \hat{\alpha}_1 = 0.295$, $\xi = 7$).

Fig. 2.18A-B show for a single MLE (implementation of the L-BFGS-B algorithm), the cumulative computation times of the iterations and the Log-Likelihood values and parameter estimates at the end of each iteration, with $\xi = 7$.

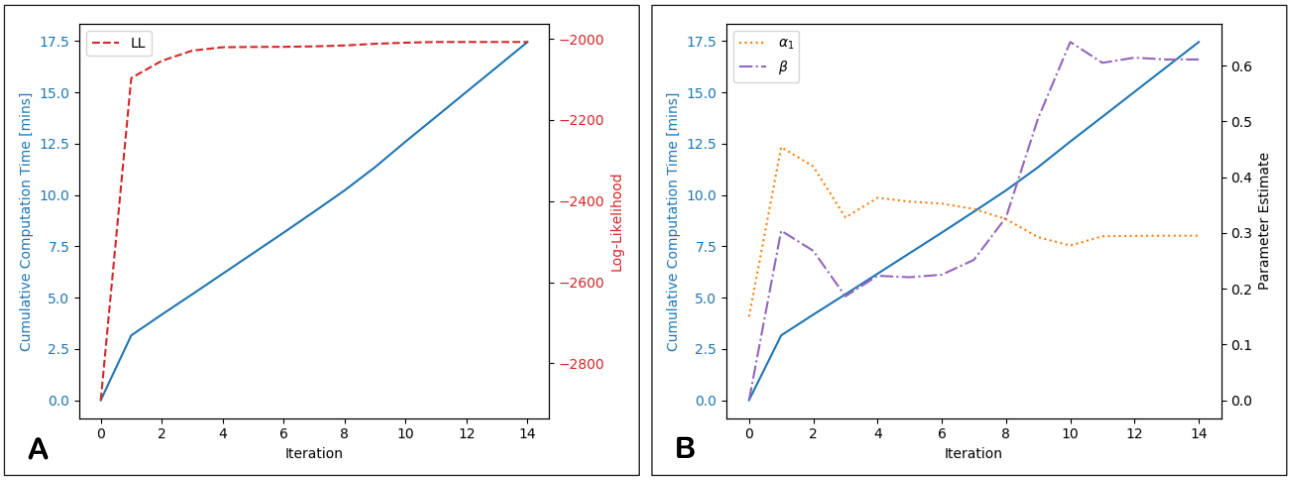

Fig. 2.18. Sioux Falls simulation study: Cumulative computation time at each iteration of a single MLE, and MLE statistics ($\xi = 7$). **A:** Log-Likelihood. **B:** Parameter estimates.

Fig. 2.19A shows the total computation times and MLE final Log-Likelihood values of different MLE runs for different settings of ξ. Fig. 2.19B shows the parameter estimates. For $\xi = 5$, the inaccuracy of the APSL choice probabilities means that more MLE iterations are required to identify the estimates. For $\xi = 6$, however, the choice probabilities are sufficiently accurate to quickly estimate the parameters. Greater values of ξ increase the number of fixed-point iterations required for the fixed-point convergences and hence the computation times of the MLE.

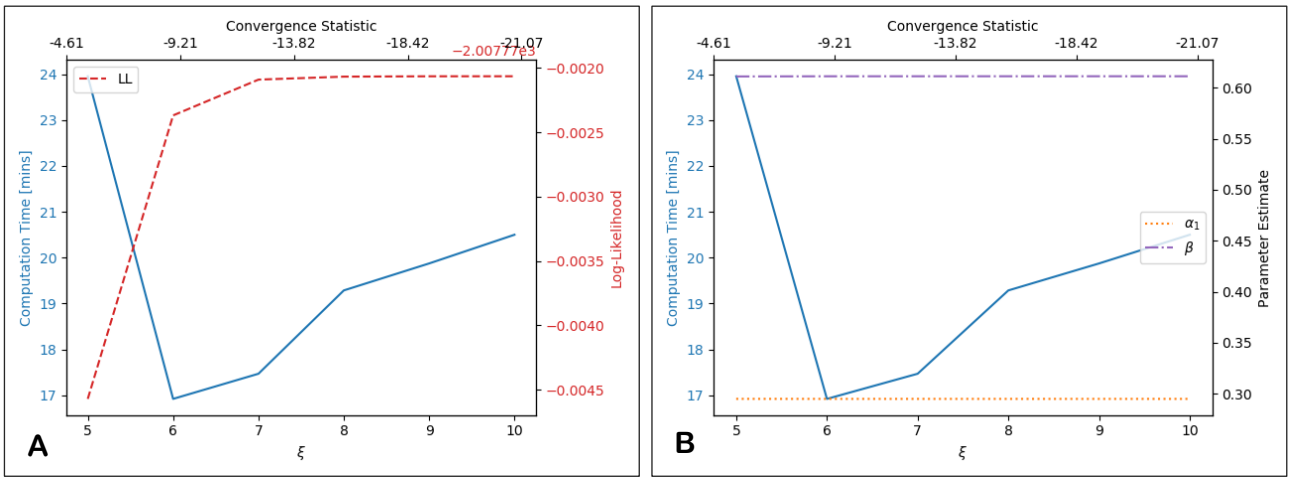

Fig. 2.19. Sioux Falls simulation study: Total computation time of MLE runs for different values of ξ, and MLE results. **A:** Final Log-Likelihood. **B:** Parameter estimates.

We also briefly investigate the impact of the τ parameter upon parameter estimation. Each OD movement m has a choice set size $N_m = 150$, and therefore supposing each OD movement has the same value for τ, the maximum value for τ is $\frac{1}{150} = 0.00\dot{6}$. Supposing τ assumes the form $\tau = 10^{-\varphi}$, Fig. 2.20 displays how the maximum likelihood parameter estimates vary as φ varies. As shown, the parameter estimates converge quickly to the limit case of $\tau \to 0$, demonstrating that we can recover the desired model APSL_0 (Section 3.1) to a high computational accuracy using the APSL model as defined in Section 3.2, with a sufficiently small value of τ.

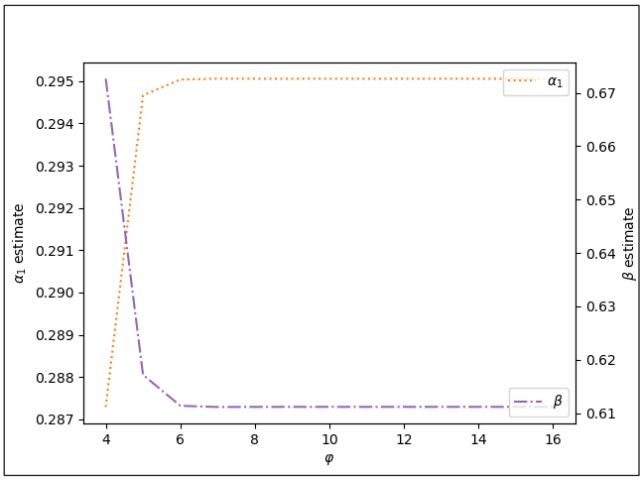

Fig. 2.20. Sioux Falls simulation study: Maximum likelihood APSL parameter estimates for different values of $\tau = 10^{-\varphi}$.

5.3.3.2 APSL Solution Uniqueness Analysis

In this subsection we briefly investigate the uniqueness of APSL choice probability solutions in the context of the Sioux Falls simulation study. Just as in Section 4.4, we plot trajectories of APSL solutions to approximate the uniqueness conditions, i.e. estimate β_{max}. A single simulation study is conducted for $\alpha_1^{true} = 0.3$, $\beta_{true} = 0.6$, and $Z = 2000$, leading to maximum likelihood estimates $\hat{\alpha}_1 = 0.306$ and $\hat{\beta} = 0.6001$. We thus investigate whether APSL solutions are unique for these parameter estimates. Fig. 2.21 displays the maximum choice probability from three trajectories of APSL solutions as the β parameter is varied for four different randomly chosen OD movements, with $\alpha_1 = \hat{\alpha}_1 = 0.306$. β was decremented by 0.01, and the initial large β value was $\beta = 2$. As shown, the $\beta_{max,m}$ values (β_{max} for OD movement m) for these OD movements can be estimated to vary between 0.86 and 0.94, suggesting that $\beta = 0.6001$ results in universally unique solutions.

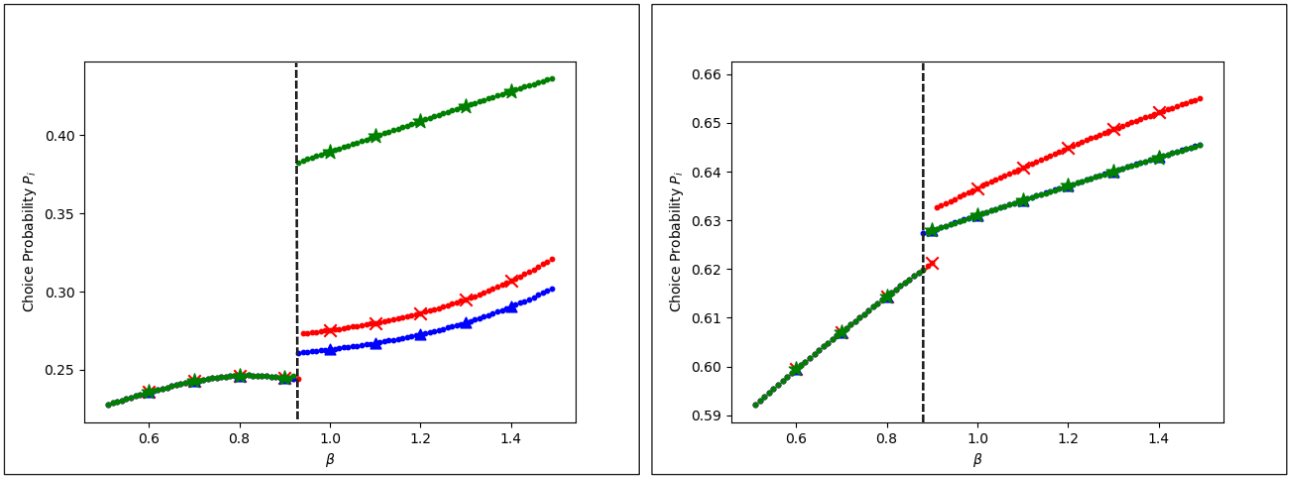

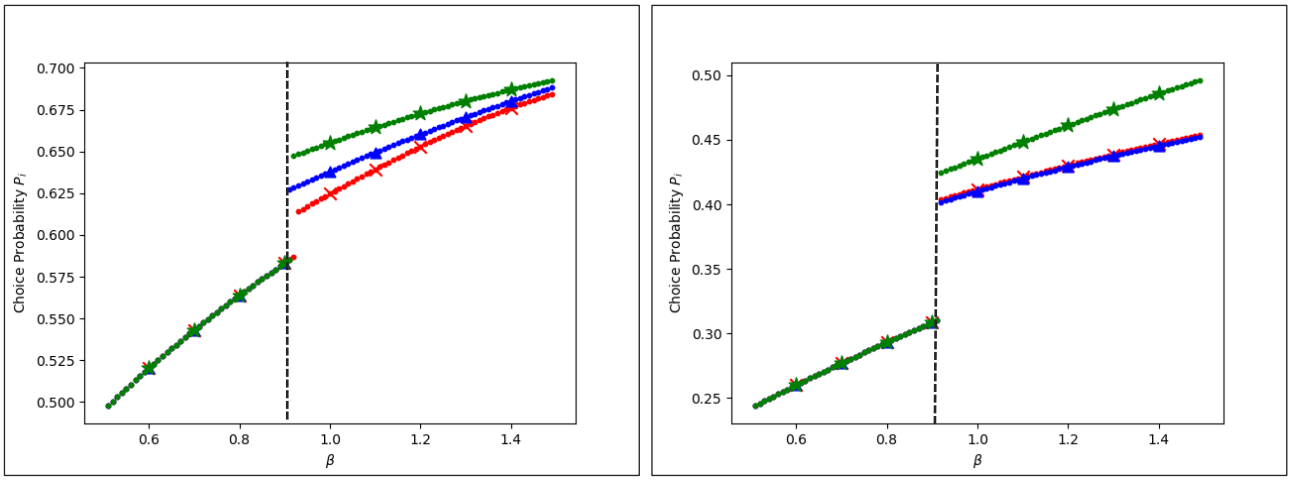

Fig. 2.21. Sioux Falls simulation study: Maximum choice probability of trajectories of APSL solutions as β is varied ($\alpha_1 = 0.306$).

5.4 Real-Life Case Study

In this section we estimate the APSL model, where the model parameters are estimated using MLE with observed route choices tracked by GPS units. The data has been collected among drivers in the eastern part of Denmark in 2011, and includes a total of 17,115 observed routes. The dataset is the same as used in Prato et al (2014) as well as Rasmussen et al (2017), and after a filtering to include only trips where the sum of travel time (in minutes) and length (in km) is at least 10, a total of 8,696 observations remain.

The GPS traces are map matched to a network, for which corresponding time-of-day dependent travel times are available on the entire network. See more details in Prato et al (2014). The network is large-scale, representing all of Denmark, and thus includes 34,251 links. With current alternative generation techniques, it is not feasible to enumerate the universal choice set for such a large network. Instead, we approximate the universal choice set by generating a choice set for each observed route by applying the doubly stochastic approach also applied in Prato et al (2014). This approach is based on repeated shortest path search in which the network attributes and parameters of the cost function is perturbated between searches (Nielsen, 2000; Bovy & Fiorenzo-Catalano, 2007). Up to 100 unique paths are generated for each observation, see the distribution of number of alternatives in Fig. 2.22.

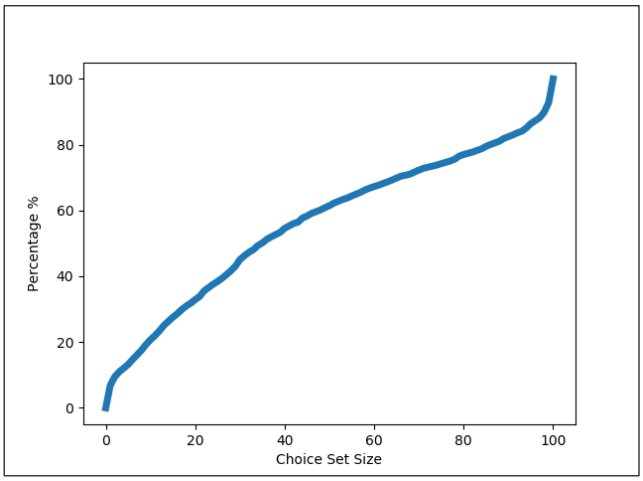

Fig. 2.22. Real-life case-study: Cumulative distribution of the choice set sizes for the 8,696 observations.

For the estimation, the travel cost of link a is specified as a weighted sum of congested travel time $w_{a,1}$ (in minutes), and length $w_{a,2}$ (in kilometres), such that:

$$t_a(\boldsymbol{w}_a; \boldsymbol{\alpha}) = w_{a,1} \cdot \alpha_1 + w_{a,2} \cdot \alpha_2$$

where $\alpha_1 > 0$ and $\alpha_2 > 0$ are the congested travel time, and length parameters, respectively. The generalised travel cost for route $i \in R_m$ is thus:

$$c_{m,i}\big(\boldsymbol{t}(\boldsymbol{w};\boldsymbol{\alpha})\big) = \sum_{a\in A_{m,i}} t_a(\boldsymbol{w}_a;\boldsymbol{\alpha}) = \sum_{a\in A_{m,i}} \big(w_{a,1}\cdot\alpha_1 + w_{a,2}\cdot\alpha_2\big) = \alpha_1 \sum_{a\in A_{m,i}} w_{a,1} + \alpha_2 \sum_{a\in A_{m,i}} w_{a,2}.$$

The model requires the specification of four parameters: α_1, α_2, θ, and β, but to ensure identification, the θ parameter is fixed at $\theta = 1$. Fig. 2.23A shows the relative travel time deviations away from the quickest routes in the choice sets for the observed routes as well as the alternative routes generated, and Fig. 2.23B shows the relative length deviations. 47% and 36% of the observed routes were the quickest and shortest routes, respectively. Moreover, there appear to be observations of unattractive route choices, where some observed routes were 2.11 times slower / 2.29 times longer than the quickest / shortest alternatives, as well as numerous potentially unrealistic routes generated, where some generated routes are 2.91 times slower / 3.22 times longer.

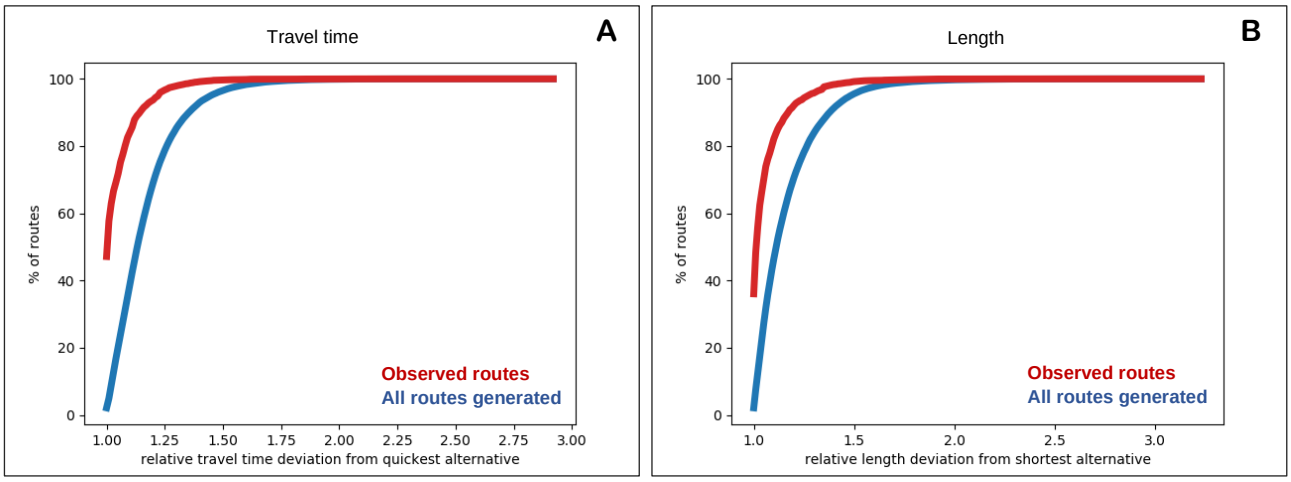

Fig. 2.23. Real-life case-study: Relative deviations away from quickest/shortest routes in the choice sets for the observed routes (red) and alternative routes generated (blue). **A:** Travel time. **B:** Length.

We estimate the models utilising the same Log-Likelihood maximisation algorithm (L-BFGS-B, see Section 5.2.2), initial conditions, and parameter bounds, where appropriate. Initial conditions: $\left(\tilde{\alpha}_1^{(1)}, \tilde{\alpha}_2^{(1)}, \tilde{\beta}^{(1)}, \tilde{\lambda}^{(1)}\right) = (0.5,0.5,0,0)$, and bounds: $\tilde{\alpha}_1, \tilde{\alpha}_2, \tilde{\beta} \in [0,2]$, $\tilde{\lambda} \in [0,200]$.

5.4.1 APSL Estimation

5.4.1.1 Results

In this subsection we provide results from estimating the three parameters of the APSL model in this case study: α_1, α_2, and β. Table 2.3 displays the APSL parameter estimates and the consequent Log-Likelihood value.

$\hat{\alpha}_1$	$\hat{\alpha}_2$	$\hat{\beta}$	LL
0.633	0.184	0.840	-18978

Table 2.3. Real-life case-study: APSL parameter estimates and Log-Likelihood.

Fig. 2.24 shows the Log-Likelihood surfaces around the three parameter estimates; as can be seen, these are smooth and maximal around the estimates.

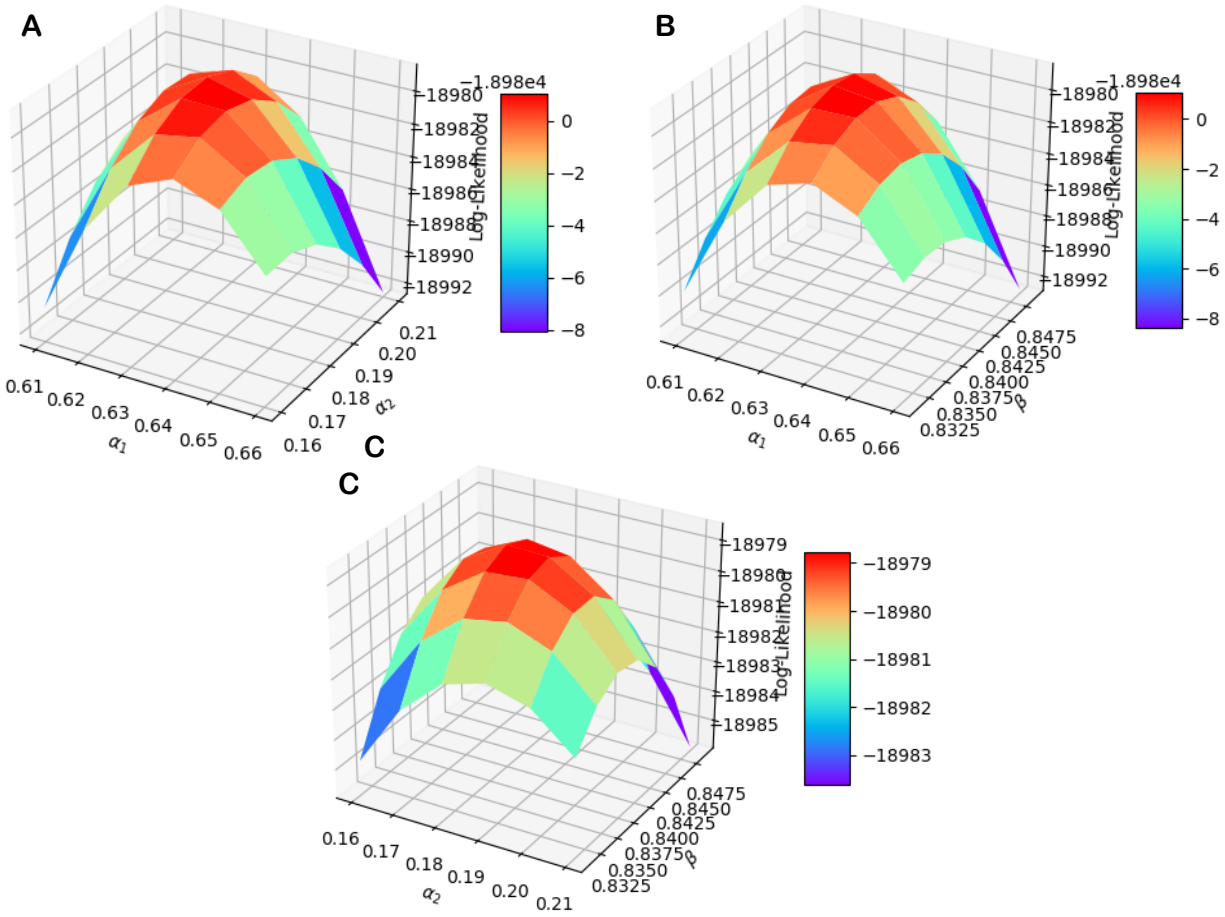

Fig. 2.24. Real-life case-study: APSL Log-Likelihood surface around parameter estimates in Table 3. **A:** α_1, α_2. **B:** α_1, β. **C:** α_2, β.

5.4.1.2 Computation Analysis

We analyse here the computational performance of the APSL model in the real-life case study. The same computer was used as in Section 5.3.2.2.

Fig. 2.25A shows for different values of the APSL choice probability convergence parameter ξ (and thus convergence statistic), the average number of fixed-point iterations per OD movement and computation time required to solve all of the 8,696 APSL fixed-point problems $\boldsymbol{P}_{m_z} = \boldsymbol{G}_{m_z}\left(\boldsymbol{g}_{m_z}\left(\boldsymbol{c}_{m_z}(\boldsymbol{t}), \boldsymbol{\gamma}_{m_z}^{APS}(\boldsymbol{t}, \boldsymbol{P}_{m_z})\right)\right)$ for $z = 1, \ldots, Z$, and consequently compute a single Log-Likelihood, with the estimated APSL parameters in Table 2.3. Fig. 2.25B shows the value of the Log-Likelihood obtained as ξ is increased. As shown, computation time and average number of fixed-point iterations per OD increase linearly as the convergence parameter is increased, and the Log-Likelihood increases in accuracy (from $\xi = 2$) as the APSL choice probabilities become more accurate. The relatively large estimated β value results in a longer computation time, as shown in Section 5.3.2.2, for lower β, the computation times are less.

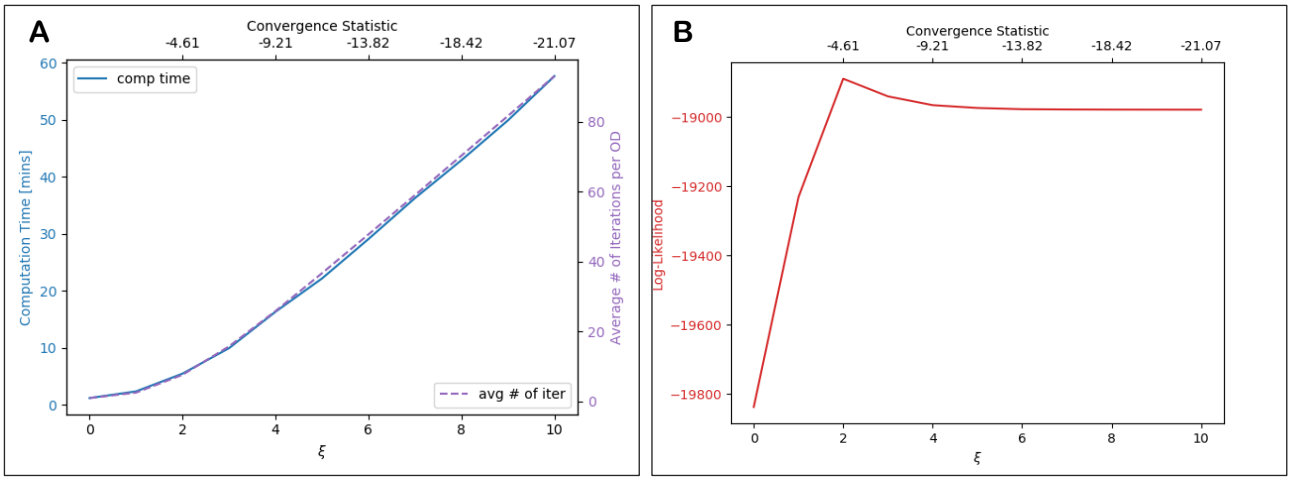

Fig. 2.25. Real-life case-study: Computational statistics for calculating APSL Log-Likelihoods as the APSL choice probability convergence parameter ξ is increased.
A: Average number of fixed-point iterations per OD / computation time [mins]. **B:** Log-Likelihood value.

Fig. 2.26A-B show for a single estimation of the APSL model (implementation of the L-BFGS-B algorithm), the cumulative computation times of the iterations and the Log-Likelihood values and parameter estimates at the end of each iteration, respectively, with $\xi = 10$. The initial conditions for solving the APSL fixed-point problems were updated at the end of each iteration with the choice probabilities obtained from the current parameter estimates.

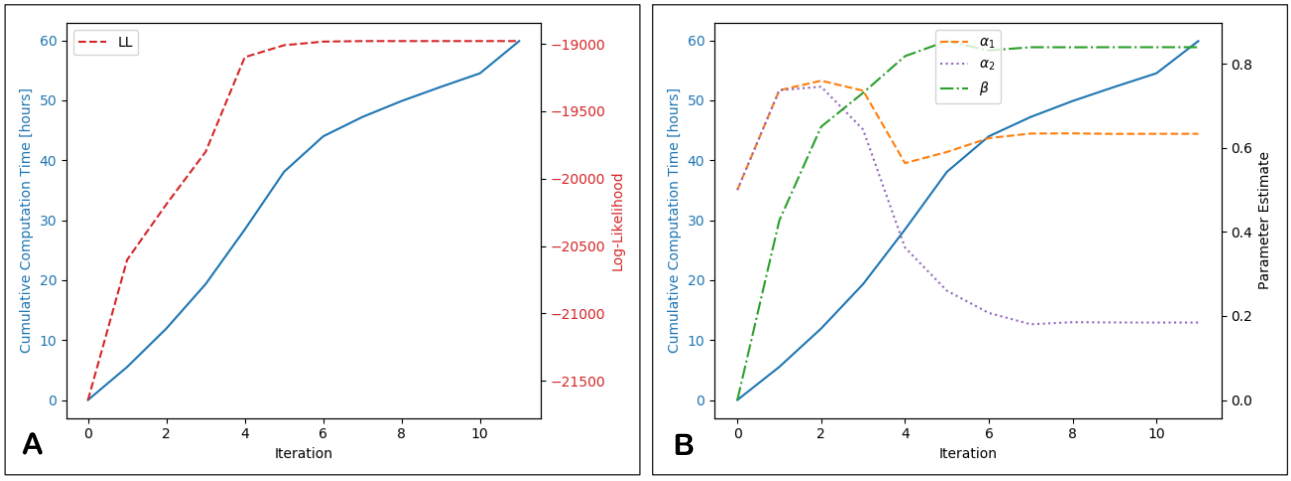

Fig. 2.26. Real-life case-study: Cumulative computation time at each iteration for a single estimation of the APSL model, and MLE statistics ($\xi = 10$). **A:** Log-Likelihood. **B:** Parameter estimates.

5.4.1.3 APSL Solution Uniqueness Analysis

We briefly investigate here the uniqueness of APSL choice probability solutions in the context of the real-life case study. Similar to the experiments conducted in Section 5.3.2.3 for the Sioux Falls simulation study, we estimate the uniqueness conditions for the network given the estimated parameters. Trajectories of APSL solutions are plotted to approximate β_{max}. Fig. 2.27 displays the maximum choice probability from trajectories of APSL solutions as the β parameter is varied for four different randomly chosen OD movements, with α_1 and α_2 as in Table 2.3. β was decremented by 0.01, and the initial large β value was $\beta = 1.5$. As shown, the $\beta_{max,m}$ values (β_{max} for OD movement m) for these OD movements are between 0.96 and 0.99, suggesting that $\beta = 0.840$ results in universally unique solutions.

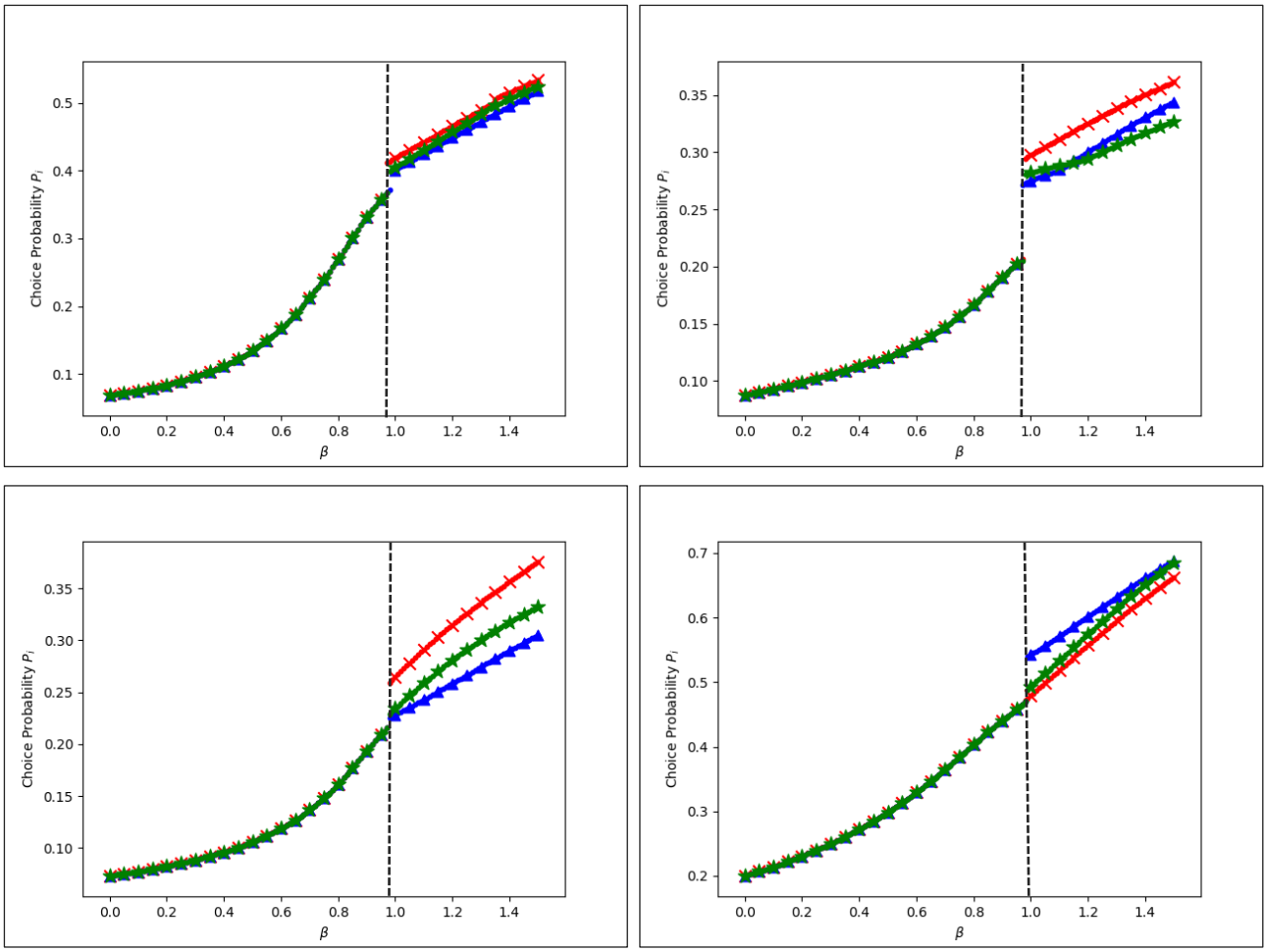

Fig. 2.27. Real-life case study: Maximum choice probability from trajectories of APSL solutions as β is varied ($\alpha_1 = 0.633$, $\alpha_2 = 0.184$).

5.4.2 Comparing Results with Other Path Size Logit Models

In this subsection we estimate models discussed in this paper and compare results. Table 2.4 shows the estimated parameters for the MNL, PSL, GPSL, GPSL$'_{(\lambda=\theta)}$, and APSL models.

	$\hat{\alpha}_1$	$\hat{\alpha}_2$	$\hat{\beta}$	$\hat{\lambda}$	LL
MNL	0.777	0.330			-21308
PSL	0.966	0.306	1.347		-20581
GPSL	0.415	0.085	1.186	91.95	-17874
GPSL$'_{(\lambda=\theta)}$	0.691	0.154	1.807		-19152
APSL	0.633	0.184	0.840		-18978

Table 2.4. Real-life case-study: Estimation results and stability statistics from all Path Size Logit models.

To compare the estimation results of the models, we apply the approach in Swait & Ben-Akiva (1984) based on the non-nested test in Horowitz (1983) in combination with the results in Table 2.4. The adjusted rho-squared for model h with estimated parameters $\hat{\boldsymbol{\omega}}_h$ is given by:

$$\bar{\rho}_h^2 = 1 - \frac{LL_h(\hat{\boldsymbol{\omega}}_h) - K_h}{LL^*},$$

where $LL_h(\hat{\boldsymbol{\omega}})$ is the Log-Likelihood for model h given the estimated parameters $\hat{\boldsymbol{\omega}}_h$, K_h is the number of model h parameters, and LL^* is the equal choice probability Log-Likelihood which in this case study is: $LL^* =$

$\ln\left(\prod_{z=1}^{Z}\frac{1}{N_{m_z}}\right) = -\sum_{z=1}^{Z}\ln(N_{m_z}) = -28200$. The distribution of the difference between $\bar{\rho}^2_{h_1}$ and $\bar{\rho}^2_{h_2}$ for models h_1 and h_2, respectively, (which are possibly non-nested) is given by:

$$\Pr\left(\bar{\rho}^2_{h_2} - \bar{\rho}^2_{h_1} > y\right) \leq \Phi\left(-\left[-2yLL^* + \left(K_{h_2} - K_{h_1}\right)\right]^{\frac{1}{2}}\right),$$

where $y > 0$ is the test statistic. To test the null hypothesis that the MNL model outperforms the PSL, GPSL, GPSL$'_{(\lambda=\theta)}$, and APSL models, we compute the test statistics $y_{PS} = \bar{\rho}^2_{PS} - \bar{\rho}^2_{MNL}$, $y_{GPS} = \bar{\rho}^2_{GPS} - \bar{\rho}^2_{MNL}$, $y_{GPS'} = \bar{\rho}^2_{GPS'} - \bar{\rho}^2_{MNL}$, and $y_{APS} = \bar{\rho}^2_{APS} - \bar{\rho}^2_{MNL}$. Similarly, we compute the corresponding $Y_{PS} = -[-2y_{PS}LL^* + (K_{PS} - K_{MNL})]^{\frac{1}{2}}$, $Y_{GPS} = -[-2y_{GPS}LL^* + (K_{GPS} - K_{MNL})]^{\frac{1}{2}}$, $Y_{GPS'} = -[-2y_{GPS'}LL^* + (K_{GPS'} - K_{MNL})]^{\frac{1}{2}}$, and $Y_{APS} = -[-2y_{APS}LL^* + (K_{APS} - K_{MNL})]^{\frac{1}{2}}$. The results are shown in Table 2.5. $\Pr(y_h \leq Y_h)$ is the probability that the MNL model outperforms model h, but these values are too small for computer precision to calculate. This exemplifies the necessity of capturing the correlation between routes. One can identify however that $\Pr(y_{PS} \leq Y_{PS}) > \Pr(y_{GPS'} \leq Y_{GPS'}) > \Pr(y_{APS} \leq Y_{APS}) > \Pr(y_{GPS} \leq Y_{GPS})$. In another comparison of fit test, Table 2.6 shows the penalised-likelihood criteria.

In both tests, the GPSL$'_{(\lambda=\theta)}$ and APSL models outperform the PSL model with the same number of parameters, where APSL outperforms GPSL$'_{(\lambda=\theta)}$. This suggests that there is value in including a measure of distinctiveness within the path size contribution factors. The GPSL model outperforms all models due to the greater flexibility the λ parameter provides. Several case studies have found that larger values of λ increase the goodness-of-fit of the GPSL model (Ramming, 2002; Prato, 2005; Hoogendoorn-Lanser, 2005; Bekhor & Prato, 2006), and hence it is not unusual that $\hat{\lambda} = 91.95$ is so big. We explore further below.

h	K_h	$\bar{\rho}^2_h$	y_h	Y_h
PSL	3	0.27006	0.02573	-38.1144
GPSL	4	0.36604	0.12171	-82.8673
GPSL$'_{(\lambda=\theta)}$	3	0.32074	0.07642	-65.6583
APSL	3	0.32690	0.08258	-68.2537

Table 2.5. Real-life case-study: Comparison of fit between models based on non-nested Horowitz type tests.

	AIC	BIC	CAIC
MNL	42621	42635	42637
PSL	41169	41190	41193
GPSL	35756	35784	35788
GPSL$'_{(\lambda=\theta)}$	38311	38332	38335
APSL	37963	37984	37987

Table 2.6. Real-life case-study: Comparison of fit between models based on penalised-likelihood criteria.

For very large values of λ within the GPSL path size terms, the path size contributions become extremely sensitive to differences in cost, where the contribution of route k to the path size term of route i is large if $c_i > c_k$ and small if $c_i < c_k$, and as $\lambda \to \infty$, $\left(\frac{c_i}{c_k}\right)^{\lambda} \to \infty$ if $c_i > c_k$, and $\left(\frac{c_i}{c_k}\right)^{\lambda} \to 0$ if $c_i < c_k$. The implication of this is that routes with relatively small travel costs are penalised significantly less than routes with relatively large travel costs for link sharing, and hence that low costing routes are considered much more distinct than high costing routes.

To provide some measure of the relative cost and distinctiveness of the observed routes (in comparison with the generated alternatives), Fig. 2.28A plots the percentage of generated routes with a travel cost greater than the observed route in each choice set (where the GPSL travel cost parameters are used), against the percentage of routes with PSL path size terms smaller than the observed route. The PSL path size terms provide a measure of the universal distinctiveness of the alternatives, i.e. without considering whether or not the routes are link sharing with unrealistic alternatives. The bottom right of the figure appears to be highly populated suggesting that many of the observations have relatively low travel costs but are relatively

universally indistinct, while a sizeable proportion are relatively distinct, even without the contribution weighting. Most notably though, a considerable proportion of the route observations have a low percentage of routes with greater travel costs, and many of these are relatively universally distinct (top left of figure). This perhaps suggests that many drivers have taken unattractive, relatively costly routes that are distinct. Fig. 2.28B plots the same cost percentage against the GPSL path size term percentage. As expected, the route observations with low costs are now considered much more distinct, while the observations with large costs are considered less distinct.

Fig. 2.29 displays the choice probability distribution of the observed routes under the different estimated models. For all models, a large percentage of the observed routes have small choice probabilities. This seems to also suggest that there are many observations where an unattractive route was chosen.

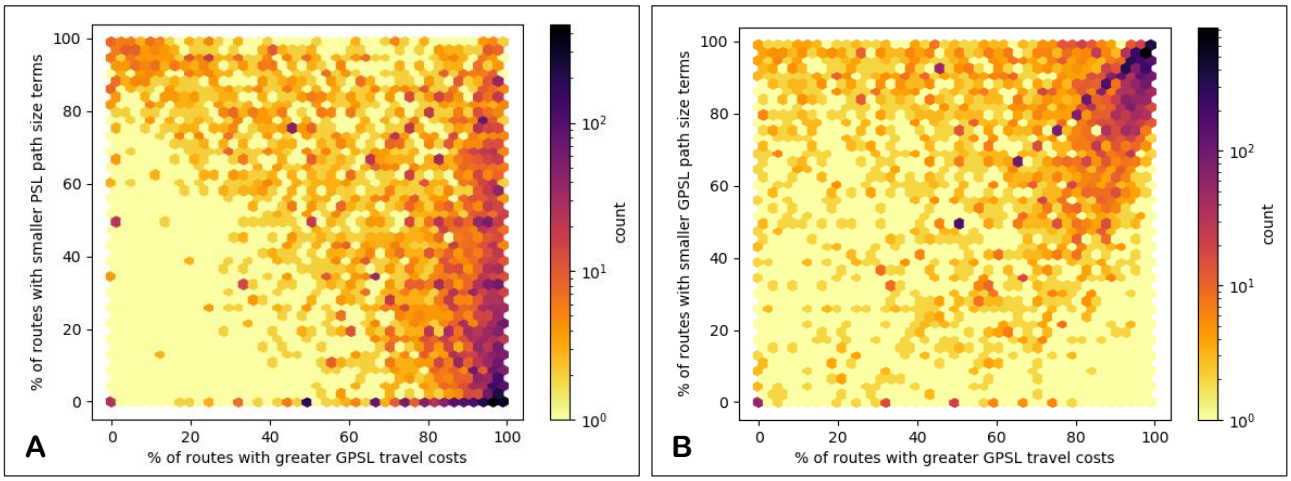

Fig. 2.28. Real-life case study: Percentage of routes in each OD movement choice set with costs greater / path size terms smaller than the observed route. **A:** PSL path size terms. **B:** GPSL path size terms.

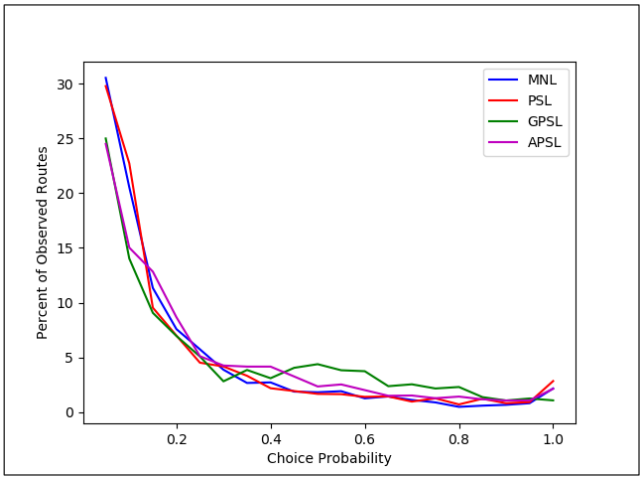

Fig. 2.29. Real-life case study: Choice probability distribution of the observed routes under the different estimated models.

The data set contains relatively costly but relatively universally distinct route observations. The GPSL model is able to provide the best fit for these observations, without compromising the fit for the low costing observations. The GPSL travel cost parameter estimates are smaller than the same estimates for the other models, which improves the relative attractiveness of the costly alternatives. To counterbalance this so that that the low costing routes still remain attractive, GPSL introduces a large λ value: routes with relatively small travel costs are penalised significantly less than routes with relatively large travel costs for link sharing. Moreover, GPSL is able to further increase the relative attractiveness of the distinct, costly routes by decreasing the attractiveness of the indistinct, costly routes with the large λ.

Fig. 2.30A & Fig. 2.31A show two route observations, which we label OD 1 and OD 2, respectively. Fig. 2.30B-D & Fig. 2.31B-D plot the consequent link choice probabilities from the MNL, PSL, GPSL, and APSL models. From first inspection it appears that the route taken by the driver in OD 1 is a high probability,

attractive route, while the route taken in OD 2 is low probability. Table 2.7 displays the choice probabilities of the observed route for OD 1 and OD 2 under the different models. The APSL model provides the largest choice probability for the observed route in OD 1, and GPSL provides the highest for OD 2, where the chosen probabilities for OD 2 are small.

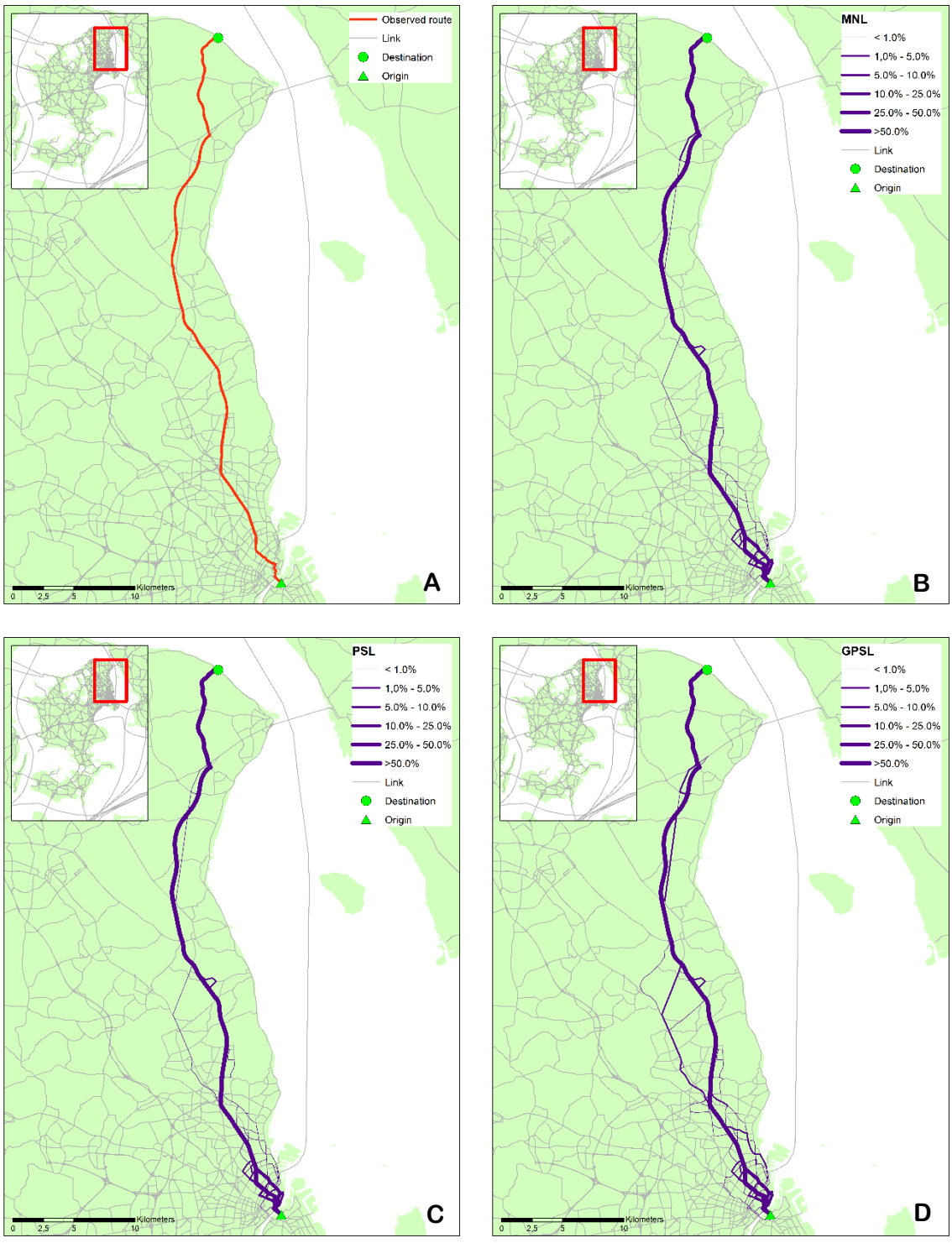
Observed route
Link
Destination
Origin
A
MNL
< 1.0%
1,0% - 5.0%
5.0% - 10.0%
10.0% - 25.0%
25.0% - 50.0%
>50.0%
Link
Destination
Origin
B
PSL
< 1.0%
1,0% - 5.0%
5.0% - 10.0%
10.0% - 25.0%
25.0% - 50.0%
>50.0%
Link
Destination
Origin
C
GPSL
< 1.0%
1,0% - 5.0%
5.0% - 10.0%
10.0% - 25.0%
25.0% - 50.0%
>50.0%
Link
Destination
Origin
D
Kilometers
0 2,5 5 10

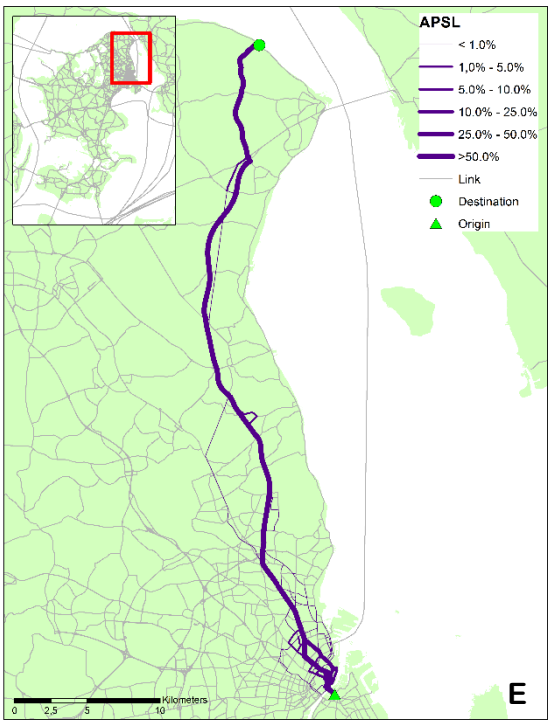

Fig. 2.30. Real-life case study: OD 1 plotted link choice probabilities from the estimated models for a single observation. **A:** Observed route. **B:** MNL. **C:** PSL. **D:** GPSL. **E:** APSL.

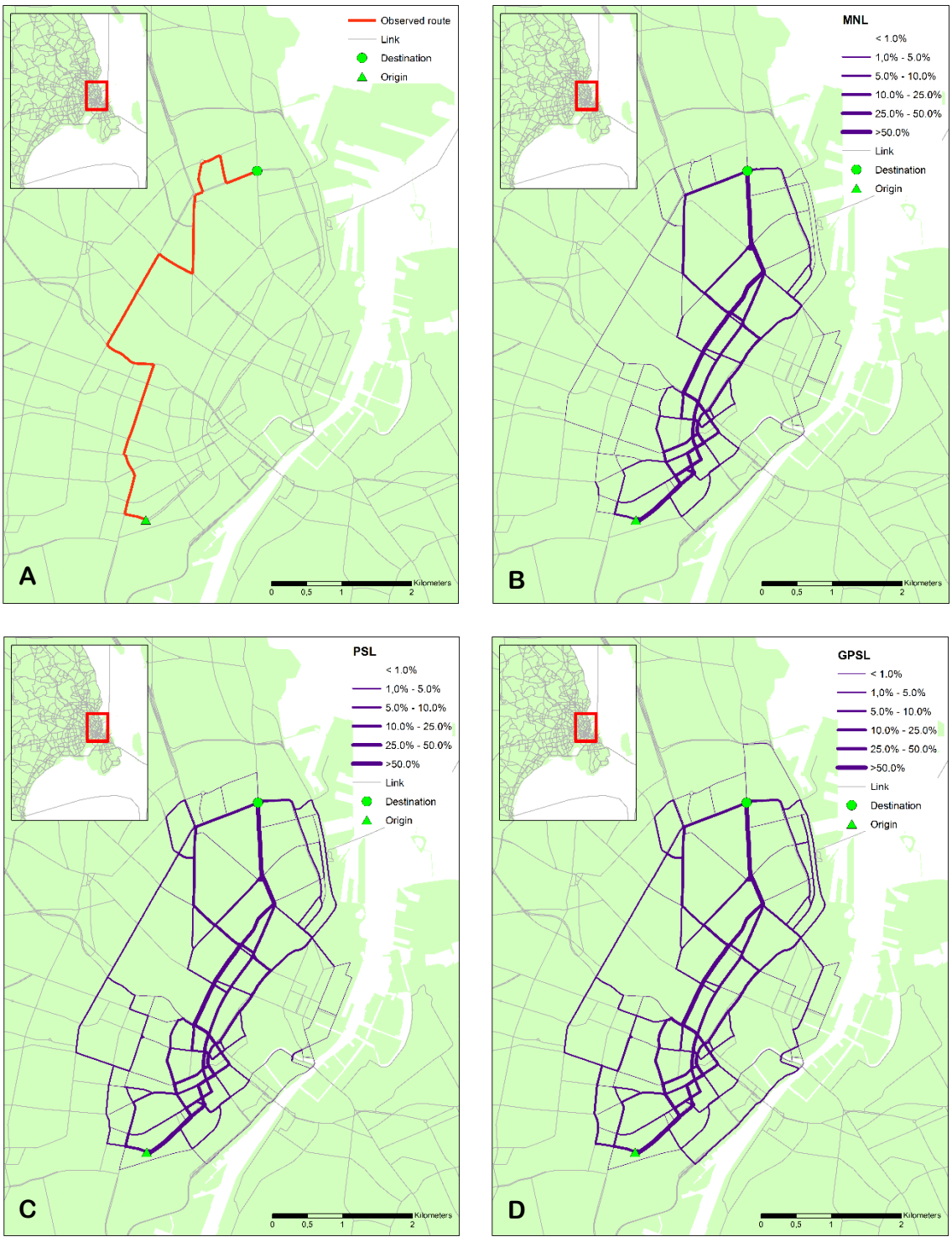
Observed route
Link
Destination
Origin
A
MNL
< 1.0%
1,0% - 5.0%
5.0% - 10.0%
10.0% - 25.0%
25.0% - 50.0%
>50.0%
Link
Destination
Origin
B
PSL
< 1.0%
1,0% - 5.0%
5.0% - 10.0%
10.0% - 25.0%
25.0% - 50.0%
>50.0%
Link
Destination
Origin
C
GPSL
< 1.0%
1,0% - 5.0%
5.0% - 10.0%
10.0% - 25.0%
25.0% - 50.0%
>50.0%
Link
Destination
Origin
D
0 0,5 1 2
Kilometers

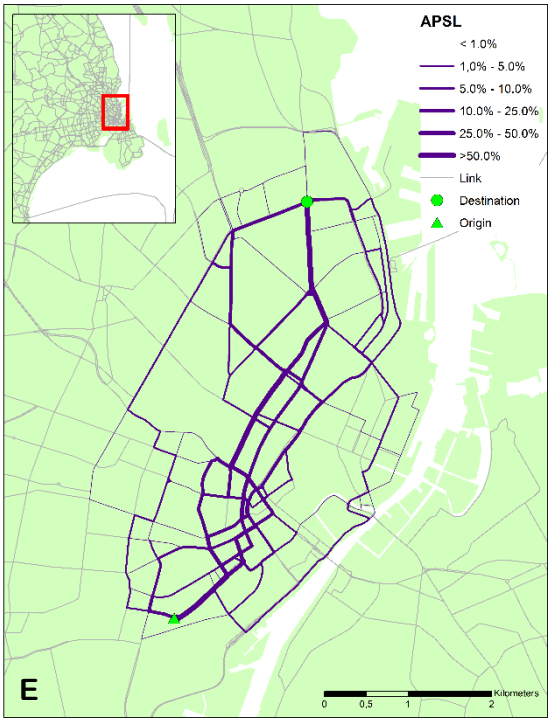

Fig. 2.31. Real-life case study: OD 2 plotted link choice probabilities from the estimated models for a single observation. **A:** Observed route. **B:** MNL. **C:** PSL. **D:** GPSL. **E:** APSL.

	MNL	PSL	GPSL	APSL
OD 1	0.101	0.110	0.150	0.261
OD 2	0.0004	0.0024	0.0042	0.0025

Table 2.7. Real-life case study: OD 1 & OD 2 observed route choice probabilities for the different estimated models.

For Path Size Logit models, the utility for route $i \in R_m$ is comprised of a cost component $-\theta c_{m,i}$ and a path-size component $\beta \ln(\gamma_{m,i})$, i.e. so that the utility is $V_{m,i} = -\theta c_i + \beta \ln(\gamma_i)$. Fig. 2.32A-B plot for OD 1 and OD 2, respectively, the cost components against path size components of the routes under the PSL, GPSL, and APSL models, where the observed route is in red. Fig. 2.33A-B plot the cost and path size components against choice probability. In both cases, universal distinctiveness tends to increase as travel cost increases. For OD 1, the observed route is universally indistinct but low costing, and is the highest choice probability route for all models. The APSL model thus provides the best fit for this observation: the path size contribution factors consider probability ratios and hence the observed route is considered the most attractive and distinct compared to its overlapping routes. The GPSL model reduces the range for the cost components and hence decreases the attractiveness of the observed route according to its cost, which is not compensated for by its distinctiveness, since it is highly correlated with other low costing routes. For OD 2, the observed route is universally distinct but high costing, and has a low choice probability for all models. As discussed above, the GPSL model is able to provide the best fit for these observations.

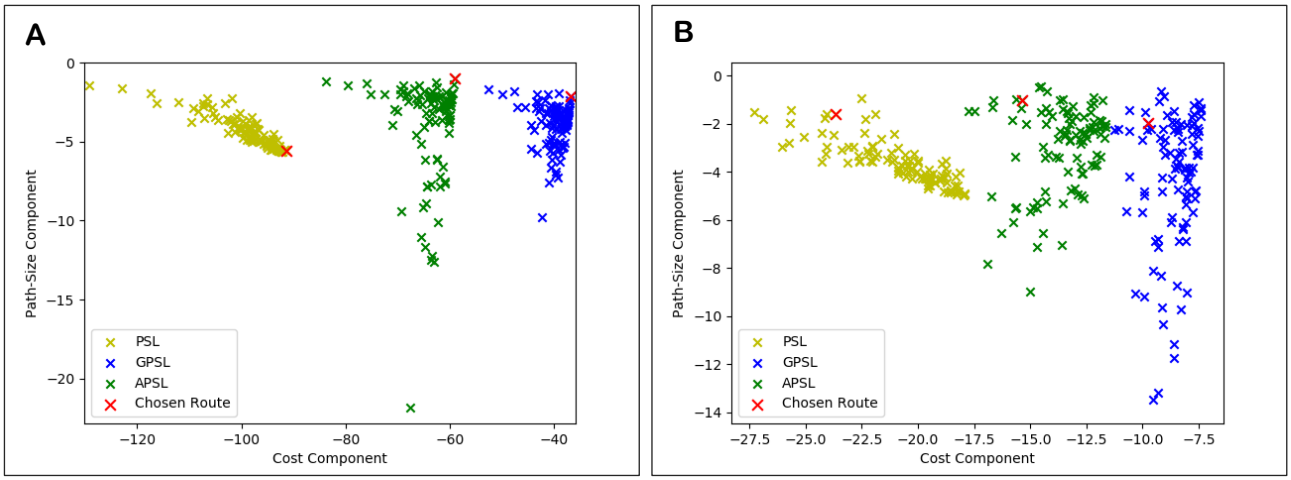

Fig. 2.32. Real-life case study: Cost / Path-Size components of the route utilities from PSL/GPSL/APSL. **A:** OD 1. **B:** OD 2.

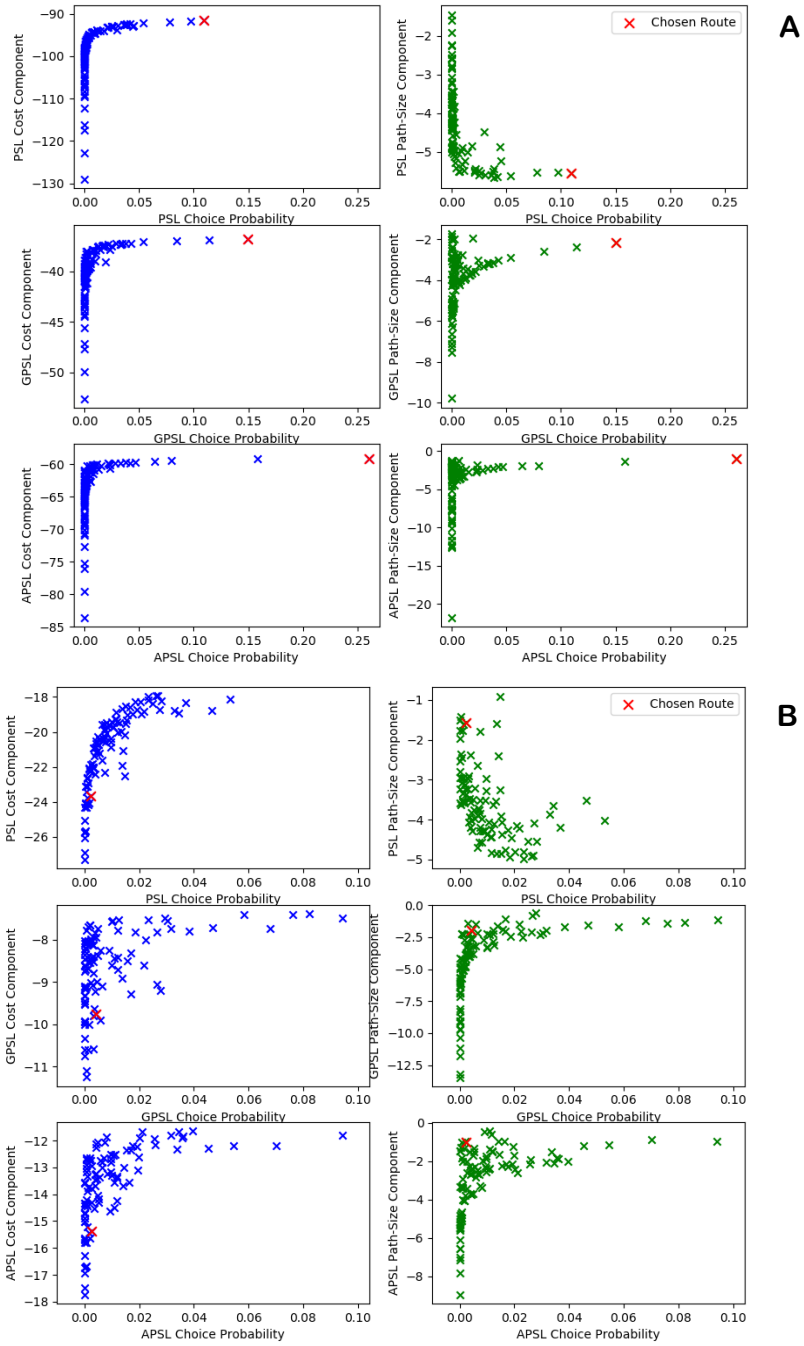

Fig. 2.33. Real-life case study: Choice probability against cost / path-size component for PSL/GPSL/APSL. **A:** OD 1. **B:** OD 2.

The consistency requirement we impose on the APSL model constrains the way that it can mimic the behaviour of the GPSL model, since if parameters are chosen to capture the high costing observations, a price is paid in terms of the feedback effect to the path size correction terms. This confirms that APSL and GPSL are quite different candidate models in the way in which they aim to capture behaviour.

The λ parameter allows the GPSL model to improve the choice probabilities of high costing, distinct route observations one might consider as being outliers / route choice decisions made according to unobserved attributes, though not by design. It seems unlikely that the GPSL model was formulated anticipating extremely large values of λ (such as 91.95) given the exponential nature of the path size contribution factors. In fact, Ramming (2002) estimates the proposed exponential formulation and finds $\lambda = \infty$ provides the best fit to the data, which does not seem reasonable. Moreover, Ramming (2002) hypothesises that the path size contribution factor should 'split the link size contributions more severely than MNL would split path shares, or counter-intuitive predictions will result', though a reason is not given. It's difficult to know what a

'sensible' restriction would be that one could impose upon the λ parameter so that the GPSL model behaves according to a more feasible theoretical interpretation. Bekhor & Prato (2006) utilise $\lambda = 9$, Hoogendoorn-Lanser (2005) utilises $\lambda = 20$, and Prato (2009) claims optimal values vary between 10 and 15, though these values still seem large. Table 2.8 displays the results from estimating the GPSL model with a restriction imposed upon λ so that $\lambda \leq 10$. As anticipated, the optimal value for λ is at the bound (equal to 10), but the Log-Likelihood value no longer beats the GPSL$'_{(\lambda=\theta)}$ and APSL models. What is also interesting is that the estimated β value is almost 2, which is very large seeming the theory suggests it should be around 1. This supports the theory that the GPSL path size components are capturing something other than the correlation.

	$\hat{\alpha}_1$	$\hat{\alpha}_2$	$\hat{\beta}$	$\hat{\lambda}$	LL
MNL	0.777	0.330			-21308
PSL	0.966	0.306	1.347		-20581
GPSL ($\lambda \leq 10$)	0.769	0.160	1.943	10	-19312
GPSL	0.415	0.085	1.186	91.95	-17874
GPSL$'_{(\lambda=\theta)}$	0.691	0.154	1.807		-19152
APSL	0.633	0.184	0.840		-18978

Table 2.8. Real-life case-study: Estimation results including GPSL with λ restricted to $\lambda \leq 10$.

6. Summary and Scope for Further Research

Due to their comparatively low computational cost and relative ease in obtaining reasonable estimates for parameters, Path Size Logit route choice models are a useful and practical approach to approximating the correlation between routes. Existing Path Size Logit models, however, have some key theoretical weaknesses: for PSL the presence of unrealistic routes in a choice set negatively impacts the choice probabilities of realistic routes when links are shared, and for GPSL there are internal inconsistency issues which can have negative implications, for example routes which are defined as unrealistic by the path size terms may not be routes with low choice probabilities. The intricacies of the issues with existing Path Size Logit models are demonstrated in the paper, and a new APSL model is proposed which provides a potential solution to these issues. The APSL model proposes that routes contribute to path size terms according to probability ratios, and choice probability solutions to the model are solutions to the fixed-point problem involving the probabilities.

The paper proves that choice probability solutions to the APSL model are guaranteed to exist, and proves that values of b exist such that APSL solutions are unique for β in the range $0 \leq \beta \leq b$. Though there are cases where solutions are unique for all $\beta \geq 0$, in most cases there is a maximum value for b (b_{max}). β in the range $0 \leq \beta \leq b_{max}$ is however only a sufficient condition for unique APSL solutions, β_{max} is the true maximum value where solutions are unique for β in the range $0 \leq \beta \leq \beta_{max}$, and a method is proposed in the paper for estimating β_{max}.

To show that the parameters of the APSL model can be estimated, a Maximum Likelihood Estimation procedure is proposed for estimating APSL with tracked route observation data. This procedure is then first investigated in a simulation study on the Sioux Falls network where it is shown that it is generally possible to reproduce assumed true parameters. The APSL model is then estimated using real tracked route GPS data on a large-scale network. Results show that the APSL outperforms the MNL and PSL models with the same number of model parameters, while the GPSL model outperforms APSL due to the added flexibility an additional parameter provides.

The APSL model requires a fixed-point algorithm to approximate solutions. The paper assesses the computational performance of the FPIM for calculating choice probabilities and estimating the parameters of the APSL model, where accuracy is compared with computation time. Results indicate that accurate choice probability solutions and parameter estimates can be obtained from feasible computation times.

Future research should explore the application of the APSL model within a Stochastic User Equilibrium framework, which could involve exploring whether one can combine the fixed-point iterations used for APSL with those used for congestion, so that they are performed simultaneously.

As noted in our numerical experiments, the consistency condition that we impose in the APSL model, while offering improvements over PSL, constrains the extent to which the model is able to compete with the

GPSL model in terms of model-fit, with the additional parameter in the GPSL model allowing it to de-couple the scale of the model from the path-size effect, albeit at the price of inconsistency. A natural path for future research could be to explore the potential for developing generalised forms of APSL, in the spirit of GPSL, allowing an extra dimension (parameter) to fit, but without sacrificing the requirement for consistency.

7. Acknowledgements

We gratefully acknowledge funding provided by the University of Leeds by awarding the corresponding author with a University of Leeds Doctoral Scholarship for PhD research, and, the financial support of the Independent Research Fund Denmark to the project "Using Big Data sources for the consistent estimation of next-generation route choice models". We would also like to thank three anonymous referees for their highly constructive criticism, which helped in improving earlier versions of this paper.

8. References

Ahipasaoglu S, Meskarian R, Magnanti T.L, & Natarajan K, (2015). Beyond normality: A cross moment stochastic user equilibrium model. Transportation Research Part B, 81(2), p.333-354.

Ahipasaoglu S, Arikan U, Natarajan K, (2016). On the flexibility of using marginal distribution choice models in traffic equilibrium. Transportation Research Part, 91, p.130-158.

Bekhor S, & Prashker J, (1999). Formulations of extended logit stochastic user equilibrium assignments. In: Proceedings of the 14th International Symposium on Transportation and Traffic Theory, Jerusalem, Israel, p.351–372.

Bekhor S, & Prashker J, (2001) Stochastic user equilibrium formulation for the generalized nested logit model. Transportation Research Record, 1752, p.84–90.

Bekhor S, & Prato C, (2006). Effects of choice set composition in route choice modeling. Proceedings of the 11th International Conference on Travel Behavior Research, Kyoto, Japan.

Bekhor S, Ben-Akiva M, & Ramming M, (2002). Adaptation of logit kernel to route choice situation. Transportation Research Record, 1805, p.78–85.

Bekhor S, Chorus C, & Toledo T, (2012). Stochastic user equilibrium for route choice model based on random regret minimization. Transportation Research Record, 2284(1), p.100-108.

Ben-Akiva M, & Ramming S, (1998). Lecture notes: discrete choice models of traveler behavior in networks. Prepared for Advanced Methods for Planning and Management of Transportation Networks. Capri, Italy.

Ben-Akiva M, & Bierlaire M, (1999). Discrete choice methods and their applications to short term travel decisions. In: Halled, R.W. (Ed.), Handbook of Transportation Science. Kluwer Publishers.

Ben-Akiva M, & Bolduc D, (1996). Multinomial probit with a logit kernel and a general parametric specification of the covariance structure. Working Paper.

Bierlaire M, (2002). The Network GEV Model. Conference paper STRC 2002.

Bovy P, & Fiorenzo-Catalano S, (2007). Stochastic Route Choice Set Generation: Behavioral and Probabilistic Foundations. Transportmetrica, 3, p.173–189.

Bovy P, Bekhor S, & Prato C, (2008). The Factor of Revisited Path Size: Alternative Derivation. Transportation Research Record: Journal of the Transportation Research Board, 2076, Transportation Research Board of the National Academies, Washington, D.C., p.132–140.

Byrd R, Lu P, Nocedal J, & Zhu C (1994). A Limited Memory Algorithm for Bound Constrained Optimization. Technical Report NAM-08, Northwestern University, Department of Electrical Engineering and Computer Science.

Cantarella G, & Binetti M, (2002). Stochastic assignment with gammit path choice models. Patriksson, M., Labbé's, M. (Eds.), Transportation Planning: State of the Art, p.53–68.

Cascetta E, Nuzzolo A, Russo F, & Vitetta A, (1996). A modified logit route choice model overcoming path overlapping problems: specification and some calibration results for interurban networks. In: Proceedings of the 13th International Symposium on Transportation and Traffic Theory, Leon, France, p.697–711.

Castillo E, Menéndez J, Jiménez P, & Rivas A, (2008). Closed form expression for choice probabilities in the Weibull case. Transportation Research Part B, 42(4), p.373–380.

Chikaraishi M, & Nakayama S, (2016). Discrete choice models with q-product random utilities. Transportation Research Part B, 93, p.576–595.

Chorus C, (2010). A New Model of Random Regret Minimization. EJTIR, 10(2), p.181-196.

Chu C, (1989). A paired combinatorial logit model for travel demand analysis. In: Proc. Fifth World Conference on Transportation Research, Ventura, Calif. 4, p.295–309.

Connors R, Hess S, & Daly A, (2014). Analytic approximations for computing probit choice probabilities, Transportmetrica A: Transport Science, 10(2), p.119-139.

Daganzo C, & Sheffi Y, (1977). On stochastic models of traffic assignment. Transportation Science, 11, p.253–274.

Daly A, & Bierlaire M, (2006). A general and operational representation of Generalised Extreme Value models. Transportation Research Part B, 40, p.285–305.

Damberg O, Lundgren J, & Patriksson M, (1996). An algorithm for the stochastic user equilibrium problem, Transportation Research, 30B, p.115–131.

Dial R, (1971). A probabilistic multipath traffic assignment model which obviates path enumeration. Transportation Research, 5(2), p.83-111.

Frejinger E, & Bierlaire M, (2007). Capturing correlation with subnetworks in route choice models. Transportation Research Part B, 41(3), p.363-378.

Fosgerau M, & Bielaire M, (2009). Discrete choice models with multiplicative error terms. Transportation Research Part B, 43, p.494-505.

Gliebe J, Koppleman F, & Ziliaskopoulos A, (1999). Route choice using a paired combinatorial logit model. Presented at the 78th Annual Meeting of the Transportation Research Board, Washington, DC.

Horowitz J, (1983). Statistical Comparison of Non-Nested Probabilistic Discrete Choice Models. Transportation Science, 17(3), p.319-350

Hoogendoorn-Lanser S, (2005). Modelling travel behaviour in multi-modal networks. Ph.D. Thesis, TRAIL Research School, Technical University of Delft, The Netherlands.

Isaacson E, & Keller H, (1966). Analysis of Numerical Methods. John Wiley & Sons, Inc., New York, USA.

Johnson L, & Scholz D, (1968). On Steffensen's Method. SIAM Journal on Numerical Analysis, 5 (2), p.296-302.

Kitthamkesorn S, & Chen A, (2013). Path-size weibit stochastic user equilibrium model. Transportation Research Part B, 57, p.378-397.

Kitthamkesorn S, & Chen A, (2014). Unconstrained weibit stochastic user equilibrium with extensions. Transportation Research Part B, 59, p.1-21.

Li B, (2011). The multinomial logit model revisited: A semi-parametric approach in discrete choice analysis. Transportation Research Part B, 45, p.461–473.

Manzo S, Prato C & Nielsen O, (2015). How uncertainty in input and parameters influences transport model outputs: a four-stage model case-study. Elsevier, Transport Policy, 38, p.64-72.

Marzano V & Papola A, (2008). On the covariance structure of the cross-nested logit model. Transportation Research Part B, 42(2), p.83–98

McFadden D, & Train K, (2000). Mixed MNL models for discrete response. Journal of Applied Econometrics, 15 (5), p.447–470.

McFadden D, (1978). Modeling the choice of residential location. In: Anders, Karlqvist., Lars, Lundqvist., Folke, Snickars., Jorgen, Weibull. (Eds.), Special interaction theory and planning models. North-Holland, Amsterdam, p.75–96.

Nakayama S, & Chikaraishi M, (2015). Unified closed-form expression of logit and weibit and its extension to a transportation network equilibrium assignment. Transportation Research Part B, 81, p.672–685.

Natarajan K, Song M, & Teo C.P, (2009). Persistency Model and Its Applications in Choice Modeling. Management Science, 55(3), p.453-469

Nielsen O, & Frederiksen R, (2006). Optimisation of timetable-based, stochastic transit assignment models based on MSA. Annals of Operations Research. 144 (1), p.263-285. Kluwer.

Nielsen O, (2000). A Stochastic Transit Assignment Model Considering Differences in Passengers Utility Functions. Transportation Research Part B Methodological, 34 (5), p.377–402. Elsevier Science Ltd.

Prashker J, & Bekhor S, (2004). Route choice models used in the stochastic user equilibrium problem: a review. Transport Reviews, 24 (4), p.437–463.

Prato C, & Bekhor S, (2006). Applying branch & bound technique to route choice set generation. Transportation Research Record, 1985, p.19-28.

Prato C, (2005). Latent factors and route choice behaviour. Ph.D. Thesis, Turin Polytechnic, Italy.

Prato C, (2009). Route choice modeling: past, present and future research directions. Journal of Choice Modelling, 2 (1), p.65–100.

Prato C, (2014). Expanding the applicability of random regret minimization for route choice analysis. Transportation, (41), p.351–375.

Prato C, Rasmussen T, & Otto N, (2014). Estimating Value of Congestion and of Reliability from Observation of Route Choice Behavior of Car Drivers. Transportation Research Record: Journal of the Transportation Research Board, 2412, p.20–27.

Pravinvongvuth S, & Chen A, (2005). Adaptation of the paired combinatorial logit model to the route choice problem. Transportmetrica, 1 (3), p.223–240.

Ramming S, (2002). Network knowledge and route choice. Ph.D. Thesis, Massachusetts Institute of Technology, Cambridge, USA.

Rasmussen T, Nielsen O, Watling D, & Prato C, (2016). The Restricted Stochastic User Equilibrium with Threshold model: Large-scale application and parameter testing. European Journal of Transport Infrastructure Research (EJTIR). 17 (1), p.1-24

Rich J, & Nielsen, O, (2015). System convergence in transport models: algorithms efficiency and output uncertainty. European Journal of Transport Infrastructure Research (EJTIR), 15 (3), p.38-62.

Sheffi Y, (1985). Urban Transportation Networks: Equilibrium Analysis with Mathematical Programming Methods. Prentice-Hall.

Swait J, & Ben-Akiva M, (1984). Incorporating Random Constraints in Discrete Choice Models: An Application to Mode Choice in Sao Paulo, Brazil. Transportation Research Part B, 21(2), p.103-115.

Vovsha P, (1997). Application of cross-nested logit model to mode choice in Tel Aviv, Israel, Metropolitan Area. Transportation Research Record 1607, p.6–15.

Watling D, Rasmussen T, Prato C, & Nielsen O, (2018). Stochastic user equilibrium with a bounded choice model. Transportation Research Part B, 114, p.254-280.

Wen C, & Koppelman F, (2001). The generalized nested logit model. Transportation Research Part B, 35 (7), p.627–641.

Xu X, Chen A, Kitthamkesorn S, Yang H, & Lo H.K, (2015). Modeling absolute and relative cost differences in stochastic user equilibrium problem. Transportation Research Part B, 81, p.686-703.

9. Appendix

9.1 Appendix A - Discontinuity issue with APSL path size terms when allowing zero choice probabilities

The APSL path size term for route $i \in R$ is given by:

$$\gamma_i^{APS}(\boldsymbol{P}) = \sum_{a \in A_i} \frac{t_a}{c_i} \frac{P_i}{\sum_{k \in R} P_k \delta_{a,k}}.$$

The issue is that there are three possible values for $\lim_{\sum_{k \in R} P_k \delta_{a,k} \to 0} \frac{P_i}{\sum_{k \in R} P_k \delta_{a,k}}$:

a) $\lim_{P_i \to 0} \left(\lim_{\sum_{k \in R; k \neq i} P_k \delta_{a,k} \to 0} \frac{P_i}{P_i + \sum_{k \in R; k \neq i} P_k \delta_{a,k}} \right) = 1,$

b) $\lim_{\sum_{k \in R; k \neq i} P_k \delta_{a,k} \to 0} \left(\lim_{P_i \to 0} \frac{P_i}{P_i + \sum_{k \in R; k \neq i} P_k \delta_{a,k}} \right) = 0,$

c) $\lim_{\substack{\sum_{k \in R_m; k \neq i} P_k \delta_{a,k} \to 0 \\ P_i \to 0}} \frac{P_i}{P_i + \sum_{k \in R; k \neq i} P_k \delta_{a,k}} = \frac{1}{\sum_{k \in R} \delta_{a,k}}.$

To demonstrate this, consider the Appendix A example network in Fig. 2.34 where there are 9 routes.

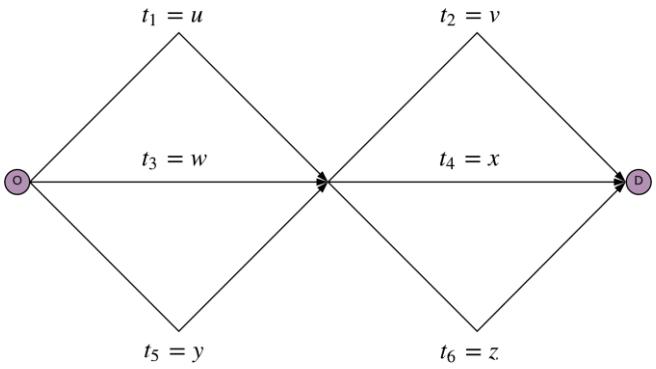

Fig. 2.34 Appendix A example network.

Route 1: 1 → 2, Route 2: 1 → 4, Route 3: 1 → 6,
Route 4: 3 → 2, Route 5: 3 → 4, Route 6: 3 → 6,
Route 7: 5 → 2, Route 8: 5 → 4, Route 9: 5 → 6.

Suppose $u = v = w = x = y = z = 1$, and let $P_1 = P_2 = P_3 = \frac{1-P_4}{3}$, $P_4 \in [0,1]$, $P_5 = P_6 = P_7 = P_8 = P_9 = 0$. As $P_4 \to 1$, $P_1 = P_2 = P_3 \to 0$, and the path size terms for Route 1, Route 2, and Route 5 as $P_4 \to 1$ are:

$$\lim_{P_4 \to 1} \gamma_1^{APS}(\boldsymbol{P}) = \lim_{P_4 \to 1} \left(\left(\frac{1}{2}\right) \cdot \left(\frac{P_1}{P_1 + P_2 + P_3} \right) + \left(\frac{1}{2}\right) \cdot \left(\frac{P_1}{P_1 + P_4 + P_7} \right) \right)$$

$$= \left(\frac{1}{2}\right) \cdot \left(\lim_{\substack{P_2 + P_3 \to 0 \\ P_1 \to 0}} \frac{P_1}{P_1 + P_2 + P_3} \right) + \left(\frac{1}{2}\right) \cdot \left(\lim_{\substack{P_4 \to 1 \\ P_1 \to 0}} \left(\lim_{P_7 \to 0} \frac{P_1}{P_1 + P_4 + P_7} \right) \right)$$

$$= \left(\frac{1}{2}\right) \cdot \left(\frac{1}{3}\right) + \left(\frac{1}{2}\right) \cdot (0) = \frac{1}{6}$$

$$\lim_{P_4 \to 1} \gamma_2^{APS}(\boldsymbol{P}) = \lim_{P_4 \to 1} \left(\left(\frac{1}{2}\right) \cdot \left(\frac{P_2}{P_1 + P_2 + P_3} \right) + \left(\frac{1}{2}\right) \cdot \left(\frac{P_2}{P_2 + P_5 + P_8} \right) \right)$$

$$= \left(\frac{1}{2}\right) \cdot \left(\lim_{\substack{P_1 + P_3 \to 0 \\ P_2 \to 0}} \frac{P_2}{P_1 + P_2 + P_3} \right) + \left(\frac{1}{2}\right) \cdot \left(\lim_{P_2 \to 0} \left(\lim_{P_5 + P_8 \to 0} \frac{P_2}{P_2 + P_5 + P_8} \right) \right)$$

$$= \left(\frac{1}{2}\right) \cdot \left(\frac{1}{3}\right) + \left(\frac{1}{2}\right) \cdot (1) = \frac{2}{3}$$

$$\lim_{P_4 \to 1} \gamma_5^{APS}(\boldsymbol{P}) = \lim_{P_4 \to 1} \left(\left(\frac{1}{2}\right) \cdot \left(\frac{P_5}{P_4 + P_5 + P_6} \right) + \left(\frac{1}{2}\right) \cdot \left(\frac{P_5}{P_2 + P_5 + P_8} \right) \right)$$

$$= \left(\frac{1}{2}\right) \cdot \left(\lim_{P_4 \to 1} \left(\lim_{\substack{P_5 \to 0 \\ P_6 \to 0}} \frac{P_5}{P_4 + P_5 + P_6} \right) \right) + \left(\frac{1}{2}\right) \cdot \left(\lim_{P_2 \to 0} \left(\lim_{\substack{P_5 \to 0 \\ P_8 \to 0}} \frac{P_5}{P_2 + P_5 + P_8} \right) \right)$$

$$= \left(\frac{1}{2}\right) \cdot (0) + \left(\frac{1}{2}\right) \cdot (0) = 0$$

Thus, at $P_4 = 1$ where $P_1 = P_2 = P_3 = P_5 = P_6 = P_7 = P_8 = P_9 = 0$, many cases of $\sum_{k \in R} P_k \delta_{a,k} = 0$ occur, but $\lim_{\sum_{k \in R} P_k \delta_{a,k} \to 0} \frac{P_i}{\sum_{k \in R} P_k \delta_{a,k}}$ either equals 1, 0, or $\frac{1}{3}$, and hence defining the path size terms as either:

$$\gamma_i^{APS}(\boldsymbol{P}) = \sum\nolimits_{a \in A_i} \frac{t_a}{c_i} \times \begin{cases} \dfrac{P_i}{\sum_{k \in R} P_k \delta_{a,k}} & if \sum_{k \in R} P_k \delta_{a,k} > 0 \\ 1 & if \sum_{k \in R} P_k \delta_{a,k} = 0 \end{cases},$$

$$\gamma_i^{APS}(\boldsymbol{P}) = \sum\nolimits_{a \in A_i} \frac{t_a}{c_i} \times \begin{cases} \dfrac{P_i}{\sum_{k \in R} P_k \delta_{a,k}} & if \sum_{k \in R} P_k \delta_{a,k} > 0 \\ 0 & if \sum_{k \in R} P_k \delta_{a,k} = 0 \end{cases},$$

or,

$$\gamma_i^{APS}(\boldsymbol{P}) = \sum\nolimits_{a \in A_i} \frac{t_a}{c_i} \times \begin{cases} \dfrac{P_i}{\sum_{k \in R} P_k \delta_{a,k}} & if \sum_{k \in R} P_k \delta_{a,k} > 0 \\ \dfrac{1}{\sum_{k \in R} \delta_{a,k}} & if \sum_{k \in R} P_k \delta_{a,k} = 0 \end{cases},$$

does not ensure continuity.

Chapter 3. Formulation and solution of Adaptive Path Size Logit Stochastic User Equilibrium – addressing choice set robustness and internal consistency

Lawrence Christopher DUNCAN [a], David Paul WATLING [a], Richard Dominic CONNORS [a,b], Thomas Kjær RASMUSSEN [c], Otto Anker NIELSEN [c]

[a] Institute for Transport Studies, University of Leeds
36-40 University Road, Leeds, LS2 9JT, United Kingdom.

[b] University of Luxembourg, Faculté des Sciences, des Technologies et de Médecine,
Maison du Nombre, 6 Avenue de la Fonte, L-4364, Esch-sur-Alzette, Luxembourg.

[c] Department of Technology, Management and Economics, Technical University of Denmark
Bygningstorvet 116B, 2800 Kgs. Lyngby, Denmark.

Highlights

- Stochastic User Equilibrium (SUE) conditions for Adaptive Path Size Logit (APSL)
- Existence proof for APSL SUE solutions & uniqueness conditions demonstrated
- Numerical experiments demonstrating computational feasibility for APSL SUE
- Internally consistent SUE formulations for correlation-based route choice models
- Computational performance and choice set robustness assessed for all SUE models

Abstract

The Stochastic User Equilibrium (SUE) traffic assignment model is a well-known approach for investigating the behaviours of travellers on congested road networks. SUE compensates for driver/modelling uncertainty of the route travel costs by supposing the costs include stochastic terms. Two key challenges for SUE modelling, however, are capturing route correlations and dealing with unrealistic routes. Numerous correlation-based SUE models have been proposed, but issues remain over both internal consistency and choice set robustness. This paper explores both internal consistency and choice set robustness for correlation-based SUE models. We formulate internally consistent SUE formulations for GEV structure and correction term correlation-based route choice models, where the functional forms in the correlation components are based upon generalised, flow-dependent congested costs, rather than e.g. length / free-flow travel time as done typically. Without explicit mechanisms for dealing with unrealistic routes in the adopted choice sets, however, there are questions on how robust these models are to choice set mis-generation.

The paper therefore develops the foundation for an SUE application of the Adaptive Path Size Logit (APSL) route choice model, as introduced by Duncan et al (2020). APSL captures correlations between routes by including correction terms within the route utilities. It offers an internally consistent approach to reducing the negative impact that unrealistic route alternatives have on the correction terms and thus on the choice probabilities of realistic routes. To do this, APSL uses choice probability ratio path size contribution factors to weight the correction terms; consequently, the model is naturally expressed as a fixed-point problem. This paper establishes SUE conditions for the APSL model, where flow-dependent, generalised costs are used consistently in all components: route costs as well as path size correction terms. The paper proves that APSL SUE solutions exist. Then it shows that the potentially onerous requirement of solving fixed-point problems to compute APSL choice probabilities can be circumvented, since at SUE the route flow proportions and choice probabilities equate. As we show, one can tune the APSL SUE algorithm by trading-off the accuracy of APSL probabilities (and thus computation times of each iteration) with rate of SUE convergence. The advantages of APSL SUE are demonstrated in numerical experiments on the Sioux Falls and Winnipeg networks, where computational performance, choice set robustness, and flow results are compared with the internally consistent SUE formulations of GEV structure and correction term correlation-based route choice models.

APSL SUE solution uniqueness is explored numerically where results suggest that uniqueness conditions exist.

Key Words: adaptive path size logit, stochastic user equilibrium, fixed-point, convergence, internal consistency, choice set robustness

1. Introduction

The Stochastic User Equilibrium (SUE) traffic assignment model proposed by Daganzo & Sheffi (1977) is a well-known approach for investigating the behaviours of travellers on congested road networks. SUE relaxes the perfect information assumption of the Deterministic User Equilibrium model by supposing that route choice is based on costs that include stochastic terms. This accounts for the differing perceptions travellers have of the attractiveness of routes. A specific challenge when developing a route choice model for SUE is capturing correlations between overlapping routes. There is a trade-off: accurately capturing route correlation in a behaviourally realistic way requires a more complex route choice model, but this results in computational challenges for solving for SUE (e.g. long computation times, sensitivity of results to sampled choice sets). The aim of this paper is hence to develop a new correlation-based SUE model that seeks to address these issues, and to demonstrate its computational feasibility for large-scale network applications.

Different stochastic route cost terms proposed in the literature give rise to three general types of correlation-based route choice models that have been applied to SUE: GEV structure models (e.g. Cross-Nested Logit (CNL), Generalised Nested Logit (GNL), Paired Combinatorial Logit (PCL)), correction term models (e.g. C-Logit (CL), Path Size Logit (PSL), Path Size Weibit (PSW), Path Size Hybrid (PSH)), and simulation models (e.g. Multinomial Probit (MNP), Multinomial Gammit (MNG)). For a detailed review of correlation-based route choice models see Duncan et al (2020). To set the background for the research in the present paper, we consider each of the categories in turn below, where we review their SUE application.

GEV structure models. Equivalent Mathematical Programming (MP) formulations for CNL, GNL, and PCL are given by Bekhor & Prashker (1999, 2001). Bekhor & Prashker (2001), Chen et al (2003) and Bekhor et al (2008) provide path-based partial linearization algorithms for solving GNL SUE, PCL SUE, and CNL SUE, respectively. However, though the PCL, CNL, and GNL models all have closed-form probability expressions, due to their two-level tree structure the choice probabilities and in particular MP formulations are complex to compute, where the computational burden escalates significantly as the scale of network / choice set sizes increase. Pre-determined, exact, and inexact line search schemes have been investigated to assess computational trade-off, i.e. where the computation time required to perform each iteration is compared with the number of iterations required for convergence (Bekhor & Prashker, 2001; Bekhor et al 2008; Chen et al, 2014).

Correction term models. Zhou et al (2012) give equivalent MP and variational inequality formulations for Length-based CL SUE (LCL SUE) and Congestion-based CL SUE (CCL SUE), where length and congestion based refers to whether the correction term is computed using length or congestion-dependent travel cost. Chen et al (2012), Kitthamkesorn & Chen (2013), and Xu et al (2015) give equivalent MP formulations for PSL SUE, PSW SUE, and PSH SUE, respectively. Chen et al (2012) present a path-based partial linearization algorithm for solving LCL SUE and PSL SUE. Zhou et al (2012) present a path-based Gradient Projection algorithm for solving LCL SUE and CCL SUE, and Xu et al (2012) and Chen et al (2013) assess the computational trade-off for different step-size strategies. Kitthamkesorn & Chen (2013) develop a path-based partial linearization algorithm for solving PSW SUE, and Kitthamkesorn & Chen (2014) propose a link-based algorithm. The main attraction of correction term models for solving SUE is that they have simple closed-form expressions, meaning the route choice probabilities and MP formulations are generally easy and quick to compute; however, more complex models can capture correlations more accurately.

Simulation models. Sheffi (1985) formulates MNP SUE as a mathematical programme and presents a flow-averaging solution algorithm. Cantarella & Binetti (2002) give flow-averaging and cost-averaging algorithms for solving MNG SUE. The issue for these models is that they do not have closed-form probability expressions, and so evaluating the route choice probabilities requires either Monte Carlo simulation or alternative methods, all of which are computationally burdensome, particularly in large-scale applications (Rasmussen et al, 2017). One specific problem is accurately computing route choice probabilities that are small, which is common when there are many routes. Increasing the accuracy of choice probability

computation substantially adds to the computational burden. Sheffi (1985) explores the computational trade-off between the number of simulation samples and SUE convergence rates.

Upon selection of which correlation-based SUE model to employ in large-scale network applications, one must trade-off the anticipated accuracy of results with the computational burden and/or convergence of applicable solution algorithms. Simulation SUE models are attractive behaviourally due to their ability to accurately capture route correlation. Moreover, solution methods do not necessarily require explicit route generation and thus the accuracy of results is not necessarily dependent upon the choice sets generated, though, without route generation, with flows being assigned in theory to all routes, unrealistic routes will still have a negative influence on results. The main issues however, are that a) due to the random nature in which the search direction is obtained in typical simulation-based algorithms, there are difficulties in suitably measuring flow convergence (Sheffi, 1985), and b) numerous studies have found very slow convergence on large-scale networks (Rich & Nielsen, 2015; Manzo et al, 2015; Rasmussen et al, 2017; Connors et al, 2014). GEV structure and correction term models on-the-other-hand do not require random simulation to compute choice probabilities, and search directions can be computed exactly. This means that convergence can be suitably measured, and more optimal step-size schemes / algorithms can be developed for better convergence. However, theoretically undesirable trade-offs are often made to improve computational performance. There are two common types of such trade-offs.

The first trade-off is between desirable behavioural features for the SUE model and the ability to solve it more efficiently. An SUE model is internally consistent if the same definition of generalised cost is used in all components of the specification. This is often overlooked in the SUE formulations of GEV structure and correction term models so that solution methods are simpler/quicker to implement. In SUE application where the travel costs within the deterministic utilities are flow-dependent (congested), for consistency, the route similarity features (PCL, CL) or link-route prominence features (CNL, GNL, PSL, PSW, PSH) in the correlation components should also be based upon the congested cost. Most studies use topological length or uncongested cost (free-flow travel time) for these features, however this may be inaccurate behaviourally since a short route can have a large congested travel cost, and vice versa.

The second trade-off is between the sizes of the choice sets generated (pre or column generated) and the ability to solve efficiently. Typical road networks have many very costly routes that should be considered unrealistic and excluded from route choice. In large-scale case studies, choice sets are typically generated to be large enough that one can be fairly certain the realistic alternatives are present, regardless of how many unrealistic routes are generated. However, for many GEV structure and correction term SUE models, the computational burden of solution algorithms increases dramatically as the number of routes increases, which limits how large the choice sets can be generated. Furthermore, many of the models are not choice set robust, and results are thus negatively influenced by the presence of unrealistic routes as well as highly sensitive to the choice set generation method adopted (Bovy et al, 2008; Bliemer & Bovy, 2008; Ramming, 2002; Ben-Akiva & Bierlaire, 1999; Duncan et al, 2020).

Motivated by the above challenges, we set out to develop a correlation-based SUE model that addresses both internal consistency and choice set robustness, and is computationally feasible in large-scale network applications. Due to the aforementioned difficulties in suitably measuring flow convergence, and the reported slow convergence on large-scale networks, we did not consider advancing simulation SUE models to be a worthwhile approach. We instead looked to advance GEV structure and/or correction term SUE models. Zhou et al (2012), Xu et al (2012), and Chen et al (2013) explore an internally consistent SUE formulation for the CL model (CCL SUE), where the CCL commonality factors capture the similarity between routes according to their shared flow-dependent congested cost. However, internally consistent SUE formulations are yet to be explored for other GEV structure and correction term models. In this paper, we address this by formulating and solving internally consistent SUE formulations for the CNL, GNL, PCL, and PSL models, where the route similarity or link-route prominence features are based upon generalised, flow-dependent congested cost. We assess the choice set robustness for these models (including CCL SUE), and evaluate their computational performances, including for different sizes of choice sets and scale of network.

None of these models, however, have explicit mechanisms for dealing with unrealistic routes within the adopted choice sets, and thus there are questions over how well these models perform in terms of choice set robustness. For the PSL model, a mechanism has been proposed for dealing with unrealistic routes: to weight

the contributions of routes to path size terms, with path size contribution factors. This relaxes the importance of obtaining accurate choice sets of realistic routes, since the negative effects of any present unrealistic routes within the choice sets are reduced. The Generalised PSL (GPSL) model (Ramming, 2002) proposes a path size contribution factor based on travel cost ratios to reduce the contributions of costly routes. However, as we discussed and demonstrated in Duncan et al (2020), GPSL is not internally consistent within the specification of the choice model, since in their definitions of unrealistic, the path size terms consider only travel cost, whereas the route choice probability relation considers disutility *including* the correction term.

Solving this, we then in Duncan et al (2020) proposed the Adaptive Path Size Logit (APSL) model where the path size contribution factors are based upon ratios of route choice probability. This ensures that APSL is internally consistent within the specification of the choice model, where routes defined as unrealistic by the path size terms – and consequently given reduced path size contributions – are exactly those with very low choice probabilities. APSL provides improved choice set robustness over PSL, and does so in a way that is internally consistent (unlike GPSL). In this paper, we thus investigate the application of APSL to SUE, where to guarantee full internal consistency in the SUE formulation of APSL we stipulate that costs in all components are defined as generalised, flow-dependent congested cost.

Since the APSL path size contribution factors depend upon the route choice probabilities, the probability relation is an implicit function, naturally expressed as a fixed-point problem. The APSL model is thus not closed-form and solving the choice probabilities requires a fixed-point algorithm to compute the solution. This has the potential to be computationally burdensome in large-scale networks even when the travel costs are fixed. However, as we show in this study, the requirement of solving fixed-point problems to compute APSL choice probabilities can be circumvented in SUE application, since at equilibrium the route flow proportions and choice probabilities equate. The useful relationship between choice probabilities and route flow proportions in SUE context allows for a considerable flexibility in solving APSL SUE, where one can trade-off the accuracy of APSL probabilities (and thus computation times of each iteration) with rate of SUE convergence.

The structure of the paper is as follows. In Section 2. we introduce congested network notation. In Section 3. we establish SUE conditions for the APSL model, prove the existence of solutions, and discuss uniqueness. In Section 4. we conduct numerical experiments to assess computational performance and choice set robustness, compare flow results, and investigate APSL SUE solution uniqueness. In Section 5. we conclude the paper.

2. Congested Network Notation

A road network consists of link set A and $m = 1, \dots, M$ OD movements. R_m is the choice set of all simple routes (no cycles) for OD movement m of size $N_m = |R_m|$, where $N = \sum_{m=1}^{M} N_m$ is the total number of routes. $A_{m,i} \subseteq A$ is the set of links belonging to route $i \in R_m$, and $\delta_{a,m,i} = \begin{cases} 1 & if\ a \in A_{m,i} \\ 0 & otherwise \end{cases}$.

The travel demand for OD movement m is $q_m \geq 0$, and $\boldsymbol{Q}_m$ is the $N_m \times N_m$ diagonal matrix of the travel demand for OD movement m (i.e. with q_m on each diagonal element). The flow on route $i \in R_m$ is $f_{m,i}$, and $\boldsymbol{f}_m$ is the N_m-length vector of route flows for OD movement m. $\boldsymbol{f}$ is the N-length vector of all OD movement route flow vectors such that $\boldsymbol{f} = (\boldsymbol{f}_1, \dots \boldsymbol{f}_M)$, where $f_{m,i}$ refers to element number $i + \sum_{k=1}^{m-1} N_k$ in $\boldsymbol{f}$. F denotes the set of all demand-feasible non-negative universal route flow vector solutions:

$$F = \left\{ \boldsymbol{f} \in \mathbb{R}_+^N : \sum_{i \in R_m} f_{m,i} = q_m, m = 1, \dots, M \right\}.$$

Furthermore, x_a denotes the flow on link $a \in A$, and $\boldsymbol{x} = \left(x_1, x_2, \dots, x_{|A|}\right)$ is the vector of all link flows. X denotes the set of all demand-feasible non-negative link flow vectors:

$$X = \left\{ \boldsymbol{x} \in \mathbb{R}_+^{|A|} : \sum_{m=1}^{M} \sum_{i \in R_m} \delta_{a,m,i} f_{m,i} = x_a, \forall a \in A, \boldsymbol{f} \in F \right\}.$$

For link $a \in A$ experiencing a flow of x_a, denote the generalised travel cost for that link as $t_a(x_a)$, where $\boldsymbol{t}(\boldsymbol{x})$ is the vector of all generalised link travel cost functions. In vector/matrix notation, let $\boldsymbol{x}$ and $\boldsymbol{f}$ be column

vectors, and define $\boldsymbol{\Delta}$ as the $|A| \times N$-dimensional link-route incidence matrix. Then the relationship between link and route flows may be written as $\boldsymbol{x} = \boldsymbol{\Delta f}$. Supposing that the travel cost for a route can be attained through summing up the total cost of its links, then the generalised travel cost for route $i \in R_m$, $c_{m,i}$, can be computed as follows: $c_{m,i}\big(\boldsymbol{t}(\boldsymbol{\Delta f})\big) = \sum_{a \in A_{m,i}} t_a(\boldsymbol{\Delta f})$, where $\boldsymbol{c}_m\big(\boldsymbol{t}(\boldsymbol{\Delta f})\big)$ is the vector of generalised travel cost functions for OD movement m.

Let the route choice probability for route $i \in R_m$ be $P_{m,i}$, where $\boldsymbol{P}_m = \big(P_{m,1}, P_{m,2}, \dots, P_{m,N_m}\big)$ is the vector of route choice probabilities for OD movement m, and D_m is the domain of possible route choice probability vectors for OD movement m, $m = 1, \dots, M$.

3. Adaptive Path Size Logit Stochastic User Equilibrium

In this section, we establish SUE conditions for the APSL route choice model, prove the existence of solutions, and discuss solution uniqueness. Since at SUE the route flow proportions and route choice probabilities are equal, APSL SUE can be defined in two different ways. These two definitions are equal at equilibrium, but not equal for any other route flow vector.

In order to appreciate the features of APSL SUE, it is helpful to contrast it with other internally consistent SUE approaches based on alternative route choice models. Therefore, these internally consistent approaches are specified in Appendix A for completeness, and we will refer to them as we introduce the proposed model below.

3.1 Definition 1: APSL SUE

The APSL model provides an internally consistent approach to reducing the negative effects unrealistic routes have on the correction terms (and thus choice probabilities) of realistic routes. To do this, path size contributions are weighted according to ratios of choice probability, and APSL is consequently naturally expressed as a fixed-point problem. Formulation of the APSL model was complicated by the desire to establish existence and uniqueness of solutions. To circumvent issues with the standard APSL formulation, a modified version was proposed where solutions are guaranteed to exist and are unique under determinable conditions. Moreover, the standard formulation can be approximated to arbitrary precision. We thus provide here the definition of and establish SUE conditions for the final proposed definition of APSL, see Duncan et al (2020) for more details on its derivation.

The APSL route choice probabilities for OD movement m, $\boldsymbol{P}_m^*$, (for a choice set of size N_m) are a solution to the fixed-point problem $\boldsymbol{P}_m = \boldsymbol{G}_m\Big(\boldsymbol{g}_m\big(\boldsymbol{c}_m(\boldsymbol{t}), \boldsymbol{\gamma}_m^{APS}(\boldsymbol{t}, \boldsymbol{P}_m)\big)\Big)$, where $G_{m,i}$ for route $i \in R_m$ is:

$$G_{m,i}\Big(g_{m,i}\big(\boldsymbol{c}_m(\boldsymbol{t}), \boldsymbol{\gamma}_m^{APS}(\boldsymbol{t}, \boldsymbol{P}_m)\big)\Big) = \tau_m + (1 - N_m\tau_m) \cdot g_{m,i}\big(\boldsymbol{c}_m(\boldsymbol{t}), \boldsymbol{\gamma}_m^{APS}(\boldsymbol{t}, \boldsymbol{P}_m)\big), \tag{3.1}$$

$g_{m,i}$ for route $i \in R_m$ is:

$$g_{m,i}\big(\boldsymbol{c}_m(\boldsymbol{t}), \boldsymbol{\gamma}_m^{APS}(\boldsymbol{t}, \boldsymbol{P}_m)\big) = \frac{\Big(\gamma_{m,i}^{APS}(\boldsymbol{t}, \boldsymbol{P}_m)\Big)^{\beta} e^{-\theta c_{m,i}(\boldsymbol{t})}}{\sum_{j \in R_m}\Big(\gamma_{m,j}^{APS}(\boldsymbol{t}, \boldsymbol{P}_m)\Big)^{\beta} e^{-\theta c_{m,j}(\boldsymbol{t})}}, \tag{3.2}$$

and, $\gamma_{m,i}^{APS}$ for route $i \in R_m$ is:

$$\gamma_{m,i}^{APS}(\boldsymbol{t}, \boldsymbol{P}_m) = \sum_{a \in A_{m,i}} \frac{t_a}{c_{m,i}(\boldsymbol{t})} \frac{1}{\sum_{k \in R_m}\left(\frac{P_{m,k}}{P_{m,i}}\right)\delta_{a,m,k}}, \qquad \forall \boldsymbol{P}_m \in D_m^{(\tau_m)}, \tag{3.3}$$

$$D_m^{(\tau_m)} = \left\{\boldsymbol{P}_m \in \mathbb{R}_{>0}^{N_m} : \tau_m \le P_{m,i} \le (1 - (N_m - 1)\tau_m), \forall i \in R_m, \sum_{j=1}^{N_m} P_{m,j} = 1\right\}.$$

$\theta > 0$ is the Logit scaling parameter, $\beta \ge 0$ is the path size scaling parameter, and $0 < \tau_m \le \frac{1}{N_m}$, $m = 1, \dots, M$, are the perturbation parameters. $\gamma_{m,i}^{APS}$ (3.3) is the APSL path size term function, $g_{m,i}$ in (3.2) is the choice probability function, and $G_{m,i}$ in (3.1) is the probability adjustment function.

As shown in (3.3), for a choice probability solution $\boldsymbol{P}_m^*$, the contribution of route k to the path size term of route i is weighted according to the ratio of choice probabilities between the routes $\left(\frac{P_{m,k}^*}{P_{m,i}^*}\right)$, and hence unrealistic route alternatives with very low choice probabilities have a diminished contribution to the path size terms of realistic routes with relatively large choice probabilities. The APSL model is thus internally consistent as the probability relation and path size terms both define a route as unrealistic if it has a relatively unattractive combination of travel cost and distinctiveness. Moreover, unlike GPSL (see Appendix A), an additional parameter to scale the path size contributions is not required as this is done implicitly and consistently through the scaling of the probabilities with θ and β. This has practical and behavioural estimation benefits compared to GPSL (Duncan et al, 2020).

The APSL model is not closed-form since the choice probabilities for each OD movement are the solution to a fixed-point problem. The τ_m parameters are not model parameters that require estimating, they are simply a mathematical construct that ensure solutions to the APSL model exist and can be unique; specifically, they ensure that the probability domain $D_m^{(\tau_m)}$ for the fixed-point function $\boldsymbol{G}_m$ is closed and bounded, while avoiding issues occurring from zero choice probabilities. Duncan et al (2020) recommend that only very small values for τ_m are used so that the fixed-point solution obtained is negligibly different to the fixed-point solution if $\tau_m = 0$ (where one would exist). We thus set $\tau_m = 10^{-16}$, $m = 1, \dots, M$, throughout this paper.

Most studies of PSL SUE (see Appendix A), or of SUE models with PSL path size terms, suppose that the link-route prominence feature is represented as the ratio of link-route length, i.e. $\frac{t_a}{c_{m,i}(\boldsymbol{t})} = \frac{l_a}{L_{m,i}}$, where l_a and $L_{m,i}$ are the lengths of link $a \in A$ and route $i \in R_m$, respectively. However, this may be inaccurate in how travellers perceive the prominence of links in a route: a short link may be highly congested and have a greater travel time than a long link that is uncongested, and hence the timely, short link may be perceived as more prominent in the route than the long, quick link. A similar argument can be made for using other uncongested costs, e.g. free-flow travel time. Thus, for internal consistency, the APSL path size term defined in (3.3) above consider generalised travel cost for the link-route prominence feature.

In the context of SUE, the generalised travel costs include congested cost and are thus flow-dependent. Adopting generalised, flow-dependent congested costs for the link-route prominence features, APSL SUE is formulated as follows:

APSL SUE: A universal route flow vector $\boldsymbol{f}^* \in F^{(\boldsymbol{\tau})}$ is an APSL SUE solution iff the route flow vector for OD movement m, $\boldsymbol{f}_m^*$, is a solution to the fixed-point problem

$$\boldsymbol{f}_m = \boldsymbol{Q}_m \boldsymbol{P}_m^*\big(\boldsymbol{t}(\boldsymbol{\Delta f})\big), \qquad m = 1, \dots, M, \tag{3.4}$$

where $\boldsymbol{P}_m^*$ is a route choice probability solution for OD movement m in $\boldsymbol{Y}_m$ to the fixed-point problem

$$\boldsymbol{Y}_m = \boldsymbol{G}_m\left(\boldsymbol{g}_m\left(\boldsymbol{c}_m\big(\boldsymbol{t}(\boldsymbol{\Delta f})\big), \boldsymbol{\gamma}_m^{APS}\big(\boldsymbol{t}(\boldsymbol{\Delta f}), \boldsymbol{Y}_m\big)\right)\right), \tag{3.5}$$

given the universal route flow vector $\boldsymbol{f}$, where $G_{m,i}$, $g_{m,i}$, and $\gamma_{m,i}^{APS}$ are as in (3.1), (3.2), and (3.3), respectively, for route $i \in R_m$, and

$$F^{(\boldsymbol{\tau})} = \left\{ \boldsymbol{f} \in \mathbb{R}_{>0}^N : \tau_m \leq \frac{f_{m,i}}{q_m} \leq (1 - (N_m - 1)\tau_m), \forall i \in R_m, \sum_{i \in R_m} f_{m,i} = q_m, m = 1, \dots, M \right\}.$$

APSL SUE is derived directly by utilising APSL as the underlying route choice model and applying flow-dependent link travel costs. For a given route flow vector and hence setting of the link costs, the APSL fixed-point system must be re-solved, so that the path size contribution factors are consistent with the relative attractiveness of the routes. This ensures that the choice model is internally consistent for all route flow vectors.

The APSL model restricts the domain for the route choice probabilities so that the probabilities for OD movement m must belong to the domain $D_m^{(\tau_m)}$, where $P_{m,i} \geq \tau_m$, $\forall i \in R_m$. Consequently, the set of all demand-feasible universal route flow vector solutions for the APSL SUE model, $F^{(\boldsymbol{\tau})}$, is also restricted, where $f_{m,i} \geq \tau_m q_m$, $\forall i \in R_m$, $m = 1, \dots, M$.

3.2 Definition 2: APSL′ SUE

APSL SUE Definition 2 (APSL′ SUE) is derived indirectly by utilising a new underlying route choice model, that is equivalent to APSL at SUE, but only at SUE. By the definition of SUE, the route flow proportions and route choice probabilities equate at equilibrium. Therefore, APSL′ SUE supposes that the path size contribution factors consider route flow proportion ratios, instead of choice probability. The underlying route choice model, APSL′, proposes that the choice probability function for route $i \in R_m$ is:

$$P_{m,i}\left(g_{m,i}\left(\boldsymbol{c}_m(\boldsymbol{t}), \boldsymbol{\gamma}_m^{APS'}(\boldsymbol{t}, \boldsymbol{f}_m)\right)\right) = \tau_m + (1 - N_m\tau_m) \cdot g_{m,i}\left(\boldsymbol{c}_m(\boldsymbol{t}), \boldsymbol{\gamma}_m^{APS'}(\boldsymbol{t}, \boldsymbol{f}_m)\right), \tag{3.6}$$

where $g_{m,i}$ for route $i \in R_m$ is:

$$g_{m,i}\left(\boldsymbol{c}_m(\boldsymbol{t}), \boldsymbol{\gamma}_m^{APS'}(\boldsymbol{t}, \boldsymbol{f}_m)\right) = \frac{\left(\gamma_{m,i}^{APS'}(\boldsymbol{t}, \boldsymbol{f}_m)\right)^{\beta} e^{-\theta c_{m,i}(\boldsymbol{t})}}{\sum_{j \in R_m}\left(\gamma_{m,j}^{APS'}(\boldsymbol{t}, \boldsymbol{f}_m)\right)^{\beta} e^{-\theta c_{m,j}(\boldsymbol{t})}}, \tag{3.7}$$

and, $\gamma_{m,i}^{APS'}$ for route $i \in R_m$ is:

$$\begin{aligned} \gamma_{m,i}^{APS'}(\boldsymbol{t}, \boldsymbol{f}_m) &= \sum_{a \in A_{m,i}} \frac{t_a}{c_{m,i}(\boldsymbol{t})} \frac{f_{m,i}/q_m}{\sum_{k \in R_m}(f_{m,k}/q_m)\delta_{a,m,k}} \\ &= \sum_{a \in A_{m,i}} \frac{t_a}{c_{m,i}(\boldsymbol{t})} \frac{f_{m,i}}{\sum_{k \in R_m} f_{m,k}\delta_{a,m,k}}, \qquad \forall \boldsymbol{f}_m \in F_m^{>0}, \end{aligned} \tag{3.8}$$

$$F_m^{>0} = \left\{ \boldsymbol{f}_m \in \mathbb{R}_{>0}^{N_m} : \sum_{i \in R_m} f_{m,i} = q_m \right\}.$$

The model parameters are again $\theta > 0$, $\beta \geq 0$, and $0 < \tau_m \leq \frac{1}{N_m}$, $m = 1, \dots, M$. As shown in (3.8), the contribution of route $k \in R_m$ to the path size term of route $i \in R_m$ is weighted according to the ratio of flow between the routes $\left(\frac{f_{m,k}}{f_{m,i}}\right)$, and hence unrealistic route alternatives with very low use/flow have a diminished contribution to the path size terms of realistic routes with relatively high use/flow.

The APSL′ choice model is closed-form and hence choice probability solutions for a given route flow vector are guaranteed to exist and be unique, assuming every route has a non-zero flow. Stipulating that the flows for OD movement m $\boldsymbol{f}_m$ belong to the set $F_m^{>0}$ ensures that: a) no routes have zero flow; b) the route flows are demand-feasible; and, c) the path size contribution factors consider ratios of route flow proportion. The APSL′ choice model need not only be considered in an SUE application; regardless of whether the link costs are flow-dependent or fixed, if information is available on the route flow proportions then the path size contribution factors can utilise this for route choice prediction.

Adopting generalised, flow-dependent congested costs for the link-route prominence features, APSL′ SUE is formulated as follows:

APSL′ SUE: A universal route flow vector $\boldsymbol{f}^* \in F^{(\boldsymbol{\tau})}$ is an APSL SUE solution iff the route flow vector for OD movement m, $\boldsymbol{f}_m^*$, is a solution to the fixed-point problem

$$\boldsymbol{f}_m = \boldsymbol{Q}_m \boldsymbol{P}_m\left(\boldsymbol{g}_m\left(\boldsymbol{c}_m\left(\boldsymbol{t}(\boldsymbol{\Delta f})\right), \boldsymbol{\gamma}_m^{APS'}(\boldsymbol{t}(\boldsymbol{\Delta f}), \boldsymbol{f}_m)\right)\right), \qquad m = 1, \dots, M, \tag{3.9}$$

where $P_{m,i}$, $g_{m,i}$, and $\gamma_{m,i}^{APS'}$ are as in (3.6), (3.7), and (3.8), respectively, for route $i \in R_m$, given the universal route flow vector $\boldsymbol{f}$, and

$$F^{(\boldsymbol{\tau})} = \left\{ \boldsymbol{f} \in \mathbb{R}_{>0}^{N} : \tau_m \leq \frac{f_{m,i}}{q_m} \leq (1 - (N_m - 1)\tau_m), \forall i \in R_m, \sum_{i \in R_m} f_{m,i} = q_m, m = 1, \dots, M \right\}.$$

The APSL′ choice model is only internally consistent for route flow vectors at SUE, since for all other route flow vectors, the relative attractiveness of routes as defined in the path size contribution factors does not match the relative attractiveness in the probability relation.

3.3 Existence & Uniqueness of Solutions

Zhou et al (2012) formulate a congestion-based CL SUE model in which the commonality factors are based on flow-dependent congested costs (see Appendix A). While such solutions can be proven to exist, uniqueness cannot be guaranteed. In a similar vein, APSL SUE solutions can be proven to exist, but it is expected that uniqueness can also not be guaranteed.

3.3.1 Existence

In this subsection, we prove that solutions are guaranteed to exist to the APSL′ SUE fixed-point system as defined in (3.9), and thus the APSL SUE fixed-point system defined in (3.4)-(3.5), due to equivalence in equilibrium.

First, we define an important function: the APSL′ SUE fixed-point function. Let $H_{m,i}(\boldsymbol{f}) = q_m P_{m,i}\left(g_{m,i}\left(\boldsymbol{c}_m\left(\boldsymbol{t}(\boldsymbol{\Delta f})\right), \boldsymbol{\gamma}_m^{APS'}(\boldsymbol{t}(\boldsymbol{\Delta f}), \boldsymbol{f}_m)\right)\right)$, where $P_{m,i}$, $g_{m,i}$, and $\gamma_{m,i}^{APS'}$ are as in (3.6), (3.7), and (3.8), respectively, for route $i \in R_m$. It is clear from (3.9) that a route flow solution $\boldsymbol{f}^*$ is an APSL′ SUE solution iff $H_{m,i}(\boldsymbol{f}^*) = f_{m,i}^*, \forall i \in R_m, m = 1, \dots, M$.

Given $H_{m,i}(\boldsymbol{f})$, we first prove that APSL′ SUE solutions are guaranteed to exist.

Proposition 1: If the link cost function $\boldsymbol{t}(\boldsymbol{\Delta f})$ is a continuous function for all $\boldsymbol{f} \in F^{(\boldsymbol{\tau})}$, then at least one APSL′ SUE fixed-point route flow solution, $\boldsymbol{f}^* \in F^{(\boldsymbol{\tau})}$, is guaranteed to exist.

Proof. From the assumption that $\boldsymbol{t}(\boldsymbol{\Delta f})$ is a continuous function for all $\boldsymbol{f} \in F^{(\boldsymbol{\tau})}$, (and thus $\boldsymbol{c}_m$, $\boldsymbol{\gamma}_m^{APS'}$, $g_{m,i}$, $P_{m,i}$, and $H_{m,i}$ are all continuous), and given that $F^{(\boldsymbol{\tau})}$ is a nonempty, convex, and compact set, and $\boldsymbol{H}$ maps $F^{(\boldsymbol{\tau})}$ into itself, then by Brouwer's Fixed-Point Theorem at least one solution $\boldsymbol{f}^*$ exists such that $H_{m,i}(\boldsymbol{f}^*) = f_{m,i}^*, \forall i \in R_m, m = 1, \dots, M$, and hence APSL′ SUE solutions are guaranteed to exist.

■

Next, we clarify the equivalence of APSL SUE and APSL′ SUE.

Lemma 1: If $\boldsymbol{f}^* \in F^{(\boldsymbol{\tau})}$ is an APSL′ SUE solution, $\boldsymbol{f}^* \in F^{(\boldsymbol{\tau})}$ is also an APSL SUE solution.

Proof. This follows by inspection from the equivalence of (3.1), (3.2), and (3.3) with (3.6), (3.7), and (3.8), respectively, when $P_{m,i} = \frac{f_{m,i}}{q_m}, \forall i \in R_m, m = 1, \dots, M$, and hence for an APSL′ SUE solution $\boldsymbol{f}^* \in F^{(\boldsymbol{\tau})}$ where $P_{m,i} = \frac{f_{m,i}^*}{q_m}$.

■

What remains is to prove the existence of APSL SUE solutions.

Proposition 2: If the link cost function $\boldsymbol{t}(\boldsymbol{\Delta f})$ is a continuous function, then at least one APSL SUE fixed-point route flow solution, $\boldsymbol{f}^* \in F^{(\boldsymbol{\tau})}$, is guaranteed to exist.

Proof. It follows from Proposition 1 and Lemma 1 that since APSL′ SUE solutions are guaranteed to exist, and an APSL′ SUE solution is also always an APSL SUE solution, then at least one APSL SUE fixed-point route flow solution $\boldsymbol{f}^* \in F^{(\boldsymbol{\tau})}$ is guaranteed to exist.

■

3.3.2 Uniqueness

The standard approach for establishing sufficient conditions for the uniqueness of APSL′ SUE solutions requires $H_{m,i}(\boldsymbol{f})$ to be a monotonic function. Assuming the link cost functions $\boldsymbol{t}(\boldsymbol{\Delta f})$ are monotonic, then the route cost functions $\boldsymbol{c}_m\left(\boldsymbol{t}(\boldsymbol{\Delta f})\right)$ are also monotonic. This is enough to establish sufficient conditions for the uniqueness of MNL SUE solutions, as well as solutions for Path Size Logit SUE models with flow-independent path size costs. However, for the APSL′ SUE model (and other Path Size Logit SUE models with flow-dependent path size costs), the path size term functions, in this case $\boldsymbol{\gamma}_m^{APS'}(\boldsymbol{t}(\boldsymbol{\Delta f}), \boldsymbol{f}_m)$, are not guaranteed to always be monotonic, and hence the approach is not applicable. This is not to say however that APSL SUE solutions cannot be unique, since the mentioned approach only establishes sufficient conditions, and in Section 4.4 we investigate this numerically.

4. Numerical Experiments

In this section, some numerical experiments are conducted to compare the computational performance of APSL & APSL′ SUE, as well as with internally consistent SUE formulations for competitor correlation-based route choice models to APSL, namely: MNL, PSL, GPSL, CL, CNL, GNL, and PCL SUE, as defined in Appendix A. We also examine how robust these SUE models are to the inclusion of unrealistic routes to the choice set, thereby mimicking choice set mis-generation. We compare flow results between the Path Size Logit SUE models, as well as investigate the uniqueness of APSL SUE solutions.

4.1 Experiment Setup

The computer used has a 2.10GHz Intel Xeon CPU and 512GB RAM, and the code was implemented in Python. In our implementation, we assume that a working set of routes is available in advance to solve the SUE models. The advantage of using a working route set (i.e. generated from a choice set generation scheme) is that it provides a common basis for the comparison of various models. Behaviourally, it has the advantage of identifying routes that would likely to be used (Cascetta et al, 1997; Bekhor et al 2006, 2008). However, a column generation procedure (e.g. Chen et al, 2001) could also be used.

In our experiments, we consider three networks: a small example network (Fig. 3.1), and two well-known networks Sioux Falls and Winnipeg. The small example network consists of 3 nodes, 4 links, and 1 OD movement (with demand 200), the Sioux Falls network consists of 24 nodes, 64 links, and 528 OD movements (with positive demands), and the Winnipeg network consists of 1052 nodes, 2836 links, and 4345 OD movements.

In general, the generalised travel cost, $t_a(x_a)$, for link $a \in A$ may consist of several flow-dependent and flow-independent attributes, for example congested travel time, length, number of left turns, etc. However, for the numerical experiments in this section and for all networks, the travel cost of link $a \in A$ is specified as the flow-dependent travel time $T_a(x_a)$ only, where the volume-delay link cost functions for all networks are based on the Bureau of Public Road (BPR) formula with link-specific parameters:

$$t_a(x_a) = T_a(x_a) = T_{0,a}\left(1 + D\left(\frac{x_a}{K_a}\right)^B\right),$$

where $T_{0,a}$ and K_a are the free-flow travel time and capacity of link $a \in A$, respectively, and $D, B \geq 0$. For the small example network, $D = 0.15$, $B = 4$, $K_a = 100$ for all links, and $T_{0,a}$ for each link is shown in Fig. 3.1. For the Sioux Falls and Winnipeg networks, the link-cost function values as well as the network and demand data are obtained from https://github.com/bstabler/TransportationNetworks.

For the small example network, the working choice set utilises all 4 routes, where the routes are Route 1: $1 \rightarrow 3$, Route 2: $1 \rightarrow 4$, Route 3: $2 \rightarrow 3$, Route 4: $2 \rightarrow 4$. For the numerical experiments in this paper, we generated new working choice sets for the Sioux Falls and Winnipeg networks. From experimenting with different settings and generation methods, we ultimately generated as large choice sets as we deemed our computational resources would allow, in order to minimise the possibility that we had excluded what would later turn out to be a plausible route from the working choice set. For the Sioux Falls network, the working choice sets were obtained by generating all routes with a free-flow travel time less than 2.5 times greater than the free-flow travel time on the quickest route for each OD movement. This technique was not viable computationally for the Winnipeg network; instead, we utilised a simulation approach (Sheffi & Powell,

1982) where the link costs were drawn randomly from a truncated normal distribution with mean value being free-flow travel time and standard deviation being 0.6 times the mean. The link costs were simulated 150 times for each OD movement and for each simulation shortest path was conducted to generate a route, where a maximum of 100 unique routes were generated for each choice set. The average and maximum free-flow travel time relative deviations from the quickest route in each choice set were 1.14 and 3.2, respectively. For Sioux Falls, 42,976 routes were generated in total, and the maximum, average, and median choice set sizes for an OD movement were 898, 116, and 6, respectively. For Winnipeg, 305,005 routes were generated in total, and the maximum, average, and median choice set sizes for an OD movement were 100, 70, and 88, respectively. In Sections 4.2 & 4.3 we investigate how varying the choice set sizes effects computational performance and flow results, respectively.

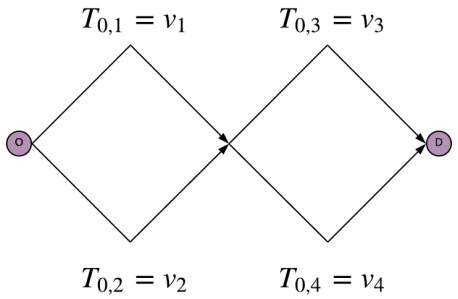

Fig. 3.1. Small example network.

It is not expected that equivalent Mathematical Programming (MP) formulations can be derived for the internally consistent SUE formulations in this paper. This is due to the correlation components being flow-dependent, e.g. based upon the flow-dependent congested costs. For example, as Zhou et al (2012) explain for congestion-based CL SUE: since the CL commonality factors are nonlinear flow-dependent functions, CL SUE cannot be formulated as an equivalent MP formulation, and thus cannot be obtained through solving some convex optimisation problem. Instead, we use a standard Flow-Averaging Algorithm (FAA) to solve all SUE models, where a step-size scheme averages the route flows between the current flow vector and an auxiliary flow vector computed from the route choice probabilities of the underlying choice model. The FAA is as follows:

$$f_{m,i}^{(n)} = (1 - \eta_n) \cdot f_{m,i}^{(n-1)} + \eta_n \cdot q_m P_{m,i}\left(\boldsymbol{f}^{(n-1)}\right), \qquad n = 1,2,3 \dots$$

such that

$$\lim_{n\to\infty} f_{m,i}^{(n)} = \lim_{n\to\infty} (1 - \eta_n) \cdot f_{m,i}^{(n-1)} + \eta_n \cdot q_m P_{m,i}\left(\boldsymbol{f}^{(n-1)}\right) = f_{m,i}^{*}, \qquad \forall i \in R_m, m = 1, \dots, M, \qquad \boldsymbol{f}^{(0)} \in F,$$

where $f_{m,i}^{(n)}$ is the flow for route $i \in R_m$ at iteration n, η_n is the step-size at iteration n, and $P_{m,i}\left(\boldsymbol{f}^{(n-1)}\right)$ is the choice probability for route $i \in R_m$ at iteration n given the route flows from iteration $n-1$. For the APSL & APSL′ SUE models, the feasible set of route flows is $F^{(\boldsymbol{\tau})}$ rather than F.

The step-size scheme we adopt in this paper is the Method of Successive Weighted Averages (MSWA) (Liu et al, 2009), which is based upon the well-known Method of Successive Averages (MSA). While being pre-defined, the MSWA allows giving higher weight to auxiliary flow patterns from later iterations, and the step-size η_n at iteration n is defined as:

$$\eta_n = \frac{n^d}{\sum_{k=1}^{n} k^d},$$

where $d \geq 0$ is the MSWA parameter. Increasing the value of d moves more flow towards the auxiliary solution. The MSA is a special case of the MSWA, namely when $d = 0$.

Convergence of the FAA is measured by the Route Mean Squared Error (RMSE) between the final route flow vector and auxiliary route flow vector at iteration n:

$$RMSE^{(n)} = \sqrt{\frac{1}{N}\sum_{m=1}^{M}\sum\nolimits_{i\in R_m}\left(f_{m,i}^{(n)} - \bar{f}_{m,i}^{(n)}\right)^2},$$

where $f_{m,i}^{(n)}$ and $\bar{f}_{m,i}^{(n)}$ are the final route flow and auxiliary route flow for route $i \in R_m$ at iteration n, and N is the total number of routes. The route flows are thus said to have converged sufficiently to a route flow vector solution $\boldsymbol{f}^* = \boldsymbol{f}^{(n)}$ if $RMSE^{(n)} < 10^{-\zeta}$, where ζ is a predetermined flow convergence parameter.

For PSL, GPSL, APSL′, CL, CNL, GNL, & PCL SUE, the auxiliary flows are computed exactly since the probability relations are closed-form. For APSL SUE, however, the accuracy of the auxiliary flows is dependent upon the accuracy of the APSL fixed-point probabilities. To ensure that APSL SUE is reached, when the RMSE convergence criteria are said to have converged, we check by computing the RMSE between the final route flow vector and an auxiliary route flow vector calculated from APSL′ probabilities, which at iteration n is:

$$RMSE^{(n)} = \sqrt{\frac{1}{N}\sum_{m=1}^{M}\sum\nolimits_{i\in R_m}\left(f_{m,i}^{(n)} - q_m P_{m,i}\left(\boldsymbol{c}_m\left(\boldsymbol{t}(\boldsymbol{\Delta f}^{(n)}), \boldsymbol{\gamma}_m^{APS'}(\boldsymbol{t}(\boldsymbol{\Delta f}^{(n)}), \boldsymbol{f}^{(n)})\right)\right)\right)^2}.$$

We continue until this RMSE satisfies the convergence criterion, or it is clear that this convergence criterion will not be satisfied.

Computing the APSL choice probabilities requires a fixed-point algorithm to compute the solution. In general, there are many fixed-point algorithms available for solving the APSL fixed-point system. In this study, we use the Fixed-Point Iteration Method (FPIM) (Isaacson & Keller, 1966). Other algorithms were considered, however the performance and convergence of the FPIM in our tests were sufficiently promising that we did not consider this worthwhile. The FPIM for solving the APSL choice probabilities for OD movement m at iteration n of the FAA is as follows:

$$P_{m,i}^{[s]} = G_{m,i}\left(g_{m,i}\left(\boldsymbol{c}_m\left(\boldsymbol{t}(\boldsymbol{\Delta f}^{(n)})\right), \boldsymbol{\gamma}_m^{APS}\left(\boldsymbol{t}(\boldsymbol{\Delta f}^{(n)}), \boldsymbol{P}_m^{[s-1]}\right)\right)\right), \qquad s = 1,2,3,\dots$$

such that

$$\lim_{s\to\infty} P_{m,i}^{[s]} = \lim_{s\to\infty} G_{m,i}\left(g_{m,i}\left(\boldsymbol{c}_m\left(\boldsymbol{t}(\boldsymbol{\Delta f}^{(n)})\right), \boldsymbol{\gamma}_m^{APS}\left(\boldsymbol{t}(\boldsymbol{\Delta f}^{(n)}), \boldsymbol{P}_m^{[s-1]}\right)\right)\right) = P_{m,i}^*, \qquad \forall i \in R_m,$$
$$\boldsymbol{P}_m^{(0)} \in D_m^{(\tau_m)},$$

where $G_{m,i}$, $g_{m,i}$, and $\gamma_{m,i}^{APS}$ are as in (3.1), (3.2), and (3.3), respectively, for route $i \in R_m$, and $\boldsymbol{f}^{(n)}$ is the route flow vector at iteration n of the FAA. The FPIM is said to have converged sufficiently to an OD movement m APSL choice probability solution $\boldsymbol{P}_m^* = \boldsymbol{P}_m^{[s]}$ if: $\sum_{i\in R_m}\left|P_{m,i}^{[s-1]} - P_{m,i}^{[s]}\right| < 10^{-\xi}$, where ξ is a predetermined APSL probability convergence parameter.

In the numerical experiments in this paper, we explore adopting two different initial conditions for the FPIM: *fixed* initial conditions where $P_{m,i}^{[0]} = \frac{1}{N_m}$, $\forall i \in R_m$, $m = 1, \dots, M$, and *follow-on* initial conditions where $P_{m,i}^{[0]} = \frac{f_{m,i}^{(n-1)}}{q_m}$, $\forall i \in R_m$, $m = 1, \dots, M$. The follow-on initial FPIM conditions utilise information from the previous FAA iteration route flows $\boldsymbol{f}^{(n-1)}$ to determine the FPIM initial conditions. The idea is to harness the useful relation between route flow proportions and route choice probabilities in SUE, where these equate at equilibrium. The hypothesis is that by utilising follow-on initial conditions, the numbers of fixed-point iterations required for APSL choice probability convergence (and thus computation time to perform each FAA iteration) should decrease as the algorithm progresses and the route flow proportions become closer to the APSL SUE route choice probabilities. This hypothesis is tested in Section 4.2.

Unless stated otherwise, the specifications are as follows. The initial SUE conditions are set as the even split route flows, i.e. $f_{m,i}^{(0)} = \frac{q_m}{N_m}$, $\forall i \in R_m$, $m = 1, \dots, M$, and the SUE route flow convergence parameter is set

as $\zeta = 3$. The MSWA parameter is set as $d = 15$. For computing APSL probabilities, the initial FPIM conditions are set as the fixed initial conditions, and the APSL probability convergence parameter is set as $\xi = 6$. The utilised model parameters for the Sioux Falls network are $\theta = 0.3$, $\beta = 0.8$, $\upsilon = -0.8$, $\lambda^{GPSL} = 10$, $\mu = 0.25$. $\theta = 0.5$, $\beta = 0.8$, $\upsilon = -0.8$, $\lambda^{GPSL} = 10$, $\mu = 0.25$, and $\lambda^{GNL} = 1$ for the Winnipeg network.

Note that for the GNL SUE model as defined in Appendix A, the model is undefined when there are routes consisting of a single link between the origin and destination. The Sioux Falls network contains numerous instances of such cases and thus we do not present results for GNL SUE on this network.

4.2 Computational Performance

We begin by analysing here the computational performance of the FAA for solving the SUE models. Table 3.1 displays for all SUE models the average computation time to perform a single FAA iteration on the Sioux Falls and Winnipeg networks. As expected, MNL probabilities are the quickest to compute. PSL/GPSL/APSL′ probabilities all take a similar amount of time to compute, but longer than MNL due to the computation of path size terms. APSL probabilities take significantly longer than the other PSL models due to the requirement of having to solve APSL probability fixed-point problems. CL probabilities take longer to compute than CNL probabilities on the Sioux Falls network, while CNL & GNL take longer than CL on the Winnipeg network. This is because the Winnipeg network has greater network depth and the routes are made up of a greater number of links. The greater the number of links, the greater the number of nests for CNL & GNL, and hence the greater the complexity of the probability expression and longer the computation times. GNL takes longer than CNL due to the computation of nesting coefficients. For CL, the commonality factors evaluate the similarity between each pair of routes, and thus despite the smaller network depth of the Sioux Falls network, there are still many routes to compare, increasing the computational burden. Due to relatively large choice set sizes and thus extremely large number of route pairs and hence nests for PCL, the probabilities for Sioux Falls and Winnipeg are very computationally burdensome and could not be computed in computationally feasible times. Due to this, we do not present computation/flow results for PCL SUE.

	MNL	PSL	GPSL	APSL	APSL′	CL	CNL	GNL
Sioux Falls	0.006	0.038	0.038	0.920	0.038	0.562	0.196	-
Winnipeg	0.089	0.208	0.208	4.199	0.208	1.611	6.806	12.921

Table 3.1. Average computation time [mins] to perform a single FAA iteration on the Sioux Falls and Winnipeg networks.

Fig. 3.2A-B display for the Sioux Falls and Winnipeg networks, respectively, the number of FAA iterations required to obtain levels of SUE convergence. Fig. 3.3A-B the display computation time required. As shown, while APSL SUE requires a similar number of FAA iterations for convergence to PSL & GPSL SUE, total computation times are significantly longer due to the requirement of solving APSL probability fixed-point problems at each iteration, and hence longer iteration times. APSL′ SUE has the same iteration computation times as for PSL & GPSL SUE, but the slow convergence also results in longer total computation times. MNL SUE is the quickest to solve due to not having to compute path size terms, while PSL SUE takes less time than GPSL SUE due to fewer iterations. For Sioux Falls, iteration times are quicker for CNL than for CL, and thus despite fewer number of iterations required for CL SUE, CNL SUE takes less time overall. For Winnipeg, iteration times are quicker for CL than for CNL & GNL, and thus CNL & GNL SUE take more time overall, where GNL SUE takes longer than CNL SUE.

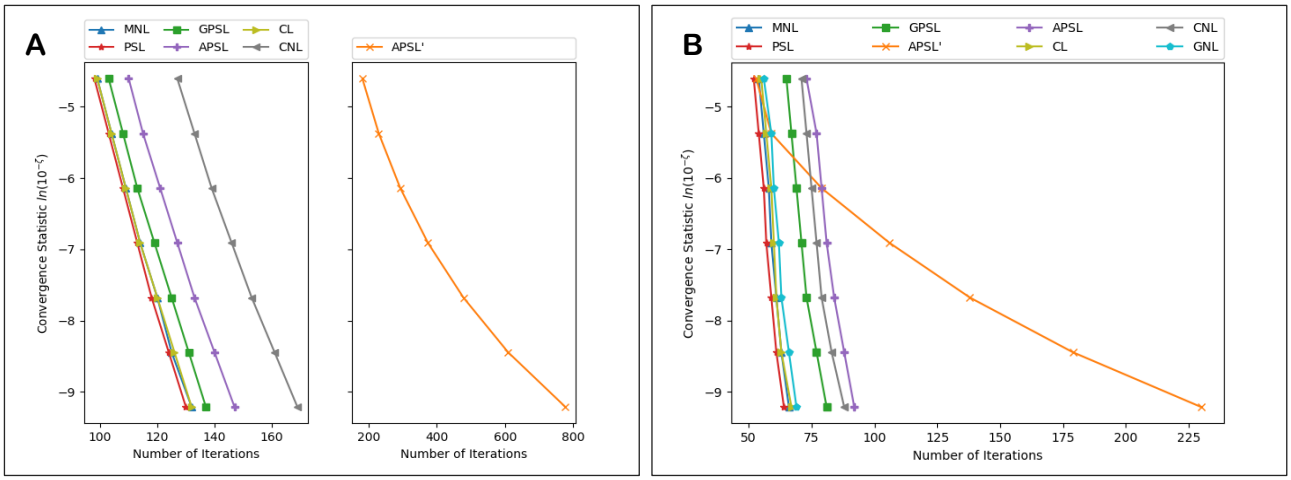

Fig. 3.2. Number of FAA iterations required to obtain levels of SUE convergence for the different SUE models. **A:** Sioux Falls. **B:** Winnipeg.

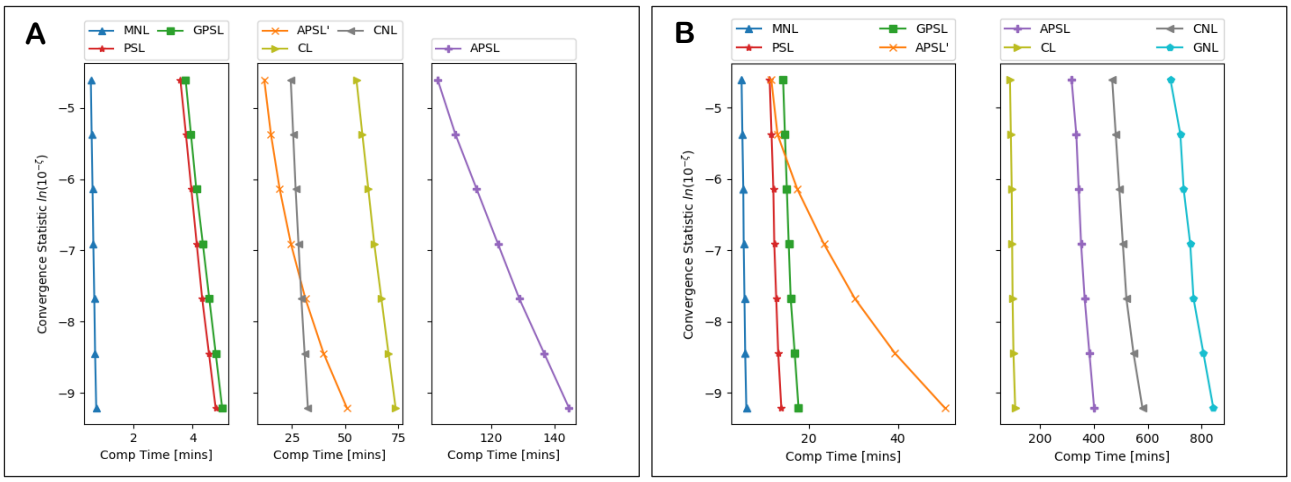

Fig. 3.3. Computation time [mins] required to obtain levels of SUE convergence for the different SUE models. **A:** Sioux Falls. **B:** Winnipeg.

As demonstrated above, further below, and in the experience of the authors, while the number of iterations required for APSL SUE convergence tend to be similar to that required for PSL & GPSL SUE convergence under identical configurations of the FAA, the requirement of solving APSL choice probability fixed-point problems at each FAA iteration results in significantly greater total computation times. On-the-other-hand, while the computational burden involved in computing the APSL′ choice probabilities during each iteration of the FAA solving APSL′ SUE is no more than that for PSL & GPSL, APSL′ SUE convergence is comparatively very slow, and thus total computational times are also longer. There are unique aspects of the APSL model however that allow for some flexibility in solving APSL SUE and consequent potential to improve computation times, as we show below.

For APSL SUE, the scale of the computational burden involved at each FAA iteration in solving the APSL choice probability fixed-point problems depends on numerous factors; some of which can be controlled by the modeller, for example the choice of fixed-point algorithm, and the fixed-point algorithm initial conditions and probability convergence parameter ξ. The current study focuses on the FPIM as the fixed-point algorithm.

Fig. 3.4A-B display for the Sioux Falls and Winnipeg networks, respectively, the cumulative computation times of the iterations during a single run of the FAA, for fixed and follow-on FPIM initial conditions. Fig. 3.5A-B shows the average number of fixed-point iterations per OD movement required for APSL choice probability convergence at each iteration of the FAA. As shown, utilising follow-on initial conditions can significantly improve overall computation time due to the reduction in the number of FPIM iterations required for APSL probability convergence as the FAA progresses.

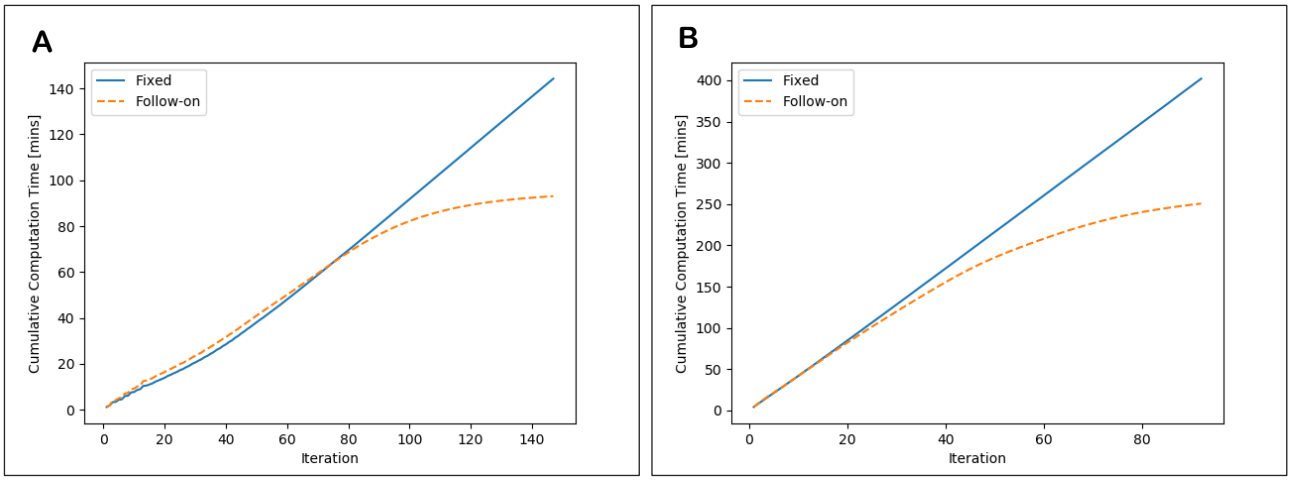

Fig. 3.4. Cumulative computation times of the iterations during a single run of the FAA solving APSL SUE with different FPIM initial conditions. **A:** Sioux Falls. **B:** Winnipeg.

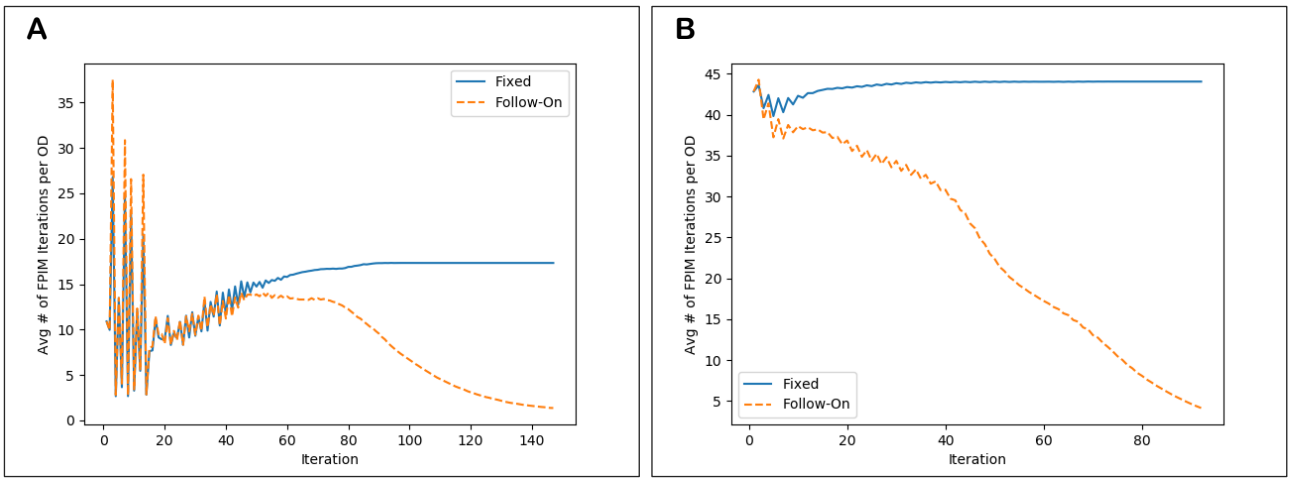

Fig. 3.5. Average number of APSL probability fixed-point iterations per OD movement at each iteration of the FAA solving APSL SUE with different FPIM initial conditions. **A:** Sioux Falls. **B:** Winnipeg.

Fig. 3.6A-B display for the Sioux Falls and Winnipeg networks, respectively, how the total computation time for solving APSL SUE varies as the FPIM probability convergence parameter ξ is increased, with follow-on and fixed FPIM initial conditions. Fig. 3.7A-B display how the average number of APSL fixed-point iterations and total number of FAA iterations vary as ξ is increased.

With fixed FPIM initial conditions, APSL SUE could not be solved for $\xi < 6$ due to the inaccuracies of the APSL probabilities. For $\xi \geq 6$, as shown, as ξ increases, while the number of iterations required for SUE convergence remains constant, greater numbers of FPIM iterations are required for APSL probability convergence and thus total computation times increase.

With follow-on FPIM initial conditions, APSL SUE could be solved for all ξ. This is because for $\xi = -1$, only single FPIM iterations are required for APSL probability convergence, and with follow-on initial FPIM conditions, solving APSL SUE this way simulates solving APSL′ SUE. Increasing ξ increases the number of FPIM iterations required for APSL probability convergence and the accuracy of the APSL probabilities, but the APSL SUE solution obtained is the same. As shown, convergence of APSL′ SUE (APSL SUE with small ξ & follow-on conditions) is slow, resulting in longer computation times. On-the-other-hand, large values of ξ result in comparatively quick APSL SUE convergence, but longer computation times at each iteration, also resulting in longer total computation times. There is thus an optimal, intermediate value of ξ whereby suitable SUE convergence meets suitable iteration computation times. As shown in Fig. 3.6A-B, the optimal values in these cases are approximately $\xi = 1$ and $\xi = 0$ for Sioux Falls and Winnipeg, respectively, yielding computation times of 32.68 minutes and 53.94 minutes, respectively.

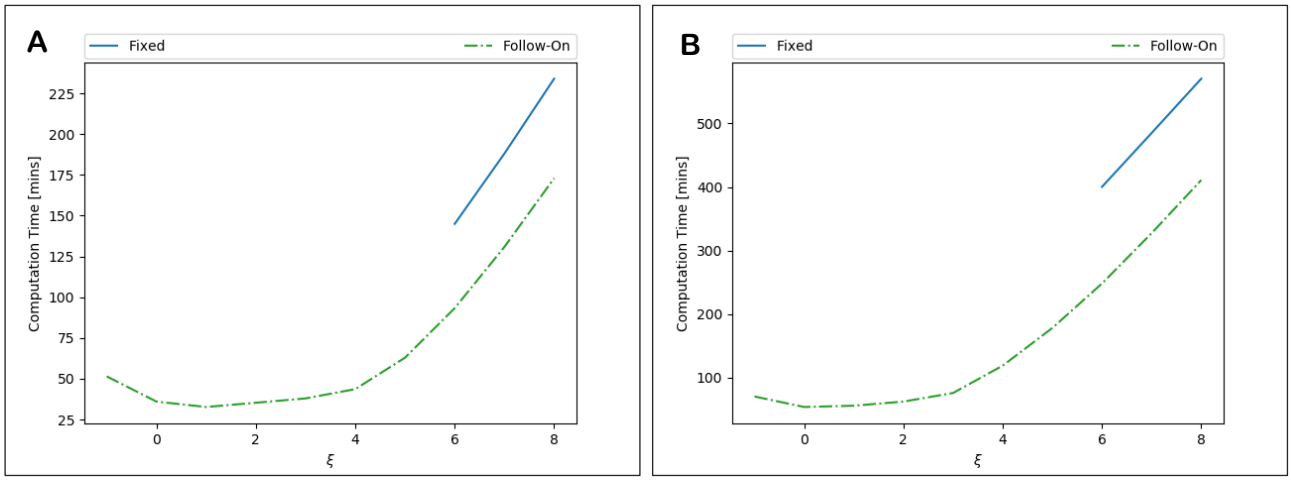

Fig. 3.6. Computation time for solving APSL SUE as the APSL probability convergence parameter ξ is increased, with fixed and follow-on initial FPIM conditions. **A:** Sioux Falls. **B:** Winnipeg.

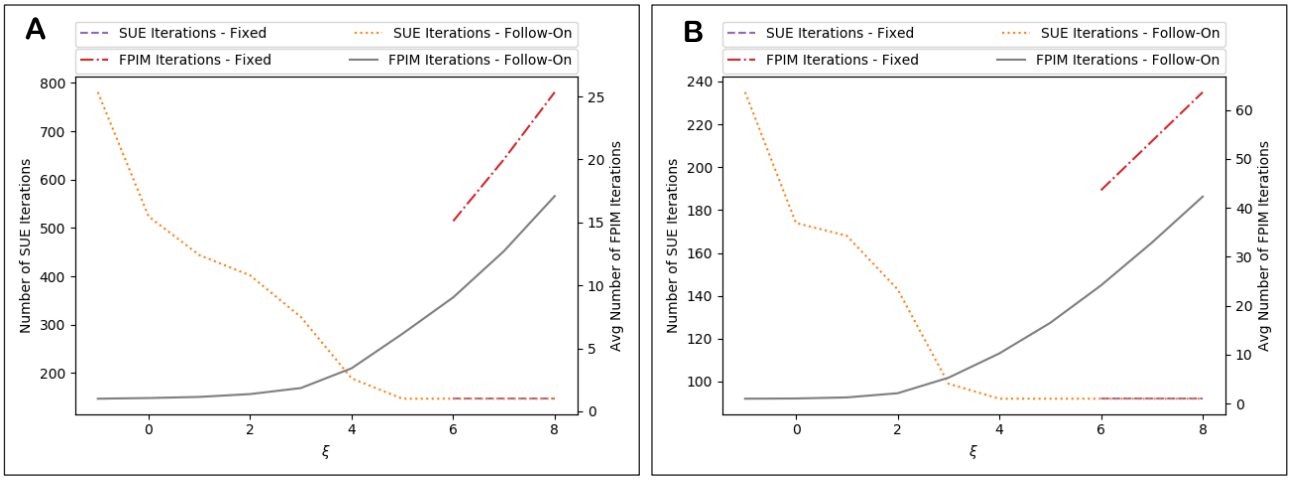

Fig. 3.7. Average number of APSL fixed-point iterations and total number of FAA iterations for solving APSL SUE as ξ is increased, with fixed and follow-on initial FPIM conditions. **A:** Sioux Falls. **B:** Winnipeg.

Alternatively, utilising follow-on conditions, one can stipulate a set number of FPIM iterations to perform at each FAA iteration. Supposing that h FPIM iterations are conducted, Fig. 3.8A-B display the total computation times and number of FAA iterations solving APSL SUE, for the Sioux Falls and Winnipeg networks, respectively. As shown, conducting just two FPIM iterations (instead of one) can significantly reduce the number of FAA iterations required for convergence, and thus total computation times. The optimal values for h appear to be 3 and 2 FPIM iterations, respectively, where suitable SUE convergence meets suitable iteration computation times. This yields computation times of 23.79 minutes for Sioux Falls and 47.17 minutes for Winnipeg.

One can also utilise a combination of both techniques for reducing APSL SUE total computation times and stipulate a maximum number of FPIM iterations to perform and a maximum level of APSL probability convergence, i.e. the FPIM is stopped if either a maximum of h iterations are conducted or the probabilities have converged sufficiently according to the set parameter ξ. This can potentially save computation times in latter FAA iterations where the stipulated amount of FPIM iterations unnecessarily overly-converges the APSL probabilities. Fig. 3.9A and Fig. 3.10A display for Sioux Falls how computation times and the number of FAA iterations / average number of FPIM iterations vary, respectively, for different settings of ξ, where a maximum of 3 FPIM iterations are conducted. Fig. 3.9B displays results for Winnipeg where a maximum of 2 FPIM iterations are conducted. As shown, optimal values of ξ with this technique are approximately $\xi = 5$ and $\xi = 4$ for Sioux Falls and Winnipeg, respectively, where a suitable number of FAA iterations meets a suitable average number of FPIM iterations. This yields computation times of 20.24 minutes for Sioux Falls and 42.25 minutes for Winnipeg.

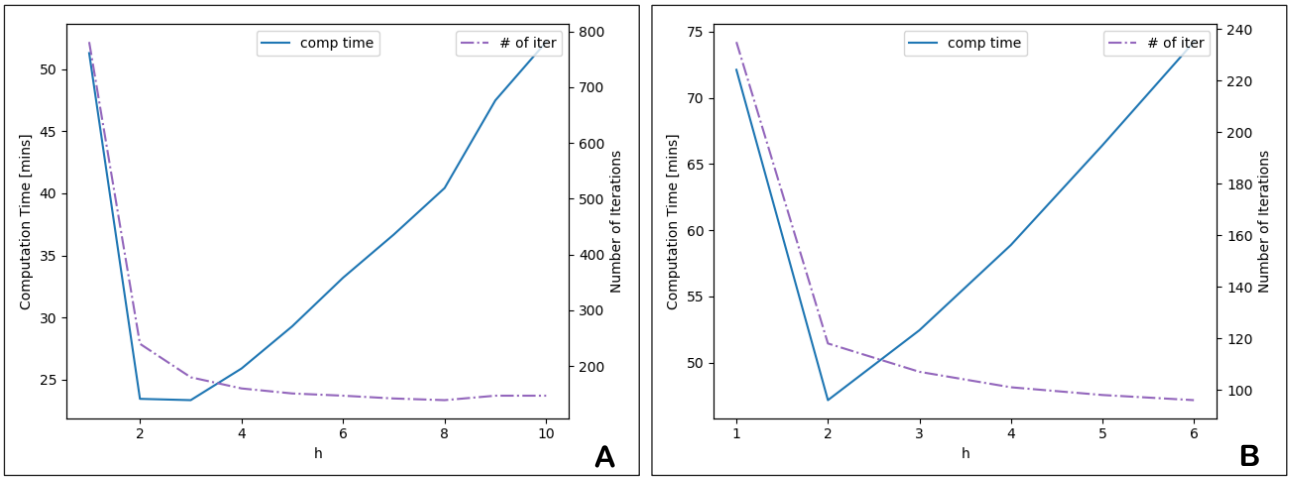

Fig. 3.8. Total computation times and number of FAA iterations for solving APSL SUE utilising follow-on conditions, with h FPIM iterations conducted. **A:** Sioux Falls. **B:** Winnipeg.

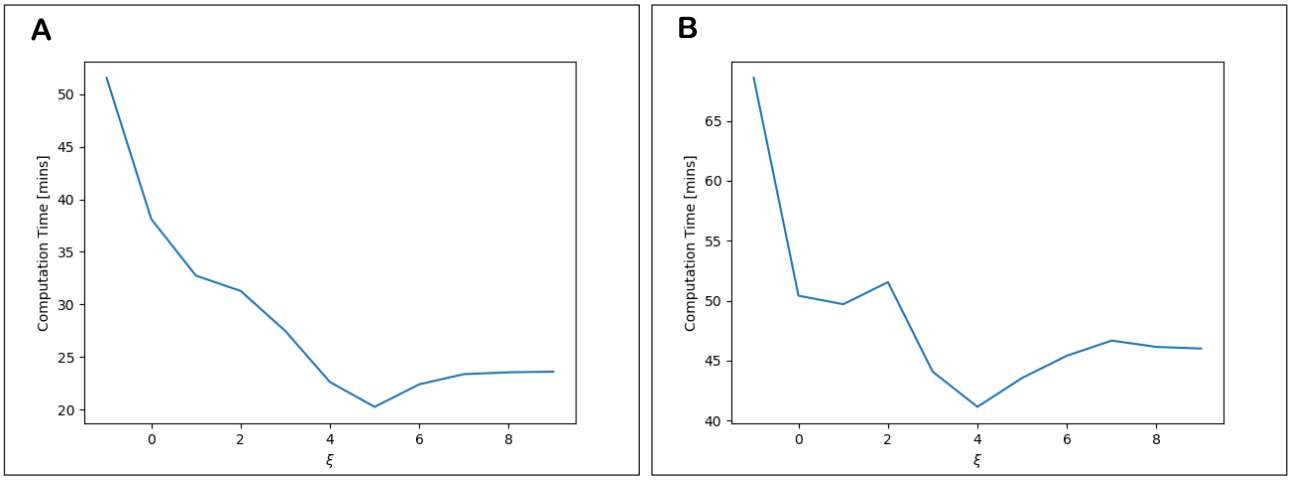

Fig. 3.9. Total computation times for solving APSL SUE utilising follow-on conditions as ξ is varied, with a max number of FPIM iterations conducted h. **A:** Sioux Falls ($h = 3$). **B:** Winnipeg ($h = 2$).

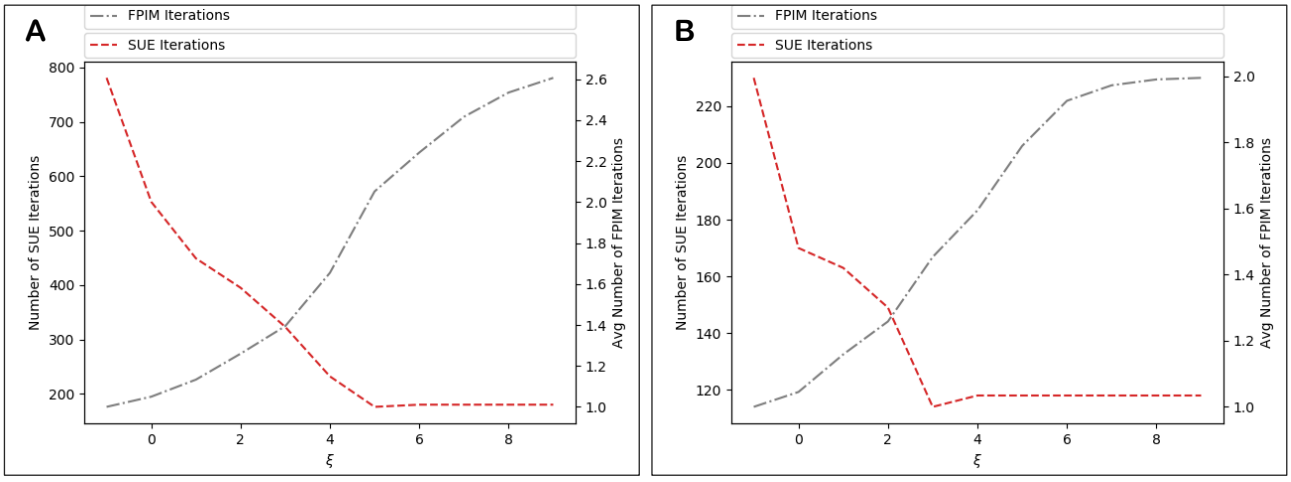

Fig. 3.10. Number of FAA iterations, and average number of FPIM iterations for solving APSL SUE utilising follow-on conditions as ξ is varied, with a max number of FPIM iterations conducted h. **A:** Sioux Falls ($h = 3$). **B:** Winnipeg ($h = 2$).

Considering the above results, for the remainder of the paper, unless stated otherwise, we solve APSL SUE by stipulating a maximum number of FPIM iterations to perform at each FAA iteration and a maximum level of APSL probability convergence. For Sioux Falls, a maximum of 3 FPIM iterations are conducted with $\xi = 5$. For Winnipeg, 2 FPIM iterations are used with $\xi = 4$. We label for reference this method APSL SUE*. This

'optimal' method for solving APSL SUE is of course particular to the network, model, and algorithm specifications, e.g. model parameters, adopted step-size scheme, choice set sizes. However, by fixing the optimised values for that particular specification, and then varying the specifications, we will show that the method is robust in its effectiveness compared to solving APSL SUE in a standard way (i.e. where the APSL fixed-point probabilities are accurately solved with non-follow-on initial conditions).

Fig. 3.11A-B and Fig. 3.12A-B add the APSL SUE* convergence statistics to the results from Fig. 3.2A-B and Fig. 3.3A-B. As shown, for APSL SUE*, the number of iterations required to obtain levels of convergence is now significantly less than for APSL′ SUE, though more than required for APSL SUE. Hence, since the iteration computation times of APSL SUE* are significantly less than for APSL SUE, total computation times are improved. Moreover, APSL SUE* outperforms CL, CNL, & GNL SUE – significantly on the larger-scale Winnipeg network.

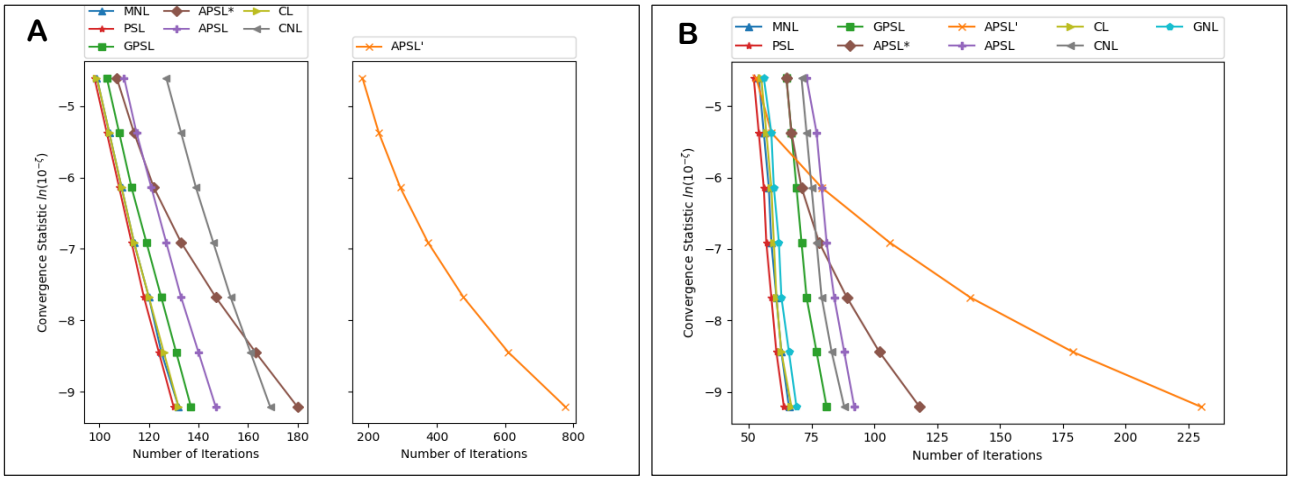

Fig. 3.11. Number of FAA iterations required to obtain levels of SUE convergence for the different SUE models, with updated APSL SUE solution method. **A:** Sioux Falls. **B:** Winnipeg.

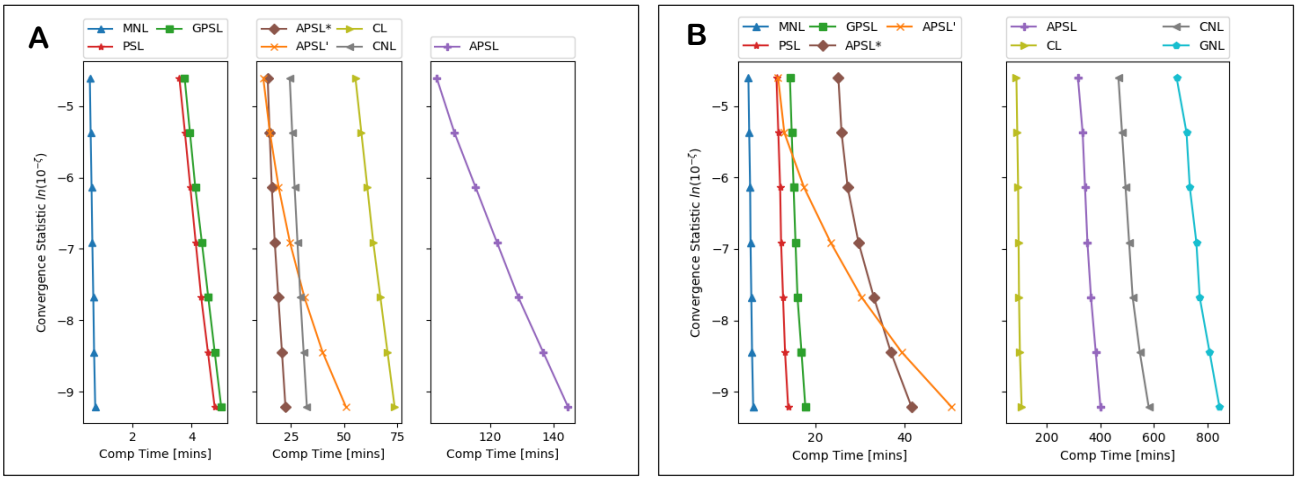

Fig. 3.12. Computation time [mins] required to obtain levels of SUE convergence for the different SUE models, with updated APSL SUE solution method. **A:** Sioux Falls. **B:** Winnipeg.

Other factors that affect the computational performance of APSL SUE, in terms of solving the APSL probability fixed-point problems, include the value of β and the choice set sizes. As shown in Duncan et al (2020), larger values of β result in a greater number of FPIM iterations being required for APSL convergence (increasing computation times), and, the greater the choice set sizes the more routes there are to capture the correlation between (escalating the computational burden involved in computing path size terms).

Fig. 3.13A-B display for the Sioux Falls and Winnipeg networks, respectively, how the computation time for APSL SUE* as well as for solving APSL SUE with follow-on and fixed initial FPIM conditions, varies as the β parameter is increased. Fig. 3.14A-B display how the average number of FPIM iterations per OD movement per FAA iteration and how the total number of FAA iterations vary as β is increased. As shown,

for APSL SUE follow-on & fixed, while the number of FAA iterations do not vary considerably, the average number of FPIM iterations increases exponentially with β and hence so do computation times. For APSL SUE*, the number of SUE iterations increases as β increases, while the average number of FPIM iterations remains low (decreasing slightly due to more SUE iterations), resulting in the technique significantly improving in effectiveness as β increases.

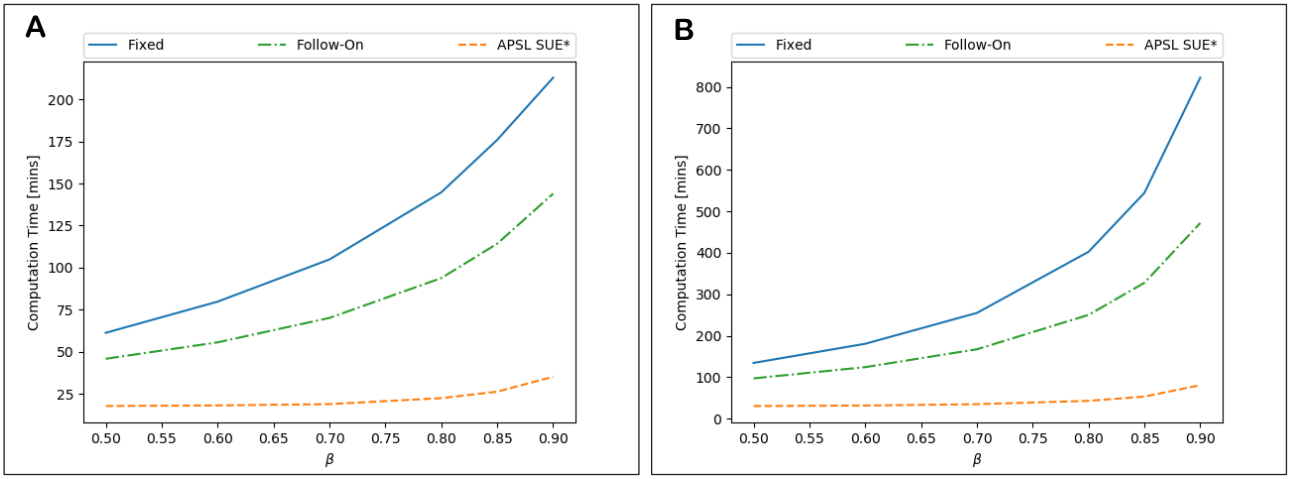

Fig. 3.13. Computation time for APSL SUE*, APSL′ SUE, and solving APSL SUE with follow-on and fixed initial FPIM conditions as β is increased. **A:** Sioux Falls. **B:** Winnipeg.

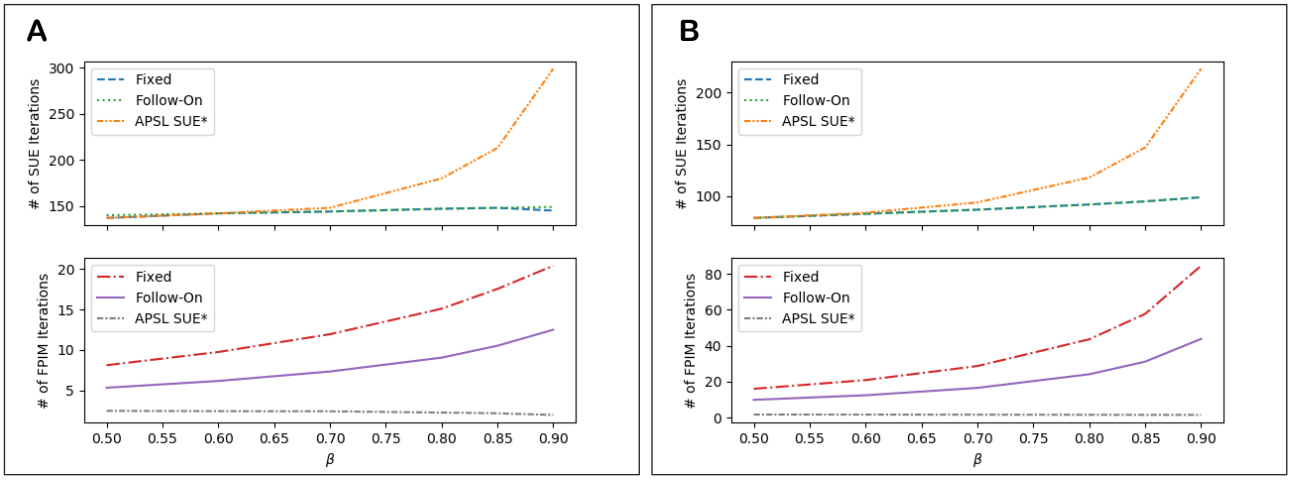

Fig. 3.14. Number of FAA iterations, and average number of FPIM iterations for APSL SUE*, APSL′ SUE, and solving APSL SUE with follow-on and fixed initial FPIM conditions as β is increased. **A:** Sioux Falls. **B:** Winnipeg.

Fig. 3.15A-B display for the Sioux Falls and Winnipeg networks, respectively, how the computation time for APSL SUE* as well as for solving APSL SUE with follow-on and fixed initial FPIM conditions, varies as the choice set sizes are increased. Fig. 3.16A-B display how the average number of FPIM iterations per OD movement per FAA iteration and how the total number of FAA iterations vary. The choice sets are obtained by generating all routes (from the master generated choice sets used throughout this section) with a free-flow travel time less than φ times greater than the free-flow travel time on the quickest generated route for each OD movement. As shown, computation times increase as the choice sets are expanded. The greater number of routes to capture the correlation between means that more FPIM iterations are required for APSL probability convergence, which, combined with a greater number of FAA iterations required for SUE convergence, results in increasing computation times (more SUE iterations that each take longer on average). It is also shown again how effective APSL SUE* can be.

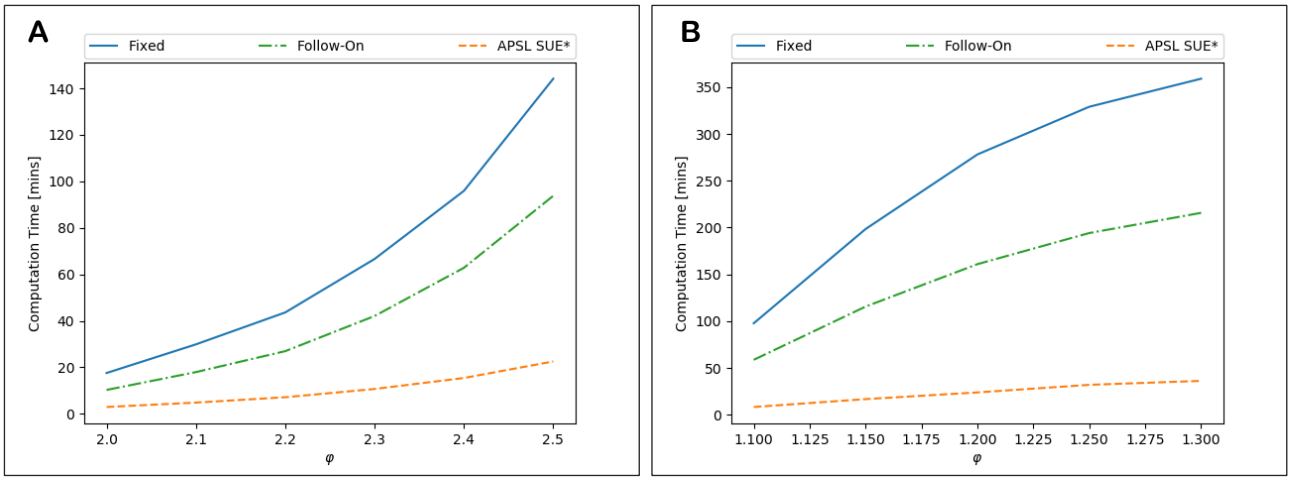

Fig. 3.15. Computation time for APSL SUE* and solving APSL SUE with follow-on and fixed initial FPIM conditions the choice set sizes are increased, scaled by φ. **A:** Sioux Falls. **B:** Winnipeg.

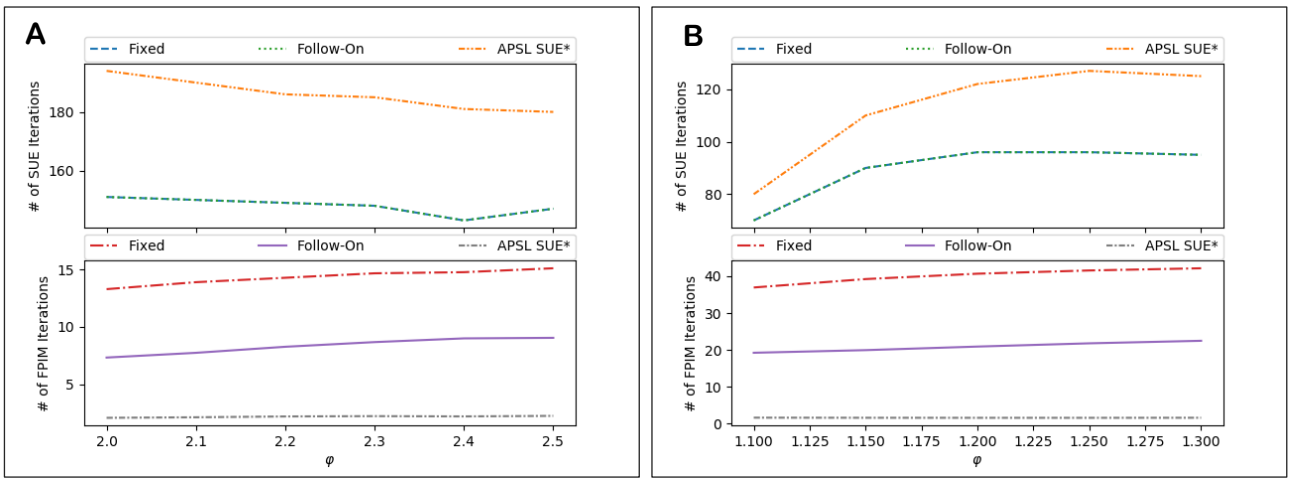

Fig. 3.16. Number of FAA iterations, and average number of FPIM iterations for APSL SUE* and solving APSL SUE with follow-on and fixed initial FPIM conditions the choice set sizes are increased, scaled by φ. **A:** Sioux Falls. **B:** Winnipeg.

Next, we investigate for all SUE models, how total computation times and number of FAA iterations vary according to different sizes of choice sets, levels of travel demand, and model parameters.

Fig. 3.17A-B display for the Sioux Falls and Winnipeg networks, respectively, how the total computation times for the different SUE models vary as the choice set sizes are increased. Fig. 3.18A-B display how the required number of FAA iterations varies. As shown, for Sioux Falls, although the number of iterations required for convergence decreases for most of the models, computation times increase due to additional burden involved in computing choice probabilities / working with more routes. For APSL SUE, computation times increase significantly due also to the more burdensome fixed-point problems (i.e. Fig. 3.15/Fig. 3.16). For Winnipeg, the number of iterations requited for SUE convergence increases, increasing to the computational burden of larger choice sets.

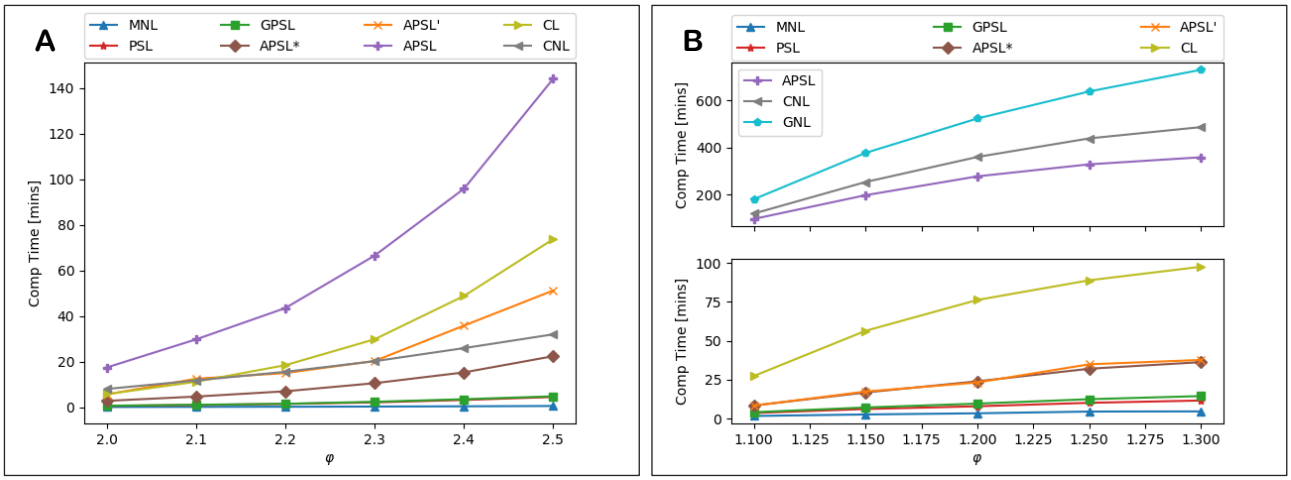

Fig. 3.17. Computation times for solving the SUE models as the choice set sizes are increased, scaled by φ. **A:** Sioux Falls. **B:** Winnipeg.

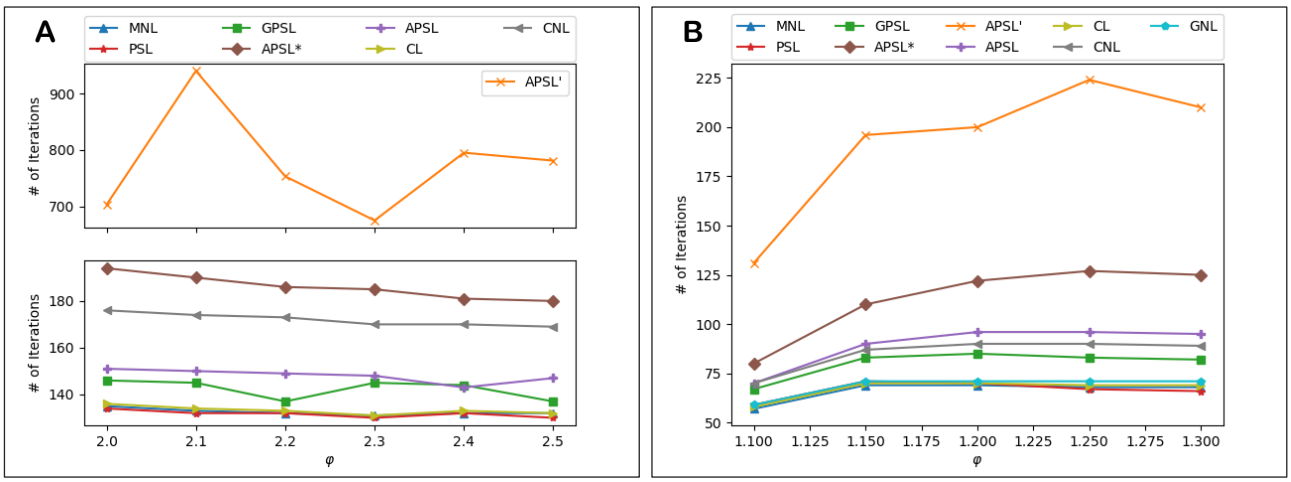

Fig. 3.18. Number of iterations required for convergence for the SUE models as the choice set sizes are increased, scaled by φ. **A:** Sioux Falls. **B:** Winnipeg.

Fig. 3.19A-B display for the Sioux Falls and Winnipeg networks, respectively, how the total computation times vary for the different SUE models as the level of travel demand is varied. Fig. 3.20A-B display how the required number of FAA iterations varies. The demand is scaled according to the parameter ω so that the demand for OD movement m is $\omega \cdot q_m$, $m = 1, \ldots, M$. As shown, and as expected, the number of iterations required for convergence increases for all SUE models as the level of demand increases, thus increasing total computation times. APSL′ SUE experiences a significant increase for large demand.

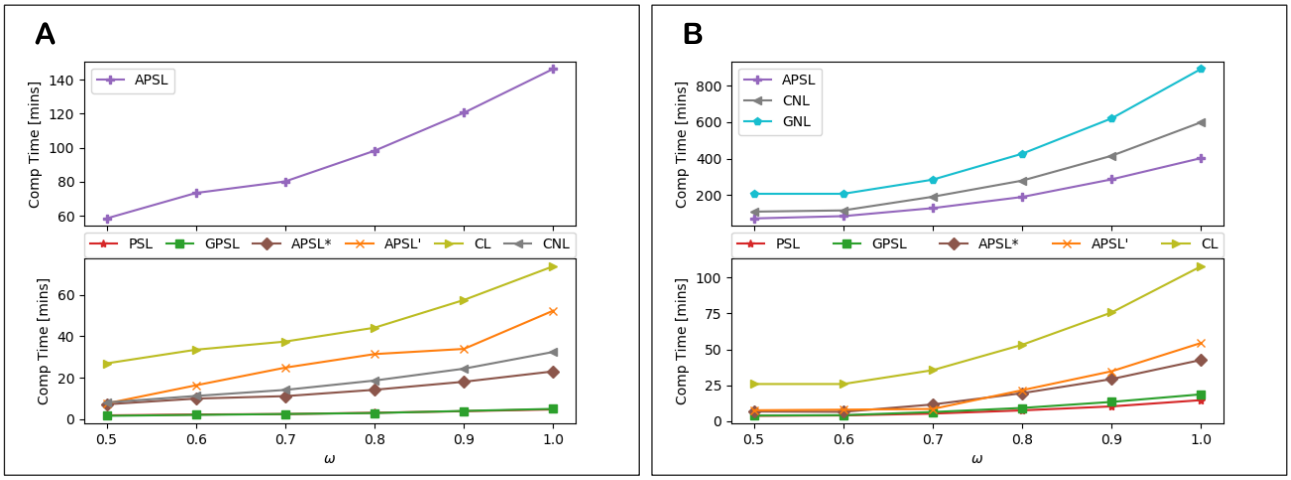

Fig. 3.19. Computation times for solving the SUE models as the level of travel demand is increased, scaled by ω. **A:** Sioux Falls. **B:** Winnipeg.

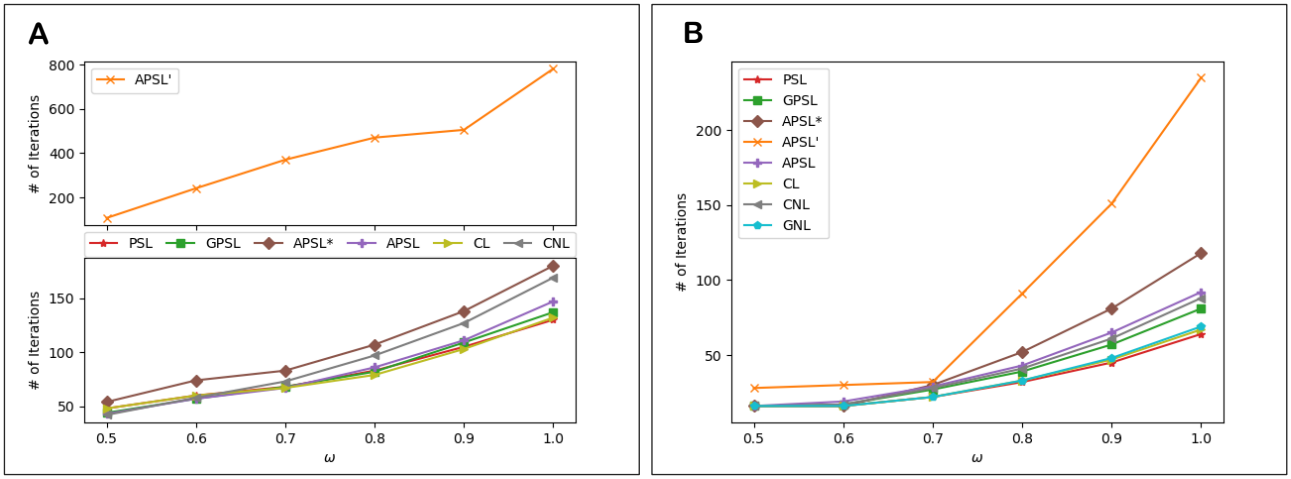

Fig. 3.20. Number of iterations required for convergence for the SUE models as the level of travel demand is increased, scaled by ω. **A:** Sioux Falls. **B:** Winnipeg.

Fig. 3.21A-B display for the Sioux Falls and Winnipeg networks, respectively, how the total computation times vary for the different SUE models as the common θ parameter is varied. Fig. 3.22A-B display how the required number of FAA iterations varies. As shown, apart from for APSL′ SUE on the Sioux Falls network, convergence for the SUE models generally gets slower as θ increases and the route cost differences are accentuated more resulting in greater flow fluctuations.

Fig. 3.23A-B and Fig. 3.24A-B display how total computation times / number of iterations vary, respectively, for the CNL SUE model as the μ parameter is varied. As shown, for both networks, the number of iterations (and thus computation time) required for convergence decreases for greater values of μ, i.e. as CNL SUE increases in similarity to MNL SUE. This is a typical finding for CNL SUE models, e.g. Bekhor et al (2008).

Fig. 3.25A-B display results for the GNL SUE model as the λ^{GNL} parameter is varied. As shown, the number of iterations (and thus computation time) required for convergence decreases for greater values of λ^{GNL}. Note that for $\lambda^{GNL} = 0$, GNL SUE is equivalent to MNL SUE (since $\lambda^{GNL} = 0$ results in $\mu_m = 1, m = 1, \dots, M$).

Fig. 3.26A-B and Fig. 3.27A-B display results for the GPSL SUE model as the λ^{GPS} parameter is varied. As shown, the number of iterations (and thus computation time) required for convergence increases for greater values of λ^{GPS}, where greater fluctuations occur within the path size contribution factors.

Fig. 3.28A-B and Fig. 3.29A-B display results for the PSL/GPSL/APSL SUE models as the common β parameter is varied. As shown, for APSL′ SUE and APSL SUE*, the number of FAA iterations increases exponentially with β. For the other models however, the effects are not as significant, though for APSL SUE – as also shown in Fig. 3.13/Fig. 3.14 – total computation times increase exponentially with β due to the fixed-point probability computation.

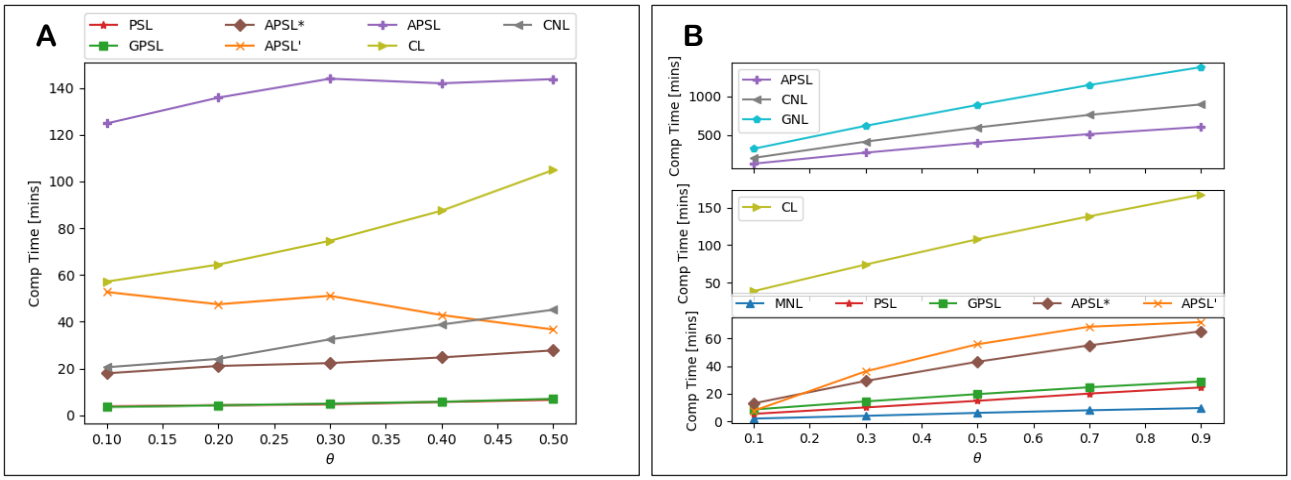

Fig. 3.21. Computation times for SUE convergence as θ is varied. **A:** Sioux Falls. **B:** Winnipeg.

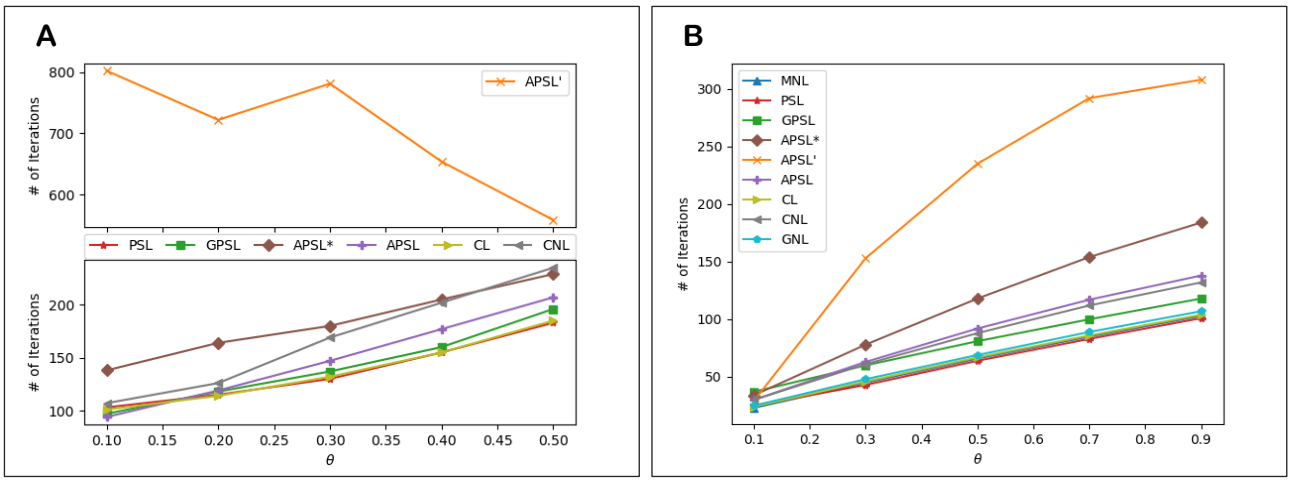

Fig. 3.22. Number of iterations required for SUE convergence as θ is varied. **A:** Sioux Falls. **B:** Winnipeg.

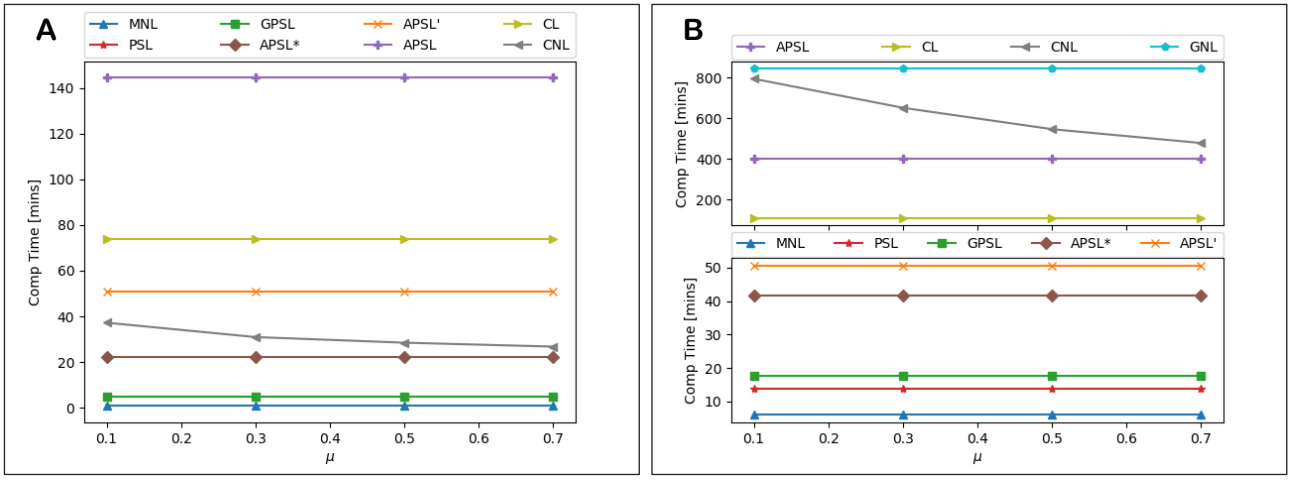

Fig. 3.23. Computation times for CNL SUE convergence as μ is varied. **A:** Sioux Falls. **B:** Winnipeg.

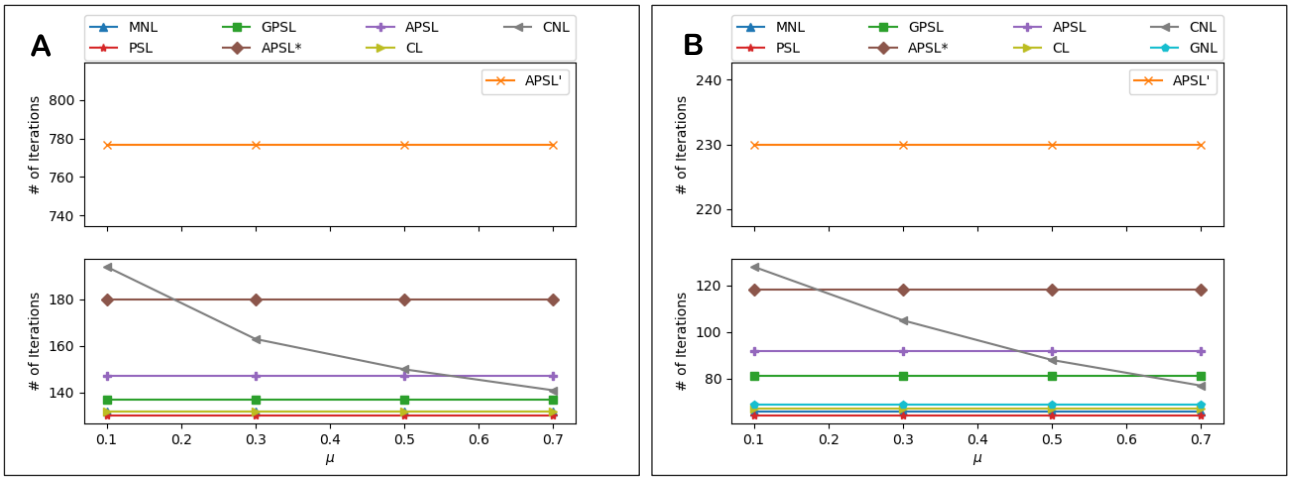

Fig. 3.24. Number of iterations required for CNL SUE convergence as μ is varied. **A:** Sioux Falls. **B:** Winnipeg.

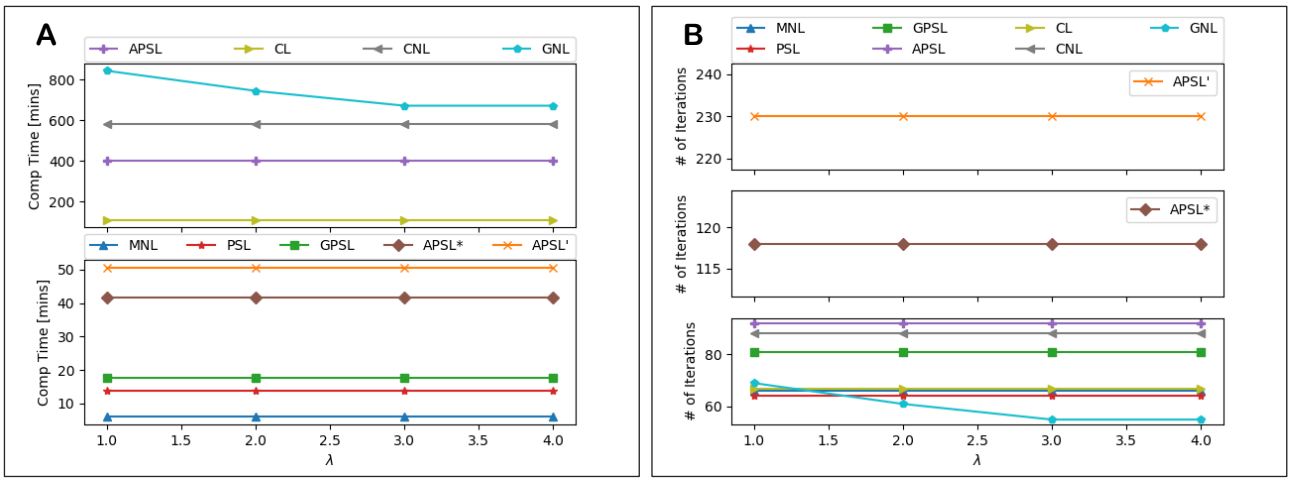

Fig. 3.25. Winnipeg: GNL SUE convergence as λ^{GNL} is varied. **A:** Computation time [mins]. **B:** Number of iterations.

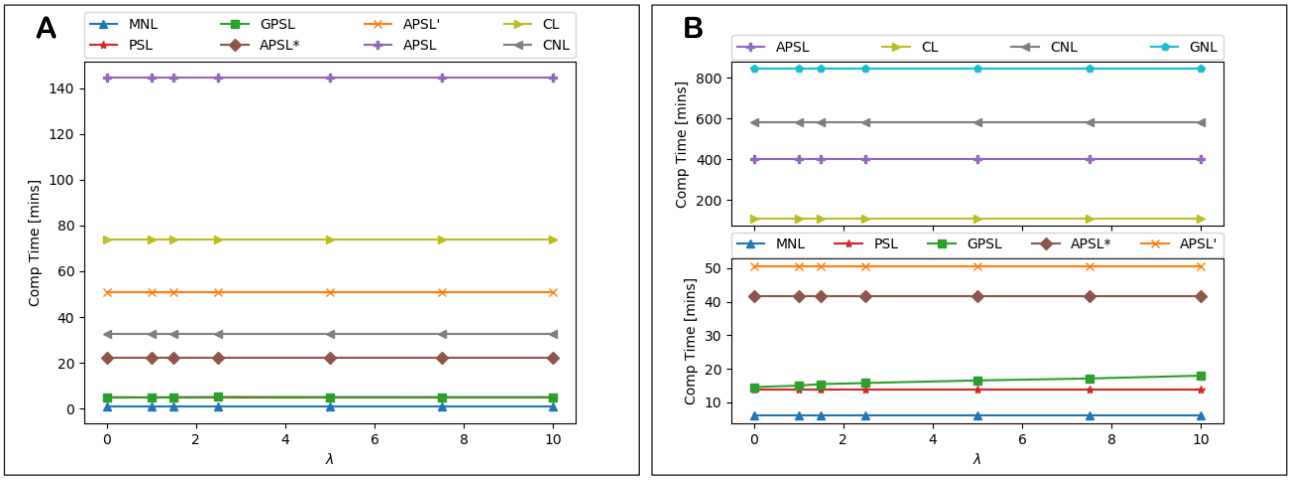

Fig. 3.26. Computation times for GPSL SUE convergence as λ^{GPS} is varied. **A:** Sioux Falls. **B:** Winnipeg.

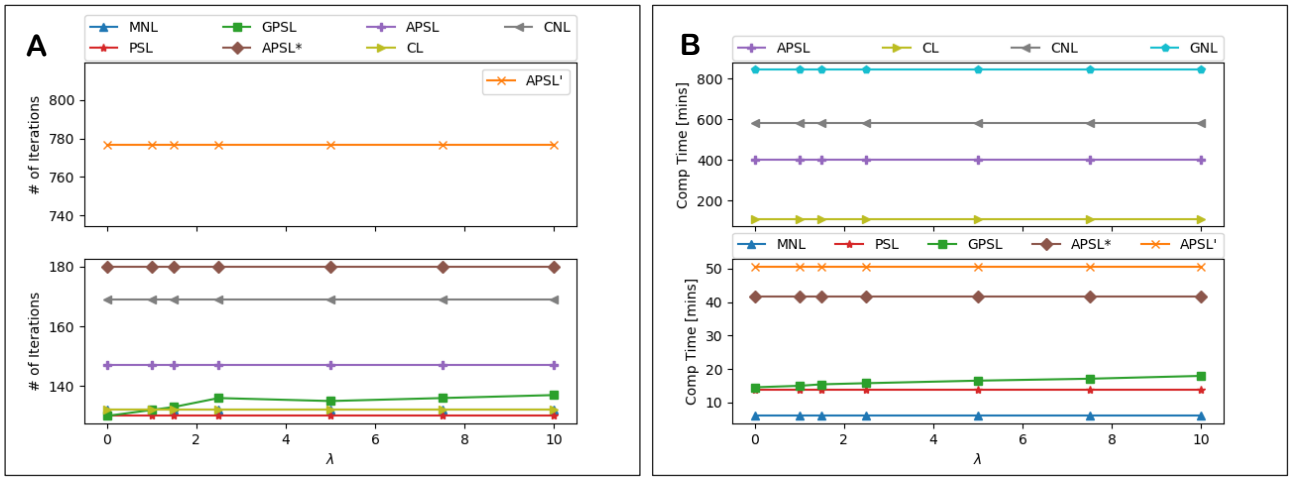

Fig. 3.27. Number of iterations required for GPSL SUE convergence as λ^{GPS} is varied. **A:** Sioux Falls. **B:** Winnipeg.

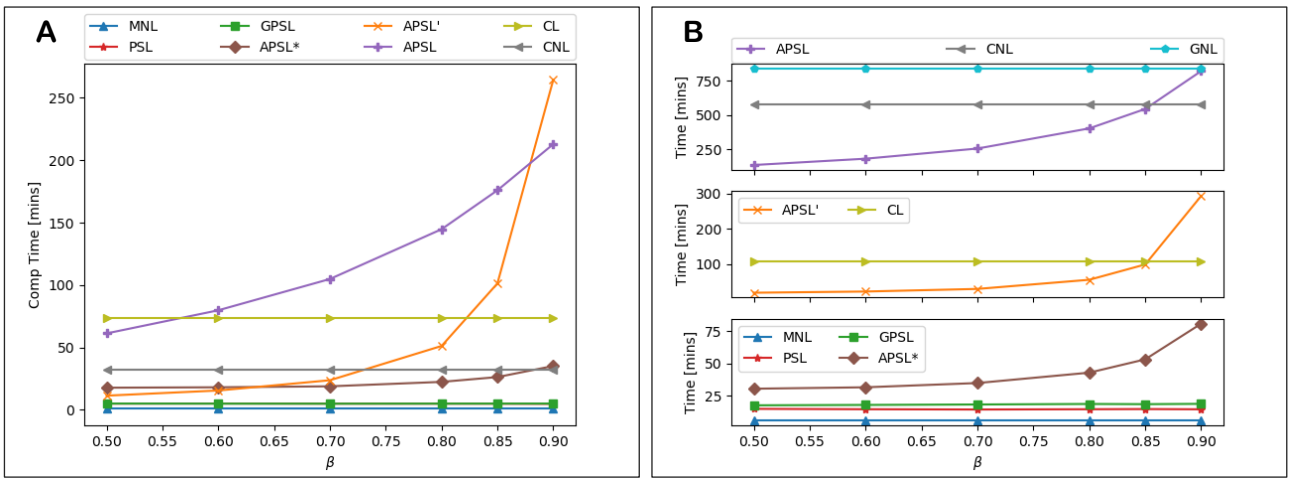

Fig. 3.28. Computation times for convergence for the Path Size Logit SUE models as β is varied. **A:** Sioux Falls. **B:** Winnipeg.

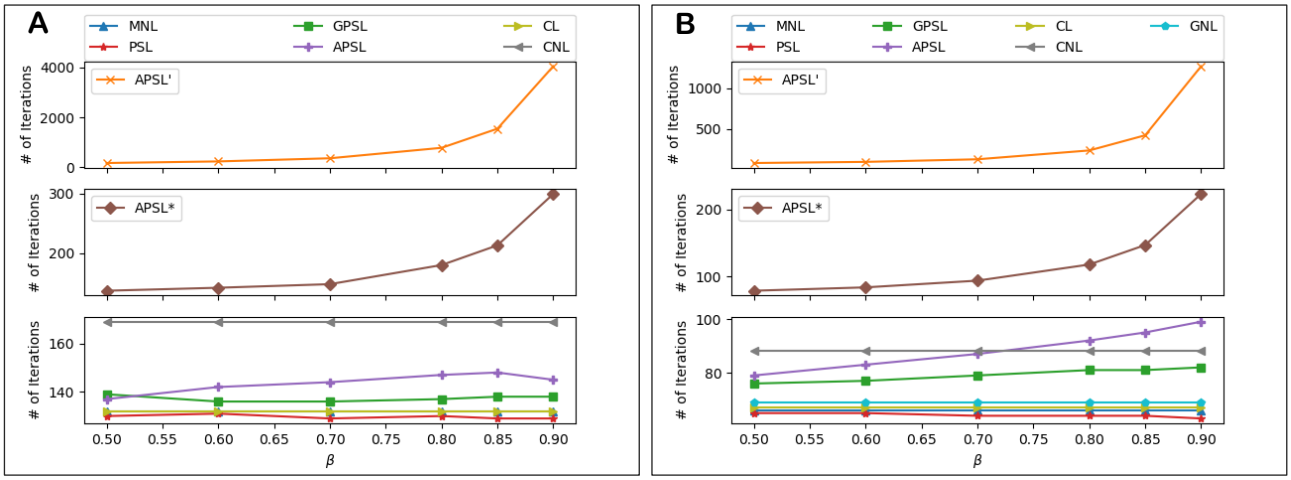

Fig. 3.29. Number of iterations required convergence for the Path Size Logit SUE models as β is varied. **A:** Sioux Falls. **B:** Winnipeg.

Lastly, Fig. 3.30A-B display for the Sioux Falls and Winnipeg networks, respectively, and for the different SUE models, how the number of iterations required for convergence varies for different settings of the MSWA parameter d. As shown, for APSL′ SUE and APSL SUE*, convergence improves significantly with greater values of d, though for APSL SUE * the number of FPIM iterations and ξ value has been optimised for $d = 5$. For APSL SUE, and MNL, PSL, & GPSL SUE, $d = 5$ and $d = 10$ provide roughly the best convergence for Sioux Falls and Winnipeg, respectively.

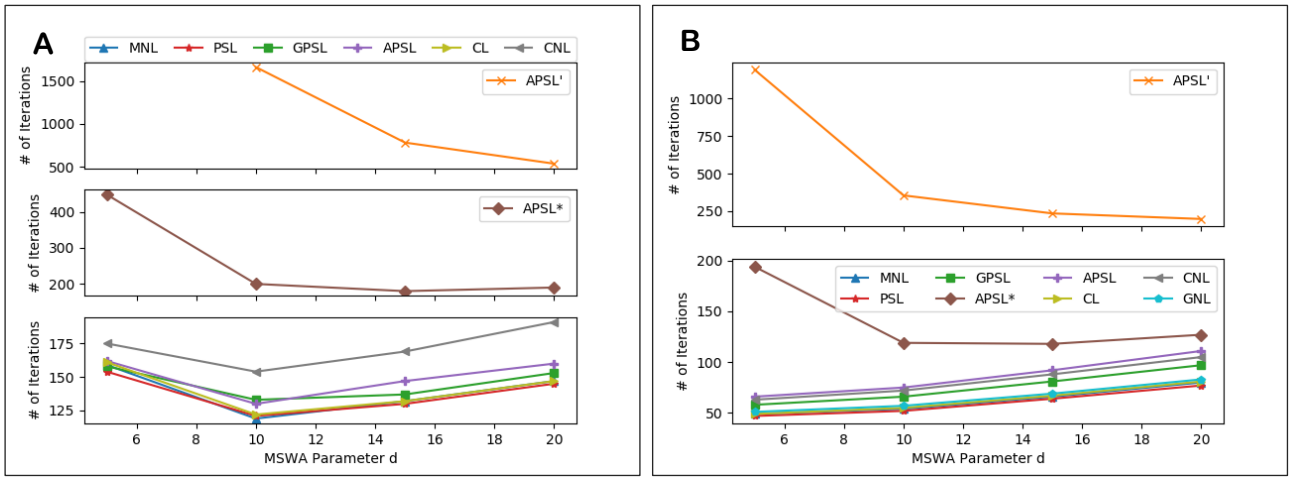

Fig. 3.30. Number of iterations required for SUE convergence for varying settings of the MSWA parameter d. **A:** Sioux Falls. **B:** Winnipeg.

4.3 Choice Set Robustness & Flow Results

In this subsection we compare the flow results from the different SUE models. To compare the flow results $\boldsymbol{f}^{*R1}$ and $\boldsymbol{f}^{*R2}$ for Result 1 and Result 2, respectively, we measure the Root Mean Squared Error (RMSE):

$$RMSE = \sqrt{\sum_{m=1}^{M} \sum_{i \in R_m} \left(f_{m,i}^{*R1} - f_{m,i}^{*R2}\right)^2 / N},$$

where N is the total number of routes. Note that for reference the RMSE between the previous and final route flows of the FAA converging to a SUE solution $\boldsymbol{f}^*$ were approximately of the order 10^{-5}.

First, we assess choice set robustness for the SUE models. Fig. 3.31A-B display for the Sioux Falls and Winnipeg networks, respectively, the impact that varying the sizes of choice sets has on the route flow results from the different models. The choice sets are obtained by generating all routes (from the pre-generated choice sets) with a free-flow travel time less than φ times greater than the free-flow travel time on the quickest route for each OD movement, and it is assumed that $\varphi = 2$ are the true choice sets, i.e. flow results are compared between the $\varphi = 2$ generated routes only. As shown, PSL SUE is the most affected by expanding the choice sets, as the path size terms of the assumed true routes are adjusted significantly attempting to capture the correlation with the added high costing routes. GPSL & APSL SUE are the least affected (and affected significantly less than PSL SUE) due to the employment of path size contribution weighting techniques, reducing the impact of the added routes.

Fig. 3.32A-B display for the Sioux Falls and Winnipeg networks, respectively, the impact varying the common θ parameter has on choice set robustness for the different SUE models. Flow results from the $\varphi = 2$ and $\varphi = 2.5$ choice sets are compared, where flows again are just compared between the $\varphi = 2$ generated routes. As shown, choice set robustness improves for all models as the θ parameter is decreased. For Sioux Falls, the relative choice set robustness between the models does not change significantly. For Winnipeg, there are more evident changes. For low θ, the choice set robustness of APSL SUE is similar to that for PSL SUE. This is because for low θ routes are considered more evenly attractive (travellers are less sensitive to differences in travel cost), and hence the APSL SUE path size contribution factors are closer to 1 (the PSL SUE factors). Increasing θ (implying the routes are less evenly attractive) accentuates the travel cost differences within the factors moving them away from 1, thereby improving choice set robustness so that for larger θ APSL SUE is the most choice set robust. For GPSL SUE, however, regardless of the θ value and consequent behavioural implications, the path size contribution factors accentuate the travel cost differences and GPSL SUE is choice set robust for all θ. This demonstrates how APSL SUE is more internally consistent and adaptable than GPSL SUE, where APSL SUE is always consistent with the behavioural implications of the model parameters.

Fig. 3.33A-B display choice set robustness for the CNL SUE model as μ is varied. As shown, for Sioux Falls, choice set robustness improves for greater values of μ, where the probabilities are closer to the MNL model, thus implying that in this case MNL is more robust than the correlation-based models. For Winnipeg,

however, choice set robustness worsens with μ, implying the opposite. Moreover, best choice set robustness occurs for μ close to 0, however as Bekhor & Prashker (2001) note, the extreme case for CNL where $\mu \to 0$ is suitable in the context of route choice only when the total route costs are equal, otherwise $\mu \to 0$ can lead to counter-intuitive results.

Fig. 3.34A-B display choice set robustness for the GNL SUE model as λ^{GNL} is varied. As shown, choice set robustness improves as λ^{GNL} increases: the nesting coefficients move away from 1 and closer 0, and thus since MNL SUE ($\mu = 1$ for CNL/GNL) on Winnipeg is not robust, robustness for GNL SUE improves for greater values of λ^{GNL}.

Fig. 3.35A-B display choice set robustness for the CL SUE model as υ is varied. As shown, for Sioux Falls, since MNL SUE is choice set robust, CL SUE is also choice set robust for low υ; however, as υ increases and the correlation component becomes more prominent, choice set robustness worsens dramatically. For Winnipeg, since MNL SUE is not robust, robustness actually improves for CL SUE as υ increases, up to a point where the correlation components become prominent enough that the adjustments from capturing similarities with new unrealistic routes begins to worsen robustness.

Fig. 3.36A-B display choice set robustness for the GPSL SUE model as λ^{GPS} is varied. As shown, and as expected, for both networks, choice set robustness is equivalent to that of PSL SUE for $\lambda^{GPS} = 0$ (where the models are equivalent), and robustness improves as λ^{GPS} increases from 0 and the path size contribution factors accentuate the cost differences more, resulting in the new more costly routes having reduced contributions and thus adjusting the realistic route probabilities less. A peak is reached in terms of choice set robustness, however, and increasing λ^{GPS} further worsens robustness.

Fig. 3.37A-B display choice set robustness for the PSL/GPSL/APSL SUE models as β is varied. As shown, for $\beta = 0$ the path size models are equal to MNL SUE, where robustness is good for Sioux Falls and bad for Winnipeg. As β increases for Sioux Falls, the increasing prominence of the correlation components worsens robustness, where the effects for PSL SUE are significantly worse than for the weighted path size contribution models. For Winnipeg, robustness improves as β increases for the weighted contribution models, but worsens for PSL SUE.

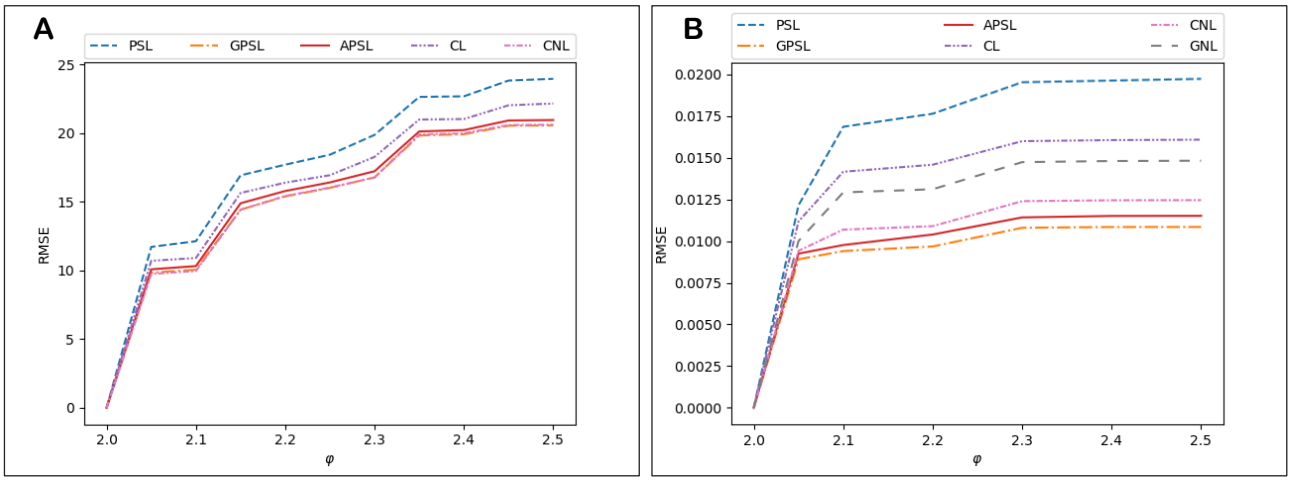

Fig. 3.31. Impact that varying the sizes of choice sets has on the route flow results of the different SUE models, scaled by φ. **A:** Sioux Falls ($\theta = 0.07$). **B:** Winnipeg.

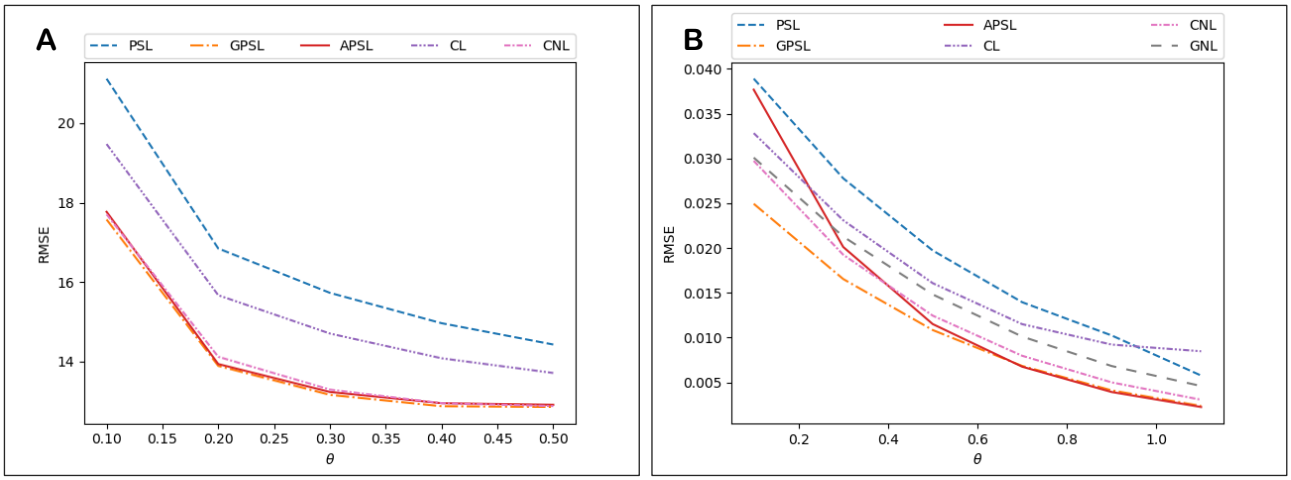

Fig. 3.32. Impact that varying the θ parameter has on choice set robustness for the different SUE models. **A:** Sioux Falls. **B:** Winnipeg.

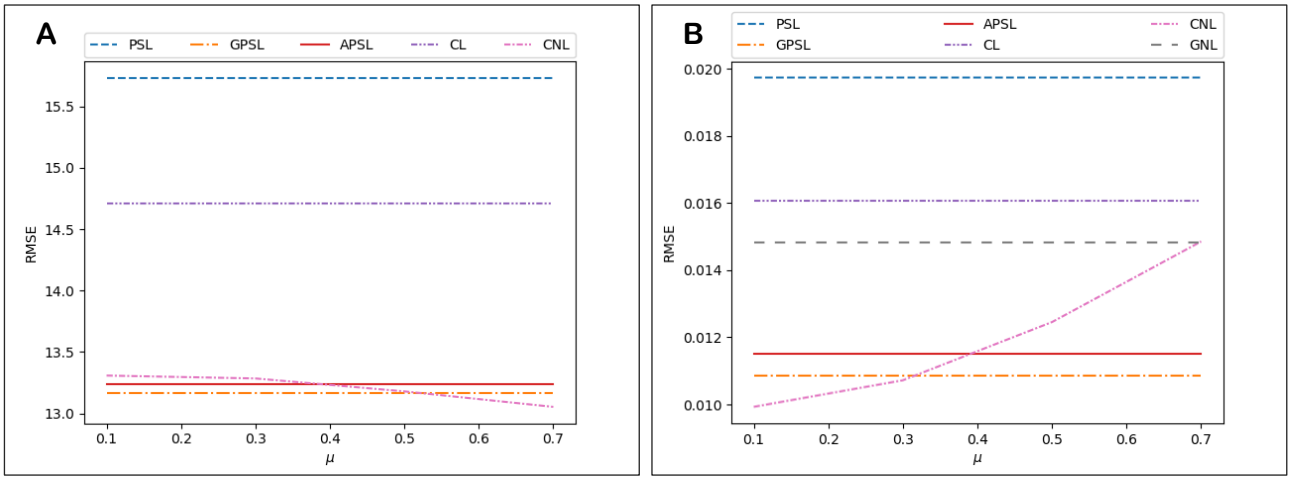

Fig. 3.33. Impact that varying the μ parameter has on choice set robustness for the CNL SUE model. **A:** Sioux Falls. **B:** Winnipeg.

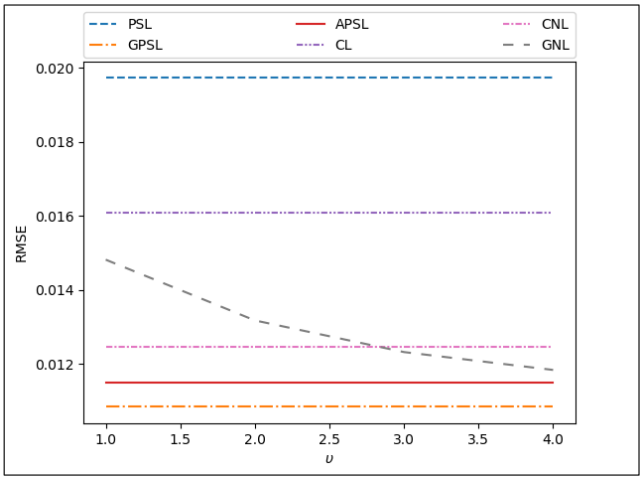

Fig. 3.34. Impact that varying the λ^{GNL} parameter has on choice set robustness for the GNL SUE model on the Winnipeg network.

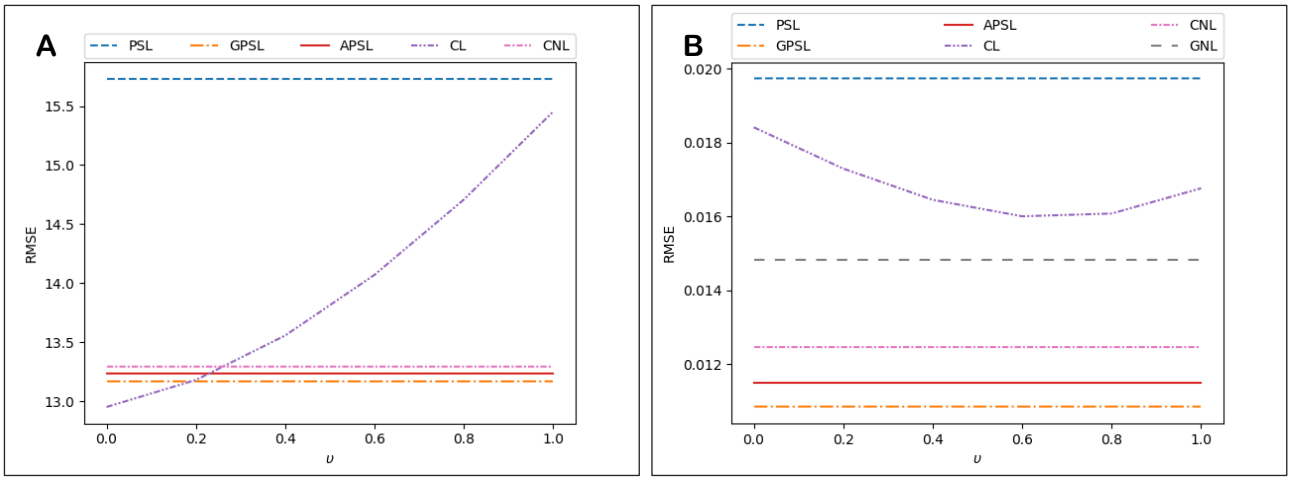

Fig. 3.35. Impact that varying the υ parameter has on choice set robustness for the CL SUE model. **A:** Sioux Falls. **B:** Winnipeg.

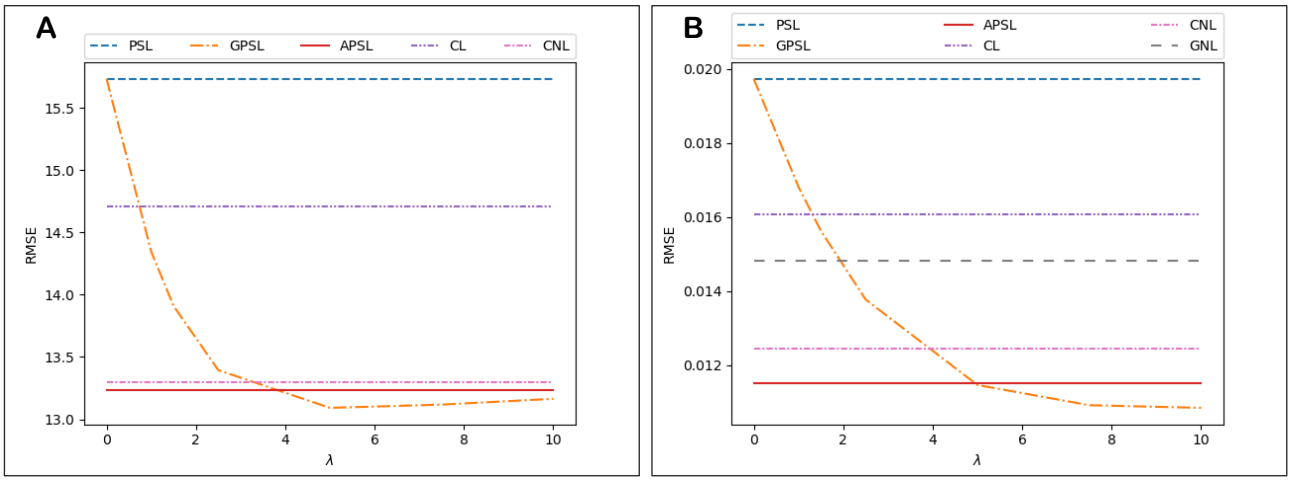

Fig. 3.36. Impact that varying the λ^{GPS} parameter has on choice set robustness for the GPSL SUE model. **A:** Sioux Falls. **B:** Winnipeg.

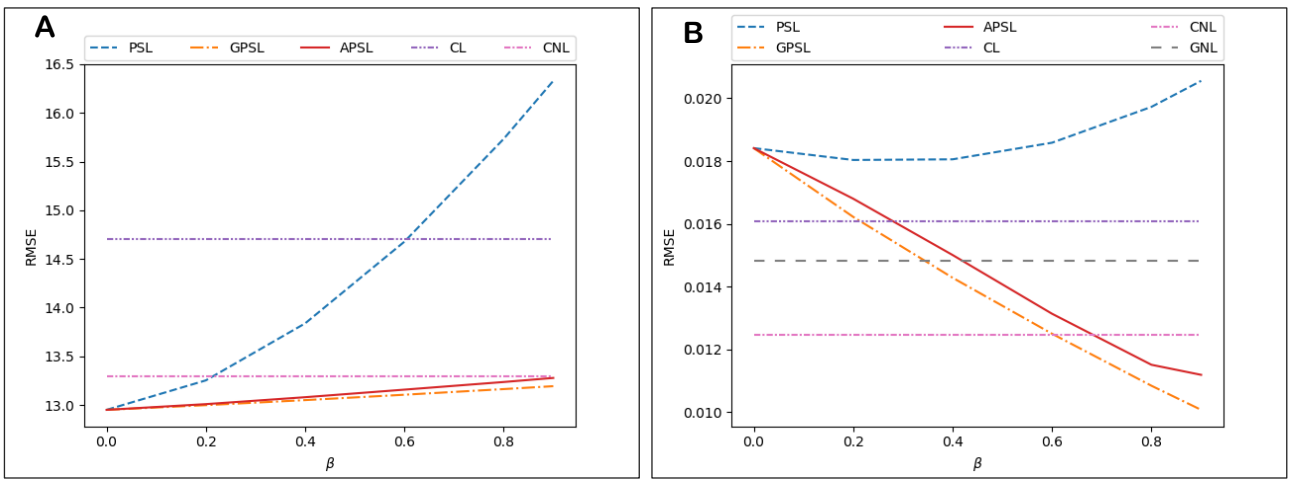

Fig. 3.37. Impact that varying the β parameter has on choice set robustness for the Path Size Logit SUE models. **A:** Sioux Falls. **B:** Winnipeg.

We next consider the differences in flow results between the Path Size Logit SUE models. Fig. 3.38A-B display for the Sioux Falls and Winnipeg networks, respectively, the impact the θ parameter has on the differences in SUE flow between the models. Most notably, in these ranges of θ, the flow differences between GPSL & APSL SUE decrease with θ (initially for Winnipeg) and the flow differences between PSL & APSL SUE increase with θ. The former is because as θ increases, the travel cost components within the APSL SUE

path size contribution factors increase in contribution influence compared to the route distinctiveness components, and hence the factors increase in similarity to the GPSL SUE factors (which only consider travel cost), and thus the SUE route flows. The flows then begin to increase in difference as the θ parameter begins to accentuate the travel cost differences for APSL more than the λ parameter does for GPSL within the contribution factors. The latter occurs since for low θ routes are considered more evenly attractive and hence the APSL SUE path size contribution factors are closer to 1 (the PSL SUE factors), and increasing θ accentuates the travel cost differences within the factors moving them away from 1. A peak is reached and further increasing θ results in the travel cost components within the PSL & APSL probability relations dominating the distinctiveness components where the difference lies.

Fig. 3.39A-B display the impact of the β parameter. As shown, the flow differences all increase as β increases, which is logical since the differences between the SUE models are the different path size correction terms scaled by β. GPSL & APSL SUE are amongst the least different due to their similarity in adopting path size contribution weighting techniques. What is noticeable is that the differences between the APSL SUE flows and PSL/GPSL SUE flows increase significantly for larger values of β. This is because distinctiveness increases significantly in contribution influence within the APSL SUE path size terms, moving the contribution factors away from 1 (PSL) and making the travel cost component less prominent (GPSL).

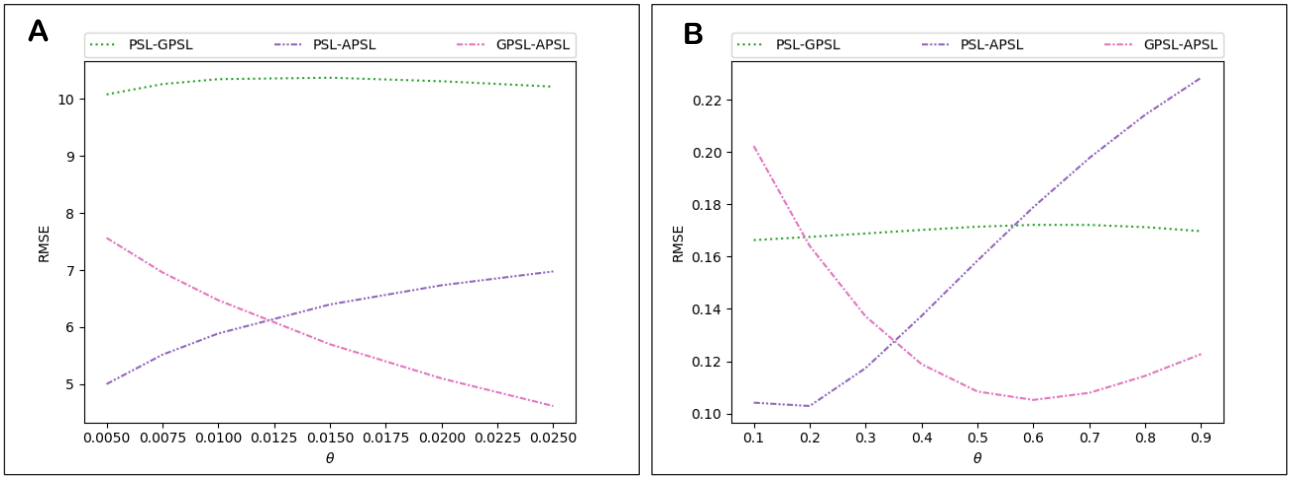

Fig. 3.38. Impact of the θ parameter on the differences in SUE flow between the Path Size Logit SUE models. **A:** Sioux Falls. **B:** Winnipeg.

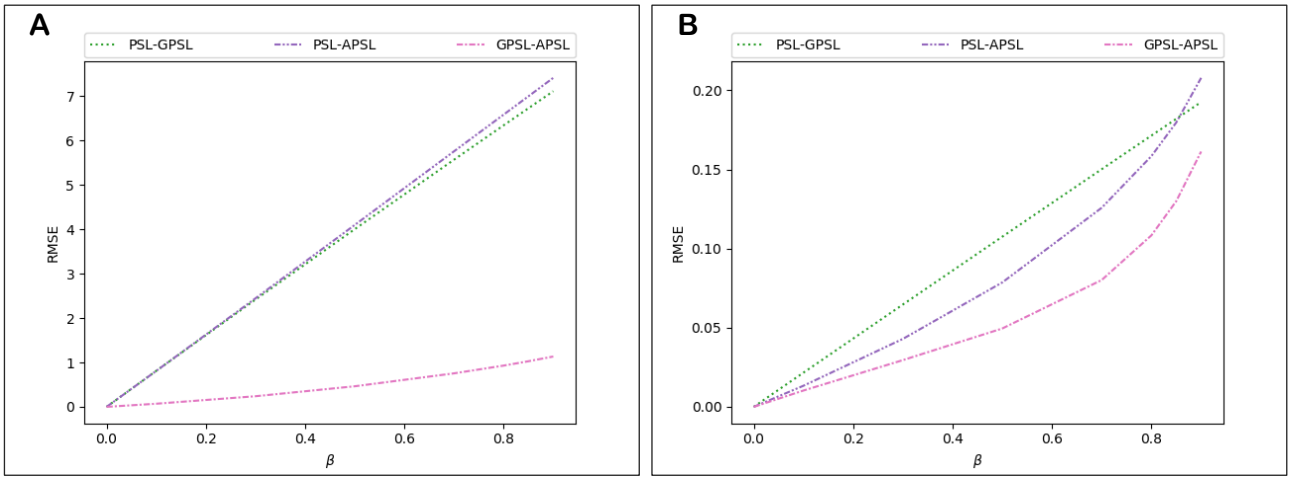

Fig. 3.39. Impact of the β parameter on the differences in SUE flow between the Path Size Logit SUE models. **A:** Sioux Falls. **B:** Winnipeg.

To explore the impact that varying the level of travel demand has on route choice (i.e. proportional route flow), we measure the RMSE of the *route choice probabilities*, i.e. by dividing the flow results by the respective OD movement demands. Fig. 3.40A-B display the impact different levels of travel demand have on the differences in choice probabilities between the Path Size Logit SUE models, with $\theta = 0.01$ for Sioux

Falls. Most notably for Sioux Falls, the differences between the GPSL & APSL SUE probabilities decrease from being the most different as the demand level increases, while the PSL & APSL SUE probability differences increase from being the least different. At zero demand, the relatively low setting of θ given the zero flow link costs dampens the travel cost differences within the APSL path size contribution factors resulting in the PSL probabilities being closer and the GPSL probabilities further away to APSL. As demand increases however and the link costs increase in scale, the travel cost differences become less dampened and the APSL contribution factors consequently move away from 1 (PSL) and closer to the GPSL factors, where the travel cost differences are accentuated. For Winnipeg, due to the overall lower level of congestion, the effects are less significant; however, the flow differences between the GPSL & APSL SUE probabilities also decrease while the PSL & APSL SUE probability differences increase. This time though the GPSL & APSL SUE probabilities are the most similar, due to the similar path size contribution weightings given the scale of travel costs.

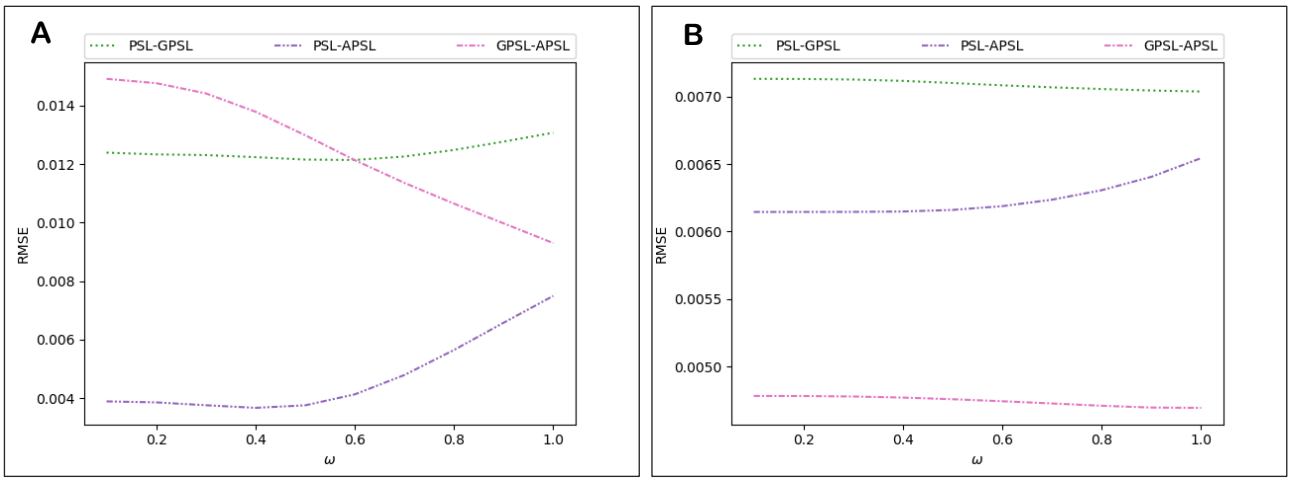

Fig. 3.40. Impact that different levels of demand has on the differences in choice probability between the Path Size Logit SUE models, demand scaled by ω. **A:** Sioux Falls. **B:** Winnipeg.

Lastly, Fig. 3.41A-B display for Sioux Falls and Winnipeg, respectively, how the SUE models differ from the CNL SUE model as the θ parameter is varied. Most interestingly, on both networks, APSL SUE is the most similar to CNL SUE for larger values of θ, even when compared with GNL SUE.

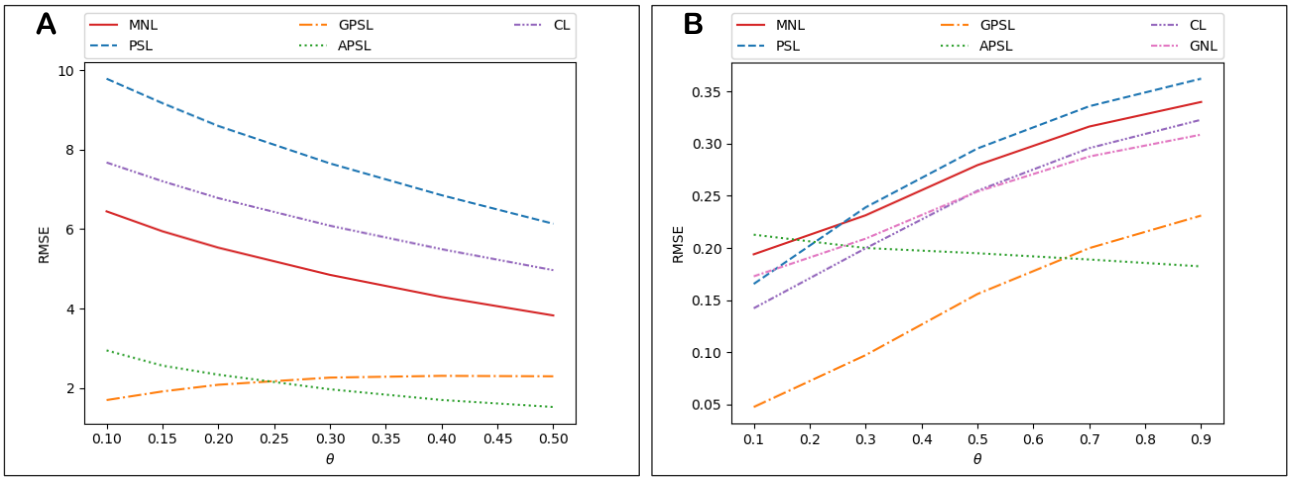

Fig. 3.41. How the SUE models differ from the CNL SUE model as the θ parameter is varied. **A:** Sioux Falls. **B:** Winnipeg.

4.4 Uniqueness of APSL SUE Solutions

As discussed in Section 3.3.2, it is not possible to prove that APSL SUE solutions can be unique according to standard approaches. Instead, we investigate here the uniqueness of APSL SUE solutions numerically.

As demonstrated in Duncan et al (2020), for a given setting of the link costs $\boldsymbol{t}$ and θ value, a β value exists, $\beta_{max,m}(\boldsymbol{t},\theta) > 0$, for OD movement m such that APSL choice probability solutions are unique for all

β in the range $0 \leq \beta \leq \beta_{max,m}(\boldsymbol{t},\theta)$. This means that a β value exists, $\beta_{max}(\boldsymbol{t},\theta) > 0$, such that solutions are unique for all OD movements for all β in the range $0 \leq \beta \leq \beta_{max}(\boldsymbol{t},\theta)$, i.e. $\beta_{max}(\boldsymbol{t},\theta) = \min\left(\beta_{max,m}(\boldsymbol{t},\theta)\right)$. And, assuming the link costs are bounded, i.e. they have a maximum and minimum value (for example due the fixed demands), for a given θ value, a β value exists, $\bar{\beta}_{max}(\theta) > 0$, such that APSL solutions are unique for all OD movements and for all feasible flow vectors (and thus costs) for all β in the range $0 \leq \beta \leq \bar{\beta}_{max}(\theta)$. Obviously, $\bar{\beta}_{max}(\theta) \leq \beta_{max}(\boldsymbol{t},\theta) \leq \beta_{max,m}(\boldsymbol{t},\theta)$.

While it is not guaranteed that in all cases APSL SUE solutions will be unique when APSL probabilities are universally unique, i.e. for β in the range $0 \leq \beta \leq \bar{\beta}_{max}(\theta)$, as we show below, it appears from numerical experiments that this is often the case.

Fig. 3.42A-B plot, for two runs, the small example network route flows at each iteration of the FAA when the initial conditions for the FPIM in Step 3 are randomly generated, for $\beta = 0.9$ and $\beta = 1.1$, respectively, $v_1 = 2$, $v_2 = v_3 = v_4 = 1$, $\theta = 1$, $\xi = 8$. The step-size is set as $\eta_n = 1$ ($n = 1,2,...$) and the algorithm is stopped after 20 iterations if convergence is not reached. As shown, for $\beta = 0.9$, because the APSL probabilities are unique for the route costs (from the flows) at each iteration, the route flows on both runs converge in the same way to the same APSL SUE solution. For $\beta = 1.1$, however, as demonstrated clearly at iteration 1, there are multiple APSL probabilities for the route costs at each iteration, and hence due to the step-size the flows fluctuate randomly and do not converge. This suggests that APSL probability solutions are universally unique for $\beta = 0.9$, but not for $\beta = 1.1$, and hence that $0.9 \leq \bar{\beta}_{max}(1) < 1.1$.

Fig. 3.43A-B plot for $\beta = 0.9$ and $\beta = 1.1$, respectively, and for multiple runs, the flows at each iteration of the FAA utilising follow-on initial conditions for the FPIM in Step 3, where the SUE initial conditions are randomly generated, $v_1 = 2$, $v_2 = v_3 = v_4 = 1$, $\theta = 1$, $\xi = 8$. As shown, for $\beta = 0.9$, all initial conditions lead to the same solution, whereas for $\beta = 1.1$, two solutions are found with different initial conditions. Fig. 3.44A-B plot the flows at each iteration of the FAA for solving APSL′ SUE. As shown, for $\beta = 0.9$, all initial conditions again lead to the same solution, whereas for $\beta = 1.1$, two solutions are found.

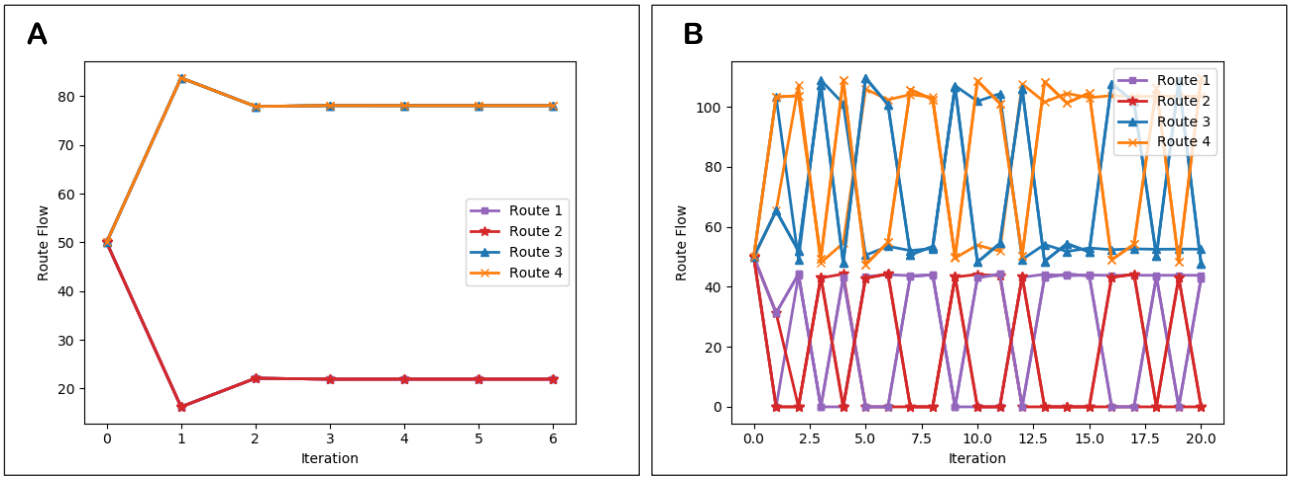

Fig. 3.42. Small example network: APSL SUE route flows at each iteration of the FAA with randomly generated FPIM initial conditions, two runs ($v_1 = 2$, $v_2 = v_3 = v_4 = 1$, $\theta = 1$, $\xi = 8$). **A:** $\beta = 0.9$. **B:** $\beta = 1.1$.

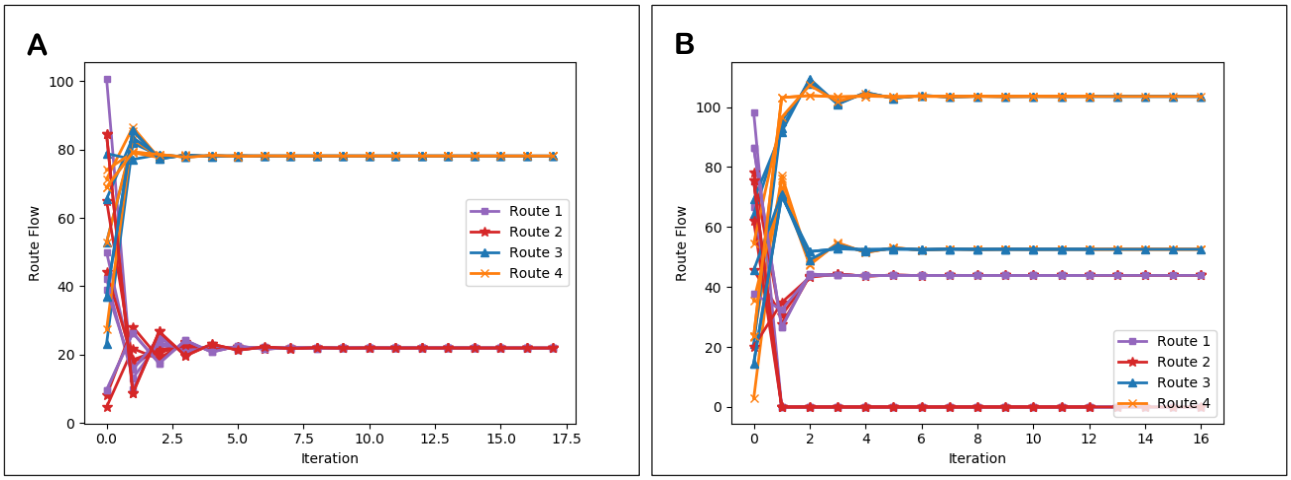

Fig. 3.43. Small example network: APSL SUE route flows at each iteration of the FAA with follow on FPIM initial conditions and randomly generated SUE initial conditions, multiple runs ($v_1 = 2$, $v_2 = v_3 = v_4 = 1$, $\theta = 1$, $\xi = 8$). **A:** $\beta = 0.9$. **B:** $\beta = 1.1$.

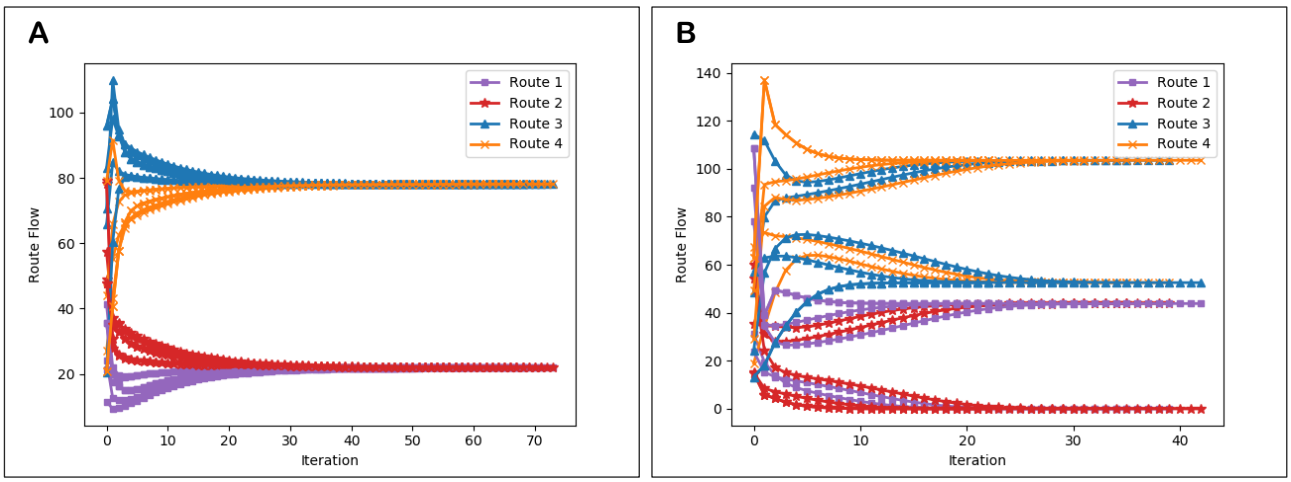

Fig. 3.44. Small example network: APSL′ SUE route flows at each iteration of the FAA with randomly generated SUE initial conditions, multiple runs ($v_1 = 2$, $v_2 = v_3 = v_4 = 1$, $\theta = 1$). **A:** $\beta = 0.9$. **B:** $\beta = 1.1$.

Fig. 3.43 & Fig. 3.44 suggest that the APSL SUE solution is unique for $\beta = 0.9$, and solutions are non-unique for $\beta = 1.1$, and Fig. 3.42 suggests that this due to the APSL choice probability solutions being universally unique for $\beta = 0.9$, but not for $\beta = 1.1$. One can imply from this that $0.9 \leq \bar{\beta}_{max}(1) < 1.1$, and potentially that APSL SUE solutions are unique for β in the range $0 \leq \beta \leq 0.9 \leq \bar{\beta}_{max}(1)$.

Duncan et al (2020) demonstrate how APSL choice probability solutions for OD movement m are unique for β in the range $0 \leq \beta \leq \beta_{max,m}(\boldsymbol{t}, \theta)$. Here, we utilise a similar method to that described in Section 4.4 of Duncan et al (2020) for the APSL model, to attempt to identify $\bar{\beta}_{max,m}(\theta)$ values and thus $\bar{\beta}_{max}(\theta) = \min\left(\bar{\beta}_{max,m}(\theta) : m = 1, \dots, M\right)$ for the APSL SUE model, where the costs are not fixed. $\bar{\beta}_{max,m}(\theta)$ is estimated by plotting trajectories of APSL SUE solutions for OD movement m for varying β, and identifying where a unique trajectory of solutions ends and multiple trajectories begin. A simple method for obtaining trajectories of APSL SUE solutions is as follows:

Step 1. Identify a suitably large value for β (where it is predicted that solutions will be non-unique).

Step 2. Solve APSL SUE for this large β with a randomly generated SUE initial condition.

Step 3. Decrement β and obtain the next APSL SUE solution with the SUE initial condition set as the solution for the previous β.

Step 4. Continue until a suitably low value of β (where it is predicted that solutions will be unique).

By plotting the route flows for OD movement m at each decremented β, and repeating this method several times, one can determine where non-unique solution trajectories end and hence estimate $\bar{\beta}_{max,m}(\theta)$. If after

several repetitions (with different randomly generated initial conditions) only a single trajectory of solutions is shown, then the initial large β value is increased. Similarly, if only multiple trajectories are shown, the stopping low β value is decreased. However, one can test beforehand whether the initial and stopping β values are suitable by solving for each a few times with random initial conditions and observing whether there are different solutions for the initial β value and the same solution for the stopping β. In the experience of the authors, the $\bar{\beta}_{max,m}(\theta)$ values typically range between 0.9 and 1.1 (usually around 1). If in large-scale networks it is computationally burdensome to solve APSL SUE once at a time for each decremented value of β, then one can instead (by possibly harnessing parallel processing) solve for different β values simultaneously, each with randomly generated initial conditions. This should also identify where solutions are and are not unique. Moreover, one can plot flow trajectories for all OD movements simultaneously, so the method does not need to be repeated for each OD movement. We illustrate the approach graphically here, but there is no need to draw graphs for general networks. One can instead observe the route flow values, where a finer grained decrement of β will provide a more accurate estimation of $\bar{\beta}_{max,m}(\theta)$.

In the case of the small example network where there is a single OD movement, we estimate $\bar{\beta}_{max}(1)$ using the above method. Fig. 3.45 displays trajectories of APSL SUE route flow solutions as the β parameter is varied for $v_1 = 2$, $v_2 = v_3 = v_4 = 1$, $\theta = 1$, $\xi = 8$. β was decremented by 0.005 and the initial large β value was 1.2. The solution trajectory plotting was repeated until multiple trajectories were shown. As shown, there is a unique trajectory of route flow solutions up until $\beta = \bar{\beta}_{max}(1)$ where there then becomes multiple trajectories. The estimated $\bar{\beta}_{max}(1)$ value is 0.995. While two APSL SUE solutions were found for $\beta = 1.1$ in Fig. 3.43B & Fig. 3.44B, Fig. 3.45 shows that there are three solutions.

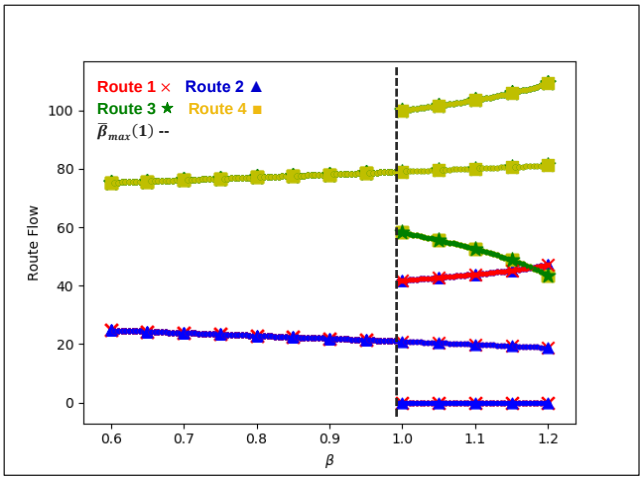

Fig. 3.45. Small example network: Trajectories of APSL SUE solutions as β is varied ($v_1 = 2$, $v_2 = v_3 = v_4 = 1$, $\theta = 1$, $\xi = 8$).

We use the same technique of plotting flow trajectories to estimate the APSL SUE uniqueness conditions for the Sioux Falls and Winnipeg networks. Fig. 3.46 displays for Sioux Falls the maximum route flow from three trajectories of APSL SUE solutions as the β parameter is varied for four different randomly chosen OD movements. β was decremented by 0.005, and the initial large β and stopping small β values were $\beta = 1.1$ and $\beta = 0.9$, respectively. As shown, the $\bar{\beta}_{max,m}(0.01)$ values for these OD movements appear to be close to 1. Fig. 3.47 display results for the Winnipeg network (two trajectories are plotted), where the $\bar{\beta}_{max,m}(0.5)$ values also appear to be close 1.

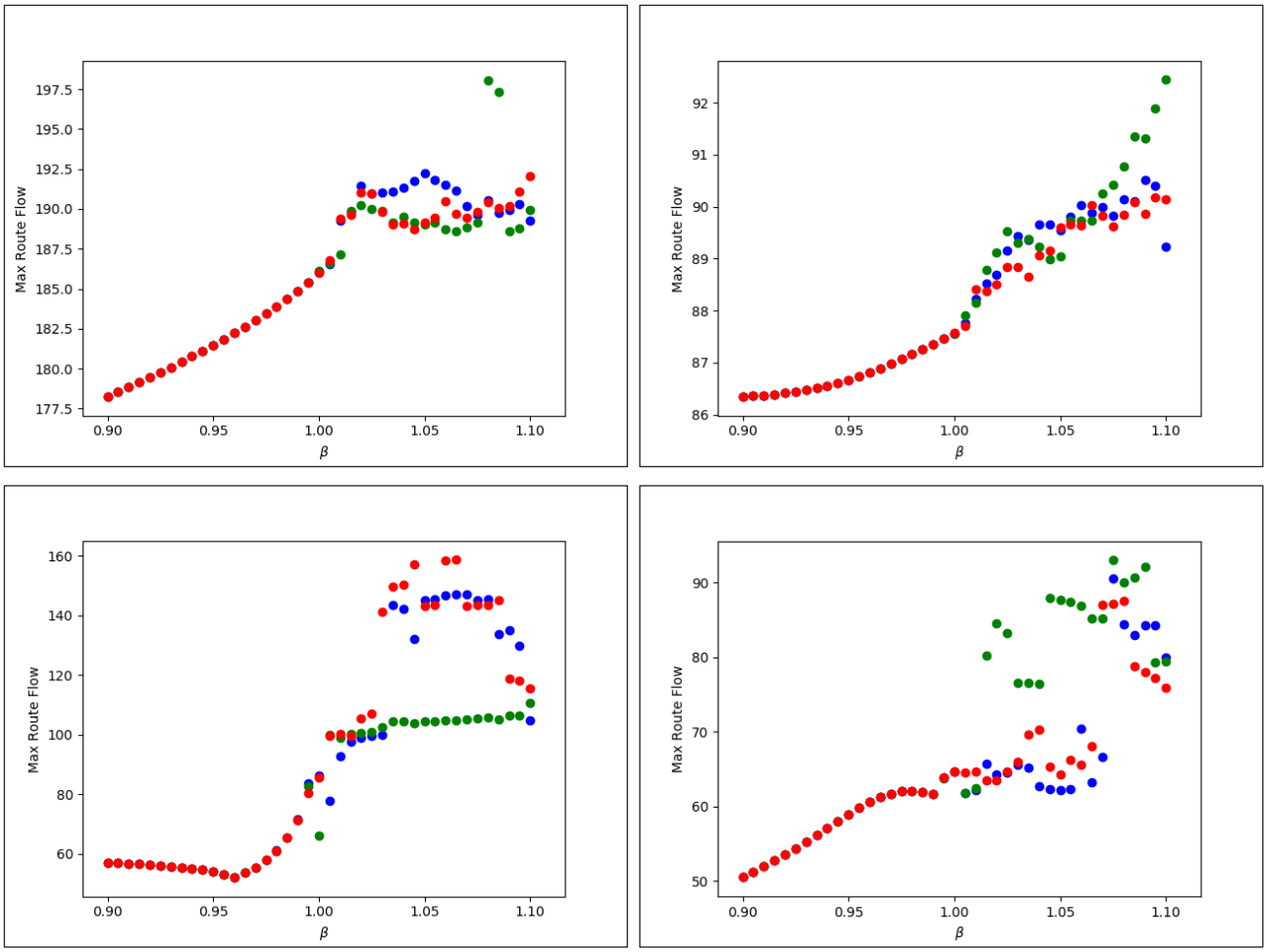

Fig. 3.46. Sioux Falls: Maximum route flow for four different OD movements from three trajectories of APSL SUE solutions as β is varied.

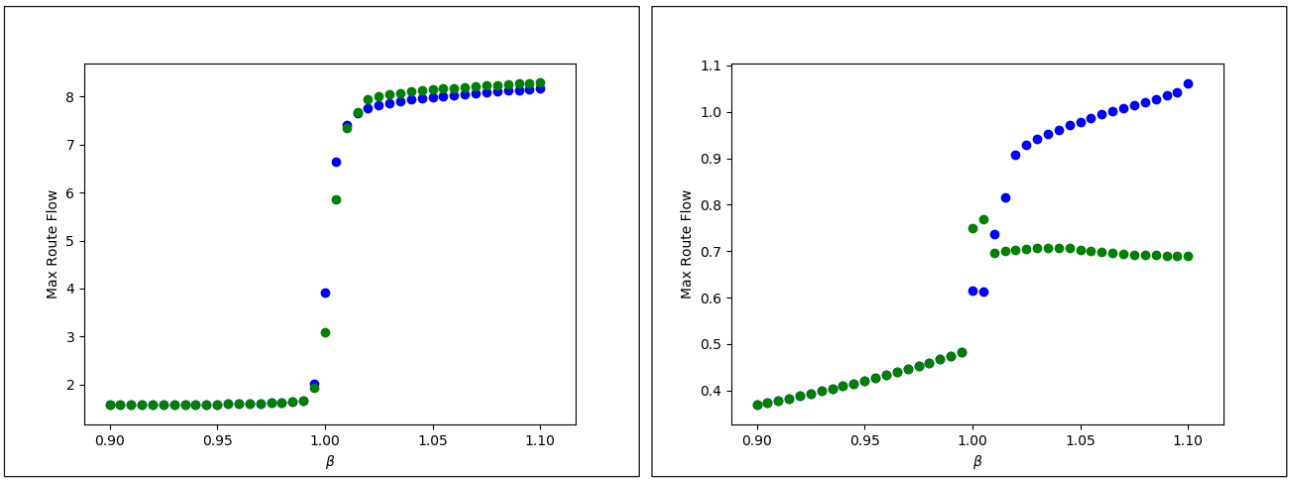

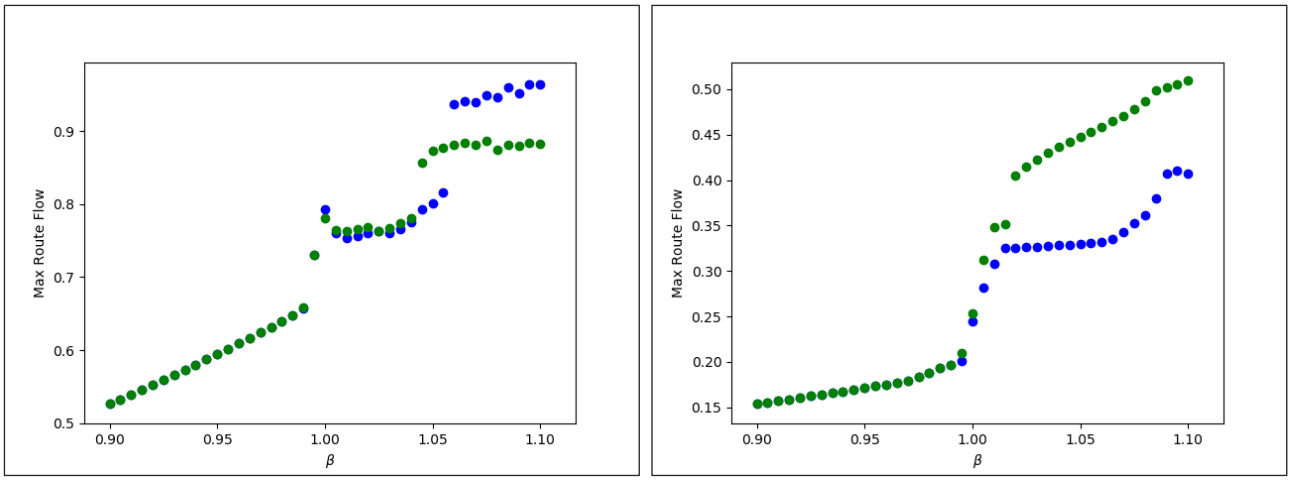

Fig. 3.47. Winnipeg: Maximum route flow for four different OD movements from two trajectories of APSL SUE solutions as β is varied.

In our experience, the ranges of β that exist for the uniqueness of APSL and APSL SUE solutions provide enough scope for fitting to behaviour, where typical β_{max} values range between 0.9 and 1.1. Duncan et al (2020) experienced no difficulties in estimating APSL on a real-life large-scale network, and obtained a maximum likelihood estimate of $\beta = 0.84$, where it was verified that this was within the uniqueness range. Although there are obvious differences in the models, we note that this 'safe' range for β for APSL uniqueness also includes values for β reported in empirical studies with PSL & GPSL (e.g. Ramming, 2002, Bovy et al, 2008, Hoogendoorn-Lanser et al, 2005; Frejinger & Bierlaire, 2007; Prato, 2013), where estimated values have been reported in the range 0.6 to 0.93.

4.5 Findings of the Numerical Experiments

To summarise, the key findings of the numerical experiments were that:

a) APSL SUE is more internally consistent than GPSL SUE in terms of dealing with unrealistic routes in the adopted choice sets.

b) APSL SUE is generally more robust than PSL, CL, CNL, & GNL SUE to the inclusion of unrealistic routes to the choice set.

c) Convergence rates for solving APSL SUE were similar to that for PSL & GPSL SUE, however the computational burden involved in computing the APSL choice probabilities for each FAA iteration resulted in much longer total computation times.

d) On-the-other-hand, the computational burden involved in computing the APSL′ choice probabilities was the same as that for PSL & GPSL (similarly closed-form), but the APSL′ SUE convergence rate was comparatively slow, and thus total computation times were also longer.

e) In general, the FPIM convergence parameter ξ (and thus the accuracy of the APSL choice probabilities) must be at a certain level for convergence of the FAA to the APSL SUE solution.

f) However, by utilising 'follow-on' initial FPIM conditions – where the initial conditions for solving the APSL probabilities at iteration n of the FAA are set as the route flow proportions from iteration $n-1$ – the FAA will converge to the APSL SUE solution regardless for all ξ.

g) There was a computational trade-off between solving APSL & APSL′ SUE: solving APSL SUE with low ξ and follow-on initial conditions simulated solving APSL′ SUE where the convergence rate was slow, while larger values of ξ resulted in comparatively quick convergence rates but lengthy computation times for the iterations.

h) There was an 'optimal' intermediate value of ξ for solving APSL SUE with follow-on initial FPIM conditions whereby a suitable SUE convergence rate meets suitable computation times for each iteration. Optimal values for the examples in this study were $\xi = 1$ for Sioux Falls and $\xi = 0$ for Winnipeg.

i) Another technique that improved APSL SUE computation times was to stipulate a set number of FPIM iterations to perform at each FAA iteration: optimal values were 3 and 2 FPIM iterations for Sioux Falls and Winnipeg, respectively.

j) Best computation times for solving APSL SUE were found when utilising a combination of a maximum number of FPIM iterations and an intermediate value of ξ: 3 FPIM iterations and $\xi = 5$ for Sioux Falls, 2 FPIM iterations and $\xi = 4$ for Winnipeg.

k) APSL SUE can be thus solved in feasible computation times – typically longer than PSL & GPSL SUE, but quicker than CL, CNL, GNL, & PCL SUE (significantly on the larger-scale Winnipeg network).

l) Uniqueness conditions appeared to exist for APSL SUE: for β in the range $0 \leq \beta \leq \bar{\beta}_{max}(\theta)$, where APSL probability solutions are unique.

m) $\bar{\beta}_{max,m}(\theta)$ values (uniqueness for OD movement m) in experiments were all close 1.

The 'optimal' values for the methods in h)-i) for solving APSL SUE are particular to the network, model, and algorithm specifications, e.g. model parameters, adopted step-size scheme, choice set sizes. However, by fixing the optimised values for a given specification, and then varying the specifications, it was shown that the method was robust in its effectiveness compared to solving APSL SUE in a standard way (i.e. where the APSL fixed-point probabilities are accurately solved with non-follow-on initial conditions). Future research could explore an intelligent, adaptive process whereby the optimal values of ξ and the maximum number of FPIM iterations to perform at each FAA iteration are learnt / worked out as the FAA progresses.

5. Conclusion

This paper investigates the integration of the Adaptive Path Size Logit (APSL) route choice model within a Stochastic User Equilibrium (SUE) model. The APSL model captures correlations between overlapping routes by including correction terms within the route utilities, and offers an internally consistent approach to reducing the negative impact that unrealistic routes have on the correction terms of realistic routes. To do this, the APSL model proposes that routes contribute to path size terms according to choice probability ratios; consequently, the probability relation is an implicit function, naturally expressed as a fixed-point problem. APSL is thus not closed-form and calculating the choice probabilities requires a fixed-point algorithm that can compute the solution. This has the potential to be computationally burdensome in large-scale networks even when the travel costs are fixed. As explored in the paper, however, the requirement of solving fixed-point problems to compute APSL choice probabilities can be circumvented in SUE application, since at equilibrium the route flow proportions and choice probabilities equate.

The paper proves that APSL SUE solutions exist, but uniqueness cannot be guaranteed. Instead, the paper investigates the uniqueness of APSL SUE solutions numerically, where experiments on the Sioux Falls and Winnipeg networks suggest that uniqueness conditions exist. These conditions are analogous to those for the uniqueness of APSL probability solutions, and APSL SUE solutions appear to be unique when APSL solutions are unique.

The advantages of APSL SUE are demonstrated in numerical experiments on the Sioux Falls and Winnipeg networks. Computational performance, choice set robustness, and flow results are compared with internally consistent SUE formulations of competitor correlation-based route choice models to APSL, namely: Path Size Logit (PSL), Generalised Path Size Logit (GPSL), C-Logit (CL), Cross-Nested Logit (CNL), Generalised Nested Logit (GNL), and Paired Combinatorial Logit (PCL), where the functional forms in the correlation components are based upon generalised, flow-dependent congested costs, rather than e.g. length / free-flow travel time. A flow-averaging algorithm with Method of Successive Weighted Averages step-size scheme is used to solve the SUE models. The paper demonstrates how for APSL SUE one can trade-off the accuracy of APSL probabilities (and thus computation times of each iteration) with rate of SUE convergence, and as such, it is shown that APSL SUE can be solved in feasible computation times. The key findings from the numerical experiments were that:

a) APSL SUE is generally more robust than PSL, CL, CNL, & GNL SUE to the inclusion of unrealistic routes to the choice set.

b) APSL SUE is more internally consistent than GPSL SUE in terms of dealing with unrealistic routes in the adopted choice sets.

c) APSL SUE can be solved in feasible computation times – typically longer than PSL & GPSL SUE, but quicker than CL, CNL, GNL, & PCL SUE (considerably on the larger-scale Winnipeg network).

Further research could compare APSL SUE / the internally consistent correlation-based SUE models in the paper with other network equilibrium modelling approaches, for example Probit, Markovian traffic equilibrium (Baillon & Cominetti, 2008), or Recursive Logit with choice aversion by Knies & Melo (2020), who provide an extensive comparison with APSL as the reference model.

6. Acknowledgements

We gratefully acknowledge funding provided by the University of Leeds by awarding the corresponding author with a University of Leeds Doctoral Scholarship for PhD research.

7. References

Baillon J & Cominetti R, (2008). Markovian traffic equilibrium. Mathematical Programming, 111(1-2), p.33-56.

Bekhor S & Prashker J, (1999). Formulations of extended logit stochastic user equilibrium assignments. In: Proceedings of the 14th International Symposium on Transportation and Traffic Theory, Jerusalem, Israel, p.351–372.

Bekhor S & Prashker J, (2001). Stochastic user equilibrium formulation for the generalized nested logit model. Transportation Research Record 1752, p.84–90.

Bekhor S, Toledo T, & Prashker J, (2006). Implementation issues of route choice models in path-based algorithms. Paper presented at the 11th international conference on travel behaviour research, Kyoto, Japan p.13–19.

Bekhor S, Toledo T, & Reznikova L, (2008). A path-based algorithm for the cross-nested logit stochastic user equilibrium. Computer-Aided Civil and Infrastructure Engineering, 24(1), p.15–25.

Ben-Akiva M, & Ramming S, (1998). Lecture notes: discrete choice models of traveler behavior in networks. Prepared for Advanced Methods for Planning and Management of Transportation Networks. Capri, Italy.

Ben-Akiva M, & Bierlaire M, (1999). Discrete choice methods and their applications to short term travel decisions. In: Halled, R.W. (Ed.), Handbook of Transportation Science. Kluwer Publishers.

Bliemer M & Bovy P, (2008). Impact of Route Choice Set on Route Choice Probabilities. Transportation Research Record: Journal of the Transportation Research Board, 2076, p.10–19.

Bovy P, Bekhor S, & Prato C, (2008). The Factor of Revisited Path Size: Alternative Derivation. Transportation Research Record: Journal of the Transportation Research Board, 2076, Transportation Research Board of the National Academies, Washington, D.C., p.132–140.

Cantarella G & Binetti M, (2002). Stochastic assignment with gammit path choice models. Patriksson, M., Labbé's, M. (Eds.), Transportation Planning: State of the Art, p.53–68.

Cascetta E, Nuzzolo A, Russo F, & Vitetta A, (1996). A modified logit route choice model overcoming path overlapping problems: specification and some calibration results for interurban networks. In: Proceedings of the 13th International Symposium on Transportation and Traffic Theory, Leon, France, p.697–711.

Cascetta E, Russo F, & Vitetta A, (1997). Stochastic user equilibrium assignment with explicit path enumeration: comparison of models and algorithms. In: Proceedings of the international federation of automatic control: Transportation systems, Chania, Greece, p.1078–1084.

Chen A, Lo H, & Yang H, (2001). A self-adaptive projection and contraction algorithm for the traffic assignment problem with path-specific costs. European Journal of Operational Research, 135(1), p.27–41.

Chen A, Lee D-H, & Jayakrishnan R, (2002). Computational study of state-of-the-art path-based traffic assignment algorithms. Mathematics and Computers in Simulation, 59, p.509–518.

Chen A, Kasikitwiwat P, & Ji Z, (2003). Solving the overlapping problem in route choice with paired combinatorial logit model. Transportation Research Record 1857, p.65–73.

Chen A, Pravinvongvuth S, Xu X, Ryu S, & Chootinan P, (2012). Examining the scaling effect and overlapping problem in logit-based stochastic user equilibrium models. Transportation Research Part A, 46, p.1343-1358.

Chen A, Xu X, Ryu S, & Zhou Z, (2013). A self-adaptive Armijo stepsize strategy with application to traffic assignment models and algorithms. Transportmetrica A: Transport Science, 9(8), p.695–712.

Chen A, S Ryu, Xu X, & Choi K, (2014). Computation and Application of the Paired Combinatorial Logit Stochastic User Equilibrium Problem. Computers and Operations Research, 43, p.68–77.

Connors R, Hess S, & Daly A, (2014). Analytic approximations for computing probit choice probabilities, Transportmetrica A: Transport Science, 10(2), p.119-139.

Daganzo C & Sheffi Y, (1977). On stochastic models of traffic assignment. Transportation Science, 11, p.253–274.

Duncan L, Watling D, Connors R, Rasmussen T, & Nielsen O, (2020). Path Size Logit Route Choice Models: Issues with Current Models, a New Internally Consistent Approach, and Parameter Estimation on a Large-Scale Network with GPS Data. Transportation Research Part B, 135, p.1-40.

Frejinger E, & Bierlaire M, (2007). Capturing correlation with subnetworks in route choice models. Transportation Research Part B, 41(3), p.363-378.

Hoogendoorn-Lanser S, van Nes R, & Bovy P, (2005). Path Size Modeling in Multimodal Route Choice Analysis. Transportation Research Record: Journal of the Transportation Research Board, 1921, p.27–34.

Isaacson E, & Keller H, (1966). Analysis of Numerical Methods. John Wiley & Sons, Inc., New York, USA.

Jayakrishnan R, et al., (1994). Faster path-based algorithm for traffic assignment. Transportation Research Record, 1443, p.75–83.

Kitthamkesorn S & Chen A, (2013). Path-size weibit stochastic user equilibrium model. Transportation Research Part B, 57, p.378-397.

Kitthamkesorn S & Chen A, (2014). Unconstrained weibit stochastic user equilibrium model with extensions. Transportation Research Part B, 59, p.1–21.

Knies A & Melo E, (2020). A Recursive Logit model with choice aversion and its application to route choice analysis. https://arxiv.org/pdf/2010.02398.pdf.

Liu H, He X, & He B, (2009). Method of successive weighted averages (MSWA) and self regulated averaging schemes for solving stochastic user equilibrium problem. Networks and Spatial Economics, 9(4), p.485–503.

Manzo S, Prato C & Nielsen O, (2015). How uncertainty in input and parameters influences transport model outputs: a four-stage model case-study. Elsevier, Transport Policy, 38, p.64-72.

Prato C, (2014). Expanding the applicability of random regret minimization for route choice analysis. Transportation, (41), p.351–375.

Ramming S, (2002). Network knowledge and route choice. Ph.D. Thesis, Massachusetts Institute of Technology, Cambridge, USA.

Rich J & Nielsen, O (2015). System convergence in transport models: algorithms efficiency and output uncertainty. European Journal of Transport Infrastructure Research (EJTIR), 15 (3), p.38-62.

Sheffi Y & Powell W, (1982). An algorithm for the equilibrium assignment problem with random link times. Network: An International Journal, 12(2), p.191-207.

Sheffi Y, (1985). Urban Transportation Networks: Equilibrium Analysis with Mathematical Programming Methods. Prentice-Hall.

Xu X, Chen A, Zhou Z, & Behkor S, (2012). Path-based algorithms for solving C-logit stochastic user equilibrium assignment problem. Transportation Research Record, 2279, p.21–30.

Xu X, Chen A, Kitthamkesorn S, Yang H, & Lo H, (2015). Modeling absolute and relative cost differences in stochastic user equilibrium problem. Transportation Research Part B, 81, p.686-703.

Zhou Z & Chen A, (2006). A self-adaptive gradient projection algorithm for solving the nonadditive traffic equilibrium problem. Paper presented at the 85th annual meeting of the transportation board, Washington, D.C., USA.

Zhou Z, Chen A, & Bekhor S, (2012). C-logit stochastic user equilibrium model: formulations and solution algorithm. Transportmetrica, 8(1), p.17–41.

8. Appendix

8.1 Appendix A: Internally Consistent SUE Formulations for Correlation-Based Route Choice Models

8.1.1 Correction Term Models

Correction term models capture correlations between routes by including heuristic correction terms within the deterministic utilities. The deterministic utility of route $i \in R_m$ is thus $V_{m,i} = -\theta c_{m,i}(\boldsymbol{t}) + \kappa_{m,i}$, where $\theta > 0$ is the Logit scaling parameter and $\kappa_{m,i} \leq 0$ is the correction term for route $i \in R_m$. The choice probability for route $i \in R_m$ is then:

$$P_{m,i}(\boldsymbol{c}_m(\boldsymbol{t}), \boldsymbol{\kappa}_m) = \frac{e^{-\theta c_{m,i}(\boldsymbol{t}) + \kappa_{m,i}}}{\sum_{j \in R_m} e^{-\theta c_{m,j}(\boldsymbol{t}) + \kappa_{m,j}}}.$$

8.1.1.1 Path Size Logit SUE Models

Path Size Logit models propose that the correction terms adopt the form $\kappa_{m,i} = \beta \ln(\gamma_{m,i})$, where $\beta \geq 0$ is the path size scaling parameter, and $\gamma_{m,i} \in (0,1]$ is the path size term for route $i \in R_m$. A distinct route with no shared links has a path size term equal to 1, resulting in no penalisation. Less distinct routes have smaller

path size terms and incur greater penalisation. The path size terms are often based upon link lengths and thus $\gamma_{m,i}$ (in those cases) is not dependent upon the link/route generalised travel costs. However, this leads to internal inconsistency (as we discuss in more detail below) and in this study we base the path size terms upon on generalised link travel costs (i.e. $\gamma_{m,i} = \gamma_{m,i}(\boldsymbol{t})$), which in SUE application are congested, flow-dependent costs. The choice probability function for route $i \in R_m$ is thus:

$$P_{m,i}\left(\boldsymbol{c}_m(\boldsymbol{t}), \boldsymbol{\gamma}_m(\boldsymbol{t})\right) = \frac{e^{-\theta c_{m,i}(\boldsymbol{t}) + \beta \ln\left(\gamma_{m,i}(\boldsymbol{t})\right)}}{\sum_{j \in R_m} e^{-\theta c_{m,j}(\boldsymbol{t}) + \beta \ln\left(\gamma_{m,j}(\boldsymbol{t})\right)}} = \frac{\left(\gamma_{m,i}(\boldsymbol{t})\right)^{\beta} e^{-\theta c_{m,i}(\boldsymbol{t})}}{\sum_{j \in R_m} \left(\gamma_{m,j}(\boldsymbol{t})\right)^{\beta} e^{-\theta c_{m,j}(\boldsymbol{t})}}. \quad (3.10)$$

The general form for the path size term is as follows:

$$\gamma_{m,i}(\boldsymbol{t}) = \sum_{a \in A_{m,i}} \frac{t_a}{c_{m,i}(\boldsymbol{t})} \frac{1}{\sum_{k \in R_m} \left(\frac{W_{m,k}(\boldsymbol{t})}{W_{m,i}(\boldsymbol{t})}\right) \delta_{a,m,k}}, \quad (3.11)$$

where $W_{m,k}(\boldsymbol{t}) > 0$ is the path size contribution weighting of route $i \in R_m$ to path size terms (different for each model), so that the contribution of route $k \in R_m$ to the path size term of route $i \in R_m$ (the path size contribution factor) is $\frac{W_{m,k}(\boldsymbol{t})}{W_{m,i}(\boldsymbol{t})}$. To dissect the path size term: each link a in route $i \in R_m$ is penalised (in terms of decreasing the path size term and hence the utility of the route) according to the number of routes in the choice set that also use that link $\left(\sum_{k \in R_m} \delta_{a,m,k}\right)$, where each contribution is weighted (i.e. $\sum_{k \in R_m} \left(\frac{W_{m,k}(\boldsymbol{t})}{W_{m,i}(\boldsymbol{t})}\right) \delta_{a,m,k}$), and the significance of the penalisation is also weighted according to how prominent link a is in route $i \in R_m$, i.e. the cost of route a in relation to the total cost of route $i \in R_m$ $\left(\frac{t_a}{c_{m,i}(\boldsymbol{t})}\right)$.

The Path Size Logit (PSL) model (Ben-Akiva & Bierlaire, 1998) proposes that $W_{m,k}(\boldsymbol{t}) = 1$ so that all routes contribute equally to path size terms. This is problematic with the mis-generation of realistic route choice sets, however, as the correction terms and thus the choice probabilities of realistic routes are affected by link sharing with unrealistic routes. To combat this, Ramming (2002) proposed the Generalised Path Size Logit (GPSL) model where $W_{m,k}(\boldsymbol{t}) = \left(c_{m,k}(\boldsymbol{t})\right)^{-\lambda}$, $\lambda \geq 0$, and routes contribute according to travel cost ratios, so that routes with large travel costs have a diminished impact upon the correction terms of routes with small travel costs, and consequently the choice probabilities of those routes.

Most studies of PSL SUE, or of SUE models with PSL path size terms, suppose that the link-route prominence feature is represented as the ratio of link-route length, i.e. $\frac{t_a}{c_{m,i}(\boldsymbol{t})} = \frac{l_a}{L_{m,i}}$, where l_a and $L_{m,i}$ are the lengths of link $a \in A$ and route $i \in R_m$, respectively. However, this may be inaccurate in how travellers perceive the prominence of links in a route: a short link may be highly congested and have a greater travel time than a long link that is uncongested, and hence the timely, short link may be perceived as more prominent in the route than the long, quick link. A similar argument can be made for using other uncongested costs, e.g. free-flow travel time. SUE for a Path Size Logit model – where for internal consistency the link-route prominence feature considers flow-dependent congested cost – can be formulated as follows:

Path Size Logit model SUE: A universal route flow vector $\boldsymbol{f}^* \in F$ is an SUE solution for a Path Size Logit model iff the route flow vector for OD movement m, $\boldsymbol{f}_m^*$, is a solution to the fixed-point problem

$$\boldsymbol{f}_m = \boldsymbol{Q}_m \boldsymbol{P}_m \left(\boldsymbol{c}_m\left(\boldsymbol{t}(\boldsymbol{\Delta f})\right), \boldsymbol{\gamma}_m\left(\boldsymbol{t}(\boldsymbol{\Delta f}), \boldsymbol{W}_m\left(\boldsymbol{t}(\boldsymbol{\Delta f})\right)\right)\right), \qquad m = 1, \dots, M, \quad (3.12)$$

where $P_{m,i}$ and $\gamma_{m,i}$ are as in (3.10) and (3.11), respectively, for route $i \in R_m$, given the universal route flow vector $\boldsymbol{f}$.

8.1.1.2 C-Logit SUE

C-Logit (CL) proposes that the correction terms adopt the form $\kappa_{m,i} = \ln(\sigma_{m,i})$, where $\upsilon \leq 0$ is the commonality scaling parameter, and $\sigma_{m,i} \in [1, \infty)$ is the commonality factor for route $i \in R_m$. The choice probability for route $i \in R_m$ is thus:

$$P_{m,i}\left(\boldsymbol{c}_m(\boldsymbol{t}),\boldsymbol{\sigma}_m(\boldsymbol{t})\right)=\frac{e^{-\theta c_{m,i}(\boldsymbol{t})+\upsilon \ln\left(\sigma_{m,i}(\boldsymbol{t})\right)}}{\sum_{j\in R_m} e^{-\theta c_{m,j}(\boldsymbol{t})+\upsilon \ln\left(\sigma_{m,j}(\boldsymbol{t})\right)}}=\frac{\left(\sigma_{m,i}(\boldsymbol{t})\right)^{\upsilon} e^{-\theta c_{m,i}(\boldsymbol{t})}}{\sum_{j\in R_m}\left(\sigma_{m,j}(\boldsymbol{t})\right)^{\upsilon} e^{-\theta c_{m,j}(\boldsymbol{t})}}. \tag{3.13}$$

Routes not similar in any way to any other route have commonality factors equal to 1 (similar only to itself) and no penalisation is incurred. Routes that are more similar to other routes (in terms of shared congested travel cost) have greater commonality factors and incur greater penalisation. Cascetta et al (1996) proposed several functional forms for the commonality factor, however the congestion-based functional form adopted by Zhou et al (2012), and thus adopted in this paper, is as follows for route $i \in R_m$:

$$\sigma_{m,i}(\boldsymbol{t})=\sum_{k\in R_m}\frac{\sum_{a\in A_{m,i}} t_a \delta_{a,m,i}\delta_{a,m,k}}{\sqrt{c_{m,i}(\boldsymbol{t})}\cdot\sqrt{c_{m,k}(\boldsymbol{t})}}, \tag{3.14}$$

where $\sum_{a\in A_{m,i}} t_a \delta_{a,m,i}\delta_{a,m,k}$ is the shared congested travel cost between routes $i \in R_m$ and $k \in R_m$.

CL SUE can thus be formulated as follows:

CL SUE: A universal route flow vector $\boldsymbol{f}^* \in F$ is a CL SUE solution iff the route flow vector for OD movement m, $\boldsymbol{f}_m^*$, is a solution to the fixed-point problem

$$\boldsymbol{f}_m=\boldsymbol{Q}_m\boldsymbol{P}_m\left(\boldsymbol{c}_m\left(\boldsymbol{t}(\boldsymbol{\Delta f})\right),\boldsymbol{\sigma}_m\left(\boldsymbol{t}(\boldsymbol{\Delta f})\right)\right),\qquad m=1,\dots,M, \tag{3.15}$$

where $P_{m,i}$ and $\sigma_{m,i}$ are as in (3.13) and (3.14) for route $i \in R_m$, respectively, given the universal route flow vector $\boldsymbol{f}$.

8.1.2 GEV Structure Models

GEV structure models are those that are based on the Generalized Extreme Value (GEV) theory (McFadden, 1978), which use a multi-level tree structure to capture the similarity among routes through the random error component of the utility function.

8.1.2.1 Cross-Nested Logit SUE

The Cross-Nested Logit (CNL) model was adapted to the context of route choice by Prashker & Bekhor (1998) and Bekhor & Prasker (1999). Their adaptation uses a two-level nesting structure in which the upper level (nests) includes all the links in the network. The lower level consists of all the routes in the choice set R_m for OD movement m, and each of the routes is allocated to all the link nests that that route consists of. The nest inclusion parameters $\alpha_{a,m,i}$ represent the proportion of link a used by alternative $i \in R_m$. For more than a handful of routes and links, however, the number of independent nest inclusion parameters becomes very large, making estimation difficult. Seeking to address this, Prashker & Bekhor (1998) proposed a functional form for these parameters based on the network topology. These link-route prominence features are represented in terms of length or free-flow travel time however, which is not internally consistent. Addressing this so that the nest inclusion parameters $\alpha_{a,m,i}(\boldsymbol{t})$ are based upon flow-dependent congested cost, the choice probability for route $i \in R_m$ is:

$$P_{m,i}(\boldsymbol{t})=\sum\nolimits_{a\in A_{m,i}} P_{m,(a)}(\boldsymbol{t})\cdot P_{m,(i|a)}(\boldsymbol{t}), \tag{3.16}$$

where

$$P_{m,(i|a)}(\boldsymbol{t})=\frac{\left(\alpha_{a,m,i}(\boldsymbol{t})\exp\left(-\theta c_{m,i}(\boldsymbol{t})\right)\right)^{1/\mu}}{\sum_{j\in R_m}\left(\alpha_{a,m,j}(\boldsymbol{t})\exp\left(-\theta c_{m,j}(\boldsymbol{t})\right)\right)^{1/\mu}}, \tag{3.17}$$

and

$$P_{m,(a)}(\boldsymbol{t}) = \frac{\left(\sum_{k\in R_m}\left(\alpha_{a,m,k}(\boldsymbol{t})\exp\left(-\theta c_{m,k}(\boldsymbol{t})\right)\right)^{1/\mu}\right)^{\mu}}{\sum_{b\in A}\left(\sum_{k\in R_m}\left(\alpha_{b,m,k}(\boldsymbol{t})\exp\left(-\theta c_{m,k}(\boldsymbol{t})\right)\right)^{1/\mu}\right)^{\mu}}, \tag{3.18}$$

where $\alpha_{a,m,i}(\boldsymbol{t}) = \frac{t_a}{c_{m,i}(\boldsymbol{t})}\cdot\delta_{a,m,i}$, and $\mu \in (0,1]$ indicates the degree of nesting such that when $\mu = 1$ CNL collapses to MNL.

CNL SUE can thus be formulated as follows:

CNL SUE: A universal route flow vector $\boldsymbol{f}^* \in F$ is a CNL SUE solution iff the route flow vector for OD movement m, $\boldsymbol{f}_m^*$, is a solution to the fixed-point problem

$$\boldsymbol{f}_m = \boldsymbol{Q}_m \boldsymbol{P}_m\big(\boldsymbol{t}(\boldsymbol{\Delta f})\big), \qquad m = 1,\dots,M, \tag{3.19}$$

where $P_{m,i}$ is as in (3.16)-(3.18) for route $i \in R_m$, respectively, given the universal route flow vector $\boldsymbol{f}$.

8.1.2.2 Generalised Nested Logit SUE

Bekhor & Prashker (2001) generalise CNL by introducing a functional form for the nesting coefficient μ, to be a parameterised average value of the nest inclusion coefficients. With congestion-based inclusion coefficients, the Generalised Nested Logit (GNL) model proposes that the choice probability for route $i \in R_m$ is as in (3.16)-(3.18), where the nesting coefficient μ for link nest a and OD movement m is: $\mu_{a,m}(\boldsymbol{t}) = \left(1 - \frac{\sum_{i\in R_m}\alpha_{a,m,i}(\boldsymbol{t})}{\sum_{i\in R_m}\delta_{a,m,i}}\right)^{\lambda}$, $\lambda \geq 0$. GNL SUE is thus as in (3.19) but with flow-dependent nesting coefficients as above. Note that routes consisting of a single link between the origin and destination result in the nesting coefficient $\mu_{a,m}(\boldsymbol{t})$ for that link being equal to 0, since $\sum_{i\in R_m}\alpha_{a,m,i}(\boldsymbol{t}) = \sum_{i\in R_m}\delta_{a,m,i} = 1$. This results in the GNL model being undefined.

8.1.2.3 Paired Combinatorial Logit SUE

The Paired Combinatorial Logit (PCL) model was adapted to the context of route choice by Prashker & Bekhor (1998). Here, each pair of routes in a choice set form a nest and routes are chosen from each nest. Within each nest, $\sigma_{m,i,j}$ is the similarity index between routes $i \in R_m$ and $j \in R_m$. Like CNL/GNL, individually estimating each of these parameters for each nest becomes infeasible for more than a handful of routes. Instead, Prashker & Bekhor (1998) propose a functional form for these similarity indexes, proposing that the similarity between routes is measured according to the C-Logit commonality factor. These commonality factors are formulated in terms of shared length / uncongested travel cost however, which is not internally consistent. Addressing this so that the similarity index parameters $\sigma_{m,i,j}(\boldsymbol{t})$ are based upon flow-dependent congested cost, the choice probability for route $i \in R_m$ is

$$P_{m,i}(\boldsymbol{t}) = \sum_{j\in R_m; j\neq i} P_{m,(i,j)}(\boldsymbol{t})\cdot P_{m,(i|i,j)}(\boldsymbol{t}), \tag{3.20}$$

where

$$P_{m,(i|i,j)}(\boldsymbol{t}) = \frac{\exp\left(\frac{-\theta c_{m,i}(\boldsymbol{t})}{1-\sigma_{m,i,j}(\boldsymbol{t})}\right)}{\exp\left(\frac{-\theta c_{m,i}(\boldsymbol{t})}{1-\sigma_{m,i,j}(\boldsymbol{t})}\right) + \exp\left(\frac{-\theta c_{m,j}(\boldsymbol{t})}{1-\sigma_{m,i,j}(\boldsymbol{t})}\right)}, \tag{3.21}$$

and

$$P_{m,(i,j)}(\boldsymbol{t}) = \frac{\left(1-\sigma_{m,i,j}(\boldsymbol{t})\right)\cdot\left(\exp\left(\frac{-\theta c_{m,i}(\boldsymbol{t})}{1-\sigma_{m,i,j}(\boldsymbol{t})}\right)+\exp\left(\frac{-\theta c_{m,j}(\boldsymbol{t})}{1-\sigma_{m,i,j}(\boldsymbol{t})}\right)\right)^{1-\sigma_{m,i,j}(\boldsymbol{t})}}{\sum_{k=1}^{N_m-1}\sum_{l=k+1}^{N_m}\left(1-\sigma_{m,k,l}(\boldsymbol{t})\right)\cdot\left(\exp\left(\frac{-\theta c_{m,k}(\boldsymbol{t})}{1-\sigma_{m,k,l}(\boldsymbol{t})}\right)+\exp\left(\frac{-\theta c_{m,l}(\boldsymbol{t})}{1-\sigma_{m,k,l}(\boldsymbol{t})}\right)\right)^{1-\sigma_{m,k,l}(\boldsymbol{t})}}, \quad (3.22)$$

where $\sigma_{m,i,j}(\boldsymbol{t}) = \left(\frac{\sum_{a\in A_{m,i}} t_a \delta_{a,m,i}\delta_{a,m,j}}{\sqrt{c_{m,i}(\boldsymbol{t})}\cdot\sqrt{c_{m,j}(\boldsymbol{t})}}\right)^{\lambda}$, $\lambda \geq 0$, is the similarity index between routes $i \in R_m$ and $j \in R_m$. PCL collapses to MNL when similarity indexes are all equal to zero.

PCL SUE can thus be formulated as follows:

PCL SUE: A universal route flow vector $\boldsymbol{f}^* \in F$ is a PCL SUE solution iff the route flow vector for OD movement m, $\boldsymbol{f}_m^*$, is a solution to the fixed-point problem

$$\boldsymbol{f}_m = \boldsymbol{Q}_m \boldsymbol{P}_m\big(\boldsymbol{t}(\boldsymbol{\Delta f})\big), \qquad m = 1, \dots, M, \quad (3.23)$$

where $P_{m,i}$ is as in (3.20)-(3.22) for route $i \in R_m$, respectively, given the universal route flow vector $\boldsymbol{f}$.

Chapter 4. A bounded path size route choice model excluding unrealistic routes: Formulation and estimation from a large-scale GPS study

Lawrence Christopher DUNCAN [a], David Paul WATLING [a], Richard Dominic CONNORS [a,b], Thomas Kjær RASMUSSEN [c], Otto Anker NIELSEN [c]

[a] Institute for Transport Studies, University of Leeds
36-40 University Road, Leeds, LS2 9JT, United Kingdom.

[b] University of Luxembourg, Faculté des Sciences, des Technologies et de Médecine,
Maison du Nombre, 6 Avenue de la Fonte, L-4364, Esch-sur-Alzette, Luxembourg.

[c] Department of Technology, Management and Economics, Technical University of Denmark
Bygningstorvet 116B, 2800 Kgs. Lyngby, Denmark.

Highlights

- Identify desired properties for a Bounded Path Size (BPS) route choice model
- Derive a mathematically well-defined & theoretically desirable BPS model form
- Propose two BPS models and demonstrate properties
- Present likelihood formulations and tracked route data MLE procedure
- Estimate proposed models on a large-scale network using real GPS data

Abstract

This paper develops a new route choice modelling framework that deals with both route correlations and unrealistic routes in a consistent and robust way. To do this, we explore the integration of a correlation-based Path Size Logit model with the Bounded Choice Model (BCM) (Watling et al, 2018). We find, however, that the natural integration of these models leads to behavioural inconsistencies and/or undesirable mathematical properties. Solving these challenges, we derive a mathematically well-defined Bounded Path Size (BPS) model form that utilises a consistent criterion for assigning zero choice probabilities to unrealistic routes while eliminating their path size contributions. Two BPS models are consequently formulated: one that is closed-form and another expressed as a fixed-point problem. Subsequently, we consider parameter estimation in a simulation study and on a real-life large-scale network using GPS data, where computational feasibility is demonstrated. Estimation results show the potential of the BPS models to give improved fit relative to unbounded versions (as well as the BCM), while providing greater robustness to the assumed choice sets.

Key Words: bounded choice model, path size logit, route choice, parameter estimation, unrealistic routes

1. Introduction

There are several distinct and unique aspects about route choice modelling that makes it a more challenging task than modelling other types of transport choices. Two key aspects are that: 1) there is often a complex correlation structure between the route alternatives, which occurs due to the significant topological overlapping of routes; and 2) typical road networks have many possibilities for very long routes that should be considered unrealistic and excluded from route choice. To the best knowledge of the authors, no route choice modelling approach has been developed thus far that addresses both of these challenges in a theoretically consistent, robust, and mathematically well-defined way, and that moreover, has been shown to be both computationally feasible in large-scale networks and estimatable from revealed choice data. In this paper, we aim to address this by developing a new model framework. To set the background for the research, below, we discuss modelling approaches for 1) and 2), and how we decided upon the approach taken.

To overcome the deficiency of the Multinomial Logit (MNL) Random Utility Model (RUM) in its inability to capture correlations between routes, numerous MNL extension models have been proposed that relax the assumption that the random error terms are independently distributed. Alternative RUMs to MNL either capture route correlations implicitly or utilise concepts from extended Logit models to similarly adapt the model. For a more detailed review, see Duncan et al (2020); however, we discuss the key models and concepts relevant to this paper below:

- GEV structure models use a multi-level tree structure to capture the similarity among routes through the random error component of the utility function. Such models include: Cross-Nested Logit (CNL) (Vovsha, 1997; Bekhor & Prashker, 1999; Marzano & Papola, 2008), Paired Combinatorial Logit (Chu, 1989; Bekhor & Prashker, 1999; Gliebe et al, 1999; Pravinvongvuth & Chen, 2005), Generalized Nested Logit (GNL) (Bekhor & Prashker, 2001; Wen & Koppelman, 2001), and the Network GEV model (Bierlaire, 2002; Daly & Bierlaire, 2006).
- Simulation models include Mixed Logit models (Ben-Akiva & Bolduc, 1996; McFadden & Train, 2000) such as the Factor Analytic Logit Kernel model (Bekhor et al, 2002), as well as alternative RUMs to MNL such as Multinomial Probit (MNP) (Daganzo & Sheffi, 1977) and Multinomial Gammit (MNG) (Cantarella & Binetti, 2002). Mixed Logit models divide the error terms into two Gumbel and Gaussian distributed variable components which ensures the Logit structure is kept while allowing for capturing interdependencies between routes. MNP and MNG etc. do not suffer from the same issue as MNL, as the similarity between each pair of routes is accounted for by allowing for covariance between the error terms, and route correlations are thus captured implicitly.
- Correction term models add correction terms to the deterministic utilities / probability relations to adjust the choice probabilities in order to capture route correlations. Such models include: C-Logit (CL) (Cascetta et al, 1996), Path Size Correction Logit (PSCL) (Bovy et al, 2008), Path Size Logit (PSL) (Ben-Akiva & Ramming, 1998), Path Size Hybrid (Xu et al, 2015), and Path Size Weibit (Kitthamkesorn & Chen, 2013).

The typical route choice modelling approach for dealing with unrealistic routes – for correlation-based models and in general – is to employ some kind of heuristic method that attempts to explicitly generate a route choice set containing just the routes considered realistic. This approach, however, leads to theoretical inconsistencies, since the route generation criteria is not consistent with the calculation of the choice probabilities among chosen routes. Moreover, in large-scale case studies, for example the study of eastern Denmark in Prato et al (2014), Rasmussen et al (2016), Duncan et al (2020), as well as in Section 7.4 of this paper, it is implausible to attempt to generate the exact choice sets of realistic routes, and instead choice sets are generated large enough so that one can be fairly certain the realistic alternatives are present, regardless of how many unrealistic routes are generated. This is problematic, since many correlation-based models are not choice set robust, and results are thus negatively influenced by the presence of the unrealistic routes as well as highly sensitive to the choice set generation method adopted (Bovy et al, 2008; Bliemer & Bovy, 2008; Ramming, 2002; Ben-Akiva & Bierlaire, 1999; Bekhor et al (2008); Duncan et al, 2020).

An approach that has recently been proposed for consistently dealing with unrealistic routes is the Bounded Choice Model (BCM) (Watling et al, 2018). The BCM has a consistent criterion for determining restricted choice sets of realistic routes, and route choice probability: a bound is applied to the difference in random utility between each given route and an imaginary reference route alternative, so that routes only receive a non-zero choice probability if the difference between its random utility and the random utility of the reference alternative is within the bound. Furthermore, the probability by which each route is chosen relates to the odds associated with choosing each alternative versus the reference alternative. A special case of the BCM is where the reference alternative is that with the maximum deterministic utility i.e. the route with the cheapest generalised travel cost, so that a route only receives a non-zero probability if its cost is within some bound of the cheapest route.

The BCM does not account for route correlation however, and motivated by the desire to develop a route choice model that deals with both route correlation and unrealistic routes in a consistent and robust way, an approach we deemed promising was to explore the integration of a correlation-based model with the BCM. To determine which correlation-based model we would adopt, there were requirements: real-life application of a route choice model involves estimating the model parameters, and we thus considered it important that the proposed model could be successfully estimated, and moreover, that it would be computationally feasible to

do so on large-scale networks. Below, we consider the suitability of the correlation-based model categories in terms of potential to satisfy these requirements.

For GEV structure and simulation models, there are computational concerns: computing route choice probabilities / estimation typically requires a high computational cost on large-scale networks. Although GEV structure models have closed-form probability expressions, due to their multi-level tree structure the choice probabilities are complex to compute, where the computational burden escalates significantly as the scale of network / choice set sizes increase. This raises concerns over their applicability to large-scale networks. For example, Lai & Bierlaire (2015) estimate CNL on a medium-scale network and find significantly greater computation times than for MNL/PSL (e.g. 9.76 hours compared to 98.7/116 seconds). The problem for simulation models is that they do not have closed-form expressions and solving the choice probabilities requires either Monte Carlo simulation or alternative methods, all of which are computationally burdensome. Many analytical approximation methods have been proposed to solve the MNP model, all aiming to provide the best compromise between speed and accuracy (reviews can be seen in e.g. Rosa (2003), Connors et al (2014)); however, performance of these approaches are assessed with a very limited number of routes, typically up to just 25 alternatives. It is generally considered infeasible to accurately compute MNP, MNG etc. probabilities on large-scale networks with thousands of routes.

There are also estimation concerns for GEV structure and simulation models: numerous studies have found/discussed difficulties in obtaining reasonable estimates for parameters. There are numerous different issues involved in estimating the numerous different specifications of the CNL model for route choice, and several studies have discussed issues in detail, for example see Bierlaire (2006), Abbe et al (2007), Marzano & Papola (2008). To summarise a few of the issues documented: a) there may be infinite specifications with different choice probabilities that lead to the same covariance figures (Marzano & Papola, 2008); b) the number of unknown parameters to be estimated increases as the number of routes increases (Marzano & Papola, 2008); c) several studies have found that when estimating the nesting coefficients the model tends to collapse to MNL (Ramming, 2002; Prato, 2005; Prato & Bekhor, 2006); d) the maximum likelihood estimation functions are not concave which significantly complicates the identification of a global maximum (Bierlaire, 2006); and, e) because of d), nonlinear programming methods tend to converge towards local maxima of the log-likelihood function, and in practice, one observes a significant influence of the initial values provided to the algorithm on the estimated parameters (Abbe et al, 2007). GNL requires the estimation of an additional parameter over CNL which makes parameter estimation more difficult. There are also difficulties in estimating the parameters of the Factor Analytic Logit Kernel model: Ramming (2002) finds instable estimates of the covariance parameters, despite the very large number of random draws, while Prato (2005) discusses the difficulty in obtaining significant estimates. And, there are also issues involved in estimating the MNP model, including: identification issues arising from the number of parameters that may need to be estimated (Dansie, 1985; Bunch, 1991; Keane, 1992); and, difficulties in accurately computing small choice probabilities (Connors et al, 2014).

Correction term models are in contrast much more computationally practical than GEV structure and simulation models, and are regularly applied and estimated on large-scale networks. They have simple closed-form expressions, meaning the route choice probabilities are generally easy and quick to compute. They are thus a useful and practical approach to approximating the correlation; more complex models can capture the correlation more accurately, but due to the comparatively low computational cost and the relative ease in obtaining reasonable estimates for parameters, correction term models are the most commonly used models in practice.

Motivated by the above, we decided to explore the integration of a correction term model with the BCM. The CL model proposes that the correction terms are based upon commonality factors that measure the similarity of routes, and penalises the utilities accordingly. In contrast, the PSL model proposes that the correction terms are based upon path size terms that measure route distinctiveness: a route is penalised based on the number of other routes sharing its links, and the costs of those shared links. The PSCL model provides a modified path size term derived from an approximation of GEV models.

Developing a BCM with an integrated correction term was complicated by the desire to produce a model such that the correction terms consistently and only capture correlations between the routes the model defines as realistic. Achieving this, however, and maintaining a continuous choice probability function is far from trivial, as the research in this paper shows. Continuity is an important property, and is typically required for applications of the model that are well-behaved, for example convergent parameter estimation and existence

of network equilibria. Thus, when considering which correction term model to integrate we considered how continuity could be achieved. We found that while one can derive a BCM with an integrated CL correction term, there are uncertainties over how one can suitably maintain a continuous probability function. For the PSL model, existing research on dealing with unrealistic routes within the path size terms presented a clear direction to pursue, and while similar techniques could be translated for the PSCL model, PSL is much more widely used and we therefore chose to pursue developing a BCM with an integrated PSL-like correction term.

The pragmatic approach that has been proposed for addressing choice set robustness for PSL, is to utilise a weighted path size contribution technique along with choice set generation, to reduce the negative effects of any present unrealistic routes. The Generalised Path Size Logit (GPSL) model (Ramming, 2002) proposes a path size contribution factor based on travel cost ratios to reduce the contributions of costly routes, while the Adaptive Path Size Logit (APSL) model (Duncan et al, 2020) proposes a contribution factor based on choice probability ratios to provide internal consistency. While improving upon the choice set robustness of PSL, these approaches do not solve the issue entirely since the path size contributions of routes defined as unrealistic are only reduced instead of eliminated.

Taking the promising weighted path size contribution approach one step further, by integrating PSL concepts with the BCM, the aim is to develop a model that eliminates unrealistic route contributions entirely, as well as removing all the negative effects of unrealistic routes by also assigning them zero choice probabilities. A natural form for a Bounded Path Size (BPS) model can be derived by inserting path size choice model utilities into the standard BCM formula. However, as we show, this natural form for a BPS model is deeply problematic and there are no behaviourally and practically desirable formulations. This is because appropriately defining the path size contribution factors within the path size terms is challenging, and from demonstrating with different options we establish desired properties for a theoretically consistent, robust, and mathematically well-defined BPS model. To develop a BPS model that satisfies these properties, we then derive an alternative BPS model form and consequently propose two BPS models: one that is closed-form and another expressed as a fixed-point problem.

The structure of the paper is as follows. In Section 2 we introduce some basic network notation as well as the definitions of relevant models. In Section 3 we discuss issues with the natural form for a BPS model and consequent desired properties for a BPS model (demonstrated in detail in Appendix C), and derive an alternative BPS model form. In Sections 4&5 we propose two BPS models adopting the alternative form. We also in Section 5 provide a solution method for computing the choice probabilities, which are a solution to a fixed-point problem, and address the existence and uniqueness of solutions (where the proofs are given in Appendix D). In Section 6 we discuss/demonstrate the theoretical properties of the proposed BPS models including how they satisfy the desired properties (demonstrated in detail in Appendix E). In Section 7 we investigate parameter estimation. To show that the model parameters can be estimated we first propose a Maximum Likelihood Estimation procedure for estimation with tracked route observation data, then investigate this procedure in simulation studies on the Sioux Falls network where we show that it is generally possible to reproduce assumed true parameters. Then, in a real-life case study, we estimate the BPS models using real tracked route GPS data on a large-scale network, compare results with other models, and assess computational feasibility. Section 8 concludes the paper.

2. Notation & Model Definitions

2.1 Basic Network Notation

The model developed in this paper is applicable to general networks with multiple OD movements and flow-dependent link costs. However, without compromising the model derivation, we simplify notation by considering a single OD movement with fixed link costs. The network consists of link set A. For the OD movement, R is the choice set of all simple routes (without cycles), having size $N = |R|$. $A_i \subseteq A$ is the set of links belonging to route $i \in R$, and $\delta_{a,i} = \begin{cases} 1 & if\ a \in A_i \\ 0 & otherwise \end{cases}$. Suppose that the generalised travel cost t_a of each link $a \in A$ is a weighted sum (by parameter vector $\boldsymbol{\alpha}$) of variables $\boldsymbol{w}_a$, i.e. $t_a(\boldsymbol{w}_a; \boldsymbol{\alpha})$, and that the generalised travel cost for route $i \in R$, c_i, can be attained through summing up the total cost of its links so that $c_i\big(\boldsymbol{t}(\boldsymbol{w}; \boldsymbol{\alpha})\big) = \sum_{a \in A_i} t_a(\boldsymbol{w}_a; \boldsymbol{\alpha})$, where $\boldsymbol{t}$ is the vector of all link travel costs and $\boldsymbol{w}$ is the vector of all link variables. To simplify notation $c_i\big(\boldsymbol{t}(\boldsymbol{w}; \boldsymbol{\alpha})\big)$ is denoted just as c_i. The route choice probability for route $i \in R$

is P_i, where $\boldsymbol{P} = (P_1, P_2, \dots, P_N)$ is the vector of route choice probabilities, and D is the set of all possible route choice probability vectors:

$$D = \left\{ \boldsymbol{P} \in \mathbb{R}^N_{\geq 0} : 0 \leq P_i \leq 1, \forall i \in R, \sum_{j=1}^{N} P_j = 1 \right\}.$$

And, $D^{>0} \subset D$ is the subset of all possible route choice probability vectors where no route has zero choice probability:

$$D^{>0} = \left\{ \boldsymbol{P} \in \mathbb{R}^N_{>0} : 0 < P_i < 1, \forall i \in R, \sum_{j=1}^{N} P_j = 1 \right\}.$$

2.2 Path Size Logit Models

Path Size Logit models were developed to address the well-known deficiency of the Multinomial Logit (MNL) model in its inability to capture the correlation between routes. To do this, they include correction terms to penalise routes that share links with other routes, so that the deterministic utility of route $i \in R$ is $V_i = -\theta c_i + \kappa_i$, where $\theta > 0$ is the Logit scaling parameter and $\kappa_i \leq 0$ is the correction term for route $i \in R$. The choice probability for route $i \in R$ is:

$$P_i = \frac{e^{-\theta c_i + \kappa_i}}{\sum_{j \in R} e^{-\theta c_j + \kappa_j}}.$$

Path Size Logit correction terms adopt the form $\kappa_i = \beta \ln(\gamma_i)$, where $\beta \geq 0$ is the path size scaling parameter, and $\gamma_i \in (0,1]$ is the path size term for route $i \in R$. A distinct route with no shared links has a path size term equal to 1, resulting in no penalisation. Less distinct routes have smaller path size terms and incur greater penalisation. The choice probability for route $i \in R$ is thus:

$$P_i = \frac{e^{-\theta c_i + \beta \ln(\gamma_i)}}{\sum_{j \in R} e^{-\theta c_j + \beta \ln(\gamma_j)}} = \frac{(\gamma_i)^{\beta} e^{-\theta c_i}}{\sum_{j \in R} (\gamma_j)^{\beta} e^{-\theta c_j}}. \tag{4.1}$$

The general form for the path size term is as follows:

$$\gamma_i = \sum_{a \in A_i} \frac{t_a}{c_i} \frac{1}{\sum_{k \in R} \left(\frac{W_k}{W_i} \right) \delta_{a,k}}, \tag{4.2}$$

where $W_k > 0$ is the path size contribution weighting of route $i \in R$ to path size terms (different for each model), so that the contribution of route k to the path size term of route i (the path size contribution factor) is $\frac{W_k}{W_i}$. To dissect the path size term: each link a in route i is penalised (in terms of decreasing the path size term and hence the utility of the route) according to the number of routes in the choice set that also use that link $\left(\sum_{k \in R} \delta_{a,k} \right)$, where each contribution is weighted (i.e. $\sum_{k \in R} \left(\frac{W_k}{W_i} \right) \delta_{a,k}$), and the significance of the penalisation is also weighted according to how prominent link a is in route i, i.e. the cost of route a in relation to the total cost of route i $\left(\frac{t_a}{c_i} \right)$.

Path size terms sometimes suppose that the link-route prominence feature is represented as the ratio of link-route length, i.e. $\frac{t_a}{c_i} = \frac{l_a}{L_i}$, where l_a and L_i are the lengths of link $a \in A$ and route $i \in R$, respectively. However, this may be inaccurate in how travellers perceive the prominence of links in a route: a short link may be highly congested and have a greater travel time than a long link that is uncongested, and hence the timely, short link may be perceived as more prominent in the route than the long, quick link. Thus, for internal consistency, we suppose the link-route prominence feature is represented as the ratio of link-route generalised travel cost.

The Path Size Logit (PSL) model (Ben-Akiva & Bierlaire, 1999) proposes that $W_k = 1$ so that all routes contribute equally to path size terms. This is problematic, however, as the correction terms and thus the choice probabilities of realistic routes are affected by link sharing with unrealistic routes. To combat this, Ramming (2002) proposed the Generalised Path Size Logit (GPSL) model where $W_k = c_k^{-\lambda}$ and routes contribute

according to travel cost ratios, so that routes with excessively large travel costs have a diminished impact upon the correction terms of routes with small travel costs, and consequently the choice probabilities of those routes. Duncan et al (2020) reformulate the GPSL model (proposing the alternative GPSL model (GPSL′)) so that the contribution weighting resembles the probability relation, i.e. $W_k = e^{-\lambda c_k}$. As they discuss, however, GPSL and GPSL′ are not internally consistent in how they define routes as being unrealistic: the path size terms consider only travel cost, whereas the route choice probability relation considers disutility *including* the correction term. To address this, the Adaptive Path Size Logit (APSL) model is proposed where $W_k = P_k$ and routes contribute according to ratios of route choice probability. This ensures internal consistency, where routes defined as unrealistic by the path size terms – and consequently given reduced path size contributions – are exactly those with very low choice probabilities. Since the APSL path size contribution factors depend upon the route choice probabilities, the probability relation is an implicit function, naturally expressed as a fixed-point problem. The APSL model is thus not closed-form and solving the choice probabilities requires a fixed-point algorithm to compute the solution. Furthermore, in order to prove existence and uniqueness of solutions the APSL probability relation is modified from that in (4.1). See Duncan et al (2020) for more details on the derivation and theoretical properties of the APSL model, as well as definitions and details of the other Path Size Logit models.

2.3 Bounded Choice Model

In this subsection we briefly formulate the Bounded Choice Model (BCM), see Watling et al (2018) for more details on the derivation and theoretical properties of the model. The BCM proposes that a bound is applied to the difference in random utility between each given alternative and an imaginary reference alternative, so that an alternative only receives a non-zero choice probability if the difference between its random utility and the random utility of the reference alternative is within the bound. Furthermore, the probability each alternative is chosen relates to the odds associated with choosing each alternative versus the reference alternative. Watling et al (2018) consider a special case of the BCM where the reference alternative is the alternative with the maximum deterministic utility. While the application of the BCM can involve exerting an absolute bound upon the difference in utility from the maximum, (for example 25 units worse in deterministic utility), we consider in this paper exerting a relative bound upon the difference, i.e. where routes only receive a non-zero choice probability if they have a deterministic disutility less than φ times worse than the greatest route utility. If $V_i < 0$ is the deterministic disutility of alternative $i \in R$, then the probability of alternative $i \in R$ is chosen under the BCM is:

$$P_i = \frac{(h_i(\boldsymbol{V}) - 1)_+}{\sum_{j \in R}\left(h_j(\boldsymbol{V}) - 1\right)_+}, \tag{4.3}$$

where $h_i(\boldsymbol{V}) = \exp(V_i - \varphi \max(V_k : k \in R))$, $\varphi > 1$ is the relative bound parameter to be estimated, and $(\cdot)_+ = \max(0, \cdot)$. The BCM formulation in (4.3) is derived from an assumption that the difference random variable error terms (relative to the best alternative) follow a truncated logistic distribution, see Appendix A for details.

In a route choice context where the deterministic utility of route $i \in R$ is given by $V_i = -\theta c_i$, the choice probability relation for route $i \in R$ is:

$$P_i = \frac{(h_i(-\theta \boldsymbol{c}) - 1)_+}{\sum_{j \in R}\left(h_j(-\theta \boldsymbol{c}) - 1\right)_+}, \tag{4.4}$$

where $h_i(-\theta \boldsymbol{c}) = \exp(-\theta c_i - \varphi \max(-\theta c_l : l \in R)) = \exp\left(-\theta(c_i - \varphi \min(c_l : l \in R))\right)$. Thus, routes only receive a non-zero choice probability if they have a cost less than φ times the cost on the cheapest route. We would like to point out that although for simplification of notation c_i is denoted as a single variable, c_i is actually a weighted sum of route variables, i.e. $c_i\left(\boldsymbol{t}(\boldsymbol{w}; \boldsymbol{\alpha})\right) = \sum_{a \in A_i} t_a(\boldsymbol{w}_a; \boldsymbol{\alpha})$, for example travel time, length, number of left/right turns, toll, etc., each with an associated taste coefficient / parameter. Therefore, the bound is applied to generalised cost.

On the surface there may appear to be some similarity between the BCM and the original Random Regret Minimisation (RRM) model (Chorus et al, 2008), in that they both propose that when travellers are considering the relative attractiveness of a route, they compare the route alternative against better alternatives, and worse alternatives in some way (at least in theory) have eliminated effects on better alternatives. For the

BCM, the generalised travel cost of a route is compared against that of the lowest costing (best) alternative, and if it has a cost some order of magnitude worse, it is not considered as a realistic alternative and is assigned a zero choice probability. As such, the worse alternatives do not affect the choice probabilities of better alternatives. For the RRM model, however, each of the cost attributes of a route are individually compared against the attributes of the other routes, and if the attribute of another route is worse than the attribute from the route in question, then there is no regret. As such, the worse alternatives do not affect the systematic regrets of better alternatives. Therefore, the BCM and RRM model are very different models. They differ in many ways, but a key difference is that in the RRM model all routes receive non-zero choice probabilities, and thus unrealistic routes in the choice set negatively impact results. Moreover, RRM operates on an attribute level. Prato (2014) explores integrating correction term models with the RRM model, to also deal with route overlap.

3. Derivation of the Proposed Bounded Path Size Model Form

3.1 The Natural Form

There is a natural form for a Bounded Path Size (BPS) choice model, which is derived as follows. Path Size RUMs (with additive error terms) propose that the deterministic utility for route $i \in R$ is given by $V_i = -\theta c_i + \beta \ln(\gamma_i)$. Thus, inserting the Path Size choice model utilities into the BCM formula in (4.3), the choice probability relation for route $i \in R$ is:

$$P_i = \frac{(h_i(-\theta \boldsymbol{c} + \beta \ln(\boldsymbol{\gamma})) - 1)_+}{\sum_{j \in R}\left(h_j(-\theta \boldsymbol{c} + \beta \ln(\boldsymbol{\gamma})) - 1\right)_+}, \tag{4.5}$$

where $h_i(-\theta \boldsymbol{c} + \beta \ln(\boldsymbol{\gamma})) = \exp(-\theta c_i + \beta \ln(\gamma_i) - \varphi \max(-\theta c_l + \beta \ln(\gamma_l) : l \in R))$. So, the natural BPS model form applies a bound to the route utilities so that zero choice probabilities are assigned to routes with infeasibly low utilities (φ times worse in utility than the best alternative), where the utilities include a path size correction.

Appropriately defining the path size contribution factors within the path size terms is difficult, however, and from exploring different options, we consequently establish desired properties for a BPS model. We briefly detail and discuss these properties here, see Appendix C for demonstrations on how they are derived. While it may appear the properties are derived from issues with the specific path size term options explored, the natural BPS model form is actually deeply problematic and there are no behaviourally and practically desirable formulations, as we attempt to demonstrate. We define the *active choice set* as the set of routes with non-zero choice probabilities, otherwise known as the used routes or those considered realistic. The Desired Properties (DP) are as follows:

- **Desired Property 1 – Consistent Definitions of Unrealistic Routes:** *Routes defined as unrealistic by the choice model (assigned zero choice probabilities) should have zero path size contributions, and vice versa.*
- **Desired Property 2 – Well-Defined Functions:** *The model functions should be well-defined across their domain.*
- **Desired Property 3 – Internal Consistency:** *The model should be internally consistent, i.e. there is a consistent assessment of the feasibility of routes between probability relation and path size contribution factors.*
- **Desired Property 4 – Uniqueness:** *Route choice probability solutions are inter-active-choice-set unique (where there is only one active choice set in which solutions exist), and conditions can be established for intra-active-choice-set uniqueness (where for a given active choice set there is only one solution).*
- **Desired Property 5 – Continuity:** *The choice probability function is continuous.*

DP1 is behaviourally desirable since otherwise the assumption would be that travellers account for overlap between routes they do not consider as being realistic alternatives, or vice versa in that they do not account for the overlap between some routes they do consider realistic. Achieving this property is not trivial however as it involves zero path size contributions, which results in issues leading to DP2,4,5. DP2 is practically desirable

as it allows solutions to exist and be computed, and derives from an issue inherent with the natural BPS model form where zero path size contributions results in occurrences of $\frac{0}{0}$ and $\ln(0)$. DP3 is motivated by the key behavioural feature of the APSL model, where theoretical consistency is provided within the model's specification. We note that internal consistency also includes utilising the same generalised costs within all model components, i.e. also within the path size terms, rather than using just length. Due to inherent $\frac{0}{0}$ and $\ln(0)$ issues with the natural BPS model form, there are problems with solution uniqueness where multiple active choice sets can yield solutions. This is undesirable as then an active choice set selection procedure is required to determine which routes are considered realistic. DP4 is thus that solutions exist within a single active choice only (i.e. so that the choice model has a unique selection of which routes are considered (un)realistic), and that conditions exist for unique solutions within that active choice set (for example conditions exist for unique APSL solutions). DP5 is practically desirable as this property is required for applications of the model, for example parameter estimation and network equilibrium where the costs are not fixed.

We would like to emphasise that continuity of the choice probability function is not trivial for a choice model with implicit restriction of routes (i.e. where zero choice probabilities are assigned). For route choice models in which non-zero choice probabilities are assigned to all routes (i.e. non-bounded models), while the choice probability functions may be continuous for a given choice set, the functions are not continuous for changes to the choice set. As such, as the generalised cost of a route increases where at some point it is excluded by the choice set generation criteria, the probabilities from the choice model will not be continuous. The BCM solves this by ensuring a routes choice probability tends towards zero as its cost increases, and receives a zero probability exactly at the bound (and thus the probabilities of other routes are not adjusted when it is removed from the active choice set). For a BPS model to be continuous, the path size contributions must tend towards zero as a route approaches zero choice probability, and be eliminated exactly at zero choice probability.

DP2,4,5 are general desired properties for any route choice model, and satisfying these properties is essential for application of the model. Often, closed-form models such as MNL, PSL, GPSL, and the BCM satisfy these properties trivially. However, these models have behavioural deficiencies: PSL models do not (fully) deal with unrealistic routes, the BCM does not capture route correlations, and MNL deals with neither route overlap nor unrealistic routes. Our aim is thus to develop a model that can harness the contrasting strengths of the BCM and PSL models, thereby dealing with route overlap *and* unrealistic routes. The difficulty, however, lies in obtaining theoretical consistency, i.e. satisfying DP1&3, where overlap is considered between only and all the routes defined as realistic. While there exist natural BPS model formulations that satisfy DP2,4,5 (e.g. option 1 in Appendix C Section 10.3.1), and formulations that satisfy DP1&3 (e.g. options 2&3 in Appendix C Section 10.3.2), no formulations exist where all properties are satisfied.

As shown in Appendix A of the revised manuscript, the BCM is derived from an assumption that the random error terms follow a truncated logistic distribution, where the truncation is dependent upon the bound. For the natural BPS model form in (4.5), the bound is dependent upon the best route utility, which includes the path size correction. Therefore, during calibration the path size correction can have an indirect effect on both the deterministic utility and random error term. The natural BPS model form could thus in principle correct the relative sizes of the deterministic and random parts of the utility across different routes, and thereby has the potential to provide a means for capturing a greater part of the correlation than standard PSL models, which capture correlations through correcting the deterministic part only (Ramming, 2002; Hoogendoorn-Laser et al, 2005). As shown in Appendix C, however, the natural BPS model form is not suitable for use. In the following section we discuss how this applies to the alternative BPS model form we propose.

3.2 The Proposed Form

To circumvent these issues with the natural form for a BPS model, we derive an alternative BPS model form (henceforth just referenced as the proposed BPS model form). In Sections 4&5 we develop two BPS models that adopt the proposed form, and which satisfy desired properties, as we discuss/demonstrate in Appendix E.

The basis for the proposed BPS model form can be considered to roughly derive from the union of two models, where the probability of choosing route i relates to the probability of choosing route i under model 1

and choosing route i under model 2. Model 1 is the BCM and model 2 is a Path Size Logit model where only the correlation between routes is considered, i.e. there is no travel cost component. Let Q_i^1 and Q_i^2 be the probability of choosing route $i \in R$ under model 1 and model 2, respectively. Unionising the two models, the probability of choosing route $i \in R$ relates as:

$$P_i = Q_i^1 \times Q_i^2 \times \chi,$$

where

$$Q_i^1 = \frac{\left(\exp\left(-\theta(c_i - \varphi \min(c_l: l \in R))\right) - 1\right)_+}{\sum_{j \in R}\left(\exp\left(-\theta\left(c_j - \varphi \min(c_l: l \in R)\right)\right) - 1\right)_+}, \qquad Q_i^2 = \frac{e^{\beta \ln(\gamma_i)}}{\sum_{j \in R} e^{\beta \ln(\gamma_j)}},$$

and χ is a normalisation constant that ensures the probabilities for all routes sum up to 1. So, Q_i^1 is the BCM choice probability relation in (4.4) and Q_i^2 is the regular Path Size Logit model probability relation in (4.1) with $\theta = 0$, i.e. considering route distinctiveness only. The deterministic utilities of route i under model 1 and model 2 are $V_i^1 = -\theta c_i$ and $V_i^2 = \beta \ln(\gamma_i)$, respectively. By giving both of these utilities i.i.d Gumbel distributed random error terms, the resultant union model would be a regular Path Size Logit model. Instead, model 2 has i.i.d Gumbel distributed random error terms, and model 1 has difference random variable error terms (relative to the best alternative) that follow a truncated logistic distribution (see Appendix A).

With probability relation $P_i = Q_i^1 \times Q_i^2 \times \chi$ and the knowledge that $\sum_{i \in R} P_i = \sum_{i \in R} Q_i^1 \times Q_i^2 \times \chi = 1$, the following BPS model is derived (see Appendix B for details):

$$\begin{aligned} P_i &= \frac{\left(\exp\left(-\theta(c_i - \varphi \min(c_l: l \in R))\right) - 1\right)_+ \cdot e^{\beta \ln(\gamma_i)}}{\sum_{j \in R}\left(\exp\left(-\theta\left(c_j - \varphi \min(c_l: l \in R)\right)\right) - 1\right)_+ \cdot e^{\beta \ln(\gamma_j)}} \\ &= \frac{\left(\exp\left(-\theta(c_i - \varphi \min(c_l: l \in R))\right) - 1\right)_+ \cdot (\gamma_i)^{\beta}}{\sum_{j \in R}\left(\exp\left(-\theta\left(c_j - \varphi \min(c_l: l \in R)\right)\right) - 1\right)_+ \cdot (\gamma_j)^{\beta}}. \end{aligned}$$

Note that the proposed BPS model form approaches the regular Path Size Logit model in (4.1) in the limit as $\varphi \to \infty$ since the BCM approaches the MNL model in limit as $\varphi \to \infty$.

Assuming that the path size terms are non-zero, a route only receives a zero choice probability if $c_i > \varphi \min(c_l: l \in R)$. One can thus predetermine the unused routes by checking the fixed route travel costs against the bound, and the model can be formulated as follows. Let $\bar{R}(\boldsymbol{c}; \varphi) \subseteq R$ be the restricted choice set of all routes $i \in R$ where $c_i < \varphi \min(c_l: l \in R)$. The choice probability relation for route $i \in R$ is:

$$P_i = \begin{cases} \dfrac{\left(\exp\left(-\theta(c_i - \varphi \min(c_l: l \in R))\right) - 1\right) \cdot (\gamma_i)^{\beta}}{\sum_{j \in \bar{R}(\boldsymbol{c};\varphi)}\left(\exp\left(-\theta\left(c_j - \varphi \min(c_l: l \in R)\right)\right) - 1\right) \cdot (\gamma_j)^{\beta}} & if\ i \in \bar{R}(\boldsymbol{c}; \varphi) \\ 0 & if\ i \notin \bar{R}(\boldsymbol{c}; \varphi) \end{cases}.$$

Routes $i \in \bar{R}(\boldsymbol{c}; \varphi)$ are the used/active routes and routes $i \notin \bar{R}(\boldsymbol{c}; \varphi)$ are the unused/inactive routes.

Proposing that the routes with zero choice probabilities are exactly those with zero path size contributions (and strictly positive otherwise), the BPS model formulation can be extended as follows. Let $\bar{R}(\boldsymbol{c}; \varphi) \subseteq R$ be the restricted choice set of all routes $i \in R$ where $c_i < \varphi \min(c_l: l \in R)$. Given $\bar{R}(\boldsymbol{c}; \varphi)$, the choice probability relation for route $i \in R$ is:

$$P_i = \begin{cases} \dfrac{\left(\exp\left(-\theta(c_i - \varphi \min(c_l: l \in R))\right) - 1\right) \cdot (\bar{\gamma}_i)^{\beta}}{\sum_{j \in \bar{R}(\boldsymbol{c};\varphi)}\left(\exp\left(-\theta\left(c_j - \varphi \min(c_l: l \in R)\right)\right) - 1\right) \cdot (\bar{\gamma}_j)^{\beta}} & if\ i \in \bar{R}(\boldsymbol{c}; \varphi) \\ 0 & if\ i \notin \bar{R}(\boldsymbol{c}; \varphi) \end{cases}, \tag{4.6}$$

where the path size term for route $i \in \bar{R}(\boldsymbol{c}; \varphi)$ is:

$$\bar{\gamma}_i = \sum\nolimits_{a \in A_i} \frac{t_a}{c_i} \frac{W_i}{\sum_{k \in \bar{R}(\boldsymbol{c};\varphi)} W_k \delta_{a,k}}, \tag{4.7}$$

where $W_i > 0$ is the path size contribution weighting of route $i \in \bar{R}(\boldsymbol{c};\varphi)$ to used route path size terms, so that the contribution of used route k to the path size term of used route i is $\frac{W_k}{W_i}$. Note that the path size contribution factor is of the form $\frac{W_k}{W_i}$ so that distinct routes non-overlapping with all other routes have path size terms equal to 1. As Ramming (2002) noted, this was an issue for the original alternative PSL formulation proposed by Ben-Akiva & Bierlaire (1999). Since it is predetermined which routes are the unrealistic routes with zero probabilities, one only need consider the correlation between the realistic routes with positive probabilities (i.e. sum over routes $k \in \bar{R}(\boldsymbol{c};\varphi)$), and inactive/unused routes, i.e. routes $i \notin \bar{R}(\boldsymbol{c};\varphi)$, do not have path size term values.

For the choice probability function to be continuous for the proposed BPS model, the path size contributions weightings (W_i) must tend to zero as the route costs approach the bound from below (and consequently zero choice probability), so that when the cost of a route reaches the bound exactly (and thus receives a zero choice probability and is removed from the active choice set), there are no adjustments to the path size terms of the remaining active routes altering the probabilities and making the distribution discontinuous. This means that the W_i contribution weightings should be explicitly or implicitly dependent upon the route/link costs.

Watling et al (2018) remark that the BCM is consistent with a behavioural assumption that travellers make decisions in two stages. In the context of route choice, in the first stage travellers compare the random utility of each route against the best alternative in a pairwise manner. The bound imposed implicitly generates a choice set. In the second stage, alternatives from this choice set are compared and route choice probabilities are modelled using the log-odds from the first stage. Use of these log-odds means that choice set generation and route choice are consistent with the same underlying behavioural model.

With the natural BPS model form, the deterministic utilities comprise of a path size component and a cost component. This combined utility is used in the first stage to compare and bound, and obtain a choice set. In the second stage, the route choice probabilities are modelled by directly using the log-odds from the first stage.

With the proposed BPS model form derived here, the first stage is identical to that for the standard use of the BCM, where solely travel cost is used to compare and bound to obtain a choice set. Where the proposed BPS model form differs, however, is that in the second stage, the route choice probabilities are not modelled by directly using the log-odds from the first stage, and instead these log-odds are adjusted according to path size corrections to heuristically capture route correlation. Importantly though, the consistent criteria for determining choice sets and route choice probabilities are not violated, i.e. no route excluded from the generated choice set during the first stage can have a non-zero choice probability in the second stage, or vice versa. The key feature of the proposed BPS model form is that the measure of route correlation in the second stage only considers overlap between routes deemed realistic in the first stage.

As discussed in the previous section for the natural BPS model form, since the random error terms depend upon the bound, and the bound in that case is dependent upon the best route utility (which includes the path size correction), during calibration the path size correction can have an indirect effect on both the deterministic utility and random error term. For the proposed BPS model form in (4.6), however, the bound (in model 1) depends only upon the best route cost and is independent from the path size correction. The path size correction in this case therefore does not affect random error.

4. The Bounded Bounded Path Size Model

In this and the following sections, we formulate two BPS models that adopt the proposed form in (4.6)-(4.7). In Appendix E we discuss/demonstrate how these two models satisfy the desired properties for a BPS model established in Appendix C.

We begin by formulating the Bounded Bounded Path Size (BBPS) model, which is defined as follows. Let $\bar{R}(\boldsymbol{c};\varphi) \subseteq R$ be the restricted choice set of all active routes $i \in R$ where $c_i < \varphi \min(c_l : l \in R)$. Given $\bar{R}(\boldsymbol{c};\varphi)$, the choice probability relation for route $i \in R$ is:

$$P_i = \begin{cases} \dfrac{\left(\exp\left(-\theta(c_i - \varphi \min(c_l: l \in R))\right) - 1\right) \cdot \left(\bar{\gamma}_i^{BBPS}\right)^{\beta}}{\sum_{j \in \bar{R}(\boldsymbol{c};\varphi)} \left(\exp\left(-\theta\left(c_j - \varphi \min(c_l: l \in R)\right)\right) - 1\right) \cdot \left(\bar{\gamma}_j^{BBPS}\right)^{\beta}} & if\ i \in \bar{R}(\boldsymbol{c};\varphi) \\ 0 & if\ i \notin \bar{R}(\boldsymbol{c};\varphi) \end{cases}, \quad (4.8)$$

where the path size term for route $i \in \bar{R}(\boldsymbol{c};\varphi)$ is:

$$\bar{\gamma}_i^{BBPS} = \sum_{a \in A_i} \frac{t_a}{c_i} \frac{(h_i(-\lambda \boldsymbol{c}) - 1)}{\sum_{k \in \bar{R}(\boldsymbol{c};\varphi)} (h_k(-\lambda \boldsymbol{c}) - 1)\delta_{a,k}}, \quad (4.9)$$

where $h_i(-\lambda \boldsymbol{c}) = \exp\left(-\lambda(c_i - \varphi \min(c_l: l \in R))\right)$, and the model parameters are $\theta, \lambda > 0$, $\beta \geq 0$, $\varphi > 1$. P_i in (4.8) is the BBPS model probability relation for route $i \in R$ which adopts the proposed BPS model form in (4.6), and $\bar{\gamma}_i^{BBPS}$ in (4.9) is the BBPS model path size term for route $i \in \bar{R}(\boldsymbol{c};\varphi)$, which adopts the form of (4.7) with $W_k = h_k(-\lambda \boldsymbol{c}) - 1$.

The rationale behind formulating the BBPS path size contribution weightings as $W_k = h_k(-\lambda \boldsymbol{c}) - 1$ was to satisfy the desired properties for a BPS model. As discussed in the previous section, when deriving a BPS model from the proposed form by stipulating how the path size contribution weightings W_k are formulated, there are requirements for the consequent model to have a continuous choice probability function. To ensure a smooth removal of a route from the active choice set, the weighting W_k for each route $k \in \bar{R}(\boldsymbol{c};\varphi)$ must tend towards zero as the cost of that route tends towards the cost bound from above, i.e. as $c_k \to \varphi \min(c_l: l \in R)$, $c_k > \varphi \min(c_l: l \in R)$, and be eliminated exactly at the bound. The BBPS path size contribution weighting $W_k = h_k(-\lambda \boldsymbol{c}) - 1$ was stipulated as such so to satisfy these requirements. As can be seen, when $\lambda = \theta$, W_k matches the travel cost component in the BBPS model probability relation exactly, and thus choice probabilities and path size contributions tend towards zero concurrently and meet at zero.

An additional path size contribution scaling parameter, λ, is included, in the spirit of the GPSL and GPSL′ models, to allow for the de-coupling of the scale of the model from the path size effect. Larger values of λ accentuate the differences in cost with the contribution factors, so that the more expensive routes have more diminished (though still positive) contributions. In the same way that the GPSL′$_{(\lambda=\theta)}$ model is developed, however, one can equate the travel cost scales setting by $\lambda = \theta$ – thus formulating the BBPS$_{(\lambda=\theta)}$ model – to improve internal consistency and reduce the number of model parameters to estimate.

The attraction of the BBPS model is that it has a closed-form choice probability expression and hence route choice probability solutions are guaranteed to exist and be unique. The BBPS model is however not fully internally consistent since the path size contribution factors do not consider route distinctiveness, though consistency is improved by setting $\lambda = \theta$.

Moreover, the BBPS model approaches the GPSL′ model as $\varphi \to \infty$:

$$\sum_{a \in A_i} \frac{t_a}{c_i} \frac{(h_i(-\lambda \boldsymbol{c}) - 1)}{\sum_{k \in \bar{R}(\boldsymbol{c};\varphi)} \left(h_j(-\lambda \boldsymbol{c}) - 1\right)\delta_{a,k}} \to \sum_{a \in A_i} \frac{t_a}{c_i} \frac{e^{-\lambda c_i}}{\sum_{k \in R} e^{-\lambda c_k}\delta_{a,k}}$$

and

$$\frac{\left(\exp\left(-\theta(c_i - \varphi \min(c_l: l \in R))\right) - 1\right) \cdot (\gamma_i)^{\beta}}{\sum_{j \in \bar{R}(\boldsymbol{c};\varphi)} \left(\exp\left(-\theta(c_i - \varphi \min(c_l: l \in R))\right) - 1\right) \cdot \left(\gamma_j\right)^{\beta}} \to \frac{(\gamma_i)^{\beta} e^{-\theta c_i}}{\sum_{j \in R} \left(\gamma_j\right)^{\beta} e^{-\theta c_j}}$$

$$\text{as } \varphi \to \infty.$$

The BBPS$_{(\lambda=\theta)}$ model is thus equivalent to the GPSL′$_{(\lambda=\theta)}$ model in the limit as $\varphi \to \infty$, and the BBPS model is equivalent to the BCM for $\beta = 0$, which is equivalent to the MNL model in the limit as $\varphi \to \infty$.

5. The Bounded Adaptive Path Size Model

The Bounded Adaptive Path Size (BAPS) model adopts the proposed BPS model form derived in Section 3 and proposes that routes contribute to path size terms according choice probability ratios to ensure internal consistency and to provide a continuous choice probability function. The BAPS model route choice probability relation is thus an implicit function, naturally expressed as a fixed-point problem.

In the following two subsections we introduce two variants of the BAPS model. We first introduce in Section 5.1 the standard formulation, which is the straightforward definition. However, the probability domain is not defined on a closed set, forcing difficulties proving the existence and uniqueness of solutions. To circumvent this, we also in Section 5.2 formulate a modified version for which we can prove solution existence and establish uniqueness conditions, and where the standard BAPS formulation can be approximated to an arbitrary precision. We then provide a solution method for the modified BAPS model formulation, prove solution existence, and establish uniqueness conditions.

5.1 Standard BAPS Model Formulation

The standard BAPS model formulation (BAPS_0) is defined as follows. Let $\bar{R}(\boldsymbol{c};\varphi) \subseteq R$ be the restricted choice set of all active routes $i \in R$ where $c_i < \varphi \min(c_l: l \in R)$. Given $\bar{R}(\boldsymbol{c};\varphi)$, the BAPS_0 model route choice probabilities, $\boldsymbol{P}^*$, are a solution to the fixed-point problem $\boldsymbol{P} = \boldsymbol{f}\left(\bar{\boldsymbol{\gamma}}^{BAPS}(\boldsymbol{P})\right)$, where f_i for route $i \in R$ is:

$$f_i\left(\bar{\boldsymbol{\gamma}}^{BAPS}(\boldsymbol{P})\right) = \begin{cases} \dfrac{\left(\exp\left(-\theta(c_i - \varphi \min(c_l: l \in R))\right) - 1\right) \cdot \left(\bar{\gamma}_i^{BAPS}(\boldsymbol{P})\right)^{\beta}}{\sum_{j \in \bar{R}(\boldsymbol{c};\varphi)} \left(\exp\left(-\theta\left(c_j - \varphi \min(c_l: l \in R)\right)\right) - 1\right) \cdot \left(\bar{\gamma}_j^{BAPS}(\boldsymbol{P})\right)^{\beta}} & if\ i \in \bar{R}(\boldsymbol{c};\varphi) \\ 0 & if\ i \notin \bar{R}(\boldsymbol{c};\varphi) \end{cases}, \tag{4.10}$$

and the path size term for route $i \in \bar{R}(\boldsymbol{c};\varphi)$ is:

$$\bar{\gamma}_i^{BAPS}(\boldsymbol{P}) = \sum_{a \in A_i} \frac{t_a}{c_i} \frac{P_i}{\sum_{k \in \bar{R}(\boldsymbol{c};\varphi)} P_k \delta_{a,k}} = \sum_{a \in A_i} \frac{t_a}{c_i} \frac{1}{\sum_{k \in \bar{R}(\boldsymbol{c};\varphi)} \left(\frac{P_k}{P_i}\right) \delta_{a,k}}, \qquad \forall \boldsymbol{P} \in D^{(\bar{R}(\boldsymbol{c};\varphi))}, \tag{4.11}$$

$$D^{(\bar{R}(\boldsymbol{c};\varphi))} = \left\{ \boldsymbol{P} \in \mathbb{R}^N_{\geq 0}: 0 < P_i \leq 1, \forall i \in \bar{R}(\boldsymbol{c};\varphi), and, 0 \leq P_i \leq 1, \forall i \notin \bar{R}(\boldsymbol{c};\varphi), \sum_{j=1}^{N} P_j = 1 \right\}.$$

The model parameters are $\theta > 0$, $\beta \geq 0$, and $\varphi > 1$. $\bar{\gamma}_i^{BAPS}(\boldsymbol{P})$ in (4.11) is the BAPS model path size term function for route $i \in \bar{R}(\boldsymbol{c};\varphi)$ that is a function involving the choice probabilities of all routes, though in effect only the active routes. $f_i\left(\bar{\boldsymbol{\gamma}}^{BAPS}(\boldsymbol{P})\right)$ in (4.10) is the BAPS_0 model choice probability function for route $i \in R$ which is a function of the used route path size term functions and hence also the choice probabilities. The choice probability relation for route $i \in R$ is given by $P_i = f_i\left(\bar{\boldsymbol{\gamma}}^{BAPS}(\boldsymbol{P})\right)$, which is an implicit equation involving choice probabilities, and hence the BAPS_0 model route choice probabilities, $\boldsymbol{P}^*$, are a solution such that $P_i^* = f_i\left(\bar{\boldsymbol{\gamma}}^{BAPS}(\boldsymbol{P}^*)\right)$, $\forall i \in R$. For a BAPS_0 model route choice probability solution vector $\boldsymbol{P}^*$, $\bar{\boldsymbol{\gamma}}^{BAPS}(\boldsymbol{P}^*)$ is the BAPS model path size term for route $i \in \bar{R}(\boldsymbol{c};\varphi)$, and unused routes, i.e. routes $i \notin \bar{R}(\boldsymbol{c};\varphi)$, do not have path size term values.

$D^{(\bar{R}(\boldsymbol{c};\varphi))}$ is the domain for the fixed-point function $\boldsymbol{f}$, which is dependent upon the active choice set of routes $\bar{R}(\boldsymbol{c};\varphi)$ (and thus the route costs and bound parameter), and stipulates the feasible set of values for the fixed-point variables, which are in this case probabilities $\boldsymbol{P}$. $D^{(\bar{R}(\boldsymbol{c};\varphi))}$ stipulates that the active routes $i \in \bar{R}(\boldsymbol{c};\varphi)$ with costs below the bound must all have non-zero fixed-point variable values (i.e. $P_i > 0$, $\forall i \in \bar{R}(\boldsymbol{c};\varphi)$) ensuring that occurrences of $\frac{0}{0}$ are avoided in the BAPS model path size term functions $\bar{\gamma}_i^{BAPS}(\boldsymbol{P})$, and thus any solution to the fixed-point system also circumvents the issue. The active routes can however assume any non-zero probability value. $D^{(\bar{R}(\boldsymbol{c};\varphi))}$ then stipulates that the inactive routes $i \notin \bar{R}(\boldsymbol{c};\varphi)$ with costs above the bound can assume any probability value (zero or non-zero), though while the domain of $\boldsymbol{f}$ allows for inactive routes to have non-zero fixed-point variable values, by the definition of f_i in (4.10), any solution to the fixed-point system will have zero probabilities for all inactive routes. $D^{(\bar{R}(\boldsymbol{c};\varphi))}$ also stipulates that the fixed-point variable values should all sum up to 1, as standard for a probability domain.

As (4.11) shows, for a choice probability solution $\boldsymbol{P}^*$, the contribution of used route k to the BAPS model path size term of used route i is weighted according to the ratio of choice probabilities between the routes

$\left(\frac{P_k^*}{P_i^*}\right)$, and hence as a used route approaches zero choice probability its path size contribution approaches zero, until it is considered unrealistic, where it then receives a zero choice probability and its path size contributions are eliminated completely.

It is our belief that there is a strong theoretical and behavioural basis for the $BAPS_0$ model, and the model captures the best features of the BCM and APSL model. It appears logical that routes are judged as unrealistic (assigned zero choice probability / have zero path size contributions) if they have an excessively large travel cost, but not necessarily unrealistic if they are very indistinct. Routes are still penalised according to their indistinctiveness and the choice probability / path size contribution of route i decreases as $\bar{\gamma}_i^{BAPS}$ decreases, but routes are not bounded according to indistinctiveness.

The $BAPS_0$ model approaches the APSL model in the limits as $\tau \to 0$ and $\varphi \to \infty$:

$$G_i\left(g_i\left(\boldsymbol{\gamma}^{APS}(\boldsymbol{P})\right)\right) \to g_i\left(\boldsymbol{\gamma}^{APS}(\boldsymbol{P})\right) \text{ as } \tau \to 0,$$

and,

$$f_i\left(\bar{\boldsymbol{\gamma}}^{BAPS}(\boldsymbol{P})\right) \to g_i\left(\boldsymbol{\gamma}^{APS}(\boldsymbol{P})\right) \text{ as } \varphi \to \infty.$$

The $BAPS_0$ model is also equivalent to the BCM for $\beta = 0$, which is equivalent to the MNL model in the limit as $\varphi \to \infty$.

The $BAPS_0$ model proposes that the path size terms utilise choice probability ratio path size contribution factors; however, referring to the derivation of the proposed BPS model form in Section 3, the choice probabilities are not the model 2 probabilities (Q_i^2), but instead those obtained from the union model. Hence, the $BAPS_0$ model is not a direct union of two separate models and instead the models are interdependent.

The complication for the $BAPS_0$ model to be mathematically well-defined is that it is not in the correct form for standard proofs of solution existence and uniqueness to apply. Standard proofs for existence and uniqueness of fixed-point solutions require the domain of the fixed-point function (in this case $\boldsymbol{f}$) to be a compact convex set. The domain of $\boldsymbol{f}$, $D^{(\bar{R}(\boldsymbol{c};\varphi))}$, however, is not a compact convex set since the fixed-point variable value bounds are not closed for all routes: the lower bound for all active routes $i \in \bar{R}(\boldsymbol{c};\varphi)$ is open where these fixed-point variables cannot assume the bound value (i.e. $P_i \neq 0$). As shown in Appendix C for options 2&3, the path size terms cannot be altered to allow for zero path size contribution weightings without losing continuity of the fixed-point function (which is also required for the proofs), and hence in Section 5.2 below we modify the BAPS model so that it is in the correct form for standard proofs to apply.

5.2 Modified BAPS Model Formulation

5.2.1 Definition

The modified BAPS model is defined as follows. Let $\bar{R}(\boldsymbol{c};\varphi) \subseteq R$ be the restricted choice set (with size $\bar{N}$) of all routes i where $c_i < \varphi \min(c_l : l \in R)$. The BAPS model route choice probabilities, $\boldsymbol{P}^*$, are a solution to the fixed-point problem $\boldsymbol{P} = \boldsymbol{F}\left(\boldsymbol{f}\left(\bar{\boldsymbol{\gamma}}^{BAPS}(\boldsymbol{P})\right)\right)$, where F_i for route $i \in R$ is:

$$F_i\left(f_i\left(\bar{\boldsymbol{\gamma}}^{BAPS}(\boldsymbol{P})\right)\right) = \begin{cases} \tau + (1 - \bar{N}\tau) \cdot f_i\left(\bar{\boldsymbol{\gamma}}^{BAPS}(\boldsymbol{P})\right) & if\ i \in \bar{R}(\boldsymbol{c};\varphi) \\ 0 & if\ i \notin \bar{R}(\boldsymbol{c};\varphi) \end{cases}, \tag{4.12}$$

f_i for route $i \in R$ is:

$$f_i\left(\bar{\boldsymbol{\gamma}}^{BAPS}(\boldsymbol{P})\right) = \begin{cases} \dfrac{\left(\exp\left(-\theta(c_i - \varphi \min(c_l : l \in R))\right) - 1\right) \cdot \left(\bar{\gamma}_i^{BAPS}(\boldsymbol{P})\right)^{\beta}}{\sum_{j \in \bar{R}(\boldsymbol{c};\varphi)} \left(\exp\left(-\theta\left(c_j - \varphi \min(c_l : l \in R)\right)\right) - 1\right) \cdot \left(\bar{\gamma}_j^{BAPS}(\boldsymbol{P})\right)^{\beta}} & if\ i \in \bar{R}(\boldsymbol{c};\varphi) \\ 0 & if\ i \notin \bar{R}(\boldsymbol{c};\varphi) \end{cases}, \tag{4.13}$$

and the path size term for route $i \in \bar{R}(\boldsymbol{c};\varphi)$ is:

$$\bar{\gamma}_i^{BAPS}(\boldsymbol{P}) = \sum_{a \in A_i} \frac{t_a}{c_i} \frac{P_i}{\sum_{k \in \bar{R}(\boldsymbol{c};\varphi)} P_k \delta_{a,k}}, \qquad \forall \boldsymbol{P} \in D^{(\bar{R}(\boldsymbol{c};\varphi),\tau)}, \tag{4.14}$$

$$D^{(\bar{R}(\boldsymbol{c};\varphi),\tau)} = \left\{ \boldsymbol{P} \in \mathbb{R}^{N}_{\geq 0} : \tau \leq P_i \leq (1-\bar{N}\tau), \forall i \in \bar{R}(\boldsymbol{c};\varphi), and, 0 \leq P_i \leq (1-\bar{N}\tau), \forall i \notin \bar{R}(\boldsymbol{c};\varphi), \sum_{j=1}^{N} P_j = 1 \right\}.$$

The model parameters are $\theta > 0$, $\beta \geq 0$, $\varphi > 1$, and $0 < \tau \leq \frac{1}{\bar{N}}$, where τ is the perturbation parameter. (4.13) and (4.14) are equivalent to (4.10) and (4.11) for the standard BAPS model formulation: $\bar{\gamma}_i^{BAPS}(\boldsymbol{P})$ in (4.14) is the path size term function for route $i \in \bar{R}(\boldsymbol{c};\varphi)$ that is a function involving the choice probabilities, and $f_i\left(\bar{\boldsymbol{\gamma}}^{BAPS}(\boldsymbol{P})\right)$ in (4.13) is the unadjusted choice probability function for route $i \in R$ which is a function of the used route path size term functions and hence also the choice probabilities. The choice probability relation for route $i \in R$ is given by $P_i = F_i\left(f_i\left(\bar{\boldsymbol{\gamma}}^{BAPS}(\boldsymbol{P})\right)\right)$, which is an implicit equation involving choice probabilities, and hence the BAPS model route choice probabilities, $\boldsymbol{P}^*$, are a solution such that $P_i^* = F_i\left(f_i\left(\bar{\boldsymbol{\gamma}}^{BAPS}(\boldsymbol{P}^*)\right)\right)$, $\forall i \in R$. The key difference between this modified formulation and the standard formulation is the adjustment function F_i. $F_i\left(f_i\left(\bar{\boldsymbol{\gamma}}^{BAPS}(\boldsymbol{P})\right)\right)$ in (4.12) is the choice probability adjustment function for route $i \in R$ which adjusts the choice probability function f_i for reasons given below.

Duncan et al (2020) construct a choice probability adjustment function G_i for the APSL model motivated by some desired behaviours and required properties for proving existence and uniqueness. Similar motivations led to the construction of the adjustment function F_i for the BAPS model. The Required Properties (RP) for F_i were as follows:

1. F_i must map into itself.
2. F_i must be continuous for all $\boldsymbol{P}$.
3. F_i must be continuously differentiable with respect to $\boldsymbol{P}$ for all $\boldsymbol{P}$.
4. The domain of F_i must be closed and bounded.
5. The domain of F_i must allow the unused routes to have zero choice probabilities but not the used routes.
6. F_i should be able to approximate f_i to arbitrary precision.
7. The domain of F_i should have a lower bound for used routes that can approximate zero to arbitrary precision.

RP 1-4 are required for existence and uniqueness proofs. RP 5 is required so that the used route path size term function $\bar{\gamma}_i^{BAPS}(\boldsymbol{P})$ in (4.14) and thus $F_i\left(f_i\left(\bar{\boldsymbol{\gamma}}^{BAPS}(\boldsymbol{P})\right)\right)$ in (4.12) are defined, i.e. to avoid occurrences of $\frac{0}{0}$. RP 6 is desired as it is not our intention for the choice probabilities acquired from the modified formulation to be different to the choice probabilities from the standard BAPS model formulation (where one would exist), and we wish them to be as close as possible. RP 7 is desired as there should be no intentional bounding of the used route choice probabilities; used routes ideally should be able to assume any non-zero probability, but this must be approximated due to the requirement for the domain to be closed and bounded.

So, the formulation of F_i in (4.12) and its domain $D^{(\bar{R}(\boldsymbol{c};\varphi),\tau)}$ have been constructed to satisfy RP 1-7. In Section 10.2 we prove that RP 1-3 are satisfied. The parameter τ is introduced, and the domain $D^{(\bar{R}(\boldsymbol{c};\varphi),\tau)}$ is such that $P_i \geq \tau$, $\forall i \in \bar{R}(\boldsymbol{c};\varphi)$, and since the choice probabilities for all routes sum up to 1: $P_i \leq (1-(\bar{N}-1)\tau)$, $\forall i \in \bar{R}(\boldsymbol{c};\varphi)$. The domain also stipulates that $0 \leq P_i \leq (1-\bar{N}\tau)$ for all $i \notin \bar{R}(\boldsymbol{c};\varphi)$. RP 4 is thus satisfied as $D^{(\bar{R}(\boldsymbol{c};\varphi),\tau)}$ is closed and bounded. τ is restricted to the range $0 < \tau \leq \frac{1}{\bar{N}}$ and thus RP 5 is satisfied as zero choice probabilities are not in the domain for the used routes, and unused routes can have zero probabilities. As $\tau \to 0$, $F_i \to f_i$ satisfying RP 6 and the lower bound for P_i $\forall i \in \bar{R}(\boldsymbol{c};\varphi)$ in $D^{(\bar{R}(\boldsymbol{c};\varphi),\tau)}$ tends towards zero satisfying RP 7.

As is the case for the APSL model, the τ parameter is not a model parameter that requires estimating, it is simply a mathematical construct that ensures RP 1-7 are satisfied. While the modified BAPS model formulation provides the capability, it is not our intention for this model to purposefully compute different choice probabilities to those obtained from the standard formulation for any given theoretical reason. In fact, we desire the choice probabilities to be as close as possible, and hence we advise that only small values of τ are used. While bounding the non-zero choice probabilities from below results in a discontinuous choice

probability function (since used routes cannot have probabilities between 0 and τ), in practice, the range of computable values is naturally limited by computer precision, and hence choice probabilities are always in effect bounded by the smallest computable positive value. Thus, despite the known discontinuity, in applications we use the modified BAPS model formulation with τ set as a very small value (as small as feasible for computation). With the APSL model proposed in Duncan et al (2020), no difficulties are experienced in practical applications in their analogous approximation of the desired $APSL_0$ model with the parameter τ, and hence it is also expected that the approximation of the $BAPS_0$ model with the proposed BAPS model here will be similarly non-problematic. For the rest of the paper, i.e. for the demonstrations and estimation work, we use the modified BAPS model formulation with $\tau = 10^{-16}$, unless stated otherwise. In Section 7.3.2.2 we briefly investigate the impact of the τ parameter upon parameter estimation.

The modified BAPS model formulation approaches the APSL model in the limit as $\varphi \to \infty$:

$$f_i\left(\bar{\boldsymbol{\gamma}}^{BAPS}(\boldsymbol{P})\right) \to g_i\left(\boldsymbol{\gamma}^{APS}(\boldsymbol{P})\right) \text{ as } \varphi \to \infty$$

and,

$$F_i\left(f_i\left(\bar{\boldsymbol{\gamma}}^{BAPS}(\boldsymbol{P})\right)\right) \to G_i\left(g_i\left(\boldsymbol{\gamma}^{APS}(\boldsymbol{P})\right)\right) \text{ as } \varphi \to \infty.$$

Both the standard and modified BAPS model formulations are equivalent to the BCM for $\beta = 0$, which is equivalent to the MNL model in the limit as $\varphi \to \infty$.

BAPS model solutions are guaranteed to exist and are unique under certain conditions. To prove these theoretical properties, we appropriately modify the proofs for existence and uniqueness provided for the APSL model in Duncan et al (2020). We include the proofs in Appendix D. Just as for the APSL model, values of $b > 0$ exist such that BAPS model solutions are unique for β in the range $0 \le \beta \le b$. Though there are cases where solutions are unique for all $\beta \ge 0$ (for example when there are no overlapping used routes), in most cases there is a maximum value for b (b_{max}). β in the range $0 \le \beta \le b_{max}$ is however only a sufficient condition for unique BAPS model solutions, β_{max} is the true maximum value where solutions are unique for β in the range $0 \le \beta \le \beta_{max}$. In Appendix E we propose a method for estimating β_{max} (also adapted from that proposed for the APSL model) and demonstrate estimating the uniqueness conditions for the example network. In Sections 7.3.2.2.3 and 7.4.2.3 we demonstrate estimating the uniqueness conditions for the Sioux Falls simulation experiments and real-life large-scale network, respectively.

5.2.2 Solution Method

There are many fixed-point algorithms available for solving the BAPS model fixed-point system $\boldsymbol{P} = \boldsymbol{F}\left(\boldsymbol{f}\left(\bar{\boldsymbol{\gamma}}^{BAPS}(\boldsymbol{P})\right)\right)$. In the studies in this paper we utilise the simplest fixed-point algorithm available: the Fixed-Point Iteration Method (FPIM) (Isaacson & Keller, 1966). The FPIM is the most basic fixed-point algorithm, and other algorithms aim to accelerate the convergence of the FPIM, though require more complicated computations at each iteration s. The FPIM for solving the BAPS model fixed-point system $\boldsymbol{P} = \boldsymbol{F}\left(\boldsymbol{f}\left(\bar{\boldsymbol{\gamma}}^{BAPS}(\boldsymbol{P})\right)\right)$ is formulated as follows:

$$P_i^{(s+1)} = F_i\left(f_i\left(\bar{\boldsymbol{\gamma}}^{BAPS}\left(\boldsymbol{P}^{(s)}\right)\right)\right), \qquad s = 0,1,2,\dots$$

such that

$$\lim_{s\to\infty} P_i^{(s+1)} = \lim_{s\to\infty} F_i\left(f_i\left(\bar{\boldsymbol{\gamma}}^{BAPS}\left(\boldsymbol{P}^{(s)}\right)\right)\right) = P_i^*, \qquad \boldsymbol{P}^{(0)} \in D^{(\bar{R}(\boldsymbol{c};\varphi),\tau)}, \qquad \forall i \in R.$$

A standard convergence statistic we chose to observe in this study is $\ln\left(\sum_{i\in R}\left|P_i^{(s+1)} - P_i^{(s)}\right|\right)$, and the FPIM is said to have converged sufficiently to a BAPS model choice probability solution if:

$$\ln\left(\sum_{i\in R}\left|P_i^{(s+1)} - P_i^{(s)}\right|\right) < \ln\left(10^{-\xi}\right),$$

where ξ is a predetermined convergence parameter. In Sections 7.3.2.2 & 7.4.1.2 we assess the computational performance of the BAPS model in computing choice probabilities and parameter estimation.

6. Theoretical Properties

In this section, we first demonstrate on small example networks the theoretical properties of the proposed BPS models and compare with results from MNL, Path Size Logit models, and the BCM. Then, we discuss how the proposed BPS models satisfy the desired properties established for a BPS model in Section 3.1 and Appendix C, and finally illustrate how the models collapse into one another.

In demonstration 1, we demonstrate whether/how the different models deal with route overlap and unrealistic routes. To do this, we adapt the famous 'loop-hole' network (also known as the red-bus/blue-bus network) presented in Cascetta et al (1996), which is Fig. 4.1 minus link 1. Example network 1 in Fig. 4.1 has five routes: Route 1: $1 \rightarrow 3$, Route 2: $1 \rightarrow 4$, Route 3: $2 \rightarrow 3$, Route 4: $2 \rightarrow 4$, Route 5: 5. Routes 3-5 all have a travel cost of 1 while Routes 1&2 have a travel cost of $2.5 - \rho$. Route 5 is distinct while Routes 1-4 are correlated, where the degree of correlation depends on ρ. As $\rho \rightarrow 1$, Routes 1&2 and Routes 3&4 become highly correlated, and (because links 3&4 become negligible compared to links 1&2) the network is in effect reduced to 3 distinct routes consisting of links 1,2,&5. On-the-other-hand, as $\rho \rightarrow 0$, link 2 becomes negligible compared to links 3&4 and Routes 3&4 become non-overlapping routes.

Fig. 4.2 displays for example network 1 the route choice probabilities for the different models as ρ is varied between 0 and 1, $\theta = \beta = \lambda^{GPS'} = \lambda^{BBPS} = 1$, $\varphi = 2$, $\lambda^{GPS} = 5$. As ρ varies between 0 and 1, the cost of Routes 1&2 decreases from 2.5 to 1.5. Since the minimum costing route is 1, the cost bound is 2. Therefore, for $\rho < 0.5$, Routes 1&2 should be considered unrealistic (given the bound criteria) and hence given zero choice probabilities and excluded from route overlap considerations. As shown for MNL and the BCM, because these models fail to account for any route overlap, and Routes 3-5 all have travel costs of 1 for all ρ, these routes have equal choice probabilities for all ρ, while the BCM gives zero probabilities to routes considered unrealistic and MNL does not. Routes 3-5 should, however, only have equal choice probabilities at $\rho = 0$ (where these routes are all non-overlapping, equal costing, and Routes 1&2 are considered unrealistic). As ρ is increased from 0 to 0.5, the choice probabilities of Routes 3&4 should be reduced to account for the overlap between the two routes, and as ρ is increased from 0.5 to 1, overlap with Routes 1&2 should also be considered as these become realistic. For PSL, while route overlap is considered, the overlap is considered in a non-discriminatory manner between realistic and unrealistic routes, and therefore Routes 3&4 are penalised for overlapping with Routes 1&2 for $\rho < 0.5$. GPSL, GPSL′, and APSL all improve upon this shortcoming of PSL by reducing the penalisation incurred upon Routes 3&4 from Routes 1&2 for $\rho < 0.5$. All routes are given non-zero choice probabilities and path size contributions however, and therefore the effects of the unrealistic routes are not fully dealt with. As the plots for the BBPS & BAPS models show, Routes 1&2 receive zero choice probabilities for $\rho < 0.5$, and Routes 3&4 are not penalised for overlapping with Routes 1&2. For $\rho > 0.5$, Routes 1&2 receive non-zero choice probabilities and Routes 3&4 are penalised for overlapping with Routes 1&2.

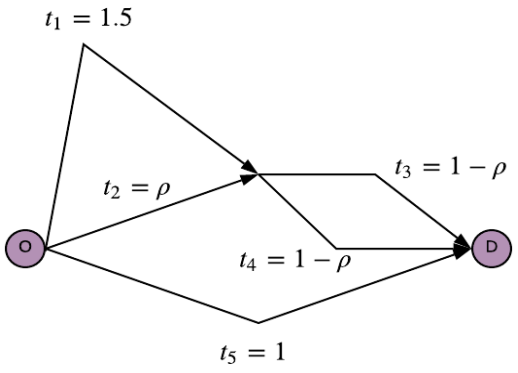

Fig. 4.1. Example network 1.

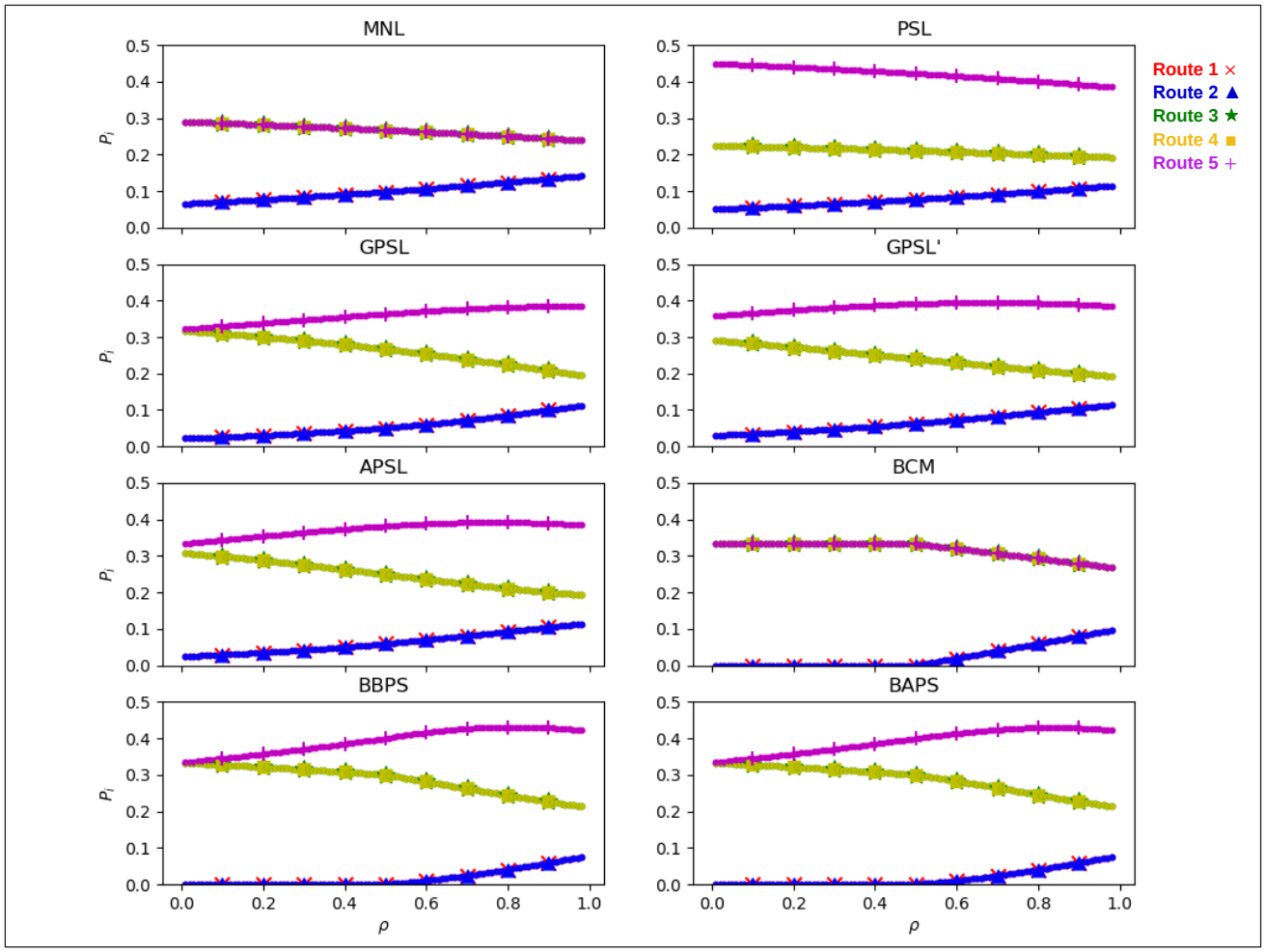

Fig. 4.2. Example network 1: Route choice probabilities for different models as ρ is varied ($\theta = \beta = \lambda^{GPS'} = \lambda^{BBPS} = 1$, $\varphi = 2$, $\lambda^{GPS} = 5$).

In demonstration 2, we demonstrate how the BPS models are able to overcome a drawback typically experienced by correction terms models on the Switching Route Network in Prashker & Bekhor (2004). Example network 2 in Fig. 4.3 (the Switching Route Network) has four routes: Route 1: $1 \rightarrow 2$. Route 2: $5 \rightarrow 6$. Route 3: $1 \rightarrow 3 \rightarrow 6$. Route 4: $5 \rightarrow 4 \rightarrow 2$. Routes 1-3 all have travel cost equal to 10 (for all η), while Route 4 has travel cost equal 4η-10. To ensure non-negative link costs, η must be between 5 and 10. For $\eta = 5$, Route 4 has equal travel cost to the other routes, and as η increases from 5, Route 4 increases in cost and consequently becomes less attractive compared to the other routes.

There are expected behaviours from the choice probabilities as η is varied between 5 and 10, where the probability of Route 3 is typically observed. For $\eta = 5$, the middle links collapse to zero and the network is in effect reduced to four identical routes. Probability for each of these routes should therefore equal $\frac{1}{4}$ at $\eta = 5$. As η increases, Route 4 becomes less attractive and the other routes should increase in choice probability. The proposition is that at some point as η is increased, Route 4 should be defined as unrealistic and beyond this point should not impact upon the probabilities of the other routes. Presuming Route 4 is defined as unrealistic before $\eta = 10$, when η reaches 10, links 1&6 collapse to zero and the network is in effect reduced to just three identical distinct routes (excluding the unrealistic route). As such, at $\eta = 10$, Route 3 (along with Routes 1&2) should have probability equal to $\frac{1}{3}$. Here, we suppose that a route is defined as unrealistic if it has a travel cost greater than or equal to twice the minimum cost route (a bound of $\varphi = 2$). This means that at and beyond $\eta = 7.5$ (where Route 4's travel cost equals 20), Route 4 should be defined as unrealistic and its impact removed.

Fig. 4.4A-B displays for example network 2 the Route 3 choice probabilities from the different models as η is varied between 5 and 10, where the parameters for Fig. 4.4A and Fig. 4.4B are $\theta = \lambda^{GPS'} = \lambda^{BBPS} = \beta =$

0.5, $\varphi = 2$, $\lambda^{GPS} = 10$ and $\theta = \lambda^{GPS'} = \lambda^{BBPS} = 0.1$, $\beta = 0.8$, $\varphi = 2$, $\lambda^{GPS} = 1$, respectively. Considering first Fig. 4.4A, as shown, for PSL, since the path size terms suppose all routes contribute equally whether realistic or unrealistic, Route 4 contributes to Routes 1&2 for all η and the PSL probability for Route 3 goes above $\frac{1}{3}$. For $\eta \geq 7.5$, however, where Route 4 should be defined as unrealistic, Route 4 should not contribute to Routes 1&2. For MNL & the BCM, Routes 1-3 receive the same probability for all η as they are equal costing and correlation is not considered. For $\eta \geq 7.5$, the BCM gives the unrealistic Route 4 zero probability (and Route 3 thus $\frac{1}{3}$ probability). MNL gives a non-zero probability, but with the θ parameter set, these probabilities are small and the BCM is approximated. With the GPSL, GPSL′, APSL, BBPS, & BAPS models, overlap correlations between Routes 1-3 are captured, where Route 3 is penalised for overlapping with both Routes 1&2, but because the path size contributions are weighted, the contribution of Route 4 to Routes 1&2 is either reduced (for GPSL, GPSL′, APSL) or eliminated (for BBPS & BAPS) for $\eta \geq 7.5$. For the parameters set, GPSL′ approximates the BBPS model and APSL approximates the BAPS model, where the contributions are weighted sufficiently for GPSL, GPSL′, & APSL such that the probability for Route 3 does not exceed $\frac{1}{3}$.

For the parameters set in Fig. 4.4B, however, the contributions are not weighted sufficiently for GPSL, GPSL′, & APSL, and the probabilities for Route 3 exceed $\frac{1}{3}$. For BBPS & BAPS, with $\varphi = 2$, the contribution of Route 4 to Routes 1&2 will be eliminated for $\eta \geq 7.5$ (rather than reduced) for all settings of the θ and β parameters. β allows for route correlations to be captured (differentiating the BPS models from the BCM), while the θ parameter scales sensitivity to travel cost.

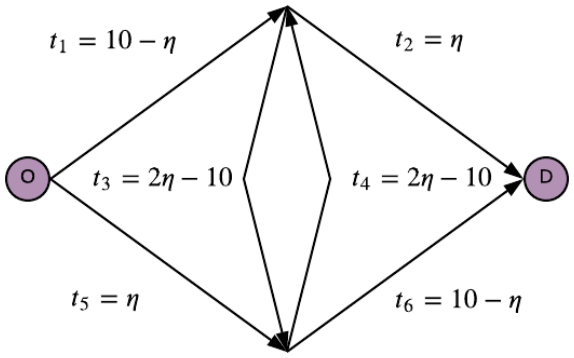

Fig. 4.3. Example network 2 (the Switching Route Network).

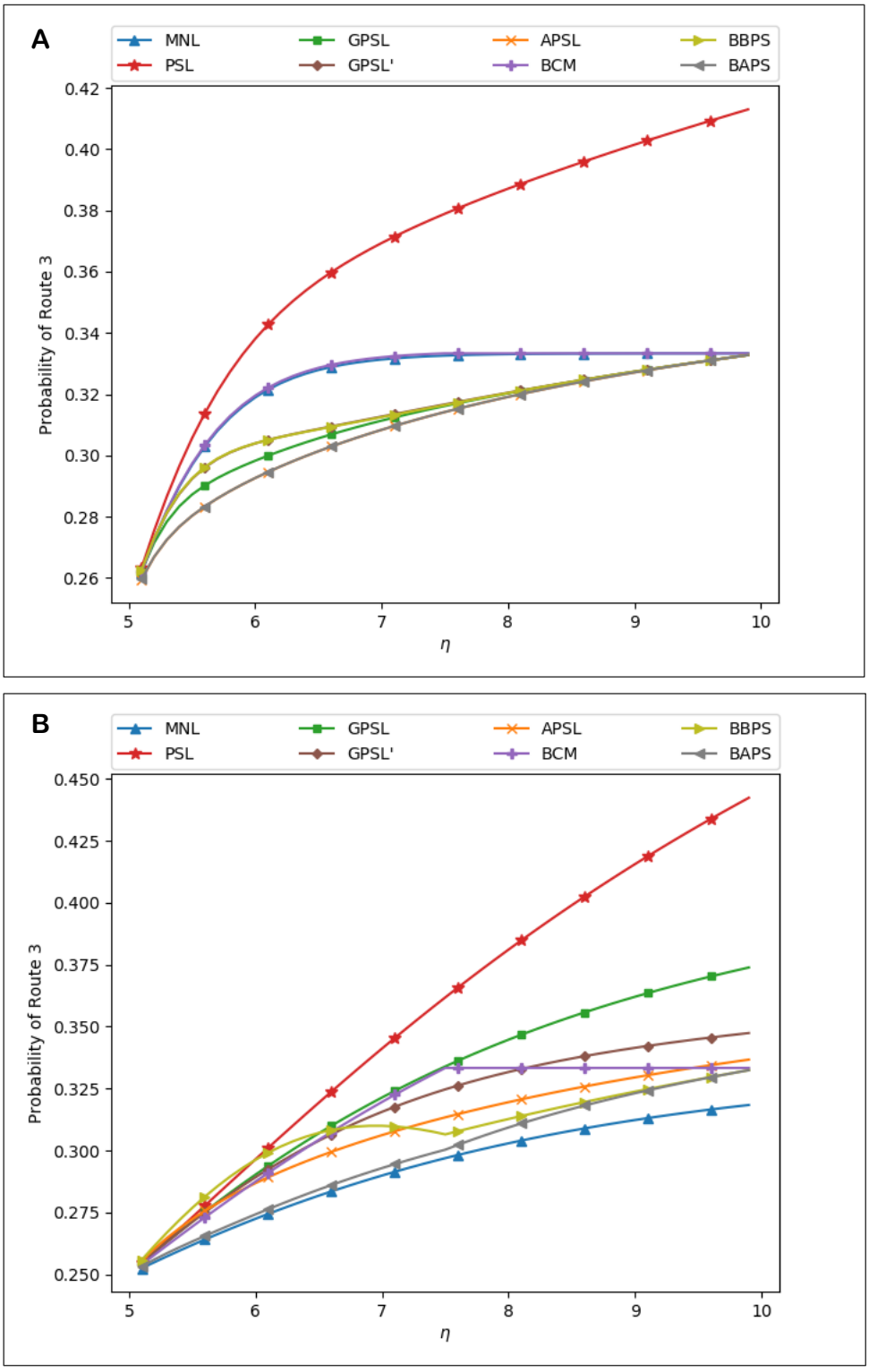

Fig. 4.4. Example network 2: Choice probability of Route 3 for the different models. **A:** $\theta = \lambda^{GPS'} = \lambda^{BBPS} = \beta = 0.5$, $\varphi = 2$, $\lambda^{GPS} = 10$. **B:** $\theta = \lambda^{GPS'} = \lambda^{BBPS} = 0.1$, $\beta = 0.8$, $\varphi = 2$, $\lambda^{GPS} = 1$.

In demonstration 3, we demonstrate how the parameters of the BAPS model impact upon the route choice probabilities. Example network 5 in Fig. 4.5A has seven routes: Route 1: 1, Route 2: 2, Route 3: 3, Route 4: 4 → 5, Route 5: 4 → 6, Route 6: 7 → 8, Route 7: 7 → 9. Routes 1&7 have travel cost 2, Routes 2&6 have travel cost 1.5, and Routes 3-5 have travel cost 1. Routes 1-3 are distinct routes, while Routes 4&5 and Routes 6&7 are correlated. The minimum costing routes are Routes 3-5 costing 1. For different ranges of the bound parameter φ, the active choice set of realistic routes varies, and the network can in effect be reduced as

follows: for $\varphi > 2$ the full network in Fig. 4.5A of all 7 seven routes; for $1.5 < \varphi \leq 2$ the reduced network in Fig. 4.5B excluding Routes 1&7; and, for $1 < \varphi \leq 1.5$ the reduced network in Fig. 4.5C excluding Routes 1&7 and Routes 2&6.

Fig. 4.6A-E display, for different settings of the θ and β parameters, how the BAPS model choice probabilities vary as φ is varied between 1 and 3. Considering first Fig. 4.6C where $\theta = \beta = 1$, as shown, for $\varphi = 3$, all routes have costs below the bound and thus all have non-zero choice probabilities, (here the APSL probabilities are approximated). As φ is decreased to 2, the costs of Routes 1&7 approach the bound, and their choice probabilities thus tend towards zero. Moreover, as Route 7 tends towards zero probability, its path size contribution to Route 6 tends to zero, and thus when $\varphi = 2$ and Route 7 receives zero probability / its contribution to Route 6 is eliminated, the probabilities remain smooth and continuous.

For $\varphi > 2$, despite having the same travel cost, Route 6 has a lower probability than Route 2 as Route 6 is penalised for overlapping with Route 7, while Route 2 is distinct. For $1.5 < \varphi \leq 2$, however, Route 6 is not penalised for overlapping with the unrealistic Route 7, and thus Routes 2&6 have the same probability. As φ is decreased to 1.5, Routes 2&6 approach the cost bound and zero probability.

For $1 < \varphi \leq 1.5$, only the minimum costing Routes 3-5 are within the cost bound are thus receive non-zero probabilities. Routes 4&5 have a lower probability than Route 3 since Routes 4&5 are penalised for overlapping.

Now, considering Fig. 4.5A-C where β equals 0, 0.5, and 1, respectively, the effect of the β parameter (and thus path size correction) upon route choice can be seen. In Fig. 4.5A where $\beta = 0$, the BCM probabilities are displayed. As can be seen, Routes 1&7, Routes 2&6, and Routes 3-5 have equal probabilities for all φ since these routes have equal costs and route correlation is not considered. Routes 4&5 and Routes 6&7 should be penalised (when considered realistic), however, as they overlap. As Fig. 4.5B-C show for $\beta = 0.5$ and $\beta = 1$, respectively, the BAPS model probabilities penalises overlapping routes (when they are considered realistic), while the penalisation is more significant for greater values of β.

Now, considering Fig. 4.5C-E where θ equals 1, 0.1, and 2, respectively, the effect of the θ parameter upon route choice can be seen. Lower θ values dampen the travel cost differences for routes within the active choice set, and routes with different costs have closer probabilities. Larger θ values accentuate the travel cost differences so that the higher costing routes receive lower probabilities. Decreasing probabilities with greater θ values also results in the path size contributions for those routes being reduced, which is why the probabilities between routes with the same cost have closer probabilities for larger θ.

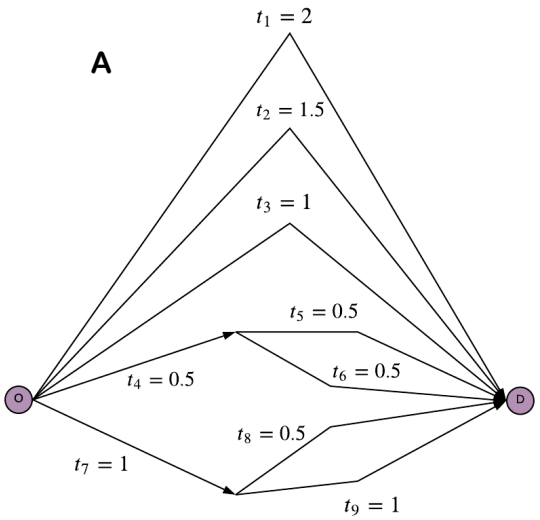

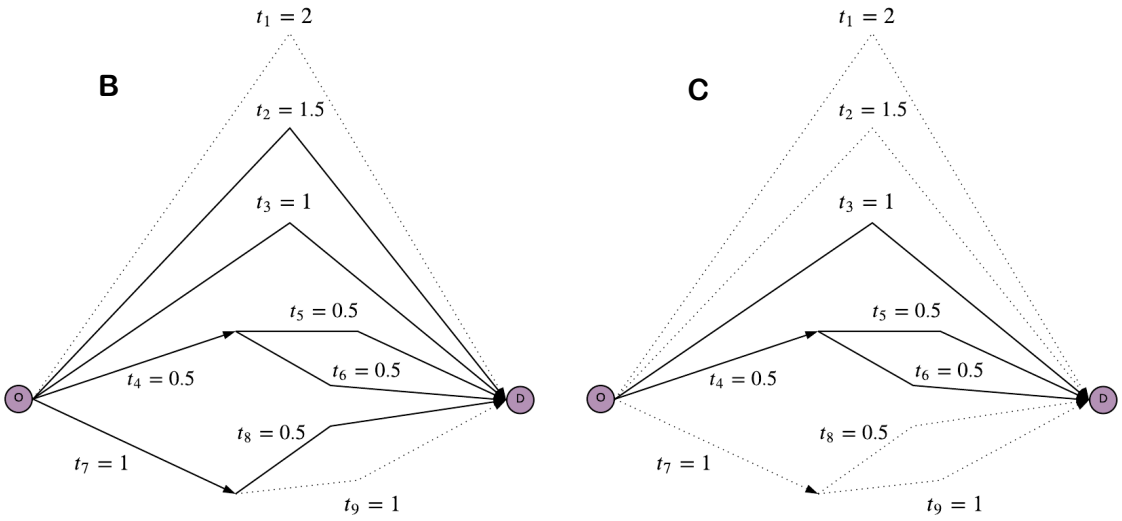

Fig. 4.5. Example network 3. **A:** Full network (for $\varphi > 2$). **B:** Reduced network (for $1.5 < \varphi \leq 2$). **C:** Reduced network (for $1 < \varphi \leq 1.5$).

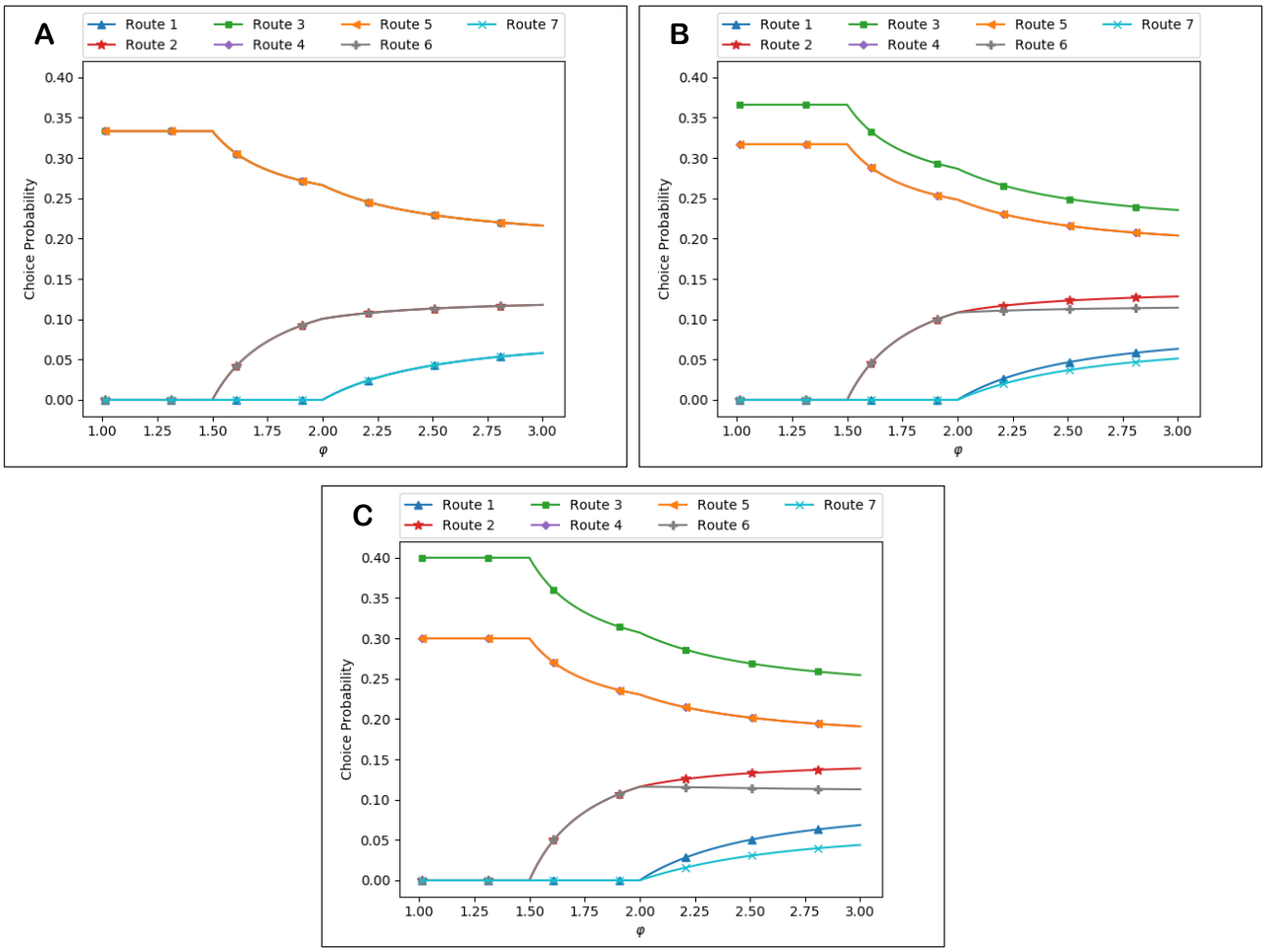

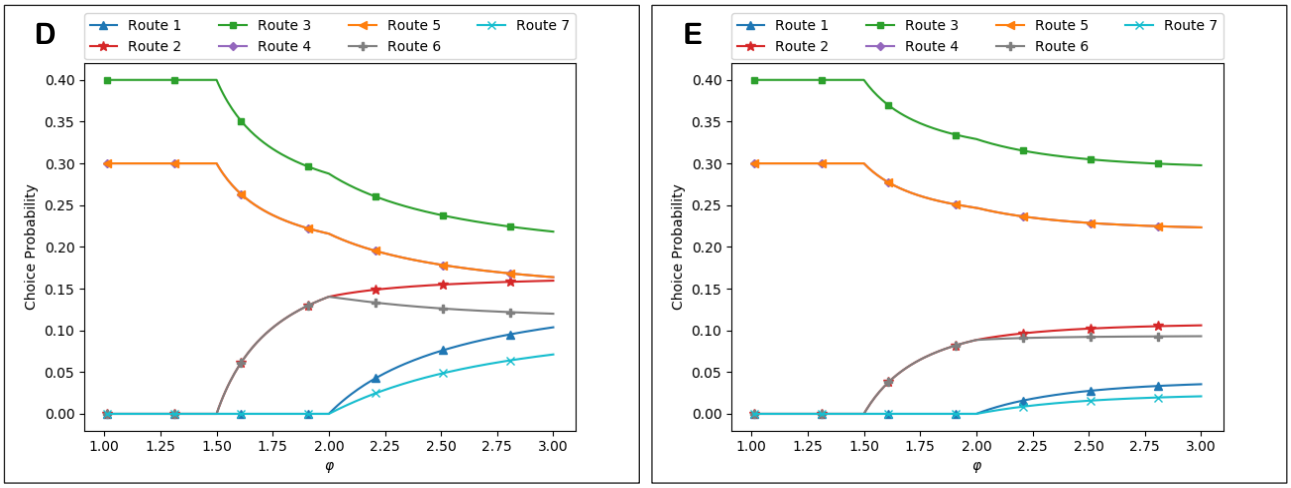

Fig. 4.6. Example network 3: BAPS model choice probabilities as the bound parameter φ is varied. **A:** $\theta = 1, \beta = 0$. **B:** $\theta = 1, \beta = 0.5$. **C:** $\theta = \beta = 1$. **D:** $\theta = 0.1, \beta = 1$. **E:** $\theta = 2, \beta = 1$.

Table 4.1 summarises whether the BBPS, $BAPS_0$, & BAPS models satisfy the established desired properties for a BPS model. We briefly discuss the results below, see Appendix E for a detailed discussion and demonstrations.

Since the BBPS, $BAPS_0$, & BAPS models all adopt the proposed BPS model form as derived in Section 3, DP1 & DP2 are automatically satisfied as the form has a consistent definition for unrealistic routes (which is whether the cost bound is violated) and ensures all functions are defined.

The BBPS model is not internally consistent since route distinctiveness is not considered within the path size contribution factors, while the $BAPS_0$ & BAPS model contribution factors consider choice probability and the models are thus internally consistent. The $BAPS_0$ & BAPS models thus satisfy DP3 while the BBPS model does not.

The BBPS model satisfies DP4 since the BBPS model has a closed-form probability relation guaranteeing solution uniqueness. As discussed in Section 5.1, the $BAPS_0$ model is not in the correct form for standard proofs of solution existence and uniqueness to apply. That is not to say that in all cases solutions are not guaranteed to exist or are not unique, or that it is not the case that solutions do not always exist or there are not always conditions under which solutions are unique. Thus, generally, the $BAPS_0$ model does not satisfy DP4, but this is not necessarily always the case, and is neither proven nor disproven. As proven in Section 10.2, BAPS model solutions are guaranteed to exist and uniqueness conditions can be established, thus satisfying DP4.

The BBPS & $BAPS_0$ model path size contribution weightings tend towards zero as route costs approach the bound from below, and when a route cost reaches the bound exactly, that route receives a zero choice probability / path size contribution. The BBPS & $BAPS_0$ models thus have continuous choice probability functions and hence satisfy DP5. $BAPS_0$ model solutions are not necessarily guaranteed to exist, however, which puts a caveat on whether this is true. The BAPS model does not have a continuous probability function since no route can have a choice probability between 0 and τ, and hence DP5 is not satisfied. The caveat however is that continuity of the BAPS model can be approximated with small values of τ (the perturbation parameter) such that discontinuity is not an issue in practice.

In conclusion, the benefit of the BBPS model is that solutions are guaranteed to exist and be unique and continuity is guaranteed, while the negative is internal inconsistency. The $BAPS_0$ & BAPS models achieve internal consistency, but the drawbacks are that $BAPS_0$ model solutions are not guaranteed to exist or be unique and the BAPS model choice probability function is not continuous, though both of these drawbacks are not issues in practice. Due to its greater theoretical appeal, and since its lack of discontinuity is not an issue in practice, our recommended is that the BAPS model is used were it is computationally feasible to do so. The BBPS model offers a more computationally practical alternative.

Desired Property (DP)	BBPS	$BAPS_0$	BAPS
DP1 – Consistent Definitions of Unrealistic Routes	Yes	Yes	Yes
DP2 – Well-Defined Functions	Yes	Yes	Yes
DP3 – Internal Consistency	No	Yes	Yes
DP4 – Uniqueness	Yes	Neither proven nor disproven	Yes
DP5 – Continuity	Yes	Yes, if solutions exist (neither proven nor disproven)	Yes, in the limit as the 'perturbation parameter' τ tends to zero

Table 4.1. Summary of how the BBPS, $BAPS_0$, & BAPS models satisfy the established desired properties for a BPS model.

Fig. 4.7 displays a schematic diagram of how the models in this paper collapse into one another.

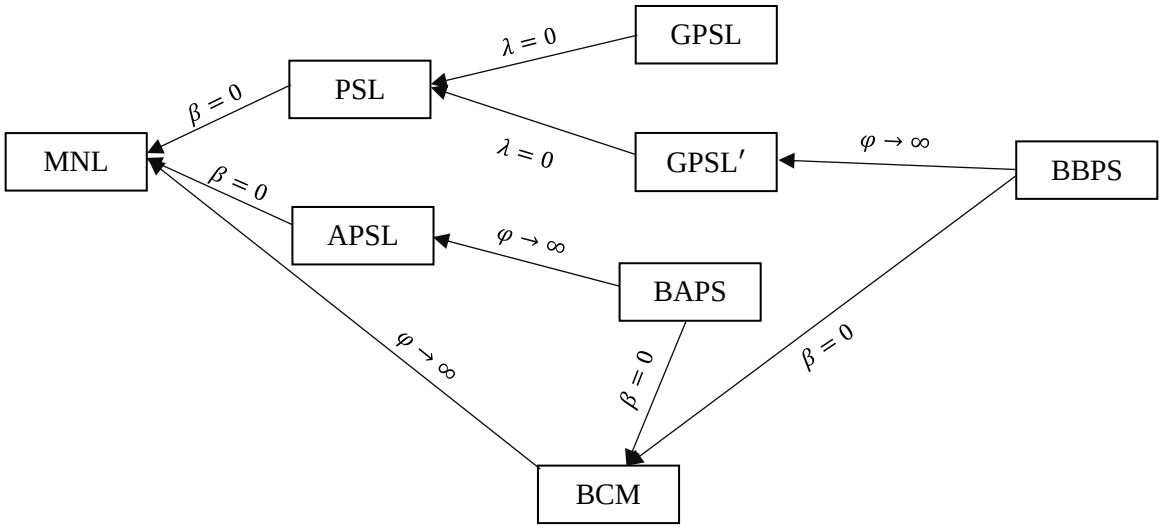

Fig. 4.7. Schematic diagram of how the models collapse into one another.

7. Estimating BPS Models

In this section, we provide a Maximum Likelihood Estimation (MLE) procedure for estimating the BBPS & BAPS models with tracked route observations. This procedure is then investigated in simulation studies, and the possibility of reproducing assumed true parameter estimates is assessed. The BBPS & BAPS models are then estimated on a large-scale network using real route choice observation data tracked with GPS units, and results are compared with MNL, Path Size Logit models, and the BCM. As discussed in the Section 5.2.1, in applications, we propose that the modified BAPS model formulation, defined in (4.12)-(4.14) is used, with the τ parameter set as a very small value.

7.1 Notation and Definitions for Estimation with Multiple OD Movements

7.1.1 Notation

To consider the estimation of the BBPS & BAPS models as well as other models, we extend definitions here for estimation on a network with multiple OD movements, but where the travel costs remain fixed. The road network consists of link set A and $m = 1, \dots, M$ OD movements. R_m is the choice set of all simple routes (no cycles) for OD movement m of size $N_m = |R_m|$, and $A_{m,i} \subseteq A$ is the set of links belonging to route $i \in R_m$, and $\delta_{a,m,i} = \begin{cases} 1 & if\ a \in A_{m,i} \\ 0 & otherwise \end{cases}$. Suppose that the generalised travel cost t_a of each link $a \in A$ is a weighted

sum (by parameter vector $\boldsymbol{\alpha}$) of variables $\boldsymbol{w}_a$, i.e. $t_a(\boldsymbol{w}_a;\boldsymbol{\alpha})$, and that the generalised travel cost for route $i \in R_m$, $c_{m,i}$, can be attained through summing up the total cost of its links so that $c_{m,i}\big(\boldsymbol{t}(\boldsymbol{w};\boldsymbol{\alpha})\big) = \sum_{a\in A_{m,i}} t_a(\boldsymbol{w}_a;\boldsymbol{\alpha})$, where $\boldsymbol{t}$ is the vector of all link travel costs and $\boldsymbol{w}$ is the vector of all link variables. Let the route choice probability for route $i \in R_m$ be $P_{m,i}$, where $\boldsymbol{P}_m = \big(P_{m,1}, P_{m,2}, \dots, P_{m,N_m}\big)$ is the vector of route choice probabilities for OD movement m, and D_m is the domain of possible route choice probability vectors for OD movement m, $m = 1, \dots, M$.

7.1.2 Model Definitions

For multiple OD movement definitions of the MNL, PSL, GPSL, GPSL′, and APSL models for parameter estimation, see Section 5.1.2 in Duncan et al (2020). For the APSL model, the τ_m parameters are also set here as $\tau_m = 10^{-16}$, $m = 1, \dots, M$, and APSL choice probability solutions are computed using the FPIM with initial conditions set as the MNL route choice probabilities, and convergence statistic set at $\xi = 10$ (see Section 3.4 in Duncan et al (2020)).

We provide here multiple OD movement definitions of the BCM, and the BBPS & BAPS models for parameter estimation.

7.1.2.1 Bounded Choice Model

The BCM choice probability relation for route $i \in R_m$:

$$P_{m,i}(\boldsymbol{t}) = \frac{\Big(\exp\Big(-\theta\big(c_{m,i}(\boldsymbol{t}) - \varphi \min\big(c_{m,l}(\boldsymbol{t}): l \in R_m\big)\big)\Big) - 1\Big)_+}{\sum_{j\in R_m}\Big(\exp\Big(-\theta\big(c_{m,j}(\boldsymbol{t}) - \varphi \min\big(c_{m,l}(\boldsymbol{t}): l \in R_m\big)\big)\Big) - 1\Big)_+}. \tag{4.15}$$

7.1.2.2 Bounded Bounded Path Size Model

Let $\bar{R}_m(\boldsymbol{c}_m(\boldsymbol{t});\varphi) \subseteq R_m$ be the restricted choice set (with size $\bar{N}_m$) of all routes $i \in R_m$ where $c_{m,i}(\boldsymbol{t}) < \varphi \min\big(c_{m,l}(\boldsymbol{t}): l \in R_m\big)$ for OD movement m. The BBPS choice probability relation for route $i \in R_m$ is:

$$P_{m,i}(\boldsymbol{t}) = \begin{cases} \dfrac{\big(h_{m,i}\big(-\theta \boldsymbol{c}_m(\boldsymbol{t})\big) - 1\big) \cdot \big(\bar{\gamma}_{m,i}^{BBPS}(\boldsymbol{t})\big)^{\beta}}{\sum_{j\in \bar{R}_m(\boldsymbol{c}_m(\boldsymbol{t});\varphi)}\big(h_{m,j}\big(-\theta \boldsymbol{c}_m(\boldsymbol{t})\big) - 1\big) \cdot \big(\bar{\gamma}_{m,j}^{BBPS}(\boldsymbol{t})\big)^{\beta}} & if\ i \in \bar{R}_m(\boldsymbol{c}_m(\boldsymbol{t});\varphi) \\ 0 & if\ i \notin \bar{R}_m(\boldsymbol{c}_m(\boldsymbol{t});\varphi) \end{cases}, \tag{4.16}$$

where $h_{m,i}\big(-\theta \boldsymbol{c}_m(\boldsymbol{t})\big) = \exp\Big(-\theta\big(c_{m,i}(\boldsymbol{t}) - \varphi \min\big(c_{m,l}(\boldsymbol{t}): l \in R_m\big)\big)\Big)$, and the path size term for route $i \in \bar{R}_m(\boldsymbol{c}_m(\boldsymbol{t});\varphi)$ is:

$$\bar{\gamma}_{m,i}^{BBPS}(\boldsymbol{t}) = \sum_{a\in A_{m,i}} \frac{t_a}{c_{m,i}(\boldsymbol{t})} \frac{\big(h_{m,i}\big(-\lambda \boldsymbol{c}_m(\boldsymbol{t})\big) - 1\big)}{\sum_{k\in \bar{R}_m(\boldsymbol{c}_m(\boldsymbol{t});\varphi)}\big(h_{m,k}\big(-\lambda \boldsymbol{c}_m(\boldsymbol{t})\big) - 1\big)\delta_{a,m,k}}. \tag{4.17}$$

7.1.2.3 Bounded Adaptive Path Size Model

Let $\bar{R}_m(\boldsymbol{c}_m(\boldsymbol{t});\varphi) \subseteq R_m$ be the restricted choice set (with size $\bar{N}_m$) of all routes $i \in R_m$ where $c_{m,i}(\boldsymbol{t}) < \varphi \min\big(c_{m,l}(\boldsymbol{t}): l \in R_m\big)$ for OD movement m. The BAPS model route choice probabilities for OD movement m, $\boldsymbol{P}_m^*(\boldsymbol{t})$, are a solution to the fixed-point problem $\boldsymbol{P}_m = \boldsymbol{F}_m\Big(\boldsymbol{f}_m\big(\boldsymbol{c}_m(\boldsymbol{t}), \bar{\boldsymbol{\gamma}}_m^{BAPS}(\boldsymbol{t}, \boldsymbol{P}_m)\big)\Big)$, given the link cost vector $\boldsymbol{t}$, where $F_{m,i}$ for route $i \in R_m$ is:

$$\begin{aligned} &F_{m,i}\Big(f_{m,i}\big(\boldsymbol{c}_m(\boldsymbol{t}), \bar{\boldsymbol{\gamma}}_m^{BAPS}(\boldsymbol{t}, \boldsymbol{P}_m)\big)\Big) \\ &= \begin{cases} \tau_m + (1 - \bar{N}_m\tau_m) \cdot f_{m,i}\big(\boldsymbol{c}_m(\boldsymbol{t}), \bar{\boldsymbol{\gamma}}_m^{BAPS}(\boldsymbol{t}, \boldsymbol{P}_m)\big) & if\ i \in \bar{R}_m(\boldsymbol{c}_m(\boldsymbol{t});\varphi) \\ 0 & if\ i \notin \bar{R}_m(\boldsymbol{c}_m(\boldsymbol{t});\varphi)' \end{cases} \end{aligned} \tag{4.18}$$

$f_{m,i}$ for route $i \in R_m$ is:

$$f_{m,i}\left(\boldsymbol{c}_m(\boldsymbol{t}), \bar{\boldsymbol{\gamma}}_m^{BAPS}(\boldsymbol{t}, \boldsymbol{P}_m)\right) = \begin{cases} \dfrac{\left(h_{m,i}\left(-\theta \boldsymbol{c}_m(\boldsymbol{t})\right) - 1\right) \cdot \left(\bar{\gamma}_{m,i}^{BAPS}(\boldsymbol{t}, \boldsymbol{P}_m)\right)^{\beta}}{\sum_{j \in \bar{R}_m(\boldsymbol{c}_m(\boldsymbol{t});\varphi)} \left(h_{m,i}\left(-\theta \boldsymbol{c}_m(\boldsymbol{t})\right) - 1\right) \cdot \left(\bar{\gamma}_{m,j}^{BAPS}(\boldsymbol{t}, \boldsymbol{P}_m)\right)^{\beta}} & if\ i \in \bar{R}_m(\boldsymbol{c}_m(\boldsymbol{t});\varphi) \\ 0 & if\ i \notin \bar{R}_m(\boldsymbol{c}_m(\boldsymbol{t});\varphi) \end{cases}, \tag{4.19}$$

where $h_{m,i}\left(-\theta \boldsymbol{c}_m(\boldsymbol{t})\right) = \exp\left(-\theta\left(c_{m,i}(\boldsymbol{t}) - \varphi \min\left(c_{m,l}(\boldsymbol{t}): l \in R_m\right)\right)\right)$, and the path size term for route $i \in \bar{R}_m(\boldsymbol{c}_m(\boldsymbol{t});\varphi)$ is:

$$\bar{\gamma}_{m,i}^{BAPS}(\boldsymbol{t}, \boldsymbol{P}_m) = \sum_{a \in A_{m,i}} \frac{t_a}{c_{m,i}(\boldsymbol{t})} \frac{P_{m,i}}{\sum_{k \in \bar{R}_m(\boldsymbol{c}_m(\boldsymbol{t});\varphi)} P_{m,k} \delta_{a,m,k}}, \qquad \forall \boldsymbol{P}_m \in D_m^{\left(\bar{R}_m(\boldsymbol{c}_m(\boldsymbol{t});\varphi)\right)}, \tag{4.20}$$

$$D_m^{\left(\bar{R}_m(\boldsymbol{c}_m(\boldsymbol{t});\varphi),\tau_m\right)} = \left\{ \boldsymbol{P}_m \in \mathbb{R}_{\geq 0}^{N_m}: \tau_m \leq P_{m,i} \leq (1 - (\bar{N}_m - 1)\tau_m), \forall i \in \bar{R}_m(\boldsymbol{c}_m(\boldsymbol{t});\varphi), and, 0 \leq P_{m,i} \leq (1 - \bar{N}_m \tau_m), \forall i \notin \bar{R}_m(\boldsymbol{c}_m(\boldsymbol{t});\varphi), \sum_{j=1}^{N_m} P_{m,j} = 1 \right\},$$

The model parameters are $\theta > 0$, $\beta \geq 0$, $\varphi > 1$, and $0 < \tau_m \leq \frac{1}{\bar{N}_m}$, $m = 1, \dots, M$. Each OD movement has its own range restrictions for τ_m based on the number of routes in the active choice set, but the τ_m parameters are not model parameters that require estimating, and we set $\tau_m = 10^{-16}$, $m = 1, \dots, M$. BAPS model choice probability solutions are computed using the FPIM with initial conditions set as the BCM route choice probabilities, and convergence statistic set at $\xi = 10$ (see Section 5.2.2), unless stated otherwise.

7.2 Likelihood Formulations, Existence/Uniqueness, & Estimation Procedure

7.2.1 Likelihood Formulations

Suppose that we have available a set of Z observed routes, e.g. collected through GPS units or smart phones, and consider a situation where it is not needed to distinguish individuals in their preferences (the approach is, of course, readily generalised to permit multiple user classes differing in their parameters). Let m_z denote the OD movement of route observation z, and for each trip observation $z = 1,2, \dots, Z$, let R_{m_z} be the choice set of all simple routes between the origin and destination of the trip. Suppose that the observation data is contained in a vector $\boldsymbol{x}$ of size Z where:

$$x_z = i \quad \text{if alternative } i \in R_{m_z} \text{ is chosen,} \qquad z = 1, \dots, Z.$$

The BBPS model Likelihood, L_{BBPS}, for a sample of size Z is:

$$L_{BBPS}(\boldsymbol{\alpha}, \theta, \beta, \varphi, \lambda | \boldsymbol{x}) = \prod_{z=1}^{Z} P_{m_z,x_z}(\boldsymbol{t}(\boldsymbol{w};\boldsymbol{\alpha}); \theta, \beta, \varphi, \lambda), \tag{4.21}$$

where $P_{m_z,x_z}(\boldsymbol{t})$ is the BBPS model choice probability function given by (4.16) for route $x_z \in R_{m_z}$.

The BAPS model Likelihood, L_{BAPS}, for a sample of size Z is:

$$L_{BAPS}(\boldsymbol{\alpha}, \theta, \beta, \varphi | \boldsymbol{x}) = \prod_{z=1}^{Z} P_{m_z,x_z}^{*}(\boldsymbol{t}(\boldsymbol{w};\boldsymbol{\alpha}); \theta, \beta, \varphi), \tag{4.22}$$

where $P_{m_z,x_z}^{*}(\boldsymbol{t})$ is the BAPS model choice probability solution for route $x_z \in R_{m_z}$ to the fixed-point problem $\boldsymbol{P}_{m_z} = \boldsymbol{F}_{m_z}\left(\boldsymbol{f}_{m_z}\left(\boldsymbol{c}_{m_z}(\boldsymbol{t}), \bar{\boldsymbol{\gamma}}_{m_z}^{BAPS}(\boldsymbol{t}, \boldsymbol{P}_{m_z})\right)\right)$ for OD movement m_z, given the link cost vector $\boldsymbol{t}$, where $F_{m,i}$ and $f_{m,i}$ are as in (4.18) and (4.19), respectively, for route $i \in R_m$, and $\bar{\gamma}_{m,i}^{BAPS}$ is as in (4.20) for route $i \in \bar{R}_m(\boldsymbol{c}_m(\boldsymbol{t});\varphi)$.

If for a given setting of the travel cost and bound parameters $\tilde{\boldsymbol{\alpha}}$ and $\tilde{\varphi}$, there is an observation z such that $c_{m_z,x_z}\left(\boldsymbol{t}(\boldsymbol{w};\tilde{\boldsymbol{\alpha}})\right) \geq \tilde{\varphi}\min\left(c_{m_z,l}\left(\boldsymbol{t}(\boldsymbol{w};\tilde{\boldsymbol{\alpha}})\right): l \in R_{m_z}\right)$, the BBPS & BAPS model Likelihood values are zero. This means that the maximum likelihood estimates $\left(\hat{\boldsymbol{\alpha}},\hat{\theta},\hat{\beta},\hat{\varphi},\hat{\lambda}\right)$ for the BBPS model and $\left(\hat{\boldsymbol{\alpha}},\hat{\theta},\hat{\beta},\hat{\varphi}\right)$ for the BAPS model will always be such that $c_{m_z,x_z}\left(\boldsymbol{t}(\boldsymbol{w};\hat{\boldsymbol{\alpha}})\right) < \hat{\varphi}\min\left(c_{m_z,l}\left(\boldsymbol{t}(\boldsymbol{w};\hat{\boldsymbol{\alpha}})\right): l \in R_{m_z}\right)$ for $z = 1,\dots,Z$.

The BBPS model Log-Likelihood function, LL_{BBPS}, to be maximised is:

$$L_{BBPS}(\boldsymbol{\alpha},\theta,\beta,\varphi,\lambda|\boldsymbol{x}) = \ln\left(\prod_{z=1}^{Z} P_{m_z,x_z}(\boldsymbol{t}(\boldsymbol{w};\boldsymbol{\alpha});\theta,\beta,\varphi,\lambda)\right) = \sum_{z=1}^{Z}\ln\left(P_{m_z,x_z}(\boldsymbol{t}(\boldsymbol{w};\boldsymbol{\alpha});\theta,\beta,\varphi,\lambda)\right), \quad (4.23)$$

$$subject\ to \quad c_{m_z,x_z}\left(\boldsymbol{t}(\boldsymbol{w};\boldsymbol{\alpha})\right) < \varphi\min\left(c_{m_z,l}\left(\boldsymbol{t}(\boldsymbol{w};\boldsymbol{\alpha})\right): l \in R_{m_z}\right), \qquad z = 1,\dots,Z,$$

where $P_{m_z,x_z}(\boldsymbol{t})$ is the BBPS model choice probability relation in (4.16) for route $x_z \in R_{m_z}$.

The BAPS model Log-Likelihood function, LL_{BAPS}, to be maximised is:

$$LL_{BAPS}(\boldsymbol{\alpha},\theta,\beta,\varphi|\boldsymbol{x}) = \ln\left(\prod_{z=1}^{Z} P^{*}_{m_z,x_z}(\boldsymbol{t}(\boldsymbol{w};\boldsymbol{\alpha});\theta,\beta,\varphi)\right) = \sum_{z=1}^{Z}\ln\left(P^{*}_{m_z,x_z}(\boldsymbol{t}(\boldsymbol{w};\boldsymbol{\alpha});\theta,\beta,\varphi)\right), \quad (4.24)$$

$$subject\ to \quad c_{m_z,x_z}\left(\boldsymbol{t}(\boldsymbol{w};\boldsymbol{\alpha})\right) < \varphi\min\left(c_{m_z,l}\left(\boldsymbol{t}(\boldsymbol{w};\boldsymbol{\alpha})\right): l \in R_{m_z}\right), \qquad z = 1,\dots,Z,$$

where $P^{*}_{m_z,x_z}(\boldsymbol{t})$ is the BAPS model choice probability solution for route $x_z \in R_{m_z}$ to the fixed-point problem $\boldsymbol{P}_{m_z} = \boldsymbol{F}_{m_z}\left(\boldsymbol{f}_{m_z}\left(\boldsymbol{c}_{m_z}(\boldsymbol{t}),\bar{\boldsymbol{\gamma}}^{BAPS}_{m_z}(\boldsymbol{t},\boldsymbol{P}_{m_z})\right)\right)$ for OD movement m_z, given the link cost vector $\boldsymbol{t}$.

7.2.2 Existence & Uniqueness of Solutions

The typical sufficient conditions for the *existence* of Maximum Likelihood Estimation (MLE) solutions are that: a) the parameter space is compact (closed and bounded), and b) the Likelihood function is a continuous function.

Consider first the BBPS model. Since the BBPS probability function in (4.16)-(4.17) is a continuous closed-form function, the BBPS Likelihood function in (4.21) is in turn also continuous. The range restrictions for the model parameters are $\theta > 0$, $\beta \geq 0$, $\varphi > 1$, $\lambda > 0$, and the travel cost parameters $\boldsymbol{\alpha}$ may have e.g. positive, negative, or no restrictions. Define Ω_{BBPS} as the parameter space obtained from these range restrictions. Ω_{BBPS} is not a compact set and thus for this general parameter space the typical sufficient conditions do not apply. This is the same for estimating MNL, PSL, etc. In practice however it is commonplace to enforce some sensible bounds upon the parameter ranges. Define then $\Omega'_{BBPS} \subseteq \Omega_{BBPS}$ as a closed-bounded parameter subspace of Ω_{BBPS}. For any Ω'_{BBPS}, since the BBPS Likelihood function is continuous, the typical sufficient conditions can be applied, and solutions are guaranteed to exist.

The BBPS Likelihood function in (4.21) can be rewritten as follows:

$$L_{BBPS}(\boldsymbol{\alpha},\theta,\beta,\varphi,\lambda|\boldsymbol{x}) = \prod_{z=1}^{Z}\begin{cases} 0 & if\ c_{m_z,x_z}\left(\boldsymbol{t}(\boldsymbol{w};\boldsymbol{\alpha})\right) \geq \varphi\min\left(c_{m_z,l}\left(\boldsymbol{t}(\boldsymbol{w};\boldsymbol{\alpha})\right): l \in R_{m_z}\right)\ for\ any\ z \\ P_{m_z,x_z}(\boldsymbol{t}(\boldsymbol{w};\boldsymbol{\alpha});\theta,\beta,\varphi,\lambda) & otherwise \end{cases}. \quad (4.25)$$

For a closed-bounded parameter space $\Omega'_{BBPS} \subseteq \Omega_{BBPS}$, there are three scenarios:

i) For *all* $\left(\tilde{\boldsymbol{\alpha}},\tilde{\theta},\tilde{\beta},\tilde{\varphi},\tilde{\lambda}\right) \in \Omega'_{BBPS}$ the observed routes have travel costs greater than the bound and the Likelihood L_{BBPS} is zero.

ii) For *some* $\left(\tilde{\boldsymbol{\alpha}},\tilde{\theta},\tilde{\beta},\tilde{\varphi},\tilde{\lambda}\right) \in \Omega'_{BBPS}$ the observed routes have travel costs greater than the bound and the Likelihood L_{BBPS} is zero.

iii) For *no* $\left(\tilde{\boldsymbol{\alpha}},\tilde{\theta},\tilde{\beta},\tilde{\varphi},\tilde{\lambda}\right) \in \Omega'_{BBPS}$ the observed routes have travel costs greater than the bound and the Likelihood L_{BBPS} is zero.

Obviously, parameter spaces resulting in i) are not suitable; however, i) occurs only when the upper limit for the bound parameter $\tilde{\varphi}$ is set too low. For any closed-bounded range for the travel cost parameters $\tilde{\boldsymbol{\alpha}}$, upper limits for $\tilde{\varphi}$ will exist such that Ω'_{BBPS} is either ii) or iii) (since it is always possible to expand the bound φ to include at least one observed route). Suppose then that the upper limit for $\tilde{\varphi}$ is set suitably high to avoid i), and we now have case ii). Define $\overline{\Omega}'_{BBPS}$ as the parameter subspace of Ω'_{BBPS} where no observed routes have travel costs greater than the bound. Since if a MLE solution is to exist, it will exist within the parameter subspace $\overline{\Omega}'_{BBPS}$, and solutions are guaranteed to exist, solutions are guaranteed to exist in $\overline{\Omega}'_{BBPS}$. For case iii), $\overline{\Omega}'_{BBPS} = \Omega'_{BBPS}$ and MLE solutions will exist and can exist in the whole closed-bounded parameter subspace.

For the BAPS model, the BAPS probability function in (4.18)-(4.20) is not technically continuous, and thus the BAPS Likelihood function in (4.22) is not continuous. Existence of MLE solutions thus cannot be guaranteed for the BAPS model. Nevertheless, as discussed in Sections 5.2&6, continuity of the BAPS probability function is not an issue in practice, since continuity can be approximated to arbitrary precision with the τ parameter. It is therefore believed that the BAPS Log-Likelihood function can also be continuous in practice, and indeed this appeared to be the case in our numerical experiments. When MLE solutions exist, they will exist in $\overline{\Omega}'_{BAPS}$ if case ii) above or in $\overline{\Omega}'_{BAPS} = \Omega'_{BAPS}$ if case iii) above.

The typical sufficient conditions for the uniqueness of MLE solutions are that, given an MLE solution exists: a) the parameter space is convex, and b) the Likelihood function is a concave function. The issue here for the BPS models, is that the probability functions are not guaranteed to be monotonic functions, and thus the Likelihood function is not guaranteed to be concave. This is not to say however that MLE solutions for the BPS models cannot be unique, since these are only sufficient conditions, and no issues with uniqueness were experienced in the experiments in this paper.

7.2.3 Estimation Procedure

Standard MLE procedures can be used to estimate the parameters of the BBPS & BAPS models for a given network. Using a standard iterative estimation procedure, BBPS & BAPS model parameters can be found that maximise the Log-Likelihood functions as formulated in (4.23) and (4.24) above for a given set of data. Duncan et al (2020) outline algorithm pseudo-code for a tracked route observation data estimation procedure for the APSL model. Using a similar approach, Algorithm 4.1 below outlines pseudo-code for the BBPS & BAPS model estimation procedure.

Maximising Log-Likelihood for the BPS models is complicated by the constraints that require all chosen routes to have costs less than the cost bound, otherwise the Log-Likelihood functions are undefined. It is possible to pre-determine the parameter space $\overline{\Omega}'$ for MLE (where there Log-Likelihood will always be defined), by identifying (for a given closed-bounded range for the cost parameters) the lower limit for the bound parameter φ before it is possible for any chosen route to violate the cost bound. Or, one can incorporate corresponding constraints for the optimisation algorithm, like those in (4.23) and (4.24) but adjusted to include equivalence. However, since identifying the existence parameter space / incorporating the corresponding constraints is not always straightforward, we detail in Algorithm 4.1 and adopt in our experiments an easier to implement approach.

Step 1: Initialisation. For each route observation $z = 1, \dots, Z$, generate the corresponding universal choice set and store the link attributes and link-route information. Define an initial set of parameter values $\left(\tilde{\boldsymbol{\alpha}}^{(1)}, \tilde{\theta}^{(1)}, \tilde{\beta}^{(1)}, \tilde{\varphi}^{(1)}, \tilde{\lambda}^{(1)}\right)$ for the BBPS model or $\left(\tilde{\boldsymbol{\alpha}}^{(1)}, \tilde{\theta}^{(1)}, \tilde{\beta}^{(1)}, \tilde{\varphi}^{(1)}\right)$ for the BAPS model for MLE, and set $n = 1$.

Step 2: Bound violation check. Given the travel cost parameters $\tilde{\boldsymbol{\alpha}}^{(n)}$ for iteration n, calculate the link costs $\boldsymbol{t}\left(\boldsymbol{w}; \tilde{\boldsymbol{\alpha}}^{(n)}\right)$ and consequently the route costs $\boldsymbol{c}_{m_z}\left(\boldsymbol{t}\left(\boldsymbol{w}; \tilde{\boldsymbol{\alpha}}^{(n)}\right)\right)$, $z = 1, \dots, Z$, for iteration n. Given the route costs, and the bound parameter value $\tilde{\varphi}^{(n)}$ for iteration n, check whether $c_{m_z,x_z}\left(\boldsymbol{t}\left(\boldsymbol{w}; \tilde{\boldsymbol{\alpha}}^{(n)}\right)\right) \geq \tilde{\varphi}^{(n)} \min\left(c_{m_z,l}\left(\boldsymbol{t}\left(\boldsymbol{w}; \tilde{\boldsymbol{\alpha}}^{(n)}\right)\right) : l \in R_{m_z}\right)$ for any z. If so, set the Log-Likelihood value $LL^{(n)}_{BBPS}$ or $LL^{(n)}_{BAPS}$ for iteration n as an appropriate large and negative value (since $\ln(0)$ is undefined), and skip to Step 4. Otherwise, continue to Step 3.

Step 3: Recalculate choice probabilities and LL.

BBPS Model: Given the set of parameter values $\left(\tilde{\boldsymbol{\alpha}}^{(n)}, \tilde{\theta}^{(n)}, \tilde{\beta}^{(n)}, \tilde{\varphi}^{(n)}, \tilde{\lambda}^{(n)}\right)$ and the link and route costs for iteration n, compute the BBPS model choice probabilities P_{m_z,x_z} according to (4.16) and (4.17) above for $z = 1, \dots, Z$. Given these probabilities, calculate the BBPS model Log-Likelihood $LL_{BBPS}^{(n)}\left(\tilde{\boldsymbol{\alpha}}^{(n)}, \tilde{\theta}^{(n)}, \tilde{\beta}^{(n)}, \tilde{\varphi}^{(n)}, \tilde{\lambda}^{(1)} \middle| \boldsymbol{x}\right)$ for iteration n.

BAPS Model: Given the set of parameter values $\left(\tilde{\boldsymbol{\alpha}}^{(n)}, \tilde{\theta}^{(n)}, \tilde{\beta}^{(n)}, \tilde{\varphi}^{(n)}\right)$ and the link and route costs for iteration n, solve each of the fixed-point problems

$$\boldsymbol{P}_{m_z} = \boldsymbol{f}_{m_z}\left(\boldsymbol{c}_{m_z}\left(\boldsymbol{t}\left(\boldsymbol{w}; \tilde{\boldsymbol{\alpha}}^{(n)}\right)\right), \overline{\boldsymbol{\gamma}}_{m_z}^{BAPS}\left(\boldsymbol{t}\left(\boldsymbol{w}; \tilde{\boldsymbol{\alpha}}^{(n)}\right), \boldsymbol{P}_{m_z}\right); \tilde{\theta}^{(n)}, \tilde{\beta}^{(n)}, \tilde{\varphi}^{(n)}\right)$$

for $z = 1, \dots, Z$. Given the fixed-point choice probability solutions P_{m_z,x_z}^{*} for each of the route observations $z = 1, \dots, Z$, calculate the BAPS model Log-Likelihood $LL_{BAPS}^{(n)}\left(\tilde{\boldsymbol{\alpha}}^{(n)}, \tilde{\theta}^{(n)}, \tilde{\beta}^{(n)}, \tilde{\varphi}^{(n)} \middle| \boldsymbol{x}\right)$ for iteration n.

Step 4: Compute new set of parameters.

BBPS Model: Based on $LL_{BBPS}^{(s)}$ and the associated parameters $\left(\tilde{\boldsymbol{\alpha}}^{(s)}, \tilde{\theta}^{(s)}, \tilde{\beta}^{(s)}, \tilde{\varphi}^{(s)}, \tilde{\lambda}^{(s)}\right)$ for all $s \leq n$, compute a new set of parameters $\left(\tilde{\boldsymbol{\alpha}}^{(n+1)}, \tilde{\theta}^{(n+1)}, \tilde{\beta}^{(n+1)}, \tilde{\varphi}^{(n+1)}, \tilde{\lambda}^{(n+1)}\right)$ to test in the following iteration.

BAPS Model: Based on $LL_{BAPS}^{(s)}$ and the associated parameters $\left(\tilde{\boldsymbol{\alpha}}^{(s)}, \tilde{\theta}^{(s)}, \tilde{\beta}^{(s)}, \tilde{\varphi}^{(s)}\right)$ for all $s \leq n$, compute a new set of parameters $\left(\tilde{\boldsymbol{\alpha}}^{(n+1)}, \tilde{\theta}^{(n+1)}, \tilde{\beta}^{(n+1)}, \tilde{\varphi}^{(n+1)}\right)$ to test in the following iteration.

Step 5: Stopping criteria. If $\left|LL_{BBPS}^{(n)} - LL_{BBPS}^{(n-1)}\right| < \zeta$ or $\left|LL_{BAPS}^{(n)} - LL_{BAPS}^{(n-1)}\right| < \zeta$ stop. Otherwise, set $n = n + 1$ and return to Step 2.

Algorithm 4.1: Pseudo-code for estimating the BBPS and BAPS models.

As discussed in Section 7.2.2 above, for a closed-bounded parameter space Ω' where for some settings of the parameters the Likelihood is zero, the MLE solution will always lie in the parameter subspace $\overline{\Omega}'$ where no observed routes have travel costs greater than the bound and the Likelihood is non-zero. Thus, the idea for Algorithm 4.1 is simply to tell the algorithm to search for solutions within $\overline{\Omega}'$ only, by setting nonoptimal values for the objective function when testing parameters not in $\overline{\Omega}'$.

To do this, in Algorithm 4.1 we include a bound violation check in Step 2. In this step, given the route travel costs from the current cost parameters $\tilde{\boldsymbol{\alpha}}^{(n)}$ and the current bound parameter $\tilde{\varphi}^{(n)}$, a check is performed to see whether any chosen route currently violates the cost bound. If any chosen route does violate the bound, then an appropriate large and negative value is set for the Log-Likelihood value. For the experiments in this paper, supposing that Z' is the set of observations that violate the bound, we set the appropriate large and negative value as

$$LL = \sum_{z=1}^{Z} \begin{cases} -999 & if\ z \in Z' \\ \ln\left(P_{m_z,x_z}^{BCM}\right) & otherwise' \end{cases}$$

where P_{m_z,x_z}^{BCM} is the BCM choice probability for route $x_z \in R_{m_z}$ given the current $\tilde{\boldsymbol{\alpha}}^{(n)}$ and $\tilde{\varphi}^{(n)}$ parameter values. Setting the appropriate large and negative value in this way, rather than as some constant arbitrary number, means that some information can be gathered on the relevance of the parameters even when bound violating parameters are tested. For more accurate information, the BBPS or BAPS probabilities can be used instead of the BCM probabilities. We use the BCM probabilities however to avoid having to compute BAPS model fixed-point probabilities for non-relevant parameter tests, thereby reducing computation times.

In general, Step 4 could apply procedures from standard numerical optimisation methods to identify the parameters to evaluate in the next iteration. For cases where there is a single variable in the generalised link travel cost function (for example in the Sioux Falls simulation experiments in Section 7.3.2 below), it is possible to adopt gradient approaches such as Newton-Raphson or BHHH. In this case, the singular cost parameter can be factored out from the cost functions, so that the minimum cost route is fixed (e.g. the route with the quickest free-flow travel time). The min operator component within the bounded model probability functions (see e.g. equations (4.15), (4.16), and (4.19)) can thus be treated as a constant and is independent from any parameters. Therefore, in this case, in the parameter space $\overline{\Omega}'$, the Log-Likelihood objective function

is continuously differentiable with respect to the parameters, and gradient minimisation algorithms can be adopted.

For cases where there are multiple variables in the generalised link travel cost function (for example in the real-life case study in Section 7.4 below), however, it is not guaranteed that gradient minimisation algorithms can be directly adopted, since in this case, the minimum cost routes are not guaranteed to be fixed for every OD movement. If for all values of the cost parameters in the stipulated cost parameter space and for all OD movements the minimum cost routes are always the same routes, then the Log-Likelihood objective function is continuously differentiable in the parameter space $\overline{\Omega}'$. It is possible that one could potentially stipulate a cost parameter space to ensure as such. Alternatively, one could smooth out the min operator, at the kinks or by adopting a logsum operator to approximate the min function.

For the BAPS model, however, regardless of whether or not the Log-Likelihood function is continuously differentiable, utilising gradient approaches is complicated by the difficulties in differentiating the BAPS model Log-Likelihood function, which involves differentiating the fixed-point choice probabilities with respect to the parameters, which is not straightforward. Other optimisation algorithms such as BFGS and alternative quasi-Newton algorithms use finite difference to approximate the differentials, and while are more computationally burdensome and typically less accurate, are readily useable. Thus, for the experiments in this paper, we estimate the BBPS and BAPS models utilising the L-BFGS-B bound-constraint, quasi-Newton minimisation algorithm (Byrd et al, 1995) for Steps 2-4 of Algorithm 4.1 (where we minimise $-LL$). The L-BFGS-B algorithm was implemented using the scipy.optimize.minimize package in Python. The parameter bounds and initial conditions are given in each study.

In Fig. 4.12 and Fig. 4.23, we demonstrate how the adopted L-BFGS-B algorithm converges to the parameter estimates for the BAPS model, given the initial conditions. Other initial conditions were tested to see whether different solutions would be found but the solution was the same. Although it is not necessarily a requirement, our recommendation is that initial conditions are set such that none of the chosen route cost bounds are violated, i.e. $\left(\tilde{\boldsymbol{\alpha}}^{(1)}, \tilde{\theta}^{(1)}, \tilde{\beta}^{(1)}, \tilde{\varphi}^{(1)}, \tilde{\lambda}^{(1)}\right) \in \overline{\Omega}'_{BBPS}$ or $\left(\tilde{\boldsymbol{\alpha}}^{(1)}, \tilde{\theta}^{(1)}, \tilde{\beta}^{(1)}, \tilde{\varphi}^{(1)}\right) \in \overline{\Omega}'_{BAPS}$. This can be done simply by setting an intuitively large bound value, or by calculating $B\left(\tilde{\boldsymbol{\alpha}}^{(1)}\right) = \max\left(\frac{c_{m_z,x_z}\left(\boldsymbol{t}\left(\boldsymbol{w};\tilde{\boldsymbol{\alpha}}^{(1)}\right)\right)}{\min\left(c_{m_z,l}\left(\boldsymbol{t}\left(\boldsymbol{w};\tilde{\boldsymbol{\alpha}}^{(1)}\right)\right): l \in R_{m_z}\right)} : z = 1, \dots, Z\right)$ (the lower limit for φ before any chosen route violates the bound) given the initial conditions for the cost parameters $\tilde{\boldsymbol{\alpha}}^{(1)}$, and choosing a larger value than $B\left(\tilde{\boldsymbol{\alpha}}^{(1)}\right)$.

Note that Algorithm 4.1 computes one set of parameter estimates, estimated from one set of observations. It is not possible to calculate standard errors for the estimates analytically for the BBPS or BAPS model. This is because the models violate the regularity conditions that establish asymptotic standard errors of the Maximum Likelihood Estimates as the inverse of the Fisher information. Instead, the robustness of the parameters estimated (variation of the estimates) can be investigated numerically by applying Algorithm 4.1 multiple times through resampling-approaches such as Bootstrap or Jackknife.

7.3 Simulation Studies

In this section we investigate the formulated Likelihood functions for the BBPS & BAPS models in simulation studies, evaluating the Likelihood-surfaces and assessing the possibility of estimating reasonable parameters that reproduces observed behaviour.

7.3.1 Experiment Setup

A similar approach is adopted to that utilised for the APSL model in Duncan et al (2020). In general, the approach is to sample observations according to an assumed 'true' model, and then use these in combination with the Log-Likelihood function to evaluate the ability to reproduce the assumed 'true' parameters. The simulation study consists of three steps:

(iv) Postulate a true BBPS / BAPS model including specification and parameter values. For each relevant OD movement, identify a corresponding choice set of routes to be used for estimation.

(v) Sample a set of observed route choices according to the true model using the specified link travel costs.

(vi) Apply MLE approach to obtain parameter estimates based on the observed route choices.

Step (ii) mimics estimating the models with tracked route observation data (e.g. GPS traces). The estimation procedure in principle needs to enumerate and store the universal choice sets in order to allow for evaluating the Log-likelihood for very large values of the bound φ (e.g. in cases when the BBPS model approaches GPSL′ or the BAPS model approaches APSL). For larger networks this is not feasible and a subset consisting of routes with costs below some value being considerably larger than the bounding cost of the true model can be used.

The generic estimation procedure in Algorithm 4.1 is altered for simulation studies, by modifying **Step 1: Initialisation** as outlined in Algorithm 4.1 (Step 1) below to reflect (i) and (ii) in the above.

Step 1: Initialisation.

1.1 Postulate a true set of parameters $(\boldsymbol{\alpha}^{true}, \theta_{true}, \beta_{true}, \varphi_{true}, \lambda_{true})$ for the BBPS model or $(\boldsymbol{\alpha}^{true}, \theta_{true}, \beta_{true}, \varphi_{true})$ for the BAPS model, and given these parameters generate/approximate the universal choice sets for OD movements $m = 1, \dots, M$, and store the link attributes and link-route information.

1.2.
BBPS model: Given the assumed true parameters and the generated choice sets, compute the BBPS model choice probabilities $\boldsymbol{P}_m$ for $m = 1, \dots, M$.
BAPS model: Given the assumed true parameters and the generated choice sets, solve each of the fixed-point problems

$$\boldsymbol{P}_m = \boldsymbol{F}_m\left(\boldsymbol{f}_m\left(\boldsymbol{c}_m\left(\boldsymbol{t}(\boldsymbol{w};\boldsymbol{\alpha}^{true})\right), \overline{\boldsymbol{\gamma}}_m^{BAPS}(\boldsymbol{t}(\boldsymbol{w};\boldsymbol{\alpha}^{true}), \boldsymbol{P}_m); \theta_{true}, \beta_{true}, \varphi_{true}\right)\right)$$

for $m = 1, \dots, M$.

1.3. Based on the BBPS model probabilities $\boldsymbol{P}_m$ or the BAPS model fixed-point choice probability solutions $\boldsymbol{P}_m^*$ for $m = 1, \dots, M$ (obtained in 1.2), sample Z observed routes.

1.4. Define an initial set of parameter values $\left(\tilde{\boldsymbol{\alpha}}^{(1)}, \tilde{\theta}^{(1)}, \tilde{\beta}^{(1)}, \tilde{\varphi}^{(1)}, \tilde{\lambda}^{(1)}\right)$ for the BBPS model or $\left(\tilde{\boldsymbol{\alpha}}^{(1)}, \tilde{\theta}^{(1)}, \tilde{\beta}^{(1)}, \tilde{\varphi}^{(1)}\right)$ for the BAPS model for MLE, and set $n = 1$.

Algorithm 4.1 (Step 1): pseudo-code for initialisation of simulation experiments.

The number of observed routes to sample, Z, is exogenously defined. The robustness of the estimated parameters estimated can be investigated numerically by applying Algorithm 4.1 multiple times and then analysing the variation of the estimated parameters.

7.3.2 Sioux Falls Application

The Sioux Falls network consists of 76 links, 528 OD movements with non-zero travel demands, and 1,632,820 total routes. Details of the network were obtained from https://github.com/bstabler/TransportationNetworks. The travel cost of link a is specified as the free-flow travel time $w_{a,1}$ only, such that:

$$t_a(\boldsymbol{w}_a;\boldsymbol{\alpha}) = w_{a,1} \cdot \alpha_1,$$

where $\alpha_1 > 0$ is the free-flow travel time parameter, and thus the travel cost for route $i \in R_m$ is:

$$c_{m,i}\left(\boldsymbol{t}(\boldsymbol{w};\boldsymbol{\alpha})\right) = \sum_{a \in A_{m,i}} t_a(\boldsymbol{w}_a;\boldsymbol{\alpha}) = \alpha_1 \sum_{a \in A_{m,i}} w_{a,1}.$$

The model requires the specification of four parameters: α_1, θ, β, and φ but to ensure identification θ is fixed at $\theta = 1$ throughout.

Since the travel costs of the links (and thus routes) correspond to a single variable, to approximate the universal choice sets, we generate all routes with a free-flow travel time less than 2.5 times greater than the free-flow travel time on the quickest route for each OD movement (since the assumed true bound parameters are much less than 2.5). We also remove all OD movements where there are less than 5 routes. The result is

that there are 370 remaining OD movements and a total of 42,976 routes, where the minimum, maximum, and average choice set sizes are 5, 898, and 116, respectively.

7.3.2.1 BBPS Model Experiment Results

We present results here from simulation studies estimating the $BBPS_{(\lambda=\theta)}$ model, and then investigate how estimating the λ parameter effects simulation results.

The $BBPS_{(\lambda=\theta)}$ model Log-Likelihood function in (4.23) depends on three parameters α_1, β, and φ, which can be visualised through three 3-dimensional projections of this 4-dimensional relationship. Fig. 4.8A-C display the $BBPS_{(\lambda=\theta)}$ model Log-Likelihood surface for a single estimation experiment, with $\alpha_1^{true} = 0.2$, $\beta_{true} = 1$, $\varphi_{true} = 1.5$ and $Z = 2000$. As Fig. 4.8A-C show, the Log-Likelihood surface is smooth and maximal around the true parameters, where the estimated parameters are $\hat{\alpha}_1 = 0.208 \pm 0.008$, $\hat{\beta} = 1.04 \pm 0.04$, and, $\hat{\varphi} = 1.5 \pm 0.002$.

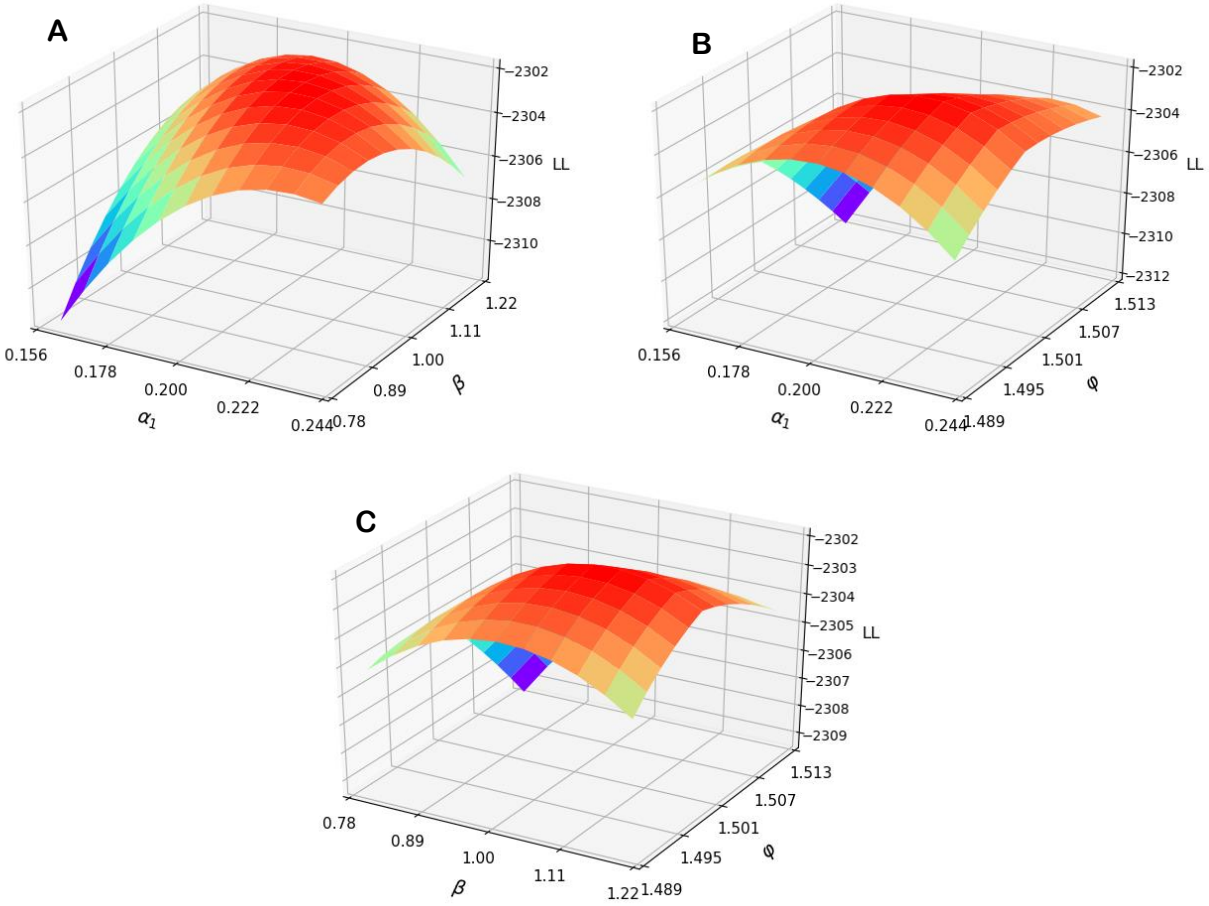

Fig. 4.8. Sioux Falls simulation study: $BBPS_{(\lambda=\theta)}$ Log-Likelihood surface ($\alpha_1^{true} = 0.2$, $\beta_{true} = 1$, $\varphi_{true} = 1.5$, $\hat{\alpha}_1 = 0.208$, $\hat{\beta} = 1.04$, $\hat{\varphi} = 1.5$). **A:** LL vs (α_1, β). **B:** LL vs (α_1, φ). **C:** LL vs (β, φ).

Next, we investigate the stability of the estimated parameters for the $BBPS_{(\lambda=\theta)}$ model over multiple experiment replications. Each experiment utilises a Log-Likelihood maximisation algorithm (see Section 7.2.2) to obtain the parameter estimates with initial conditions $\left(\tilde{\alpha}_1^{(0)}, \tilde{\beta}^{(0)}, \tilde{\varphi}^{(0)}\right) = (0.15,0,1.1)$, and bounds $\tilde{\alpha}_1 \in [0,1]$, $\tilde{\beta} \in [0,2]$, $\tilde{\varphi} \in [1.01,2.5]$.

Table 4.2 reports, for various settings of the true parameters, the mean Bias, Standard Error, and Route Mean Squared Error $\left(RMSE = \sqrt{(Bias)^2 + (S.E)^2}\right)$, of the estimates across $r = 25$ experiment replications with $Z = 1500$ simulated observations. Table 4.3 displays the estimated covariances between the α_1, β, and φ parameters. As shown, the mean bias of the estimates of α_1, β, and φ are small for all settings of the true

parameters tested, with max absolute percentage biases of 7% ($\frac{0.014}{0.2} \times 100\%$), 6.4%, & 0.5%, respectively. There is thus no evidence of bias in the parameter estimates – the estimates are all close to the true values. However, as measured by the RMSE, the precision of estimating α_1 and β decrease as α_1^{true} and β_{true} decrease. This seems reasonable as increasing α_1 corresponds to lower perception error of travel cost and decreasing β corresponds to lower perception of distinctiveness. Moreover, a lower perception error of travel cost also results in less precise estimations of the bound parameter φ since fewer simulated observations are close to the bound. The RMSEs of the estimated bound parameters $\hat{\varphi}$ suggest though that the bound, at least for these settings of φ_{true}, can be estimated to a reasonably high level of precision.

Table 4.3 indicates that, with this network and the generated choice sets, there appears to be some negative correlation between the $\hat{\alpha}_1$ and $\hat{\beta}$ estimates since both scale negative utility components. There also appears to be some positive correlation between the $\hat{\alpha}_1$ and $\hat{\varphi}$ estimates, which is logical since both these parameters scale travel cost, where an increase in α_1 or a decrease in φ gives more probability to lower costing routes.

α_1^{true}	β_{true}	φ_{true}	$\hat{\alpha}_1$			$\hat{\beta}$			$\hat{\varphi}$		
			Bias	S.E	RMSE	Bias	S.E	RMSE	Bias	S.E	RMSE
0.2	0.8	1.5	-0.008	0.031	0.0320	-0.029	0.146	0.1489	-0.003	0.0061	0.0068
0.2	1	1.4	0.002	0.027	0.0271	-0.024	0.162	0.1638	-0.004	0.0078	0.0088
0.2	1	1.5	-0.014	0.023	0.0269	0.012	0.147	0.1475	-0.008	0.0075	0.0110
0.2	1	1.6	-0.001	0.017	0.0170	0.064	0.132	0.1467	-0.001	0.0091	0.0092
0.1	1	1.5	-0.007	0.028	0.0289	-0.017	0.099	0.1004	-0.004	0.0068	0.0079

Table 4.2. Sioux Falls simulation study: Stability of estimated $\text{BBPS}_{(\lambda=0)}$ parameters across multiple experiment replications ($Z = 1500$, $r = 25$).

α_1^{true}	β_{true}	φ_{true}	$cov(\hat{\boldsymbol{\alpha}}_1, \hat{\boldsymbol{\beta}})$	$cov(\hat{\boldsymbol{\alpha}}_1, \hat{\boldsymbol{\varphi}})$	$cov(\hat{\boldsymbol{\beta}}, \hat{\boldsymbol{\varphi}})$
0.2	0.8	1.5	-0.00306	0.00007	-0.00003
0.2	1	1.4	-0.00045	0.00007	0.00082
0.2	1	1.5	-0.00183	0.00004	-0.00004
0.2	1	1.6	-0.00085	0.00003	0.00042
0.1	1	1.5	-0.00101	0.00010	0.00010

Table 4.3. Sioux Falls simulation study: Estimated covariances between $\text{BBPS}_{(\lambda=0)}$ model parameters from multiple experiments ($Z = 1500$, $r = 25$).

We also explore estimating the additional λ parameter of the BBPS model. For the Log-Likelihood maximisation algorithm, the initial condition and bounds for λ were $\tilde{\lambda}^{(0)} = 1$ and $\tilde{\lambda} \in [0,20]$, respectively. Table 4.4 displays for different settings of λ_{true} the stability statistics of the estimates $\hat{\alpha}_1$, $\hat{\beta}$, $\hat{\varphi}$, and $\hat{\lambda}$ across $r = 25$ experiment replications with $Z = 1500$ simulated observations, where $\alpha_1^{true} = 0.2$, $\beta_{true} = 1$, and $\varphi_{true} = 1.5$. Table 4.4 also displays the estimated covariances between the α_1 and λ parameters. As shown, as measured by the MSE, the precision of estimating all parameters generally appears to decrease as λ_{true} increases. Most notably, the precision of estimating λ appears particularly poor for large λ_{true}, and the mean bias for λ worsens as λ_{true} increases where the percentage bias is 39% for $\lambda_{true} = 8$ and 34% for $\lambda_{true} = 10$, providing evidence of positive bias. There also appears to be some negative correlation between the $\hat{\alpha}_1$ and $\hat{\lambda}$ estimates, which makes sense since both scale travel cost within the path size contribution factors.

λ_{true}	$\hat{\alpha}_1$			$\hat{\beta}$			$\hat{\varphi}$			$\hat{\lambda}$			$cov(\hat{\boldsymbol{\alpha}}_1, \hat{\boldsymbol{\lambda}})$
	Bias	S.E	RMSE	Bias	S.E	RMSE	Bias	S.E	RMSE	Bias	S.E	RMSE	
2	-0.014	0.032	0.0349	-0.011	0.092	0.0927	-0.007	0.008	0.0106	0.67	1.226	1.397	-0.0347
5	-0.014	0.042	0.0443	0.035	0.121	0.1260	-0.006	0.010	0.0117	1.06	1.391	1.749	-0.0397
8	-0.028	0.044	0.0522	0.035	0.157	0.1609	-0.009	0.008	0.0120	3.15	4.168	5.224	-0.0647
10	-0.024	0.043	0.0492	0.003	0.130	0.1300	-0.008	0.011	0.0136	3.43	3.791	5.112	-0.0899

Table 4.4. Sioux Falls simulation study: Stability of estimated BBPS model parameters across multiple experiment replications with different settings of λ ($Z = 1500$, $r = 25$).

7.3.2.2 BAPS Model

7.3.2.2.1 Experiment Results

The BAPS model Log-Likelihood function in (4.24) depends on three parameters α_1, β, and φ, which can again be visualised through three 3-dimensional projections of this 4-dimensional relationship. Fig. 4.9A-C display the BAPS model Log-Likelihood surface for a single estimation experiment, with $\alpha_1^{true} = 0.2$, $\beta_{true} = 0.7$, $\varphi_{true} = 1.5$ and $Z = 2000$. As Fig. 4.9A-C show, the Log-Likelihood surfaces are smooth and approximately maximal around the true parameters, where the estimated parameters are $\hat{\alpha}_1 = 0.2 \pm 0.02$, $\hat{\beta} = 0.66 \pm 0.04$, and, $\hat{\varphi} = 1.496 \pm 0.004$.

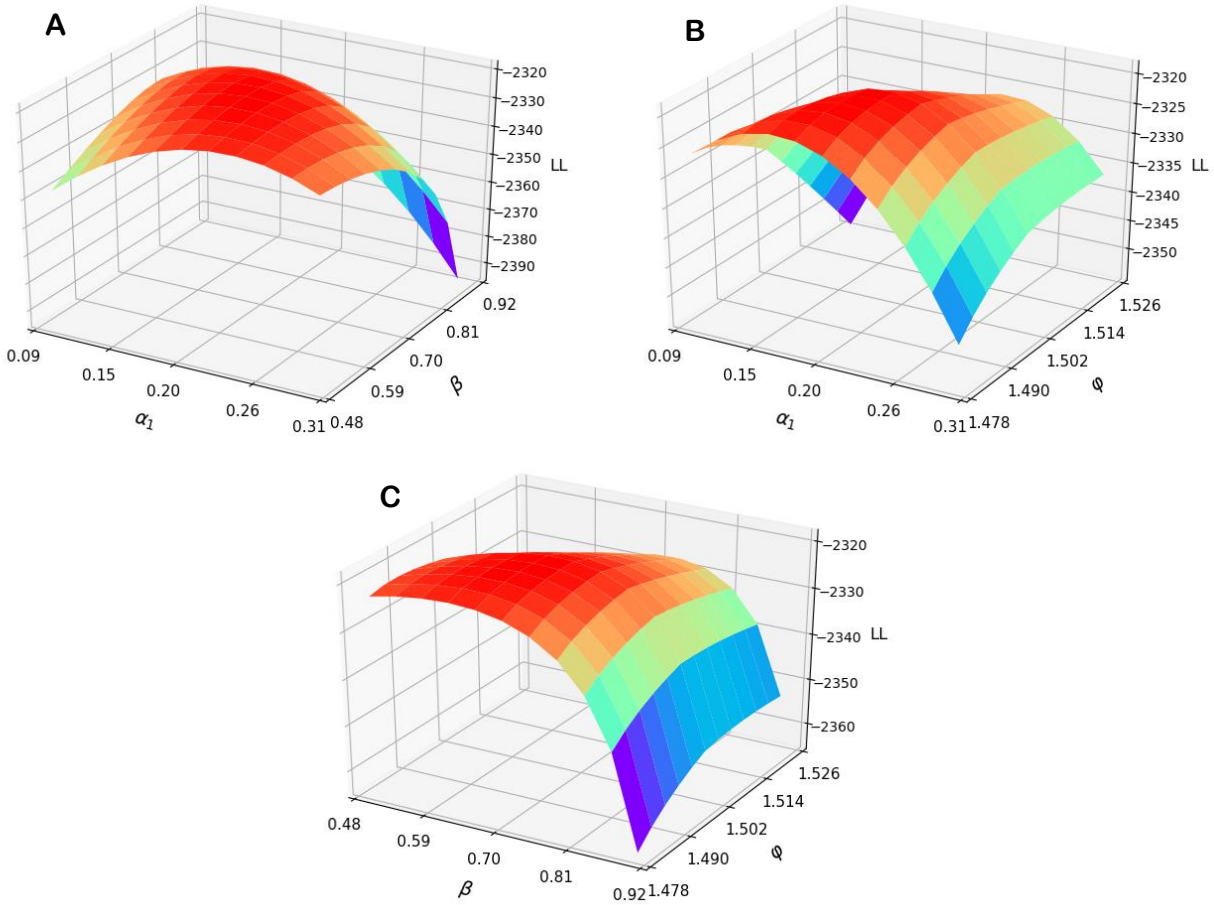

Fig. 4.9. Sioux Falls simulation study: BAPS model Log-Likelihood surface. ($\alpha_1^{true} = 0.2$, $\beta_{true} = 0.7$, $\varphi_{true} = 1.5$, $\hat{\alpha}_1 = 0.20$, $\hat{\beta} = 0.66$, $\hat{\varphi} = 1.496$). **A:** LL vs (α_1, β). **B:** LL vs (α_1, φ). **C:** LL vs (β, φ).

Next, we investigate the stability of the estimated parameters over multiple experiment replications. Each experiment utilises a Log-Likelihood maximisation algorithm (see Section 7.2.2) to obtain the parameter estimates with initial conditions $\left(\tilde{\alpha}_1^{(0)}, \tilde{\beta}^{(0)}, \tilde{\varphi}^{(0)}\right) = (0.15,0,2)$, and bounds $\tilde{\alpha}_1 \in [0.05,1]$, $\tilde{\beta} \in [0,1]$, $\tilde{\varphi} = [1.01,2.5]$.

Table 4.5 reports, for various settings of the true parameters the mean bias, standard error, and RMSE of the estimates across $r = 25$ experiment replications with $Z = 1500$ simulated observations. Table 4.6 displays the estimated covariance between the α_1, β, and φ parameters. As shown, as for the BBPS model, the mean bias of the estimates of α_1, β, and φ are small for all settings of the true parameters tested, with max absolute percentage biases of 13%, 4.6%, & 0.6%, respectively. There is thus again no evidence of bias in the parameter estimates – the estimates are all close to the true values. The precision of estimating α_1 and β decrease as α_1^{true} and β_{true} decrease, as anticipated. And, a lower perception error of travel cost again results in less precise estimations of the bound parameter φ. The RMSEs of $\hat{\beta}$ compared to those for the $BBPS_{(\lambda=\theta)}$

model in Table 4.2 suggest that the β parameter can be estimated more accurately with the BAPS model. Table 4.6 indicates that there also appears to be some negative correlation between the $\hat{\alpha}_1$ and $\hat{\beta}$ estimates, as well as some positive correlation between the $\hat{\alpha}_1$ and $\hat{\varphi}$ estimates.

α_1^{true}	β_{true}	φ_{true}	$\hat{\alpha}_1$			$\hat{\beta}$			$\hat{\varphi}$		
			Bias	S.E	RMSE	Bias	S.E	RMSE	Bias	S.E	RMSE
0.2	0.8	1.5	0.000	0.018	0.0180	0.000	0.108	0.1080	-0.003	0.0047	0.0056
0.2	0.7	1.4	-0.004	0.030	0.0303	-0.032	0.134	0.1378	-0.004	0.0067	0.0078
0.2	0.7	1.5	-0.003	0.014	0.0143	-0.023	0.112	0.1143	-0.004	0.0058	0.0070
0.2	0.8	1.7	-0.004	0.017	0.0175	0.006	0.115	0.1152	-0.002	0.0101	0.0103
0.1	0.7	1.5	-0.013	0.022	0.0256	0.006	0.126	0.1261	-0.004	0.0052	0.0066

Table 4.5. Sioux Falls simulation study: Stability of estimated BAPS model parameters across multiple experiment replications ($Z = 1500$, $r = 25$).

α_1^{true}	β_{true}	φ_{true}	$cov(\hat{\boldsymbol{\alpha}}_1, \hat{\boldsymbol{\beta}})$	$cov(\hat{\boldsymbol{\alpha}}_1, \hat{\boldsymbol{\varphi}})$	$cov(\hat{\boldsymbol{\beta}}, \hat{\boldsymbol{\varphi}})$
0.2	0.8	1.5	-0.00090	0.00004	-0.00015
0.2	0.7	1.4	-0.00198	0.00003	0.00029
0.2	0.7	1.5	-0.00104	0.00002	0.00008
0.2	0.8	1.7	-0.00104	0.00007	0.00026
0.1	1	1.5	-0.00155	0.00005	-0.00002

Table 4.6. Sioux Falls simulation study: Estimated covariance of BAPS model parameters from multiple experiment replications ($Z = 1500$, $r = 25$).

7.3.2.2.2 Computation Analysis

Due to the requirement of having to solve fixed-point problems to compute choice probabilities, in this subsection we analyse the computational performance of the BAPS model in the Sioux Falls MLE application. We The computer used has a 2.10GHz Intel Xeon CPU, 512GB RAM, and 64 Logical Processors (of which 50 were utilised). The code was implemented in Python. Results are reported throughout this section for a single simulation experiment where $Z = 1000$ route choice observations were simulated from the true model $\alpha_1^{true} = 0.2$, $\beta_{true} = 0.7$, $\varphi_{true} = 1.5$. $\hat{\alpha}_1 = 0.208$, $\hat{\beta} = 0.703$, and $\hat{\varphi} = 1.493$ were the consequent maximum likelihood estimates. Unless stated otherwise, the BAPS model choice probability convergence parameter ξ was set as $\xi = 10$ (see Section 5.2.2).

Fig. 4.10A shows for different values of the BAPS model choice probability convergence parameter ξ (and thus convergence statistic), the average number of fixed-point iterations per OD movement and computation time required to solve all of the 370 BAPS model fixed-point problems $\boldsymbol{P}_m = \boldsymbol{F}_m\left(\boldsymbol{f}_m\left(\boldsymbol{c}_m(\boldsymbol{t}), \bar{\boldsymbol{\gamma}}_m^{BAPS}(\boldsymbol{t}, \boldsymbol{P}_m)\right)\right)$, and consequently compute the Log-Likelihood value of the maximum likelihood estimates. As shown, computation time and average number of fixed-point iterations per OD increase roughly linearly as the convergence parameter is increased. As expected, computation times relate to the number of iterations required for convergence. Fig. 4.10B shows the value of the Log-Likelihood obtained as ξ is increased. As shown, the Log-Likelihood increases in accuracy as the BAPS model choice probabilities become more accurate.

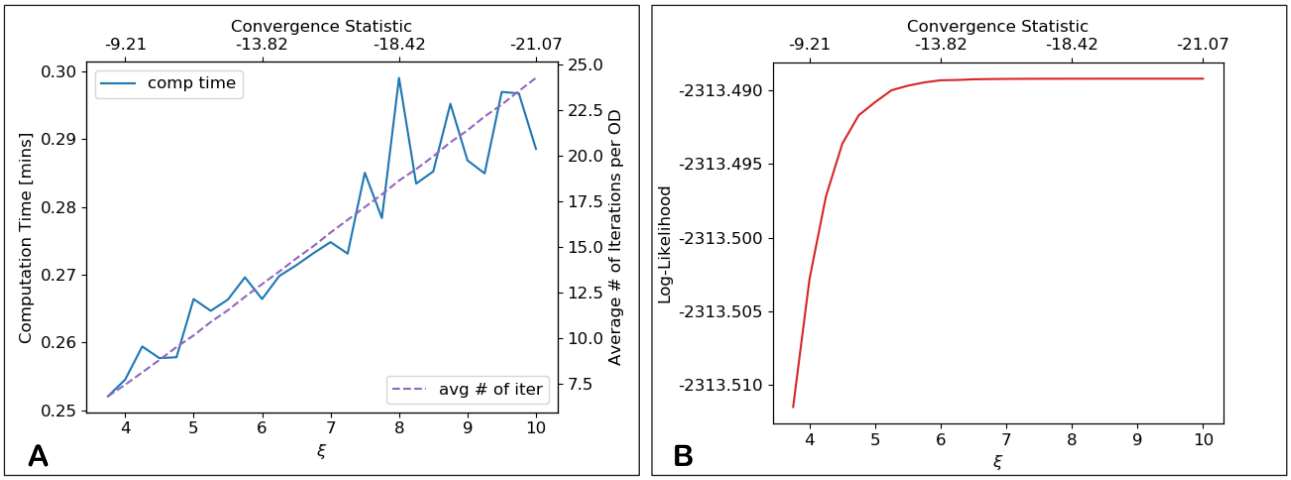

Fig. 4.10. Sioux Falls simulation study: Computational statistics for calculating a BAPS model Log-Likelihood as the BAPS model choice probability convergence parameter ξ is increased. **A:** Average number of fixed-point iterations per OD / computation time [mins]. **B:** Log-Likelihood value.

Fig. 4.11 shows for different values of $\tilde{\varphi}$ the average number of fixed-point iterations per OD movement and computation time required to calculate the Log-Likelihood. As shown, the average number of iterations per OD required for convergence increases as $\tilde{\varphi}$ increases, and thus so do the required computation times. This is because the number of routes with a cost below the bound increases as the bound becomes less restrictive, and there are thus more routes to calculate the correlation between. This shows that the BAPS model can improve upon the computational performance of the APSL model in computing choice probabilities.

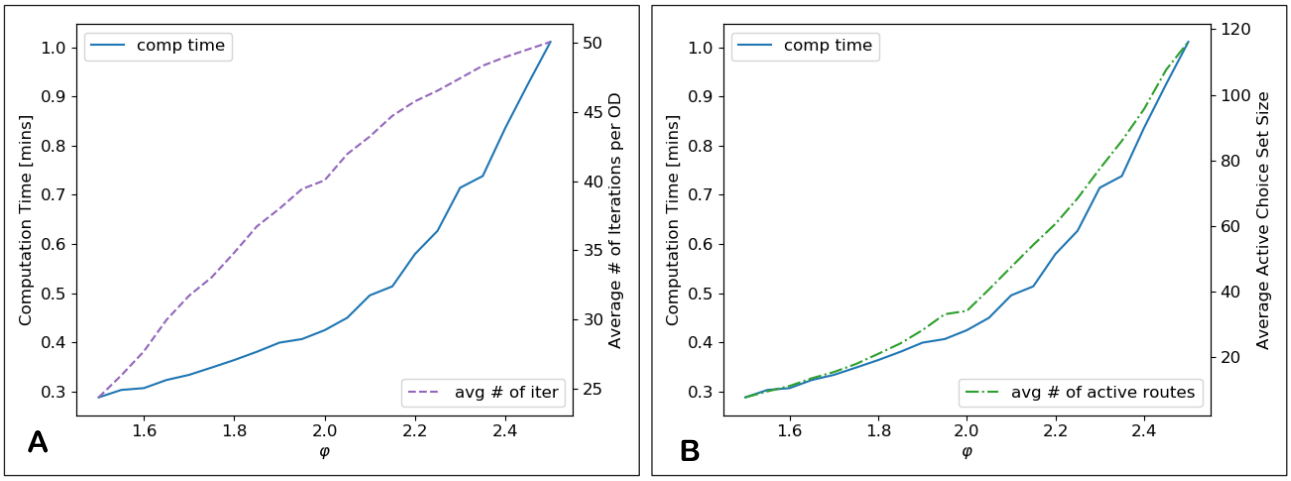

Fig. 4.11. Sioux Falls simulation study: Average number of fixed-point iterations (**A**) / active routes (**B**) per OD movement and computation time required to calculate the BAPS model Log-Likelihood for different $\tilde{\varphi}$ values.

Fig. 4.12A-B show for a single MLE (implementation of the L-BFGS-B algorithm), the cumulative computation times of the iterations and the BAPS model Log-Likelihood values and parameter estimates at the end of each iteration.

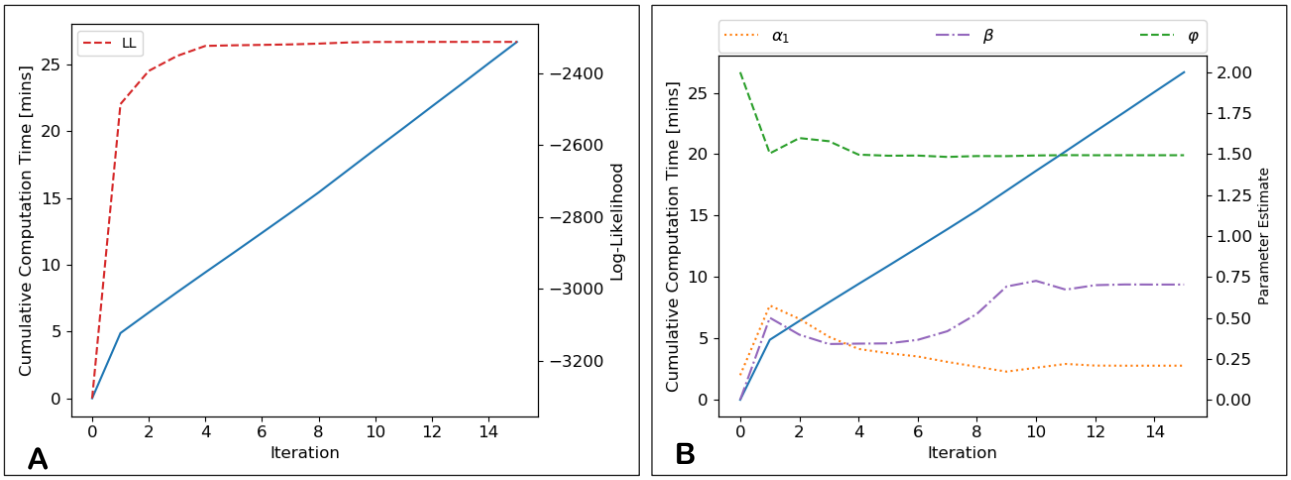

Fig. 4.12. Sioux Falls simulation study: Cumulative computation time at each iteration of a single BAPS model MLE, and MLE statistics. **A:** Log-Likelihood. **B:** Parameter estimates.

We also briefly investigate the impact of the τ parameter upon parameter estimation. For $\varphi = 1.5$, the largest choice set size is 898; thus, supposing that $\tau_m = \tau$, $m = 1, \dots, M$, the maximum value for τ is $\frac{1}{898} \cong 10^{-3}$. Supposing τ assumes the form $\tau = 10^{-\nu}$, Fig. 4.13 displays how the maximum likelihood parameter estimates vary as ν varies. Unlike the APSL model, the BAPS model probability function is not continuous, and continuity is approximated by setting a small τ value. MLE requires a continuous probability function, and hence a small τ value is not only desired to approximate the standard formulation (like APSL), but is required so that the model is well behaved. For $\nu = 4$ and $\nu = 5$, MLE could not run successfully due to the discontinuity; however, as Fig. 4.13 shows for $\nu > 5$, MLE runs successfully and the parameter estimates are extremely close / roughly converge to the limit case of $\tau \to 0$. This demonstrates that we can recover the desired BAPS_0 model (Section 5.1) to a high computational accuracy using the BAPS model as defined in Section 5.2, with a sufficiently small value of τ.

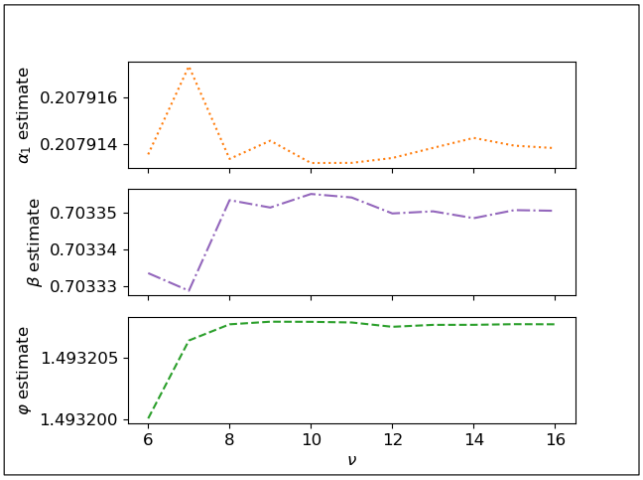

Fig. 4.13. Sioux Falls simulation study: Maximum likelihood BAPS model parameter estimates for different values of $\tau = 10^{-\nu}$.

7.3.2.2.3 BAPS Model Solution Uniqueness Analysis

In this subsection we briefly investigate the uniqueness of BAPS model choice probability solutions in the context of the Sioux Falls simulation study. To do this, we utilise the method proposed in Section 10.3.4, where we plot trajectories of BAPS model solutions to approximate the uniqueness conditions, i.e. estimate β_{max}. A single simulation study is conducted for $\alpha_1^{true} = 0.2$, $\beta_{true} = 0.7$, $\varphi_{true} = 1.5$, and $Z = 2000$, leading to maximum likelihood estimates $\hat{\alpha}_1 = 0.200$, $\hat{\beta} = 0.747$, and $\hat{\varphi} = 1.499$. We thus investigate whether BAPS model solutions are unique for these parameter estimates. Fig. 4.14 displays the maximum choice probability from three trajectories of BAPS model solutions as the β parameter is varied for four different randomly chosen OD movements, with $\alpha_1 = \hat{\alpha}_1 = 0.200$ and $\varphi = \hat{\varphi} = 1.499$. β was decremented

by 0.01, and the initial large β value was $\beta = 2$. As shown, the $\beta_{max,m}$ values (β_{max} for OD movement m) for these OD movements can be estimated to vary between 0.86 and 0.94, suggesting that $\beta = 0.747$ results in universally unique solutions.

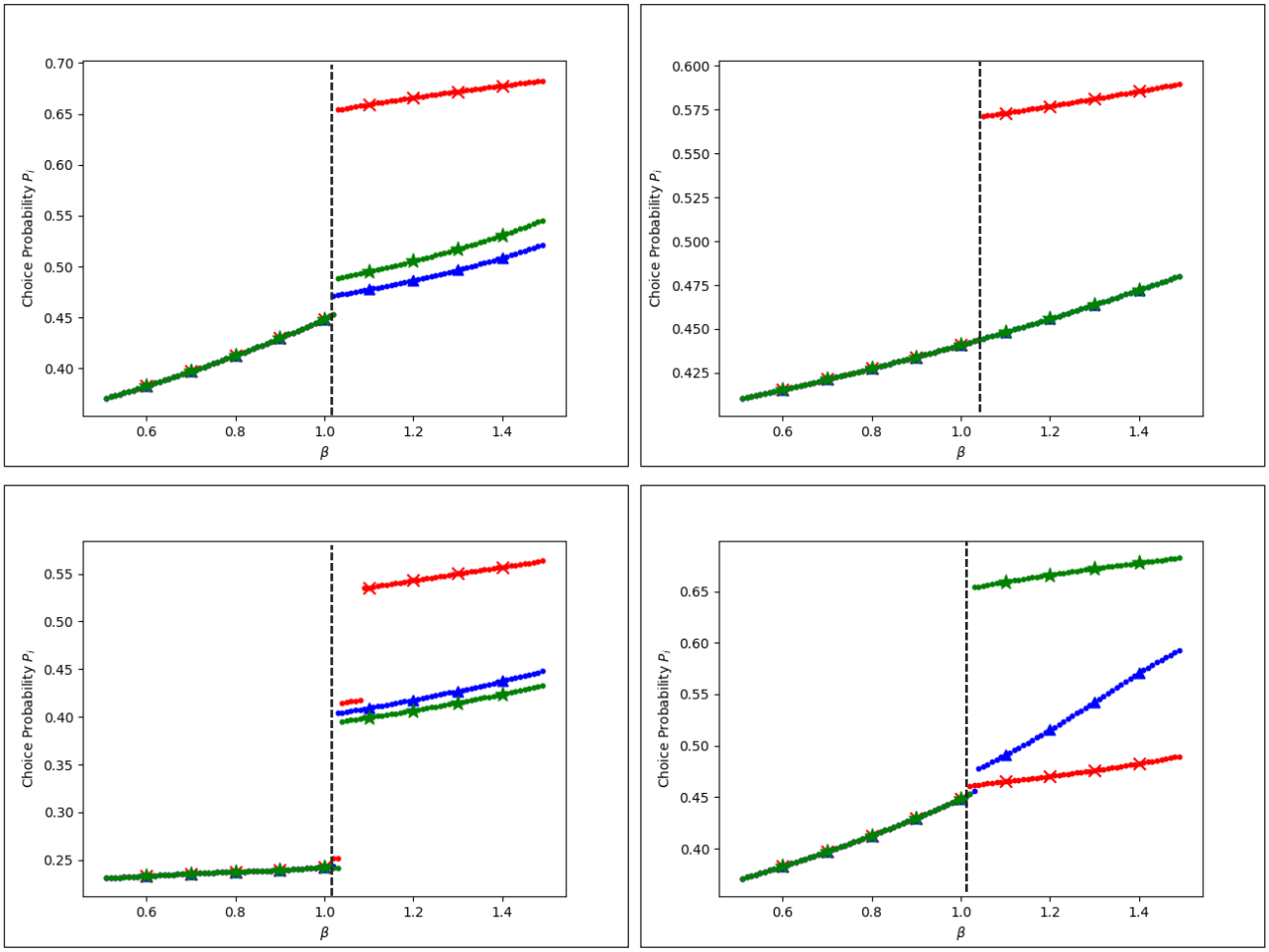

Fig. 4.14. Sioux Falls simulation study: Maximum choice probability of trajectories of BAPS model solutions as β is varied.

7.3.2.3 Model Robustness to the Adopted Choice Sets

We briefly evaluate here on the Sioux Falls network the robustness of the BBPS & BAPS models to the adopted choice sets. Fig. 4.15A-B display the impact that varying the sizes of choice sets has on the route choice probabilities from the different models. The choice sets are generated using k-shortest path, with increasing values of k. It is assumed that the true active choice sets are those containing all routes with a free-flow travel time less than 2 and 2.5 times greater, respectively, than the free-flow travel time on the quickest route for each OD movement, and probability results are compared between these routes only (probability is zero if not generated). The model parameters are assumed known: $\alpha_1 = 0.2$, $\beta = 0.8$, $\lambda^{GPSL} = 10$, $\lambda^{BBPS} = 1$, and $\varphi = 2{,}2.5$ for Fig. 4.15A,B, respectively, and to compare the probability result $\boldsymbol{P}^{\{k\}}$ for the k-shortest path choice sets with the assumed true probabilities $\boldsymbol{P}^{true}$, we measure the Route Mean Squared Error (RMSE):

$$RMSE = \sqrt{\sum_{m=1}^{M} \sum_{i \in R_m} \left(P_{m,i}^{\{k\}} - P_{m,i}^{true}\right)^2 / N},$$

where N is the total number of routes (12,844 for $\varphi = 2$, 42,976 for $\varphi = 2.5$). Fig. 4.16A-B show how the percentage of routes generated with a cost greater than the 2 and 2.5 relative cost bound varies, respectively, as k varies, as well as the percentage of routes that should be generated but were not (non-generated routes with a relative cost less the bound).

As shown, the choice probability results for the MNL and PSL models both decrease in similarity to the respective assumed true probabilities as the choice sets are expanded and more unrealistic routes (with relative cost deviations greater than the bound) are present with the choice sets (shown in Fig. 4.16). The GPSL and APSL model results remain fairly stable in similarity due to the weighted contributions. The probability results for the bounded models, however, all increase in similarity since these models implicitly restrict the choice sets and perform better as more realistic routes are generated, regardless of how many generated unrealistic routes. As anticipated, GPSL & APSL are more robust than PSL due to the employment of path size contribution weighting techniques, while the BBPS & BAPS models are significantly more robust due to path size contribution elimination.

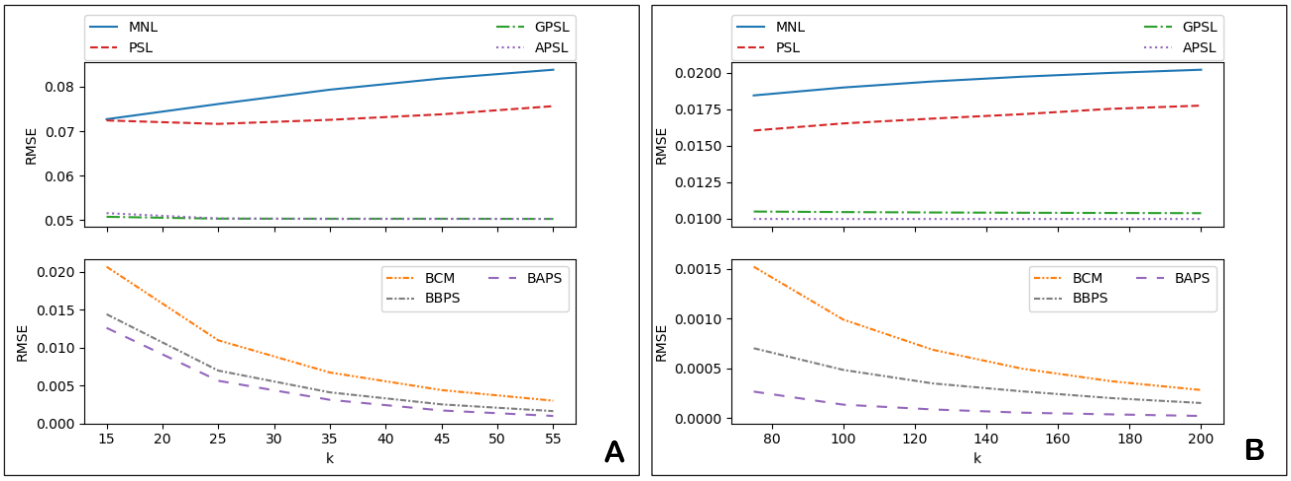

Fig. 4.15. Sioux Falls network: Impact that varying the sizes of choice sets has on the choice probabilities from different models, k-shortest path. **A:** $\varphi = 2$. **B:** $\varphi = 2.5$.

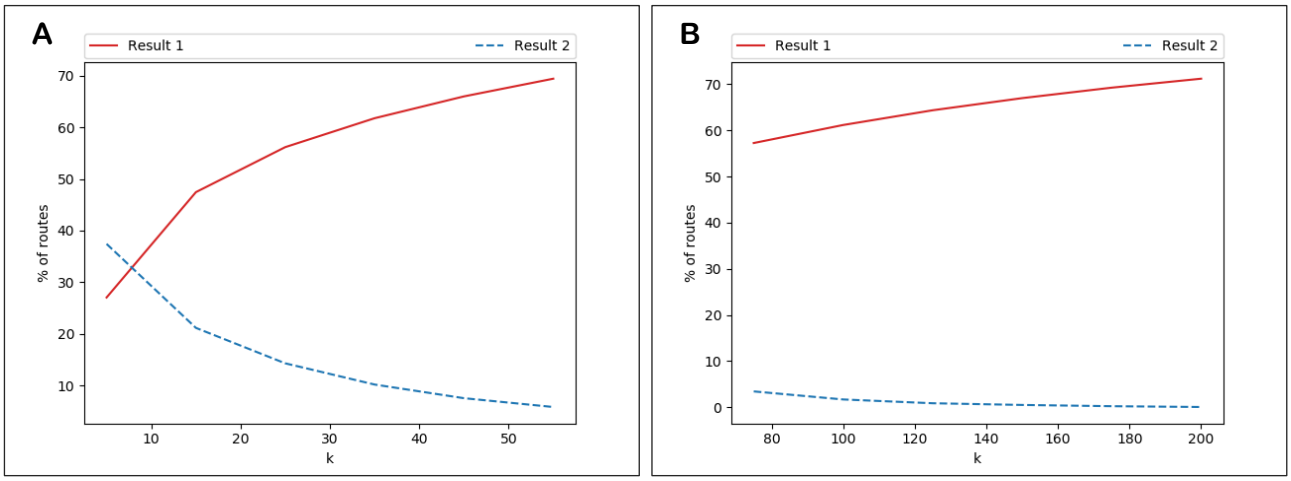

Fig. 4.16. Sioux Falls network: Percentage of routes in the choice sets with a free-flow travel time greater than or equal to the φ relative cost bound (Result 1) and percentage of routes that should be generated but were not as k varies (Result 2). **A:** $\varphi = 2$. **B:** $\varphi = 2.5$.

7.4 Real-Life Large-Scale Case Study

In this section we estimate the BBPS and BAPS models, where the model parameters are estimated using MLE with observed route choices tracked by GPS units. The data has been collected among drivers in the eastern part of Denmark in 2011, and includes a total of 17,115 observed routes. The dataset is the same as used in Prato et al (2014), Rasmussen et al (2017), and Duncan et al (2020), and after a filtering to include only trips where the sum of travel time (in minutes) and length (in km) is at least 10, a total of 8,696 observations remain.

The GPS traces are map matched to a network, for which corresponding time-of-day dependent travel times are available on the entire network. See more details in Prato et al (2014). The network is large-scale, representing all of Denmark, and thus includes 34,251 links. With current alternative generation techniques, it

is not feasible to enumerate the universal choice set for such a large network, and even enumerating all alternatives with a cost below a rather large relative bound (e.g. $\varphi = 2$) is not feasible. Instead, we approximate the universal choice set by generating a choice set for each observed route by applying the doubly stochastic approach also applied in Prato et al (2014). This approach is based on repeated shortest path search in which the network attributes and parameters of the cost function are perturbated between searches (Nielsen, 2000; Bovy & Fiorenzo-Catalano, 2007). To reduce the risk of bias in estimation, care was taken to ensure a large variety of alternatives with different characteristics were generated, by assuming large variance in the parameters of the cost function. Up to 100 unique paths are generated for each observation, and for 591 observations only the observed route was generated, so these are removed from the data set, leaving 8105 observations.

For the estimation, the travel cost of link a is specified as a weighted sum of congested travel time $w_{a,1}$ (in minutes), and length $w_{a,2}$ (in kilometres), such that:

$$t_a(\boldsymbol{w}_a; \boldsymbol{\alpha}) = w_{a,1} \cdot \alpha_1 + w_{a,2} \cdot \alpha_2$$

where $\alpha_1 > 0$ and $\alpha_2 > 0$ are the congested travel time, and length parameters, respectively. The generalised travel cost for route $i \in R_m$ is thus:

$$c_{m,i}\big(\boldsymbol{t}(\boldsymbol{w}; \boldsymbol{\alpha})\big) = \sum_{a \in A_{m,i}} t_a(\boldsymbol{w}_a; \boldsymbol{\alpha}) = \sum_{a \in A_{m,i}} \big(w_{a,1} \cdot \alpha_1 + w_{a,2} \cdot \alpha_2\big) = \alpha_1 \sum_{a \in A_{m,i}} w_{a,1} + \alpha_2 \sum_{a \in A_{m,i}} w_{a,2}.$$

The model requires the specification of five parameters: α_1, α_2, θ, β, and φ but to ensure identification, the θ parameter is fixed at $\theta = 1$. There are some outlying observations in the data where the relative travel time / length deviation of the observed route away from the quickest/shortest route is high. So that the estimation results are not influenced significantly by these outliers, and to improve the analysis of results, we remove 82 route observations where either the relative travel time or length deviation is over 1.5, leaving 8023 observations, see the distribution of the choice set sizes in Fig. 4.17.

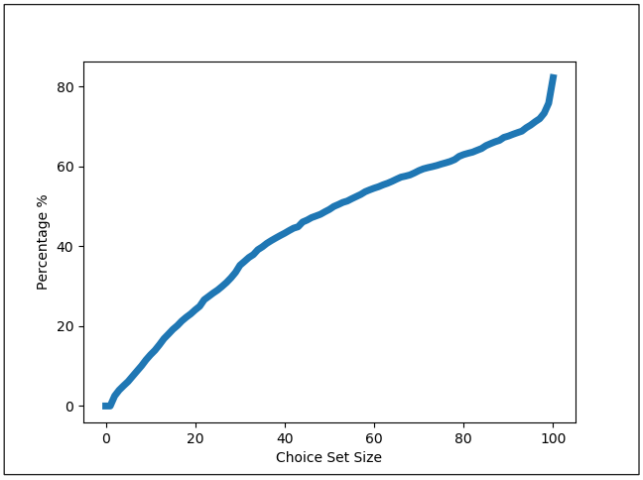

Fig. 4.17. Real-life case-study: Cumulative distribution of the choice set sizes for the 8,023 observations.

Fig. 4.18A shows the relative travel time deviations away from the quickest routes in the choice sets for the observed routes as well as the alternative routes generated, and Fig. 4.18B shows the relative length deviations.

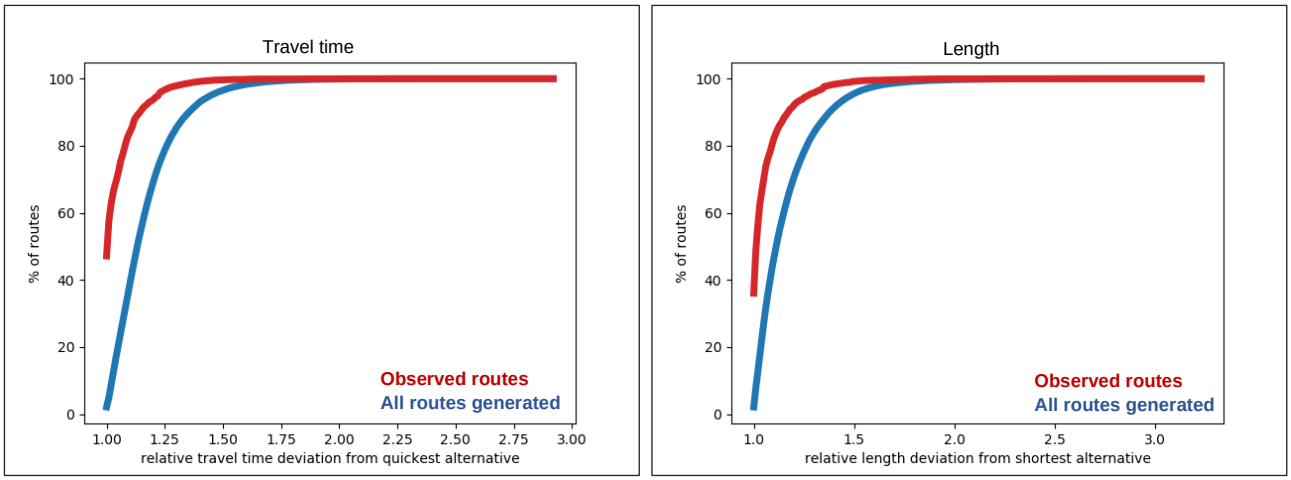

Fig. 4.18. Real-life case-study: Relative deviations away from quickest/shortest routes in the choice sets for the observed routes (red) and alternative routes generated (blue).

We estimate the models utilising the same Log-Likelihood maximisation algorithm (L-BFGS-B, see Section 7.2.2), initial conditions, and parameter bounds, where appropriate. Initial conditions are: $\left(\tilde{\alpha}_1^{(1)}, \tilde{\alpha}_2^{(1)}, \tilde{\beta}^{(1)}, \tilde{\varphi}^{(1)}, \tilde{\lambda}^{(1)}\right) = (0.5,0.5,0,1.6,0)$, and bounds: $\tilde{\alpha}_1, \tilde{\alpha}_2 \in [0,1]$, $\tilde{\beta} \in [0,2]$, $\tilde{\varphi} \in [1.01,5]$, $\tilde{\lambda} \in [0,200]$. For the APSL and BAPS models the bounds are: $\tilde{\alpha}_1, \tilde{\alpha}_2 \in [0.1,1]$, $\tilde{\beta} \in [0,1]$, $\tilde{\varphi} \in [1.01,5]$.

7.4.1 BBPS Model Estimation

Table 4.7 displays the $\text{BBPS}_{(\lambda=\theta)}$ and BBPS model parameter estimates, and the consequent Log-Likelihood values. The BBPS model appears to outperform the $\text{BBPS}_{(\lambda=\theta)}$ model due to the greater flexibility the λ parameter provides; however, the estimated bound is very large considering the relative deviations in Fig. 4.18, which results in every route having a cost within the bound and the BBPS approximating the GPSL′ model. This suggests that the GPSL′ model with a large λ value is outperforming more internally consistent models by capturing something other than the correlation between the realistic routes. We explore this further in Section 7.4.3.

	$\hat{\alpha}_1$	$\hat{\alpha}_2$	$\hat{\beta}$	$\hat{\lambda}$	$\hat{\varphi}$	LL
$\text{BBPS}_{(\lambda=\theta)}$	0.690	0.209	1.786		1.495	-18556
BBPS	0.433	0.148	0.970	10.277	3.834	-17463

Table 4.7. Real-life case-study: $\text{BBPS}_{(\lambda=\theta)}$ & BBPS parameter estimates and Log-Likelihood values.

Fig. 4.19A-F visualise the $\text{BBPS}_{(\lambda=\theta)}$ model Log-Likelihood surface around the four parameter estimates; as can be seen, these are smooth.

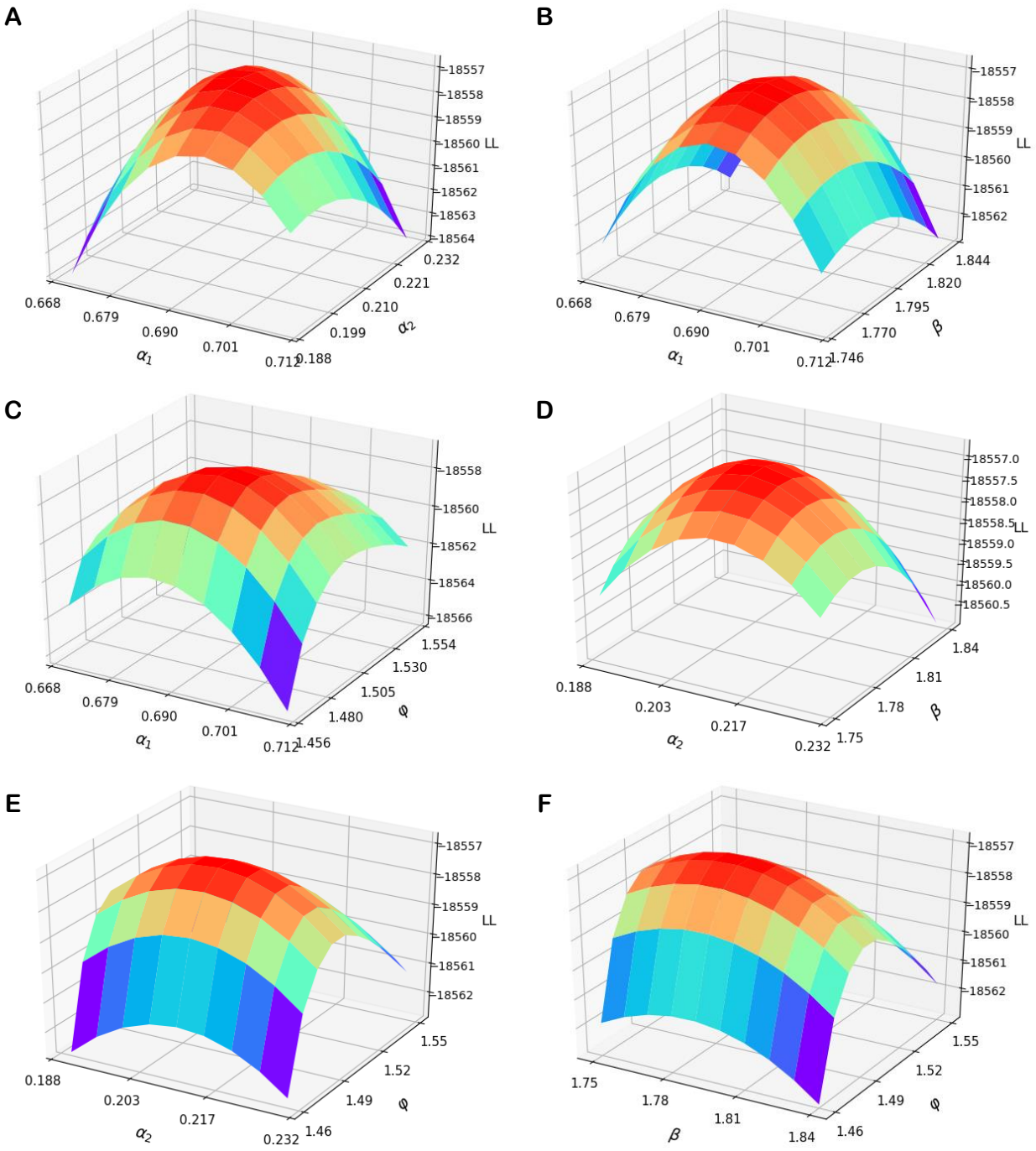

Fig. 4.19. Real-life case-study: $BBPS_{(\lambda=\theta)}$ model Log-Likelihood surface around parameter estimates in Table 4.7. **A:** LL vs (α_1, α_2). **B:** LL vs (α_1, β). **C:** LL vs (α_1, φ). **D:** LL vs (α_2, β). **E:** LL vs (α_2, φ). **F:** LL vs (β, φ).

7.4.2 BAPS Model Estimation

7.4.2.1 Results

Table 4.8 displays the BAPS model parameter estimates and the consequent Log-Likelihood value. As shown, the estimates all seem reasonable and the BAPS model appears to provide better fit over the $BBPS_{(\lambda=\theta)}$ model in Table 4.7.

$\hat{\alpha}_1$	$\hat{\alpha}_2$	$\hat{\beta}$	$\hat{\varphi}$	LL
0.629	0.250	0.844	1.506	-18308

Table 4.8. Real-life case-study: BAPS model parameter estimates and Log-Likelihood.

Fig. 4.20A-F visualise the Log-Likelihood surface around the four parameter estimates; as can be seen, these are smooth.

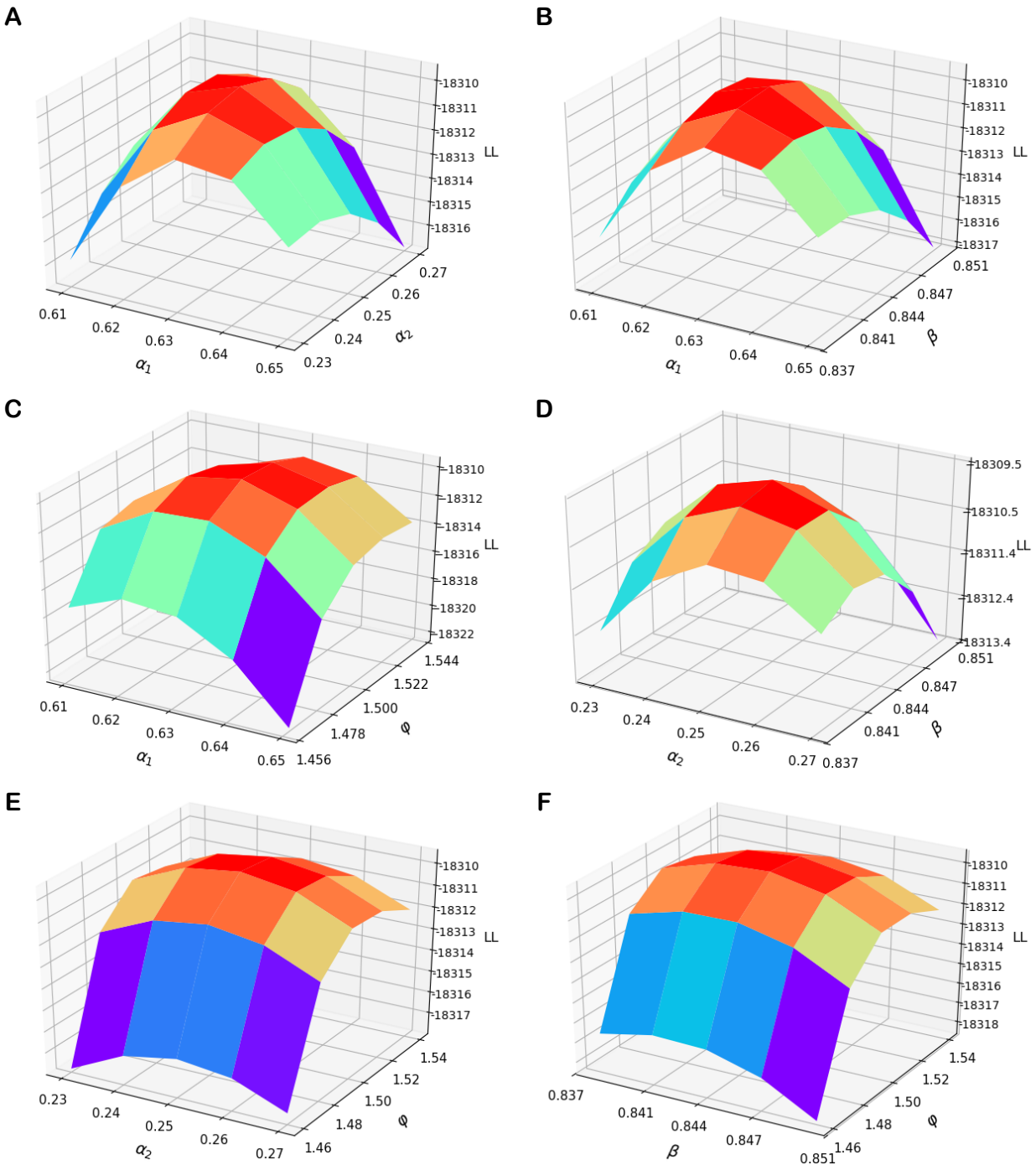

Fig. 4.20. Real-life case-study: BAPS model Log-Likelihood surface around parameter estimates in Table 4.8. **A:** LL vs (α_1, α_2). **B:** LL vs (α_1, β). **C:** LL vs (α_1, φ). **D:** LL vs (α_2, β). **E:** LL vs (α_2, φ). **F:** LL vs (β, φ).

7.4.2.2 Computation Analysis

We analyse here the computational performance of the BAPS model in the real-life case study. The same computer was used as in Section 7.3.2.2.2. Unless stated otherwise, the BAPS model choice probability convergence parameter ξ was set as $\xi = 7$.

Fig. 4.21A shows for different values of the BAPS model choice probability convergence parameter ξ (and thus convergence statistic), the average number of fixed-point iterations per OD movement and

computation time required to solve all of the 8,023 BAPS model fixed-point problems $\boldsymbol{P}_{m_z} = \boldsymbol{F}_{m_z}\left(\boldsymbol{f}_{m_z}\left(\boldsymbol{c}_{m_z}(\boldsymbol{t}), \overline{\boldsymbol{\gamma}}_{m_z}^{BAPS}(\boldsymbol{t}, \boldsymbol{P}_{m_z})\right)\right)$ for $z = 1, \dots, Z$, and consequently compute a single Log-Likelihood, with the estimated BAPS model parameters in Table 4.8. Fig. 4.21B shows the value of the Log-Likelihood obtained as ξ is increased. As shown, computation time and average number of fixed-point iterations per OD increase linearly as the convergence parameter is increased, and the Log-Likelihood increases in accuracy (from $\xi = 2$) as the BAPS model choice probabilities become more accurate.

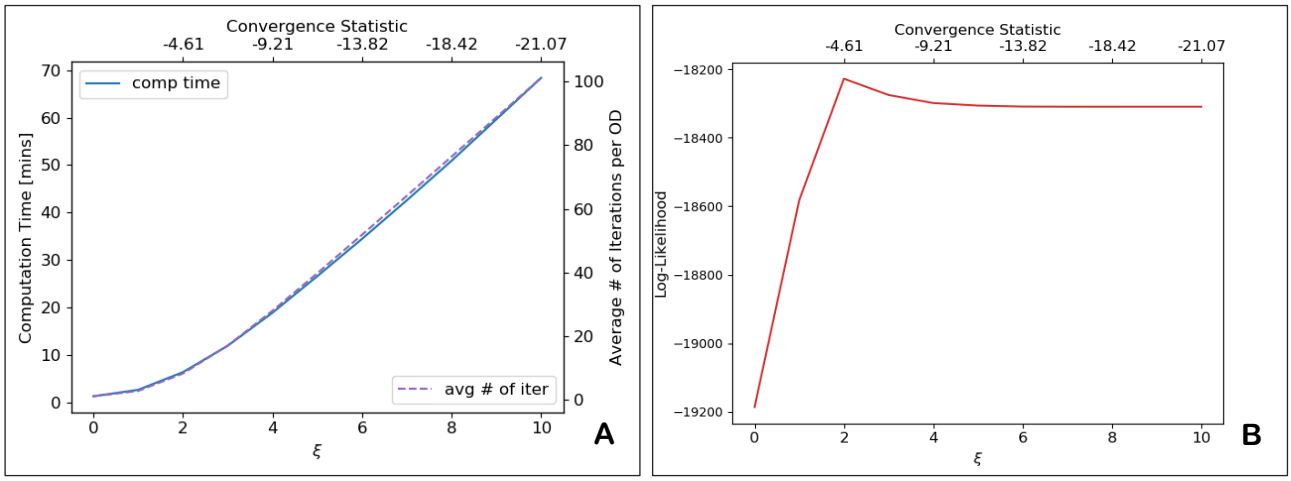

Fig. 4.21. Real-life case-study: Computational statistics for calculating the estimated BAPS model Log-Likelihood as the BAPS model choice probability convergence parameter ξ is increased. **A:** Average number of fixed-point iterations per OD / computation time [mins]. **B:** Log-Likelihood value.

Fig. 4.22A shows for different values of φ the average number of fixed-point iterations per OD movement and computation time required to solve the BAPS model, with α_1, α_2, and β set as the estimated BAPS model parameters in Table 4.8. Fig. 4.22B shows the average active choice set size as φ increases. As shown, the average number of iterations per OD required for convergence and average active choice set size increases as φ increases, and thus so do the required computation times.

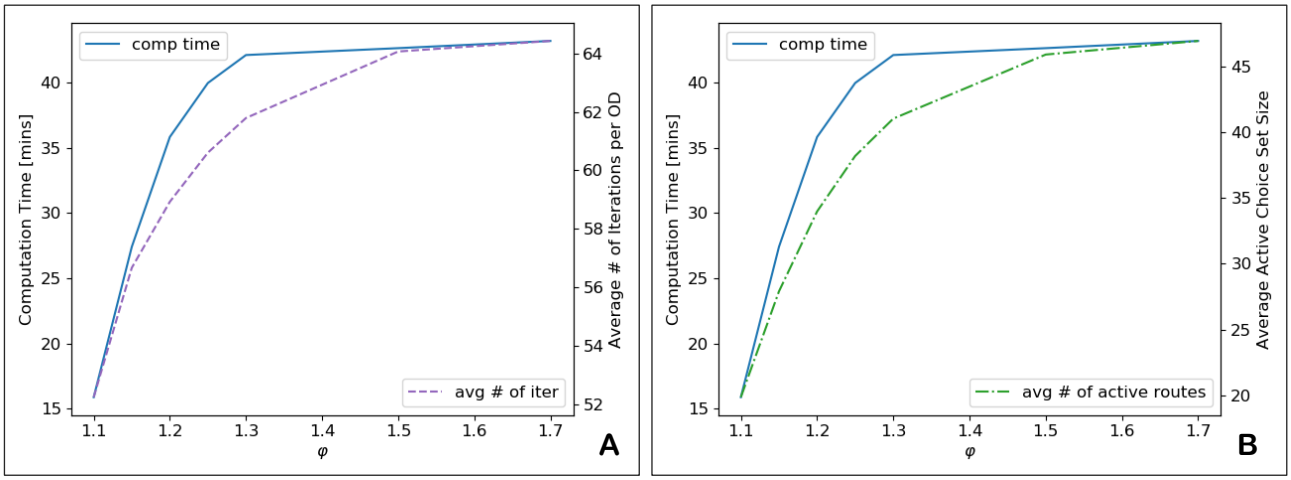

Fig. 4.22. Real-life case study: The impact of φ on computation statistics for solving the BAPS model with α_1, α_2, β as the parameter estimates in Table 4.8. Computation time [mins] and **A:** Average number of fixed-point iterations per OD movement. **B:** Average active choice set size.

Fig. 4.23A-B show for a single estimation of the BAPS model (implementation of the L-BFGS-B algorithm), the cumulative computation times of the iterations and the Log-Likelihood values and parameter estimates at the end of each iteration, respectively.

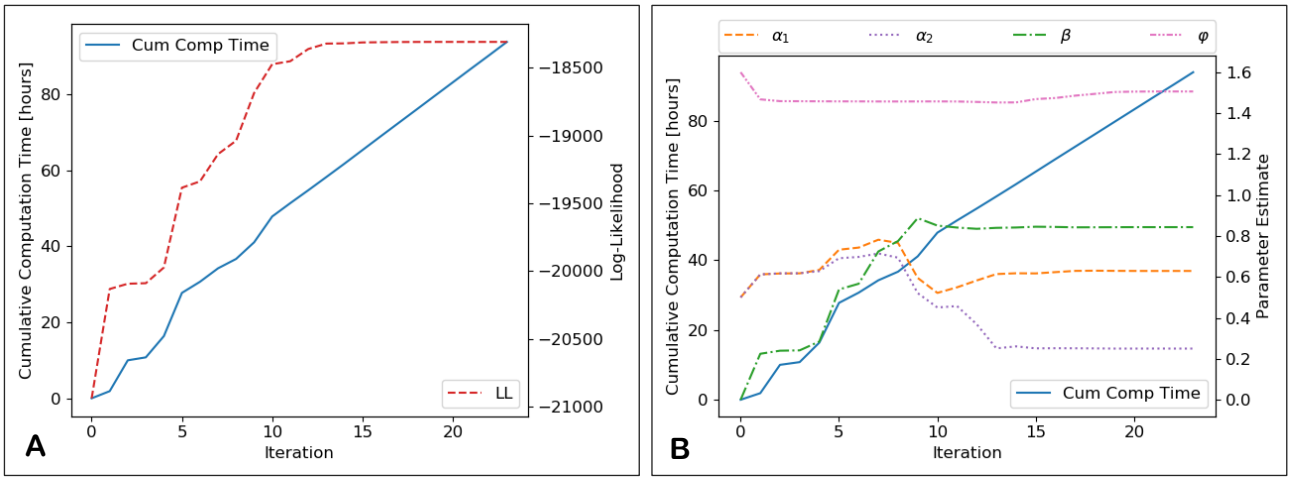

Fig. 4.23. Real-life case-study: Cumulative computation time at each iteration for a single estimation of the BAPS model, and MLE statistics. **A:** Log-Likelihood. **B:** Parameter estimates.

7.4.2.3 BAPS Model Solution Uniqueness Analysis

We briefly investigate here the uniqueness of BAPS model choice probability solutions in the context of the real-life case study. Similar to the experiments conducted in Section 7.3.2.2.3 for the Sioux Falls simulation study, we estimate the uniqueness conditions for the network given the estimated parameters. Trajectories of BAPS model solutions are plotted to approximate β_{max}. Fig. 4.24 displays the maximum choice probability from trajectories of BAPS model solutions as the β parameter is varied for four different randomly chosen OD movements, with α_1, α_2, and φ as in Table 4.8. β was decremented by 0.01, and the initial large β value was $\beta = 1.5$. As shown, the $\beta_{max,m}$ values for these OD movements are around 1, suggesting that $\beta = 0.844$ results in universally unique solutions.

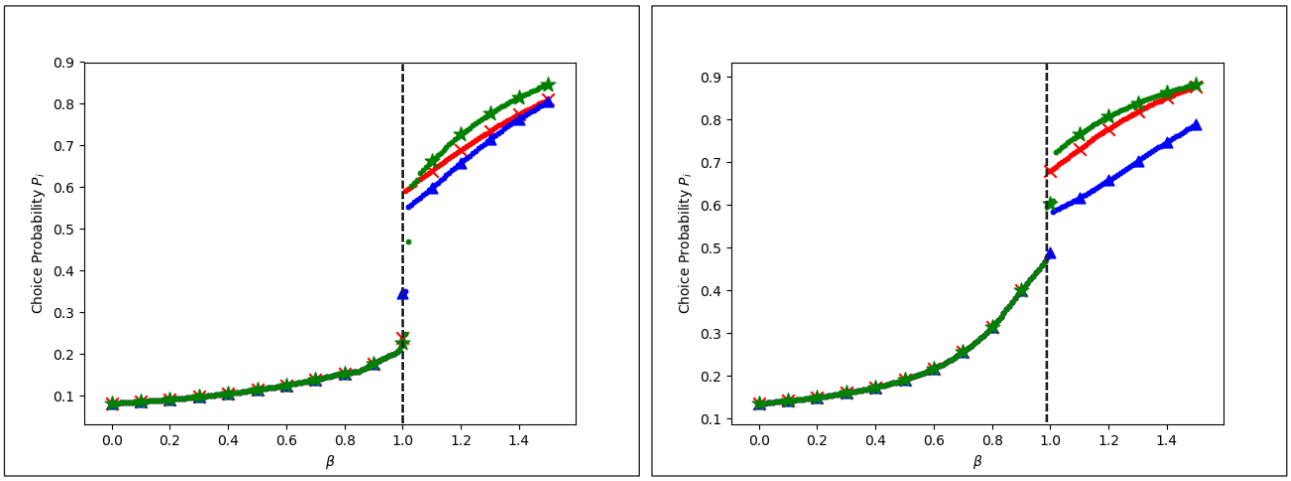

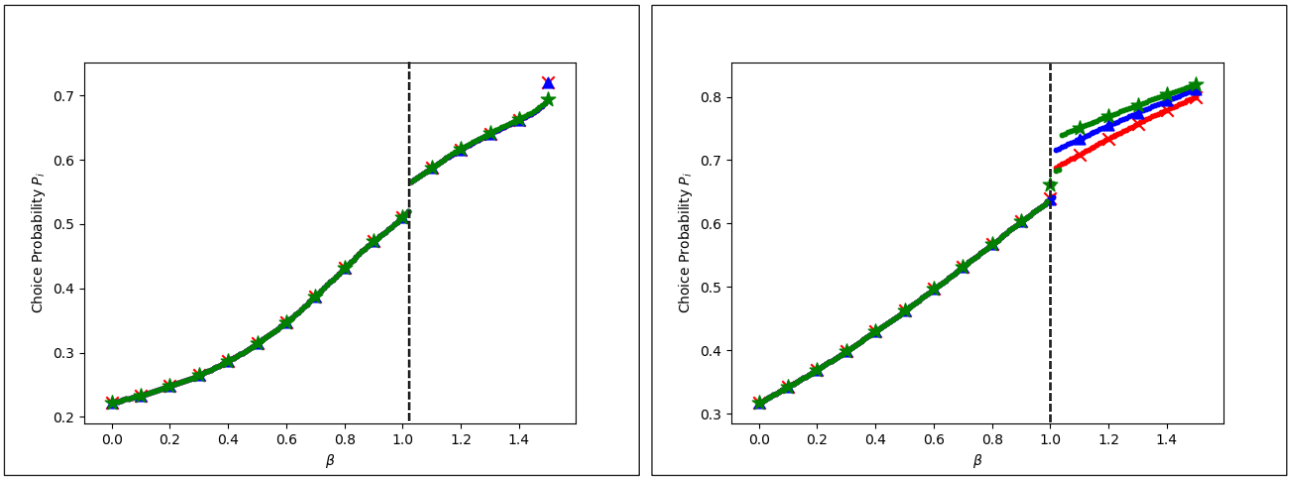

Fig. 4.24. Real-life case study: Maximum choice probability from trajectories of BAPS model solutions as β is varied.

7.4.3 Comparing Results with Other Models

In this subsection we estimate models discussed in this paper and compare results. Table 4.9 shows the estimated parameters and Log-Likelihood values for the MNL, PSL, GPSL, GPSL′, GPSL′$_{(\lambda=\theta)}$, & APSL models, as well as the BCM, BBPS$_{(\lambda=\theta)}$, BBPS, & BAPS models. As anticipated, the estimated bounds for the BCM, and BBPS$_{(\lambda=\theta)}$ and BAPS models are all around 1.5; however, the estimated bound for the BBPS model is much larger than 1.5 and while the given value is 3.834 it is approximating $\varphi \to \infty$ where the BBPS model collapses to the GPSL′ model, which is evident from the same estimated parameters and Log-Likelihood value. We discuss this result in more detail below.

	$\hat{\alpha}_1$	$\hat{\alpha}_2$	$\hat{\beta}$	$\hat{\lambda}$	$\hat{\varphi}$	LL
MNL	0.799	0.441				-20573
PSL	0.990	0.405	1.335			-19907
GPSL	0.431	0.126	1.133	103.89		-17327
GPSL′	0.433	0.148	0.970	10.277		-17463
GPSL′$_{(\lambda=\theta)}$	0.701	0.212	1.780			-18571
APSL	0.642	0.251	0.842			-18323
BCM	0.786	0.439			1.486	-20565
BBPS$_{(\lambda=\theta)}$	0.690	0.209	1.786		1.495	-18556
BBPS	0.433	0.148	0.970	10.277	3.834	-17463
BAPS	0.629	0.250	0.844		1.506	-18308

Table 4.9. Real-life case-study: Estimation results.

To compare the fits of the estimated models, Table 4.10 shows the penalised-likelihood criteria. As expected, the MNL model provides the worst fit, and the Path Size models all perform significantly better. APSL outperforms GPSL′$_{(\lambda=\theta)}$ and the BAPS model outperforms the BBPS$_{(\lambda=\theta)}$ model suggesting that internal consistency can improve model fit, but more specifically by including a measure of distinctiveness within the path size contribution factors. By applying a relative bound of around 1.5 to the route costs, the BCM, and BBPS$_{(\lambda=\theta)}$ & BAPS models all improve upon the fit of their limit models MNL, GPSL′$_{(\lambda=\theta)}$, and APSL, respectively, showing the value in excluding the influence of unrealistic routes. The BBPS model, however, cannot improve upon the fit of its limit model despite it being known that unrealistic routes are present in the choice sets.

GPSL and GPSL′ (also BBPS with $\varphi \to \infty$) outperform all models, however this appears not to be by design. The PSL′ model introduced by Ben-Akiva & Bierlaire (1999) and then the GPSL model by Ramming (2002) were constructed so that, as Ramming (2002) notes, “arbitrarily long paths – which would likely not be considered by travelers – do not reduce the size of other, more reasonable paths that use the same link”, which loosely translates as so that the path size terms are attempting the capture the correlation between the realistic

alternatives only. So, if these models are aiming to reduce the contributions of unrealistic routes to the path size terms of realistic routes, then eliminating the contributions completely should improve performance. However, when the GPSL′ model is given the opportunity to eliminate contributions, i.e. with the BBPS model, the option is not taken, and the best fit comes from an unbounding φ and a large λ value. This clearly indicates that the GPSL and GPSL′ models are able to provide better fits to real data by capturing something other than the correlation between the realistic routes within the path size terms.

Duncan et al (2020) estimate the GPSL model with the same data set but without excluding the 82 route observations with relatively large travel times / lengths. As they note, the data set contains relatively costly but relatively universally distinct route observations (i.e. without considering whether or not the routes are link sharing with unrealistic alternatives), and the GPSL model is able to provide the best fit for these observations, without compromising the fit for the low costing observations. The GPSL travel cost parameter estimates are smaller than the same estimates for the other models, which improves the relative attractiveness of the costly alternatives. To counterbalance this so that that the low costing routes still remain attractive, GPSL introduces a large λ value: routes with relatively small travel costs are penalised significantly less than routes with relatively large travel costs for link sharing. Moreover, GPSL is able to further increase the relative attractiveness of the distinct, costly routes by decreasing the attractiveness of the indistinct, costly routes with the large λ. It appears then that for the GPSL and GPSL′ models to work well, they require the presence of costly routes in the choice sets so that the counterbalancing can occur, which is why the bound is all-inclusive.

What is noticeable about the estimated GPSL parameters with this reduced data set is that the travel cost parameters are slightly larger (than $\hat{\alpha}_1 = 0.415$ and $\hat{\alpha}_1 = 0.085$ from full data set), which make sense since the most relatively costly observations have been removed. The estimated λ parameter is also larger (than $\hat{\lambda} = 91.95$) which fits with the arguments above: a larger λ is required to counterbalance the small travel cost parameters (but greater than before) for the low costing routes.

Furthermore, as reported in Section 7.3.2.1 in the Sioux Falls simulation experiments, larger values of λ for the BBPS model makes estimation more unreliable/unstable. Due to the clear similarities with analogous additional λ parameters, it would be natural to assume that this is also the case for the GPSL models, further adding to the undesirability of estimating GPSL/BBPS with large λ.

The reason why the relative improvement in fit from BCM to $BBPS_{(\lambda=\theta)}$ is greater than from MNL to PSL is because PSL does not deal with unrealistic routes in the path size terms at all. It is therefore not just limited in how it can adjust for correlation compared to the bounded path size models, but also the weighted path size contribution models. When comparing relative improvement in fit from the BCM to $BBPS_{(\lambda=\theta)}$ with MNL to $GPSL'_{(\lambda=\theta)}$ (the limit model of $BBPS_{(\lambda=\theta)}$), however, the effects are of the same order of magnitude, across the range of tests i.e. for the primary estimation results in Table 4.9&Table 4.10 and re-estimation results below in Table 4.11.

	AIC	BIC	CAIC
MNL	41150	41164	41166
PSL	39820	39841	39844
GPSL	34662	34690	34694
GPSL′	34934	34961	34966
$GPSL'_{(\lambda=\theta)}$	37148	37168	37172
APSL	36652	36673	36676
BCM	41136	41157	41160
$BBPS_{(\lambda=\theta)}$	37120	37148	37152
BBPS	34936	34970	34976
BAPS	36624	36651	36656

Table 4.10. Real-life case-study: Comparison of fit between models based on penalised-likelihood criteria.

As shown in Fig. 4.18A-B, only a very small percentage of the generated routes have a relative travel time and/or length deviation greater than 1.5 (3.4% for travel time, 4.4% for length). Hence, since there are route observations with relative cost deviations close to 1.5 and thus the estimated bound parameters are close to

1.5, only a small percentage of routes generated are defined as unrealistic by the bounded models and consequently assigned zero choice probabilities / path size contributions eliminated. This restricts how effective the bounded models are at improving upon the fit of their limit models. The bounded models are however more robust (than the unbounded models) to changes in the adopted choice sets. If the choice sets are expanded, all routes generated with a relative cost deviation greater than 1.5 will have no effect upon the estimation and resultant choice probabilities of the bounded models. The unbounded models will however all be affected, and some potentially quite significantly (e.g. MNL, PSL). Generating routes with a relative cost deviation less than 1.5 will though affect the bounded models. This means though that either the choice sets were mis-generated initially, outlier observations have resulted in a large estimated bound, or the universal bound mis-represents actual OD-specific relative cost bounds, or all of these. Obtaining multiple route choice observations from the OD movements and estimating OD-specific bounds would lead to far more accurate estimated bounded models, and far greater goodness-of-fit improvements over the limit models. Moreover, it would improve robustness to the adopted choice sets.

To demonstrate how the bounded models can be more effective at improving the fit of their limit models, we re-estimate the models after removing a further 872 route observations from the data set where either the relative travel time or length deviation is over 1.2, leaving 7151 observations. This means that there are now 30.4% and 27.4% of the generated routes that have a relative travel time and length deviation, respectively, greater than the expected estimated bound of 1.2 (as opposed to previously 3.4% and 4.4% for 1.5). Hence, with more routes within the choice sets judged as being unrealistic, the negative effects of not excluding these from route choice should be greater. Table 4.11 shows the estimated parameters and Log-Likelihood values for the re-estimated models, as well as the penalised-likelihood criteria. As expected, the estimated bound parameters are approximately 1.2, apart from for the BBPS model where the estimate is very large, again approximating $\varphi \to \infty$ and the GPSL′ model. As shown, the BCM, and $BBPS_{(\lambda=\theta)}$ & BAPS models now all improve significantly more upon the fit of their limit models MNL, $GPSL'_{(\lambda=\theta)}$, and APSL, respectively.

As noted above, when 82 of the most costly observations are removed from the full data set and the GPSL model is re-estimated, the travel cost parameters increase slightly not having to provide fit for the costly observations, and the λ parameter becomes slightly larger to counterbalance within the contribution factors. As can be seen from Table 4.11 after removing a further 872 costly observations, the GPSL travel cost parameters increase significantly and hence the λ parameter increases dramatically too, supporting the trend.

	$\hat{\alpha}_1$	$\hat{\alpha}_2$	$\hat{\beta}$	$\hat{\lambda}$	$\hat{\varphi}$	LL	AIC	BIC	CAIC
MNL	1.066	1.161				-15159	30322	30336	30337
PSL	1.231	1.079	1.149			-14883	29772	29793	29796
GPSL	0.621	0.477	0.811	203.43		-13254	26516	26544	26548
GPSL′	0.633	0.519	0.696	10.962		-13301	26610	26638	26642
$GPSL'_{(\lambda=\theta)}$	0.832	0.589	1.548			-14146	28298	28319	28322
APSL	0.792	0.606	0.825			-13771	27548	27569	27572
BCM	0.973	1.049			1.194	-15050	30106	30127	30130
$BBPS_{(\lambda=\theta)}$	0.731	0.481	1.631		1.197	-13960	27928	27956	27960
BBPS	0.633	0.519	0.696	10.962	3.940	-13301	26612	26646	26651
BAPS	0.681	0.505	0.838		1.201	-13582	27172	27199	27204

Table 4.11. Real-life case-study: Re-estimation results after removing observations with relative travel time or length deviations greater than 1.2, and penalised-likelihood criteria.

8. Conclusion

This paper develops a new route choice modelling framework that deals with both route overlap and unrealistic routes in a theoretically consistent, robust, and mathematically well-defined way, and demonstrates its computational feasibility and estimatibility on large-scale networks. Path Size Logit route choice models capture the correlation between routes by including correction terms within the route utility functions. This provides a convenient closed-form solution for implementation in traffic network models. The deficiency of based Path Size Logit (PSL) model, in its sensitivity to unrealistic routes in the adopted choice sets, is well established. By weighting the contributions of routes to path size terms, current PSL model variants (e.g.

Generalised PSL (GPSL), alternative GPSL (GPSL′), & Adaptive PSL (APSL)) reduce the negative impact the unrealistic routes have upon the correction factors and thus choice probabilities of realistic routes. However, the effectiveness of this technique worsens as the choice sets are expanded and more unrealistic routes are included. In this study we develop a path size choice model that entirely eliminates the path size contributions and undesirable effects of unrealistic routes.

To tackle this, we explored the integration of PSL concepts with the recently developed Bounded Choice Model (BCM). The BCM provides a consistent criterion for determining restricted choice sets of feasible routes and route choice probability, though route correlation is not considered. This paper derives the natural form for a Bounded Path Size (BPS) model whereby path size choice model utilities are inserted into the BCM formula; however, this led to behavioural inconsistencies and/or undesirable mathematical properties, which were demonstrated by a series of examples. Five desirable properties are consequently established for a mathematically well-defined BPS model that utilises a consistent criterion for assigning zero choice probabilities to unrealistic routes while eliminating their path size contributions.

In order to solve these challenges, an alternative form for a BPS model is derived and two models are consequently formulated that adopt this form: the Bounded Bounded Path Size (BBPS) model and Bounded Adaptive Path Size (BAPS) model, which satisfy many of the desired properties, as discussed/demonstrated.

1. The BBPS model has a consistent criterion for assigning zero choice probabilities to unrealistic routes and eliminating path size contributions, but is not internally consistent. The attraction of the BBPS model, however, is that the probability relation is closed-form.
2. The BAPS model has a consistent criterion for assigning zero choice probabilities to unrealistic routes, eliminating the path size contributions of unrealistic routes, and determining route choice probabilities and path size contributions (internally consistent). The BAPS model is, however, not closed-form since the path size contribution factors are based upon choice probability ratios, and hence the probability relation is an implicit function, naturally expressed as a fixed-point problem. Two formulations for the BAPS model are given: one that has a continuous choice probability function but no formal proofs for solution existence and uniqueness, and one modified version that does not have a continuous distribution, but solutions can be proven to exist and be unique, and the proofs are given. The modified version can approximate the standard version to an arbitrary precision (i.e. by setting a very small value for the parameter τ), however, thus approximating continuity, and hence in practice we use the modified formulation with a small value of τ.

This paper proves that choice probability solutions to the BAPS model are guaranteed to exist, and provides conditions under which solutions are unique. These conditions are only sufficient conditions for uniqueness, however, and a method is proposed and demonstrated for estimating the actual uniqueness conditions.

To show that the parameters of the BBPS & BAPS models can be estimated, a Maximum Likelihood Estimation procedure is proposed for estimating the BBPS & BAPS models with tracked route observation data. Application to the Sioux Falls network shows it is generally possible to reproduce assumed true parameters. The BBPS & BAPS models are then estimated using real tracked route GPS data on a large-scale network. Results show that the $\text{BBPS}_{(\lambda=\theta)}$ and BAPS models outperform their limit models $\text{GPSL}'_{(\lambda=\theta)}$ and APSL, respectively, but that the BBPS model approximates the GPSL′ model. This indicates that the GPSL′ and GPSL models provide better fits to real data not by design but by capturing something other than the correlation between the realistic routes within the path size terms.

The BAPS model requires a fixed-point algorithm to approximate solutions. The paper assesses the computational performance of the Fixed-Point Iteration Method for calculating choice probabilities and estimating the parameters of the BAPS model, where accuracy is compared with computation time. Results indicate that accurate choice probability solutions and parameter estimates can be obtained by feasible computation times. It is also shown that BAPS model choice probability computation times can be quicker than for APSL, due to its implicit restriction of choice sets to having fewer routes.

The theory suggests that the BAPS model is more behaviourally realistic than the BBPS model, which is supported by the estimation results, and thus our recommendation is that the BAPS model is used where it is computationally feasible to do so. The BBPS model offers a more computationally practical alternative.

9. References

Abbe E, Bierlaire M, & Toledo T, (2007). Normalization and correlation of cross-nested logit models. Transportation Research Part B, 41(7), p.795-808.

Bekhor S, & Prashker J, (1999). Formulations of extended logit stochastic user equilibrium assignments. In: Proceedings of the 14th International Symposium on Transportation and Traffic Theory, Jerusalem, Israel, p.351–372.

Bekhor S, & Prashker J, (2001) Stochastic user equilibrium formulation for the generalized nested logit model. Transportation Research Record, 1752, p.84–90.

Bekhor S, Ben-Akiva M, & Ramming M, (2002). Adaptation of logit kernel to route choice situation. Transportation Research Record, 1805, p.78–85.

Bekhor S, Toledo T, & Prashker J, (2008). Effects of choice set size and route choice models on path-based traffic assignment. Transportmetrica, 4(2), p.117-133.

Ben-Akiva M, & Bolduc D, (1996). Multinomial probit with a logit kernel and a general parametric specification of the covariance structure. Working Paper.

Ben-Akiva M, & Ramming S, (1998). Lecture notes: discrete choice models of traveler behavior in networks. Prepared for Advanced Methods for Planning and Management of Transportation Networks. Capri, Italy.

Ben-Akiva M, & Bierlaire M, (1999). Discrete choice methods and their applications to short term travel decisions. In: Halled, R.W. (Ed.), Handbook of Transportation Science. Kluwer Publishers.

Bierlaire M, (2002). The Network GEV Model. Conference paper STRC 2002.

Bierlaire M, (2006). A theoretical analysis of the cross-nested logit model. Annals of operations research, 144, p.287-300.

Bliemer M & Bovy P, (2008). Impact of Route Choice Set on Route Choice Probabilities. Transportation Research Record: Journal of the Transportation Research Board, 2076, p.10–19.

Bovy P, & Fiorenzo-Catalano S, (2007). Stochastic Route Choice Set Generation: Behavioral and Probabilistic Foundations. Transportmetrica, 3, p.173–189.

Bovy P, Bekhor S, & Prato C, (2008). The Factor of Revisited Path Size: Alternative Derivation. Transportation Research Record: Journal of the Transportation Research Board, 2076, Transportation Research Board of the National Academies, Washington, D.C., p.132–140.

Bunch, D, (1991). Estimability in the multinomial probit model. Transportation Research Part B: Methodological, 25, p.1–12.

Byrd R, Lu P, Nocedal J, & Zhu C, (1995). A limited memory algorithm for bound constrained optimization. J. Sci. Comput. 16(5), p.1190–1208.

Cantarella G, & Binetti M, (2002). Stochastic assignment with gammit path choice models. Patriksson, M., Labbé's, M. (Eds.), Transportation Planning: State of the Art, p.53–68.

Cascetta E, Nuzzolo A, Russo F, & Vitetta A, (1996). A modified logit route choice model overcoming path overlapping problems: specification and some calibration results for interurban networks. In: Proceedings of the 13th International Symposium on Transportation and Traffic Theory, Leon, France, p.697–711.

Chorus C, Arentze T, & Timmermans H, (2008). A random regret-minimization model of travel choice. Transportation Research Part B, 42, p.1–18.

Chu C, (1989). A paired combinatorial logit model for travel demand analysis. In: Proc. Fifth World Conference on Transportation Research, Ventura, Calif. 4, p.295–309.

Connors R, Hess S, & Daly A, (2014). Analytic approximations for computing probit choice probabilities, Transportmetrica A: Transport Science, 10(2), p.119-139.

Daganzo C, & Sheffi Y, (1977). On stochastic models of traffic assignment. Transportation Science, 11, p.253–274.

Daly A, & Bierlaire M, (2006). A general and operational representation of Generalised Extreme Value models. Transportation Research Part B, 40, p.285–305.

Dansie, B, (1985). Parameter estimability in the multinomial probit model. Transportation Research Part B: Methodological, 19, p526–528.

Duncan L, Watling D, Connors R, Rasmussen T, & Nielsen O, (2020). Path Size Logit Route Choice Models: Issues with Current Models, a New Internally Consistent Approach, and Parameter Estimation on a Large-Scale Network with GPS Data. Transportation Research Part B, 135, p.1-40.

Gliebe J, Koppleman F, & Ziliaskopoulos A, (1999). Route choice using a paired combinatorial logit model. Presented at the 78th Annual Meeting of the Transportation Research Board, Washington, DC.

Hoogendoorn-Lanser S, van Nes R, & Bovy P, (2005). Path Size and overlap in multi-modal transport networks, a new interpretation. In Mahmassani, H.S. (Ed.), Flow, Dynamics and Human Interaction, Proceedings of the 16th International Symposium on Transportation and Traffic Theory. Elsevier, NY. p.63–84.

Isaacson E, & Keller H, (1966). Analysis of Numerical Methods. John Wiley & Sons, Inc., New York, USA.

Keane M, (1992). A note on identification in the multinomial probit model. Journal of Business & Economic Statistics, 10, p.193–200.

Kitthamkesorn S, & Chen A, (2013). Path-size weibit stochastic user equilibrium model. Transportation Research Part B, 57, p.378-397.

Lai X & Bierlaire M, (2015). Specification of the cross-nested logit model with sampling of alternatives for route choice models. Transportation Research Part B, 80, p.220-234.

Marzano V & Papola A, (2008). On the covariance structure of the cross-nested logit model. Transportation Research Part B, 42(2), p.83–98.

McFadden D, & Train K, (2000). Mixed MNL models for discrete response. Journal of Applied Econometrics, 15 (5), p.447–470.

Nielsen O, (2000). A Stochastic Transit Assignment Model Considering Differences in Passengers Utility Functions. Transportation Research Part B Methodological, 34(5), p.377–402. Elsevier Science Ltd.

Prashker J & Bekhor S, (2004). Route choice models used in the stochastic user equilibrium problem: a review. Transport reviews, 24(4), p.437-463.

Prato C, (2005). Latent factors and route choice behaviour. Ph.D. Thesis, Turin, Polytechnic, Italy.

Prato C, (2014). Expanding the applicability of random regret minimization for route choice analysis. Transportation, 41, p.351–375.

Prato C, Rasmussen T, & Nielsen O, (2014). Estimating Value of Congestion and of Reliability from Observation of Route Choice Behavior of Car Drivers. Transportation Research Record: Journal of the Transportation Research Board, 2412, p.20-27.

Prato C & Bekhor S, (2006). Applying branch & bound technique to route choice set generation. Transportation Research Record, 1985, p.19-28.

Pravinvongvuth S, & Chen A, (2005). Adaptation of the paired combinatorial logit model to the route choice problem. Transportmetrica, 1 (3), p.223–240.

Ramming S, (2002). Network knowledge and route choice. Ph.D. Thesis, Massachusetts Institute of Technology, Cambridge, USA.

Rasmussen T, Nielsen O, Watling D, & Prato C, (2016). The Restricted Stochastic User Equilibrium with Threshold model: Large-scale application and parameter testing. European Journal of Transport Infrastructure Research (EJTIR). 17 (1), p.1-24

Rosa, A (2003). Probit based methods in traffic assignment and discrete choice modelling, (unpublished PhD Thesis), Napier University.

Vovsha P, (1997). Application of cross-nested logit model to mode choice in Tel Aviv, Israel, Metropolitan Area. Transportation Research Record 1607, p.6–15.

Watling D, Rasmussen T, Prato C, & Nielsen O, (2018). Stochastic user equilibrium with a bounded choice model. Transportation Research Part B, 114, p.254-280.

Wen C, & Koppelman F, (2001). The generalized nested logit model. Transportation Research Part B, 35 (7), p.627–641.

Xu X, Chen A, Kitthamkesorn S, Yang H, & Lo H.K, (2015). Modeling absolute and relative cost differences in stochastic user equilibrium problem. Transportation Research Part B, 81, p.686-703.

10. Appendix

10.1 Appendix A – Derivation of the Bounded Choice Model

First, we define the pdf's and cdf's of relevant probability distributions. The pdf of a Gumbel distribution with mode ζ and scale θ^{-1} ($\theta > 0$) is:

$$f_G(x;\zeta,\theta) = \theta \exp\Big(-\big(\theta(x-\zeta) + \exp\big(-\theta(x-\zeta)\big)\big)\Big), \qquad (-\infty < x < \infty),$$

and the cdf is:

$$F_G(x;\zeta,\theta) = \exp\big(-\exp\big(-\theta(x-\alpha)\big)\big), \qquad (-\infty < x < \infty).$$

Supposing that ϵ_1 and ϵ_2 are individually and identically distributed Gumbel random variables, the difference random variable $\varepsilon = \epsilon_1 - \epsilon_2$ is a logistic distribution with pdf (for mean μ and scale θ^{-1}) equal to:

$$f_L(x;\mu,\theta) = \theta \exp\big(-\theta(x-\mu)\big)\big(1+\exp\big(-\theta(x-\mu)\big)\big)^{-2}, \qquad (-\infty < x < \infty),$$

and cdf:

$$F_L(x;\mu,\theta) = \big(1+\exp\big(-\theta(x-\mu)\big)\big)^{-1}, \qquad (-\infty < x < \infty).$$

If ϵ_1 and ϵ_2 have mode 0 and scale θ^{-1} it follows that ε has mean 0 and scale θ^{-1}.

The BCM proposes that each route $i \in R$ is compared with an imaginary reference alternative r^* in terms of difference in random utility, and imposes a bound, ψ, upon this random utility difference. In this study, the reference alternative is the route with the best utility. If U_i and V_i are the random and deterministic utilities for route $i \in R$, respectively, the difference in random utility relative to the reference alternative for route $i \in R$ is:

$$U_{r^*} - U_i = V_{r^*} + \epsilon_{r^*} - V_i - \epsilon_i = \max(V_l : l \in R) - V_i + \epsilon_{r^*} - \epsilon_i = \max(V_l : l \in R) - V_i + \varepsilon_i,$$

where ϵ_i is the individually and identically distributed random variable error term for route $i \in R$, and ε_i is the difference random variable for route $i \in R$ with the reference alternative. The MNL model can be derived by assuming the ϵ_i error terms are Gumbel distributed and thus the ε_i difference random error terms assume the logistic distribution. The BCM, however, proposes that the difference random variable error terms ε_i assume a truncated logistic distribution, obtained by left-truncating a logistic distribution with mean 0 and scale θ^{-1} at a lower bound of $-\psi$ for some $\psi \geq 0$. Each of these variables thus has pdf:

$$f_T(x;\mu,\theta,\psi) = \begin{cases} 0 & -\infty < x < -\psi \\ \dfrac{f_L(x;\mu,\theta)}{1-F_L(-\psi;\mu,\theta)} & x \geq -\psi \end{cases},$$

and cdf:

$$F_T(x;\mu,\theta,\psi) = \begin{cases} 0 & -\infty < x < -\psi \\ \dfrac{F_L(x;\mu,\theta) - F_L(-\psi;\mu,\theta)}{1-F_L(-\psi;\mu,\theta)} & x \geq -\psi \end{cases}.$$

The probability of choosing route $i \in R$ versus the reference alternative is therefore:

$$\Pr(\text{choosing } i \text{ from } \{i, r^*\}) = \Pr(U_i \geq U_{r^*}) = \Pr(U_{r^*} - U_i \leq 0)$$
$$= \Pr(\max(V_l : l \in R) - V_i + \varepsilon_i \leq 0) = \Pr(\varepsilon_i \leq V_i - \max(V_l : l \in R))$$
$$= F_T(V_i - \max(V_l : l \in R)\,; 0, \theta, \psi)$$
$$= \begin{cases} 0 & -\infty < V_i - \max(V_l : l \in R) < -\psi \\ \dfrac{F_L(V_i - \max(V_l : l \in R)\,; 0, \theta) - F_L(-\psi; 0, \theta)}{1-F_L(-\psi; 0, \theta)} & V_i - \max(V_l : l \in R) \geq -\psi \end{cases},$$
$$= \begin{cases} 0 & -\infty < V_i - \max(V_l : l \in R) < -\psi \\ \dfrac{\big(1+\exp\big(-\theta(V_i - \max(V_l : l \in R))\big)\big)^{-1} - (1+\exp(\theta\psi))^{-1}}{1-(1+\exp(\theta\psi))^{-1}} & V_i - \max(V_l : l \in R) \geq -\psi \end{cases}.$$

The odds ratio for route $i \in R$ versus the reference alternative $r^* \in R$ is then:

$$\eta_i = \frac{\Pr(\text{choosing } i \text{ from } \{i, r^*\})}{1 - \Pr(\text{choosing } i \text{ from } \{i, r^*\})} = \frac{F_T(V_i - \max(V_l : l \in R)\,; 0, \theta, \psi)}{1 - F_T(V_i - \max(V_l : l \in R)\,; 0, \theta, \psi)}.$$

For $V_i - \max(V_l : l \in R) \geq -\psi$, η_i can be re-arranged as follows:

$$\frac{\frac{1}{\left(1+\exp\left(-\theta(V_i-\max(V_l:l\in R))\right)\right)}-\frac{1}{(1+\exp(\theta\psi))}}{\frac{1}{1}-\frac{1}{(1+\exp(\theta\psi))}}}{1-\frac{\frac{1}{\left(1+\exp\left(-\theta(V_i-\max(V_l:l\in R))\right)\right)}-\frac{1}{(1+\exp(\theta\psi))}}{\frac{1}{1}-\frac{1}{(1+\exp(\theta\psi))}}}$$

$$=\frac{\frac{\exp(\theta\psi)-\exp\left(-\theta(V_i-\max(V_l:l\in R))\right)}{\left(1+\exp\left(-\theta(V_i-\max(V_l:l\in R))\right)\right)(1+\exp(\theta\psi))}}{\frac{\exp(\theta\psi)}{(1+\exp(\theta\psi))}}}{1-\frac{\frac{\exp(\theta\psi)-\exp\left(-\theta(V_i-\max(V_l:l\in R))\right)}{\left(1+\exp\left(-\theta(V_i-\max(V_l:l\in R))\right)\right)(1+\exp(\theta\psi))}}{\frac{\exp(\theta\psi)}{(1+\exp(\theta\psi))}}}$$

$$=\frac{\frac{\left(\exp(\theta\psi)-\exp\left(-\theta(V_i-\max(V_l:l\in R))\right)\right)}{\left(1+\exp\left(-\theta(V_i-\max(V_l:l\in R))\right)\right)\exp(\theta\psi)}}{\frac{1}{1}-\frac{\left(\exp(\theta\psi)-\exp\left(-\theta(V_i-\max(V_l:l\in R))\right)\right)}{\left(1+\exp\left(-\theta(V_i-\max(V_l:l\in R))\right)\right)\exp(\theta\psi)}}$$

$$=\frac{\frac{\left(\exp(\theta\psi)-\exp\left(-\theta(V_i-\max(V_l:l\in R))\right)\right)}{\left(1+\exp\left(-\theta(V_i-\max(V_l:l\in R))\right)\right)\exp(\theta\psi)}}{\frac{\exp\left(-\theta(V_i-\max(V_l:l\in R))\right)\exp(\theta\psi)+\exp\left(-\theta(V_i-\max(V_l:l\in R))\right)}{\left(1+\exp\left(-\theta(V_i-\max(V_l:l\in R))\right)\right)\exp(\theta\psi)}}$$

$$=\frac{\exp(\theta\psi)-\exp\left(-\theta(V_i-\max(V_l:l\in R))\right)}{\exp\left(-\theta(V_i-\max(V_l:l\in R))\right)\exp(\theta\psi)+\exp\left(-\theta(V_i-\max(V_l:l\in R))\right)}$$

$$=\frac{\exp(\theta\psi)\exp\left(\theta(V_i-\max(V_l:l\in R))\right)-1}{\exp(\theta\psi)+1}$$

$$=\frac{\exp\left(\theta(V_i-\max(V_l:l\in R)+\psi)\right)-1}{\exp(\theta\psi)+1}.$$

Thus, given the above re-arranging, the odds ratio η_i for route $i\in R$ versus the reference alternative $r^*\in R$ is:

$$\eta_i=\begin{cases}0 & -\infty<V_i-\max(V_l:l\in R)<-\psi\\ \dfrac{\exp\left(\theta(V_i-\max(V_l:l\in R)+\psi)\right)-1}{\exp(\theta\psi)+1} & V_i-\max(V_l:l\in R)\geq-\psi\end{cases},$$

which can be written succinctly as:

$$\eta_i=\frac{\left(\exp\left(\theta(V_i-\max(V_l:l\in R)+\psi)\right)-1\right)_+}{\exp(\theta\psi)+1},$$

where $(\cdot)_+=\max(0,\cdot)$.

Now, due to the Independence from Irrelevant Alternatives (IIA) property, the probability ratio between any two routes $i,j\in R$ where $P_i>0$ and $P_j>0$ is the ratio of the odds ratios:

$$\frac{P_i}{P_j}=\frac{\eta_i}{\eta_j}=\frac{\frac{\Pr(\text{choosing } i \text{ from } \{i,r^*\})}{1-\Pr(\text{choosing } i \text{ from } \{i,r^*\})}}{\frac{\Pr(\text{choosing } j \text{ from } \{j,r^*\})}{1-\Pr(\text{choosing } j \text{ from } \{j,r^*\})}}$$

$$= \frac{\left(\exp\left(\theta\left(V_i - \max(V_l : l \in R) + \psi\right)\right) - 1\right)_+}{\left(\exp\left(\theta\left(V_j - \max(V_l : l \in R) + \psi\right)\right) - 1\right)_+}.$$

Thence, since the non-zero probabilities must add up to 1, the BCM probability for route $i \in R$ is:

$$P_i = \frac{\left(\exp\left(\theta\left(V_i - \max(V_l : l \in R) + \psi\right)\right) - 1\right)_+}{\sum_{j \in R}\left(\exp\left(\theta\left(V_j - \max(V_l : l \in R) + \psi\right)\right) - 1\right)_+}.$$

Finally, setting $\psi = (1 - \varphi)\max(V_l : l \in R)$:

$$P_i = \frac{\left(\exp\left(-\theta\left(V_i - \varphi \max(V_l : l \in R)\right)\right)\right)_+}{\sum_{j \in R}\left(\exp\left(-\theta\left(V_j - \varphi \max(V_l : l \in R)\right)\right)\right)_+}.$$

10.2 Appendix B – Derivation of Proposed BPS Model Form

Suppose the probability of choosing route $i \in R$ relates as:

$$P_i = Q_i^1 \times Q_i^2 \times \chi,$$

where

$$Q_i^1 = \frac{\left(\exp\left(-\theta\left(c_i - \varphi \min(c_l : l \in R)\right)\right) - 1\right)_+}{\sum_{j \in R}\left(\exp\left(-\theta\left(c_j - \varphi \min(c_l : l \in R)\right)\right) - 1\right)_+}, \qquad Q_i^2 = \frac{e^{\beta \ln(\gamma_i)}}{\sum_{j \in R} e^{\beta \ln(\gamma_j)}},$$

and χ is a normalisation constant. The probabilities for all routes $r \in R$ must add up to 1:

$$\sum_{r \in R} P_r = \sum_{r \in R} Q_r^1 \times Q_r^2 \times \chi = \left(\sum_{r \in R} \frac{\left(\exp\left(-\theta\left(c_r - \varphi \min(c_l : l \in R)\right)\right) - 1\right)_+ e^{\beta \ln(\gamma_r)}}{\sum_{j \in R}\left(\exp\left(-\theta\left(c_j - \varphi \min(c_l : l \in R)\right)\right) - 1\right)_+ \sum_{j \in R} e^{\beta \ln(\gamma_j)}}\right) \times \chi = \left(\sum_{r \in R} \frac{X_r}{L}\right) \times \chi = 1,$$

where to simplify notation:

$$X_r = \left(\exp\left(-\theta\left(c_r - \varphi \min(c_l : l \in R)\right)\right) - 1\right)_+ e^{\beta \ln(\gamma_r)},$$

and

$$L = \sum\nolimits_{j \in R}\left(\exp\left(-\theta\left(c_j - \varphi \min(c_l : l \in R)\right)\right) - 1\right)_+ \sum\nolimits_{j \in R} e^{\beta \ln(\gamma_j)}.$$

By rearranging, the normalisation constant χ is thus:

$$\chi = \left(\sum_{r \in R} \frac{X_r}{L}\right)^{-1}.$$

Substituting χ back into the probability relation for route $i \in R$:

$$P_i = Q_i^1 \times Q_i^2 \times \chi = \frac{X_i}{L} \times \left(\sum_{r \in R} \frac{X_r}{L}\right)^{-1} = \frac{X_i}{L} \times \left(\frac{1}{L}\sum_{r \in R} X_r\right)^{-1} = \frac{X_i}{L} \times \frac{L}{\sum_{r \in R} X_r} = \frac{X_i}{\sum_{r \in R} X_r}$$

$$= \frac{\left(\exp\left(-\theta\left(c_i - \varphi \min(c_l : l \in R)\right)\right) - 1\right)_+ \cdot e^{\beta \ln(\gamma_i)}}{\sum_{r \in R}\left(\exp\left(-\theta\left(c_r - \varphi \min(c_l : l \in R)\right)\right) - 1\right)_+ \cdot e^{\beta \ln(\gamma_r)}}.$$

10.3 Appendix C – Desired Properties for a Bounded Path Size Model

In this section, we establish desired properties for a BPS model by exploring different options for the path size terms for the natural BPS model in (4.5).

10.3.1 Option 1

Suppose that the path size term for route $i \in R$ is defined as follows:

$$\gamma_i^1 = \sum_{a \in A_i} \frac{t_a}{c_i} \frac{1}{\sum_{k \in R} \delta_{a,k}}. \tag{4.26}$$

The option 1 path size term, γ_i^1, is equivalent to the PSL path size term. As (4.26) shows, all routes in the choice set contribute equally to path size terms, however unattractive, and thus unrealistic routes (with zero choice probabilities) negatively impact the choice probabilities of realistic routes (with non-zero choice probabilities) if links are shared. To demonstrate this, consider example network 4 in Fig. 4.25A where there are 3 routes: Routes 2&3 have travel cost 1 and Route 1 has travel cost $0.5 + \upsilon$, Routes 1&2 are correlated while Route 3 is distinct. Fig. 4.25B displays the example network 4 option 1 BPS model route choice probabilities as υ is increased from 0.5 to 3, $\theta = \beta = 1$, $\varphi = 2.5$. For $\upsilon = 0.5$, Routes 1&2 have the same unshared travel cost and are thus considered equally attractive. As υ is increased, Route 1 increases in travel cost and decreases in utility. As the utility of Route 1 becomes 2.5 times smaller than the utility of Route 3 (the best alternative), Route 1 attains zero choice probability, but continues to contribute to the path size term of Route 2, which is not desired.

We thus establish the following desired property for a BPS model:

Desired Property 1 – Consistent Definitions of Unrealistic Routes: *Routes defined as unrealistic by the choice model (assigned zero choice probabilities) should have zero path size contributions, and vice versa.*

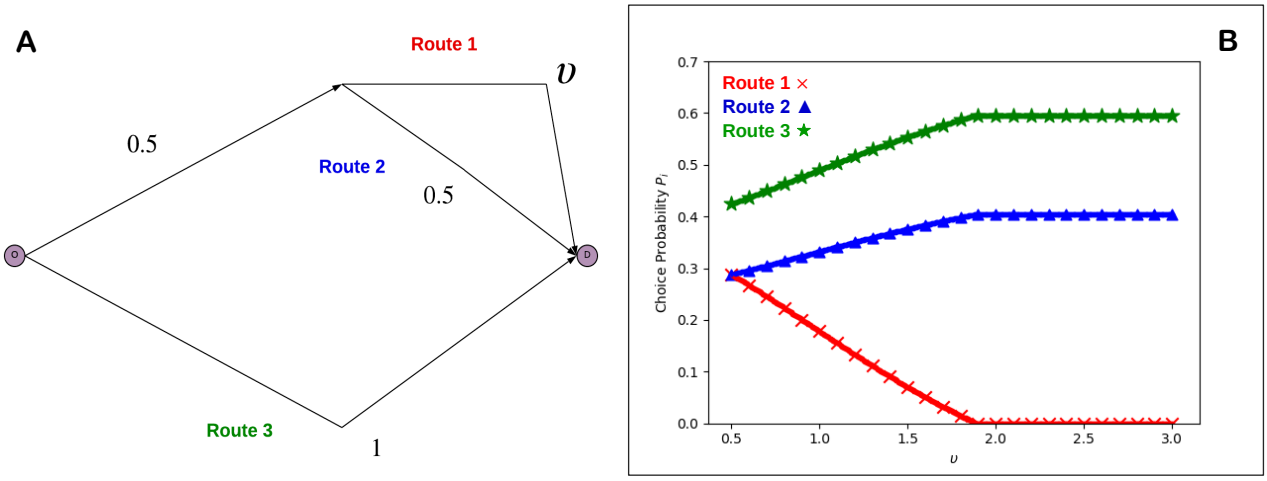

Fig. 4.25. A: Example network 4. B: Example network 4: Option 1 BPS model route choice probabilities for increasing υ ($\theta = \beta = 1$, $\varphi = 2.5$).

10.3.2 Options 2&3

Option 1 clarifies that routes defined as unrealistic by the path size terms should have no path size contributions. We explore in options 2&3 below how this might be achieved. However, there is a practical issue for both options that complicates matters. Allowing path size contributions to be zero means that: a) scenarios of $\frac{0}{0}$ can occur within the path size terms; and, b) path size terms can equal zero which consequently results in occurrences of $\ln(0)$ within the route utilities. The $\ln(0)$ issue can be circumvented by negligibly perturbing path size terms that equal zero (by $0 < \tau \ll 1$ say), so that the utility of route $i \in R$ is $V_i = -\theta c_i + \beta \ln((\gamma_i - \tau)_+ + \tau)$. $\ln(0)$ within a route utility implies that that the route is infinitely unattractive, and hence it can be concluded that the route is outside the bound and assigned zero choice probability. A suitably low value for τ will ensure utilities with zero path size terms are finite but small enough to violate the bound, and for the demonstrations below we set $\tau = 10^{-16}$. The $\frac{0}{0}$ issue, however, cannot be completely circumvented. In order to use options 2&3, one must specify how the path size terms deal with $\frac{0}{0}$, and with each option there is no single formulation that ensures continuity, as we will show. Nevertheless, we present here their formulations as simply as possible for pedagogical purposes only.

10.3.2.1 Option 2

Suppose that the path size term for route $i \in R$ is defined as follows:

$$\gamma_i^2 = \sum\nolimits_{a\in A_i} \frac{t_a}{c_i} \frac{(h_i(-\theta \boldsymbol{c};\omega)-1)_+}{\sum_{k\in R}(h_k(-\theta \boldsymbol{c};\omega)-1)_+\delta_{a,k}}, \tag{4.27}$$

where $h_i(-\theta \boldsymbol{c};\omega) = \exp(-\theta c_i - \omega \max(-\theta c_l: l \in R)) = \exp\big(-\theta(c_i - \omega \min(c_l: l \in R))\big)$, and $\omega > 1$ is the path size contribution bound parameter. Option 2 supposes that routes only contribute to path size terms if they have a cost less than ω times the cost on the cheapest route, and the path size contribution factors consider ratios of the odds that routes are within this path size contribution bound. As (4.27) shows, route k only contributes to path size terms if $c_k < \omega \min(c_l: l \in R)$, and as the cost of a route decreases below the contribution bound its path size contribution increases.

Option 2 has two main failings. The first main failing is the practical issue discussed above. If no routes using link a have a cost within the contribution bound, then $\sum_{k\in R}(h_k(-\theta \boldsymbol{c};\omega)-1)_+\delta_{a,k} = 0$ and $\frac{0}{0}$ occurs. Furthermore, if route i has a cost above the contribution bound (i.e. $(h_i(-\theta \boldsymbol{c};\omega)-1)_+ = 0$) but for all links in route i at least one route has a cost within the contribution bound (i.e. $\sum_{k\in R}(h_k(-\theta \boldsymbol{c};\omega)-1)_+\delta_{a,k} > 0$, $\forall a \in A_i$), then $\gamma_i^2 = 0$ and $\ln(0)$ occurs in V_i. In order to use option 2, one must specify how γ_i^2 is formulated for $\sum_{k\in R}(h_k(-\theta \boldsymbol{c};\omega)-1)_+\delta_{a,k} = 0$ (to avoid occurrences of $\frac{0}{0}$). There are three alternative formulations for γ_i^2:

$$\gamma_i^2 = \sum\nolimits_{a\in A_i} \frac{t_a}{c_i} \times \begin{cases} \dfrac{(h_i(-\theta \boldsymbol{c};\omega)-1)_+}{\sum_{k\in R}(h_k(-\theta \boldsymbol{c};\omega)-1)_+\delta_{a,k}} & if \sum_{k\in R}(h_k(-\theta \boldsymbol{c};\omega)-1)_+\delta_{a,k} > 0 \\ Y & if \sum_{k\in R}(h_k(-\theta \boldsymbol{c};\omega)-1)_+\delta_{a,k} = 0 \end{cases},$$

where Y has three alternative values, equal to either 0, 1, or $\frac{1}{\sum_{k\in R}\delta_{a,k}}$, depending on how $\frac{(h_i(-\theta \boldsymbol{c};\omega)-1)_+}{\sum_{k\in R}(h_k(-\theta \boldsymbol{c};\omega)-1)_+\delta_{a,k}} \to \frac{0}{0}$.

The second main failing is that the model is internally inconsistent with how routes are defined as being (un)realistic. The natural BPS model probability relation in (4.5) bounds the route utilities so that routes with a relatively unattractive combination of travel cost and distinctiveness are assigned zero choice probabilities. The option 2 path size terms, however, define a route as unrealistic if it has a large travel cost only, and subsequently bound the route costs so that expensive routes have zero path size contributions. The option 2 path size terms thus potentially result in an inconsistent model, as routes with non-zero choice probabilities may have zero path size contributions, and/or vice versa. To demonstrate, consider example network 4 in Fig. 4.25A. Fig. 4.26A-B display example network 4 option 2 BPS model choice probabilities for $\omega = 1.5$ and $\omega = 3$, respectively, as v is increased from 0.5 to 3, $Y = \theta = \beta = 1$, $\varphi = 2.5$. In Fig. 4.26A, as the path size contribution bound parameter is more restrictive than the model bound, the path size contribution of Route 1 to Route 2 is eliminated before Route 1 reaches zero choice probability. Conversely in Fig. 4.26B, as the contribution bound is less restrictive than the model bound, Route 1 reaches zero probability before its contribution to Route 2 is eliminated.

Option 2 also requires the estimation of an additional bound parameter, which makes estimation more difficult, and which can amplify the inconsistency of the model due to the different bound considerations. It is possible that the model bound and path size contribution bound could equate ($\omega = \varphi$), so that routes have zero choice probabilities and/or zero path size contributions if they have a utility/cost φ times worse than the best respective route, but there is no real theoretical basis for this. Fig. 4.26C displays example network 4 option 2 BPS model choice probabilities as v is increased from 0.5 to 3, with $\omega = \varphi = 2.5$, $Y = \theta = \beta = 1$. As shown, internal inconsistency still occurs with equated bounds. This does though at least decrease the number of parameters for estimation. The inconsistency of the resultant option 2 model is amplified if the two bound parameters φ and ω have significantly different restrictions on the assessed feasibility of routes, as Fig. 4.26A-B show. If the model bound φ is restrictive so that very few routes have non-zero choice probabilities, but the contribution bound is unrestrictive so that many routes have non-zero path size contributions, or vice versa, then the model is clearly more inconsistent than if the two bound parameters were similarly restricting.

From exploring option 2, we establish the following desired properties for a BPS model:

Desired Property 2 – Well-Defined Functions: *The model functions should be well-defined across their domain.*

Desired Property 3 – Internal Consistency: *The model should be internally consistent, i.e. there is a consistent assessment of the feasibility of routes between probability relation and path size contribution factors.*

Specifically, Desired Property 2 covers the avoidance of occurrences of $\frac{0}{0}$ in the path size terms / $\ln(0)$ within the route utilities, which occur naturally when routes have zero path size contributions, as shown above and below. It is worth noting that satisfying Desired Property 3 – Internal Consistency is enough to satisfy Desired Property 1 – Consistent Definitions of Unrealistic Routes, but the vice versa is not true, as shown in Section 10.3.3.

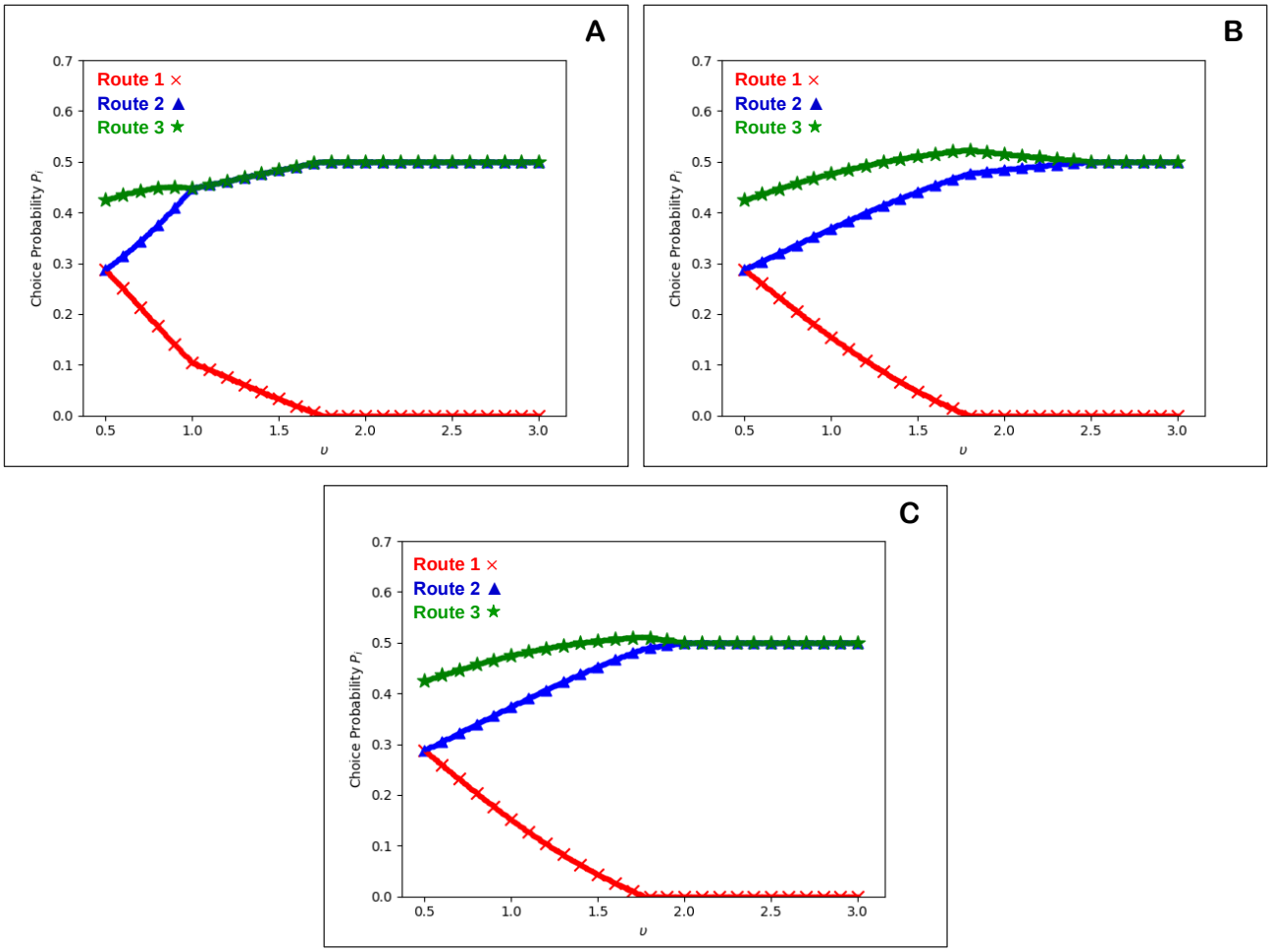

Fig. 4.26. Example network 4: Option 2 BPS model route choice probabilities for increasing υ ($Y = \theta = \beta = 1$, $\varphi = 2.5$). **A:** $\omega = 1.5$. **B:** $\omega = 3$. **C:** $\omega = 2.5$

10.3.2.2 Option 3

Suppose that the path size term for route $i \in R$ is defined as follows:

$$\gamma_i^3(\boldsymbol{P}) = \sum_{a \in A_i} \frac{t_a}{c_i} \frac{P_i}{\sum_{k \in R} P_k \delta_{a,k}} = \sum_{a \in A_i} \frac{t_a}{c_i} \frac{1}{\sum_{k \in R} \left(\frac{P_k}{P_i}\right) \delta_{a,k}}, \tag{4.28}$$

where $\boldsymbol{P}$ is a route choice probability vector, and the option 3 BPS model choice probabilities, $\boldsymbol{P}^*$, are a solution to the fixed-point problem $\boldsymbol{P} = \boldsymbol{H}\left(\boldsymbol{\gamma}^3(\boldsymbol{P})\right)$ in D, where:

$$H_i\left(\boldsymbol{\gamma}^3(\boldsymbol{P})\right) = \frac{\left(h_i\left(-\theta \boldsymbol{c} + \beta \ln\left(\boldsymbol{\gamma}^3(\boldsymbol{P})\right)\right) - 1\right)_+}{\sum_{j \in R}\left(h_j\left(-\theta \boldsymbol{c} + \beta \ln\left(\boldsymbol{\gamma}^3(\boldsymbol{P})\right)\right) - 1\right)_+}, \qquad \forall i \in R.$$

The option 3 path size terms propose that routes contribute according to ratios of choice probability, and thus the resultant model is internally consistent. The probability relation is an implicit function involving the

choice probabilities, and solutions to the model are solutions to the fixed-point problem. Whereas the APSL domain for choice probability solutions, $D^{(\tau)}$, does not allow routes to have zero choice probabilities, the option 3 BPS model domain, D, does allow for zero probabilities. This is a requirement since the model assigns zero choice probabilities / eliminates the path size contributions of routes with infeasibly low utilities. With this though, $\frac{0}{0}$ occurs in the path size terms when $\sum_{k\in R} P_k\delta_{a,k} = 0$, and $\ln(0)$ occurs in the route utilities when $P_i = 0$ and $\sum_{k\in R;k\neq i} P_k\delta_{a,k} > 0$ for all $a \in A_i$. In order to use option 3. one must specify how γ_i^3 is formulated for $\sum_{k\in R} P_k\delta_{a,k} = 0$. There are again three alternative formulations for γ_i^3:

$$\gamma_i^3 = \sum_{a\in A_i} \frac{t_a}{c_i} \times \begin{cases} \frac{P_i}{\sum_{k\in R} P_k\delta_{a,k}} & if \sum_{k\in R} P_k\delta_{a,k} > 0 \\ Y & if \sum_{k\in R} P_k\delta_{a,k} = 0 \end{cases},$$

where Y has three alternative values, equal to either 0, 1, or $\frac{1}{\sum_{k\in R}\delta_{a,k}}$, depending on how $\frac{P_i}{\sum_{k\in R} P_k\delta_{a,k}} \to \frac{0}{0}$.

Option 3 has two other main failings. The first of which is the unconditional non-uniqueness of solutions. The 'active choice set' is the restricted choice set of routes with non-zero choice probabilities. In the case of the option 3 BPS model, there are two types of solution non-uniqueness: *inter-active-choice-set non-uniqueness* and *intra-active-choice-set non-uniqueness*. Intra-active-choice-set non-uniqueness is where there are multiple choice probability solutions within the active choice sets, and inter-active-choice-set non-uniqueness is where there are multiple solutions between active choice sets. Inter-active-choice-set non-uniqueness is much more problematic than intra-active-choice-set non-uniqueness, and having a single active choice set where multiple choice probability solutions exist is more manageable than having multiple active choice sets where solutions exist. If there is just one active choice set where solutions exist, then at least it is known which routes are defined as unrealistic, and it's possible that there will be some conditions under which solutions within the active choice set are unique. However, if it is possible for multiple active choice sets to have solutions, then it is unlikely that uniqueness conditions can be established (conditions under which there is only ever one active choice set with solutions), and an active choice set selection procedure is required.

Inter-active-choice-set non-uniqueness occurs extensively for the option 3 BPS model due to the route utilities not being fixed and the potential for them to vary massively according to the active choice set. Without fixed utilities, the maximum utility route(s) and value can vary, and different routes can have utilities within the bound. To demonstrate, consider example network 5 in Fig. 4.27 where there are 5 routes; Table 4.12 gives the route information. As Fig. 4.27 shows, Routes 1-4 are correlated, and Route 5 is distinct. Using an exhaustive search for active choice set solutions, Table 4.13, Table 4.14, & Table 4.15 display all of the BPS model option 3 choice probability solutions for $Y = 0$, $Y = 1$, and $Y = \frac{1}{\sum_{k\in R}\delta_{a,k}}$, respectively, for $\theta = \beta = 1$, $\varphi = 2$. $\bar{R} \subseteq R$ is the restricted choice set of active routes. There are 17, 3, and 5 active choice sets in which solutions exist for $Y = 0$, $Y = 1$, and $Y = \frac{1}{\sum_{k\in R}\delta_{a,k}}$, respectively. For these parameter settings there is intra-active-choice-set uniqueness. However, to demonstrate how there can also be intra-active-choice-set non-uniqueness, Table 4.16 displays two BPS model option 3 choice probability solutions for the active choice set $\bar{R} = \{1,2,5\}$, with $Y = 0$, $\theta = 1$, and $\beta = \varphi = 5$.

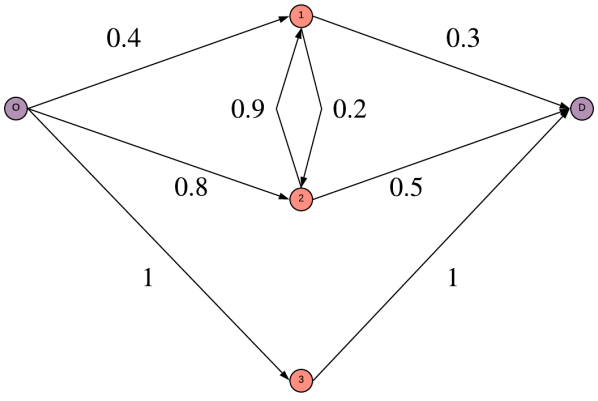

Fig. 4.27. Example network 5.

Route	Node Traversal	Travel Cost
1	$O \to 1 \to D$	0.7
2	$O \to 1 \to 2 \to D$	1.1
3	$O \to 2 \to 1 \to D$	2
4	$O \to 2 \to D$	1.3
5	$O \to 3 \to D$	2

Table 4.12. Example network 5 route information.

$\bar{R}$	P_1	P_2	P_3	P_4	P_5	$\bar{R}$	P_1	P_2	P_3	P_4	P_5
{5}	0	0	0	0	1	{2,4}	0	0.590	0	0.410	0
{4}	0	0	0	1	0	{2,4,5}	0	0.498	0	0.346	0.156
{4,5}	0	0	0	0.765	0.235	{2,3}	0	0.901	0.099	0	0
{3}	0	0	1	0	0	{2,3,5}	0	0.819	0.09	0	0.09
{3,5}	0	0	0.5	0	0.5	{2,3,4}	0	0.610	0.026	0.365	0
{3,4}	0	0	0.101	0.899	0	{2,3,4,5}	0	0.517	0.022	0.309	0.153
{3,4,5}	0	0	0.076	0.676	0.249	{1}	1	0	0	0	0
{2}	0	1	0	0	0	{1,4}	0.906	0	0	0.094	0
{2,5}	0	0.901	0	0	0.099						

Table 4.13. Example network 5: All option 3 BPS model choice probabilities solutions ($Y = 0$, $\theta = \beta = 1$, $\varphi = 2$).

$\bar{R}$	P_1	P_2	P_3	P_4	P_5
{2,3,5}	0	0.819	0.09	0	0.09
{2,3,4,5}	0	0.517	0.022	0.309	0.153
{1,4}	0.906	0	0	0.094	0

Table 4.14. Example network 5: All option 3 BPS model choice probabilities solutions ($Y = 1$, $\theta = \beta = 1$, $\varphi = 2$).

$\bar{R}$	P_1	P_2	P_3	P_4	P_5
{2,5}	0	0.901	0	0	0.099
{2,3,5}	0	0.819	0.09	0	0.09
{2,3,4,5}	0	0.517	0.022	0.309	0.153
{1}	1	0	0	0	0
{1,4}	0.906	0	0	0.094	0

Table 4.15. Example network 5: All option 3 BPS model choice probabilities solutions ($Y = \frac{1}{\sum_{k \in R} \delta_{a,k}}$, $\theta = \beta = 1$, $\varphi = 2$).

P_1	P_2	P_3	P_4	P_5
0.009	0.703	0	0	0.288
0.698	0.066	0	0	0.235

Table 4.16. Example network 5: Option 3 BPS model choice probabilities solutions for $\bar{R} = \{1,2,5\}$ ($Y = 0$, $\theta = 1$, $\beta = \varphi = 5$).

Another main failing for the option 3 model is that the choice probability function is not always continuous. The option 3 BPS model has trajectories of choice probability solutions as the φ bound parameter is varied. For a given trajectory of solutions, as φ is decreased, route utilities approach the bound from below resulting in the choice probabilities and thus path size contributions approaching zero. However, since the utilities are not fixed, and are dependent upon φ, it is possible for the utility of a route to meet the bound (as φ is decreased) before its path size contribution to routes meets zero, and as a consequence, the choice probability function is not always continuous in φ. To demonstrate, consider again example network 5 in Fig. 4.27. To identify a trajectory of option 3 BPS model solutions for varying φ we utilise the following method.

Step 1. Identify a suitably large value for φ such that the option 3 BPS model solution will have a non-zero choice probability for all routes.

Step 2. Solve the option 3 BPS model fixed-point problem for this large φ with a randomly generated initial condition.

Step 3. Decrement φ and obtain the next solution with initial condition set as the solution for the previous φ.

Step 4. Continue until $\varphi = 1$.

Utilising the above method and plotting the probabilities at each decremented φ, Fig. 4.28 displays a trajectory of option 3 BPS model choice probability solutions as φ is varied, $Y = \theta = \beta = 1$. As φ is decreased, the utility of Route 3 approaches the bound and zero choice probability. However, the utility of Route 3 reaches the bound before the path size contribution of Route 3 to Routes 1&4 reaches zero. Thus, due to the sizeable adjustment of the utilities when Route 3 is removed from the active choice set, the choice probability function is not continuous.

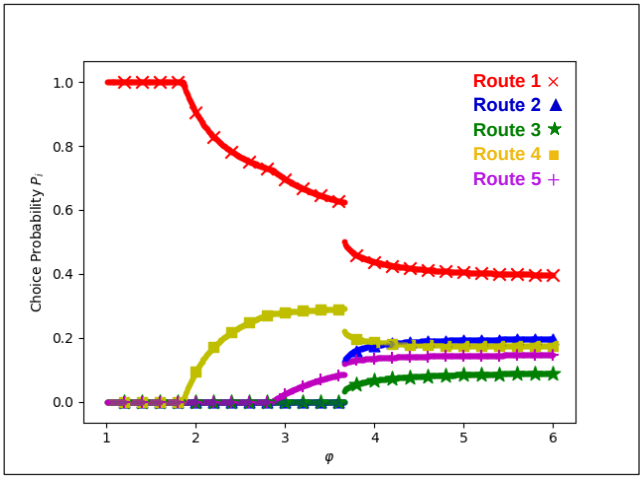

Fig. 4.28. Example network 5: Trajectory of option 3 BPS model choice probability solutions for varying φ ($Y = \theta = \beta = 1$)

From exploring option 3, we establish the following desired properties for a BPS model:

Desired Property 4 – Uniqueness: *Route choice probability solutions are inter-active-choice-set unique (where there is only one active choice set in which solutions exist), and conditions can be established for intra-active-choice-set uniqueness (where for a given active choice set there is only one solution).*

Desired Property 5 – Continuity: *The choice probability function is continuous.*

10.4 Appendix D – Existence and Uniqueness of BAPS Model Solutions

In this section we establish a series of theoretical results concerning the BAPS model as defined in (4.18), (4.19), and (4.20), where the guaranteed existence of solutions is proven, and sufficient conditions for the uniqueness of solutions are detailed.

10.4.1 Properties

We begin by providing two important properties of the fixed-point function $\boldsymbol{F}$. In Lemma 1 we establish the continuity property of $\boldsymbol{F}$.

Lemma 1. *$F_i\left(f_i\left(\bar{\boldsymbol{\gamma}}^{BAPS}(\boldsymbol{P})\right)\right)$ is a continuous function for $\boldsymbol{P} \in D^{(\bar{R}(\boldsymbol{c};\varphi),\tau)}$, $\forall i \in R$.*

Proof. From the definition (4.20) above it follows that $\bar{\boldsymbol{\gamma}}^{BAPS}$ is continuous in $\boldsymbol{P}$ for all $\boldsymbol{P} \in D^{(\bar{R}(\boldsymbol{c};\varphi),\tau)}$:

$$\lim_{\boldsymbol{P}\to\boldsymbol{P}_0} \bar{\boldsymbol{\gamma}}^{BAPS}(\boldsymbol{P}) = \bar{\boldsymbol{\gamma}}^{BAPS}(\boldsymbol{P}_0), \qquad \forall \boldsymbol{P}_0 \in D^{(\bar{R}(\boldsymbol{c};\varphi),\tau)}. \tag{4.29}$$

If we let $\bar{\Gamma}$ be the set of possible path size terms:

$$\bar{\Gamma} = \left\{\bar{\boldsymbol{\gamma}}^{BAPS} \in \mathbb{R}^{\bar{N}}_{>0} : 0 < \bar{\gamma}_i^{BAPS} \leq 1, \forall i \in \bar{R}(\boldsymbol{c};\varphi)\right\},$$

then from definition (4.19) above it follows that f_i is continuous in $\bar{\boldsymbol{\gamma}}^{BAPS}$ for all $\bar{\boldsymbol{\gamma}}^{BAPS} \in \bar{\Gamma}$:

$$\lim_{\overline{\boldsymbol{\gamma}}^{BAPS}\to\overline{\boldsymbol{\gamma}}_0} f_i(\overline{\boldsymbol{\gamma}}^{BAPS}) = f_i(\overline{\boldsymbol{\gamma}}_0), \qquad \forall\overline{\boldsymbol{\gamma}}_0 \in \bar{\Gamma}, \qquad \forall i \in R. \tag{4.30}$$

And, from definition (4.18) above it follows that F_i is continuous in x for all $x \in [0,1]$:

$$\lim_{x\to x_0} F_i(x) = F_i(x_0), \qquad \forall x_0 \in [0,1], \qquad \forall i \in R. \tag{4.31}$$

It then follows from (4.29), (4.30), and (4.31) that $F_i\left(f_i\left(\overline{\boldsymbol{\gamma}}^{BAPS}(\boldsymbol{P})\right)\right)$, as a composition of continuous functions, is itself continuous in $\boldsymbol{P}$ for all $\boldsymbol{P} \in D^{(\bar{R}(\boldsymbol{c};\varphi),\tau)}$:

$$\lim_{\boldsymbol{P}\to\boldsymbol{P}_0} F_i\left(f_i\left(\overline{\boldsymbol{\gamma}}^{BAPS}(\boldsymbol{P})\right)\right) = F_i\left(f_i\left(\overline{\boldsymbol{\gamma}}^{BAPS}(\boldsymbol{P}_0)\right)\right), \qquad \forall \boldsymbol{P}_0 \in D^{(\bar{R}(\boldsymbol{c};\varphi),\tau)}, \qquad \forall i \in R.$$

■

We now in Lemma 2 show that the domain of $\boldsymbol{F}$ maps to itself.

Lemma 2. *$\boldsymbol{F}\left(\boldsymbol{f}\left(\overline{\boldsymbol{\gamma}}^{BAPS}(\boldsymbol{P})\right)\right)$ maps $D^{(\bar{R}(\boldsymbol{c};\varphi),\tau)}$ into $D^{(\bar{R}(\boldsymbol{c};\varphi),\tau)}$.*

Proof. From definition (4.20) above it follows that the function $\overline{\boldsymbol{\gamma}}^{BAPS}$ maps $D^{(\bar{R}(\boldsymbol{c};\varphi),\tau)} \to \bar{\Gamma}$, from definition (4.19) it follows that the function $\boldsymbol{f}$ maps $\bar{\Gamma} \to D^{(\bar{R}(\boldsymbol{c};\varphi))}$, and, from definition (4.18) it follows that the function $\boldsymbol{F}$ maps $D^{(\bar{R}(\boldsymbol{c};\varphi))} \to D^{(\bar{R}(\boldsymbol{c};\varphi),\tau)}$. It thus follows that the composition of the functions $\overline{\boldsymbol{\gamma}}^{BAPS}$, $\boldsymbol{f}$, and $\boldsymbol{F}$, $\boldsymbol{F}\left(\boldsymbol{f}\left(\overline{\boldsymbol{\gamma}}^{BAPS}(\boldsymbol{P})\right)\right)$, maps $D^{(\bar{R}(\boldsymbol{c};\varphi),\tau)} \to D^{(\bar{R}(\boldsymbol{c};\varphi),\tau)}$.

■

10.4.2 Existence of Solutions

Having established some properties regarding the BAPS model fixed-point function $\boldsymbol{F}$, we consider the existence of BAPS model solutions.

Proposition 1. *At least one BAPS model fixed-point solution, $\boldsymbol{P}^*$, to the system $\boldsymbol{P} = \boldsymbol{F}\left(\boldsymbol{f}\left(\overline{\boldsymbol{\gamma}}^{BAPS}(\boldsymbol{P})\right)\right)$ is guaranteed to exist in $D^{(\bar{R}(\boldsymbol{c};\varphi),\tau)}$.*

Proof. $\boldsymbol{F}\left(\boldsymbol{f}\left(\overline{\boldsymbol{\gamma}}^{BAPS}(\boldsymbol{P})\right)\right)$ is a continuous function by Lemma 1, which maps $D^{(\bar{R}(\boldsymbol{c};\varphi),\tau)}$ into $D^{(\bar{R}(\boldsymbol{c};\varphi),\tau)}$ by Lemma 2, and thus since $D^{(\bar{R}(\boldsymbol{c};\varphi),\tau)}$ is a compact convex set, and by Brouwer's Fixed-Point Theorem at least one fixed-point solution, $\boldsymbol{P}^*$, is guaranteed to exist for the system $\boldsymbol{P} = \boldsymbol{F}\left(\boldsymbol{f}\left(\overline{\boldsymbol{\gamma}}^{BAPS}(\boldsymbol{P})\right)\right)$ in $D^{(\bar{R}(\boldsymbol{c};\varphi),\tau)}$.

■

10.4.3 Uniqueness of Solutions

Having proven that BAPS model solutions are guaranteed to exist, the next question is whether sufficient conditions exist which ensure BAPS model solutions are unique. In order to do this, we must first establish two key properties of $J_{\boldsymbol{F}}(\boldsymbol{P};\beta)$ which is the Jacobian matrix of first partial derivatives of $\boldsymbol{F}$ evaluated at $\boldsymbol{P}$ and β.

Lemma 3. *The maximum Jacobian matrix norm of $\boldsymbol{F}\left(\boldsymbol{f}\left(\overline{\boldsymbol{\gamma}}^{BAPS}(\boldsymbol{P});\beta\right)\right)$ for all $\boldsymbol{P} \in D^{(\bar{R}(\boldsymbol{c};\varphi),\tau)}$ at $\beta = 0$ is equal to zero:* $\max\left(\|J_{\boldsymbol{F}}(\boldsymbol{P};0)\| : \forall \boldsymbol{P} \in D^{(\bar{R}(\boldsymbol{c};\varphi),\tau)}\right) = 0.$

Proof. From definitions (4.18) and (4.19) above it follows that:

$$F_i\left(f_i\left(\overline{\boldsymbol{\gamma}}^{BAPS}(\boldsymbol{P});0\right)\right) = \begin{cases} \tau + (1-\bar{N}\tau)\cdot\left(\dfrac{\left(\exp\left(-\theta\left(c_i - \varphi\min(c_l : l \in R)\right)\right)-1\right)}{\sum_{j\in\bar{R}(\boldsymbol{c};\varphi)}\left(\exp\left(-\theta\left(c_j - \varphi\min(c_l : l \in R)\right)\right)-1\right)}\right) & if\ i \in \bar{R}(\boldsymbol{c};\varphi) \\ 0 & if\ i \notin \bar{R}(\boldsymbol{c};\varphi) \end{cases}, \qquad \forall i \in R. \tag{4.32}$$

It then follows from (4.32) that:

$$\frac{\partial F_i\left(f_i(\bar{\boldsymbol{\gamma}}^{BAPS}(\boldsymbol{P});0)\right)}{\partial P_l}=0,\qquad \forall \boldsymbol{P}\in D^{(\bar{R}(\boldsymbol{c};\varphi),\tau)},\qquad \forall i,l\in R. \tag{4.33}$$

It thus follows from (4.33) that $\|J_{\boldsymbol{F}}(\boldsymbol{P};0)\|=0, \forall \boldsymbol{P}\in D^{(\bar{R}(\boldsymbol{c};\varphi),\tau)}$, and hence $\max\left(\|J_{\boldsymbol{F}}(\boldsymbol{P};0)\|:\forall \boldsymbol{P}\in D^{(\bar{R}(\boldsymbol{c};\varphi),\tau)}\right)=0$.

■

Lemma 4. *The maximum Jacobian matrix norm of* $\boldsymbol{F}\left(\boldsymbol{f}(\bar{\boldsymbol{\gamma}}^{BAPS}(\boldsymbol{P});\beta)\right)$, $\max\left(\|J_{\boldsymbol{F}}(\boldsymbol{P};\beta)\|:\forall \boldsymbol{P}\in D^{(\bar{R}(\boldsymbol{c};\varphi),\tau)}\right)$, is a continuous function for $\beta\in[0,\infty)$.

Proof. It follows from the definitions (4.18), (4.19), and (4.20) above that:

$$\frac{\partial F_i\left(f_i(\bar{\boldsymbol{\gamma}}^{BAPS}(\boldsymbol{P}))\right)}{\partial P_l}= \begin{cases} (1-N\tau)\cdot\left(\frac{(h_i(-\theta\boldsymbol{c})-1)\cdot\left(\bar{\gamma}_i^{BAPS}(\boldsymbol{P})\right)^{\beta}}{\sum_{j\in\bar{R}(\boldsymbol{c};\varphi)}\left(h_j(-\theta\boldsymbol{c})-1\right)\cdot\left(\bar{\gamma}_j^{BAPS}(\boldsymbol{P})\right)^{\beta}}\right)\cdot\left(\frac{\beta\frac{\partial\bar{\gamma}_i^{BAPS}(\boldsymbol{P})}{\partial P_l}}{\bar{\gamma}_i^{BAPS}(\boldsymbol{P})}-\frac{\sum_{j\in\bar{R}(\boldsymbol{c};\varphi)}\beta\left(h_j(-\theta\boldsymbol{c})-1\right)\frac{\partial\bar{\gamma}_j^{BAPS}(\boldsymbol{P})}{\partial P_l}\left(\bar{\gamma}_j^{BAPS}(\boldsymbol{P})\right)^{\beta-1}}{\sum_{j\in\bar{R}(\boldsymbol{c};\varphi)}\left(h_j(-\theta\boldsymbol{c})-1\right)\cdot\left(\bar{\gamma}_j^{BAPS}(\boldsymbol{P})\right)^{\beta}}\right) & if\ i,l\in\bar{R}(\boldsymbol{c};\varphi),\\ 0 & otherwise \end{cases} \tag{4.34}$$

$$\forall i,l\in R,$$

$$\frac{\partial\bar{\gamma}_i^{BAPS}(\boldsymbol{P})}{\partial P_i}=\sum\nolimits_{a\in A_i}\frac{t_a}{c_i}\left(\frac{\sum_{k\in\bar{R}(\boldsymbol{c};\varphi);k\neq i}P_k\delta_{a,k}}{\left(\sum_{k\in\bar{R}(\boldsymbol{c};\varphi)}P_k\delta_{a,k}\right)^2}\right),\qquad \forall i\in\bar{R}(\boldsymbol{c};\varphi), \tag{4.35}$$

and,

$$\frac{\partial\bar{\gamma}_i^{BAPS}(\boldsymbol{P})}{\partial P_l}=\begin{cases}-\sum\nolimits_{a\in A_i}\frac{t_a}{c_i}\frac{P_i\delta_{a,l}}{\left(\sum_{k\in\bar{R}(\boldsymbol{c};\varphi)}P_k\delta_{a,k}\right)^2} & if\ l\in\bar{R}(\boldsymbol{c};\varphi)\\ 0 & if\ l\notin\bar{R}(\boldsymbol{c};\varphi)\end{cases}, \tag{4.36}$$

$$\forall i\in\bar{R}(\boldsymbol{c};\varphi), l\in R, l\neq i.$$

From the definitions (4.35) and (4.36) above it follows that $\frac{\partial\bar{\boldsymbol{\gamma}}^{BAPS}(\boldsymbol{P})}{\partial\boldsymbol{P}}$ is continuous in $\boldsymbol{P}$ for all $\boldsymbol{P}\in D^{(\bar{R}(\boldsymbol{c};\varphi),\tau)}$:

$$\lim_{\boldsymbol{P}\to\boldsymbol{P}_0}\frac{\partial\bar{\boldsymbol{\gamma}}^{BAPS}(\boldsymbol{P})}{\partial\boldsymbol{P}}=\frac{\partial\bar{\boldsymbol{\gamma}}^{BAPS}(\boldsymbol{P}_0)}{\partial\boldsymbol{P}},\qquad \forall\boldsymbol{P}_0\in D^{(\bar{R}(\boldsymbol{c};\varphi),\tau)}. \tag{4.37}$$

It then follows from (4.29) and (4.37) that $\frac{\partial F_i\left(f_i(\bar{\boldsymbol{\gamma}}^{BAPS}(\boldsymbol{P}))\right)}{\partial P_l}$ as defined in (4.34), being a composition of continuous functions, is itself continuous in $\boldsymbol{P}$ for all $\boldsymbol{P}\in D^{(\bar{R}(\boldsymbol{c};\varphi),\tau)}$:

$$\lim_{\boldsymbol{P}\to\boldsymbol{P}_0}\frac{\partial F_i\left(f_i(\bar{\boldsymbol{\gamma}}^{BAPS}(\boldsymbol{P}))\right)}{\partial P_l}=\frac{\partial F_i\left(f_i(\bar{\boldsymbol{\gamma}}^{BAPS}(\boldsymbol{P}_0))\right)}{\partial P_l},\qquad \forall\boldsymbol{P}_0\in D^{(\bar{R}(\boldsymbol{c};\varphi),\tau)},\qquad \forall i,l\in R.$$

Since $\frac{\partial F_i\left(f_i(\bar{\boldsymbol{\gamma}}^{BAPS}(\boldsymbol{P}))\right)}{\partial P_l}$ is a continuous function for $\boldsymbol{P}\in D^{(\bar{R}(\boldsymbol{c};\varphi),\tau)}$, $\forall i,l\in R$, $\frac{\partial F_i\left(f_i(\bar{\boldsymbol{\gamma}}^{BAPS}(\boldsymbol{P});\beta)\right)}{\partial P_l}$ is also a continuous function for $\beta\in[0,\infty)$, $\forall i,l\in R$:

$$\lim_{\beta\to\beta_0}\left(\frac{\partial F_i\left(f_i(\bar{\boldsymbol{\gamma}}^{BAPS}(\boldsymbol{P});\beta)\right)}{\partial P_l}\right)=\frac{\partial F_i\left(f_i(\bar{\boldsymbol{\gamma}}^{BAPS}(\boldsymbol{P});\beta_0)\right)}{\partial P_l},\qquad \forall\beta_0\in[0,\infty),\qquad \forall i,l\in R.$$

Hence, since $\max\left(\|J_{\boldsymbol{F}}(\boldsymbol{P};\beta)\|:\forall\boldsymbol{P}\in D^{(\bar{R}(\boldsymbol{c};\varphi),\tau)}\right)$ is a composition of continuous functions then it itself is a continuous function for $\beta\in[0,\infty)$:

$$\lim_{\beta \to \beta_0} \left(\max\left(\|J_{\boldsymbol{F}}(\boldsymbol{P};\beta)\| : \forall \boldsymbol{P} \in D^{(\bar{R}(\boldsymbol{c};\varphi),\tau)}\right)\right) = \max\left(\|J_{\boldsymbol{F}}(\boldsymbol{P};\beta_0)\| : \forall \boldsymbol{P} \in D^{(\bar{R}(\boldsymbol{c};\varphi),\tau)}\right), \qquad \forall \beta_0 \in [0,\infty).$$

■

These two key properties of $J_{\boldsymbol{F}}(\boldsymbol{P};\beta)$ allow us to establish conditions for the uniqueness of solutions.

Proposition 2. *There always exist values of $b > 0$ such that when the β parameter is within the range $0 \leq \beta \leq b$, there are unique BAPS model fixed-point solutions, $\boldsymbol{P}^*$, to the system $\boldsymbol{P} = \boldsymbol{F}\left(\boldsymbol{f}(\bar{\boldsymbol{\gamma}}^{BAPS}(\boldsymbol{P});\beta)\right)$ in $D^{(\bar{R}(\boldsymbol{c};\varphi),\tau)}$.*

Proof. $\boldsymbol{F}$ is a *contraction mapping* on the domain $D^{(\bar{R}(\boldsymbol{c};\varphi),\tau)}$ if:

a) $\boldsymbol{F}$ maps $D^{(\bar{R}(\boldsymbol{c};\varphi),\tau)}$ into itself, so $\boldsymbol{F}\left(\boldsymbol{f}(\bar{\boldsymbol{\gamma}}^{BAPS}(\boldsymbol{P}_0);\beta)\right) \in D^{(\bar{R}(\boldsymbol{c};\varphi),\tau)}, \forall \boldsymbol{P}_0 \in D^{(\bar{R}(\boldsymbol{c};\varphi),\tau)}$, and

b) There exists a constant $0 \leq \sigma < 1$ such that:

$$\|J_{\boldsymbol{F}}(\boldsymbol{P};\beta)\| \leq \sigma, \qquad \forall \boldsymbol{P} \in D^{(\bar{R}(\boldsymbol{c};\varphi),\tau)},$$

where $J_{\boldsymbol{F}}(\boldsymbol{P};\beta)$ is the Jacobian matrix of first partial derivatives of $\boldsymbol{F}$ evaluated at $\boldsymbol{P}$.

If the link cost vector $\boldsymbol{t}$ is fixed (and thus the route cost vector $\boldsymbol{c}$ is fixed), and θ, φ are fixed, then for any given β, if $\boldsymbol{F}$ is a contraction mapping, then since $D^{(\bar{R}(\boldsymbol{c};\varphi),\tau)}$ is a compact convex set, and by Lemma 1, Lemma 2, and the Contraction Mapping Theorem, $\boldsymbol{F}$ emits a unique fixed-point solution $\boldsymbol{P}^* \in D^{(\bar{R}(\boldsymbol{c};\varphi),\tau)}$.

It remains to establish the conditions under which $\boldsymbol{F}$ is a contraction mapping. Since by Lemma 3 the maximum Jacobian matrix norm of $\boldsymbol{F}$ for all $\boldsymbol{P} \in D^{(\bar{R}(\boldsymbol{c};\varphi),\tau)}$ at $\beta = 0$ is equal to zero $\left(\max\left(\|J_{\boldsymbol{F}}(\boldsymbol{P};0)\| : \forall \boldsymbol{P} \in D^{(\bar{R}(\boldsymbol{c};\varphi),\tau)}\right) = 0\right)$, and by Lemma 4 $\max\left(\|J_{\boldsymbol{G}}(\boldsymbol{P};\beta)\| : \forall \boldsymbol{P} \in D^{(\bar{R}(\boldsymbol{c};\varphi),\tau)}\right)$ is a continuous function for $\beta \in [0,\infty)$, then there must always exist values $b > 0$ such that when β is within the range $0 \leq \beta \leq b$ $\boldsymbol{F}$ is a contraction mapping and the sufficient conditions for unique BAPS model solutions are always met.

■

There are cases where the BAPS model has unique solutions for all $\beta > 0$ (i.e. for all values of b), for example where all active routes are non-overlapping and the path size terms are consequently all 1 so that F_i collapses to (4.32), and hence in these cases a maximum value for b does not exist. However, in most cases BAPS model solutions are not unique for all values of β and in these cases a maximum value for b exists (denoted b_{max}) such that Proposition 2 holds. However, Proposition 2 is only a sufficient condition for unique BAPS model solutions and solutions are not necessarily non-unique for $\beta > b_{max}$. In Section 10.5 below we demonstrate how the true maximum range $0 \leq \beta \leq \beta_{max}$ for which BAPS model solutions are unique can be estimated.

10.5 Appendix E – Satisfying the Desired Properties for a BPS Model

In this section we discuss/demonstrate how the BBPS and BAPS models satisfy the desired properties for a BPS model established in Appendix C.

10.5.1 Desired Property 1 – Consistent Definitions of Unrealistic Routes

Property: *Routes defined as unrealistic by the choice model (assigned zero choice probabilities) should have zero path size contributions, and vice versa.*

The BBPS and BAPS models both satisfy Desired Property 1 since the proposed BPS model form stipulates that a route has both a zero choice probability and zero path size contributions if and only if it has a travel cost above the bound. This is demonstrated in Section 10.5.3 below.

10.5.2 Desired Property 2 – Well-Defined Functions

Property: *The model functions should be well-defined across their domain.*

The BBPS and BAPS models both satisfy Desired Property 2, which, specifically, is established so that occurrences of $\frac{0}{0}$ in the path size terms / $\ln(0)$ within the route utilities are avoided. Generally, the path size correction factor for route $i \in R$ is $\kappa_i = \beta \ln(\gamma_i)$, and the path size term of route $i \in R$ is defined as follows:

$$\gamma_i = \sum_{a \in A_i} \frac{t_a}{c_i} \frac{W_i}{\sum_{k \in R} W_k \delta_{a,k}},$$

where W_k is the path size contribution weighting of route $k \in R$. If allowing for the weightings to be zero as to eliminate contributions, then $\frac{0}{0}$ occurs when $W_i = \sum_{k \in R} W_k \delta_{a,k} = 0$, and $\gamma_i = 0$ occurs (resulting in $\ln(0)$) when $W_i = 0$ and $\sum_{k \in R; k \neq i} W_k \delta_{a,k} > 0$. Two key features of the proposed BPS model form – of which the BBPS and BAPS model adopt – are that: a) only the realistic routes have path size terms; and, b) the realistic route path size terms only consider the path size contributions of other realistic routes. These two features ensure that the proposed BPS model form has well-defined functions. The form stipulates that the realistic routes are those which have a travel cost less than the bound (φ times the cost on the cheapest route), and that the path size contribution weightings of these routes are non-zero. The proposed BPS model path size term definition in (4.7) thus only considers the path size contribution weightings of routes $k \in R$ that have costs below the bound (routes $k \in \bar{R}(\boldsymbol{c}; \varphi)$), since it is known that these are the realistic routes and have non-zero weightings, and hence occurrences of $\frac{0}{0}$ are avoided. Moreover, since path size terms are only defined for realistic routes where $W_i > 0$, occurrences of $\gamma_i = 0$ and thus $\ln(0)$ are avoided, although (4.7) precludes occurrences of $\ln(\gamma_i)$ regardless.

10.5.3 Desired Property 3 – Internal Consistency

Property: *The model should be internally consistent, i.e. there is a consistent assessment of the feasibility of routes for both the probability relation and the path size contribution factors.*

The BAPS model satisfies Desired Property 3 since the BAPS model path size contribution factors assess the feasibility of routes according to their route choice probability, and hence the model is internally consistent. The BBPS model is not internally consistent, however, since the contribution factors assess routes according to their travel cost, with no consideration of distinctiveness, and hence Desired Property 3 is not satisfied.

To demonstrate, consider example network 4 in Fig. 4.25A. Fig. 4.29A-B display the example network 4 BBPS model $\lambda = 8$ and BAPS model choice probabilities, respectively, as υ is increased from 0.5 to 3, $\theta = \beta = 1$, $\varphi = 2.5$. As Fig. 4.29B shows for the BAPS model, as the travel cost of Route 1 increases, its choice probability and consequently path size contribution to Route 2 decreases. As the cost of Route 1 approaches the bound, Route 1 approaches zero choice probability / path size contribution. When $\upsilon = 2$, the travel cost of Route 1 is exactly 2.5 times the cost on the cheapest routes (Routes 2&3), and hence Route 1 is assigned zero choice probability, and its path size contribution is eliminated. In Fig. 4.29A, however, for the BBPS model, the large λ value accentuates the travel cost differences and the contribution of Route 1 to Route 2 diminishes to zero well before the cost of Route 1 reaches the bound and obtains zero probability.

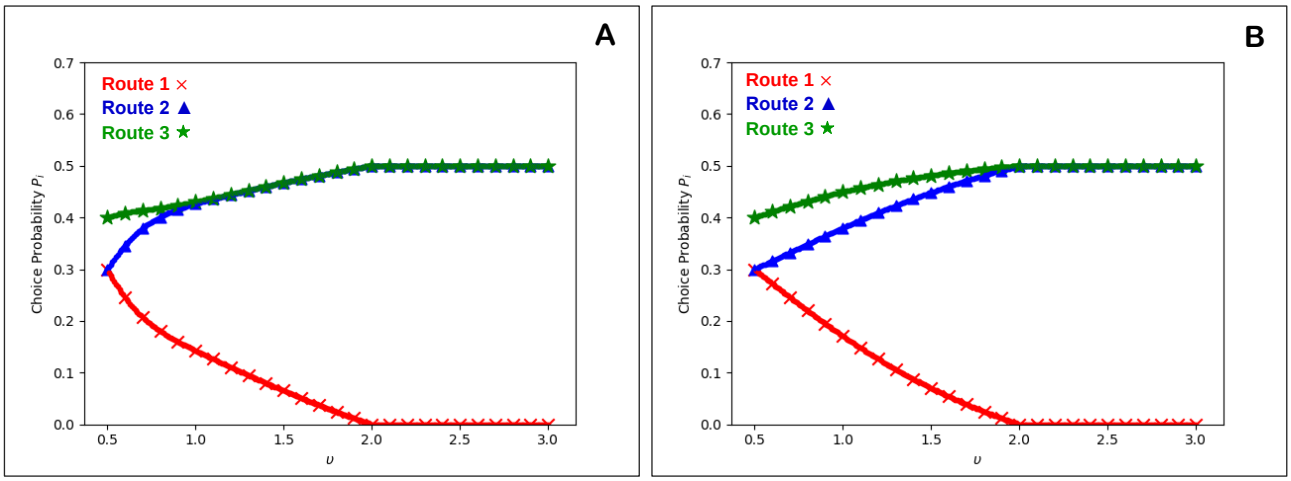

Fig. 4.29. Example network 4: Route choice probabilities for increasing υ ($\theta = \beta = 1$, $\varphi = 2.5$). **A:** BBPS model, $\lambda = 8$. **B:** BAPS model.

10.5.4 Desired Property 4 – Uniqueness

Property: *Route choice probability solutions are inter-active-choice-set unique (where there is only one active choice set in which solutions exist), and conditions can be established for intra-active-choice-set uniqueness (where for a given active choice set there is only one solution).*

For the proposed BPS model form, there is only one active choice set in which solutions exist: the zero choice probability routes are exactly the routes with travel costs greater than or equal to the bound, and, routes with travel costs below the bound will receive non-zero choice probabilities. This is in contrast to the option 2&3 BPS models in Section 10.1.2 where there are multiple active choice sets in which solutions exist. BBPS & BAPS model choice probability solutions are thus inter-active-choice-set unique, and, since the BBPS model is closed-form, solutions are also intra-active-choice-set unique. BAPS model choice probability solutions are however not intra-active-choice-set unique, though conditions exist under which solutions are.

Duncan et al (2020) demonstrate how APSL choice probability solutions are unique for β in the range $0 \leq \beta \leq \beta_{max}$. A similar range exists for the BAPS model. We shall show here: a) that multiple BAPS model solutions can exist; b) that there is a range $0 \leq \beta \leq \beta_{max}$ for β in which solutions are unique; and, c) how β_{max} can be estimated. To do this, we utilise the same method to that described in Section 4.4 of Duncan et al (2020) for the APSL model. β_{max} is estimated by plotting trajectories of BAPS model solutions for varying β, and identifying where a unique trajectory of solutions ends and multiple trajectories begin. A simple method for obtaining trajectories of BAPS model solutions is as follows:

Step 1. Identify a suitably large value for β.

Step 2. Solve the BAPS model fixed-point system for this large β with a randomly generated initial condition (see Section 5.2.2).

Step 3. Decrement β and obtain the next BAPS model solution with initial condition set as the solution for the previous β.

Step 4. Continue until $\beta = 0$.

By plotting the choice probabilities at each decremented β, and repeating this method several times, one can determine where non-unique solution trajectories end and hence estimate β_{max}. If after several repetitions (with different randomly generated initial conditions) only a single trajectory of solutions is shown, then the initial large β value is increased. We illustrate the approach graphically, but there is no need to draw graphs for general networks. One can instead observe the choice probability values, where a finer grained decrement of β will provide a more accurate estimation of β_{max}.

To demonstrate, consider again example network 5 in Fig. 4.27; Fig. 4.30A-B display trajectories of BAPS model solutions as the β parameter is varied for $\varphi = 7$ and $\varphi = 2.5$, respectively, with $\theta = 1$. β was decremented by 0.01, and the initial large β values were $\beta = 1.5$ for Fig. 4.30A and $\beta = 10$ for Fig. 4.30B. The solution trajectory plotting was repeated until multiple clear trajectories were shown. As shown, there is a unique trajectory of choice probability solutions up until $\beta = \beta_{max}$ where there then becomes multiple trajectories. The estimated β_{max} values are 0.97 for Fig. 4.30A and 4.61 for Fig. 4.30B.

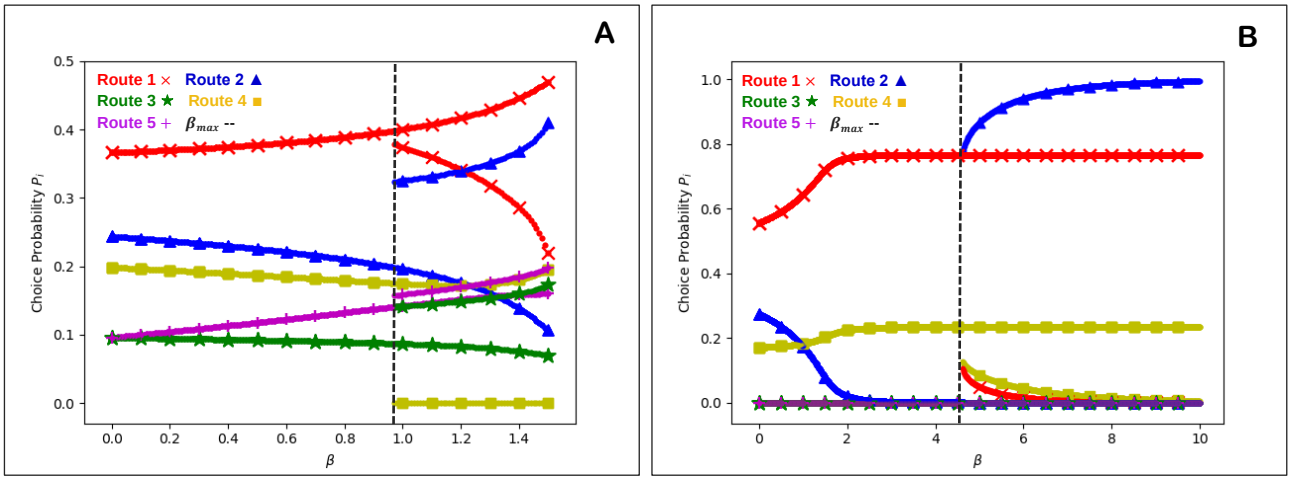

Fig. 4.30. Example network 5: Trajectories of BAPS model choice probability solutions as β is varied ($\theta = 1$). **A:** $\varphi = 7$. **B:** $\varphi = 2.5$.

10.5.5 Desired Property 5 – Continuity

Property: *The choice probability function is continuous.*

The BBPS model has a continuous choice probability function: it is closed-form, and as the cost of a route approaches the bound from below, its choice probability and path size contributions approach zero, and meet exactly at zero. While the modified BAPS model formulation is known to be discontinuous, the standard BAPS model formulation has a continuous choice probability function (if assumed solutions always exist), and the modified version approximates the standard version, thus approximating continuity. Despite having similar path size terms, the standard BAPS model formulation does not suffer from the same discontinuity issue as the option 3 BPS model in Section 10.1. Whereas with the option 3 model the feature that is bounded (route utility) varies as φ varies, the feature that is bounded with the BAPS model (route cost) is constant for all φ. As a consequence, choice probabilities / path size contributions approach zero as routes approach the bound from below, and meet exactly at zero. To demonstrate, consider example network 5 in Fig. 4.27; Fig. 4.31A-B display the trajectories of $BBPS_{(\lambda=\theta)}$ and BAPS model choice probability solutions, respectively, as φ is varied, $\theta = \beta = 1$. As Fig. 4.31A-B show, as the bound decreases and the route costs approach the bound from below, the choice probabilities approach zero and meet zero at the bound. Since the path size contributions also approach zero as the route costs approach the bound, then there is no adjustment amongst the active route probabilities once a route becomes inactive and hence the choice probability functions are continuous in φ, and thus travel cost (as shown in Fig. 4.29).

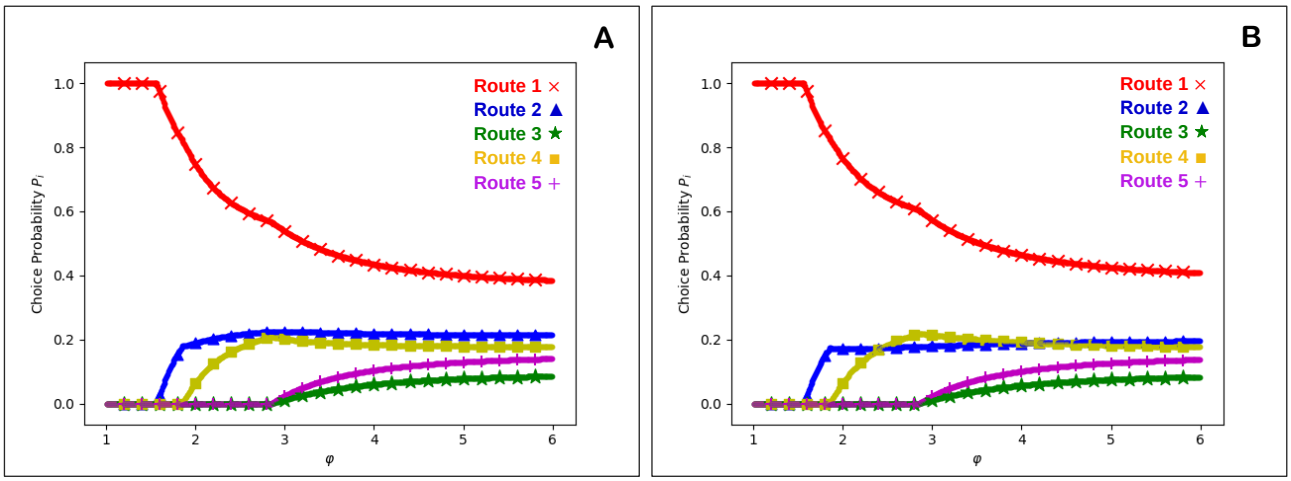

Fig. 4.31. Example network 5: Route choice probabilities for varying φ ($\theta = \beta = 1$). **A:** $BBPS_{(\lambda=\theta)}$ model. **B:** BAPS model.

Chapter 5. Formulation and solution of bounded path size stochastic user equilibrium models – consistently addressing route overlap and unrealistic routes

Lawrence Christopher DUNCAN [a], David Paul WATLING [a], Richard Dominic CONNORS [a,b], Thomas Kjær RASMUSSEN [c], Otto Anker NIELSEN [c]

[a] Institute for Transport Studies, University of Leeds
36-40 University Road, Leeds, LS2 9JT, United Kingdom.

[b] University of Luxembourg, Faculté des Sciences, des Technologies et de Médecine, Maison du Nombre, 6 Avenue de la Fonte, L-4364, Esch-sur-Alzette, Luxembourg.

[c] Department of Technology, Management and Economics, Technical University of Denmark Bygningstorvet 116B, 2800 Kgs. Lyngby, Denmark.

Highlights

- Stochastic User Equilibrium (SUE) conditions for Bounded Path Size (BPS) models
- Proof of existence for BPS SUE solutions and BPS SUE solution algorithm
- Computation/flow results compared between BPS SUE models and with PS SUE models
- Computational feasibility & insensitivity to unrealistic routes in the choice sets shown
- Uniqueness conditions for BPS SUE solutions demonstrated numerically

Abstract

The Bounded Path Size (BPS) route choice model form, as introduced in Duncan et al (2021b), offers a theoretically consistent and practical approach to dealing with both route overlap and unrealistic routes. It captures correlations between overlapping routes by including correction terms within the probability relations, and has a consistent criterion for assigning zero choice probabilities to unrealistic routes while eliminating their path size contributions. Two BPS models are proposed: one that is closed-form and another expressed as a fixed-point problem. This paper establishes Stochastic User Equilibrium (SUE) conditions for these BPS models, where the choice sets of realistic routes are equilibrated along with the route flows. SUE solution existence is proven for the closed-form BPS model. A generic algorithm is proposed for solving BPS SUE models, where the realistic route choice sets are equilibrated from a master pre-generated set of routes. For the BPS SUE algorithm solving the fixed-point BPS model, we show how the potentially onerous requirement of solving fixed-point problems to compute choice probabilities can be circumvented, by harnessing the relationship between choice probability and route flow proportion in SUE context. This allows one to trade-off the accuracy of the fixed-point probabilities (and thus computation times of each iteration) with rate of SUE convergence. Numerical experiments on the Sioux Falls and Winnipeg networks show that the BPS SUE models can be solved in feasible computation times compared to non-bounded versions, while providing the potential for significantly improved robustness to the adopted master route choice set. Solution uniqueness for the fixed-point BPS SUE model is explored numerically where results suggest that uniqueness conditions exist.

Key Words: bounded path size, stochastic user equilibrium, solution algorithm, fixed-point, convergence, equilibrated choice sets

1. Introduction

The Stochastic User Equilibrium (SUE) traffic assignment model proposed by Daganzo & Sheffi (1977) is a well-known approach for investigating the behaviours of travellers on congested road networks. SUE relaxes the perfect information assumption of the Deterministic User Equilibrium model by supposing that route

choice is based on costs that include stochastic terms. This accounts for the differing perceptions travellers have of the attractiveness of routes. Two specific challenges for SUE modelling are: 1) capturing correlations between overlapping routes, and 2) dealing with unrealistic routes. In this paper, we develop a new SUE modelling approach that addresses both of these challenges in a theoretically consistent, robust, and mathematically well-defined way, and demonstrate its computational feasibility on large-scale networks. To set the background for the research, we discuss existing SUE modelling approaches for 1) and 2) below.

When developing a correlation-based route choice model for SUE, there is a trade-off: accurately capturing route correlation in a behaviourally realistic way requires a more complex route choice model, but this results in computational challenges for solving for SUE (e.g. long computation times, difficulties measuring convergence). Different stochastic route cost terms proposed in the literature give rise to three general types of correlation-based route choice models that have been applied to SUE: GEV structure models (e.g. Cross-Nested Logit, Generalised Nested Logit, Paired Combinatorial Logit), simulation models (e.g. Multinomial Probit, Multinomial Gammit), and correction term models (e.g. C-Logit, Path Size Logit (PSL), Path Size Weibit, Path Size Hybrid). For a detailed review of correlation-based route choice models, with literature references, see Duncan et al (2020, 2021b), and for a detailed review of SUE applications of correlation-based models, with literature references, see Duncan et al (2021a). We briefly discuss here, without the literature references, the key characteristics and strengths/weaknesses of the different correlation-based SUE model categories.

GEV structure models use a multi-level tree structure to capture the similarity among routes through the random error component of the utility function. This means that despite having closed-form probability expressions, due to their multi-level tree structure the choice probabilities and in particular Mathematical Programming (MP) formulations are complex to compute, where the computational burden escalates significantly as the scale of network / choice set sizes increase. Simulation models capture route correlation implicitly, as the similarity between each pair of routes is accounted for by allowing for covariance between the error terms. The issue for these models is that they do not have closed-form probability expressions, and so evaluating the route choice probabilities requires either Monte Carlo simulation or alternative methods, all of which are computationally burdensome. Correction term models add correction terms to the deterministic utilities / probability relations to adjust the choice probabilities in order to capture route correlations. Their main attraction is that they have simple closed-form expressions, meaning the route choice probabilities and MP formulations are generally easy and quick to compute; however, more complex models can capture correlations more accurately.

Upon selection of which correlation-based SUE model to employ in large-scale network applications, one must compare the anticipated accuracy of results with the computational burden and/or convergence of applicable solution algorithms. Simulation SUE models are attractive behaviourally due to their ability to accurately capture route correlations. However, due to the random nature in which the search direction is obtained in typical simulation-based algorithms, there are difficulties in suitably measuring flow convergence. Moreover, numerous studies have found convergence very slow on large-scale networks, while there are also difficulties in accurately computing small probabilities/flows. GEV structure and correction term models do not require random simulation to compute choice probabilities, and search directions can be computed exactly. This means that convergence can be suitably measured, and more optimal step-size schemes / algorithms can be developed for better convergence. As discussed above, due to their increasing computational burden as network scale increases, there are questions over the suitability of GEV structure models for SUE on large-scale networks, while in Duncan et al (2020b), we discuss internal consistency issues. Correction term models, although are typically less accurate in capturing route correlations, are more computationally practical and are regularly applied to SUE on large-scale networks.

Historically, SUE models – correlation-based and in general – have had a theoretical need to enumerate the universal set of routes, however nonsensical they may be (Daganzo & Sheffi, 1977). This is behaviourally unrealistic and computationally infeasible, as the set contains millions of routes even in medium-sized networks (Watling et al, 2015; Rasmussen et al, 2015), the majority of which are very long and should be considered unrealistic. The typical approach for dealing with this is to employ some kind of heuristic method that attempts to explicitly generate a route choice set containing just the routes considered realistic. This approach leads to theoretical inconsistencies however, since the route generation criteria is not consistent with the calculation of the flows among generated routes. Moreover, generating the exact choice sets of realistic routes is very difficult to do, especially on large-scale networks, and this problematic for many correlation-

based SUE models as many are not choice set robust (Bovy et al, 2008; Bliemer & Bovy, 2008; Ramming, 2002; Ben-Akiva & Bierlaire, 1999; Bekhor et al, 2008; Duncan et al, 2020,2021b). For simulation SUE models, typical solution methods do not require explicit route generation and thus the accuracy of results is not dependent upon the choice sets generated, although the routes generated may vary from different algorithm runs.

Recent years have seen the emergence of some promising SUE approaches for dealing with unrealistic routes in a consistent way. Watling et al (2015) and Rasmussen et al (2015) develop a Restricted Stochastic User Equilibrium approach whereby the choice set of used routes is determined by some explicit constraint that is dependent on the equilibrium solution. Rasmussen et al (2015) further extend the approach to include a second restriction, determined partly by an exogenously defined cost threshold. PSL correction terms are added to both of these approaches to also deal with the route overlap problem. The disadvantage with these approaches, however, is that equilibrium solutions are not guaranteed to exist, and even in cases where solutions do exist, there is no guarantee of the uniqueness of the solution. This lack of theoretical guarantee of existence and uniqueness is a major price to pay when one considers the typical use of such models in policy testing, meaning that one cannot guarantee to attribute a unique forecasted benefit to any tested measure. Furthermore, the lack of a mathematically well-defined underlying route choice model with a continuous choice probability distribution means that the approach is not robust (i.e. potentially sensitive to small changes to network/model specifications).

Motivated by the desire to develop an SUE model that consistently addresses unrealistic routes but has guaranteed existence and uniqueness of solutions, as well as a mathematically well-defined underlying route choice model, Watling et al (2018) formulate the Bounded Choice Model (BCM), and consequently Bounded SUE. The BCM has a consistent criterion for determining restricted choice sets of feasible routes, and route choice probability: a bound is applied to the difference in random utility between each given route and an imaginary reference route alternative, so that routes only receive a non-zero choice probability if the difference between its random utility and the random utility of the reference alternative is within the bound. Furthermore, the probability each route is chosen relates to the odds associated with choosing each alternative versus the reference alternative. A special case of the BCM is where the reference alternative is that with the maximum deterministic utility i.e. the route with the cheapest generalised travel cost, so that a route only receives a non-zero probability if its cost is within some bound of the cheapest route.

The BCM, however, does not account for route correlations. To address this, in Duncan et al (2021b), our own previous work, we considered the integration of a correlation-based route choice model with the BCM. Upon selection of which correlation-based model to adopt, we had some requirements: real-life application of a route choice model involves estimating the model parameters, and we thus considered it important that the proposed model could be successfully estimated, and moreover, that it would be computationally feasible to do so (as well as apply it) on large-scale networks. As we discussed, there are computational and estimation concerns that raise questions whether GEV structure and simulation models may satisfy these requirements. Due to the comparatively low computational cost and the relative ease in obtaining reasonable estimates for parameters, we thus chose to explore the integration of correction term models with the BCM.

The real-life application of a route choice model on congested road networks involves applying it to SUE, and thus, although it was not discussed in the paper, our other requirement was that the proposed model would be suitable for SUE on large-scale networks. As discussed above, and demonstrated in Duncan et al (2021a), there are also questions over the suitability of GEV structure and simulation models for large-scale SUE applications, while correction term models are suitable. Furthermore, although it is always desirable for a route choice model to be mathematically well-defined, this is essential for SUE application, and thus although it was not explicitly discussed in the paper as for SUE, it was important the proposed model was well-defined.

Inspired by existing research on dealing with unrealistic routes for the PSL model (e.g. Generalised PSL (Ramming, 2002), Adaptive PSL (APSL) (Duncan et al, 2020)), we chose to pursue integration of PSL model concepts with the BCM. In the paper, we consequently derived a mathematically well-defined Bounded Path Size (BPS) model form that utilises a consistent criterion for assigning zero probabilities to unrealistic routes while eliminating their path size contributions. Two BPS models were proposed: one that is closed-form, and another expressed as a fixed-point problem.

In this paper, we investigate the application of these BPS models to SUE. For the fixed-point BPS model, solving the choice probabilities requires a fixed-point algorithm to compute the solution. This has the potential to be computationally burdensome in large-scale networks even when the travel costs are fixed. However, as

we explore in this study, the requirement of solving fixed-point problems to compute the probabilities can be circumvented in SUE application, since at equilibrium the route flow proportions and choice probabilities equate. In an analogous way to that described/explored for the APSL SUE model in Duncan et al (2021a), the useful relationship between choice probabilities and route flow proportions in SUE context allows for a considerable flexibility in solving the fixed-point BPS SUE model, where one can trade-off the accuracy of the probabilities (and thus computation times of each iteration) with rate of SUE convergence.

The structure of the paper is as follows. In Section 2 we introduce congested network notation as well as provide definitions of relevant SUE models. In Section 3 we establish SUE conditions for BPS models and address solution existence/uniqueness. In Section 4 we detail a solution algorithm, which has two variants for cases where there are and are not approximated or actual pre-generated universal choice sets. In Section 5 we conduct numerical experiments to assess computational performance, compare flow results, and investigate BPS SUE solution uniqueness. Section 6 concludes the paper.

2. Notation & Model Definitions

2.1 Congested Network Notation

A road network consists of link set A and $m = 1, \dots, M$ OD movements. R_m is the choice set of all simple routes (no cycles) for OD movement m of size $N_m = |R_m|$, where $N = \sum_{m=1}^{M} N_m$ is the total number of routes. $A_{m,i} \subseteq A$ is the set of links belonging to route $i \in R_m$, and $\delta_{a,m,i} = \begin{cases} 1 & if\ a \in A_{m,i} \\ 0 & otherwise \end{cases}$.

The travel demand for OD movement m is $q_m > 0$, and $\boldsymbol{Q}_m$ is the $N_m \times N_m$ diagonal matrix of the travel demand for OD movement m (i.e. with q_m on each diagonal element). The flow on route $i \in R_m$ is $f_{m,i}$, and $\boldsymbol{f}_m$ is the N_m-length vector of route flows for OD movement m. $\boldsymbol{f}$ is the N-length vector of all OD movement route flow vectors such that $\boldsymbol{f} = (\boldsymbol{f}_1, \dots \boldsymbol{f}_M)$, where $f_{m,i}$ refers to element number $i + \sum_{k=1}^{m-1} N_k$ in $\boldsymbol{f}$. F denotes the set of all demand-feasible non-negative universal route flow vector solutions:

$$F = \left\{ \boldsymbol{f} \in \mathbb{R}_+^N : \sum_{i \in R_m} f_{m,i} = q_m, m = 1, \dots, M \right\}.$$

Furthermore, x_a denotes the flow on link $a \in A$, and $\boldsymbol{x} = \left(x_1, x_2, \dots, x_{|A|}\right)$ is the vector of all link flows. X denotes the set of all demand-feasible non-negative link flow vectors:

$$X = \left\{ \boldsymbol{x} \in \mathbb{R}_+^{|A|} : \sum_{m=1}^{M} \sum_{i \in R_m} \delta_{a,m,i} f_{m,i} = x_a, \forall a \in A, \boldsymbol{f} \in F \right\}.$$

For link $a \in A$ experiencing a flow of x_a, denote the generalised travel cost for that link as $t_a(x_a)$, where $\boldsymbol{t}(\boldsymbol{x})$ is the vector of all generalised link travel cost functions. In vector/matrix notation, let $\boldsymbol{x}$ and $\boldsymbol{f}$ be column vectors, and define $\boldsymbol{\Delta}$ as the $|A| \times N$-dimensional link-route incidence matrix. Then the relationship between link and route flows may be written as $\boldsymbol{x} = \boldsymbol{\Delta f}$. Supposing that the travel cost for a route can be attained through summing up the total cost of its links, then the generalised travel cost for route $i \in R_m$, $c_{m,i}$, can be computed as follows: $c_{m,i}\left(\boldsymbol{t}(\boldsymbol{\Delta f})\right) = \sum_{a \in A_{m,i}} t_a(\boldsymbol{\Delta f})$, where $\boldsymbol{c}_m\left(\boldsymbol{t}(\boldsymbol{\Delta f})\right)$ is the vector of generalised travel cost functions for OD movement m.

Let the route choice probability for route $i \in R_m$ be $P_{m,i}$, where $\boldsymbol{P}_m = \left(P_{m,1}, P_{m,2}, \dots, P_{m,N_m}\right)$ is the vector of route choice probabilities for OD movement m, and D_m is the domain of possible route choice probability vectors for OD movement m, $m = 1, \dots, M$.

2.2 Path Size Logit SUE Models

We briefly detail definitions of SUE for Path Size Logit models with flow-dependent path size terms here, we direct the reader to Duncan et al (2021a) for more details and solution methods.

Path Size Logit models were developed to address the well-known deficiency of the Multinomial Logit (MNL) model in its inability to capture the correlation between routes. To do this, they include correction terms to penalise routes that share links with other routes, so that the deterministic utility of route $i \in R_m$ is

$V_{m,i} = -\theta c_{m,i}(\boldsymbol{t}) + \kappa_{m,i}$, where $\theta > 0$ is the Logit scaling parameter and $\kappa_{m,i} \leq 0$ is the correction term for route $i \in R_m$. The choice probability for route $i \in R_m$ is:

$$P_{m,i}(\boldsymbol{c}_m(\boldsymbol{t}), \boldsymbol{\kappa}_m) = \frac{e^{-\theta c_{m,i}(\boldsymbol{t}) + \kappa_{m,i}}}{\sum_{j \in R_m} e^{-\theta c_{m,j}(\boldsymbol{t}) + \kappa_{m,j}}}.$$

Path Size Logit correction terms adopt the form $\kappa_{m,i} = \beta \ln(\gamma_{m,i})$, where $\beta \geq 0$ is the path size scaling parameter, and $\gamma_{m,i} \in (0,1]$ is the path size term for route $i \in R_m$. A distinct route with no shared links has a path size term equal to 1, resulting in no penalisation. Less distinct routes have smaller path size terms and incur greater penalisation. The path size terms are often based upon link lengths and thus $\gamma_{m,i}$ (in those cases) is not dependent upon the link/route generalised travel costs. However, this leads to internal inconsistency (see Duncan et al (2021a)), and in this study we base the path size terms upon on generalised link travel costs (i.e. $\gamma_{m,i} = \gamma_{m,i}(\boldsymbol{t})$), which in SUE application are congested, flow-dependent costs. The choice probability for route $i \in R_m$ is thus:

$$P_{m,i}\big(\boldsymbol{c}_m(\boldsymbol{t}), \boldsymbol{\gamma}_m(\boldsymbol{t})\big) = \frac{e^{-\theta c_{m,i}(\boldsymbol{t}) + \beta \ln\left(\gamma_{m,i}(\boldsymbol{t})\right)}}{\sum_{j \in R_m} e^{-\theta c_{m,j}(\boldsymbol{t}) + \beta \ln\left(\gamma_{m,j}(\boldsymbol{t})\right)}} = \frac{\left(\gamma_{m,i}(\boldsymbol{t})\right)^{\beta} e^{-\theta c_{m,i}(\boldsymbol{t})}}{\sum_{j \in R_m} \left(\gamma_{m,j}(\boldsymbol{t})\right)^{\beta} e^{-\theta c_{m,j}(\boldsymbol{t})}}. \quad (5.1)$$

The general form for the path size term is as follows:

$$\gamma_{m,i}(\boldsymbol{t}) = \sum_{a \in A_{m,i}} \frac{t_a}{c_{m,i}(\boldsymbol{t})} \frac{1}{\sum_{k \in R_m} \left(\frac{W_{m,k}}{W_{m,i}}\right) \delta_{a,m,k}}, \quad (5.2)$$

where $W_{m,k} > 0$ is the path size contribution weighting of route $i \in R_m$ to path size terms (different for each model), so that the contribution of route $k \in R_m$ to the path size term of route $i \in R_m$ (the path size contribution factor) is $\frac{W_{m,k}}{W_{m,i}}$. To dissect the path size term: each link a in route $i \in R_m$ is penalised (in terms of decreasing the path size term and hence the utility of the route) according to the number of routes in the choice set that also use that link $\left(\sum_{k \in R_m} \delta_{a,m,k}\right)$, where each contribution is weighted (i.e. $\sum_{k \in R_m} \left(\frac{W_{m,k}}{W_{m,i}}\right) \delta_{a,m,k}$), and the significance of the penalisation is also weighted according to how prominent link a is in route $i \in R_m$, i.e. the cost of route a in relation to the total cost of route $i \in R_m$ $\left(\frac{t_a}{c_{m,i}(\boldsymbol{t})}\right)$.

The Path Size Logit (PSL) model (Ben-Akiva & Bierlaire, 1999) proposes that $W_{m,k} = 1$ so that all routes contribute equally to path size terms. This is problematic, however, as the correction terms and thus the choice probabilities of realistic routes are affected by link sharing with unrealistic routes.

To combat this, Ramming (2002) proposed the Generalised Path Size Logit (GPSL) model where $W_{m,k} = \left(c_{m,k}(\boldsymbol{t})\right)^{-\lambda}$ and routes contribute according to travel cost ratios, so that routes with excessively large travel costs have a diminished impact upon the correction terms of routes with small travel costs, and consequently the choice probabilities of those routes.

Duncan et al (2020) reformulate the GPSL model (proposing the alternative GPSL model (GPSL′)) so that the contribution weighting resembles the probability relation, i.e. $W_{m,k} = e^{-\lambda c_{m,k}(\boldsymbol{t})}$. As they discuss, however, GPSL and GPSL′ are not internally consistent in how they define routes as being unrealistic: the path size terms consider only travel cost, whereas the route choice probability relation considers disutility *including* the correction term.

To address this, the Adaptive Path Size Logit (APSL) model is proposed where $W_{m,k} = P_{m,k}$ and routes contribute according to ratios of route choice probability. This ensures internal consistency, where routes defined as unrealistic by the path size terms – and consequently given reduced path size contributions – are exactly those with very low choice probabilities. Since the APSL path size contribution factors depend upon the route choice probabilities, the probability relation is an implicit function, naturally expressed as a fixed-point problem. The APSL model is thus not closed-form and solving the choice probabilities requires a fixed-point algorithm to compute the solution. Furthermore, in order to prove existence and uniqueness of solutions the APSL probability relation is modified from that in (5.1). See Duncan et al (2020) for more details on the

derivation and theoretical properties of the APSL model, as well as definitions and details of the other Path Size Logit models.

SUE for a Path Size Logit model with flow-dependent path size terms can be formulated as follows:

Path Size Logit model SUE: A universal route flow vector $\boldsymbol{f}^* \in F$ is an SUE solution for a Path Size Logit model iff the route flow vector for OD movement m, $\boldsymbol{f}_m^*$, is a solution to the fixed-point problem

$$\boldsymbol{f}_m = \boldsymbol{Q}_m \boldsymbol{P}_m\left(\boldsymbol{c}_m\big(\boldsymbol{t}(\boldsymbol{\Delta f})\big), \boldsymbol{\gamma}_m\big(\boldsymbol{t}(\boldsymbol{\Delta f})\big)\right), \qquad m = 1, \dots, M, \tag{5.3}$$

where $P_{m,i}$ and $\gamma_{m,i}$ are as in (5.1) and (5.2) for route $i \in R_m$, respectively, given the universal route flow vector $\boldsymbol{f}$.

For APSL SUE, the probabilities in (5.3) are fixed-point probabilities. As shown in Duncan et al (2021a), since the route choice probabilities and route flow proportions equate at SUE, the APSL path size contribution factors can be instead expressed in terms of route flow proportions, i.e. where $W_{m,k} = \frac{f_{m,k}}{q_m}$. This underlying route choice model is denoted APSL′ and is closed-form. This alternative definition of APSL SUE is hence denoted APSL′ SUE, and APSL SUE and APSL′ SUE are equivalent for route flow vectors at SUE only. Since the APSL probabilities are fixed-point, and the APSL′ probabilities are closed-form, APSL SUE and APSL′ SUE have different computational performances: the increased computational burden involved in computing each iteration solving APSL SUE means that total computation times are long, while convergence is very slow for APSL′ SUE also resulting in longer total computation times. As explored in Duncan et al (2021a), one can trade-off the accuracy of APSL choice probabilities with rate of SUE convergence, and several techniques are developed that significantly improve total computation times. This manipulation of the APSL SUE model as well as the developed solution techniques are highly relevant for the SUE application of the fixed-point BPS model as detailed in Section 3.2.

2.3 Bounded SUE

Bounded SUE (BSUE) is derived with the Bounded Choice Model (BCM) as the underlying route choice model. In this subsection we briefly formulate the BCM, see Watling et al (2018) and Duncan et al (2021b) for more details on the derivation and theoretical properties of the model. The BCM proposes that a bound is applied to the difference in random utility between each given alternative and an imaginary reference alternative, so that an alternative only receives a non-zero choice probability if the difference between its random utility and the random utility of the reference alternative is within the bound. Furthermore, the probability each alternative is chosen relates to the odds associated with choosing each alternative versus the reference alternative. Watling et al (2018) consider a special case of the BCM where the reference alternative is the alternative with the maximum deterministic utility. While the application of the BCM can involve exerting an absolute bound upon the difference in utility from the maximum, (for example 25 units worse in deterministic utility), we consider in this paper exerting a relative bound upon the difference, i.e. where routes only receive a non-zero choice probability if they have a deterministic disutility less than φ times worse than the greatest route utility. If $V_{m,i} < 0$ is the deterministic disutility of alternative $i \in R_m$, then the probability alternative $i \in R_m$ is chosen under the BCM is:

$$P_{m,i}(\boldsymbol{V}_m) = \frac{\big(h_{m,i}(\boldsymbol{V}_m) - 1\big)_+}{\sum_{j \in R_m}\big(h_{m,j}(\boldsymbol{V}_m) - 1\big)_+}, \tag{5.4}$$

where $h_{m,i}(\boldsymbol{V}_m) = \exp\big(V_{m,i} - \varphi \max\big(V_{m,k} : k \in R_m\big)\big)$, $\varphi > 1$ is the relative bound parameter to be estimated, and $(\cdot)_+ = \max(0, \cdot)$. In a route choice context where the deterministic utility of route $i \in R_m$ is given by $V_{m,i} = -\theta c_{m,i}$, the probability of choosing route $i \in R_m$ is:

$$P_{m,i}\big(\boldsymbol{c}_m(\boldsymbol{t})\big) = \frac{\big(h_{m,i}\big(-\theta \boldsymbol{c}_m(\boldsymbol{t})\big) - 1\big)_+}{\sum_{j \in R_m}\big(h_{m,j}\big(-\theta \boldsymbol{c}_m(\boldsymbol{t})\big) - 1\big)_+}, \tag{5.5}$$

where $h_{m,i}(-\theta \boldsymbol{c}_m(\boldsymbol{t})) = \exp(-\theta c_{m,i}(\boldsymbol{t}) - \varphi \max(-\theta c_{m,l}(\boldsymbol{t}): l \in R_m)) = \exp\left(-\theta\left(c_{m,i}(\boldsymbol{t}) - \varphi \min(c_{m,l}(\boldsymbol{t}): l \in R_m)\right)\right)$. Thus, routes only receive a non-zero choice probability if they have a cost less than φ times the cost on the cheapest route, and the probability each route is chosen relates to the odds that that route has a cost within the bound.

BSUE can be formulated as follows:

BSUE: A universal route flow vector $\boldsymbol{f}^* \in \Omega$ is a BSUE solution iff the route flow vector for OD movement m, $\boldsymbol{f}_m^*$, is a solution to the fixed-point problem

$$\boldsymbol{f}_m = \boldsymbol{Q}_m \boldsymbol{P}_m\left(\boldsymbol{c}_m\left(\boldsymbol{t}(\boldsymbol{\Delta f})\right)\right), \qquad m = 1, \dots, M, \tag{5.6}$$

where $P_{m,i}$ is as in (5.5), respectively, for route $i \in R_m$, given the universal route flow vector $\boldsymbol{f}$.

3. Bounded Path Size Stochastic User Equilibrium Models

The PSL model is problematic in that results are sensitive to unrealistic routes in the adopted choice sets. PSL variants such as GPSL, GPSL′, and APSL weight the contributions of routes to path size terms so that the negative impact that unrealistic routes have upon the corrections factors of realistic routes is reduced, and thus the choice probabilities of those routes. This technique, however, does not solve this problem entirely and only worsens in effectiveness as the choice sets are expanded and more unrealistic routes are included. Duncan et al (2021) investigate developing a path size route choice model that eliminates the path size contributions of unrealistic routes entirely, and once more, that removes all the negative effects of unrealistic routes, thereby fully solving the issue.

To tackle this, the integration of PSL concepts with the BCM was explored. The BCM provides a consistent criterion for determining restricted choice sets of feasible routes and route choice probability, though route correlation is not considered. The natural form for a Bounded Path Size (BPS) choice model is derived from inserting path size choice model utilities into the BCM formula in (5.4). As Duncan et al (2021b) show, however, appropriately defining the path size contribution factors within the path size terms is problematic, as demonstrated with examples. A series of desired properties are consequently established for a mathematically well-defined BPS model formulation that utilises a consistent criterion for assigning zero choice probabilities to unrealistic routes while eliminating their path size contributions.

Solving these challenges, an alternative form for a BPS model is proposed and two models are consequently formulated that adopt this form: the Bounded Bounded Path Size (BBPS) model and Bounded Adaptive Path Size (BAPS) model, which satisfy desired properties, as discussed/demonstrated. In this section, we provide SUE definitions for the BBPS & BAPS models, then address the existence and uniqueness of solutions.

Just like the BCM, the BPS models propose that routes are defined as unrealistic if they have generalised travel costs greater than the cost bound, i.e. routes $i \in R_m$ such that $c_{m,i}(\boldsymbol{t}) \geq \varphi \min(c_{m,l}(\boldsymbol{t}): l \in R_m)$, where $\varphi > 1$ is the bound parameter. For a given setting of the link/route costs (and bound parameter), $\bar{R}_m(\boldsymbol{c}_m(\boldsymbol{t}); \varphi) \subseteq R_m$ is defined as the restricted choice set (for OD movement m) of all routes $i \in R_m$ where $c_{m,i}(\boldsymbol{t}) < \varphi \min(c_{m,l}(\boldsymbol{t}): l \in R_m)$. $\bar{R}_m$ is the active choice set of the realistic/used routes that will receive non-zero probabilities. Unrealistic routes $i \notin \bar{R}_m(\boldsymbol{c}_m(\boldsymbol{t}); \varphi)$ with costs above the bound receive zero choice probabilities.

Where the BPS models differ from the BCM is with the inclusion of path size correction factors within the probability relation, to adjust the probabilities to capture route correlations. Moreover, the key behavioural feature of the BPS models is that route correlations are considered between only the routes defined as realistic. Thus, only the realistic routes $i \in \bar{R}_m(\boldsymbol{c}_m(\boldsymbol{t}); \varphi)$ have path size terms and contribute to / impact the path size terms of other realistic routes. Unrealistic routes $i \notin \bar{R}_m(\boldsymbol{c}_m(\boldsymbol{t}); \varphi)$ do not have path size terms and do not contribute to / impact the path size terms of realistic routes.

In SUE application, the travel costs are flow-dependent, and therefore the routes defined as (un)realistic depend upon the flows set. The restricted choice sets of realistic routes for the BPS models in SUE are thus equilibrated along with the route flows. The theoretical difference between the BBPS model and BAPS model is in how the path size contribution factors are formulated, as we discuss below.

3.1 Bounded Bounded Path Size SUE

The BBPS model proposes that the path size contribution factors consider ratios of the odds that routes are within the bound. Given $\bar{R}_m(\boldsymbol{c}_m(\boldsymbol{t});\varphi)$ for OD movement m, the BBPS model choice probability relation for route $i \in R_m$ is:

$$P_{m,i}\left(\boldsymbol{c}_m(\boldsymbol{t}), \bar{\boldsymbol{\gamma}}_m^{BBPS}(\boldsymbol{t})\right) = \begin{cases} \dfrac{\left(h_{m,i}\left(-\theta \boldsymbol{c}_m(\boldsymbol{t})\right)-1\right)\cdot\left(\bar{\gamma}_{m,i}^{BBPS}(\boldsymbol{t})\right)^{\beta}}{\sum_{j\in\bar{R}_m(\boldsymbol{c}_m(\boldsymbol{t});\varphi)}\left(h_{m,j}\left(-\theta \boldsymbol{c}_m(\boldsymbol{t})\right)-1\right)\cdot\left(\bar{\gamma}_{m,j}^{BBPS}(\boldsymbol{t})\right)^{\beta}} & if\ i \in \bar{R}_m(\boldsymbol{c}_m(\boldsymbol{t});\varphi) \\ 0 & if\ i \notin \bar{R}_m(\boldsymbol{c}_m(\boldsymbol{t});\varphi) \end{cases}, \quad (5.7)$$

where $h_{m,i}\left(-\theta \boldsymbol{c}_m(\boldsymbol{t})\right) = \exp\left(-\theta\left(c_{m,i}(\boldsymbol{t}) - \varphi \min\left(c_{m,l}(\boldsymbol{t}): l \in R_m\right)\right)\right)$, and the path size term for route $i \in \bar{R}_m(\boldsymbol{c}_m(\boldsymbol{t});\varphi)$ is:

$$\bar{\gamma}_{m,i}^{BBPS}(\boldsymbol{t}) = \sum\nolimits_{a\in A_{m,i}} \frac{t_a}{c_{m,i}(\boldsymbol{t})} \frac{\left(h_{m,i}\left(-\lambda \boldsymbol{c}_m(\boldsymbol{t})\right)-1\right)}{\sum_{k\in\bar{R}_m(\boldsymbol{c}_m(\boldsymbol{t});\varphi)}\left(h_{m,k}\left(-\lambda \boldsymbol{c}_m(\boldsymbol{t})\right)-1\right)\delta_{a,m,k}}. \quad (5.8)$$

$\theta > 0$ is the Logit scaling parameter, $\beta \geq 0$ is the path size scaling parameter, $\varphi > 1$ is the universal bound parameter, and $\lambda > 0$ is the path size contribution scaling parameter.

The BBPS path size contribution weighting $W_{m,k} = h_{m,k}\left(-\lambda \boldsymbol{c}_m(\boldsymbol{t})\right) - 1$ is stipulated as such so to satisfy the desired properties for a BPS model established in Duncan et al (2021b). This includes ensuring the choice probability function is continuous, which is vital for SUE application. As can be seen, when $\lambda = \theta$, $W_{m,k}$ matches the travel cost component in the BBPS model probability relation exactly, and thus choice probabilities and path size contributions tend towards zero concurrently and meet at zero. This ensures the smooth removal of a route from the active choice set as it's travel cost is decreased below the bound.

An additional path size contribution scaling parameter, λ, is included, in the spirit of the GPSL and GPSL' models, to allow for the de-coupling of the scale of the model from the path size effect. Larger values of λ accentuate the differences in cost within the contribution factors, so that the more expensive routes have more diminished (though still positive) contributions. In the same way that the GPSL$'_{(\lambda=\theta)}$ model is developed, however, one can equate the travel cost scales setting by $\lambda = \theta$ – thus formulating the BBPS$_{(\lambda=\theta)}$ model – to improve internal consistency and reduce the number of model parameters to estimate. In Duncan et al (2020) and Duncan et al (2021b), through theoretical and empirical analysis, the credibility of large λ values for BBPS/GPSL models is questioned.

The attraction of the BBPS model is that it has a closed-form choice probability expression and hence route choice probability solutions are guaranteed to exist and be unique. The BBPS model is however not fully internally consistent since the path size contribution factors do not consider route distinctiveness, though consistency is improved by setting $\lambda = \theta$.

The BBPS model approaches the GPSL$'$ model as $\varphi \to \infty$, and thus the BBPS$_{(\lambda=\theta)}$ model is also equivalent to the GPSL$'_{(\lambda=\theta)}$ model in the limit as $\varphi \to \infty$. This provides the BBPS model with a theoretical connection to the family of PSL models. The BBPS model is also equivalent to the BCM for $\beta = 0$, which is equivalent to the MNL model in the limit as $\varphi \to \infty$.

BBPS SUE can be formulated as follows:

BBPS SUE: A universal route flow vector $\boldsymbol{f}^* \in \Omega$ is a BBPS SUE solution iff the route flow vector for OD movement m, $\boldsymbol{f}_m^*$, is a solution to the fixed-point problem

$$\boldsymbol{f}_m = \boldsymbol{Q}_m \boldsymbol{P}_m\left(\boldsymbol{c}_m\left(\boldsymbol{t}(\boldsymbol{\Delta f})\right), \bar{\boldsymbol{\gamma}}_m^{BBPS}\left(\boldsymbol{t}(\boldsymbol{\Delta f})\right)\right), \qquad m = 1, \ldots, M, \quad (5.9)$$

where $P_{m,i}$ is as in (5.7) for route $i \in R_m$ and $\bar{\gamma}_{m,i}^{BBPS}$ is as in (5.8) for route $i \notin \bar{R}_m(\boldsymbol{c}_m(\boldsymbol{t});\varphi)$, given the universal route flow vector $\boldsymbol{f}$.

3.2 Bounded Adaptive Path Size SUE

Like the APSL model, the BAPS model proposes that the path size contribution factors consider choice probability ratios, and as such BAPS SUE can also be defined in two different ways.

3.2.1 Definition 1: BAPS SUE

By adopting choice probability ratio path size contribution factors, the BAPS model has a consistent criterion for assigning zero choice probabilities to unrealistic routes, eliminating the path size contributions of unrealistic routes, and determining route choice probabilities and path size contributions (internally consistent). The BAPS model is, however, not closed-form and the probability relation is an implicit function, naturally expressed as a fixed-point problem.

As discussed in more detail in Duncan et al (2021b), the standard formulation for the BAPS model is problematic, since the probability domain is not defined on a closed set, forcing difficulties proving the existence and uniqueness of solutions. To circumvent this, a modified version is formulated for which solutions are proven to exist and uniqueness conditions are established. The modified BAPS model formulation does not have a continuous probability distribution, but the standard formulation can be approximated to arbitrary precision, thus also approximating continuity. In practice the modified version is used and hence we formulate SUE conditions for this formulation.

The modified BAPS formulation is defined as follows, see Duncan et al (2021b) for more details on the derivation and theoretical properties of the model. Given $\bar{R}_m(\boldsymbol{c}_m(\boldsymbol{t});\varphi)$, the BAPS model route choice probabilities for OD movement m, $\boldsymbol{P}_m^*(\boldsymbol{t})$, are a solution to the fixed-point problem $\boldsymbol{P}_m = \boldsymbol{Z}_m\left(\boldsymbol{z}_m\left(\boldsymbol{c}_m(\boldsymbol{t}), \bar{\boldsymbol{\gamma}}_m^{BAPS}(\boldsymbol{t}, \boldsymbol{P}_m)\right)\right)$, given the link cost vector $\boldsymbol{t}$, where:

$$Z_{m,i}\left(z_{m,i}\left(\boldsymbol{c}_m(\boldsymbol{t}), \bar{\boldsymbol{\gamma}}_m^{BAPS}(\boldsymbol{t}, \boldsymbol{P}_m)\right)\right) = \begin{cases} \tau_m + (1 - \bar{N}_m\tau_m)\cdot z_{m,i}\left(\boldsymbol{c}_m(\boldsymbol{t}), \bar{\boldsymbol{\gamma}}_m^{BAPS}(\boldsymbol{t}, \boldsymbol{P}_m)\right) & if\ i \in \bar{R}_m(\boldsymbol{c}_m(\boldsymbol{t});\varphi) \\ 0 & if\ i \notin \bar{R}_m(\boldsymbol{c}_m(\boldsymbol{t});\varphi) \end{cases}, \tag{5.10}$$

$$z_{m,i}\left(\boldsymbol{c}_m(\boldsymbol{t}), \bar{\boldsymbol{\gamma}}_m^{BAPS}(\boldsymbol{t}, \boldsymbol{P}_m)\right) = \begin{cases} \dfrac{\left(h_{m,i}\left(-\theta\boldsymbol{c}_m(\boldsymbol{t})\right) - 1\right)\cdot\left(\bar{\gamma}_{m,i}^{BAPS}(\boldsymbol{t}, \boldsymbol{P}_m)\right)^{\beta}}{\sum_{j\in\bar{R}_m(\boldsymbol{c}_m(\boldsymbol{t});\varphi)}\left(h_{m,j}\left(-\theta\boldsymbol{c}_m(\boldsymbol{t})\right) - 1\right)\cdot\left(\bar{\gamma}_{m,j}^{BAPS}(\boldsymbol{t}, \boldsymbol{P}_m)\right)^{\beta}} & if\ i \in \bar{R}_m(\boldsymbol{c}_m(\boldsymbol{t});\varphi) \\ 0 & if\ i \notin \bar{R}_m(\boldsymbol{c}_m(\boldsymbol{t});\varphi) \end{cases}, \tag{5.11}$$

where $h_{m,i}\left(-\theta\boldsymbol{c}_m(\boldsymbol{t})\right) = \exp\left(-\theta\left(c_{m,i}(\boldsymbol{t}) - \varphi\min\left(c_{m,l}(\boldsymbol{t}): l \in R_m\right)\right)\right)$, and the path size term for route $i \in \bar{R}_m(\boldsymbol{c}_m(\boldsymbol{t});\varphi)$ is:

$$\bar{\gamma}_{m,i}^{BAPS}(\boldsymbol{t}, \boldsymbol{P}_m) = \sum_{a\in A_{m,i}} \frac{t_a}{c_{m,i}(\boldsymbol{t})} \frac{P_{m,i}}{\sum_{k\in\bar{R}_m(\boldsymbol{c}_m(\boldsymbol{t});\varphi)} P_{m,k}\delta_{a,m,k}}, \forall \boldsymbol{P}_m \in D^{(\bar{R}_m(\boldsymbol{c}_m(\boldsymbol{t});\varphi),\tau_m)}, \tag{5.12}$$

$$D_m^{(\bar{R}_m(\boldsymbol{c}_m(\boldsymbol{t});\varphi),\tau_m)} = \Big\{\boldsymbol{P}_m \in \mathbb{R}_{\geq 0}^{N_m}: \tau_m \leq P_{m,i} \leq (1 - (\bar{N}_m - 1)\tau_m), \forall i \in \bar{R}_m(\boldsymbol{c}_m(\boldsymbol{t});\varphi), and, 0 \leq P_{m,i} \leq (1 - \bar{N}_m\tau_m), \forall i \notin \bar{R}_m(\boldsymbol{c}_m(\boldsymbol{t});\varphi), \sum_{j=1}^{N_m} P_{m,j} = 1\Big\}.$$

The model parameters are $0 < \tau_m \leq \frac{1}{\bar{N}_m}$, $m = 1, \dots, M$, $\theta > 0$, $\beta \geq 0$, $\varphi > 1$, where τ_m is the perturbation parameter for OD movement m, which does not require estimating, but is introduced so that BAPS models solutions can be proven to exist and be unique. $Z_{m,i}$ in (5.10) is the probability adjustment function also introduced for existence and uniqueness proofs.

As (5.12) shows, for a choice probability solution $\boldsymbol{P}_m^*$, the contribution of used route $k \in \bar{R}_m(\boldsymbol{c}_m(\boldsymbol{t});\varphi)$ to the BAPS model path size term of used route $i \in \bar{R}_m(\boldsymbol{c}_m(\boldsymbol{t});\varphi)$ is weighted according to the ratio of choice

probabilities between the routes $\left(\frac{P^*_{m,k}}{P^*_{m,i}}\right)$, and hence as a used route approaches zero choice probability its path size contributions approach zero, until it is considered unrealistic, where it then receives a zero choice probability and its path size contributions are eliminated completely. This ensures that *in practice* the choice probability function is continuous, (when setting arbitrarily small τ_m values, see Duncan et al (2021b) for details).

The modified BAPS model formulation approaches the APSL model in the limit as $\varphi \to \infty$, and is equivalent to the BCM for $\beta = 0$, which is equivalent to the MNL model in the limit as $\varphi \to \infty$.

BAPS SUE can be formulated as follows:

BAPS SUE: A universal route flow vector $\boldsymbol{f}^* \in \Omega$ is a BAPS SUE solution iff the route flow vector for OD movement m, $\boldsymbol{f}^*_m$, is a solution to the fixed-point problem

$$\boldsymbol{f}_m = \boldsymbol{Q}_m \boldsymbol{P}^*_m\big(\boldsymbol{t}(\boldsymbol{\Delta f})\big), \qquad m = 1, \dots, M, \tag{5.13}$$

where $\boldsymbol{P}^*_m$ is a route choice probability solution for OD movement m in $\boldsymbol{Y}_m$ to the fixed-point problem:

$$\boldsymbol{Y}_m = \boldsymbol{Z}_m\left(\boldsymbol{z}_m\left(\boldsymbol{c}_m\big(\boldsymbol{t}(\boldsymbol{\Delta f})\big), \bar{\boldsymbol{\gamma}}^{BAPS}_m\big(\boldsymbol{t}(\boldsymbol{\Delta f}), \boldsymbol{Y}_m\big)\right)\right), \tag{5.14}$$

given the universal route flow vector $\boldsymbol{f}$, where $Z_{m,i}$ and $z_{m,i}$ are as in (5.10) and (5.11), respectively, for route $i \in R_m$, and $\bar{\gamma}^{BAPS}_{m,i}$ is as in (5.12) for route $i \in \bar{R}_m(\boldsymbol{c}_m(\boldsymbol{t}); \varphi)$.

3.2.2 Definition 2: BAPS′ SUE

Like APSL SUE Definition 2 (APSL′ SUE), BAPS SUE Definition 2 (BAPS′ SUE) is derived indirectly by utilising a different underlying route choice model, that is equivalent to the BAPS model at SUE, but only at SUE. By the definition of SUE, the route flow proportions and route choice probabilities equate at equilibrium. Therefore, the BAPS′ choice model supposes that the path size contribution factors consider route flow proportion ratios, instead of choice probability.

The BAPS′ model is defined as follows. Given $\bar{R}_m(\boldsymbol{c}_m(\boldsymbol{t}); \varphi)$, the BAPS′ model choice probability relation for route $i \in R_m$ is:

$$P_{m,i}\left(z_{m,i}\left(\boldsymbol{c}_m(\boldsymbol{t}), \bar{\boldsymbol{\gamma}}^{BAPS'}_m(\boldsymbol{t}, \boldsymbol{f}_m)\right)\right) = \begin{cases} \tau_m + (1 - \bar{N}_m \tau_m) \cdot z_{m,i}\left(\boldsymbol{c}_m(\boldsymbol{t}), \bar{\boldsymbol{\gamma}}^{BAPS'}_m(\boldsymbol{t}, \boldsymbol{f}_m)\right) & if\ i \in \bar{R}_m(\boldsymbol{c}_m(\boldsymbol{t}); \varphi) \\ 0 & if\ i \notin \bar{R}_m(\boldsymbol{c}_m(\boldsymbol{t}); \varphi) \end{cases}, \tag{5.15}$$

$$z_{m,i}\left(\boldsymbol{c}_m(\boldsymbol{t}), \bar{\boldsymbol{\gamma}}^{BAPS'}_m(\boldsymbol{t}, \boldsymbol{f}_m)\right) = \begin{cases} \dfrac{\left(h_{m,i}\left(-\theta \boldsymbol{c}_m(\boldsymbol{t})\right) - 1\right) \cdot \left(\bar{\gamma}^{BAPS'}_{m,i}(\boldsymbol{t}, \boldsymbol{f}_m)\right)^{\beta}}{\sum_{j \in \bar{R}_m(\boldsymbol{c}_m(\boldsymbol{t}); \varphi)} \left(h_{m,i}\left(-\theta \boldsymbol{c}_m(\boldsymbol{t})\right) - 1\right) \cdot \left(\bar{\gamma}^{BAPS'}_{m,j}(\boldsymbol{t}, \boldsymbol{f}_m)\right)^{\beta}} & if\ i \in \bar{R}_m(\boldsymbol{c}_m(\boldsymbol{t}); \varphi) \\ 0 & if\ i \notin \bar{R}_m(\boldsymbol{c}_m(\boldsymbol{t}); \varphi) \end{cases}, \tag{5.16}$$

where $h_{m,i}\left(-\theta \boldsymbol{c}_m(\boldsymbol{t})\right) = \exp\left(-\theta\left(c_{m,i}(\boldsymbol{t}) - \varphi \min\left(c_{m,l}(\boldsymbol{t}) : l \in R_m\right)\right)\right)$, and the path size term for route $i \in \bar{R}_m(\boldsymbol{c}_m(\boldsymbol{t}); \varphi)$ is:

$$\bar{\gamma}^{BAPS'}_{m,i}(\boldsymbol{t}, \boldsymbol{f}_m) = \sum_{a \in A_{m,i}} \frac{t_a}{c_{m,i}(\boldsymbol{t})} \frac{f_{m,i}}{\sum_{k \in \bar{R}_m(\boldsymbol{c}_m(\boldsymbol{t}); \varphi)} f_{m,k} \delta_{a,m,k}}, \forall \boldsymbol{f}_m \in \Omega_m^{(\bar{R}_m(\boldsymbol{c}_m(\boldsymbol{t}); \varphi), \tau_m)}, \tag{5.17}$$

$$\Omega_m^{(\bar{R}_m(\boldsymbol{c}_m(\boldsymbol{t});\varphi),\tau_m)} = \left\{ \boldsymbol{f}_m \in \mathbb{R}_+^{N_m} : \tau_m \le \frac{f_{m,i}}{q_m} \le (1-(\bar{N}_m-1)\tau_m), \forall i \in \bar{R}_m(\boldsymbol{c}_m(\boldsymbol{t});\varphi), and, 0 \le \frac{f_{m,i}}{q_m} \le (1-\bar{N}_m\tau_m), \forall i \notin \bar{R}_m(\boldsymbol{c}_m(\boldsymbol{t});\varphi), \sum_{i\in R_m} f_{m,i} = q_m \right\}.$$

$0 < \tau_m \le \frac{1}{\bar{N}_m}$, $m = 1, \dots, M$, $\theta > 0$, $\beta \ge 0$, $\varphi > 1$. As shown in (5.17), the contribution of route $k \in \bar{R}_m(\boldsymbol{c}_m(\boldsymbol{t});\varphi)$ to the path size term of route $i \in \bar{R}_m(\boldsymbol{c}_m(\boldsymbol{t});\varphi)$ is weighted according to the ratio of flow between the routes $\left(\frac{f_{m,k}}{f_{m,i}}\right)$, and hence less feasible route alternatives with very low use/flow have a diminished contribution to the path size terms of more feasible routes with relatively high use/flow.

The BAPS′ choice model is closed-form and hence choice probability solutions for a given flow vector are guaranteed to exist and be unique, assuming every route with a travel cost below the bound has a non-zero flow. Stipulating that the flows for OD movement m $\boldsymbol{f}_m$ belong to the set $\Omega_m^{(\bar{R}_m(\boldsymbol{c}_m(\boldsymbol{t});\varphi),\tau_m)}$ ensures that: a) routes with costs below the bound have a non-zero flow; b) routes with costs above the bound can have a zero flow; c) the route flows are demand-feasible; d) the path size contribution factors consider ratios of route flow proportion (where the demands q_m cancel out), and, e) the BAPS′ model flow domain matches the BAPS model probability domain $D_m^{(\bar{R}_m(\boldsymbol{c}_m(\boldsymbol{t});\varphi),\tau_m)}$.

BAPS′ SUE can be formulated as follows:

BAPS′ SUE: Let $\Omega' \subseteq \Omega$ be the subset of demand-feasible universal route flow vectors $\boldsymbol{f}$ that satisfy the following conditions:

$$\tau_m \le \frac{f_{m,i}}{q_m} \le (1-(\bar{N}_m-1)\tau_m) \Leftrightarrow c_{m,i}(\boldsymbol{t}(\boldsymbol{\Delta f})) < \varphi \min\left(c_{m,l}(\boldsymbol{t}(\boldsymbol{\Delta f})) : l \in R_m\right), \quad \forall i \in R_m, m = 1, \dots, M, \tag{5.18}$$

$$f_{m,i} = 0 \Leftrightarrow c_{m,i}(\boldsymbol{t}(\boldsymbol{\Delta f})) \ge \varphi \min\left(c_{m,l}(\boldsymbol{t}(\boldsymbol{\Delta f})) : l \in R_m\right), \quad \forall i \in R_m, m = 1, \dots, M. \tag{5.19}$$

A universal route flow vector $\boldsymbol{f}^* \in \Omega'$ is a BAPS′ SUE solution iff the route flow vector for OD movement m, $\boldsymbol{f}_m^*$, is a solution to the fixed-point problem

$$\boldsymbol{f}_m = \boldsymbol{Q}_m \boldsymbol{P}_m \left(\boldsymbol{z}_m \left(\boldsymbol{c}_m(\boldsymbol{t}(\boldsymbol{\Delta f})), \boldsymbol{\gamma}_m^{BAPS'}(\boldsymbol{t}(\boldsymbol{\Delta f}), \boldsymbol{f}_m) \right) \right), \quad m = 1, \dots, M, \tag{5.20}$$

where $P_{m,i}$ and $z_{m,i}$ are as in (5.15) and (5.16), respectively, for route $i \in R_m$, and $\bar{\gamma}_{m,i}^{BAPS'}$ is as in (5.17) for route $i \in \bar{R}_m(\boldsymbol{c}_m(\boldsymbol{t}(\boldsymbol{\Delta f})); \varphi)$.

The feasible set of flows Ω' for all OD movements prohibits route flow vectors that lead to routes having non-zero flows and cost that violates the cost bound. This ensures that $\Omega_m^{(\bar{R}_m(\boldsymbol{c}_m(\boldsymbol{t});\varphi),\tau_m)}$ is satisfied for each OD movement $m = 1, \dots, M$, where a route with a cost below the bound must have a non-zero flow ($\ge q_m\tau_m$).

The BAPS′ choice model is only internally consistent for flow distributions at SUE, since for all other flow distributions, the relative attractiveness of routes as defined in the path size contribution factors does not match the relative attractiveness in the probability relation.

The BAPS′ choice model in (5.15)-(5.17) above is defined including the BAPS model adjustment functions $z_{m,i}$ and perturbation parameters τ_m, so that the definitions of BAPS SUE and BAPS′ SUE are equivalent. However, since the BAPS′ model is closed-form, these modifications are not required for solution existence/uniqueness, and the BAPS′ model can be simplified and be formulated as follows (denoted BAPS″). Given $\bar{R}_m(\boldsymbol{c}_m(\boldsymbol{t});\varphi)$, the BAPS″ model choice probability relation for route $i \in R_m$ is:

$$P_{m,i}\left(\boldsymbol{c}_m(\boldsymbol{t}), \bar{\boldsymbol{\gamma}}_m^{BAPS''}(\boldsymbol{t}, \boldsymbol{f}_m)\right) = \begin{cases} \dfrac{\left(h_{m,i}\left(-\theta \boldsymbol{c}_m(\boldsymbol{t})\right) - 1\right) \cdot \left(\bar{\gamma}_{m,i}^{BAPS''}(\boldsymbol{t}, \boldsymbol{f}_m)\right)^{\beta}}{\sum_{j \in \bar{R}_m(\boldsymbol{c}_m(\boldsymbol{t});\varphi)} \left(h_{m,i}\left(-\theta \boldsymbol{c}_m(\boldsymbol{t})\right) - 1\right) \cdot \left(\bar{\gamma}_{m,j}^{BAPS''}(\boldsymbol{t}, \boldsymbol{f}_m)\right)^{\beta}} & if\ i \in \bar{R}_m(\boldsymbol{c}_m(\boldsymbol{t});\varphi) \\ 0 & if\ i \notin \bar{R}_m(\boldsymbol{c}_m(\boldsymbol{t});\varphi) \end{cases}, \quad (5.21)$$

where $h_{m,i}\left(-\theta \boldsymbol{c}_m(\boldsymbol{t})\right) = \exp\left(-\theta\left(c_{m,i}(\boldsymbol{t}) - \varphi \min\left(c_{m,l}(\boldsymbol{t}): l \in R_m\right)\right)\right)$, and the path size term for route $i \in \bar{R}_m(\boldsymbol{c}_m(\boldsymbol{t});\varphi)$ is:

$$\bar{\gamma}_{m,i}^{BAPS''}(\boldsymbol{t}, \boldsymbol{f}_m) = \sum\nolimits_{a \in A_{m,i}} \frac{t_a}{c_{m,i}(\boldsymbol{t})} \frac{f_{m,i}}{\sum_{k \in \bar{R}_m(\boldsymbol{c}_m(\boldsymbol{t});\varphi)} f_{m,k} \delta_{a,m,k}}, \qquad \forall \boldsymbol{f}_m \in \Omega_m^{\left(\bar{R}_m(\boldsymbol{c}_m(\boldsymbol{t});\varphi)\right)}, \quad (5.22)$$

$$\Omega_m^{\left(\bar{R}_m(\boldsymbol{c}_m(\boldsymbol{t});\varphi)\right)} = \left\{ \boldsymbol{f}_m \in \mathbb{R}_+^{N_m}: f_{m,i} > 0, \forall i \in \bar{R}_m(\boldsymbol{c}_m(\boldsymbol{t});\varphi), and, f_{m,i} = 0, \forall i \notin \bar{R}_m(\boldsymbol{c}_m(\boldsymbol{t});\varphi), \sum_{i \in R_m} f_{m,i} = q_m \right\}.$$

$\theta > 0, \beta \geq 0, \varphi > 1$.

BAPS$''$ SUE can thus be formulated as follows:

BAPS$''$ SUE: Let $\Omega'' \subseteq \Omega$ be the subset of demand-feasible universal route flow vectors $\boldsymbol{f}$ that satisfy the following conditions:

$$f_{m,i} > 0 \Leftrightarrow c_{m,i}\left(\boldsymbol{t}(\boldsymbol{\Delta f})\right) < \varphi \min\left(c_{m,l}\left(\boldsymbol{t}(\boldsymbol{\Delta f})\right): l \in R_m\right), \qquad \forall i \in R_m, m = 1, \dots, M, \quad (5.23)$$

$$f_{m,i} = 0 \Leftrightarrow c_{m,i}\left(\boldsymbol{t}(\boldsymbol{\Delta f})\right) \geq \varphi \min\left(c_{m,l}\left(\boldsymbol{t}(\boldsymbol{\Delta f})\right): l \in R_m\right), \qquad \forall i \in R_m, m = 1, \dots, M. \quad (5.24)$$

A universal route flow vector $\boldsymbol{f}^* \in \Omega''$ is a BAPS$''$ SUE solution iff the route flow vector for OD movement m, $\boldsymbol{f}_m^*$, is a solution to the fixed-point problem

$$\boldsymbol{f}_m = \boldsymbol{Q}_m \boldsymbol{P}_m\left(\boldsymbol{c}_m\left(\boldsymbol{t}(\boldsymbol{\Delta f})\right), \boldsymbol{\gamma}_m^{BAPS''}(\boldsymbol{t}(\boldsymbol{\Delta f}), \boldsymbol{f}_m)\right), \qquad m = 1, \dots, M, \quad (5.25)$$

where $P_{m,i}$ is as in (5.21) for route $i \in R_m$, and $\bar{\gamma}_{m,i}^{BAPS''}$ is as in (5.22) for route $i \in \bar{R}_m\left(\boldsymbol{c}_m\left(\boldsymbol{t}(\boldsymbol{\Delta f})\right);\varphi\right)$.

3.3 Existence & Uniqueness of Solutions

In this subsection, we prove the existence of BBPS SUE solutions. However, since the BAPS model probability relation is modified so that BAPS probability solutions can be proven to exist, and the probability function is consequently discontinuous, BAPS SUE solutions (and therefore BAPS$'$ SUE solutions) cannot be proven to exist. We note that since continuity of the BAPS/BAPS$'$ probability functions can be approximated in the limits as $\tau_m \to 0$, we do not anticipate there to be issues with non-existence of BAPS/BAPS$'$ SUE solutions, as long as τ_m is set suitably small, and no issues were experienced in our experiments. Although the BAPS$''$ model does have a continuous probability function, Ω'' is not a convex set, and thus standard proofs for solution existence also do not apply.

First, we define an important function: the BBPS SUE fixed-point function. Let $H_{m,i}(\boldsymbol{f}) = q_m P_{m,i}\left(\boldsymbol{c}_m\left(\boldsymbol{t}(\boldsymbol{\Delta f})\right), \bar{\boldsymbol{\gamma}}_m^{BBPS}\left(\boldsymbol{t}(\boldsymbol{\Delta f})\right)\right)$, where $P_{m,i}$ is as in (5.7) for route $i \in R_m$ and $\bar{\gamma}_{m,i}^{BBPS}$ is as in (5.8) for route $i \in \bar{R}_m\left(\boldsymbol{c}_m\left(\boldsymbol{t}(\boldsymbol{\Delta f})\right);\varphi\right)$. It is clear from (5.9) that a route flow solution $\boldsymbol{f}^*$ is a BBPS SUE solution iff $H_{m,i}(\boldsymbol{f}^*) = f_{m,i}^*, \forall i \in R_m, m = 1, \dots, M$.

Given $H_{m,i}(\boldsymbol{f})$, we prove that BBPS SUE model solutions are guaranteed to exist.

Proposition 1: If the link cost function $\boldsymbol{t}(\boldsymbol{\Delta f})$ is a continuous function for all $\boldsymbol{f} \in \Omega$, then at least one BBPS SUE fixed-point route flow solution, $\boldsymbol{f}^* \in \Omega$, is guaranteed to exist.

Proof. From the assumptions that $\boldsymbol{t}(\boldsymbol{\Delta f})$ is a continuous function for all $\boldsymbol{f} \in \Omega$, (and thus $H_{m,i}$ is a continuous function), and given that Ω is a nonempty, convex, and compact set, and $\boldsymbol{H}$ maps Ω into itself, then by

Brouwer's Fixed-Point Theorem at least one solution $\boldsymbol{f}^*$ exists such that $H_{m,i}(\boldsymbol{f}^*) = 0, \forall i \in R_m, m = 1, \dots, M$, and hence BBPS SUE solutions are guaranteed to exist.

■

The standard approach for establishing sufficient conditions for the uniqueness of BBPS SUE solutions requires $H_{m,i}(\boldsymbol{f})$ to be a monotonic function. Assuming the link cost functions $\boldsymbol{t}(\boldsymbol{\Delta f})$ are monotonic, then the route cost functions $\boldsymbol{c}_m\big(\boldsymbol{t}(\boldsymbol{\Delta f})\big)$ are also monotonic. However, the used route path size term functions $\overline{\boldsymbol{\gamma}}_m^{BBPS}\big(\boldsymbol{t}(\boldsymbol{\Delta f})\big)$, are not guaranteed to always be monotonic, and hence the approach is not applicable. This is not to say however that BBPS SUE solutions cannot be unique, since the mentioned approach only establishes sufficient conditions. Due to the probability In Section 5.4 we investigate the uniqueness of BAPS SUE solutions numerically, since it is a fixed-point .

4. Solution Algorithm

In this section, we propose a generic algorithm for solving BPS SUE models. The algorithm is an adaptation of the generic algorithm proposed by Watling et al (2018) for the BSUE model, which is in turn an adaptation of the generic algorithm proposed by Rasmussen et al (2015) for the Restricted SUE (RSUE) model. Since it is typically not feasible to generate and operate with the universal set of routes, these algorithms propose that routes are generated from the network as the algorithm progresses. At each iteration, given the route costs from the current route flows, a column generation approach is used to find, for each OD movement, all the routes in the network that have a travel cost below the current cost bound. As Watling et al (2018) discuss, however, with the current techniques available for generating all such routes, there are questions over the suitability of the approach for large-scale networks. For example, the computational burden of the Constrained Enumeration approach (e.g. Prato & Bekhor, 2006; Hoogendoorn-Lanser et al, 2006), which they adopt, increases exponentially as the bound parameter, size of network, and network depth increase. For use of the column generation approach, more computationally efficient methods for consistent route generation may need to be adopted.

The approach we adopt in this paper for the proposed BPS SUE algorithm and its application, is to pre-generate approximated universal choice sets and make an assumption that these routes contain at least all those considered realistic. Usually, for non-bounded route choice models, it is crucial for the accuracy of results that the pre-generated choice sets contain only the routes considered realistic, as the presence of unrealistic routes can significantly and negatively affect realistic route choice probabilities. For the bounded models, however, the presence of unrealistic routes in the pre-generated choice sets have no effect upon the probabilities of realistic routes (as defined by the model). Hence, choice sets can be generated as large as the computational resources allow, in order to minimise the possibility of excluding what would later turn out to be a plausible route from the choice sets. From the approximated universal choice sets, the BPS SUE algorithm equilibrates the restricted choice sets of the realistic route alternatives and assigns flows to these routes in a way that is consistent. The computational benefit of having pre-generated choice sets is that at each iteration of the BPS SUE algorithm, the travel costs for all routes can be computed and the column generation phase becomes trivial. The proposed BPS SUE algorithm given here can however be easily adapted so that routes are generated as the algorithm progresses, just like the BSUE algorithm in Watling et al (2018).

As discussed in Section 3 in Duncan et al (2021b), a 'natural' form for the BPS model was initially explored, where path size utilities are inserted into the BCM formula in (5.4). This bounds routes according their utility (i.e. combination of cost and path size correction), rather than just cost. However, as demonstrated, appropriately defining the path size contribution factors within the path size terms is difficult. Instead, to circumvent this issue, an alternative BPS model form was derived, which proposes that routes are bounded according to their travel cost (like the BCM), while the probability relations for routes with costs below the bound include path size correction factors to adjust for route correlations. This means that the BCM and BPS model both have the same definition for unrealistic routes: those with travel costs above the bound. This has the benefit that the algorithm and gap measures proposed for solving BSUE are applicable for solving BPS SUE with only a few minor adjustments.

The main adaptation of the BPS SUE algorithm from the BSUE algorithm is the addition of a *Flow Allocation for New Routes* phase, which ensures that the allocation of flow to new routes generated from the *Column Generation Phase* is done so in a way that satisfies the feasible set of flows.

The BPS SUE algorithm can be summarised as follows: **Step 0:** Initialise by performing all-or-nothing assignments to obtain the initial sets of used routes (where there is a single route in each used route choice set); **Step 1:** Search for routes with a cost below the current bound and add them to the used route choice sets; **Step 2:** Allocate flow to new routes in a way that satisfies flow feasibility; **Step 3:** Compute the relevant BPS model choice probabilities for the current used routes given the current flow vector and thus link costs (knowing all of these routes will receive a non-zero probability); **Step 4:** Compute auxiliary route flow vector given the probabilities; **Step 5:** Compute the next route flow vector by averaging the previous and auxiliary flow vectors according to chosen averaging scheme; **Step 6:** Given the new flow vector, compute the link/route costs; **Step 7:** Compute the *used above bound* relative gap measure which when satisfied ensures no routes with costs *above* the cost bound are *used*; **Step 8:** Remove routes that have costs above the bound (and thus should not be used / have flow), redistribute the flows, and update costs; **Step 9:** Compute the *unused below bound* and *used below bound* relative gap measures, which when satisfied ensure that no routes with costs *below* the cost bound are *unused* and that flow is allocated across the used routes in a way that fulfils the underlying choice model, respectively. Stop if all relative gap measures are satisfied, else return to Step 1.

Step 0: Initialisation. Perform deterministic all-or-nothing assignments for all OD movements $m = 1, \dots, M$ and obtain the used route choice sets $\bar{R}_m^{(0)}$ for OD movements $m = 1, \dots, M$, and the universal route flow vector $\boldsymbol{f}^{(0)}$, where all unused routes have zero flow. Given $\boldsymbol{f}^{(0)}$, compute the link travel cost vector $\boldsymbol{t}^{(1)} = \boldsymbol{t}\left(\boldsymbol{\Delta f}^{(0)}\right)$ for iteration $n = 1$, and hence also the route cost vectors $\boldsymbol{c}_m^{(1)} = \boldsymbol{c}_m\left(\boldsymbol{t}^{(1)}\right) = \boldsymbol{c}_m\left(\boldsymbol{t}\left(\boldsymbol{\Delta f}^{(0)}\right)\right)$, $m = 1, \dots, M$, for iteration $n = 1$. Set $n = 1$.

Step 1: Column Generation Phase. Let $\bar{N}_m^{(n-1)}$ be the number of routes in the choice set for OD movement m at iteration $n - 1$. For each OD movement $m = 1, \dots, M$, given route cost vector $\boldsymbol{c}_m^{(n)}$ for iteration n, add all routes with costs below the current bound to the used route choice sets $\bar{R}_m^{(n)}$ for iteration n.

Step 2: Flow Allocation for New Routes. Allocate a flow to each of the new routes generated in Step 1 (and adjust existing route flows if required) in a way that satisfies the feasible set for route flows Ω, and thus obtain $\boldsymbol{f}^{(n)}$ for iteration n. If required, update $\boldsymbol{t}^{(n)} = \boldsymbol{t}\left(\boldsymbol{\Delta f}^{(n)}\right)$ and $\boldsymbol{c}_m^{(n)} = \boldsymbol{c}_m\left(\boldsymbol{t}^{(n)}\right)$, $m = 1, \dots, M$, for iteration n.

Step 3: Compute Route Choice Probabilities. Given the choice sets $\bar{R}_m^{(n)}$ for OD movements $m = 1, \dots, M$ and the link cost vector $\boldsymbol{t}^{(n)}$ for iteration n, and the route flow vector $\boldsymbol{f}^{(n)}$ for iteration n (or otherwise), compute the route choice probability vectors $\boldsymbol{P}_m^{(n)}$, $m = 1, \dots, M$, for iteration n.

Step 4: Compute Auxiliary Route Flow Vector. Given the route choice probability vectors $\boldsymbol{P}_m^{(n)}$, $m = 1, \dots, M$, for iteration n, compute the auxiliary route flow vector $\tilde{\boldsymbol{f}}^{(n)}$ for iteration n: $\tilde{f}_{m,i}^{(n)} = q_m P_{m,i}^{(n)}, \forall i \in \bar{R}_m^{(n)}, m = 1, \dots, M$.

Step 5: Flow-Averaging Phase. Given the route flow vector $\boldsymbol{f}^{(n)}$ and the auxiliary route flow vector $\tilde{\boldsymbol{f}}^{(n)}$ for iteration n, perform flow-averaging to find the route flow vector $\boldsymbol{f}^{(n+1)}$ for iteration $n + 1$.

Step 6: Compute Link/Route Costs. Given $\boldsymbol{f}^{(n+1)}$, compute the link travel cost vector $\boldsymbol{t}^{(n+1)} = \boldsymbol{t}\left(\boldsymbol{\Delta f}^{(n+1)}\right)$ and hence also the route cost vectors $\boldsymbol{c}_m^{(n+1)} = \boldsymbol{c}_m\left(\boldsymbol{t}^{(n+1)}\right)$, $m = 1, \dots, M$, for iteration $n = n + 1$.

Step 7: Used Above Bound Convergence Evaluation. Compute the *used above bound* relative gap measure, and if this is equal to zero, continue to Step 9. Otherwise, continue to Step 8.

Step 8: Bound Condition Phase. Given the used route choice sets $\bar{R}_m^{(n)}$ for all OD movements $m = 1, \dots, M$, check whether the condition $c_{m,i}^{(n+1)} < \varphi \min\left(c_{m,j}^{(n+1)} : j \in \bar{R}_m^{(n)}\right)$ is violated for any $i \in \bar{R}_m^{(n)}$ for $m = 1, \dots, M$. Update the choice sets $\bar{R}_m^{(n)}$ by removing violating routes, and update $\boldsymbol{f}^{(n+1)}$ by redistributing the flow on

routes removed among the remaining routes in the respective choice sets, ensuring the OD travel demands are still satisfied. Update $\boldsymbol{t}^{(n+1)} = \boldsymbol{t}\left(\boldsymbol{\Delta f}^{(n+1)}\right)$ and $\boldsymbol{c}_m^{(n+1)} = \boldsymbol{c}_m\left(\boldsymbol{t}^{(n+1)}\right)$, $m = 1, \dots, M$, for iteration $n+1$.

Step 9: Below Bound Convergence Evaluation. Compute the *below bound* relative gap measures, and if all gap measures (including the *used above bound* measure) satisfy their pre-specified convergence value, output the route flow vector $\boldsymbol{f}^{(n)}$. Otherwise, set $n = n+1$ and return to Step 1.

Algorithm 5.1. Generic solution algorithm for Bounded Path Size SUE models, for when there are pre-generated approximated or actual universal choice sets.

4.1 Step 2: Flow Allocation for New Routes

For BPS SUE models in general – such as BBPS SUE – this step is straightforward: allocate all new routes zero flow. However, for the BAPS′ model, allocating new routes zero flows violates the set of feasible flows $\Omega^{(\varphi,\tau)}$ since these routes may have costs within the bound. Therefore, to satisfy feasible flows, we propose that these new routes are each allocated τ_m flow (where τ_m is the BAPS/BAPS′ perturbation parameter, see Section 3.2), and the flows of routes already existing in the choice set adjusted accordingly:

$$f_{m,i}^{(n)} = \begin{cases} f_{m,i}^{(n)} - \dfrac{\left(\bar{N}_m^{(n)} - \bar{N}_m^{(n-1)}\right)}{\bar{N}_m^{(n-1)}} \cdot \tau_m & if\ i \in \bar{R}_m^{(n)} \cap \bar{R}_m^{(n-1)} \\ \tau_m & if\ i \in \bar{R}_m^{(n)} \backslash \bar{R}_m^{(n-1)} \end{cases}, \qquad \forall i \in \bar{R}_m^{(n)},$$

where $\bar{R}_m^{(n)}$ is the OD movement m used route choice set at this stage of iteration n (after the *column generation phase*) of size $\left|\bar{R}_m^{(n)}\right| = \bar{N}_m^{(n)}$, and $\bar{R}_m^{(n-1)}$ is the OD movement m used route choice set at the end of iteration $n-1$ (after the *bound condition phase*) of size $\left|\bar{R}_m^{(n-1)}\right| = \bar{N}_m^{(n-1)}$, $m = 1, \dots, M$. This is also required for solving BAPS SUE with follow-on initial conditions (see Section 4.2); however, otherwise (with non-follow-on conditions), new routes can be allocated zero flow. If the flows are adjusted, then the link/route costs should in theory be updated. However, in practice, the τ_m values are so small that the effects are insignificant and updating the costs is not necessary.

4.2 Step 3: Compute Route Choice Probabilities

For BBPS and BAPS′ SUE, this step is straightforward and involves a simple computation of the closed-form probability expressions.

BBPS SUE: Given the used route choice set $\bar{R}_m^{(n)}$ for OD movement m, the link cost vector $\boldsymbol{t}^{(n)}$, and the route flow vector $\boldsymbol{f}^{(n)}$ at this stage of iteration n, the choice probability for route $i \in R_m$ for iteration n is:

$$P_{m,i}^{(n)} = P_{m,i}\left(\boldsymbol{c}_m\left(\boldsymbol{t}^{(n)}\right), \bar{\boldsymbol{\gamma}}_m^{BBPS}\left(\boldsymbol{t}^{(n)}\right); \bar{R}_m^{(n)}\right), \qquad \forall i \in R_m,$$

where $P_{m,i}$ is as in (5.7) for route $i \in R_m$, and $\bar{\gamma}_{m,i}^{BBPS}$ is as in (5.8) for route $i \in \bar{R}_m^{(n)}$, $m = 1, \dots, M$.

BAPS′ SUE: Given the used route choice set $\bar{R}_m^{(n)}$ for OD movement m, the link cost vector $\boldsymbol{t}^{(n)}$, and the route flow vector $\boldsymbol{f}^{(n)}$ at this stage of iteration n, the choice probability for route $i \in R_m$ for iteration n is:

$$P_{m,i}^{(n)} = P_{m,i}\left(z_{m,i}\left(\boldsymbol{c}_m\left(\boldsymbol{t}^{(n)}\right), \bar{\boldsymbol{\gamma}}_m^{BAPS'}\left(\boldsymbol{t}^{(n)}, \boldsymbol{f}^{(n)}\right)\right); \bar{R}_m^{(n)}\right),$$

where $P_{m,i}$ and $z_{m,i}$ are as in (5.15) and (5.16), respectively, for route $i \in R_m$, and $\bar{\gamma}_{m,i}^{BAPS'}$ is as in (5.17) for route $i \in \bar{R}_m^{(n)}$, $m = 1, \dots, M$.

For BAPS SUE, computing the BAPS model choice probabilities requires a fixed-point algorithm to compute the solution. In general, there are many fixed-point algorithms available for solving the BAPS fixed-point system. In this study, we use the Fixed-Point Iteration Method (FPIM) (Isaacson & Keller, 1966). Other algorithms were considered, however the performance and convergence of the FPIM in our initial tests (not reported here) were sufficiently promising that we did not consider this worthwhile. Given the used route choice set $\bar{R}_m^{(n)}$ for OD movement m, the link cost vector $\boldsymbol{t}^{(n)}$, and the route flow vector $\boldsymbol{f}^{(n)}$ at this stage of

iteration n, the FPIM for solving the BAPS model choice probabilities for OD movement m at iteration n of the BPS SUE algorithm is as follows:

$$P_{m,i}^{[s]} = Z_{m,i}\left(z_{m,i}\left(\boldsymbol{c}_m\left(\boldsymbol{t}^{(n)}\right), \bar{\boldsymbol{\gamma}}_m^{BAPS}\left(\boldsymbol{t}^{(n)}, \boldsymbol{P}_m^{[s-1]}\right)\right); \bar{R}_m^{(n)}\right), \qquad s = 1,2,3,\dots$$

such that

$$\lim_{s\to\infty} P_{m,i}^{[s]} = \lim_{s\to\infty} Z_{m,i}\left(z_{m,i}\left(\boldsymbol{c}_m\left(\boldsymbol{t}^{(n)}\right), \bar{\boldsymbol{\gamma}}_m^{BAPS}\left(\boldsymbol{t}^{(n)}, \boldsymbol{P}_m^{[s-1]}\right)\right); \bar{R}_m^{(n)}\right) = P_{m,i}^{*}, \qquad \forall i \in R_m,$$
$$\boldsymbol{P}_m^{(0)} \in D_m^{\left(\bar{R}_m^{(n)}, \tau_m\right)},$$

where $Z_{m,i}$, $z_{m,i}$, and $\gamma_{m,i}^{APS}$ are as in (5.10), (5.11), and (5.12), respectively, for route $i \in R_m$, and $\boldsymbol{f}^{(n)}$ is the route flow vector at this stage of iteration n of the BPS SUE algorithm. The FPIM is said to have converged sufficiently to an OD movement m BAPS choice probability solution $\boldsymbol{P}_m^{*} = \boldsymbol{P}_m^{[s]}$ if: $\sum_{i\in R_m}\left|P_{m,i}^{[s-1]} - P_{m,i}^{[s]}\right| < 10^{-\xi}$, where ξ is a predetermined BAPS probability convergence parameter.

In the numerical experiments in Section 5 of this paper, we explore adopting two different initial conditions for the FPIM: *fixed* initial conditions where $P_{m,i}^{[0]} = \frac{1}{\bar{N}_m}$, $\forall i \in R_m$, $m = 1,\dots,M$, and *follow-on* initial conditions where $P_{m,i}^{[0]} = \frac{f_{m,i}^{(n)}}{q_m}$, $\forall i \in R_m$, $m = 1,\dots,M$. The follow-on initial FPIM conditions utilise information from the previous BPS SUE algorithm iteration route flows $\boldsymbol{f}^{(n)}$ to determine the FPIM initial conditions. The idea is to harness the useful relation between route flow proportions and route choice probabilities in SUE, where these equate at equilibrium. In Duncan et al (2021), it was shown that utilising follow-on initial FPIM conditions for computing APSL probabilities solving APSL SUE, the numbers of fixed-point iterations required for APSL choice probability convergence (and thus computation times for each of the iterations) decreased as the flow-averaging algorithm progressed and the route flow proportions became closer to the APSL SUE route choice probabilities. For BAPS SUE, the set of used routes varies as the BPS SUE algorithm progresses, and therefore it is less clear how follow-on initial FPIM conditions will perform. We anticipate, however, that once the used route choice sets have equilibrated, the number of fixed-point iterations required for BAPS model choice probability convergence will decrease as the algorithm progresses (like as for APSL SUE). We test this hypothesis in Section 5.2.

4.3 Step 5: Flow-Averaging Phase

In Step 3, the route choice probabilities are computed given the current route flows, and these are used in Step 4 to obtain an auxiliary route flow vector. In Step 5, the flow-averaging phase consists of weighting the current iteration route flow vector $\boldsymbol{f}^{(n)}$ with the auxiliary route flow vector $\tilde{\boldsymbol{f}}^{(n)}$, according to some step-size η_n, to find the next route flow vector:

$$f_{m,i}^{(n+1)} = (1-\eta_n)\cdot f_{m,i}^{(n)} + \eta_n \cdot \tilde{f}_{m,i}^{(n)}, \qquad \forall i \in R_m, \qquad m = 1,\dots,M,$$

where $0 \le \eta_n \le 1$. There are numerous flow-averaging step-size schemes available, all based on the famous pre-defined Method of Successive Averages (MSA). Liu et al (2009) test different alternative pre-defined averaging schemes, and introduce the Method of Successive Weighted Averages (MSWA), which we adopt for the experiments in this paper. While being pre-defined, the MSWA allows giving higher weight to auxiliary flow patterns from later iterations, and the step-size η_n at iteration n is defined as:

$$\eta_n = \frac{n^d}{\sum_{k=1}^{n} k^d},$$

where $d > 0$ is a real number. Increasing the value of d moves more flow towards the auxiliary solution. The MSA is a special case of the MSWA, namely when $d = 0$.

4.4 Steps 7&9: Convergence Evaluation Phases

In this subsection, we propose three gap measures to monitor convergence of the BPS-SUE algorithm to a solution satisfying the BPS SUE conditions. These gap measures are similar to those detailed for the BSUE

model in Watling et al (2018). Two parts monitor convergence of the equilibrated choice sets and one part monitors the convergence of the allocation of flow to fulfil the underlying choice model.

Step 7: Used Above Bound Convergence Evaluation: Given the route cost vectors $\boldsymbol{c}_m^{(n+1)}$, $m = 1, \dots, M$, and the route flow vector $\boldsymbol{f}^{(n+1)}$ (for iteration $n+1$) at this stage of iteration n, the *used above bound* relative gap measure is as follows:

$$Rel.\,gap^{(n)}_{used\ above\ bound} = \frac{\sum_{m=1}^{M}\sum_{i\in R_m} f_{m,i}^{(n+1)} \cdot \left(c_{m,i}^{(n+1)} - \varphi \min\left(\boldsymbol{c}_m^{(n+1)}\right)\right)_+}{\sum_{m=1}^{M}\sum_{i\in R_m} f_{m,i}^{(n+1)} \cdot c_{m,i}^{(n+1)}}. \tag{5.26}$$

This gap measure in (5.26) ensures that (at convergence) no routes with a cost *above* the cost bound are *used*. Moreover, it measures the total violation relative to the total costs across all routes. When across all OD movements, no used routes have costs above the bound, then the gap is zero, and the convergence criteria are satisfied.

Step 9: Below Bound Convergence Evaluation: Given the current used route choice sets $\bar{R}_m^{(n)}$ and thus also the unused route choice sets $R_m \backslash \bar{R}_m^{(n)}$, $m = 1, \dots, M$, at this stage of iteration n, and the route cost vectors $\boldsymbol{c}_m^{(n+1)}$, $m = 1, \dots, M$, (for iteration $n+1$) at this stage of iteration n, the *unused below bound* relative gap measure for iteration n is as follows:

$$Rel.\,gap^{(n)}_{unused\ below\ bound} = \frac{\sum_{m=1}^{M} q_m \cdot \max\left(\varphi \min\left(\boldsymbol{c}_m^{(n+1)}\right) - c_{m,i}^{(n+1)} : i \in R_m \backslash \bar{R}_m^{(n)}\right)}{(\varphi - 1) \cdot \sum_{m=1}^{M} q_m \cdot \min\left(\boldsymbol{c}_m^{(n+1)}\right)}, \tag{5.27}$$

This gap measure in (5.27) ensures that no routes with a cost *below* the cost bound are *unused*. Moreover, for each OD movement, it measures the average relative non-violation of the bound for the unused routes not violating the bound the most. When across all OD movements, no unused routes have a cost below the bound, then the gap is zero, and the convergence criteria are satisfied.

Given the current used route choice sets $\bar{R}_m^{(n)}$, $m = 1, \dots, M$, at this stage of iteration n, and the route flow vector $\boldsymbol{f}^{(n+1)}$ (for iteration $n+1$) at this stage of iteration n, the *used below bound* relative gap measure for iteration n is as follows:

$$Rel.\,gap^{(n)}_{used\ below\ bound} = \frac{\sum_{m=1}^{M}\sum_{i\in \bar{R}_m^{(n)}} f_{m,i}^{(n+1)} \cdot \left(\tilde{c}_{m,i}\left(\boldsymbol{f}^{(n+1)}\right) - \min\left(\tilde{c}_{m,j}\left(\boldsymbol{f}^{(n+1)}\right) : j \in \bar{R}_m^{(n)}\right)\right)}{\sum_{m=1}^{M}\sum_{i\in \bar{R}_m^{(n)}} f_{m,i}^{(n+1)} \cdot \tilde{c}_{m,i}\left(\boldsymbol{f}^{(n+1)}\right)}. \tag{5.28}$$

This gap measure in (5.28) ensures that flow is allocated across used routes in a way that fulfils the underlying choice model. For this we extend ideas from Rasmussen et al (2015) and Watling et al (2018), where transformed cost measures $\tilde{c}_{m,i}\left(\boldsymbol{f}^{(n+1)}\right)$ were defined for the MNL choice model and the BCM, respectively, and convergence was proven for when (5.28) is equal to zero using this. For BPS models, we define $\tilde{c}_{m,i}\left(\boldsymbol{f}^{(n+1)}\right)$ to be used in (5.28) instead to be:

$$\tilde{c}_{m,i}\left(\boldsymbol{f}^{(n+1)}\right) = \frac{f_{m,i}^{(n+1)}}{\left(h_{m,i}\left(-\theta \boldsymbol{c}_m\left(\boldsymbol{t}\left(\boldsymbol{\Delta} \boldsymbol{f}^{(n+1)}\right)\right)\right) - 1\right) \cdot \left(\bar{\gamma}_{m,i}\left(\boldsymbol{t}\left(\boldsymbol{\Delta} \boldsymbol{f}^{(n+1)}\right), \boldsymbol{W}_m\left(\boldsymbol{f}^{(n+1)}\right)\right)\right)^{\beta}}, \tag{5.29}$$

where $\bar{\gamma}_{m,i}$ is the used route path size term for route $i \in \bar{R}_m^{(n)}$, and $W_{m,i}\left(\boldsymbol{f}^{(n+1)}\right) = \left(h_{m,i}\left(-\theta \boldsymbol{c}_m\left(\boldsymbol{t}\left(\boldsymbol{\Delta} \boldsymbol{f}^{(n+1)}\right)\right)\right) - 1\right)$ for the BBPS model, and $W_{m,i}\left(f_{m,i}^{(n+1)}\right) = f_{m,i}^{(n+1)}$ for the BAPS & BAPS′ models. At equilibrium, $\tilde{c}_{m,i}\left(\boldsymbol{f}^{(n+1)}\right)$ will be the same across all utilised routes for OD movement m, and the gap is zero. However, the convergence criteria is said to be satisfied if $Rel.\,gap^{(n)}_{used\ below\ bound} < 10^{-\zeta}$, where ζ is a predetermined convergence parameter. Although for the BAPS model $W_{m,i}\left(\boldsymbol{f}^{(n)}\right) = P^*_{m,i}\left(\boldsymbol{t}\left(\boldsymbol{\Delta} \boldsymbol{f}^{(n)}\right)\right)$ for the underlying choice model, this requires solving choice probability fixed-point

problems just for computing the gap measures, and instead we recommend that this is circumvented by utilising the route flow proportions, which will be equal to the choice probabilities at convergence.

5. Numerical Experiments

In this section, some numerical experiments are conducted to compare the computational performance and flow results of bounded SUE models (namely BSUE, BBPS, BAPS, & BAPS′ SUE) as well as with other SUE models (namely MNL, PSL, GPSL, GPSL′, APSL, & APSL′ SUE, as defined in Duncan et al (2021a) with flow-dependent path size terms). We examine results in the case where there are pre-generated approximated universal choice sets. Bounded SUE models are solved with the BPS SUE algorithm in Algorithm 5.1, and non-bounded SUE models are solved with a Flow-Averaging Algorithm (FAA) (see Duncan et al, 2021a). The BPS SUE algorithm can be seen as an extension of the FAA, where *column generation*, *flow allocation for new routes*, and *bound condition* phases are added for the equilibration of choice sets. We also investigate the uniqueness of BAPS SUE solutions.

5.1 Experiment Setup

The computer used has a 2.10GHz Intel Xeon CPU and 512GB RAM, and the code was implemented in Python. In our experiments, we consider three networks: a small example network (Fig. 5.1), and two well-known networks Sioux Falls and Winnipeg. The small example network consists of 3 nodes, 4 links, and 1 OD movement (with demand 200), the Sioux Falls network consists of 24 nodes, 64 links, and 528 OD movements (with positive demands), and the Winnipeg network consists of 1052 nodes, 2836 links, and 4345 OD movements.

In general, the generalised travel cost, $t_a(x_a)$, for link $a \in A$ may consist of several flow-dependent and flow-independent attributes, for example congested travel time, length, number of left turns, etc. However, for the numerical experiments in this section and for all networks, the travel cost of link $a \in A$ is specified as the flow-dependent travel time $T_a(x_a)$ only, where the volume-delay link cost functions for all networks are based on the Bureau of Public Road (BPR) formula with link-specific parameters:

$$t_a(x_a) = T_a(x_a) = T_{0,a}\left(1 + D\left(\frac{x_a}{K_a}\right)^B\right),$$

where $T_{0,a}$ and K_a are the free-flow travel time and capacity of link $a \in A$, respectively, and $D, B \geq 0$. For the small example network, $D = 0.15$, $B = 4$, $K_a = 100$ for all links, and $T_{0,a}$ for each link is shown in Fig. 3.1. For the Sioux Falls and Winnipeg networks, the link-cost function values as well as the network and demand data are obtained from https://github.com/bstabler/TransportationNetworks.

For the small example network, the pre-generated choice set is the actual universal set of all 4 routes, where the routes are Route 1: $1 \to 3$, Route 2: $1 \to 4$, Route 3: $2 \to 3$, Route 4: $2 \to 4$. For Sioux Falls and Winnipeg, we utilise choice sets generated in Duncan et al (2021). For the Sioux Falls network, the choice sets were obtained by generating all routes with a free-flow travel time less than 2.5 times greater than the free-flow travel time on the quickest route for each OD movement. For Winnipeg, a simulation approach was adopted (Sheffi & Powell, 1982), where the link costs were drawn randomly from a truncated normal distribution with mean value being free-flow travel time and standard deviation being 0.6 times the mean. The link costs were simulated 150 times for each OD movement and for each simulation shortest path was conducted to generate a route, where a maximum of 100 unique routes were generated for each choice set. The average and maximum free-flow travel time relative deviations from the quickest route in each choice set were 1.15 and 3.3, respectively. For Sioux Falls, 42,976 routes were generated in total, and the maximum, average, and median choice set sizes for an OD movement were 898, 116, and 6, respectively. For Winnipeg, 305,005 routes were generated in total, and the maximum, average, and median choice set sizes for an OD movement were 100, 70, and 88, respectively.

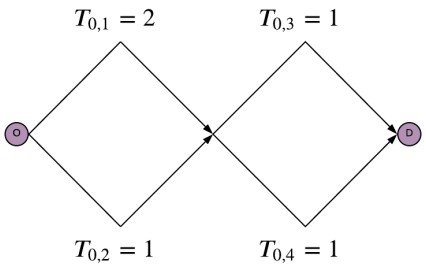

Fig. 5.1. Small example network.

Convergence for the bounded SUE models is measured with the *used below bound*, *used above boun*d, and *unused below bound* relative gap measures in Section 4.4, where convergence is said to be reached when $Rel.\,gap^{(n)}_{used\ above\ bound} = 0$, $Rel.\,gap^{(n)}_{unused\ below\ bound} = 0$, and $Rel.\,gap^{(n)}_{used\ below\ bound} < 10^{-4}$ ($\zeta = 4$).

For non-bounded SUE models, SUE convergence is measured using the *used below bound* relative gap measure (where all routes are used), which is as follows for iteration n:

$$Rel.\,gap^{(n)}_{used\ below\ bound} = \frac{\sum_{m=1}^{M}\sum_{i\in R_m} f_{m,i}^{(n+1)} \cdot \left(\tilde{c}_{m,i}\left(\boldsymbol{f}^{(n+1)}\right) - \min\left(\tilde{c}_{m,j}\left(\boldsymbol{f}^{(n+1)}\right): j \in R_m\right)\right)}{\sum_{m=1}^{M}\sum_{i\in R_m} f_{m,i}^{(n+1)} \cdot \tilde{c}_{m,i}\left(\boldsymbol{f}^{(n+1)}\right)}. \tag{5.30}$$

where,

$$\tilde{c}_{m,i}\left(\boldsymbol{f}^{(n+1)}\right) = \frac{f_{m,i}^{(n+1)}}{\exp\left(-\theta c_{m,i}\left(\boldsymbol{t}(\boldsymbol{\Delta f}^{(n+1)})\right)\right) \cdot \left(\gamma_{m,i}(\boldsymbol{f}^{(n+1)})\right)^{\beta}}. \tag{5.31}$$

$\gamma_{m,i}\left(\boldsymbol{f}^{(n+1)}\right)$ is the flow-dependent path size term for route $i \in R_m$, different for each Path Size Logit SUE model, and equal to 1 for MNL SUE. For APSL SUE, the APSL′ SUE path size terms are used (to avoid solving fixed-point problems), since these are equal at convergence. Convergence is said to be reached also when $Rel.\,gap^{(n)}_{used\ below\ bound} < 10^{-4}$.

Unless stated otherwise, specifications are also as follows. The initial conditions for non-bounded SUE models are set as the even split route flows, i.e. $f_{m,i} = \frac{q_m}{N_m}$, $\forall i \in R_m$, $m = 1, \ldots, M$. The MSWA parameter is set as $d = 15$. For computing BAPS and APSL probabilities with the FPIM, the probability convergence parameter is set as $\xi = 6$. The utilised model parameters for the Sioux Falls network are $\theta = \lambda^{BBPS} = 0.3$, $\beta = 0.8$, $\lambda^{GPS} = 10$, and $\varphi = 2$. $\theta = 0.5$, $\beta = 0.8$, $\lambda^{GPS} = 10$, and $\varphi = 2$ for the Winnipeg network.

5.2 Computational Performance

We begin the numerical experiments by analysing here the computational performance of the BPS SUE algorithm for solving the bounded SUE models, and comparing computational performance with that for solving non-bounded Path Size Logit SUE models with the FAA.

First, Table 5.1 displays for all SUE models, during a single run of the solution algorithm, the average computation times to compute the choice probabilities / perform an iteration on the Sioux Falls and Winnipeg networks.

As shown and as expected for the non-bounded SUE models, the MNL probabilities are the quickest to compute, followed by the PSL, GPSL, GPSL′, and APSL′ probabilities, which have similar computation times. APSL probabilities take significantly longer due to solving the fixed-point probabilities. Furthermore, for the non-bounded SUE models, computing the probabilities takes up a significant proportion of the computation time for each iteration. Computing the convergence measure takes up most of the rest of the computation time.

For the bounded SUE models, there are additional steps in the BPS SUE algorithm compared to the FAA for equilibrating the used route choice sets. Thus, computing the probabilities takes up a smaller proportion of the computation time for each iteration. As shown by the probability computation times, the bounded model probabilities are slightly more complex to compute compared to their associated non-bounded model, i.e. the limit models (BCM & MNL, BBPS & GPSL′, BAPS & APSL, BAPS′ & BAPS′). Like APSL, the fixed-point BAPS model probabilities are computationally expensive to compute. For BAPS′, as discussed below, a greater proportion of the total iterations during a BPS SUE algorithm run are performed with the choice sets equilibrated where the computational burden is less than for pre-equilibrated. Therefore, the average computation time to perform an iteration across the iterations is less for BAPS′ than for BBPS, despite similar probability computation times.

	MNL	PSL	GPSL	GPSL′	APSL	APSL′	BCM	BBPS	BAPS	BAPS′
Sioux Falls	0.003/ 0.010	0.034/ 0.049	0.034/ 0.049	0.034/ 0.049	1.465/ 1.478	0.034/ 0.049	0.004/ 0.069	0.017/ 0.087	0.844/ 0.909	0.017/ 0.066
Winnipeg	0.02/ 0.05	0.14/ 0.22	0.14/ 0.22	0.14/ 0.22	4.33/ 4.40	0.14/ 0.22	0.05/ 0.16	0.19/ 0.72	5.85/ 6.38	0.19/ 0.55

Table 5.1. Average computation time [mins] to compute the probabilities / perform an iteration on the Sioux Falls and Winnipeg networks.

Fig. 5.2A-B display for the Sioux Falls and Winnipeg networks, respectively, the convergence patterns for the bounded SUE models for a single run of the BPS SUE algorithm. Fig. 5.3A-B display results in terms of computation time, and Fig. 5.4A-B display how the average used route choice set size varies as the algorithm progresses. Fig. 5.5A-B display for Winnipeg the convergence patterns for the non-bounded SUE models for a single run of the FAA in terms of iterations and computation time, respectively.

As shown in Fig. 5.2/Fig. 5.3, the convergence patterns for the BSUE, BBPS SUE, & BAPS SUE models are different but not drastically different, and converge in similar numbers of SUE iterations. BBPS SUE takes longer to solve than BSUE, however, due to the longer choice probability computation times from computing path size terms. BAPS SUE takes significantly longer than BSUE / BBPS SUE, due to the computationally expensive fixed-point probabilities. For the BAPS′ SUE model, as is evident from the BAPS′ SUE convergence patterns being more concentrated to the left of the figures, while the number of iterations required to equilibrate the used route choice sets is similar to BSUE / BBPS SUE / BAPS SUE (can also be seen in Fig. 5.4), once the choice sets are equilibrated, convergence of the flows is slow compared to BSUE / BBPS SUE / BAPS SUE.

Comparing the corresponding convergence patterns in Fig. 5.2 and Fig. 5.3, under close inspection one can observe that the region where the *unused below bound* and *used above bound* relative gap measures are non-zero appear more concentrated to the left of the figures in Fig. 5.2 than in Fig. 5.3 (more evident in Fig. 5.2A/Fig. 5.3A for Sioux Falls). This indicates that the earlier iterations are more time consuming than later iterations, which is as expected since the steps for equilibrating the choice sets in earlier iterations are more active e.g. redistributing the flows of violating routes in the *Bound Violation Check* phase.

As shown in Fig. 5.4, the average used route choice set sizes for the bounded SUE models generally expand as the BPS SUE algorithm progresses, up until choice set equilibration. Again, the average choice set size patterns are different for each model, but not drastically different.

As shown in Fig. 5.5 for Winnipeg, in analogous results to the bounded versions of the non-bounded SUE models, the number of iterations required for MNL, PSL, GPSL, GPSL′, & APSL SUE convergence are similar, while APSL′ SUE convergence is comparatively slow. PSL/GPSL/GPSL′ SUE take longer than MNL SUE due to the path size term computation. APSL′ SUE takes longer than PSL/GPSL/GPSL′ SUE due to slower convergence, and APSL SUE takes significantly longer due to the fixed-point probabilities. The APSL′ SUE convergence patterns are also concentrated to the left of the figures, indicating that the slow convergence arises in achieving higher levels of convergence (i.e. convergence gets increasingly slow as the convergence measure is made more strict). Unlike for the bounded SUE models, the convergence patterns with respect to the iterations (Fig. 5.5A) appear in the figures similar to the convergence patterns with respect to computation time (Fig. 5.5B), i.e. the patterns are not skewed left or right of each other. This is because the computational burden is roughly uniform across the iterations, with the same number of active routes in each iteration.

Interestingly, the bounded SUE models in this case converge in similar numbers of iterations to the non-bounded versions. APSL′ SUE is significantly slower than BAPS′ SUE, however, and APSL SUE actually takes longer than BAPS′ SUE. Otherwise, the bounded SUE models take longer than the non-bounded versions.

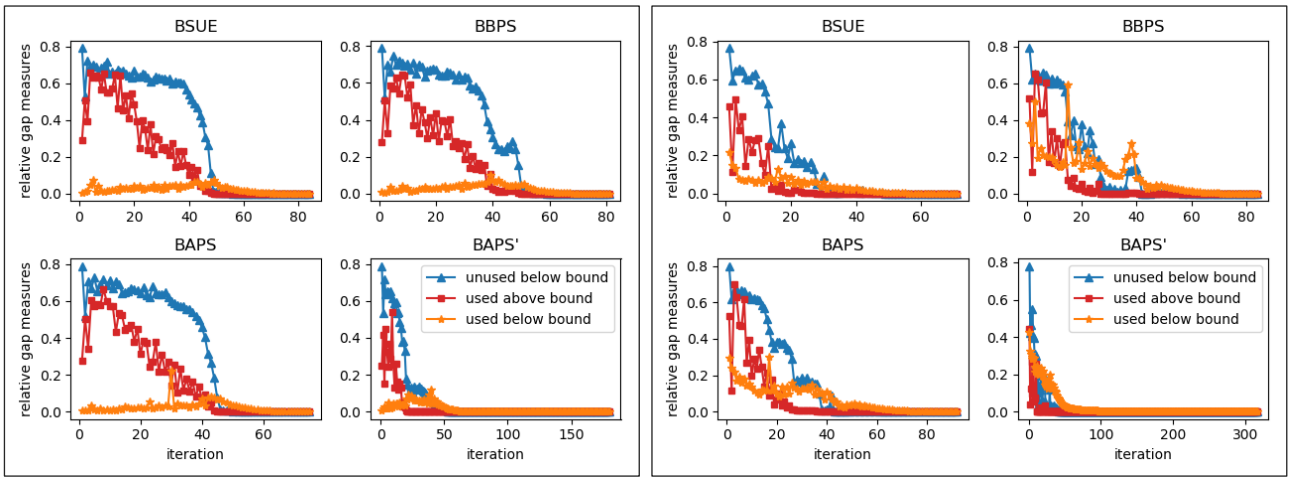

Fig. 5.2. Relative gap measures for the bounded SUE models at each iteration of the BPS SUE Algorithm. **A:** Sioux Falls. **B:** Winnipeg.

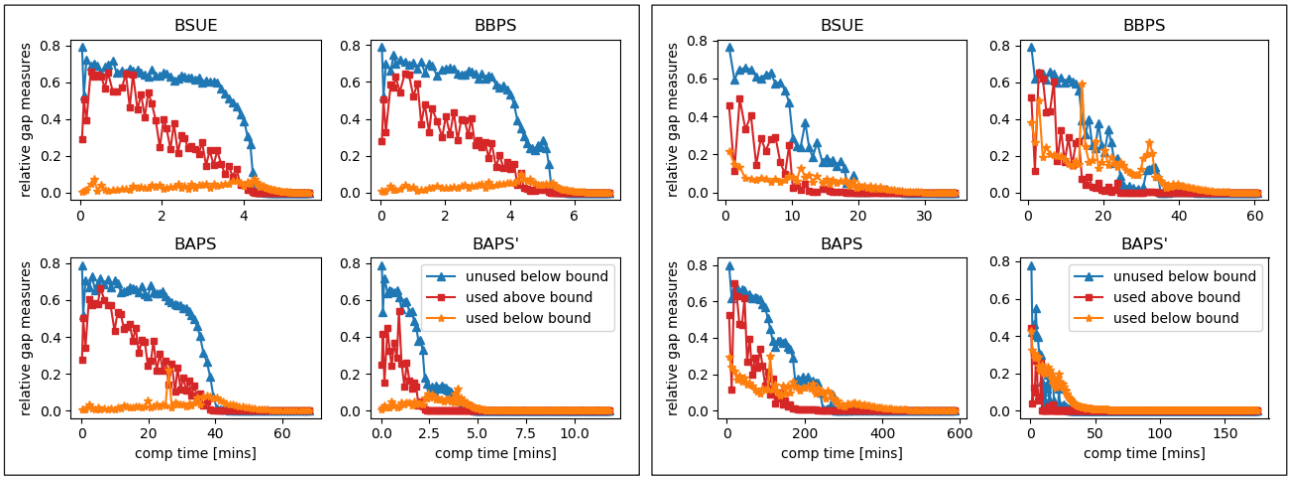

Fig. 5.3. Relative gap measures for the bounded SUE models in computation time [mins] of the BPS SUE Algorithm. **A:** Sioux Falls. **B:** Winnipeg.

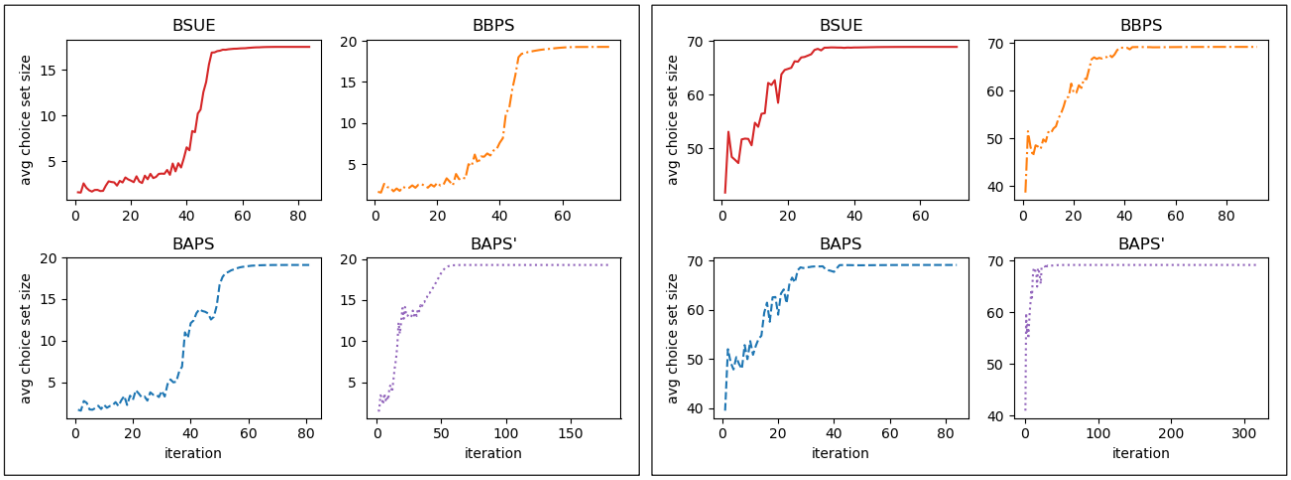

Fig. 5.4. Average used route choice set sizes for the bounded SUE models at each iteration of BPS SUE algorithm. **A:** Sioux Falls. **B:** Winnipeg.

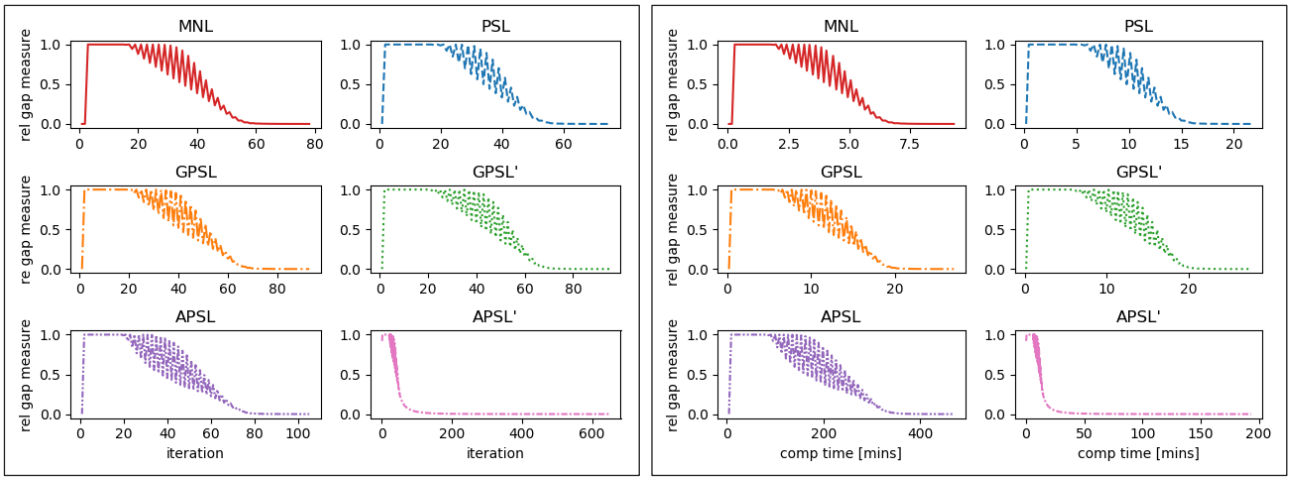

Fig. 5.5. Winnipeg: Relative gap measures for the non-bounded SUE models at each iteration (**A**) / in computation time [mins] (**B**) of the FAA.

Duncan et al (2021) demonstrated that while the number of iterations required for APSL SUE convergence tended to be similar to that required for MNL, PSL, & GPSL SUE under identical configurations of the FAA, the requirement of solving APSL choice probability fixed-point problems at each iteration resulted in significantly greater total computation times. On-the-other-hand, while the computational burden involved in computing the APSL′ choice probabilities during each iteration solving APSL′ SUE was no more than that for PSL & GPSL, APSL′ SUE convergence was comparatively very slow, and thus total computational times were also much longer. As they showed however, tuning the APSL SUE algorithm showed how one can trade-off the accuracy of APSL probabilities (and thus computation times of each iteration) with rate of SUE convergence. Several tuning techniques were explored, and it was shown how total computation times can be greatly improved. We shall now explore the success of these techniques for solving BAPS SUE.

For BAPS SUE, the scale of the computational burden involved at each BPS SUE algorithm iteration in solving the BAPS model choice probability fixed-point problems depends on numerous factors; some of which can be controlled by the modeller, for example the choice of fixed-point algorithm, and the fixed-point algorithm initial conditions and probability convergence parameter ξ. The current study focuses on the FPIM as the fixed-point algorithm.

Fig. 5.6A-B display for the Sioux Falls and Winnipeg networks, respectively, the cumulative computation times of the iterations during a single run of the BPS SUE algorithm solving BAPS SUE, with fixed and follow-on FPIM initial conditions (see Section 4.2). Fig. 5.7A-B shows the average number of fixed-point iterations per OD movement required for BAPS choice probability convergence at each iteration of the BPS SUE algorithm. As shown for Sioux Falls, once the choice sets have equilibrated, utilising follow-on initial conditions improves the computation times of each iteration due to the reduction in the number of FPIM iterations required for probability convergence. Before the choice sets have equilibrated, however, more FPIM iterations are required for follow-on initial conditions, due to the oscillations in flow. For Winnipeg, utilising follow-on conditions is significantly more effective.

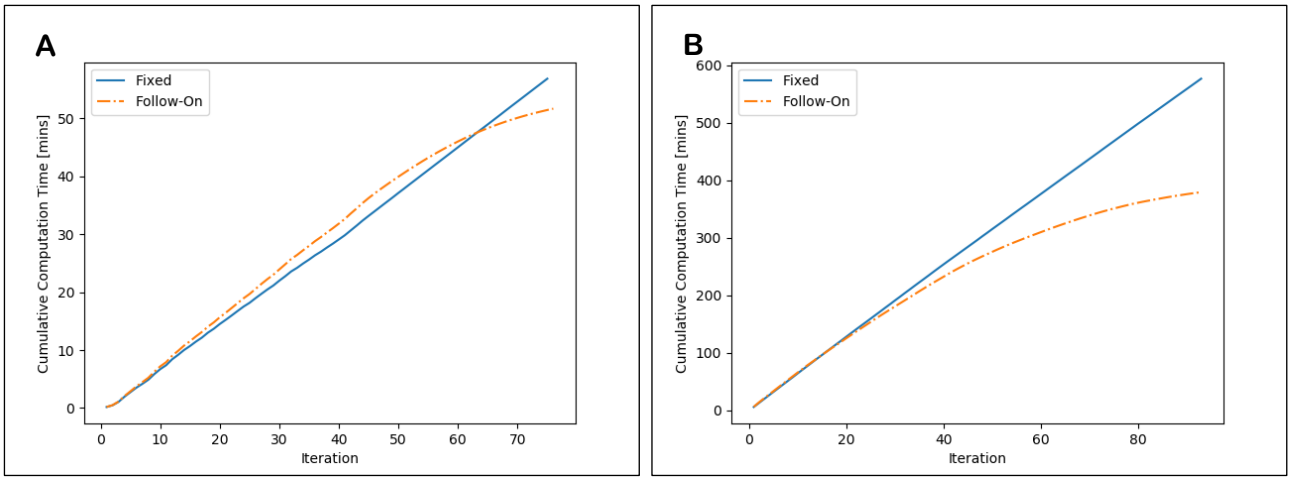

Fig. 5.6. Cumulative computation times of the iterations during a single run of the BPS SUE algorithm solving BAPS SUE with fixed and follow initial FPIM conditions. **A:** Sioux Falls. **B:** Winnipeg.

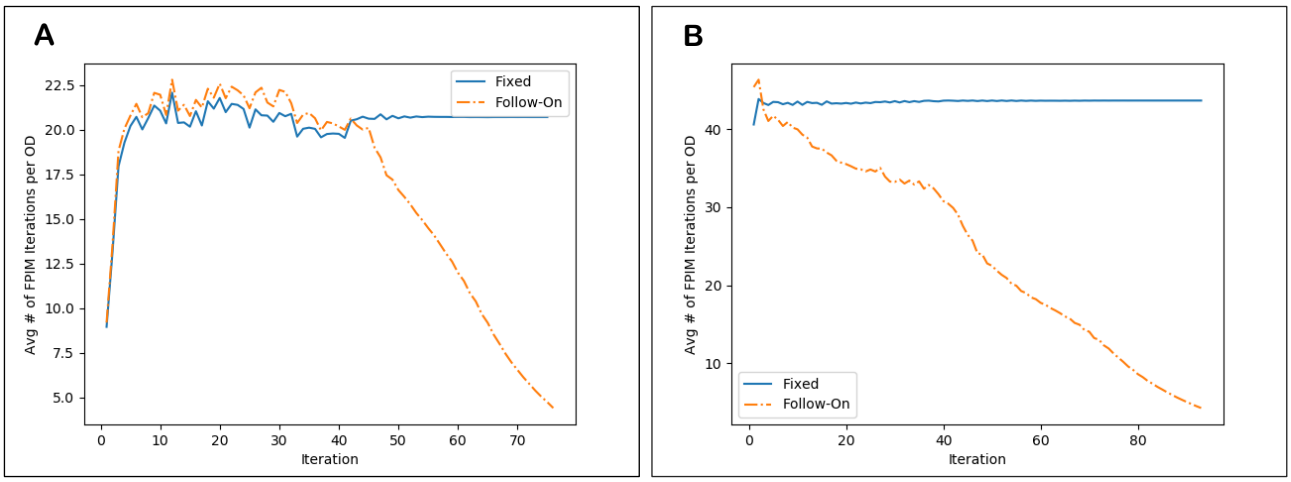

Fig. 5.7. Average number of BAPS probability fixed-point iterations at each iteration of the BPS SUE algorithm solving BAPS SUE with fixed and follow-on initial conditions. **A:** Sioux Falls. **B:** Winnipeg.

Fig. 5.8A-B display for the Sioux Falls and Winnipeg networks, respectively, how the total computation time for solving BAPS SUE varies as the FPIM probability convergence parameter ξ is increased, with fixed and follow-on initial FPIM conditions. Fig. 5.9A-B display how the average number of BAPS fixed-point iterations and total number of BPS SUE algorithm iterations vary as ξ is increased.

With fixed FPIM initial conditions, BAPS SUE could not be solved for $\xi < 6$ due to the inaccuracies of the BAPS probabilities. For $\xi \geq 6$, as shown, as ξ increases, while the number of iterations required for SUE convergence remains constant, greater numbers of FPIM iterations are required for APSL probability convergence and thus total computation times increase.

With follow-on FPIM initial conditions, like as for APSL SUE, BAPS SUE could be solved for all ξ. For $\xi = -1$, only single FPIM iterations are required for BAPS probability convergence, and with follow-on initial FPIM conditions, solving BAPS SUE this way simulates solving BAPS′ SUE. Increasing ξ increases the number of FPIM iterations required for BAPS probability convergence and the accuracy of the BAPS probabilities, but the BAPS SUE solution obtained is the same. As shown, convergence of BAPS′ SUE (BAPS SUE with small ξ & follow-on conditions) is slow. Increasing ξ (generally) improves SUE convergence, with exceptions at small ξ, up until a minimum number of BPS SUE algorithm iterations is reached for solving with accurate BAPS probabilities. With these algorithm and model specifications, the convergence of BAPS′ SUE is not so slow that total computation times are high. However, best total computation times come from intermediate values of ξ whereby suitable SUE convergence meets suitable iteration computation times, approximately $\xi = 1$ and $\xi = 0$ for Sioux Falls and Winnipeg, respectively.

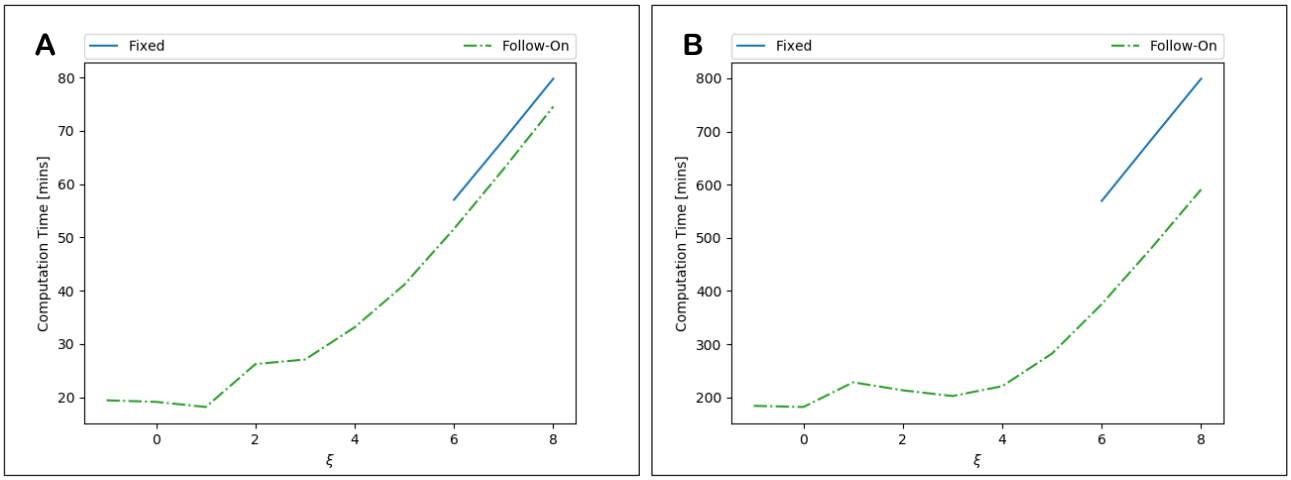

Fig. 5.8. Computation time for solving BAPS SUE as the BAPS model probability convergence parameter ξ is increased, with fixed and follow-on initial FPIM conditions. **A:** Sioux Falls. **B:** Winnipeg.

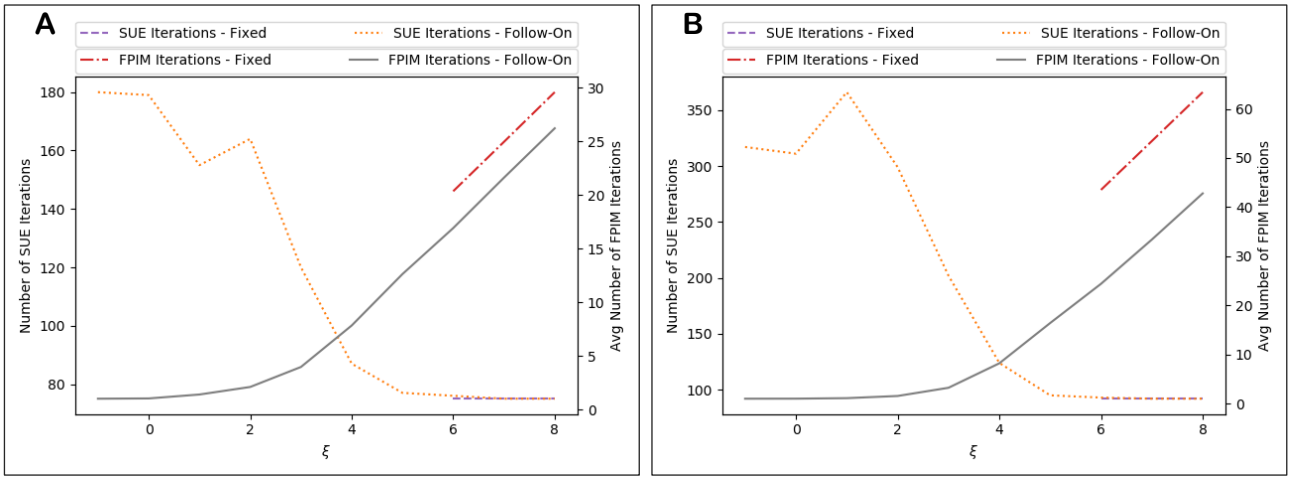

Fig. 5.9. Average number of BAPS model fixed-point iterations and total number of BPS SUE algorithm iterations solving BAPS SUE as ξ is increased. **A:** Sioux Falls. **B:** Winnipeg.

Alternatively, utilising follow-on conditions, one can stipulate a set number of FPIM iterations to perform at each BPS SUE algorithm iteration. Supposing that k FPIM iterations are conducted, Fig. 5.10A-B display the total computation times and number of BPS SUE algorithm iterations solving BAPS SUE, for the Sioux Falls and Winnipeg networks, respectively. As shown, conducting just two FPIM iterations (instead of one) can significantly reduce the number of BPS SUE algorithm iterations required for convergence, and thus total computation times. The optimal values for k appear to be 2 and 3 FPIM iterations, respectively, where suitable SUE convergence meets suitable iteration computation times.

One can also utilise a combination of both techniques for reducing BAPS SUE total computation times and stipulate a maximum number of FPIM iterations to perform and a maximum level of BAPS probability convergence, i.e. the FPIM is stopped if either a maximum of h iterations are conducted or the probabilities have converged sufficiently according to the set parameter ξ. This can potentially save computation times in latter BPS SUE algorithm iterations where the stipulated amount of FPIM iterations unnecessarily overly-converges the BAPS probabilities. Fig. 5.11A and Fig. 5.12A display for Sioux Falls how computation times and the number of BPS SUE algorithm iterations / average number of FPIM iterations vary, respectively, for different settings of ξ, where a maximum of 2 FPIM iterations are conducted. Fig. 5.11B and Fig. 5.12B display results for Winnipeg where a maximum of 3 FPIM iterations are conducted. As shown, best total computation times come from larger ξ values and the time saved in latter iterations is not significant compared to a greater number of iterations being required for SUE convergence. This is different from the results for APSL SUE in Duncan et al (2021a), and is likely due to the iterations being more complex in the BPS SUE algorithm than the FAA. Optimal values of ξ with this technique are approximately $\xi = 7$ and $\xi = 8$ for Sioux Falls and Winnipeg, respectively.

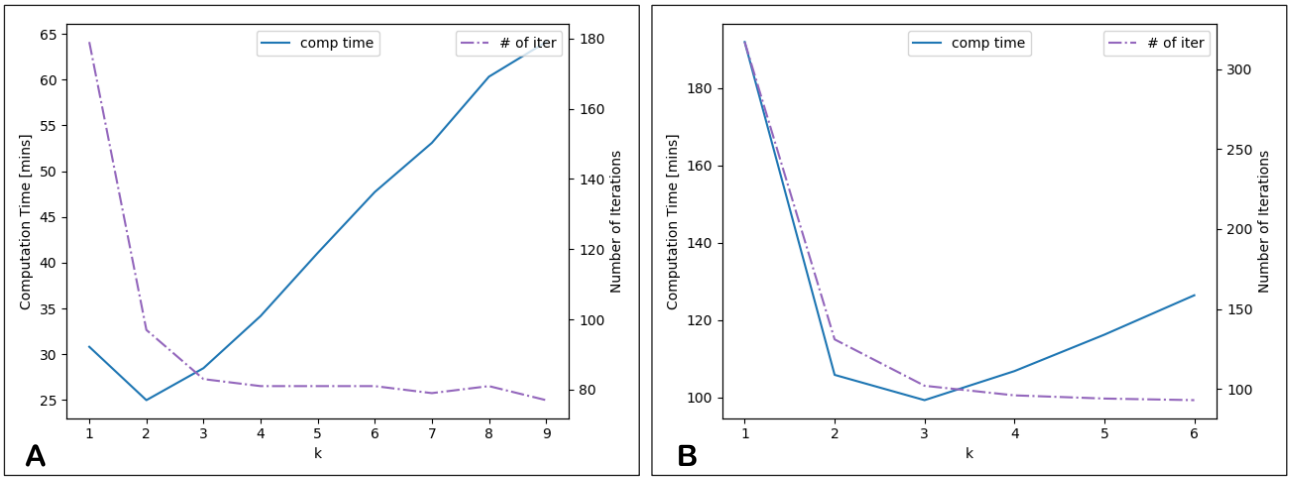

Fig. 5.10. Total computation times and number of BPS SUE algorithm iterations for solving BAPS SUE utilising follow-on conditions, with h FPIM iterations conducted. **A:** Sioux Falls. **B:** Winnipeg.

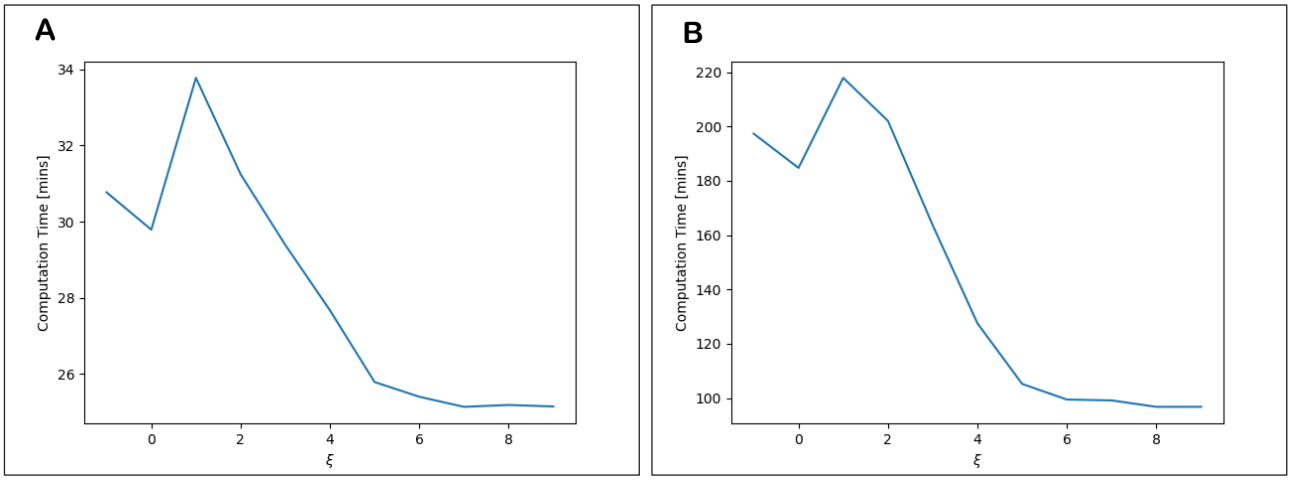

Fig. 5.11. Total computation times for solving BAPS SUE utilising follow-on conditions as ξ is varied, with a max number of FPIM iterations conducted h. **A:** Sioux Falls ($h = 2$). **B:** Winnipeg ($h = 3$).

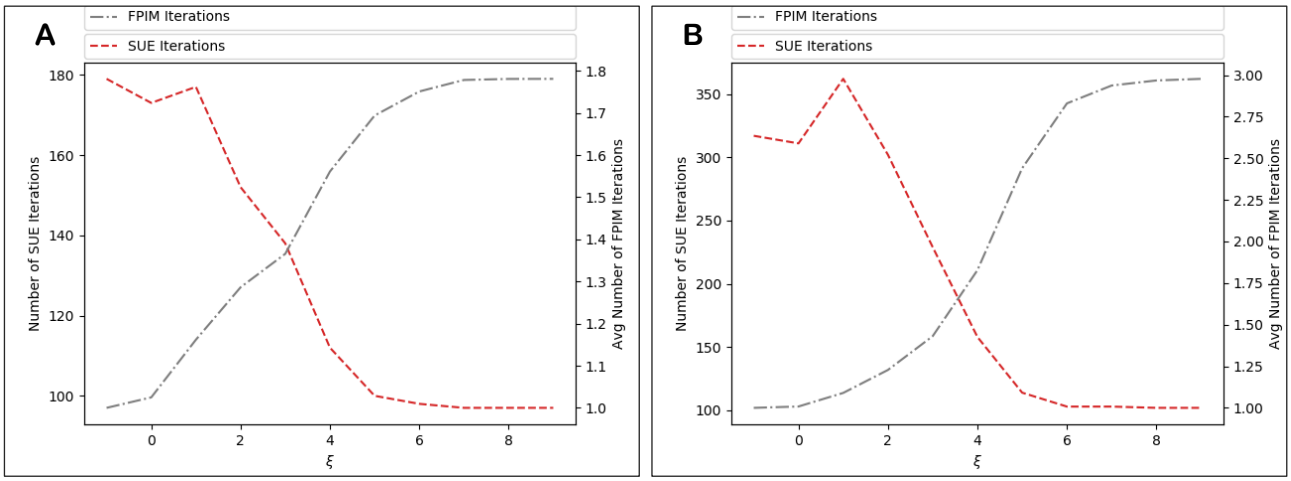

Fig. 5.12. Number of BPS SUE algorithm iterations, and average number of FPIM iterations for solving BAPS SUE utilising follow-on conditions as ξ is varied, with a max number of FPIM iterations conducted h. **A:** Sioux Falls ($h = 2$). **B:** Winnipeg ($h = 3$).

Considering the above results, for the remainder of the paper, unless stated otherwise, we solve BAPS SUE by stipulating a maximum number of FPIM iterations to perform at each BPS SUE algorithm iteration and a maximum level of BAPS model probability convergence. For Sioux Falls, a maximum of 2 FPIM iterations are conducted with $\xi = 7$. For Winnipeg, 3 FPIM iterations are used with $\xi = 8$. We label for reference this

method BAPS SUE*. This ‘optimal’ method for solving BAPS SUE is of course particular to the network, model, and algorithm specifications, e.g. model parameters, adopted step-size scheme, sizes of the approximated universal choice sets. However, by fixing the optimised values for that particular specification, and then varying the specifications, we will show that the method is robust in its effectiveness compared to solving BAPS SUE in a standard way (i.e. where the BAPS fixed-point probabilities are accurately solved with non-follow-on initial conditions).

Fig. 5.13A-B display for the Sioux Falls and Winnipeg networks, respectively, the convergence patterns for BAPS SUE* for a single run of the BPS SUE algorithm. Fig. 5.14A-B display results in terms of computation time, and Fig. 5.15A-B display how the average used route choice set size varies as the algorithm progresses. As shown, for BAPS SUE*, the number of iterations required to obtain levels of convergence is now less than for BAPS′ SUE, though more than required for BAPS SUE (see Fig. 5.2). Hence, since the computation times for each iteration of BAPS SUE* are significantly less than for BAPS SUE, total computation times are improved.

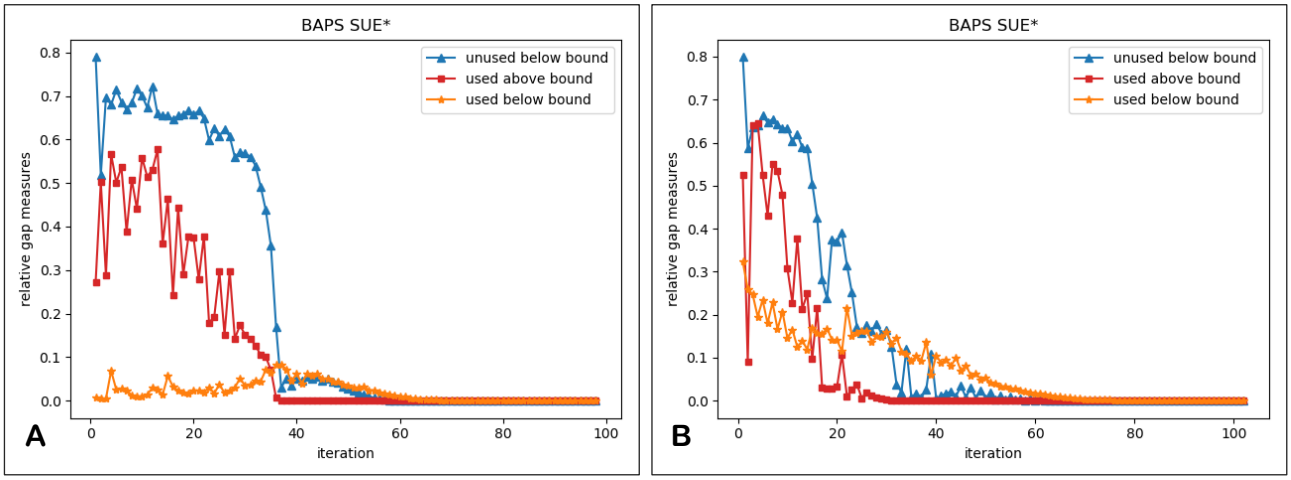

Fig. 5.13. Relative gap measures for BAPS SUE* at each iteration of the BPS SUE algorithm. **A:** Sioux Falls. **B:** Winnipeg.

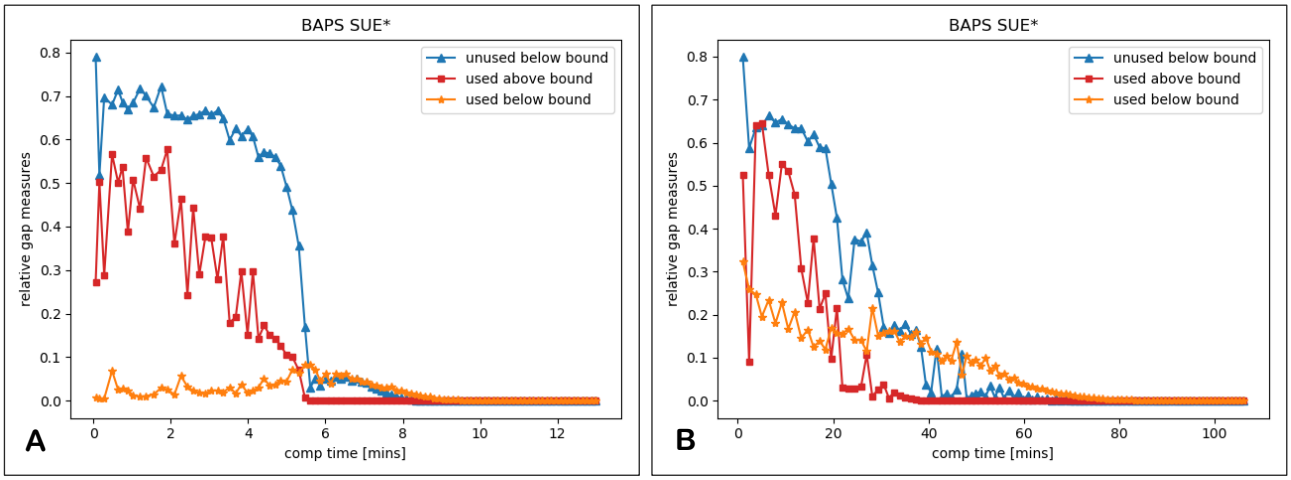

Fig. 5.14. Relative gap measures for BAPS SUE* in computation time [mins] of the BPS SUE algorithm. **A:** Sioux Falls. **B:** Winnipeg.

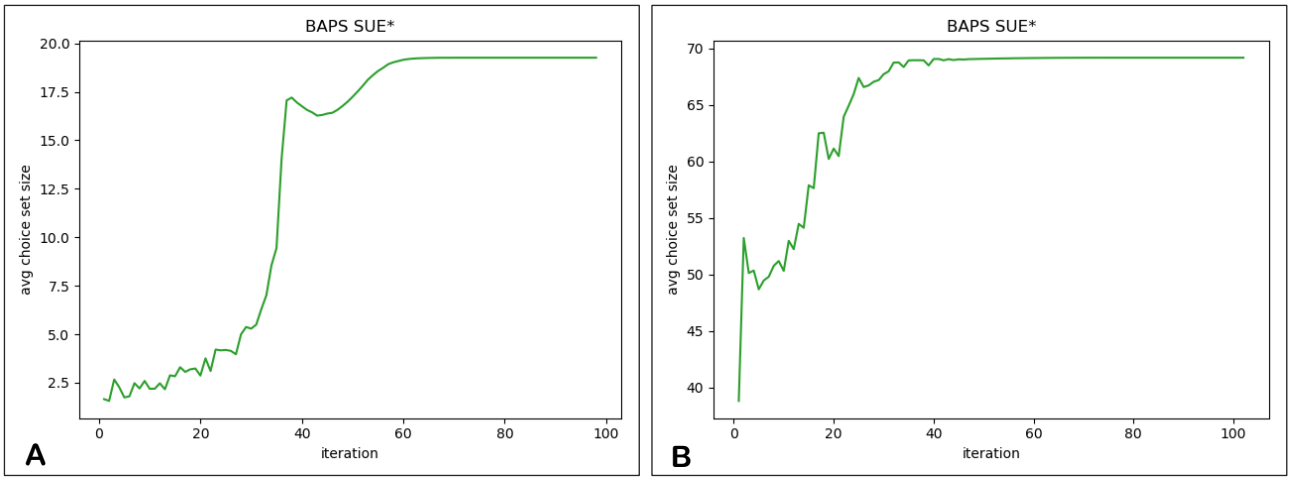

Fig. 5.15. Average used route choice set size for BAPS SUE* at each iteration of BPS SUE algorithm. **A:** Sioux Falls. **B:** Winnipeg.

Other factors that affect the computational performance of BAPS SUE, in terms of solving the BAPS probability fixed-point problems, include the values of β and φ. As shown in Duncan et al (2021b), larger values of β and φ result in greater numbers of FPIM iterations being required for BAPS probability convergence (increasing computation times).

Fig. 5.16A-B display for the Sioux Falls and Winnipeg networks, respectively, how the computation time for BAPS SUE* as well as for solving BAPS SUE with follow-on and fixed initial FPIM conditions, varies as the β parameter is increased. Fig. 5.17A-B display how the average number of FPIM iterations per OD movement per BPS SUE algorithm iteration and how the total number of BPS SUE algorithm iterations vary as β is increased. As shown, for BAPS SUE follow-on & fixed, while the number of BPS SUE algorithm iterations do not vary considerably, the average number of FPIM iterations increases exponentially with β and hence so do computation times. For BAPS SUE*, the number of SUE iterations increases as β increases, while the average number of FPIM iterations remains low (decreasing slightly due to more SUE iterations), resulting in the technique significantly improving in effectiveness as β increases.

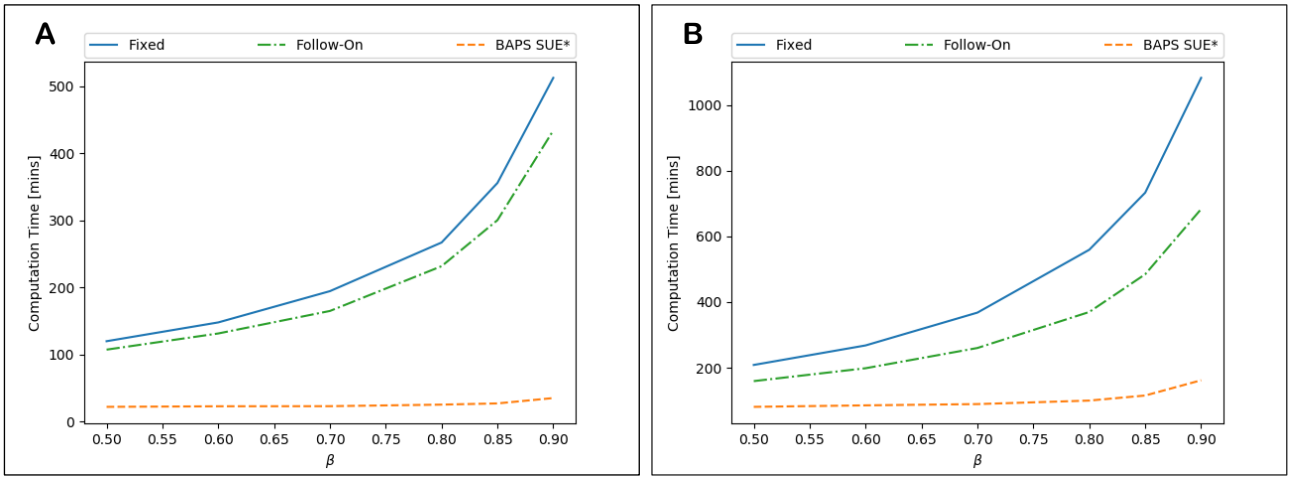

Fig. 5.16. Computation time for BAPS SUE* and solving BAPS SUE with follow-on and fixed initial FPIM conditions as β is increased. **A:** Sioux Falls. **B:** Winnipeg.

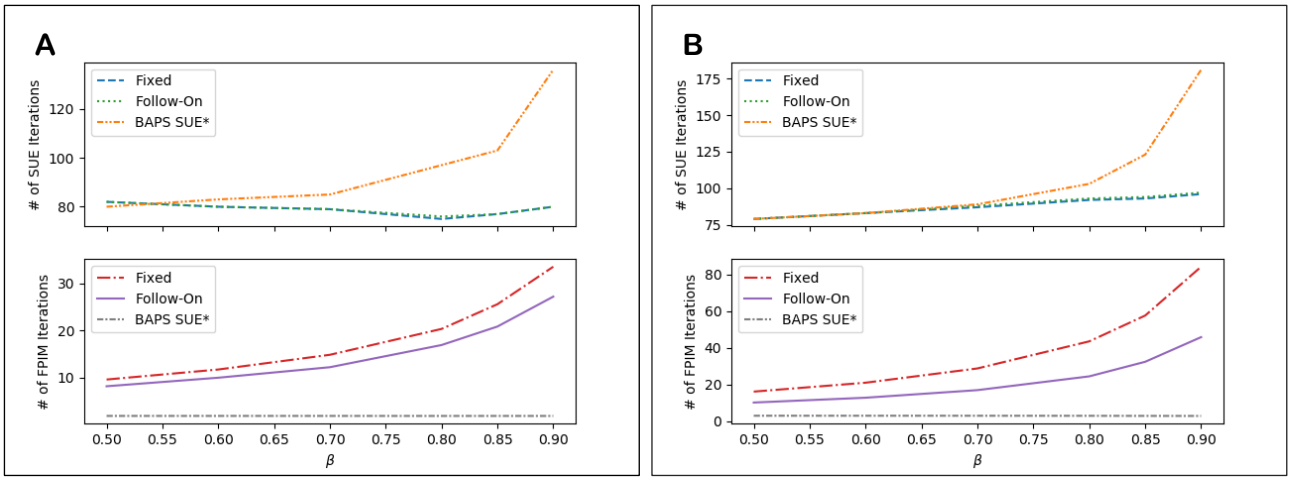

Fig. 5.17. Number of BPS SUE algorithm iterations, and average number of FPIM iterations for BAPS SUE*, and solving BAPS SUE with follow-on and fixed initial FPIM conditions as β is increased. **A:** Sioux Falls. **B:** Winnipeg.

Fig. 5.18A-B display for the Sioux Falls and Winnipeg networks, respectively, how the computation time for BAPS SUE* as well as for solving BAPS SUE with follow-on and fixed initial FPIM conditions, varies as the φ parameter is increased. Fig. 5.19A-B display how the average number of FPIM iterations per OD movement per BPS SUE algorithm iteration and how the total number of BPS SUE algorithm iterations vary as φ is increased. As shown for Sioux Falls, for this range of φ, there are no clear trends for the SUE convergence rates as φ is varied, though the average number of FPIM iterations increases with φ, as expected. For Winnipeg, however, there is a clear trend that the number of iterations required for SUE convergence decreases as φ increases. This is due to a greater number of iterations being required to equilibrate the choice sets, which are more restrictive for smaller φ. Total computation times for the bounded SUE models thus decrease with φ in this range, despite greater numbers of FPIM iterations being required for BAPS probability convergence.

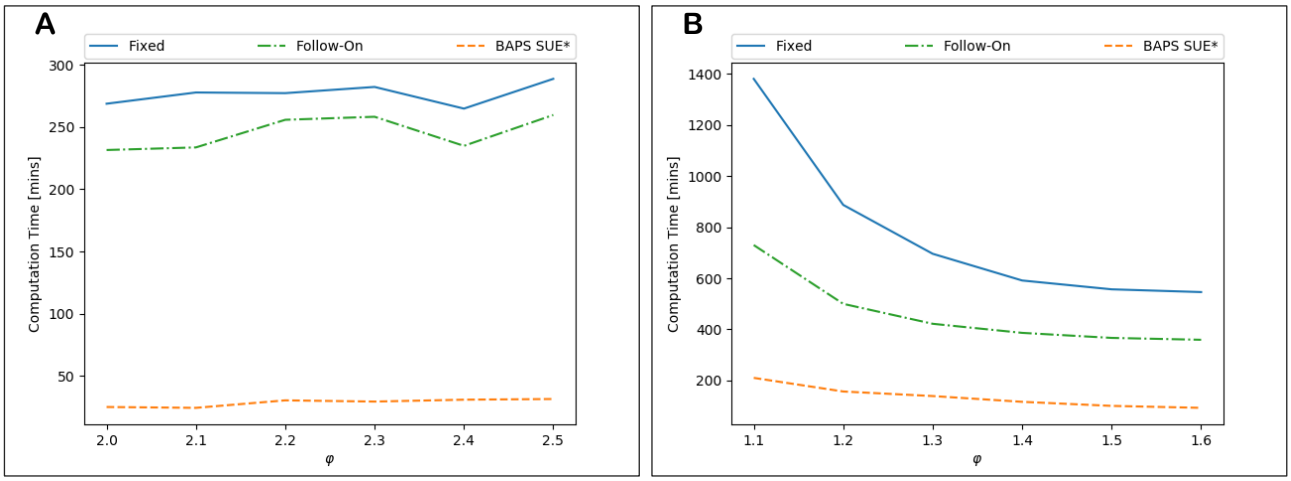

Fig. 5.18. Computation time for BAPS SUE* and solving BAPS SUE with follow-on and fixed initial FPIM conditions as φ is increased. **A:** Sioux Falls. **B:** Winnipeg.

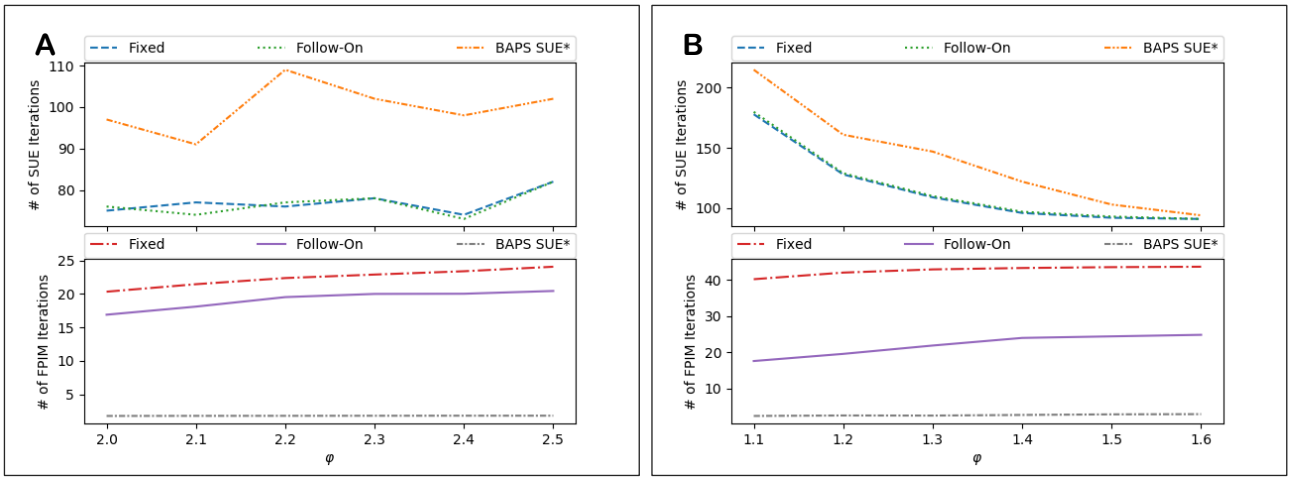

Fig. 5.19. Number of BPS SUE algorithm iterations, and average number of FPIM iterations for BAPS SUE* and solving BAPS SUE with follow-on and fixed initial FPIM conditions and φ is increased. **A:** Sioux Falls. **B:** Winnipeg.

Next, we investigate for the bounded SUE models, how total computation times, number of BPS SUE algorithm iterations, and average used route choice set sizes vary according to levels of travel demand and the model parameters.

Fig. 5.20A-B display for the Sioux Falls and Winnipeg networks, respectively, how the number of iterations required for SUE convergence varies for the bounded SUE models as the level of travel demand is varied, where the demand is scaled according to the parameter ω so that the demand for OD movement m is $\omega \cdot q_m, m = 1, \dots, M$. Fig. 5.21A-B display results in terms of computation time, and Fig. 5.22A-B display how the average used route choice set size varies. As shown, and as expected, the number of iterations required for convergence generally increases for the bounded SUE models as the level of demand increases, resulting in longer computation times.

A surprising result is that (at least towards larger demand on Winnipeg) the average used route choice set sizes decrease as the demand level increases. If one considers what one might expect under Deterministic User Equilibrium (Wardrop, 1952), for low demand only the best costing routes are used, and increasing demand results in the used route choice sets expanding. For Winnipeg, the choice set sizes do expand initially as the demand level is increased, but then they decrease in size more significantly. For Sioux Falls, the more heavily congested network, the choice sets decrease in size quite significantly for ω in this range. The suspected reason for this is that for high levels of congestion the costs on all links are inflated, and routes that are used for one OD movement are likely inflating the costs so that routes in other OD movements are then too costly to be used. Sioux Falls is also potentially more susceptible to this due to the way the network is structured, i.e. heavily overlapping OD movements.

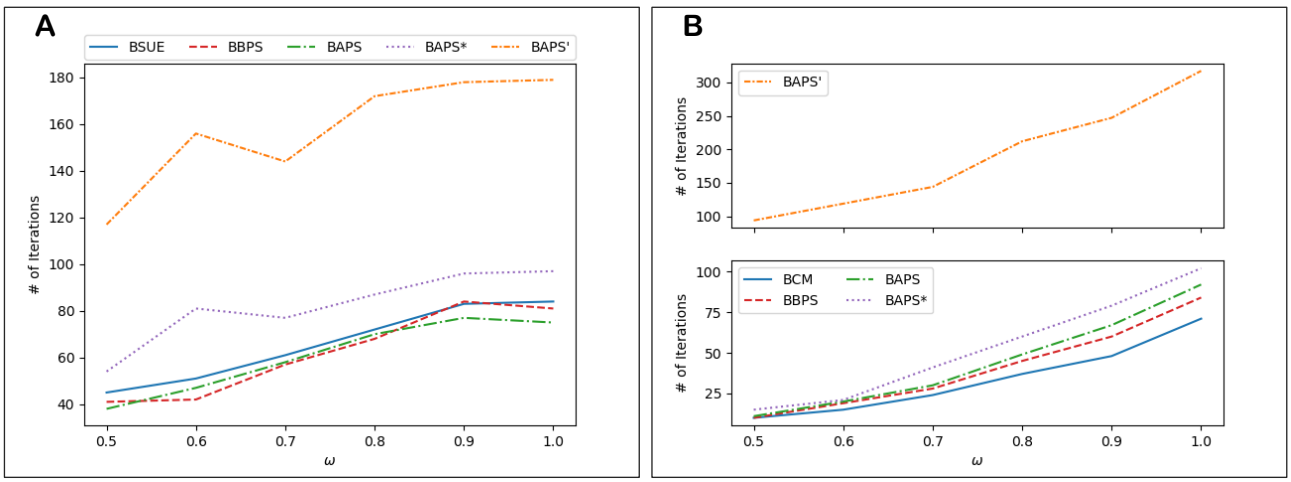

Fig. 5.20. Number of iterations required for SUE convergence for varying levels of travel demand, scaled by ω. **A:** Sioux Falls. **B:** Winnipeg.

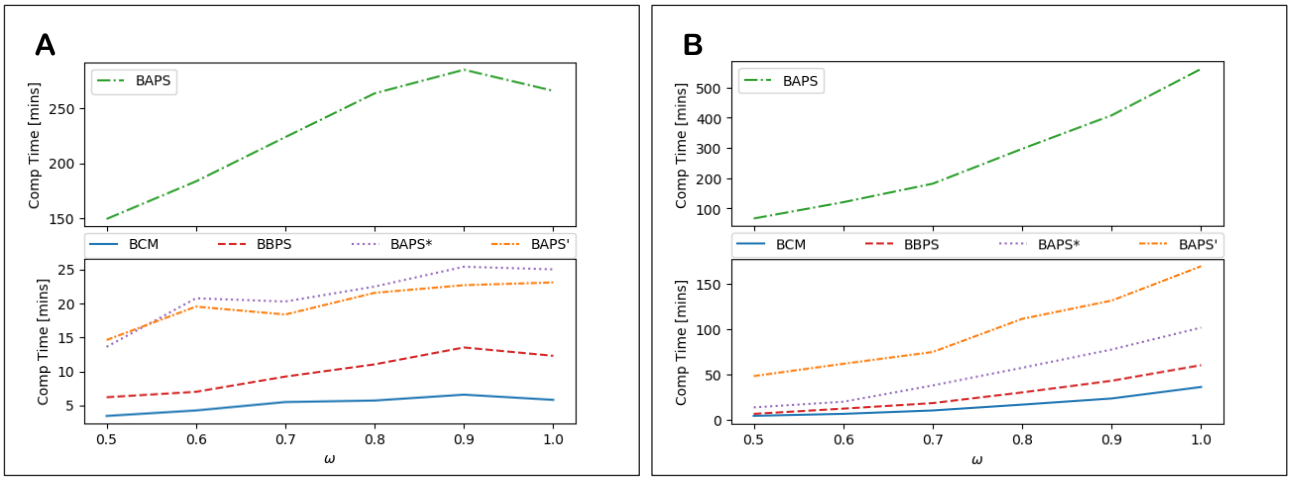

Fig. 5.21. Computation time [mins] required for SUE convergence for varying levels of travel demand, scaled by ω. **A:** Sioux Falls. **B:** Winnipeg.

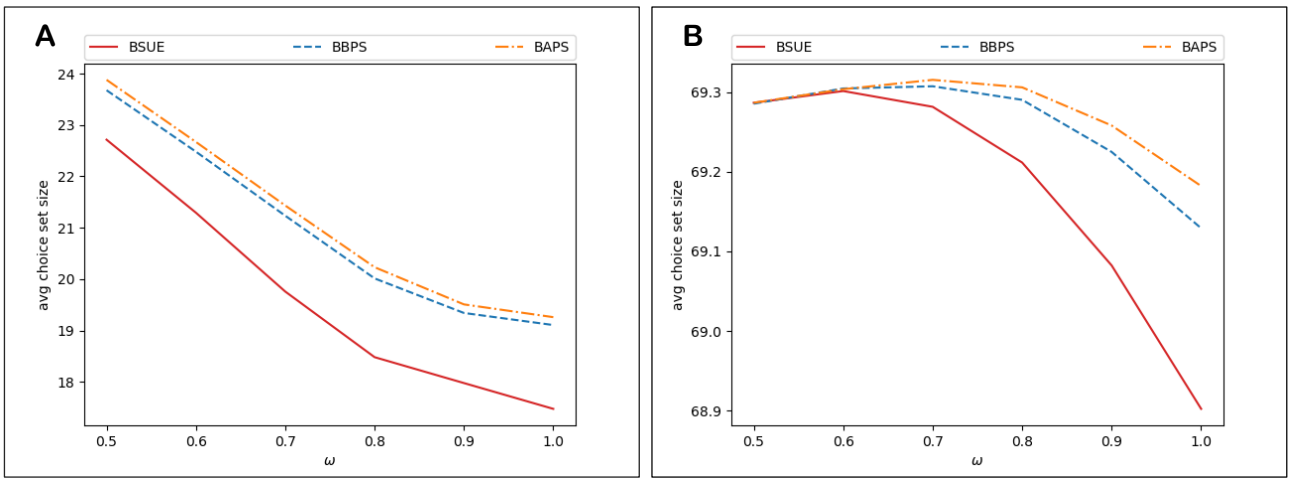

Fig. 5.22. Average used route choice set size for the bounded SUE models with different levels of travel demand, scaled by ω. **A:** Sioux Falls. **B:** Winnipeg.

Fig. 5.23A-B display for the Sioux Falls and Winnipeg networks, respectively, how the number of iterations required for SUE convergence varies for the BPS SUE models as the β parameter is varied. Fig. 5.24A-B display results in terms of computation time, and Fig. 5.25A-B display how the average used route choice set size varies. As shown, for BBPS SUE and BAPS SUE, only a small increase in the number of iterations required for convergence occurs as β is increased, though for BAPS SUE – as also shown in Fig. 5.16/Fig. 5.17 – total computation times increase exponentially with β due to the fixed-point probability computation. For BAPS′ SUE and BAPS SUE*, the number of BPS SUE algorithm iterations increases exponentially with β, and for $\beta = 0.9$ on Winnipeg, BAPS′ SUE actually takes longer than BAPS SUE. Albeit marginally, the average used route choice set sizes increase for the BBPS/BAPS SUE models as β increases. As shown in Fig. 5.22 & Fig. 5.28, BSUE tends to equilibrate smaller used route choice sets than the BPS SUE models. Decreasing β tends the BPS SUE models towards BSUE and thus it makes sense that decreasing β results in smaller choice sets. The reason that BSUE is equilibrating smaller used route choice sets than the BPS SUE models, must be due to the path size correction factors in the probability relations pushing flow to the low costing route(s), thus expanding the bound and including more used routes.

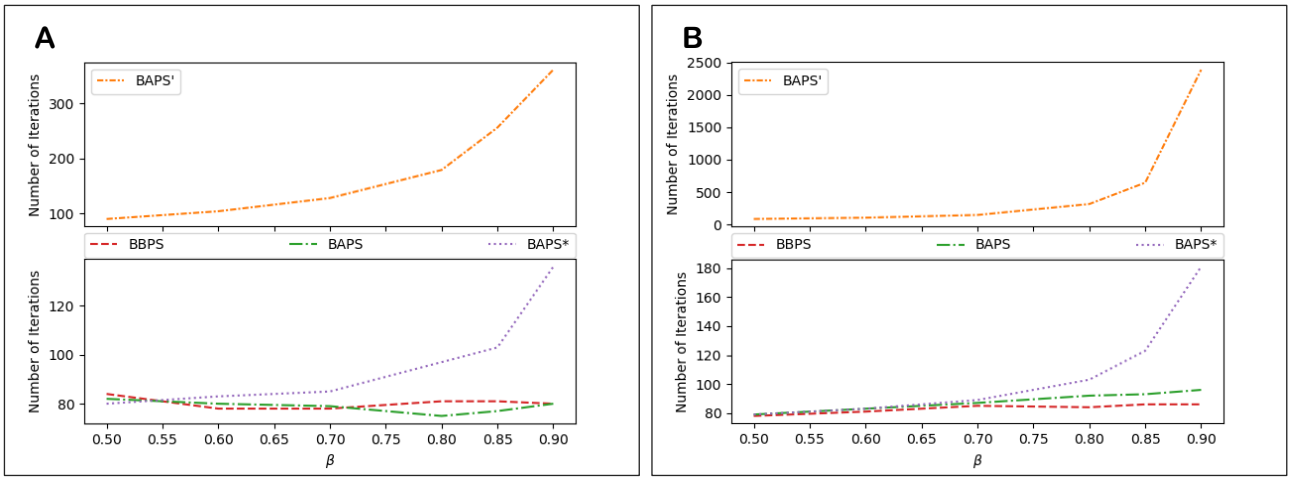

Fig. 5.23. Number of iterations required for SUE convergence as the β parameter is varied. **A:** Sioux Falls. **B:** Winnipeg.

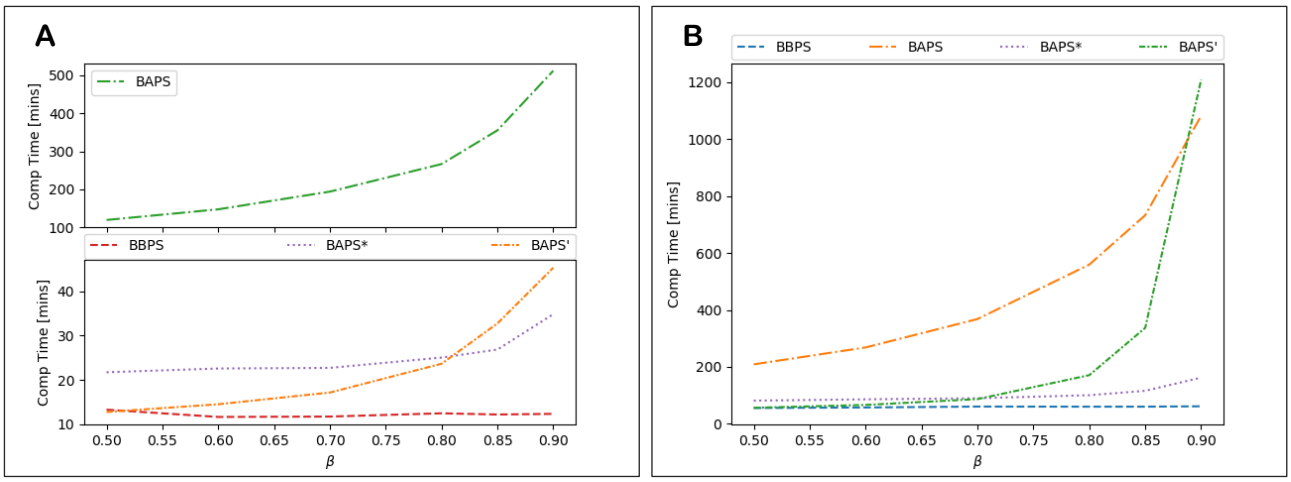

Fig. 5.24. Computation time [mins] required for SUE convergence as the β parameter is varied. **A:** Sioux Falls. **B:** Winnipeg.

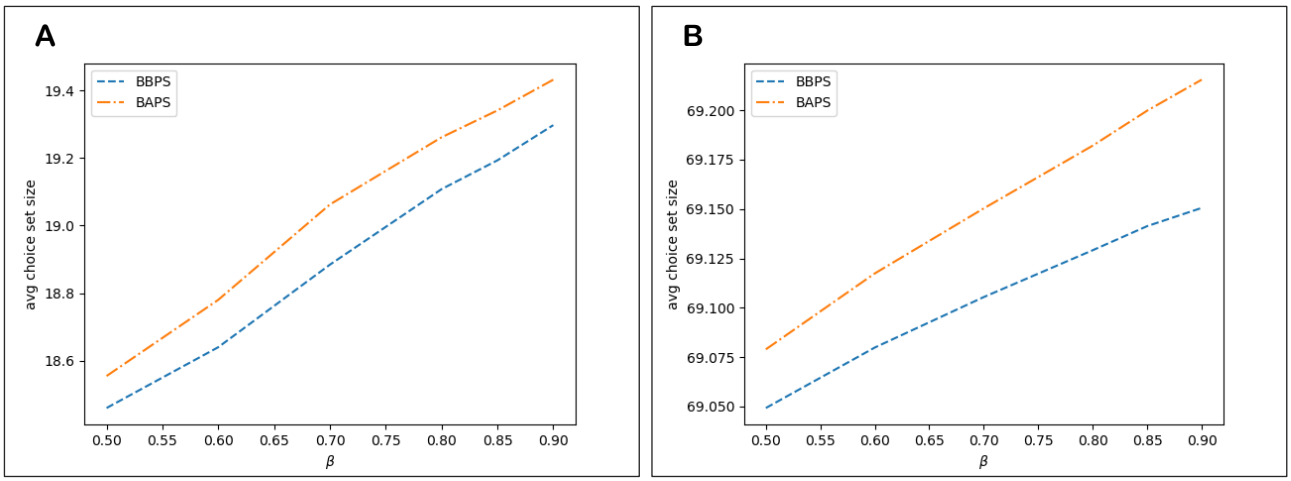

Fig. 5.25. Average choice set size for the BPS SUE models as the β parameter is varied. **A:** Sioux Falls. **B:** Winnipeg.

Fig. 5.26A-B display for the Sioux Falls and Winnipeg networks, respectively, how the number of iterations required for SUE convergence varies for the BPS SUE models as the φ parameter is varied. Fig. 5.27A-B display results in terms of computation time, and Fig. 5.28A-B display how the average used route choice set size varies. As expected, the used route choice set sizes expand as the bound parameter φ increases. As shown for Sioux Falls, there appears to be no clear trend for the SUE convergence rates in this range of φ, though computation times generally increase due to the greater number of active routes. For Winnipeg, the SUE convergence rates improve as φ increases in this range, improving computation times.

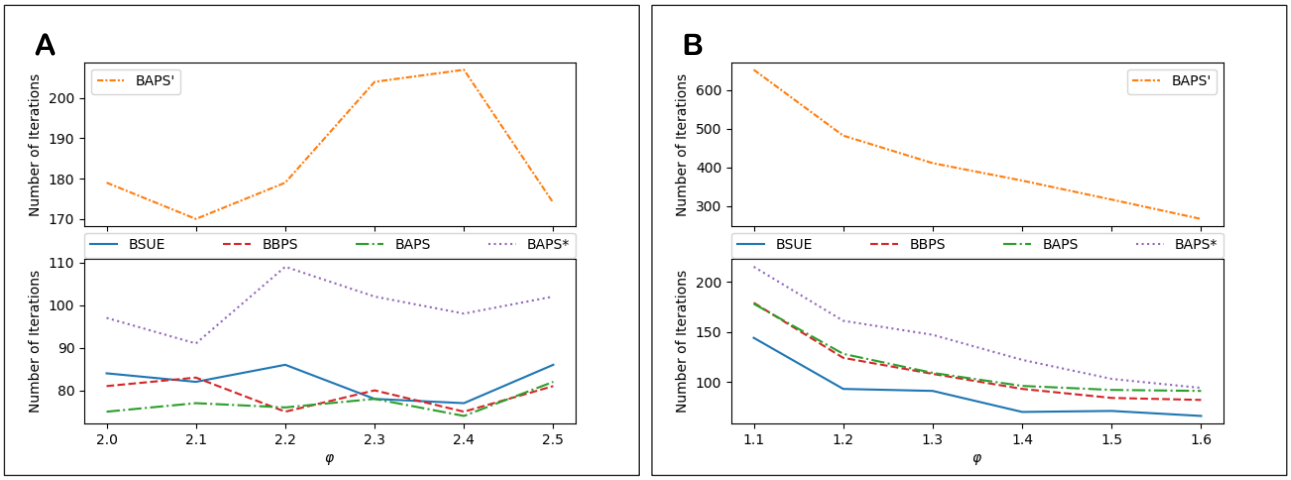

Fig. 5.26. Number of iterations required for SUE convergence as the φ parameter is varied. **A:** Sioux Falls. **B:** Winnipeg.

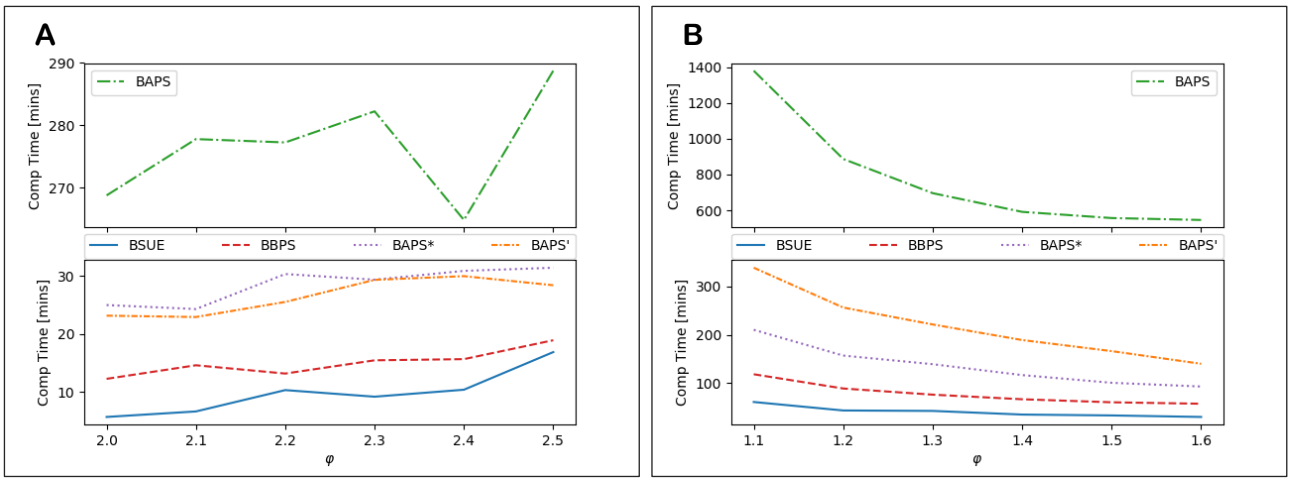

Fig. 5.27. Computation time [mins] required for SUE convergence as the φ parameter is varied. **A:** Sioux Falls. **B:** Winnipeg.

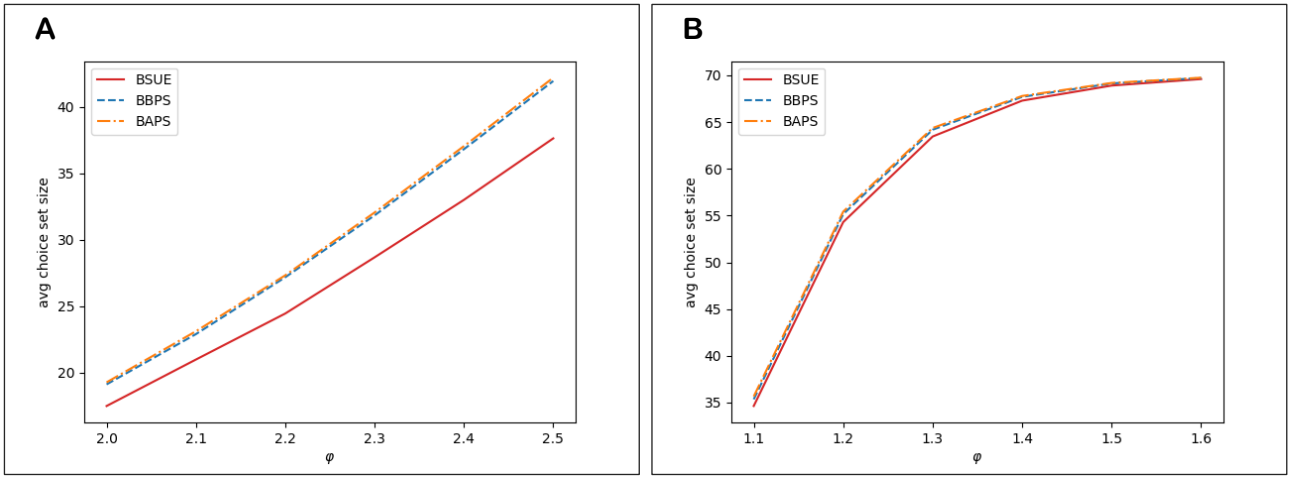

Fig. 5.28. Average choice set size for the bounded SUE models as the φ parameter is varied. **A:** Sioux Falls. **B:** Winnipeg.

The figures are omitted from the paper, but in similar experiments, for Sioux Falls and Winnipeg the SUE convergence rate worsened for the bounded SUE models as the θ parameter was increased, resulting in longer computation times. This is because the route cost differences are accentuated more with large θ resulting in greater flow fluctuations.

5.3 Flow Results

In this subsection we compare the flow results from the different SUE models. To compare the flow results $\boldsymbol{f}^{*R1}$ and $\boldsymbol{f}^{*R2}$ for Result 1 and Result 2, respectively, we measure the Root Mean Squared Error (RMSE):

$$RMSE = \sqrt{\sum_{m=1}^{M} \sum_{i \in R_m} \left(f_{m,i}^{*R1} - f_{m,i}^{*R2}\right)^2 / N},$$

where N is the total number of routes.

We begin by demonstrating the relationships between the bounded and non-bounded SUE models. The bounded models all approach limit models as the bound $\varphi \to \infty$ and all routes become used. MNL is the limit model of the BCM, GPSL′ is the limit model of the BBPS model, and APSL is the limit model of the BAPS model. Fig. 5.29 thus displays the differences between MNL SUE & BSUE, GPSL′ SUE & BBPS SUE, and APSL SUE & BAPS SUE respectively, as φ is increased, A: Sioux Falls, B: Winnipeg. As expected, similarity to the limit models increases as φ increases.

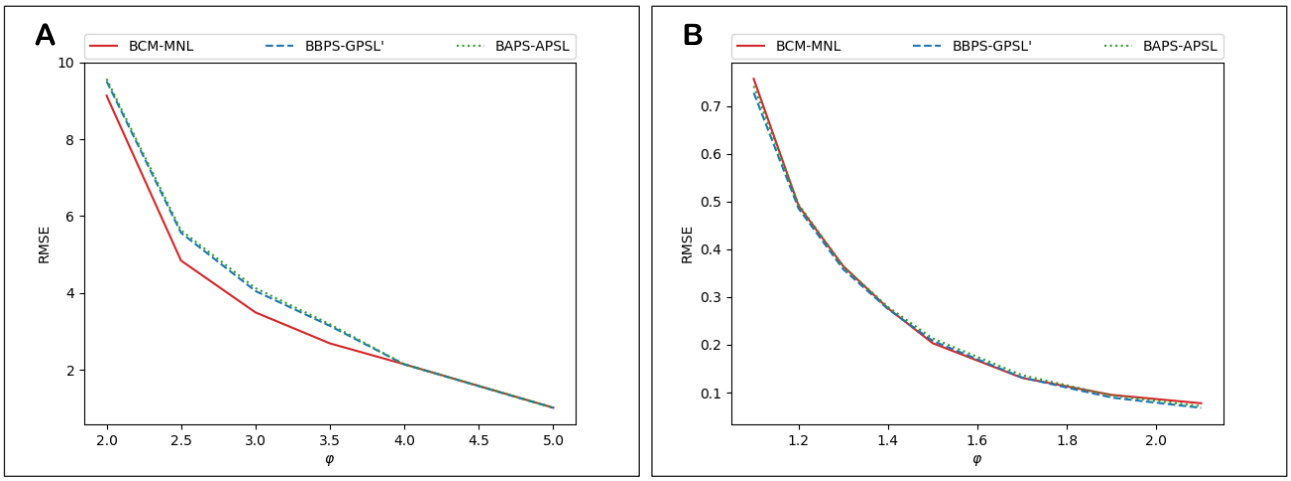

Fig. 5.29. Difference between MNL SUE & BSUE, GPSL′ SUE & BBPS SUE, and APSL SUE & BAPS SUE as the bound φ is increased. **A:** Sioux Falls. **B:** Winnipeg.

We next consider the differences in flow results between the bounded SUE models. Fig. 5.30A-B display for Sioux Falls and Winnipeg, respectively, the impact the φ parameter has on the differences in SUE flow between the models. As shown, BBPS & BAPS SUE as expected are the most similar, while BAPS SUE is the most different to BSUE. The similarity between BSUE and BBPS/BAPS SUE decreases as φ increases. This is likely because there are more routes to capture the correlation between as φ increases, and thus the path size terms have a greater impact upon the probability relations.

Fig. 5.31A-B display the impact of the θ parameter. As shown, the similarity between BBPS & BAPS SUE increases initially as θ increases: increasing θ increases the prominence of the travel cost components in the BAPS path size contribution factors, for low θ the distinctiveness components are more prominent increasing the difference to the BBPS factors.

Fig. 5.32A-B display the impact of the β parameter. As shown, the flow differences all increase as β increases, which is logical since the differences between the SUE models are the different path size correction terms scaled by β. For BAPS SUE, the impact is more significant for larger β, where the contribution influence of distinctiveness is more significant within the BAPS path size terms.

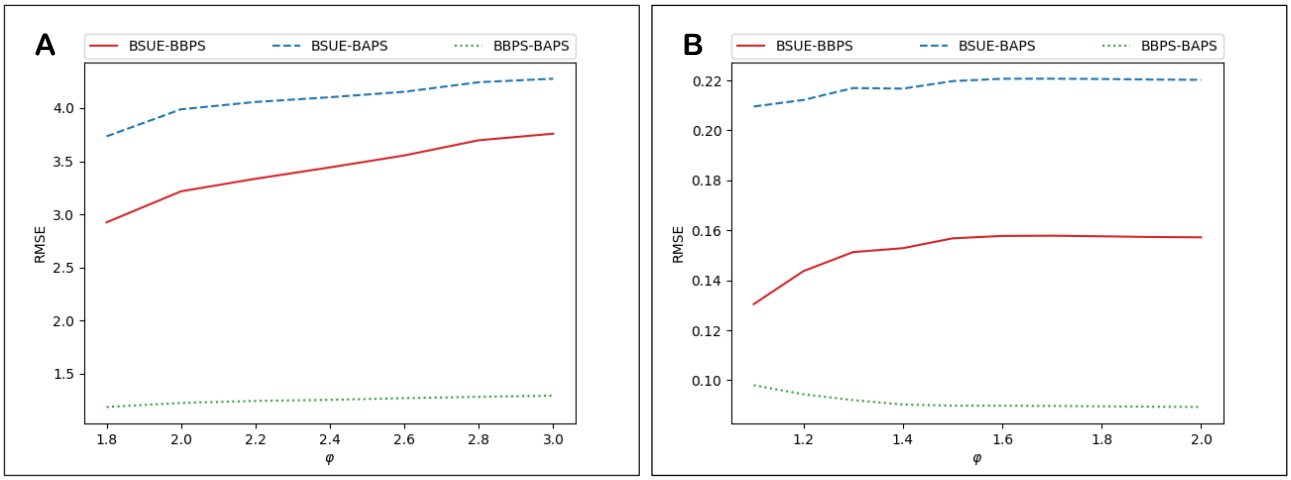

Fig. 5.30. Impact of the φ parameter on the difference in SUE flow between the bounded SUE models. **A:** Sioux Falls. **B:** Winnipeg.

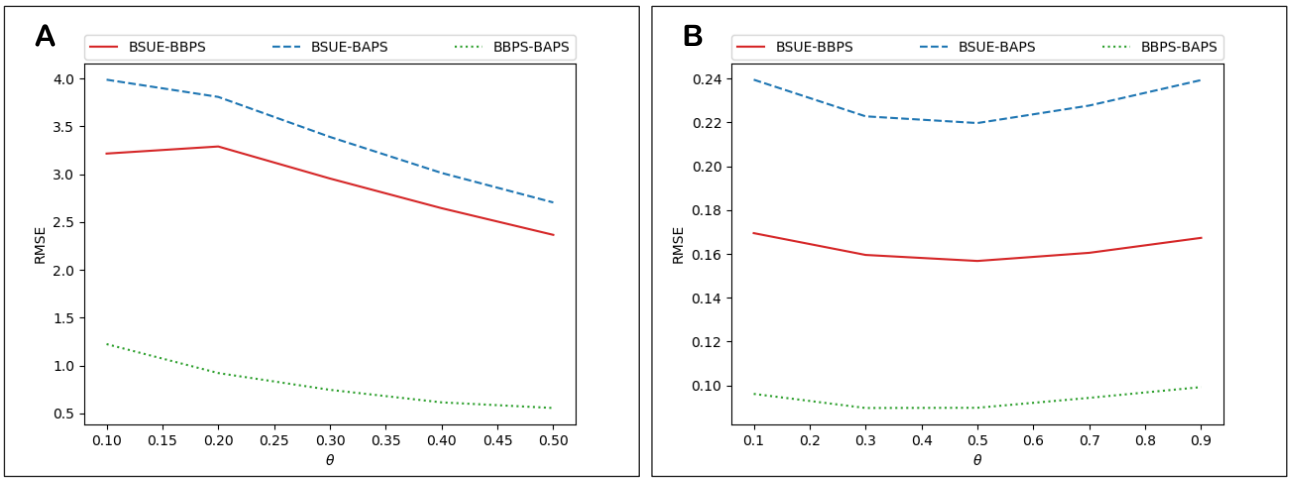

Fig. 5.31. Impact of the θ parameter on the difference in SUE flow between the bounded SUE models. **A:** Sioux Falls. **B:** Winnipeg.

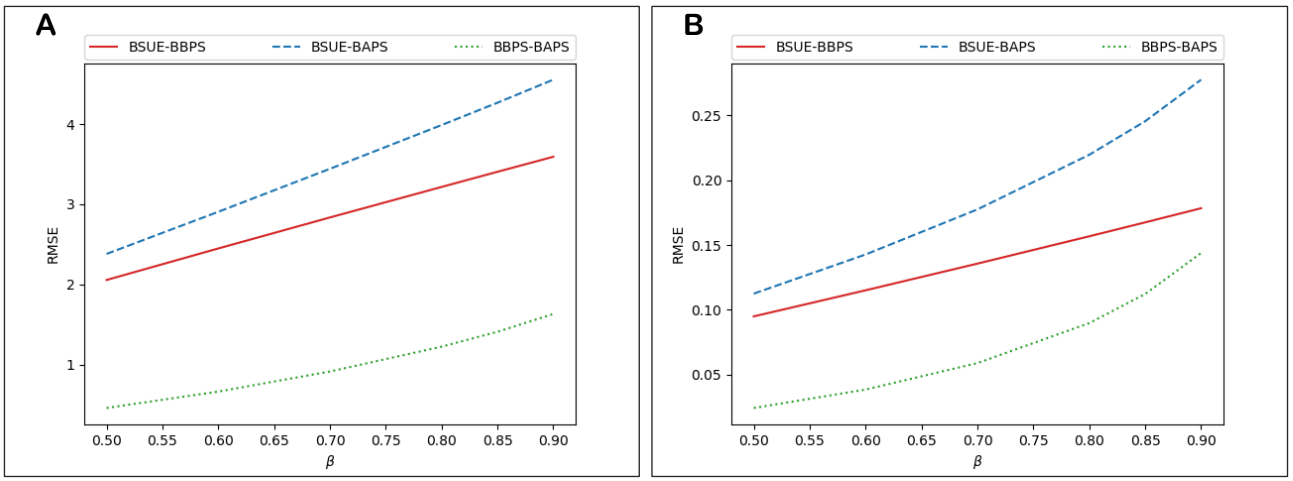

Fig. 5.32. Impact of the β parameter on the difference in SUE flow between the bounded SUE models. **A:** Sioux Falls. **B:** Winnipeg.

Next, we assess choice set robustness for the bounded SUE models (robustness to the approximated universal choice sets). In Duncan et al (2021a) we assessed choice set robustness for internally consistent SUE formulations of numerous correlation-based route choice models, namely: PSL, GPSL, APSL, C-Logit (CL), Cross-Nested Logit (CNL), and Generalised Nested Logit (GNL). It was shown that GPSL & APSL SUE generally performed the best due to having explicit mechanisms for dealing with unrealistic routes in the correlation components. All routes receive non-zero flows however, and the mechanisms only reduce the

effects of unrealistic routes. The BPS SUE models have significantly greater potential to be more effective in dealing with unrealistic routes, and we anticipate that choice set robustness should be significantly improved.

Adopting a similar experiment to that in Duncan et al (2021a), Fig. 5.33A-B display for the Sioux Falls and Winnipeg networks, respectively, the impact that varying the bound parameter φ has on choice set robustness for the bounded SUE models. To assess choice set robustness, flow results are compared between two different approximated universal choice sets, where the second set of choice sets expands the first, thus mimicking choice set mis-generation and the inclusion of unrealistic routes. The two choice sets are obtained by generating all routes (from the full pre-generated choice sets) with a free-flow travel time less than ψ times greater than the free-flow travel time on the quickest route for each OD movement. For Sioux Falls, the base-level choice sets are those obtained with $\psi = 2.3$, and the expanded choice sets are those obtained with $\psi = 2.5$ (i.e. in this case the full the pre-generated choice sets). For Winnipeg, the equivalent values are $\psi = 1.4$ and $\psi = 2.5$, respectively. Fig. 5.34A-B display for the Sioux Falls and Winnipeg networks, respectively, the average used route choice set sizes vary for the bounded SUE models as φ is varied, for the base-level and expanded approximated universal choice sets. Note that for Sioux Falls the $\psi = 2.3$ and $\psi = 2.5$ universal choice sets have average sizes 54.8 and 81.9, respectively. For Winnipeg, the $\psi = 1.4$ and $\psi = 2.5$ choice sets have average sizes 67.9 and 70.2, respectively.

As Fig. 5.33A-B show, the bounded SUE models do indeed have significant potential to improve choice set robustness. As $\varphi \to \infty$, BSUE tends towards MNL SUE, BBPS SUE tends towards GPSL′ SUE, and BAPS SUE tends towards APSL SUE. As can be seen, decreasing the bound parameter φ from large φ (where $\varphi \to \infty$ is approximated), improves choice set robustness for the bounded SUE models. For large bound values, the additional routes in the expanded choice sets have equilibrated costs within the bound and thus receive non-zero flows. This means that for the expanded choice sets solutions, the flows on the non-additional routes (those in the base-level choice sets) are adjusted from the base SUE solution. Lower bound values assign additional routes zero flows which reduces the impact they have on the non-additional route flows, thereby improving choice set robustness. As Fig. 5.34A-B show, decreasing φ reduces the difference between the equilibrated used routes from the base-level and the expanded approximated universal choice sets.

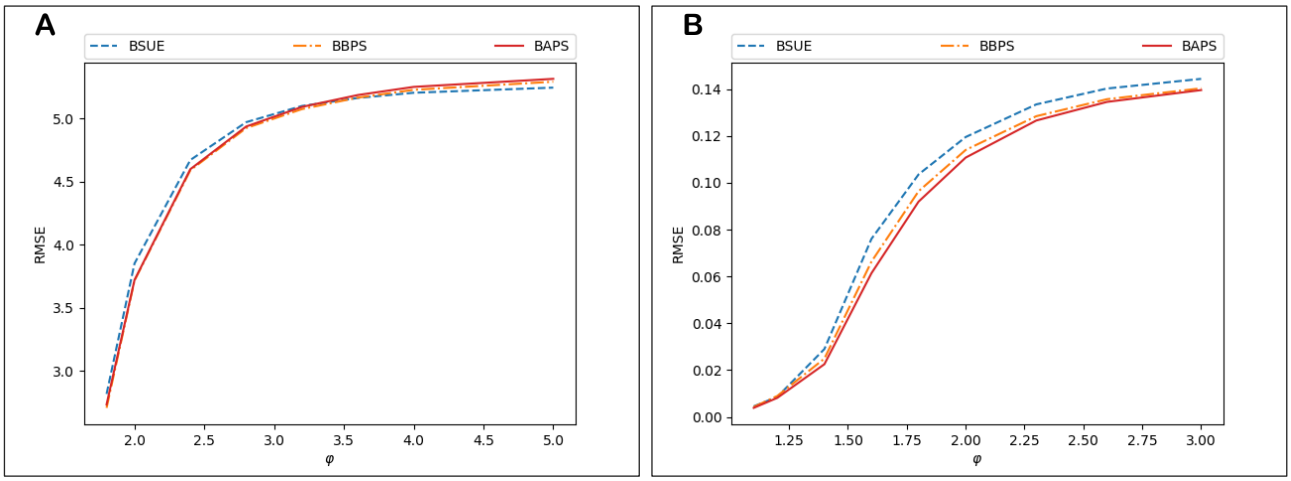

Fig. 5.33. Impact of the φ parameter on choice set robustness for the bounded SUE models. **A:** Sioux Falls. **B:** Winnipeg.

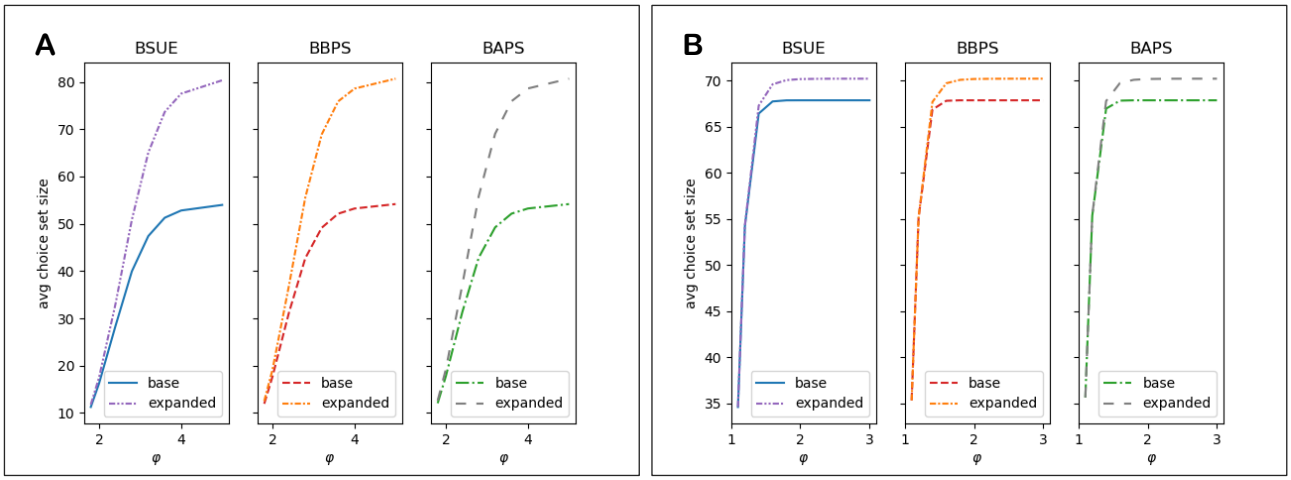

Fig. 5.34. How the average equilibrated used route choice set sizes vary for the bounded SUE models as the bound parameter φ is varied, for the base-level and expanded approximated universal choice sets. **A:** Sioux Falls. **B:** Winnipeg.

5.4 Uniqueness of BAPS SUE Solutions

As discussed in Section 3.3, it is not possible to prove that BBPS SUE or BAPS SUE solutions can be unique according to standard approaches. In Duncan et al (2021a), the uniqueness of APSL SUE solutions was investigated numerically, where the results suggested uniqueness conditions exist. Due to the similarities between the APSL SUE and BAPS SUE models, we conduct similar experiments to investigate the uniqueness of BAPS SUE solutions numerically.

As demonstrated in Duncan et al (2021b), for a given setting of the link costs $\boldsymbol{t}$ and θ and φ values, a β value exists, $\beta_{max,m}(\boldsymbol{t},\theta,\varphi) > 0$, for OD movement m such that BAPS model choice probability solutions are unique for all β in the range $0 \leq \beta \leq \beta_{max,m}(\boldsymbol{t},\theta,\varphi)$. This means that a β value exists, $\beta_{max}(\boldsymbol{t},\theta,\varphi) > 0$, such that solutions are unique for all OD movements for all β in the range $0 \leq \beta \leq \beta_{max}(\boldsymbol{t},\theta,\varphi)$, i.e. $\beta_{max}(\boldsymbol{t},\theta,\varphi) = \min\left(\beta_{max,m}(\boldsymbol{t},\theta,\varphi)\right)$. And, assuming the link costs are bounded, i.e. they have a maximum and minimum value (for example due the fixed demands), for a given θ value, a β value exists, $\bar{\beta}_{max}(\theta,\varphi) > 0$, such that BAPS model solutions are unique for all OD movements and for all feasible flow vectors (and thus costs) for all β in the range $0 \leq \beta \leq \bar{\beta}_{max}(\theta,\varphi)$. Obviously, $\bar{\beta}_{max}(\theta,\varphi) \leq \beta_{max}(\boldsymbol{t},\theta,\varphi) \leq \beta_{max,m}(\boldsymbol{t},\theta,\varphi)$.

In Duncan et al (2021a) it was found that APSL SUE solutions appeared to be unique when APSL probabilities were universally unique. Thus, while it is not guaranteed that in all cases BAPS SUE solutions will be unique when BAPS models probabilities are universally unique, i.e. for β in the range $0 \leq \beta \leq \bar{\beta}_{max}(\theta,\varphi)$, as we show below, it appears from numerical experiments that this is also often the case.

Fig. 5.35A-B plot, for two runs, the small example network route flows at each iteration of the BPS SUE algorithm solving BAPS SUE, when the initial conditions for the FPIM computing the BAPS model probabilities are randomly generated, for $\beta = 0.9$ and $\beta = 1.1$, respectively, $\theta = 1$, $\varphi = 1$, $\xi = 10$. The MSWA step-size scheme is adopted with $d = 10$, and the algorithm is stopped after 20 iterations if convergence is not reached. As shown, for $\beta = 0.9$, because the BAPS model probabilities are unique for the route costs (from the flows) at each iteration, the route flows on both runs converge in the same way to the same BAPS SUE solution. For $\beta = 1.1$, however, as demonstrated clearly at iteration 12, there are multiple BAPS model probabilities for the route costs at each iteration, and hence due to the step-size the flows fluctuate randomly and do not converge. This suggests that BAPS model probability solutions are universally unique for $\beta = 0.9$, but not for $\beta = 1.1$, and hence that $0.9 \leq \bar{\beta}_{max}(1) < 1.1$.

Fig. 5.36A-B plot for $\beta = 0.9$ and $\beta = 1.1$, respectively, and for multiple runs, the flows at each iteration of the BPS SUE algorithm solving BAPS SUE utilising follow-on initial conditions for the FPIM computing the BAPS model probabilities, where the SUE initial conditions are randomly generated, $\theta = 1$, $\varphi = 1$, $\xi = 10$. The initial SUE conditions for the BPS SUE algorithm in Algorithm 5.1 are All-Or-Nothing assignments. To instead randomly generate initial SUE conditions here, we first suppose all routes are used and randomly generate flows for these routes (maintaining demand-feasibility). A bound condition phase is then conducted

to remove routes with consequent costs above the bound and redistribute the flows accordingly. As shown, for $\beta = 0.9$, all initial SUE conditions lead to the same solution, whereas for $\beta = 1.1$, two solutions are found with different initial conditions. Fig. 5.37A-B plot the flows at each iteration of the BPS SUE algorithm for solving BAPS′ SUE. As shown, for $\beta = 0.9$, all initial conditions again lead to the same solution, whereas for $\beta = 1.1$, two solutions are found.

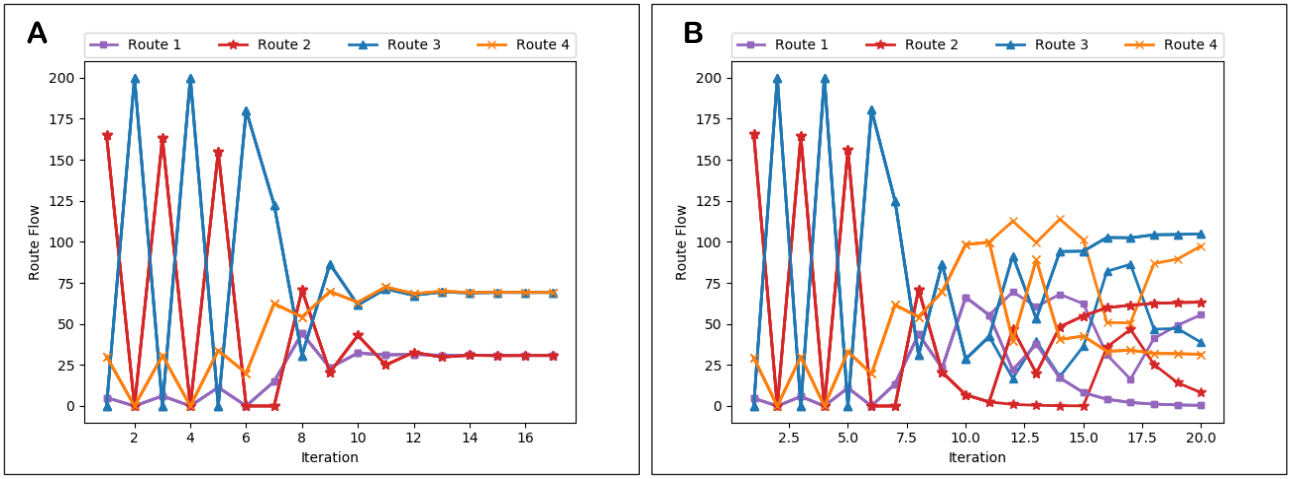

Fig. 5.35. Small example network: BAPS SUE route flows at each iteration of the BPS SUE algorithm with randomly generated initial FPIM conditions, two runs ($\theta = 1$, $\varphi = 2$, $\xi = 10$). **A:** $\beta = 0.9$. **B:** $\beta = 1.1$.

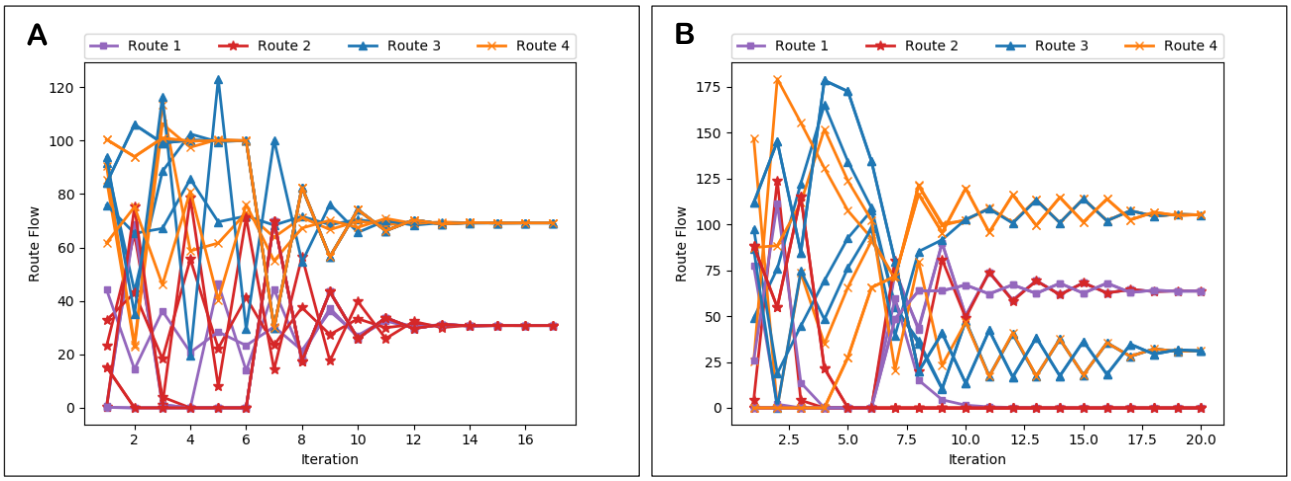

Fig. 5.36. Small example network: BAPS SUE route flows at each iteration of the BPS SUE algorithm with follow-on initial FPIM conditions and randomly generated initial SUE conditions, multiple runs ($\theta = 1$, $\varphi = 2$, $\xi = 10$). **A:** $\beta = 0.9$. **B:** $\beta = 1.1$.

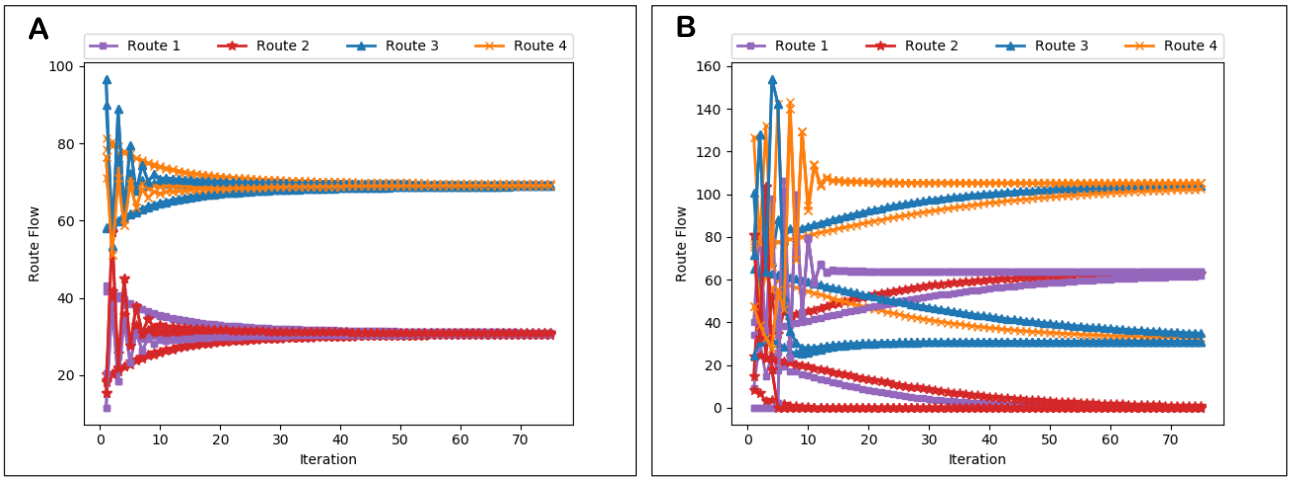

Fig. 5.37. Small example network: BAPS′ SUE route flows at each iteration of the BPS SUE algorithm with randomly generated initial SUE conditions, multiple runs ($\theta = 1$, $\varphi = 2$). **A:** $\beta = 0.9$. **B:** $\beta = 1.1$.

Fig. 5.36 & Fig. 5.37 suggest that the BAPS SUE solution is unique for $\beta = 0.9$, and solutions are non-unique for $\beta = 1.1$, and Fig. 5.35 suggests that this due to the BAPS choice probability solutions being universally unique for $\beta = 0.9$, but not for $\beta = 1.1$. One can imply from this that $0.9 \leq \bar{\beta}_{max}(1,2) < 1.1$, and potentially that BAPS SUE solutions are unique for β in the range $0 \leq \beta \leq 0.9 \leq \bar{\beta}_{max}(1,2)$.

Duncan et al (2021a) describe a method for identifying the uniqueness conditions for APSL SUE solutions. Here, we utilise a similar method, to attempt to identify $\bar{\beta}_{max,m}(\theta, \varphi)$ values and thus $\bar{\beta}_{max}(\theta, \varphi) = \min(\bar{\beta}_{max,m}(\theta, \varphi): m = 1, \dots, M)$ for the BAPS SUE model. $\bar{\beta}_{max,m}(\theta, \varphi)$ is estimated by plotting trajectories of BAPS SUE solutions for OD movement m for varying β, and identifying where a unique trajectory of solutions ends and multiple trajectories begin. A simple method for obtaining trajectories of BAPS SUE solutions is as follows:

Step 1. Identify a suitably large value for β (where it is predicted that solutions will be non-unique).

Step 2. Solve BAPS SUE for this large β with a randomly generated initial SUE condition.

Step 3. Decrement β and obtain the next BAPS SUE solution with the initial SUE condition set as the solution for the previous β.

Step 4. Continue until a suitably low value of β (where it is predicted that solutions will be unique).

The randomly generated initial SUE conditions for the BPS SUE algorithm are obtained by the same method as described above: by randomly generating a non-zero flow for all routes (maintaining demand-feasibility), and performing a bound condition phase to remove routes with consequent costs above the bound, redistributing the flows accordingly. Since the φ parameter is fixed, a bound condition phase is not required for Step 3 when using the solution to the previous β.

By plotting the route flows for OD movement m at each decremented β, and repeating this method several times, one can determine where non-unique solution trajectories end and hence estimate $\bar{\beta}_{max,m}(\theta, \varphi)$. If after several repetitions (with different randomly generated initial conditions) only a single trajectory of solutions is shown, then the initial large β value is increased. Similarly, if only multiple trajectories are shown, the stopping low β value is decreased. However, one can test beforehand whether the initial and stopping β values are suitable by solving for each a few times with random initial conditions and observing whether there are different solutions for the initial β value and the same solution for the stopping β. In the experience of the authors, the $\bar{\beta}_{max,m}(\theta, \varphi)$ values typically range between 0.9 and 1.1 (usually around 1).

If in large-scale networks it is computationally burdensome to solve BAPS SUE once at a time for each decremented value of β, then one can instead (by possibly harnessing parallel processing) solve for different β values simultaneously, each with randomly generated initial conditions. This should also identify where solutions are and are not unique. Moreover, one can plot flow trajectories for all OD movements simultaneously, so the method does not need to be repeated for each OD movement. We illustrate the approach graphically here, but there is no need to draw graphs for general networks. One can instead observe the route flow values, where a finer grained decrement of β will provide a more accurate estimation of $\bar{\beta}_{max,m}(\theta, \varphi)$.

In the case of the small example network where there is a single OD movement, we estimate $\bar{\beta}_{max}(1,2)$ using the above method. Fig. 5.38 displays trajectories of BAPS SUE route flow solutions as the β parameter is varied for $\theta = 1$, $\varphi = 2$, $\xi = 10$. β was decremented by 0.005 and the initial large β value was 1.2. The solution trajectory plotting was repeated until multiple trajectories were shown. As shown, there is a unique trajectory of route flow solutions up until $\beta = \bar{\beta}_{max}(1,2)$ where there then becomes multiple trajectories. The estimated $\bar{\beta}_{max}(1,2)$ value is 0.995.

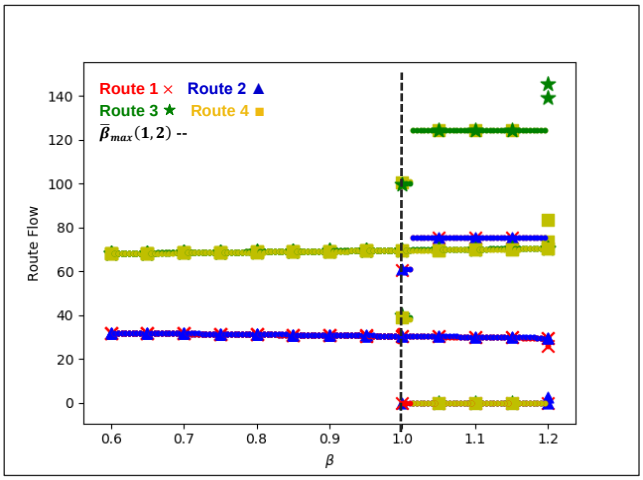

Fig. 5.38. Small example network: Trajectories of BAPS SUE solutions as β is varied ($\theta = 1$, $\varphi = 2$, $\xi = 8$).

We use the same technique of plotting flow trajectories to estimate the BAPS SUE uniqueness conditions for the Sioux Falls network. Fig. 5.39 displays for Sioux Falls the maximum route flow from two trajectories of BAPS SUE solutions as the β parameter is varied for two different randomly chosen OD movements. β was decremented by 0.01, and the initial large β and stopping small β values were $\beta = 1.1$ and $\beta = 0.9$, respectively. As shown, the $\bar{\beta}_{max,m}(0.1,2)$ values for these OD movements appear to be greater than 0.9.

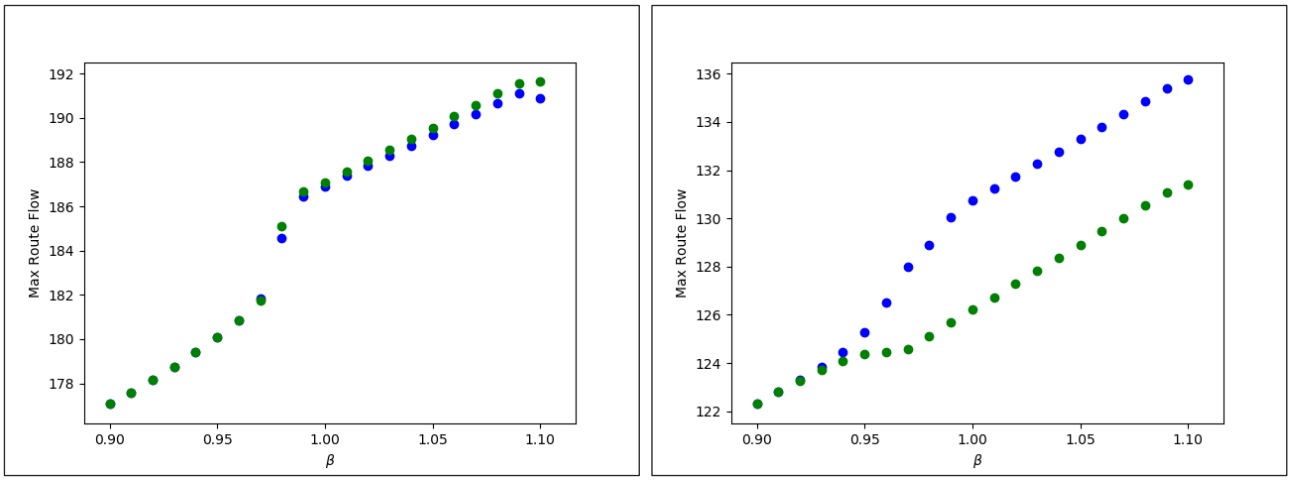

Fig. 5.39. Sioux Falls: Maximum route flow for two different OD movements from two trajectories of BAPS SUE solutions as β is varied.

5.5 Findings of the Numerical Experiments

To summarise, the key findings of the numerical experiments were that:

a) Flow results from the bounded SUE models converged towards their non-bounded limit models as the bound parameter was increased towards infinity.

b) Bounded SUE models have the potential to be significantly more robust than non-bounded SUE models to the inclusion of unrealistic routes to the adopted choice sets.

c) The BPS SUE models tended to equilibrate marginally larger used route choice set sizes than BSUE.

d) BBPS SUE converged in a similar number of BPS SUE algorithm iterations to BSUE, but total computation times were longer due to the more complex probability expression.

e) The features of solving APSL/APSL′ SUE explored in Duncan et al (2021a) could be transferred to solving the analogous BAPS/BAPS′ SUE:

f) Convergence rates for solving BAPS SUE were similar to that for BSUE & BBPS SUE, however the computational burden involved in computing the fixed-point BAPS model choice probabilities for each BPS SUE algorithm iteration resulted in much longer total computation times.

g) On-the-other-hand, the computational burden involved in computing the BAPS′ model choice probabilities was similar to that for the BBPS model (similarly closed-form), but the BAPS′ SUE convergence rate was comparatively slow, and thus total computation times were also longer.

h) In general, the FPIM convergence parameter ξ (and thus the accuracy of the BAPS model choice probabilities) must be at a certain level for convergence of the BPS SUE algorithm to the BAPS SUE solution.

i) However, by utilising 'follow-on' initial FPIM conditions – where the initial conditions for solving the BAPS probabilities at iteration n of the BPS SUE algorithm are set as the route flow proportions from iteration $n-1$ – the BPS SUE algorithm will converge to the BAPS SUE solution for all ξ.

j) There was a computational trade-off between solving BAPS & BAPS′ SUE: solving BAPS SUE with low ξ and follow-on initial conditions simulated solving BAPS′ SUE where the convergence rate was slow, while larger values of ξ resulted in comparatively quick convergence rates but lengthy computation times for the iterations.

k) One can thereby, with ξ, trade-off SUE convergence rates with computation times for each of the BPS SUE algorithm iterations, to improve total computation times for solving BAPS SUE.

l) Also to improve BAPS SUE total computation times, one can stipulate a set number FPIM iterations to perform at each BPS SUE algorithm iteration, or utilise a combination of a maximum number of FPIM iterations to perform and a maximum level of BAPS probability convergence (controlled with ξ).

m) BAPS SUE can be thus solved in feasible computation times, though typically longer than BSUE & BBPS SUE.

n) Uniqueness conditions appeared to exist for BAPS SUE: for β in the range $0 \leq \beta \leq \bar{\beta}_{max}(\theta)$, where BAPS probability solutions are unique.

o) $\bar{\beta}_{max,m}(\theta)$ values (uniqueness for OD movement m) in experiments were greater than 0.9.

The 'optimal' values for the methods in j)-k) for solving BAPS SUE are particular to the network, model, and algorithm specifications, e.g. model parameters, adopted step-size scheme, choice set sizes. However, by fixing the optimised values for a given specification, and then varying the specifications, it was shown that the method was robust in its effectiveness compared to solving BAPS SUE in a standard way (i.e. where the BAPS fixed-point probabilities are accurately solved with non-follow-on initial conditions). Future research could explore an intelligent, adaptive process whereby the optimal values of ξ and the maximum number of FPIM iterations to perform at each BPS SUE algorithm iteration are learnt / worked out as the BPS SUE algorithm progresses.

6. Conclusion

This paper investigates the integration of Bounded Path Size (BPS) route choice models within a Stochastic User Equilibrium (SUE) model. The BPS model form offers a theoretically consistent and practical approach for dealing with both route overlap and unrealistic routes on large-scale networks. It captures correlations between overlapping routes by including correction terms within the probability relations, and has a consistent criterion for assigning zero choice probabilities to unrealistic routes while eliminating their path size contributions. Two BPS models are proposed: one that is closed-form (the BBPS model), and another expressed as a fixed-point problem (the BAPS model). For the BAPS model, solving the choice probabilities requires a fixed-point algorithm to compute the solution. This has the potential to be computationally burdensome in large-scale networks even when the travel costs are fixed. As explored in the paper, however, the requirement of solving fixed-point problems to compute the BAPS model choice probabilities can be circumvented in SUE application, since at equilibrium the route flow proportions and choice probabilities equate.

The paper proves the existence of BBPS SUE solutions. BAPS SUE solution existence cannot be guaranteed by the standard proofs since the BAPS choice probability function is not technically continuous, though this is not an issue in practice and thus in practice BAPS SUE solution existence is not an issue. Uniqueness for BBPS SUE or BAPS SUE cannot be guaranteed. Instead, the paper investigates the uniqueness of BAPS SUE model solutions numerically, where experiments on the Sioux Falls and Winnipeg networks suggest that uniqueness conditions exist. These conditions are analogous to those for the uniqueness of BAPS model probability solutions, and BAPS SUE solutions appear to be unique when BAPS model solutions are unique.

The paper proposes a generic algorithm for solving BPS SUE models. The algorithm is an adaptation of the generic algorithm proposed by Watling et al (2018) for the Bounded SUE (BSUE) model. To equilibrate the choice sets of realistic routes, the BSUE algorithm generates realistic routes from the network as the algorithm progresses. With the current techniques available for generating these routes, there are questions over the suitability of the approach for large-scale networks. For the proposed BPS SUE algorithm, we thus take a more heuristic approach, by pre-generating approximated universal choice sets. From these routes, the restricted choice sets of realistic routes are equilibrated. The algorithm can however be easily adapted so that routes are generated as the algorithm progresses, just like the BSUE algorithm.

Adopting the Method of Successive Weighted Averages (MSWA) step-size scheme, the computational performance of the BPS SUE algorithm for solving BBPS & BAPS SUE is assessed in numerical experiments on the Sioux Falls and Winnipeg networks. The paper demonstrates how for BAPS SUE one can trade-off the accuracy of BAPS model probabilities (and thus computation times of each iteration) with rate of SUE convergence, and as such, it is shown that BAPS SUE can be solved in feasible computation times. Computational performance and flow results are also compared with BSUE and standard Path Size Logit (PSL) SUE models (solved with a flow-averaging algorithm and MSWA). The key findings of the numerical experiments were that:

a) Flow results from the bounded SUE models converged towards their associated non-bounded limit SUE model as the bound parameter was increased towards infinity.

b) The bounded SUE models have the potential to be significantly more choice set robust that non-bounded SUE models, i.e. less sensitive to the inclusion of unrealistic routes to the adopted choice sets.

c) BBPS SUE could be solved quicker than BAPS SUE, due to the closed-form BBPS probability expression, but BAPS SUE was more internally consistent (greater behavioural realism).

d) BPS SUE models can be solved in feasible computation times, though typically longer than non-bounded models.

7. References

Bekhor S, Toledo T, & Prashker J, (2008). Effects of choice set size and route choice models on path-based traffic assignment. Transportmetrica, 4(2), p.117-133.

Ben-Akiva M, & Bierlaire M, (1999). Discrete choice methods and their applications to short term travel decisions. In: Halled, R.W. (Ed.), Handbook of Transportation Science. Kluwer Publishers.

Bliemer M & Bovy P, (2008). Impact of Route Choice Set on Route Choice Probabilities. Transportation Research Record: Journal of the Transportation Research Board, 2076, p.10–19.

Bovy P, Bekhor S, & Prato C, (2008). The Factor of Revisited Path Size: Alternative Derivation. Transportation Research Record: Journal of the Transportation Research Board, 2076, Transportation Research Board of the National Academies, Washington, D.C., p.132–140.

Daganzo C & Sheffi Y, (1977). On stochastic models of traffic assignment. Transportation Science, 11, p.253–274.

Duncan L, Watling D, Connors R, Rasmussen T, & Nielsen O, (2020). Path Size Logit Route Choice Models: Issues with Current Models, a New Internally Consistent Approach, and Parameter Estimation on a Large-Scale Network with GPS Data. Transportation Research Part B, 135, p.1-40.

Duncan L, Watling D, Connors R, Rasmussen T, & Nielsen O, (2021a). Formulation and solution of Adaptive Path Size Logit Stochastic User Equilibrium – addressing choice set robustness and internal consistency. Status: Currently under review at Transportation Research Part B: Methodological.

Duncan L, Watling D, Connors R, Rasmussen T, & Nielsen O, (2021b). A bounded path size route choice model excluding unrealistic routes: Formulation and estimation from a large-scale GPS study. Transportmetrica A: Transport Science.

Hoogendoorn-Lanser S, van Nes R, & Bovy P, (2006). A constrained enumeration approach to multi-modal choice set generation. In: Proceedings, 11th International Conference on Travel Behaviour Research (CD-ROM), Kyoto, Japan.

Isaacson E, & Keller H, (1966). Analysis of Numerical Methods. John Wiley & Sons, Inc., New York, USA.

Liu H, He X, & He B, (2009). Method of successive weighted averages (MSWA) and self regulated averaging schemes for solving stochastic user equilibrium problem. Networks and Spatial Economics, 9(4), p.485–503.

Prato C & Bekhor S, (2006). Applying branch & bound technique to route choice set generation. Transport. Res. Rec. 1985, p.19–28.

Ramming S, (2002). Network knowledge and route choice. Ph.D. Thesis, Massachusetts Institute of Technology, Cambridge, USA.

Rasmussen T, Nielsen O, Watling D, & Prato C, (2015). Stochastic user equilibrium with equilibrated choice sets: Part II – Solving the restricted SUE for the logit family. Transportation Research Part B, 77, p.146–165.

Sheffi Y & Powell W, (1982). An algorithm for the equilibrium assignment problem with random link times. Network: An International Journal, 12(2), p.191-207.

Wardrop J, (1952). Some theoretical aspects of road traffic research. Proc. Institute of Civil Engineers, Part II, 1, p.325-378.

Watling D, Rasmussen T, Prato C, & Nielsen O, (2015). Stochastic user equilibrium with equilibrated choice sets: Part I – Model formulations under alternative distributions and restrictions. Transportation Research Part B (77), p.166-181.

Watling D, Rasmussen T, Prato C, & Nielsen O, (2018). Stochastic user equilibrium with a bounded choice model. Transportation Research Part B, 114, p.254-280.

Chapter 6. Conclusion

It is essential that decision processes related to improving transport infrastructure, are supported by a well-functioning transport model which gives a realistic representation of the route choices of travellers. The ability to predict driver route choice means that route flows can be calculated and areas of potentially high levels of congestion can be identified, in turn allowing us to investigate many eventualities, and assess any possible remedial measures.

There are, however, several distinct and unique aspects about route choice modelling that makes it a more challenging task than modelling other types of transport choices. The literature highlights four key aspects in particular: allowing for driver/modelling uncertainty, capturing correlations between overlapping routes, dealing with unrealistic routes, and incorporating the effects of congestion. Numerous modelling approaches have been developed to address these challenges; however, as discussed/uncovered/demonstrated in this thesis, some of the models/approaches have issues with theoretical consistency, robustness, and/or being mathematically well-defined. This thesis addresses this by developing two new route choice modelling approaches, and demonstrates their computationally feasibility and estimatability on real-life large-scale networks. Chapters 2&3 of this thesis developed the first modelling approach, and Chapters 4&5 developed the second. Below, the two modelling approaches are reviewed, by reviewing the findings of each chapter in turn, followed by discussions of scope for further research. Some wider concluding remarks then finalise the conclusion chapter and thesis. Fig. 6.1 collates the highlights from the thesis chapters (the papers).

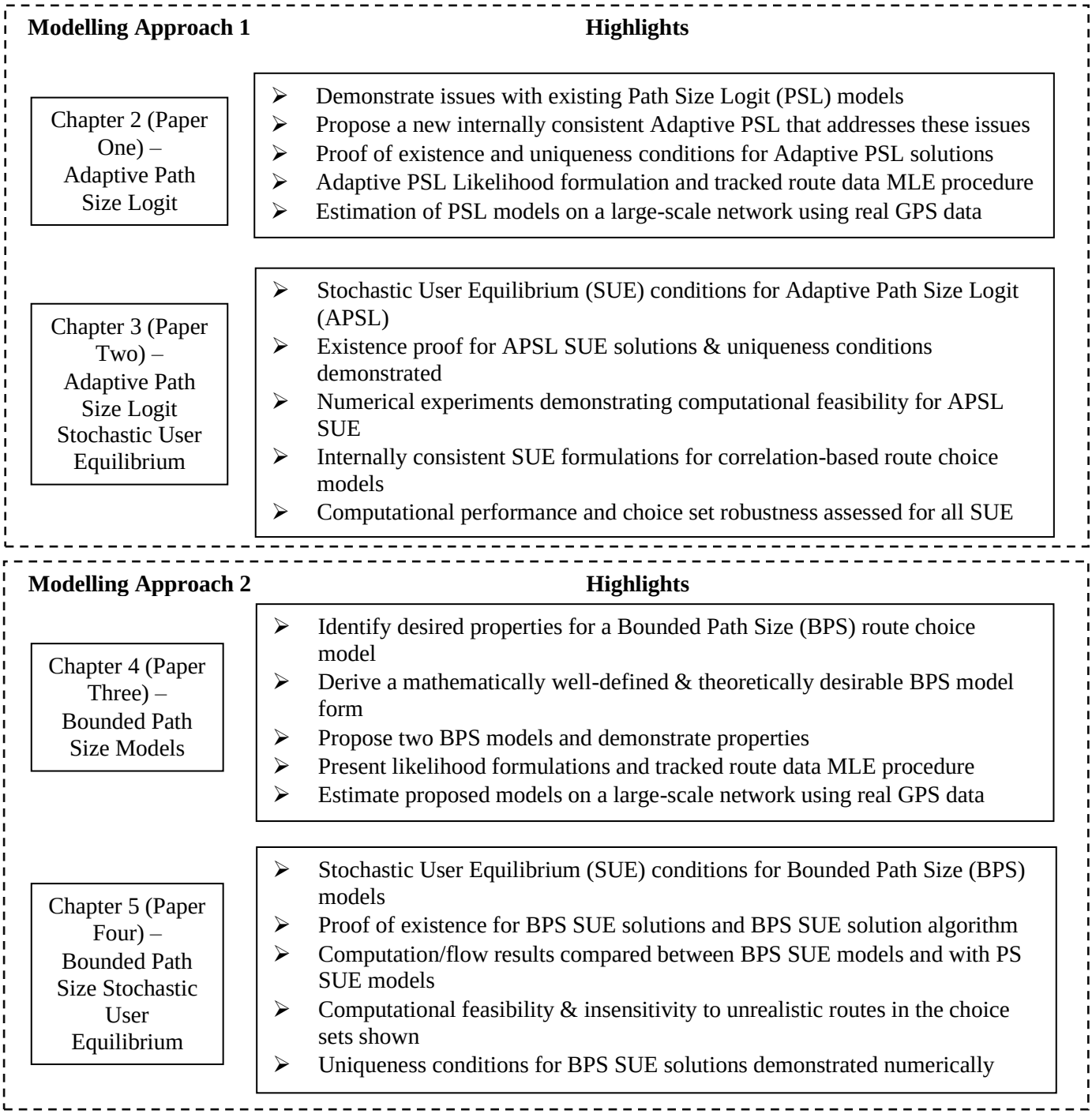

Fig. 6.1. Thesis chapter highlights.

1. Modelling Approach 1 – A New Internally Consistent Weighted Path Size Contribution Technique

1.1 Chapter 2 – Adaptive Path Size Logit

1.1.1 Review of Findings

The Path Size Logit (PSL) route choice model captures correlations between overlapping routes by including correction terms within the route utility functions. This provides a convenient closed-form solution for implementation in traffic network models, where the model has been shown to be both computationally feasible and estimatable on real-life large-scale networks.

The correction terms depend upon path size terms which measure the distinctiveness of routes: a route is penalised based on the number of other routes sharing its links, and the costs of those shared links. The key issue for PSL, however, is that all routes contribute equally to path size terms, meaning that unrealistic routes have a considerable and negative effect on the choice probabilities of the realistic routes when links are shared. The typical way of dealing with unrealistic routes for PSL is to employ some kind of heuristic method that attempts to explicitly generate a route choice set containing just the routes considered realistic. This approach, however, leads to theoretical inconsistencies, since the route generation criteria is not consistent with the calculation of the choice probabilities among generated routes, while generating the exact choice sets of realistic routes is very difficult to do, especially on large-scale networks.

Acknowledging the difficulties in obtaining exact choice sets of realistic routes for PSL to be suitable, a pragmatic approach that has been proposed is to utilise a weighted path size contribution technique along with choice set generation, to attempt to reduce the impact any present unrealistic routes may have on the choice probabilities of realistic routes. The idea is that instead of all routes having equal path size contributions to the path size terms of other routes (i.e. PSL), the contributions are weighted so that the probabilities of realistic routes are only minorly adjusted from link sharing with generated unrealistic routes. This is a promising approach as it relaxes the importance of generating exact choice sets of realistic routes.

The Generalised PSL (GPSL) model proposes that the path size contribution factor is based upon ratios of travel cost between routes, and hence routes with large travel costs have a diminished impact upon the correction terms of routes with small travel costs. However, as discussed and demonstrated on example networks in Chapter 2 (the first journal manuscript), GPSL has some theoretical and practical issues. Firstly, GPSL is not internally consistent in how it defines routes as unrealistic: the path size terms consider the travel cost of the route, while the probability relation considers disutility *including* the correction term. Secondly, due to the way in which the contribution factor is formulated – as travel cost ratios – an additional scaling parameter, λ, is required to scale these contributions, which makes parameter estimation more difficult, while there are questions over its behavioural interpretation.

To address these issues, Chapter 2 then formulated two new PSL models. Firstly, addressing the second issue, the GPSL contribution factors were re-formulated to resemble the travel cost component in the probability relation, thus proposing an alternative GPSL (GPSL$'$) model. This means that one can equate the path size scaling parameter (λ) with the Logit parameter (θ), formulating the GPSL$'_{(\lambda=\theta)}$ model, thereby improving internal consistency, reducing the number of parameters for estimation, and removing the concerns over behavioural interpretation of the path size scaling parameter.

However, although the GPSL$'_{(\lambda=\theta)}$ model provides improved internal consistency over GPSL, the path size contribution factors do not consider route distinctiveness. Addressing this, the Adaptive Path Size Logit (APSL) model was then formulated, where the contribution factors consider ratios of route choice probability between routes, thus ensuring that routes defined as unrealistic by the path size terms, are exactly those with very low choice probabilities. APSL is hence internally consistent in how routes are defined as (un)realistic. Also, by defining the path size contribution factor as the ratio of choice probabilities, the scaling of the path size contributions is controlled implicitly through the scaling of the route choice probabilities (i.e. with the Logit parameter and path size parameter), and hence there is no additional path size contribution parameter for estimation.

The APSL route choice probability relation is an implicit function involving the choice probabilities, and solutions to the model are solutions to the fixed-point problem. Formulation of the APSL model was complicated by the desire to establish existence and uniqueness of solutions. The straightforward, desired APSL formulation was not in the correct format for standard proofs of existence and uniqueness of fixed-point solutions to apply. The proposed APSL formulation modifies the desired model so that the proofs apply.

Critically though, the desired APSL formulation can be approximated to arbitrary precision with the 'perturbation parameter' τ, i.e. the proposed APSL definition is equivalent to the desired APSL definition in the limit as $\tau \to 0$. It is therefore advised that in application of the APSL model, τ is set as a very small number, e.g. as small as computational precision will allow.

Solutions to the APSL fixed-point problem are proven to exist, and it is proven that values of b exist such that APSL solutions are unique for β (the path size parameter) in the range $0 \leq \beta \leq b$. Though there are cases where solutions are unique for all $\beta \geq 0$, in most cases there is a maximum value for b (b_{max}). β in the range $0 \leq \beta \leq b_{max}$ is however only a sufficient condition for unique APSL solutions, β_{max} is the true maximum value where solutions are unique for β in the range $0 \leq \beta \leq \beta_{max}$, and a method is proposed for estimating β_{max}. These sufficient and actual uniqueness conditions are specific to each setting of the travel costs and Logit scaling parameter. However, in the writer's experience and experiments in this thesis, the actual uniqueness conditions provide enough scope for fitting to behaviour, where typical β_{max} values range between 0.9 and 1.1. No difficulties were experienced in estimating APSL on the real-life large-scale network (discussed below), and a maximum likelihood estimate of $\hat{\beta} = 0.84$ was obtained, where it was verified that this was within the uniqueness range.

Reflection. It remains uncertain under which conditions solutions to the straightforward, desired APSL formulation do not exist, and it has not been ruled out that a fixed-point theorem exists to prove existence. A considerable amount of time was spent formulating the modified version and exploring conditions for the uniqueness of solutions. It was a real struggle trying to work out why the mathematical uniqueness conditions (identified from max Jacobians) did not match the conditions found numerically, until it was realised that the conditions were only sufficient conditions.

To show that the parameters of the APSL model can be estimated, a Maximum Likelihood Estimation (MLE) procedure was proposed for estimating APSL with tracked route observation data. This procedure was then first investigated in a simulation study on the Sioux Falls network where it was shown that it is generally possible to reproduce assumed true parameters. The APSL model was then estimated using real tracked route GPS data on a large-scale network.

Estimation results show that APSL outperforms MNL and PSL in goodness-of-fit to the data, both showing the value in and highlighting the efficacy of APSL in capturing route correlations and dealing with unrealistic routes. Moreover, APSL outperforms the GPSL$'_{(\lambda=\theta)}$ model, suggesting that there is value in having an internally consistency model / value in including a measure of distinctiveness within the path size contribution factors. The GPSL model outperforms all models due to the greater flexibility the additional path size contribution scaling parameter λ provides. However, as typically found in estimations of GPSL, the estimate for λ is extremely large ($\hat{\lambda} = 91.95$), which is investigated.

After conducting some analysis, it was postulated that the reason GPSL is able to provide better fit to the data is that the λ parameter allows GPSL to improve the choice probabilities of high costing, distinct route observations one might consider as being outliers / route choice decisions made according to unobserved attributes, without compromising the fit for the low costing observations, though this is not done by design.

Reflection. Before the estimation experiments were conducted there were question marks over the computational feasibility of estimating APSL, especially for the real-life large-scale network. After some initial experiments in Python on a personal laptop, it became clear that utilising parallel processing was going to be necessary, and perhaps a better computer too. Initially, I learnt how to operate the High-Performance Computing system at University of Leeds. However, the real-life observation data could not be shared with me for ethical reasons, and the Danish Technical University (DTU) were kind enough to offer use of their super-computer, accessed via VPN, where I could access and use the data. After a significant amount of time and many difficulties working out how to parallel process in Python, it became possible to split APSL probability computation for different OD movements across multiple cores, improving computation times considerably. There were also concerns of whether APSL solution non-uniqueness would be an issue in estimation. The general approach adopted was to not allow for values of β greater than around 0.9-0.95, a 'safe range' determined from experience, and as non-uniqueness would typically become an issue towards $\beta = 1$. With this, non-uniqueness was never an issue, and the estimate for β in the real-life estimation was within the uniqueness range. It was also learned the hard way how a code error can ruin months of work. For several months, slightly strange results were reported from the estimation experiments, until it was realised that there was an index error and all the experiments had to be done again.

1.1.2 Future Research

Future research should explore estimating the APSL model with more complex route utility functions, than just considering travel time and length, to explore how APSL performs when there are fewer unobserved attributes / a better representation of route choices. Moreover, further research should also explore formulating and estimating APSL with different utilities/parameters for different user classes / vehicle types. One could also investigate estimating the models for different choice sets to assess their robustness.

The APSL model requires a fixed-point algorithm to compute solutions. The paper assesses the computational performance of the Fixed-Point Iteration Method (FPIM) for calculating choice probabilities and estimating the parameters of the APSL model, where accuracy is compared with computation time. Results indicate that accurate choice probability solutions and parameter estimates can be obtained from feasible computation times. The FPIM, however, is the simplest fixed-point algorithm with the slowest convergence, and many fixed-point algorithms have been proposed to accelerate convergence. Further research could explore solving APSL utilising different fixed-point algorithms, such as Steffenson's Method or Newton Raphson's Method.

Although these algorithms are designed to reduce the number of iterations required for fixed-point convergence, performing each iteration requires computing a more complicated function. Performance of these algorithms in terms of total computation time is therefore a trade-off between the number of iterations saved and the computation times for each of the iterations. As shown with the FPIM, the number of iterations required for APSL fixed-point convergence increases exponentially as β increases. The performances of the more complex fixed-point algorithms (compared to the FPIM) are therefore likely to improve for larger values of β, where more iterations will be saved. As the scale of network / choice set sizes increase, however, the greater the computational burden of the more complex iteration functions, and after conducting some early experiments on the Sioux Falls networks, it was found that Steffensen's Method and Newton Raphson's Method did not improve total computation times compare to the FPIM.

Scope for further research also includes modifying APSL, or integrating adaptive path size concepts within a different RUM, to also address the scaling problem. APSL, as it is currently formulated, does not distinguish between different lengths of trip. This can lead to imprecisions since travellers usually have more accurate perceptions of the route characteristics for a short trip than they do for very long trips, where a greater amount of uncertainty comes with knowing for example the exact travel time / distance. The thorough way of addressing this is to individually estimate a Logit scaling parameter for each OD movement, however this is potentially impractical and could lead to identification issues as the number of parameters to estimate may be huge. Alternatively, one could instead, for each OD movement, adjust the Logit scaling parameter according to the OD-specific scaling factor as proposed by Gliebe et al (1999). An interesting approach could be to explore altering the path size correction factors within the Path Size Weibit and Path Size Hybrid models to be adaptive path size, since both address the scaling problem.

1.2 Chapter 3 – Adaptive Path Size Logit Stochastic User Equilibrium

1.2.1 Review of Findings

Chapter 3 explored the integration of APSL within a Stochastic User Equilibrium (SUE) model. On congested road networks, the travel times for the available routes are dependent upon the vehicle flow along them (where travel time increases with flow), and there is thus a feedback effect: drivers make decisions on which routes to take according to the travel times they perceive for the routes, which in turn depend upon the route choice decisions and the consequent route and link flows. SUE is a well-known approach for modelling this feedback effect, where an SUE route flow solution and the consequent route travel costs are such that, for each OD movement, the proportion of the flow on each route is equal to the probability that that route has a perceived utility greater than or equal to the perceived utility of all alternative routes. The distribution of the route flows is thus dependent on the underlying route choice model, which in this case is APSL.

Reflection. APSL comes at a price of needing to solve a fixed-point problem even to compute route choice probabilities at given travel cost/utility levels. Thus, before the research was conducted, there was a question of whether it would be computationally feasible to implement such a method within an SUE framework, since it apparently needs to embed a fixed-point problem (for calculating choice probabilities) within another fixed-point problem (for equilibrating flows). Thankfully, harnessing the useful relationship between route choice probability and flow proportion in the context of SUE opened up a range of possibilities

for solving APSL SUE, and the potentially onerous requirement of solving fixed-point problems to compute APSL choice probabilities could be circumvented/controlled when solving SUE (discussed below).

APSL SUE can be defined in two different ways: Definition 1 is consistent with the APSL choice model for every setting of the route flows, and Definition 2 (APSL′ SUE) is just consistent at equilibrium, where the APSL′ path size contribution factors are instead presented as ratios of route flow. Definition 1 involves solving choice probability fixed-point problems for each given setting of the route flows, while Definition 2 is closed-form.

Typical SUE formulations of PSL models utilise an uncongested variable such as length or free-flow travel time for the link-route prominence features within the path size terms, so that they are not flow-dependent. The advantages of this are that: a) solution existence and uniqueness can be proven according to standard proofs; b) an equivalent MP formulation can easily be derived; and, c) the path size terms are constants and hence only need to be computed once at the initial rather than at every iteration of an SUE algorithm. However, for APSL/APSL′, these advantages are not applicable, since the APSL/APSL′ path size terms are flow-dependent regardless of whether or not flow-independent variables are used for the link-route prominence features. Moreover, the key feature of the APSL model is internal consistency, and utilising flow-independent costs within the path size terms would violate this claim, since they would be inconsistent with the flow-dependent travel costs in other components. Therefore, for full internal consistency, the definitions of APSL & APSL′ SUE utilise the same flow-dependent, generalised costs in all components: route costs as well as path size terms.

APSL′ SUE solutions are proven to exist, and thus by proving the equivalence of APSL SUE and APSL′ SUE, APSL SUE solutions are also proven to exist. Uniqueness of solutions, however, cannot be guaranteed by standard proofs, due to the flow-dependent path size terms, though that is not to say solutions cannot be unique, which is explore numerically. Experiments on the Sioux Falls and Winnipeg networks suggest that uniqueness conditions exist. These conditions are analogous to those for the uniqueness of APSL probability solutions, and APSL SUE solutions appear to be unique when APSL solutions are unique.

Reflection. Like for estimation of APSL, there were concerns of whether non-uniqueness of APSL solutions would be an issue for a) solving APSL SUE and b) non-uniqueness of APSL SUE solutions. The conditions for unique APSL solutions depend upon the link/route travel costs, which in the context of SUE can vary significantly depending on the flows, and it is not feasible to determine the uniqueness conditions for all possible settings of the flows / costs. However, using again the general rule of restricting β to no greater than 0.9-0.95 (a safe range), the non-uniqueness of APSL probability solutions was not an issue, and as the experiments found, APSL SUE solutions were unique when APSL probability solutions were unique (in those cases).

To establish APSL SUE as a worthwhile approach, APSL SUE was compared to an array of competitor correlation-based SUE models. Like as discussed for PSL models above, typical SUE formulations for correlation-based models utilise uncongested costs for the functional forms in the correlation components. Addressing this, internally consistent SUE formulations for the competitor correlation-based models to APSL were formulated, namely: PSL, Generalised PSL (GPSL), C-Logit (CL), Cross-Nested Logit (CNL), Generalised Nested Logit (GNL), and Paired Combinatorial Logit (PCL). Only an internally consistent formulation for CL had previously been explored in the literature.

Numerical experiments were conducted on the well-known Sioux Falls and Winnipeg networks to assess computational performance, choice set robustness, and internal consistency. APSL SUE outperformed GPSL SUE in terms of internal consistency (when dealing with unrealistic routes in the adopted choice sets), generally outperformed PSL, CL, CNL, & GNL SUE in terms of choice set robustness, and outperformed CL, CNL, GNL, & PCL SUE in terms of computational performance (considerably on the larger-scale Winnipeg network).

A standard Flow-Averaging Algorithm (FAA) was used to solve the SUE models. The simplicity of the FAA is attractive for solving APSL SUE, where computing accurate choice probabilities is not straightforward/quick. The Method of Successive Weighted Averages (MSWA) step-size scheme was employed, however numerous other averaging step-size schemes could be adopted. Other inexact step-size schemes are applicable, however these are potentially complex / not computationally feasible for APSL SUE. For example, it may require gradient information which would involve differentiating the fixed-point APSL choice probabilities, which is not straightforward. Or, it may require accurately computing the APSL choice

probabilities which has the potential to be very computationally burdensome. Optimal step-size approaches are not applicable since there are no equivalent MP formulations.

Since computing APSL probabilities involves solving fixed-point problems, and the APSL′ probability relation is closed-form, it was anticipated that APSL SUE and APSL′ SUE would have very different computational performances. Experiments on the Sioux Falls and Winnipeg networks found that, while the number of iterations required for APSL SUE convergence tended to be similar to that required for PSL & GPSL SUE convergence under identical configurations of the flow-averaging algorithm, the requirement of solving APSL choice probability fixed-point problems at each algorithm iteration resulted in significantly greater total computation times. On-the-other-hand, while the computational burden involved in computing the APSL′ choice probabilities during each iteration of the flow-averaging algorithm solving APSL′ SUE was no more than that for PSL & GPSL, APSL′ SUE convergence was comparatively very slow, and thus total computational times were also much longer.

In this thesis, the accuracy of the APSL probabilities is controlled exogenously by the FPIM probability convergence parameter ξ, where accuracy increases as ξ increases. Thus, in general, increasing ξ increased the accuracy of the APSL SUE solution, but this resulted in longer computation times, as more FPIM iterations were required for probability convergence.

However, as explored, the useful relationship between route flow proportions and choice probabilities in SUE context (where these are equal at equilibrium) allows for a considerable flexibility in solving APSL SUE, where one can trade-off the accuracy of APSL probabilities (and thus computation times of each iteration) with rate of SUE convergence. By utilising as termed 'follow-on' initial conditions for the FPIM – where the initial conditions for solving the APSL probabilities at iteration n of the flow-averaging algorithm were set as the route flow proportions from iteration $n-1$ – the same APSL SUE solution was obtained regardless of ξ. For low ξ, solving APSL SUE with follow-on initial conditions simulated solving APSL' SUE, where there was just a single FPIM iteration conducted (and hence the APSL probabilities were very inaccurate) at every flow-averaging algorithm iteration. Increasing ξ increased the accuracy of the APSL probabilities, which improved the rate of SUE convergence: more FPIM iterations were required for APSL probability convergence, but fewer flow-averaging algorithm iterations were required for SUE convergence.

Thus, solving APSL SUE with low ξ and follow-on initial conditions resulted in long total computation times due to the slow SUE convergence rate, while larger values of ξ resulted in comparatively quick SUE convergence rates but lengthy computation times for each of the algorithm iterations, thus also resulting in long total computation times. There was therefore an 'optimal' intermediate value of ξ for solving APSL SUE with follow-on initial FPIM conditions, whereby a suitable SUE convergence rate met suitable computation times for each iteration.

Another technique that improved APSL SUE computation times was to utilise follow-on initial FPIM conditions and stipulate a set number of FPIM iterations to perform at each iteration of the flow-averaging algorithm. Conducting just two FPIM iterations (instead of one) significantly reduced the number of iterations required for SUE convergence, and thus total computation times.

Best computation times for solving APSL SUE were found when utilising a combination of a maximum number of FPIM iterations to perform and a maximum level of APSL probability convergence (controlled with ξ) at each SUE iteration. This saved computation times in latter SUE iterations where the stipulated amount of FPIM iterations would unnecessarily overly-converge the APSL probabilities.

Reflection. Due to the scale of the Winnipeg network, some careful thought was required to pre-process the network data and code up the SUE solution algorithm to optimise computational performance. In the pre-processing, for example, link-route incidence matrices were generated and stored in Python dictionaries for quick access, where the matrices were trimmed to remove redundant links for that OD movement. And, for the solution algorithm, a way to compute path size terms using matrix manipulation was constructed, which improved computation times considerably. Due to the overhead involved in parallel processing in Python, parallel processing only improved computation times when accurately computing the fixed-point APSL probabilities. The best APSL SUE solution times were found when not accurately computing the APSL probabilities and thus for consistency across the models, parallel processing was not adopted. The work was also set back by another error: all experiments for the Winnipeg network had to be redone because the zone nodes were included as through nodes in the network, whereas they should be setup as connector nodes.

In conclusion, the proposed APSL SUE model succeeds in addressing all four of the key challenging aspects of route choice modelling in a theoretically consistent, robust, and mathematically well-defined way.

As discussed/demonstrated, APSL SUE offers improved internal consistency and choice set robustness compared to competitor models. APSL SUE solutions are proven to exist, and though uniqueness is not guaranteed, numerical experiments suggest that uniqueness conditions exist. Moreover, as shown, the model is estimatable from revealed choice data and can be solved in computationally feasible times on real-life large-scale networks.

1.2.2 Future Research

The 'optimal' values for the methods described above for solving APSL SUE are particular to the network, model, and algorithm specifications, e.g. model parameters, adopted step-size scheme, choice set sizes. However, by fixing the optimised values for a given specification, and then varying the specifications, it was shown that the method was robust in its effectiveness compared to solving APSL SUE in a standard way (i.e. where the APSL fixed-point probabilities are accurately solved with non-follow-on initial conditions). Future research could explore an intelligent, adaptive process whereby the optimal values of ξ and the maximum number of FPIM iterations to perform at each SUE algorithm iteration are learnt / worked out as the algorithm progresses.

Future research could also explore utilising a different fixed-point algorithm (to the FPIM) for computing the APSL probabilities within the SUE algorithm, or perhaps a combination of fixed-point algorithms could be used, e.g. Newton Raphson's Method for early iterations, Steffenson's Method for middle iterations, and the FPIM for latter iterations, as the initial conditions for the probabilities become closer to the solution through the use of follow-on initial conditions.

Future research could also explore utilising different averaging step-size schemes, such as the self-regulated averaging method Liu et al (2009), which has been applied with success in various SUE models (e.g. Yang et al, 2013; Xu & Chen, 2013; Kitthamkesorn & Chen, 2013, 2014; Chen et al, 2014; Yao et al, 2014). It has not yet been explored whether similar techniques to those described above for solving APSL SUE – where the APSL probabilities need not be computed accurately – are applicable for some inexact step-size schemes, such as the self-adaptive method (e.g. Chen et al, 2012, 2013; Xu et al, 2012; Zhou et al, 2012). Furthermore, future research could explore alternative algorithms, such as the New Self-Adaptive Gradient Projection algorithm (Zhou & Chen, 2006), which has been applied with success to solve SUE for the C-Logit model with flow-dependent correction terms.

Future research could also investigate under what conditions APSL SUE solutions are not unique when APSL solutions are universally unique, and/or identify uniqueness conditions and a proof.

2. Modelling Approach 2 – A Bounded Path Size Route Choice Model

2.1 Chapter 4 – Bounded Path Size Models

2.1.1 Review of Findings

Although the weighted path contribution technique is a promising approach for addressing the deficiency of the PSL model, in its sensitivity to unrealistic routes in the adopted choice sets, it does not solve the issue entirely, since the path size contributions of routes defined as unrealistic are only reduced instead of eliminated. Moreover, as well as non-zero path size contributions, unrealistic routes also receive non-zero choice probabilities. Thus, while under the GPSL, GPSL′, and APSL models each unrealistic route may only have a small path size contribution / choice probability, the total sum of these unrealistic route contributions / probabilities may be significant, consequently impacting the accuracy of results. This problem becomes greater as the scale of network increases and a greater amount of uncertainty comes with choice set generation, where, typically, choice sets are generated as large as the computational resources are deemed to allow, in order to minimise the possibility of excluding what would later turn out to be a plausible route.

The second modelling approach in this thesis was thus to take the weighted path size contribution technique one step further by exploring how one might eliminate unrealistic route path size contributions entirely. Moreover, in order to fully solve the issue, it was explored how one could also assign zero choice probabilities to unrealistic routes, as well as zero path size contributions.

An approach that was deemed promising to investigate was the integration of PSL model concepts with the Bounded Choice Model (BCM). The BCM proposes that a bound is applied to the difference in utility / travel cost between each route and the highest utility / lowest costing route, so that routes with utilities/costs less/greater than the bound are considered unrealistic and assigned zero choice probabilities. Furthermore, the

probability each route is chosen relates to the odds associated with choosing each route versus the highest utility / lowest costing route, and the BCM thus has a consistent criterion for determining restricted choice sets of realistic routes and route choice probability. The BCM does not account for route correlations, however, and hence the aim was to develop a Bounded Path Size (BPS) route choice model that harnesses the contrasting strengths of the two approaches.

In Chapter 4, a natural form for a BPS model was derived whereby path size choice model utilities (which include path size corrections) were inserted into the BCM formula. This, however, led to behavioural inconsistencies and/or undesirable mathematical properties, which were demonstrated by a series of examples. By utilising path size terms where all contributions were non-zero, a mathematically well-defined BPS model could be derived from the natural BPS model form, but this would mean that the contributions of unrealistic routes were not eliminated, as desired. On-the-other-hand, allocating zero path size contributions to routes defined as unrealistic resulted in occurrences of $\frac{0}{0}$ and $\ln(0)$, and the path size term functions were thus not guaranteed to be defined. Moreover, these $\frac{0}{0}$ and $\ln(0)$ issues led to problems with non-uniqueness of solutions and discontinuity of the choice probability function. Although these issues were derived from specific path size term options explored, the aim was to demonstrate that the natural BPS model is actually deeply problematic and there are no behaviourally and practically desirable formulations.

Reflection. The best part of a year was spent trying to get the natural BPS form to work, by thinking of ways to work round the $\frac{0}{0}$ and $\ln(0)$ issues. Numerous different approaches were proposed to deal with non-uniqueness, i.e. different rules/methods for identifying the active choice set, for example decreasing from a high bound value and systematically removing routes. No approach however could achieve a continuous probability function. It was an enjoyable yet frustrating experience experimenting.

From the investigation into issues with the natural BPS model form, five desirable properties were consequently established for a mathematically well-defined BPS model that utilises a consistent criterion for assigning zero choice probabilities to unrealistic routes while eliminating their path size contributions. Solving these challenges, an alternative form for a BPS model was derived. Here, path size correction factors are added directly to the BCM probability relation rather than the route utilities to adjust the probabilities to capture route correlations. Like the BCM, routes are defined as unrealistic if they have a travel cost greater than a cost bound. This means that for a setting of the costs, the realistic routes are identified as those with costs below the bound, and correlations are only considered between these routes, as only and exactly these will have non-zero choice probabilities, and unrealistic routes with costs greater than the bound do not have path size term values / path size contributions.

Deriving a BPS model from the proposed form involves defining the path size contribution factors for the realistic/used routes. Care must be taken, however, to ensure that the chosen factors lead to a continuous choice probability function (a desired property): as the cost of a route approaches the bound (from below) its path size contribution must approach zero and be eliminated exactly at the bound. Two BPS models were thus proposed: the Bounded Bounded Path Size (BBPS) model and the Bounded Adaptive Path Size (BAPS) model. The BBPS model proposes that the contribution factors consider ratios of the odds that routes are within the bound, and the BAPS model proposes ratios of route choice probability (like APSL). Although the BBPS model is consistent in its definitions of which routes are considered (un)realistic, it does not have a consistent criterion for determining route choice probabilities and path size contributions, since the contribution factors do not consider route distinctiveness. The BAPS model has a consistent criterion for assigning zero choice probabilities to unrealistic routes, eliminating their path size contributions, and determining route choice probabilities and path size contributions, since the contributions are the probabilities. The BAPS model is thus fully internally consistent. The limit models for the BBPS & BAPS models are the GPSL′ and APSL models, respectively, where the bound is large enough so that all routes have non-zero choice probabilities, i.e. BBPS $\rightarrow$ GPSL′ and BAPS $\rightarrow$ APSL in the limit as the bound $(\varphi) \rightarrow \infty$.

The attraction of the BBPS model is that it has a closed-form probability relation, and therefore probability solutions are automatically guaranteed to exist and be unique and computing solutions is quick and simple, while the BBPS model also has a continuous choice probability function.

The BAPS model, however, just like APSL, is not closed-form since the path size contribution factors are a function of the choice probabilities, and hence the probability relation is an implicit function, naturally expressed as a fixed-point problem. As was the case for APSL, formulation of the BAPS model was similarly complicated by the desire to establish existence and uniqueness of solutions. Although it also remains

uncertain under which conditions solutions do not exist / there are not uniqueness conditions, the straightforward, desired BAPS model formulation was not in the correct format for standard proofs of existence and uniqueness of fixed-point solutions to apply. The proposed BAPS model formulation, in an analogous way to APSL, modifies the desired model so that the proofs apply, and the desired BAPS model formulation can be approximated to arbitrary precision with the 'perturbation parameter' τ, i.e. the proposed BAPS model definition is equivalent to the desired BAPS model definition in the limit as $\tau \to 0$.

Unlike for APSL, however, the proposed formulation for the BAPS model does not have a continuous choice probability function, since, unlike APSL, routes can have zero choice probabilities, and consequently due to the modification with the perturbation parameter, routes cannot have probabilities between 0 and τ. Nonetheless, although this is undesirable theoretically, it is not an issue in practice, since continuity can be approximated to arbitrary precision by the setting of τ as a very small value, e.g. as small as computational precision will allow.

By adapting the proofs of existence and uniqueness for APSL solutions, solutions to the BAPS model fixed-point problem were proven to exist, and it was proven that values of b exist such that BAPS model solutions are unique for β (the path size parameter) in the range $0 \leq \beta \leq b$, where b_{max} is the maximum value of b. Just like APSL, β in the range $0 \leq \beta \leq b_{max}$ is only a sufficient condition for unique BAPS model solutions, β_{max} is the true maximum value where solutions are unique for β in the range $0 \leq \beta \leq \beta_{max}$, and a method is proposed for estimating β_{max}. These sufficient and actual uniqueness conditions are specific to each setting of the travel costs, Logit scaling parameter, and bound parameter. However, in the experience of the author and experiments in this thesis, the actual uniqueness conditions provide enough scope for fitting to behaviour, where typical β_{max} values range between 0.9 and 1.1. No difficulties were experienced in estimating the BAPS model on the real-life large-scale network (discussed below), and obtained maximum likelihood estimates of $\hat{\beta} = 0.844$ and $\hat{\beta} = 0.838$, where it was verified that the former estimate was within the uniqueness range.

To show that the parameters of the BBPS & BAPS models can be estimated, an MLE procedure was proposed, similar to that for APSL, for estimating the BBPS & BAPS models with tracked route observation data. Application to the Sioux Falls network showed it is generally possible to reproduce assumed true parameters. The BBPS & BAPS models were then estimated using real tracked route GPS data on a large-scale network. Results found that the $\text{BBPS}_{(\lambda=\theta)}$ and BAPS models outperformed their limit models $\text{GPSL}'_{(\lambda=\theta)}$ and APSL, respectively, suggesting that there is value in fully dealing with unrealistic routes by eliminating their path size contributions / assigning them zero choice probabilities, rather than just reducing contributions / assigning small probabilities. Moreover, just as APSL outperformed the $\text{GPSL}'_{(\lambda=\theta)}$ model, the BAPS model outperformed the $\text{BBPS}_{(\lambda=\theta)}$ model, further suggesting that there is value in having a fully internally consistency model / value in including a measure of distinctiveness within the path size contribution factors.

Reflection. For the BPS model MLE procedure, a pragmatic approach was proposed to avoid issues with $\ln(0)$ when an observed route has a cost above the bound (Likelihood equal to zero). The approach was to set a large and negative Log-Likelihood value when observed routes have a zero probability, the aim simply just to tell the optimisation algorithm to return to searching for maximum likelihood estimates within the parameter space the solution was known to lie. There was some uncertainty in how effective the approach would work, solutions might somehow get trapped in the large negative Log-Likelihood space, but the approach worked without any real problems.

In Chapter 2, it was postulated that the GPSL/GPSL′ models provided the best fit to the data not by design. As investigated, the very large estimate for the additional path size scaling parameter, λ, seemed to allow GPSL to improve the choice probabilities of high costing, distinct route observations one might consider as being outliers / route choice decisions made according to unobserved attributes, without compromising the fit for the low costing observations.

An interesting result found when estimating the BBPS model in Chapter 4 was that the parameter estimates approximated the GPSL′ model, where the estimate for the bound parameter, $\hat{\varphi}$, was very large approximating $\hat{\varphi} \to \infty$. The GPSL(/GPSL′) model was constructed with the aim of reducing the path size contributions of unrealistic, costly routes, so that the path size correction terms and thus the choice probabilities of realistic routes are not undesirably adjusted for overlapping with unrealistic routes. In other words, so that the path size terms of realistic routes capture the correlation between the realistic alternatives only. So, if these models are aiming to reduce the contributions of unrealistic routes to the path size terms of

realistic routes, then eliminating the contributions completely should improve performance. However, when the GPSL′ model was given the opportunity to eliminate contributions, i.e. with the BBPS model, the option was not taken, and the best fit came from an unbounding φ and a large λ value.

This indicates that the GPSL and GPSL′ models were able to in this case provide better fits to real data by capturing something other than the correlation between the realistic routes within the path size terms. This could potentially be an important finding, since many studies either estimate GPSL and find best fit with a very large λ value (e.g. $\hat{\lambda} = \infty$ Ramming, (2002)) or estimate GPSL with a fixed large λ value (e.g. $\lambda = 20$ Hoogendoorn-Lanser et al, 2005)). Studies have speculated as to why large λ values provide the best fits, however no study (to the best knowledge of the author) has investigated this in detail. The typical interpretation is that when comparing routes and the overlap between them, drivers make a binary decision according to which route has the greater cost, and perceive the route with the lower cost as being distinct. This reasoning, however, is questionable, and it seems unlikely that driver psychology would be as such.

2.1.2 Future Research

The experiments in this thesis provide new insights into why GPSL/GPSL′ are best fitted with large λ values, and why GPSL/GPSL′ consequently outperform other PSL models. Further research should explore this in more detail. For example, how the GPSL models perform with more complex utility functions and hence there are fewer unobserved attributes.

In reality, rather than a universal bound for all OD movements, there are likely to be OD-specific bounds and even traveller-specific bounds (as well as other-specific bounds) that travellers apply upon travel cost to consider routes unrealistic, and future research could investigate estimating such non-universal bounds. To estimate such bounds, however, one requires numerous observations from the same OD movement / traveller. Moreover, MLE exponentiates in difficulty as the number of parameters increases. This makes estimating a universal bound attractive. However, this can limit how effective the bounded models are at improving the fit of their limit models. The estimated universal bound will always at least be the supremum of the route observation cost deviations meaning that outlier observations will significantly limit the performance of the bounded models. As shown in Chapter 4, when there are route observations with large cost deviations and only a very small percentage of the generated routes have costs above the estimated bound, the bounded models only marginally improved upon the fit of their limit models. When the most relatively costly observations were removed, however, improved fit increased significantly. Theoretically, for any given estimated bound, the choice sets should include all routes with cost deviations less than this bound, as these routes are considered realistic, under the definition of the model. Future research could investigate how the re-generation of choice sets effects re-estimation results, and further explore the effects of and how to deal with outlier observations, potentially through some systematic procedure.

With the bounded models, a route is only defined unrealistic if it has a travel cost greater than the cost bound. However, in reality there may be routes that have travel costs below the bound but would also be considered unrealistic. For example, routes that repeatedly use on-off-ramps on motorways, which may have total travel costs below the bound but large local detour travel costs. Clearly, such alternatives with long local detours would not be considered in the mental map that travellers build in their mind when making their route choice decisions, and hence these routes should also be excluded from the choice sets. This could be done within the choice set pre-generation before implementation, however future research could investigate how to do this in an implicit, consistent way, for example by applying some consistent bound upon local detour cost, like as that for total travel cost. Moreover, one could investigate other forms of route choice bounds, for example for cyclist route choice, riders may have a bound upon the steepness of a route.

As discussed for APSL, scope for further research for the BPS models also includes also addressing the scaling problem. This could again be through individually estimating a Logit scaling parameter for each OD movement, or adjusting the Logit scaling parameters according to the OD-specific scaling factor as proposed by Gliebe et al (1999). A more interesting approach would be to first investigate formulating a bounded choice model with Weibull distributed random error terms, then explore integrating appropriate path size correction factors, as done for the BCM in Chapter 4. Following on from this, it would also be interesting to explore formulating bounded choice models with other distributions for the random error terms, for example a Normal or Gamma distribution, or with GEV structure models e.g. Cross-Nested Logit.

2.2 Chapter 5 – Bounded Path Size Stochastic User Equilibrium

2.2.1 Review of Findings

Chapter 5 explored the integration of BPS models within a SUE model. SUE conditions are established for the BBPS & BAPS models where – for internal consistency – the link-route prominence features within the used route path size terms are based upon flow-dependent congested travel cost. A BPS SUE route flow solution and the consequent route travel costs are such that unused routes with zero flows have costs greater than or equal to the flow-dependent cost bound, while used routes with non-zero flows have costs below the bound. The restricted choice sets of realistic routes are thus equilibrated along with the flows.

The BBPS SUE model has a closed-form underlying route choice model, while the BAPS SUE model has an underlying route choice model formulated as a fixed-point problem. However, since the path size contribution factors are based upon ratios of choice probability, (just like APSL), the potentially onerous requirement of solving fixed-point problems to compute the BAPS model choice probabilities can be circumvented, since at SUE the route flow proportions and choice probabilities equate. BAPS SUE can thus also be defined in two different ways: Definition 1 is consistent with the BAPS choice model for every setting of the route flows, and Definition 2 (BAPS′ SUE) is just consistent at equilibrium, where the BAPS′ model path size contribution factors are instead presented as ratios of route flow. Definition 1 involves solving choice probability fixed-point problems for each given setting of the route flows, while Definition 2 is closed-form.

BBPS SUE solutions are proven to exist, however existence of BAPS/BAPS′ SUE solutions could not be proven, since the underlying choice models do not have continuous probability functions (as routes cannot have probabilities between 0 and τ). Although this is theoretically undesirable, solution existence is not a problem in practice since continuity can be approximated to arbitrary precision with small values of τ. The modification of the desired BAPS model probability relation with the adjustment functions and perturbation parameter τ was required to establish existence and uniqueness of the fixed-point probability solutions. However, this is not necessary for the BAPS′ model since it is closed-form. BAPS′ SUE can thus be simplified and re-formulated (denoted BAPS′′) without the modifications so that it does have a continuous probability function. Nonetheless, solution existence could still not be proven since the set of feasible flows for the BAPS′′ model – which must be modified to avoid occurrences of $\frac{0}{0}$ within the path size terms – is not a convex set, a requirement of standard proofs.

Due to the flow-dependent path size terms, uniqueness of solutions for the BBPS & BAPS SUE models could not be guaranteed by standard proofs. That is not to say that solutions cannot be unique, however, and this is explored numerically for the BAPS SUE model. Experiments on a small-scale network and the Sioux Falls network suggest that uniqueness conditions exist. Like for APSL, these conditions are analogous to those for the uniqueness of probability solutions, and BAPS SUE solutions appear to be unique when BAPS model solutions are unique.

A generic algorithm is proposed for solving BPS SUE models. The algorithm is an adaptation of the generic algorithm proposed by Watling et al (2018) for the Bounded SUE (BSUE) model, i.e. SUE with the BCM. To equilibrate the choice sets of realistic routes, the BSUE algorithm generates realistic routes from the network as the algorithm progresses. With the current techniques available for generating these routes, there are questions over the suitability of the approach for large-scale networks. For the proposed BPS SUE algorithm, a more practical approach is taken, by pre-generating approximated universal choice sets. From these routes, the restricted choice sets of realistic routes are equilibrated. The algorithm can however be easily adapted so that routes are generated as the algorithm progresses, just like the BSUE algorithm.

The natural BPS model form originally explored in Chapter 4 bounds routes according their utility (i.e. combination of cost and path size correction), rather than just cost. This approach was found to be challenging, and instead, to circumvent the issues, an alternative BPS model form was derived, where routes are bounded according to their travel cost, but path size correction factors are included in the probability relations (rather than route utilities) to adjust for route correlations. The benefit of this is that the BCM and BPS model both have the same definition for unrealistic routes: those with travel costs above the bound, and the algorithm and gap measures proposed for solving BSUE are applicable for solving BPS SUE with only a few minor adjustments.

The BPS SUE algorithm can be seen as an extension of the flow-averaging algorithm used in Chapter 3 for solving the internally consistent SUE formulations of the correlation-based models, where *column*

generation, *flow allocation for new routes*, and *bound condition* phases are added for the equilibration of the used route choice sets. Numerous averaging step-size schemes can be employed, where the simplicity of the averaging method is also attractive for solving BAPS SUE, where computing accurate choice probabilities is not straightforward/quick. Other inexact step-size schemes are applicable, however, like for solving APSL SUE, these are potentially complex / not computationally feasible for BAPS SUE. The Method of Successive Weighted Averages step-size scheme was adopted in Chapter 3 for the flow-averaging algorithm where it proved successful, moreover Watling et al (2018) adopt this scheme to solve BSUE, and thus this approach was also adopted for the BPS SUE numerical experiments.

Using similar SUE convergence criteria for the flow-averaging and BPS SUE algorithms, experiments on the Sioux Falls and Winnipeg networks found that, (in that case at least), although the numbers of iterations required for convergence were not notably longer for the bounded models (i.e. BSUE, BBPS, BAPS, & BAPS′ SUE) than the non-bounded models (i.e. MNL, PSL, GPSL, APSL, & APSL′ SUE), the additional computation time required during each iteration for the bounded models to perform the additional *column generation*, *flow allocation for new routes*, and *bound condition* phases, meant that (as expected) total computation times were longer. As anticipated from experiences solving APSL & APSL′ SUE, BAPS & BAPS′ SUE both had longer total computation times compared to BSUE & BBPS SUE, where BAPS SUE had long computation times for each of the iterations (due to solving fixed-point problems), and BAPS′ SUE had slow SUE convergence. However, from exploring the techniques developed for solving the APSL SUE model, it was shown how BAPS SUE can be solved in much quicker computation times.

An interesting result was that for Winnipeg, increasing the bound parameter φ led to quicker total computation times for solving BAPS SUE. This is because a greater number of iterations were required to equilibrate the choice sets for small values of the bound, which outweighed only a small saving in the average number of FPIM iterations required for BAPS probability convergence (from the smaller active choice sets).

Another interesting result was that the average used route choice set sizes for the bounded SUE models decreased as the travel demand level was increased. If one considers what one might expect under DUE, for low demand only the best costing routes are used, and increasing demand results in the used route choice sets expanding. For the bounded SUE models, however, although the used route choice sets expand initially from zero demand, they begin to decrease in size for larger demand. The suspected reason for this is that for high levels of congestion the costs on all links are inflated, and routes that are used for one OD movement are likely inflating the costs so that routes in other OD movements are then too costly to be used.

The experiments demonstrated how the bounded SUE models have the potential to be significantly more robust to the adopted choice sets than the non-bounded SUE models, with robustness improving as the bound parameter is decreased. It was also confirmed that the flow results from the bounded SUE models tend towards their limit non-bounded SUE model as the bound parameter is increased.

In conclusion, the proposed BPS SUE models succeed in addressing all four of the key challenging aspects of route choice modelling in a theoretically consistent, robust, and mathematically well-defined way. As discussed/demonstrated, the BPS SUE models offer a theoretically consistent and robust approach to realistic route choice set generation, and are significantly more robust to adopted choice sets compared to competitor non-bounded SUE models. BAPS has greater theoretical consistency compared to BBPS, and is thus in theory more behaviourally realistic, which is supported by the estimation results. BBPS SUE solutions are proven to exist, while, although not proven, solution existence is not an issue in practice for BAPS SUE, as long as the perturbation parameter is set appropriately small. Moreover, although uniqueness of solutions is not guaranteed, numerical experiments suggest that BBPS SUE solutions can be / are unique, and that uniqueness conditions exist for the BAPS SUE model. Furthermore, as shown, both models are estimatable from revealed choice data and can be solved in computationally feasible times on real-life large-scale networks, where BBPS is more computationally practical than BAPS.

There were three key motivating factors for developing the BPS SUE models: firstly, to take the weighted path size contribution technique of GPSL and APSL one step further by fully eliminating the path size contributions of unrealistic routes; secondly, to improve the behavioural realism of the BCM by incorporating a mechanism for capturing route correlations; and, thirdly, to develop a model that was mathematically well-defined, thereby addressing the shortcomings of the PSL Restricted SUE (PSL RSUE) (Watling et al, 2015; Rasmussen et al, 2015) and PSL Restricted SUE with a Threshold (PSL RSUET) (Rasmussen et al, 2017) models. PSL RSUE and PSL RSUET both offer a theoretically consistent approach to dealing with unrealistic routes and capturing route correlations within SUE context, but solution existence and uniqueness are not

guaranteed, and indeed this has been shown in examples. Although not proven, numerical experiments suggest that BBPS & BAPS SUE are mathematically well-defined in terms of solution existence and uniqueness. This is a significant result as it means they are suitable for real-life applications for traffic flow predictions.

2.2.2 Future Research

As discussed for solving APSL SUE, further research could also explore more intelligent, adaptive processes for solving BAPS SUE, as well as utilising a different fixed-point algorithm (to the FPIM) for computing the BAPS model probabilities within the SUE algorithm. Different step-size schemes should also be explored, such as the self-regulated averaging method, and if applicable the self-adaptive method. Since the BBPS model is closed-form, it would also be interesting to see whether inexact approaches requiring gradient information such as Armijo's step-size strategy are applicable, and how they perform.

In this thesis, solving BPS SUE models was explored in the case where there are pre-generated approximated universal route choice sets. Future research should also explore the case where routes are generated as the algorithm progresses. The difficulty with this approach – as discussed for BSUE in Watling et al (2018) – is that the computational burden involved in column generating all routes with costs less than the bound escalates dramatically and non-linearly as the scale of network increases / the bound increases. With this approach though, there are guaranteed to be no inconsistencies in terms of routes that were not pre-generated by the route generation criteria but would be considered realistic by the choice model criteria.

However, as discussed above, with the bounded models, a route is only defined unrealistic if it has a travel cost greater than the cost bound, yet in reality there may be many routes that have travel costs below the bound but would also be considered unrealistic. For example, routes with relatively large local detours such as on-off-ramps on motorways. Therefore, since on large-scale networks it will potentially be computationally infeasible to generate all routes less than even reasonably small bound values, yet possibly the majority of these routes may actually be unrealistic, future research could explore some theoretically consistent and computationally feasible way of removing all routes considered unrealistic.

Further research could also investigate under what conditions BAPS SUE solutions are not unique when BAPS model solutions are universally unique, and/or identify uniqueness conditions and a proof. Moreover, further research could explore under what conditions BBPS SUE solutions are not unique, and/or identify uniqueness conditions and a proof.

It would also be interesting to compare results from the BPS SUE models with results from the PSL RSUE and PSL RSUET models, and/or other RSUE models.

3. Wider Concluding Remarks

This thesis offers new approaches for modelling the route choices of drivers on road networks. This provides a means for traffic flow predictions on real-life networks. The hope is that APSL SUE and/or BBPS/BAPS SUE will be used for traffic flow predictions in real-life transport systems, e.g. for policy scenario testing.

Some further work is required before this, however. As discussed above, the models will need to be calibrated and applied with more complex route utility functions than those in this thesis, and different utilities/parameters for different e.g. user classes / vehicle types will need to be explored.

Moreover, the estimation work in this thesis concerns estimating APSL, BBPS, & BAPS as route choice models. How to estimate/calibrate these models within SUE should be explored. Traditionally, this has been done either sequentially (through estimating the link cost functions and then SUE model), or in a completely detached way (by just calibrating the underlying choice model). These approaches are potentially inconsistent, however. It would be interesting to explore whether calibration of the SUE models and link cost functions could be performed simultaneously.

There are also other behavioural realism extensions such as the scaling issue and dealing with local detour routes that could be explored to improve the accuracy of results. Moreover, a well-behaved approach for properly accounting for the effects of congestion – such as how bottlenecks lead to flow-metering and spillbacks – should be investigated, e.g. the 'quasi-dynamic' approaches of Bleimer et al (2014) and Brederode et al (2019).

Application of the models to network equilibrium with elastic travel demand should also be considered (e.g. Kitthamkesorn et al, 2015), to explicitly consider the equilibrium between supply and demand. It would be interesting to see how the equilibration of demand effects the equilibration of the choice sets.

Further, it would be interesting to know whether the APSL/BBPS/BAPS SUE models could be implemented within transport modelling software such as SATURN and VISUM, and how they perform. Both of these pieces of software have the capability of solving SUE and using it for traffic flow predictions. Most studies using SATURN for policy analysis so far, however, seem to use DUE for the traffic assignment (e.g. Mitchell et al, 2005; May et al, 2002).

It is worth noting also that, so far, standard PSL has been the most common path size approach (and also route choice modelling approach) adopted in practice, for e.g. travel behaviour adjustment prediction within a policy evaluation model. Perhaps the reason for this is due to the deficiencies of GPSL such as those highlighted in this thesis, e.g. the estimation concerns, and/or that solution of GPSL within a network equilibrium model had not yet been explored. The work in this thesis thus will (hopefully) provide practitioners with incentive to adopt an alternative path size model such APSL/BBPS/BAPS, or even GPSL.

The BPS models assume that drivers are aware of and consider the correlation between all routes / parts of the routes that they define as being realistic alternatives. This provides theoretical consistency, but perhaps it could be investigated whether the correlation network should be different to the physical network, by e.g. comparing with the subnetwork path size approaches of Frejinger & Bierlaire (2007) and Frejinger et al (2009), and thereby developing a BPS approach for the correlation subnetwork that offers continuity, consistency, robustness, and mathematical rigour (that the existing subnetwork approach currently lacks).

It would also be interesting to find out how the models and concepts developed in this thesis could be transferred to other transport or non-transport modelling topics. For example, the recently developed concept of multi-region traffic assignment modelling with Macroscopic Fundamental Diagrams (MFDs) (e.g. Yildirimoglu & Geroliminis (2014), Batista & Leclercq (2019), Mariotte et al (2020)), where the new path size models are adapted for the context of regional path choice. Or, how the new path size models could be applied to other route choice types, such as cycling route choice, where there may be different features to consider. For example, in cycling route choice, cyclists may have a bound upon the gradient of slope or energy they are willing to exert travelling uphill, which the BPS models could be adapted to remove routes. Alternatively, how the models can be adapted for path choice in multi-modal networks in contexts such as Mobility-as-a-Service (MaaS). Hoogendoorn-Lanser et al (2005) explore GPSL for multi-modal networks where trip legs are considered in the path size terms, it would be interesting to see how the BPS models apply, and there are likely to be plenty of unrealistic journey options.

Route choice modelling is a unique type of choice modelling in many respects, however it would be interesting to discover how the choice modelling concepts in this thesis could apply to other types of choice modelling. Specifically, perhaps, how the concept of imposing a consistent bound upon choice attributes could be adopted to implicitly generate choice sets, or how path size correction factors could be used to capture correlations between alternatives in other settings. One application, for example, could be in Mobility-as-a-Service bundle choice modelling, where there are potentially millions of bundle options, many of which may be considered unrealistic. There will also likely be strong correlations between alternative bundles and with such large choice sets, perhaps path size correction factors would be more suitable computationally, than nested/mixed approaches.

It would be particularly pleasing if the models and concepts developed in this thesis were used in policy analysis for reducing levels of congestion, with the objective of reducing CO_2 emissions. For example, exploring introducing a tolling scheme, where APSL/BBPS/BAPS SUE would be used for the traffic flow predictions, and some optimisation procedure would optimise the tolling price levels to minimise CO_2 emissions (whilst satisfying e.g. socio-economic benefit).

Furthermore, due to the improved possibilities of collecting new types of data, and the increased accessibility of data, the way in which we can calibrate and validate proposed route choice models is changing. Traditionally, the calibration and validation of models has been through measuring the proximity of the predicted link flows to some observed link flows collected from data. However, due to the emergence of new data types, for example GPS data and Bluetooth data, there is now an improved possibility to observe the choices of routes in which drivers take, allowing for a greater understanding of the behaviour of drivers and the calibration and validation of route choice models. It is also possible that these new data types and the increasing availability and detail of them, could be more beneficial to the models developed in this thesis than traditional models. The ability to track a large sample of observed route choices – from all travellers as well as from specific individuals / OD movements – means that significant information can be gathered on the bounds drivers have as a whole, as well as bounds that individuals, user classes etc. may have.

It is gratifying that APSL has already picked up interest in the field of route choice modelling. A recent article by Knies & Melo (2020) proposes a Recursive Logit with choice aversion model, where APSL is used as the main reference model throughout the paper. An extensive comparison is conducted in numerous experiments and the authors are quite complimentary of APSL. It will be exciting to see what other models are compared with APSL in other studies, or how other researchers use APSL in their work. Moreover, what attention the BPS models receive, now that the paper has been published.

4. References

Batista S & Leclercq L, (2019). Regional Dynamic Traffic Assignment Framework for Macroscopic Fundamental Diagram Multi-regions Models. Transportation Science, 53(6), p.1563-1590.

Bliemer M, Raadsen M, Smits E, Zhou B, & Bell M, (2014). Quasi-dynamic traffic assignment with residual point queues incorporating a first order node model. Transportation Research Part B: Methodological, 68, p.363-384.

Brederode L, Pel A, Wismans L, de Romph E, & Hoogendoorn S, (2019). Static Traffic Assignment with Queuing: model properties and applications. Transportmetrica A: Transport Science, 15(2), p.179-214.

Chen A, Pravinvongvuth S, Xu X, Ryu S, & Chootinan P, (2012). Examining the scaling effect and overlapping problem in logit-based stochastic user equilibrium models. Transportation Research Part A, 46, p.1343-1358.

Chen A, Xu X, Ryu S, & Zhou Z, (2013). A self-adaptive Armijo stepsize strategy with application to traffic assignment models and algorithms. Transportmetrica A: Transport Science, 9(8), p.695–712.

Chen A, S Ryu, Xu X, & Choi K, (2014). Computation and Application of the Paired Combinatorial Logit Stochastic User Equilibrium Problem. Computers and Operations Research, 43, p.68–77.

Gliebe J, Koppleman F, & Ziliaskopoulos A, (1999). Route choice using a paired combinatorial logit model. In: Presented at the 78th Annual Meeting of the Transportation Research Board, Washington, DC.

Kitthamkesorn S, & Chen A, (2013). Path-size weibit stochastic user equilibrium model. Transportation Research Part B, 57, p.378-397.

Kitthamkesorn S & Chen A, (2014). Unconstrained weibit stochastic user equilibrium model with extensions. Transportation Research Part B, 59, p.1–21.

Kitthamkesorn S, Chen A, & Xu X, (2015). Elastic demand with weibit stochastic user equilibrium flows and application in a motorised and non-motorised network, Transportmetrica A: Transport Science, 11(2), p.158-185.

Hoogendoorn-Lanser S, Nes R, & Bovy P, (2005). Path Size Modeling in Multimodal Route Choice Analysis. Transportation Research Record: Journal of the Transportation Research Board, 1921, p.27–34.

Liu H, He X, & He B, (2009). Method of successive weighted averages (MSWA) and self regulated averaging schemes for solving stochastic user equilibrium problem. Networks and Spatial Economics, 9(4), p.485–503.

May A, Milne D, & Shepherd A, (2002). Specification of Optimal Cordon Pricing Locations and Charges. Transportation Research Record: Journal of the Transportation Research Board, 1812(1), p.60-68.

Mariotte G, Leclercq L, Batista F, Krug J, & Paipuri M, (2020). Calibration and validation of multi-reservoir MFD models: A case study in Lyon. Transportation Research Part B, 136, p.62-86.

Mitchell G, Namdeo A, & Milne D, (2005). The air quality impact of cordon and distance based road user charging: An empirical study of Leeds, UK. Atmospheric Environment, 39(33), p.6231-6242.

Ramming S, (2002). Network knowledge and route choice. Ph.D. Thesis, Massachusetts Institute of Technology, Cambridge, USA.

Rasmussen T, Nielsen O, Watling D, & Prato C, (2015). Stochastic user equilibrium with equilibrated choice sets: Part II – Solving the restricted SUE for the logit family. Transportation Research Part B, 77, p.146–165.

Rasmussen T, Nielsen O, Watling D, & Prato C, (2017). The Restricted Stochastic User Equilibrium with Threshold model: Large-scale application and parameter testing. European Journal of Transport and Infrastructure Research, 15(1), p.1-24.

Watling D, Rasmussen T, Prato C, & Nielsen O, (2015). Stochastic user equilibrium with equilibrated choice sets: Part I – Model formulations under alternative distributions and restrictions. Transportation Research Part B (77), p.166-181.

Watling D, Rasmussen T, Prato C, & Nielsen O, (2018). Stochastic user equilibrium with a bounded choice model. Transportation Research Part B, 114, p.254-280.

Xu X, Chen A, Zhou Z, & Behkor S, (2012). Path-based algorithms for solving C-logit stochastic user equilibrium assignment problem. Transportation Research Record, 2279, p.21–30.

Xu X, & Chen A, (2013). C-logit stochastic user equilibrium model with elastic demand. Transportation Planning and Technology, 36(5), p.463–478.

Yang C, Chen A, & Xu X, (2013). Improved partial linearization algorithm for solving the combined travel-destination-mode-route choice problem. Journal of Urban Planning and Development, 139(1), p.22–32.

Yao J, Chen A, Ryu S, & Shi F, (2014). A general unconstrained optimization formulation for the combined distribution and assignment problem. Transportation Research Part B, 59, p.137–160.

Yildirimoglu M & Geroliminis N, (2014). Approximating dynamic equilibrium conditions with macroscopic fundamental diagrams. Transportation Research Part B: Methodological, 70, p.186–200.

Zhou Z & Chen A, (2006). A self-adaptive gradient projection algorithm for solving the nonadditive traffic equilibrium problem. Paper presented at the 85th annual meeting of the transportation board, Washington, D.C., USA.

Zhou Z, Chen A, & Bekhor S, (2012). C-logit stochastic user equilibrium model: formulations and solution algorithm. Transportmetrica, 8(1), p.17–41.